Wavevector-Frequency Analysis With Applications to Acoustics

Wayne A. Strawderman

Wavevector-Frequency Analysis With Applications to Acoustics

Wayne A. Strawderman

For sale by the Superintendent of
Documents, U.S. Government Printing
Office, Washington, DC 20402
Stock #008-047-00408-7

PREFACE

The preparation of this book was funded by the Independent Research/Independent Exploratory Development (IR/IED) Program of the Naval Undersea Warfare Center (NUWC), Division Newport. The sponsoring activity is the Office of Naval Research (ONR), program manager Dr. William Lukens (Code 10P6).

The author gratefully acknowledges the assistance of the following individuals during the preparation of this book: Albert Nuttall for his many helpful discussions and suggestions on numerous technical issues and for his technical review of the final document; Ronald Kneipfer for his recommendations on the treatment of certain statistical concepts and for his technical review of individual chapters; Henry Bakewell, Roy Streit, and Charles Sherman for their technical review of individual chapters; Kenneth Lima, IR/IED program manager, for his enthusiastic support of this research effort; and Karen Holt for her careful editing of the manuscript.

TABLE OF CONTENTS

TABLE OF CONTENTS (Cont'd)

TABLE OF CONTENTS (Cont'd)

LIST OF ILLUSTRATIONS

LIST OF ILLUSTRATIONS (Cont'd)

LIST OF ILLUSTRATIONS (Cont'd)

LIST OF ILLUSTRATIONS (Cont'd)

LIST OF TABLES

WAVEVECTOR-FREQUENCY ANALYSIS WITH APPLICATIONS TO ACOUSTICS

CHAPTER 1
INTRODUCTION

This monograph presents an approach to the description and analysis of acoustic fields and systems that parallels and extends one developed by electrical engineers to describe and analyze electrical signals and systems. This approach, called wavevector-frequency analysis, complements traditional methods of acoustics.

Wavevector-frequency analysis is simply the description and interpretation of a space-time field or system in terms of the Fourier conjugates of the independent spatial and temporal variables of the field or system. The Fourier conjugate of the spatial vector variable is called the wavevector, and the Fourier conjugate of the time variable is the frequency.

The formalism of this approach to acoustics evolved over the course of an extended research effort to understand and characterize certain acoustic fields associated with turbulent flow. A brief description of this research effort will put the evolution of this approach in perspective.

1.1 HISTORY AND PERSPECTIVE

When a vehicle such as an airplane, automobile, or ship is subjected to a turbulent flow, random pressure fluctuations that occur in the boundary layer of the vehicle excite a vibration field in the outer wall of the vehicle. That flow-excited vibration field in turn produces pressure fields in the fluids interior and exterior to the vehicle. Because the pressure in the turbulent boundary layer varies randomly in space and time, the turbulent flow-excited pressure and vibration fields are also random functions of space and time. Such turbulent flow-induced pressure and vibration fields have been the subject of continuing research over the past 30 years.

By necessity, this research has been a interdisciplinary effort. That is, the physics of turbulent flow is the domain of the hydrodynamicist; the vibration of the vehicle and the consequent pressure fields radiated to the interior and exterior of the vehicle are the domain of the acoustician; and the description and measurement of these random fields is the domain of the statistician or signal processor. As might be expected, the cooperative effort between researchers in these different specialties over a long period of time led to extensive crossfertilization among disciplines. This crossfertilization resulted in an entirely new set of specialties in the field of acoustics. The combinations of disciplines comprising the best known of these new specialties, hydroacoustics and aeroacoustics, are evident from their names. Some combinations of disciplines, however, did not lead to such descriptive names nor to such widespread recognition. One such combination, called wavevector-frequency analysis, designates the specialized extension of traditional linear systems and signal processing theories developed, over the course of this research effort, to describe and analyze the turbulent pressure field and the turbulent flow-excited vibration and pressure fields.

Traditional linear systems and signal processing theories were developed by electrical engineers to treat systems and fields that depend only on a single independent variable, time. In linear systems theory, it is demonstrated that the Fourier transformation of these temporal fields into corresponding fields in the frequency domain often simplifies the mathematical description of the system and thereby facilitates physical prediction and interpretation of the system. To exploit these advantages for empirical investigations, signal processing engineers developed techniques to measure the frequency characteristics of random and deterministic time fields.

It should be emphasized that the advantages of Fourier transform techniques for analysis and interpretation of linear systems have long been recognized by researchers in other branches of physics, including those in acoustics. However, the pressure and velocity fields encountered in acoustics are generally functions of four variables: three spatial coordinates (the components of the spatial position vector) and time.

Consequently, the Fourier transforms of acoustic fields are also functions of four variables: three wavenumber coordinates (the components of the wavevector) that are the Fourier conjugates of the three spatial variables, and frequency (the Fourier conjugate of the time variable). Owing to this higher dimensionality, the measurement of the wavevector-frequency characteristics of acoustic fields presented a far more difficult task than the measurement of the frequency characteristics of electrical fields that varied only with time. Prior to the development of such a measurement capability, wavevector-frequency descriptions of acoustic fields were traditionally employed only as an intermediate step in the prediction of the space-time characteristics of such fields. Nonetheless, these theoretical studies provided the mathematical foundation for the formalized extension of traditional linear systems theory to space-time fields.

In 1967, Maidanik and Jorgensen[1] proposed a method for direct measurement of the wavevector-frequency spectrum of the wall pressure fluctuations in a turbulent boundary layer. In 1971, Blake and Chase[2] employed this technique to perform such measurements. This demonstrated ability to measure the wavevector-frequency characteristics of space-time fields promoted wavevector-frequency analysis from an interesting and useful mathematical technique to a potentially powerful tool for interpretation and analysis of experimental data. It therefore prompted increased research efforts to develop new techniques for wavevector-frequency measurement and analysis. These research efforts continue today in a wide variety of scientific disciplines dealing with space-time fields.

1.2 MOTIVATION AND OBJECTIVE

Despite the demonstrated utility of wavevector-frequency analysis for characterization and interpretation of the acoustic fields generated by turbulent flow over vehicles, the application of wavevector analysis techniques in acoustics has been left to the specialist. The motivation for this monograph is to encourage a wider understanding and application of these powerful techniques by the nonspecialist.

One impediment to the adoption of these techniques by the nonspecialist

is the lack of a comprehensive tutorial treatment of wavevector-frequency analysis. The existing theoretical and experimental capabilities in this specialty are a result of research conducted in universities, government laboratories, and private industry. The objective of this monograph is to organize these disparate theoretical and experimental results into a tutorial treatment of wavevector-frequency analysis and its application to acoustics.

Because the objective of this work is to teach the fundamentals of wavevector-frequency analysis for acoustic applications, we make no attempt to exhaustively review the manifold publications of theoretical and experimental research in this field. Rather, we will meld selected results from those references into a format that mathematically defines, physically interprets, and (where possible) illustrates by experimental data, the essential aspects of wavevector-frequency analysis. It is expected that the reader interested in a particular topic will use the references cited at the end of each chapter to expand his sources of information.

1.3 ORGANIZATION

The nine chapters comprising this text treat four topics. Basic definitions and relationships are presented in chapter 2. Chapters 3, 4, and 5 present linear systems theory for space-time invariant, space-varying, and coupled systems, respectively. Chapters 6 and 7 treat the description of random space-time fields and the response of linear systems to such random fields. The problems of measurement and estimation of wavevector-frequency spectra are treated in chapters 8 and 9.

1.4 DEPTH AND PREREQUISITES

This monograph is intended as a tutorial source for practicing scientists and engineers. The level of the material presented is equivalent to that encountered in a first-year graduate course. The reader is assumed to have a basic understanding of acoustics (including vibrations), Fourier transforms and series, simple generalized functions, and statistics. Although many fundamental concepts in these subjects are reviewed in this

book, their treatment is not rigorous. Rather, such reviews are somewhat cursory and are included to reacquaint the reader with certain fundamentals or to improve the continuity of certain arguments. For comprehensive treatments of such fundamental concepts, the reader should consult standard references.

1.5 REFERENCES

1. G. Maidanik and D. W. Jorgensen, "Boundary Wave-Vector Filters for the Study of the Pressure Field in a Turbulent Boundary Layer," Journal of the Acoustical Society of America, vol. 42, no. 2, August 1967, pp. 494-501.

2. W. K. Blake and D. M. Chase, "Wavenumber-Frequency Spectra of Turbulent Boundary Layer Pressure Measured by Microphone Arrays," Journal of the Acoustical Society of America, vol. 49, no. 3, March 1971, pp. 862-877.

CHAPTER 2
WAVES AND THEIR DESCRIPTORS

This chapter defines, and physically interprets, the parameters used to describe the spatial and temporal characteristics of harmonic waves. The mathematical description of an arbitrary wave in terms of these parameters is developed.

Van Nostrand's Scientific Encyclopedia[1] defines a wave as a "disturbance which is propagated in a medium in such a manner that at any point in the medium the displacement is a function of the time, while at any instant the displacement at a point is a function of the position of the point." This general definition establishes that waves are fields in which the variation of some physical quantity is specified over some region of space and time. Note that this definition does not require any specific form of the temporal or spatial variation of the disturbance. However, the word "propagated" implies some relationship between the spatial and temporal variables. From the above, it is clear that a wave is not a specific space-time field. Rather, a wave is any member of a class of space-time fields that describes a disturbance which propagates in space and time.

One of the simplest waves is the harmonic wave. A harmonic wave is defined as one in which the disturbance varies sinusoidally in space and time. We begin our study and characterization of waves with a specific form of the harmonic wave called the plane harmonic wave.

2.1 THE PLANE HARMONIC WAVE

Consider a disturbance, say the pressure in a fluid, described by

$$p(\vec{x},t) = P \exp[i(\vec{k}\cdot\vec{x} + \omega t)] \ . \tag{2-1}$$

Here, p denotes the pressure, $\vec{x} = [x_1, x_2, x_3]$ is the spatial position vector, t designates time, P is a complex constant that represents the

amplitude of the disturbance, $\vec{k} = [k_1,k_2,k_3]$ is the (constant) wave vector, ω is the (constant) circular frequency, exp z denotes e^z, $\vec{k}\cdot\vec{x}$ denotes the inner (or dot) product of the vectors $\vec{k}$ and $\vec{x}$, and i is the square root of minus one.

The physical pressure is, of course, a real function of space and time. Therefore, when expressing the pressure in the complex form of equation (2-1), we mean that the physical pressure, $p_r(\vec{x},t)$, is the real part of the complex function. That is, we mean

$$p_r(\vec{x},t) = P_{mag} \cos(\vec{k}\cdot\vec{x} + \omega t + \phi) \ , \qquad (2\text{-}2)$$

where P_{mag} and ϕ are the absolute value and argument of the complex amplitude, P, respectively.

The argument of the cosine in equation (2-2), that is, $\vec{k}\cdot\vec{x} + \omega t + \phi$, is defined as the phase of the harmonic wave, and P_{mag} is the amplitude of the physical wave. Therefore, the effect of varying the spatial or temporal coordinates is simply to change the phase of the wave. Note that ϕ is the phase of the wave at $\vec{x} = [0,0,0]$ and $t = 0$.

The period of a harmonic wave is defined as the time difference, T, between successive repetitions, or cycles, of the wave at a fixed point in space. Recall that, in equations (2-1) and (2-2), the wavevector and frequency are constants. Thus, at any fixed point in space, say $\vec{x}_0$, the pressure varies only with time. That is,

$$p(\vec{x}_0,t) = P_{mag} \exp[i(\omega t + \vec{k}\cdot\vec{x}_0 + \phi)] \ . \qquad (2\text{-}3)$$

Mathematically, the period is defined as the smallest positive value of T for which

$$p(\vec{x}_0,t + T) = p(\vec{x}_0,t) \qquad (2\text{-}4)$$

for all t. By equations (2-3) and (2-4), it is clear that the period corresponds to the time increment required to increase the phase of the wave

by 2π radians, and it is given by

$$T = 2\pi/\omega \ . \tag{2-5}$$

It follows, then, that the circular frequency, ω, is related to the period by

$$\omega = 2\pi/T \tag{2-6}$$

and is the time rate of change of phase of the wave in radians per second.

A more familiar definition of frequency is the temporal frequency, f, which is defined as the number of repetitions, or cycles, of the wave per unit time. One cycle corresponds to a phase change of 2π radians; thus, the temporal and circular frequencies are related by

$$f = \omega/(2\pi) = 1/T \ . \tag{2-7}$$

By the above, it is evident that both circular and temporal frequency define the time rate of repetition of the wave. However, this rate is measured in different units. That is, circular frequency is the time rate of change of phase, where a phase change of 2π radians is required for one repetition. Temporal frequency, on the other hand, is the number of repetitions of the wave per unit time.

An important concept in the description and characterization of harmonic waves is that of the phase front. A phase front is defined as a surface in space over which the phase of the wave is constant. According to equations (2-1) and (2-2), when the phase is constant, the value of the pressure, $p(\vec{x},t)$, is constant. Thus, a phase front corresponds to a surface of constant pressure in space associated with a particular phase of the wave.

Consider the phase front of the wave defined by equation (2-2) associated with the constant phase, β. The phase front is then defined by

$$\vec{k}\cdot\vec{x} + \omega t + \phi = \beta \tag{2-8}$$

and is designated as phase front β. At time $t = t_0$, the surface of constant

phase associated with phase front ß is given by

$$\vec{k}\cdot\vec{x} + \omega t_0 + \phi = \beta \tag{2-9}$$

and is a function of $\vec{x}$ only. As $\vec{k}$ is a constant, equation (2-9) defines a plane in the three-dimensional space, $\vec{x}$. The constant, ß, is arbitrary. Therefore, all phase fronts of the harmonic wave defined by equations (2-1) and (2-2) are planes. Consequently, waves having the mathematical form of equations (2-1) and (2-2) are called plane harmonic waves, and their phase fronts are often referred to as phase planes.

Let $\vec{x}_A$ and $\vec{x}_B$ be vectors defining two points, A and B, in the phase plane specified by equation (2-9), as illustrated in figure 2-1.

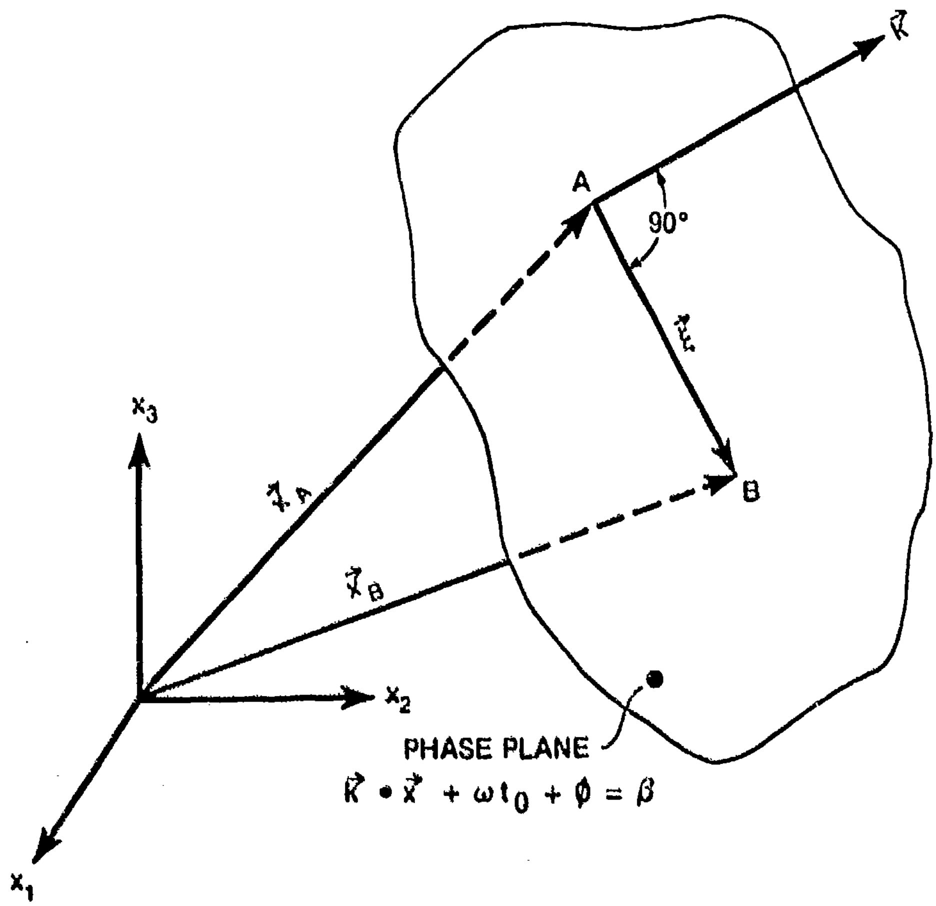

Figure 2-1. Relative Geometry Between the Wavevector and a Line in the Phase Plane

The nonzero vector $\vec{\xi} = \vec{x}_B - \vec{x}_A$ then defines a vector in the phase plane. As both $\vec{x}_A$ and $\vec{x}_B$ satisfy equation (2-9), it follows that

$$\vec{k} \cdot \vec{\xi} = 0 \, . \tag{2-10}$$

Neither $\vec{k}$ nor $\vec{\xi}$ is a zero vector. It follows, then, that the wavevector $\vec{k}$ is perpendicular to the vector $\vec{\xi}$. However, as the vectors $\vec{x}_A$ and $\vec{x}_B$ are arbitrary, the vector $\vec{\xi}$ is also arbitrary. Therefore, the wavevector, $\vec{k}$, is perpendicular to every vector in the phase plane. Consequently, the wavevector $\vec{k}$ is perpendicular to the plane of the phase front. Furthermore, as $\vec{k}$ is a constant vector, it is clear that all phase planes of our harmonic wave are parallel.

By taking the time derivative of equation (2-8), we obtain (for constant β)

$$\vec{k} \cdot \vec{v} + \omega = 0 \, , \tag{2-11}$$

where $\vec{v}$ is the velocity vector of the phase front at any point $\vec{x}$ and is defined by

$$\vec{v} = \frac{d\vec{x}}{dt} \, . \tag{2-12}$$

It is evident that there are an infinite number of velocities which satisfy equation (2-11). However, as $\vec{k}$ is a constant, all possible velocity vectors defined by equation (2-11) must have the same component normal to the phase front: that is, in the direction parallel to $\vec{k}$. If we denote the velocity normal to the phase front by $\vec{c}_p$, it follows from equation (2-11) that

$$\vec{k} \cdot \vec{v} = \vec{k} \cdot \vec{c}_p = k c_p \cos \theta = -\omega \, , \tag{2-13}$$

where k and c_p denote the magnitudes of the corresponding vectors and θ is the angle between the vectors $\vec{k}$ and $\vec{c}_p$. As $\vec{k}$ and $\vec{c}_p$ are parallel vectors, it follows from equation (2-13) that $\theta = \pi$ for $\omega > 0$ and $\theta = 0$ for $\omega < 0$. Thus, the wavevector, $\vec{k}$, is directed opposite to the normal velocity of the phase front for $\omega > 0$ and coincident to the normal velocity of the phase front for $\omega < 0$. Further, as $\vec{k}$ and ω are constants, the normal velocity, $\vec{c}_p$, is a constant and is given by

$$\vec{c}_p = \frac{-\vec{k}\omega}{k^2} \, . \tag{2-14}$$

The velocity $\vec{c}_p$ is defined as the phase velocity of the wave and is the apparent velocity at which the planar phase front propagates through the medium. The word "apparent" is used because only the normal component of the velocity of the phase plane effects an apparent change in the spatial location of the phase plane; the tangential components produce only in-plane slippage of the front. For a more comprehensive treatment of the kinematics of wavefronts, the reader is directed to reference 2.

For a known phase velocity of the plane wave, the wavevector is easily determined by

$$\vec{k} = \frac{-\vec{c}_p\omega}{c_p^2} \, . \tag{2-15}$$

Returning our attention to equations (2-1) and (2-2), it is a simple matter to show that, at any fixed time, the pressure field is periodic in space. That is, a spatial vector $\vec{\xi}$ exists such that, at the fixed time t_0,

$$p(\vec{x} + \vec{\xi}, t_0) = p(\vec{x}, t_0) \tag{2-16}$$

for all $\vec{x}$. The nonzero vectors, $\vec{\xi}$, that satisfy equation (2-16) are easily shown to be those for which

$$\vec{k}\cdot\vec{\xi} = 2n\pi \, , \quad n = \pm 1, 2, 3, \ldots \, . \tag{2-17}$$

The allowable values of $\vec{\xi}$ in equation (2-17) correspond to all vector separations between a reference phase plane and a series of other phase planes. If the phase of the reference plane is β, the phases associated with the other planes are $\beta + 2n\pi$.

The wavelength (or spatial period) is defined as the distance, measured normal to the phase plane, between successive spatial repetitions of the wave. If we denote the wavelength by λ and recall that the vector $\vec{k}$ is normal

to the wavefront, it follows from equation (2-17) that

$$\lambda = 2\pi/k \ . \tag{2-18}$$

Thus, for a known wavelength, the magnitude of the wavevector is given by

$$k = 2\pi/\lambda \ . \tag{2-19}$$

As λ is the minimum distance between successive repetitions of the wave and is measured parallel to $\vec{k}$, it follows from equation (2-19) that the wavevector can be interpreted as the magnitude and direction of the maximum rate of change of phase in space. This same interpretation of the wavevector can be obtained by considering the gradient of the phase. It is straightforward to show that the gradient of the phase, which by definition corresponds to the maximum spatial rate of change of phase, is equal to $\vec{k}$.

By returning our attention to equation (2-17), it is apparent that, if the vector $\vec{\xi}$ is taken parallel to the x_1 axis, the distance between successive repetitions of the wave is

$$\vec{\xi}_1 = 2\pi/k_1 \ . \tag{2-20}$$

This distance is defined as the projected wavelength in the x_1 coordinate direction and is designated by λ_1. Similarly, projected wavelength components may be defined in the other two coordinate directions, resulting in the relationships

$$\lambda_1 = 2\pi/k_1 \ , \quad \lambda_2 = 2\pi/k_2 \ , \quad \lambda_3 = 2\pi/k_3 \ . \tag{2-21}$$

The magnitude of the three components of the wavevector can therefore be expressed in terms of the projected wavelength components by

$$k_1 = 2\pi/\lambda_1 \ , \ k_2 = 2\pi/\lambda_2 \ , \ k_3 = 2\pi/\lambda_3 \tag{2-22}$$

and can be interpreted as the spatial rate of change of phase in the respective coordinate directions.

Some texts (see reference 3, for example) define the wavenumber components in terms of the number of cycles of the wave per unit length (which corresponds to $k_j = 1/\lambda_j$, $j = 1, 2, 3$) rather than the spatial rate of change of phase implied by equation (2-22). In this text, the wavevector will always be defined such that its components are consistent with equation (2-22). However, if one desires to express the wavenumber components in terms of cycles per unit length, the conversion is easily made by using arguments similar to those leading to equation (2-7).

2.2 MATHEMATICAL REVIEW

This section reviews some of the mathematical concepts and techniques that will be used in the course of this text. The review is included only for the purpose of reacquainting the reader with these concepts and techniques and for establishing certain conventions that we shall follow throughout this text. Therefore, this review will be conducted without any pretense of rigor, and the reader is encouraged to consult standard texts, as necessary, to supplement the material presented here.

2.2.1 Fourier Transforms

The Fourier integral theorem states that a function g(t) can be represented as an integral of its harmonic elements.[4] That is,

$$g(t) = \frac{1}{2\pi} \int_{-\infty}^{\infty} G(\omega)\exp(i\omega t)\, d\omega\ , \tag{2-23}$$

where $G(\omega)$ is the complex amplitude (within a factor of 2π) of each harmonic element and is given by

$$G(\omega) = \int_{-\infty}^{\infty} g(t)\exp(-i\omega t)\, dt\ . \tag{2-24}$$

The functions $g(t)$ and $G(\omega)$ constitute a Fourier transform pair, and the variable ω is called the Fourier conjugate of the variable t. The placement

of the factor of 2π in the definition of the transform pair is, within certain constraints, arbitrary. The choice in equations (2-23) and (2-24) is consistent with the convention used by electrical engineers.

To paraphrase Lighthill,[5] considerable literature has been devoted to determining the conditions on g(t) sufficient for equations (2-23) and (2-24) to be valid representations. For the fields, g(t), treated in this text, equations (2-23) and (2-24) are valid representations.

Sneddon[6] shows that the theory of Fourier transforms of functions of a single variable can be extended to functions of several variables. Thus, wave fields, which are functions of space and time, may be represented in terms of multidimensional Fourier transforms. For example, let $p(\vec{x},t)$ denote the space-time field associated with a pressure wave. Then, $p(\vec{x},t)$ can be represented by

$$p(\vec{x},t) = \frac{1}{(2\pi)^4} \iint_{-\infty}^{\infty} P(\vec{k},\omega)\exp[i(\vec{k}\cdot\vec{x} + \omega t)]\, d\vec{k}\, d\omega \; , \qquad (2\text{-}25)$$

where

$$P(\vec{k},\omega) = \iint_{-\infty}^{\infty} p(\vec{x},t)\exp[-i(\vec{k}\cdot\vec{x} + \omega t)]\, d\vec{x}\, dt \; . \qquad (2\text{-}26)$$

In equations (2-25) and (2-26), $d\vec{x}$ denotes $dx_1 dx_2 dx_3$ and $d\vec{k}$ denotes $dk_1 dk_2 dk_3$. The Fourier conjugate of the spatial vector variable, $\vec{x}$, is the wavevector, $\vec{k}$, and the Fourier conjugate of the time variable, t, is the circular frequency, ω.

Note that the integrand of equation (2-25) is a harmonic plane wave of the form of equation (2-1), with a complex amplitude of $P(\vec{k},\omega)$. Thus, it is evident, by equation (2-25), that expressing the pressure field as a Fourier transform is equivalent to representing that field as a summation, or superposition, of harmonic plane waves, where each harmonic component is characterized by a distinct wavevector and frequency. The wavevector-

frequency transform, $P(\vec{k},\omega)$, of the space-time field, $p(\vec{x},t)$, can be interpreted as the relative complex amplitude of each harmonic plane wave component comprising the pressure field.

It should be emphasized that the components of the wavevector, $\vec{k}$, and the circular frequency, ω, are real variables. If we require the wave field variable (e.g., the pressure in equation (2-25)) to be real also, then we require that

$$p(\vec{x},t) = p^*(\vec{x},t) \ , \tag{2-27}$$

where the asterisk denotes the complex conjugate. It follows from equations (2-25) and (2-27) that, for the pressure to be real,

$$P(\vec{k},\omega) = P^*(-\vec{k},-\omega) \ . \tag{2-28}$$

Thus, the wavevector-frequency transform of a real space-time field has conjugate symmetry in both wavevector and frequency.

2.2.2 Generalized Functions

Many of the operations involving Fourier transforms are facilitated by the use of generalized functions. Further, in some of the chapters to follow, generalized functions will be used for either notational or mathematical convenience. Therefore, before proceeding with further discussion of the Fourier transform and its properties, it is convenient to introduce the three generalized functions that will be used repeatedly throughout this text. For a more rigorous treatment of these generalized functions, the reader is referred to such texts as Lighthill[5] or Papoulis.[7]

The generalized function used most often is the Dirac delta function, denoted by δ. The delta function is defined by[8]

$$\delta(t - t_0) = 0 \ , \quad \text{for } t \neq t_0 \ , \tag{2-29}$$

and is sufficiently large in the vicinity of $t = t_0$ that

$$\int_{t_1}^{t_2} \delta(t - t_0)\, dt = 1 , \tag{2-30}$$

where $t_1 < t_0 < t_2$. The delta function has the integral property that

$$\int_{-\infty}^{\infty} g(t)\delta(t - t_0)\, dt = g(t_0) , \tag{2-31}$$

where g(t) is any function of t that is continuous at t_0. By equation (2-31), it is seen that the delta function can be used to sample a function at any discrete argument of that function.

The second generalized function we shall use is the Heaviside, or unit step, function. The Heaviside function, denoted by U, is the indefinite integral of the Dirac delta function and is defined by the discontinuous function

$$U(t - t_0) = \int_{-\infty}^{t} \delta(y - t_0)\, dy = \begin{cases} 0 , & t < t_0 , \\ 1 , & t > t_0 . \end{cases} \tag{2-32}$$

The Heaviside function has the integral property that

$$\int_{-\infty}^{\infty} U(t - t_0)g(t)\, dt = \int_{t_0}^{\infty} g(t)\, dt , \tag{2-33}$$

where g(t) is any function that is continuous at $t = t_0$.

The last of the generalized functions we require are the derivatives of the delta function. The n^{th} derivative of the delta function is denoted by

$$\delta^{(n)}(t - t_0) = \frac{d^n\delta(t - t_0)}{dt^n} . \tag{2-34}$$

The derivatives of the delta function have the property that, for any good function, g(t),

$$\int_{t_1}^{t_2} \delta^{(n)}(t - t_0)g(t)\, dt = (-1)^n \frac{d^n g(t_0)}{dt^n} , \qquad (2\text{-}35)$$

where $t_1 < t_0 < t_2$. Lighthill[9] defines a "good" function as one that is everywhere differentiable any number of times and is such that it and all its derivatives are, at most, of order $|x|^{-N}$ as $|x|$ approaches infinity for all N. Thus, a good function decays, for large $|x|$, faster than any inverse power of $|x|$.

2.2.3 Some Useful Relationships and Interpretations

By use of the generalized functions and the Fourier transform, we may deduce some relationships that will be of use in forthcoming chapters. Further, some of these mathematical relationships can be interpreted in terms of the composition and characterization of wave fields.

One especially useful relationship is the Fourier transform of the delta function. If, in equation (2-24), we set

$$g(t) = \delta(t - t_0) , \qquad (2\text{-}36)$$

then, by equation (2-31), it follows that

$$G(\omega) = \exp(-i\omega t_0) . \qquad (2\text{-}37)$$

From equations (2-23), (2-36), and (2-37), it follows that

$$\delta(t - t_0) = \frac{1}{2\pi} \int_{-\infty}^{\infty} \exp[i\omega(t - t_0)]\, d\omega . \qquad (2\text{-}38)$$

A similar relation can be developed for $\delta(\omega - \omega_0)$.

Consider now a wave field (for consistency, we will again use the pressure field, $p(\vec{x},t)$) that has the Fourier transform

$$P(\vec{k},\omega) = (2\pi)^4 P_0 \delta(\vec{k} - \vec{k}_0)\delta(\omega - \omega_0) \; , \tag{2-39}$$

where

$$\delta(\vec{k} - \vec{k}_0) = \delta(k_1 - k_{01})\delta(k_2 - k_{02})\delta(k_3 - k_{03}) \tag{2-40}$$

and P_0 is a complex constant. By equations (2-25), (2-31), (2-39), and (2-40), it is easily shown that the pressure field resulting from the wavevector-frequency transform of equation (2-39) is

$$p(\vec{x},t) = P_0 \exp[i(\vec{k}_0 \cdot \vec{x} + \omega_0 t)] \; . \tag{2-41}$$

Equations (2-39) and (2-41) constitute a four-dimensional Fourier transform pair.

Comparison of equation (2-41) with equation (2-1) reveals that the pressure field of equation (2-41) is a plane harmonic wave field characterized by the single wavevector $\vec{k}_0$, the single frequency ω_0, and the complex amplitude P_0. This example shows distinctly one of the potential advantages of expressing a wave field in terms of its wavevector-frequency transform. That is, in this example, the Fourier transform maps the plane harmonic wave field, which exists over all space and time, into a field in the Fourier conjugate, or wavevector-frequency, domain, which is nonzero only at a single point.

A particularly useful property of the Fourier transform is the property of superposition. That is, if $g(t)$ in equation (2-24) is given by

$$g(t) = \sum_{n=1}^{N} g_n(t) \; , \tag{2-42}$$

then it follows that

$$G(\omega) = \sum_{n=1}^{N} G_n(\omega) . \qquad (2\text{-}43)$$

An interesting example of superposition in four dimensions can be illustrated by considering the pressure field resulting from the wavevector-frequency spectrum given by

$$P(\vec{k},\omega) = \frac{(2\pi)^4}{2} P_0[\delta(\vec{k} - \vec{k}_0)\delta(\omega - \omega_0) + \delta(\vec{k} + \vec{k}_0)\delta(\omega + \omega_0)] , \qquad (2\text{-}44)$$

where P_0 is a real constant. By equations (2-25) and (2-44), the pressure field is

$$p(\vec{x},t) = P_0 \cos(\vec{k}_0 \cdot \vec{x} + \omega_0 t) . \qquad (2\text{-}45)$$

Note that the pressure field of equation (2-45) is of the form of equation (2-2), with θ equal to zero. In this case, the pressure field is seen to be real, and its wavevector-frequency transform consists of two discrete components. Note that the Fourier transform of the real-valued pressure field (equation (2-44)) satisfies the condition of equation (2-28).

At the risk of belaboring a point, we may use the principle of superposition to substantiate our physical interpretation of the Fourier transform of equation (2-25). That is, we have shown that a wavevector-frequency transform comprised of the product of delta functions of the form of equation (2-39) produces a plane harmonic wave in the space-time domain of the form of equation (2-41). By the principle of superposition, then, a transform comprised of a summation of many different products of delta functions will produce a space-time field comprised of a summation of the corresponding plane harmonic waves. Therefore, if we write the transform of the pressure field in the form of the weighted superposition of products of delta functions, that is,

$$P(\vec{k},\omega) = \iint_{-\infty}^{\infty} P(\vec{\mu},\Omega)\delta(\vec{k} - \vec{\mu})\delta(\omega - \Omega)\, d\vec{\mu}\, d\Omega , \qquad (2\text{-}46)$$

then the resulting pressure field is a weighted superposition of plane harmonic waves. By equations (2-25) and (2-31), that weighted superposition of plane waves is given by

$$p(\vec{x},t) = (2\pi)^{-4} \iint_{-\infty}^{\infty} P(\vec{\mu},\Omega)\exp[i(\vec{\mu}\cdot\vec{x} + \Omega t)]\, d\vec{\mu}\, d\Omega \;, \tag{2-47}$$

which is merely a restatement of the multidimensional Fourier transform of equation (2-25). Therefore, the expression of a wave field as the multidimensional Fourier transform of equation (2-25) can be physically interpreted as the representation of that wave field as a superposition of plane harmonic waves. The wavevector-frequency transform of the space-time wave field represents the relative amplitudes and phases of these various harmonic wave components.

In the forthcoming chapters, we will often require the Fourier transforms of temporal or spatial derivatives of fields. Let g(t) be given by equation (2-23) and define

$$f(t) = \frac{d^n g(t)}{dt^n} \;, \tag{2-48}$$

If $F(\omega)$ denotes the Fourier transform of f(t), it is straightforward to show, by equations (2-23) and (2-48), that

$$F(\omega) = (i\omega)^n G(\omega) \;. \tag{2-49}$$

By similar arguments, it may be shown that the inverse Fourier transform of the n^{th} derivative of $G(\omega)$ with respect to ω is equal to $(-it)^n g(t)$.

An interesting and useful application of equations (2-48) and (2-49) is illustrated by the following example. Consider the equation

$$(\omega^2 - \omega_0^2)G(\omega) = 0 \;, \tag{2-50}$$

where we wish to determine $G(\omega)$. By performing the inverse Fourier transform of equation (2-50) and by utilizing equation (2-48), equation (2-49), and the principle of superposition, we can show that

$$g(t) = A \exp(i\omega_0 t) + B \exp(-i\omega_0 t) \ , \qquad (2\text{-}51)$$

where A and B are constants. By use of equations (2-24) and (2-38), it follows that the $G(\omega)$ satisfying equation (2-50) is given by

$$G(\omega) = A\delta(\omega - \omega_0) + B\delta(\omega + \omega_0) \ . \qquad (2\text{-}52)$$

This result will prove useful in forthcoming chapters.

As a final mathematical note, consider the Fourier transform of the product of two functions, $g(t)$ and $f(t)$. If the transforms of g and f are denoted by G and F, we may use equations (2-23) and (2-38) to show that

$$\int_{-\infty}^{\infty} g(t)f(t)\exp(-i\omega t)\ dt = (2\pi)^{-1} \int_{-\infty}^{\infty} G(\omega - \Omega)F(\Omega)\ d\Omega \ . \qquad (2\text{-}53)$$

The integral on the right-hand side is called the convolution of the functions G and F. By equation (2-53), it is seen that the Fourier transform of a product is the convolution of the transforms of the functions making up the product. By similar arguments, it may be shown that the inverse transform of a product also results in a convolution. That is,

$$(2\pi)^{-1} \int_{-\infty}^{\infty} G(\omega)F(\omega)\exp(i\omega t)\ d\omega = \int_{-\infty}^{\infty} f(t - \theta)g(\theta)\ d\theta \ . \qquad (2\text{-}54)$$

2.3 WAVEVECTOR-FREQUENCY DESCRIPTION OF WAVE FIELDS

This section reviews certain physical and mathematical concepts presented in the first two sections to clarify the rationale for describing wave fields in terms of their wavevector-frequency characteristics. In addition,

wavevector-frequency descriptions of wave fields in one and two spatial dimensions will be presented and discussed.

2.3.1 Review and Perspective

The justification for the description of wave fields as a function of wavevector and frequency, rather than space and time, is found in the multidimensional Fourier transform pair of equations (2-25) and (2-26). By these transform relationships, it must be concluded that $P(\vec{k},\omega)$ and $p(\vec{x},t)$ constitute equivalent descriptions of the wave field, inasmuch as either description may be derived from the other via the appropriate Fourier transformations. Therefore, a description of a wave field as a function of wavevector and frequency is as valid and complete as the description of that field as a function of space and time.

The reader might ask, with some justification, why the kinematics of the plane harmonic wave, rather than the simple argument presented above, was the focus of the initial section of this chapter. The reason for this choice was that, in my experience, the primary impediment to the understanding of the wavevector-frequency descriptions of fields is not the concept of the Fourier transform: it is the concept of the wavevector. The scientist or engineer has no problem envisioning the pressure field, $p(\vec{x},t)$, because space and time are familiar physical concepts. Envisioning the field $P(\vec{k},\omega)$, on the other hand, is likely to prove difficult because the wavevector is an unfamiliar physical concept. The concept of frequency, however, is well understood by acousticians. For this reason, the primary emphasis in this chapter was to define and physically interpret the wavevector.

The definition and interpretation of the wavevector were addressed by studying the kinematics of a plane harmonic wave, which corresponds to a wavevector-frequency field, $P(\vec{k},\omega)$, containing a single discrete wavevector-frequency component. It was shown that the space-time field associated with a plane harmonic wave is completely determined by the amplitude and phase of the wave. The amplitude specifies only the magnitude (and, in the case of a complex wave, the initial phase) of the disturbance associated with the wave.

All information regarding the spatial and temporal variation of the wave is contained in the phase.

As was shown in equation (2-8), the phase is a linear function of the components of the spatial position vector, $\vec{x}$, and time, t. The constants of proportionality are the components of the wavevector, $\vec{k}$, and the circular frequency, ω. The wavevector components define the rate of spatial repetition of the wave in each of the corresponding spatial coordinate directions at any fixed time. The circular frequency defines the rate of temporal repetition of the wave at any fixed point in space. The direction and speed of propagation of the plane harmonic wave are determined by appropriate combinations of the wavevector and circular frequency.

By equation (2-1), it is evident that knowledge of the (complex) amplitude, the wavevector, and the circular frequency is sufficient to define the field of the plane harmonic wave over all space and time. Further, it was shown in section 2.2.3 that expressing a space-time wave field as the multiple Fourier transform of equation (2-25) is equivalent to representing that field as a superposition of plane harmonic waves. Therefore, if one knows the complex amplitude, the wavevector, and the circular frequency of each plane harmonic wave comprising that superposition, the wave field can be uniquely defined over all space and time. This is precisely the information provided by the wavevector-frequency description (or transform) of the wave field, which is denoted by $P(\vec{k},\omega)$ in equations (2-25) and (2-26).

By the arguments presented above, the wavevector-frequency description (or transform) of a wave field specifies the complex amplitudes of all harmonic plane waves comprising that field as a function of the rates of spatial repetition (in each coordinate direction) and temporal repetition corresponding to each harmonic wave component.

2.3.2 Wave Fields in One and Two Spatial Dimensions

For generality, the wave fields treated thus far in this chapter have been assumed to have three-dimensional spatial variation. In forthcoming chapters, many of the illustrative examples will treat wave fields with spatial

variation in only one or two coordinate directions. These one- and two-dimensional spatial fields are interpreted as special cases of the three-dimensional field below.

Consider the pressure field, $p(\vec{x},t)$, having the wavevector-frequency transform

$$P(\vec{k},\omega) = 2\pi\tilde{P}(\underline{k},\omega)\delta(k_3) \ , \tag{2-55}$$

where $\underline{k}$ denotes the two-dimensional wavevector (k_1,k_2). By equation (2-25), the space-time field corresponding to equation (2-55) is given by

$$p(\vec{x},t) = \tilde{p}(\underline{x},t) = (2\pi)^{-3} \int_{-\infty}^{\infty} \tilde{P}(\underline{k},\omega)\exp[i(\underline{k}\cdot\underline{x} + \omega t)] \, d\underline{k} \, d\omega \ , \tag{2-56}$$

where $\underline{x}$ denotes the two-dimensional spatial vector (x_1,x_2). By equation (2-56), it is evident that $\tilde{p}(\underline{x},t)$ is a pressure field that depends only on the two-dimensional spatial vector, $\underline{x}$, and the time, t. Further, by equations (2-55), (2-56), and (2-26), one can easily demonstrate that

$$\tilde{P}(\underline{k},\omega) = \int_{-\infty}^{\infty} \tilde{p}(\underline{x},t)\exp[-i(\underline{k}\cdot\underline{x} + \omega t)] \, d\underline{x} \, dt \ . \tag{2-57}$$

Thus, $\tilde{P}(\underline{k},\omega)$ is the three-dimensional Fourier transform of $\tilde{p}(\underline{x},t)$ and is a function of the two-dimensional wavevector, $\underline{k}$, and the circular frequency, ω.

The characteristics of the wave field in two spatial dimensions can be interpreted as a special case of the three-dimensional spatial field. Equation (2-55) describes a wavevector-frequency field in which only plane harmonic waves having a zero spatial repetition rate in the x_3 coordinate direction (i.e., $k_3 = 0$) contribute to the space-time field. The physical interpretation of a zero spatial repetition rate of a plane harmonic wave in one coordinate direction is that there is no spatial variation of the wave in that coordinate direction. This is borne out by equation (2-56), which shows the resultant space-time field to be independent of the x_3 spatial coordinate.

As the space-time dependence of a plane harmonic wave is contained in the phase of the wave, it follows that the phase of each plane harmonic wave contribution to the wave field must also be independent of x_3. This conclusion is again supported by the form of the integrand of equation (2-56). If we consider a single wavevector-frequency component of the integrand, say $\underline{k}_0 = (k_{01}, k_{02})$ and ω_0, and denote the initial phase of that component by $\phi(\underline{k}_0, \omega_0)$, the phase front associated with the single wavevector component is given by

$$\underline{k}_0 \cdot \underline{x} + \omega_0 t + \phi(\underline{k}_0, \omega_0) = \beta \ . \tag{2-58}$$

The phase front defined by equation (2-58) is a straight line in the (x_1, x_2) plane. This straight line can be interpreted as a special case of the phase plane defined by equation (2-9). Recall that the wavevector, $\vec{k}$, is perpendicular to the phase plane. The x_3 axis, in our Cartesian coordinate system, is perpendicular to the (x_1, x_2) plane. By equations (2-55) and (2-56), only plane harmonic wave components characterized by wavevectors $\vec{k} = (\underline{k}, 0)$ contribute to the space-time pressure field. For such wavevectors, it is easily shown that if $\vec{x}_3 = (0, 0, x_3)$, then $\vec{k} \cdot \vec{x}_3 = 0$. As the magnitudes of neither $\vec{k}$ nor $\vec{x}_3$ are, in general, zero, it follows that the phase planes are perpendicular to the (x_1, x_2) plane. Thus, equation (2-58) may be interpreted as the description of a phase plane oriented perpendicular to the (x_1, x_2) plane, or as a phase line characterizing the intersection of that phase plane with the (x_1, x_2) plane.

From the arguments presented above, it should be obvious that the two-dimensional wavevector, $\underline{k}$, is perpendicular to the phase line. Further, definitions and interpretations of the two-dimensional wavevector are easily obtained by specializing the relationships presented in section 2.1.1 to the case where k_3 is zero and x_3 is a constant.

The wavevector-frequency characterization of a wave field in one spatial dimension can also be developed as a special case of the three-dimensional spatial field. Consider the wave field, $p(\vec{x}, t)$, resulting from the wavevector-frequency transform

$$P(\vec{k},\omega) = (2\pi)^2 \tilde{P}(k_1,\omega)\delta(k_2)\delta(k_3) \ . \qquad (2\text{-}59)$$

By equations (2-25) and (2-59), we obtain

$$p(\vec{x},t) = \tilde{p}(x_1,t) = (2\pi)^{-2} \iint_{-\infty}^{\infty} \tilde{P}(k_1,\omega)\exp[i(k_1x_1 + \omega t) \ dk_1 \ d\omega \ . \qquad (2\text{-}60)$$

Equation (2-60) describes a space-time field, $\tilde{p}(x_1,t)$, that is a function of the single spatial variable, x_1, and time. By Fourier-transforming equation (2-60) in x_1 and t and by utilizing equation (2-38), one can easily show that

$$\tilde{P}(k_1,\omega) = \iint_{-\infty}^{\infty} \tilde{p}(x_1,t)\exp[-i(k_1x_1 + \omega t)] \ dx_1 \ dt \ . \qquad (2\text{-}61)$$

Equations (2-60) and (2-61) constitute a Fourier transform pair.

As in the case of the wave field in two spatial dimensions, the wave field in one spatial dimension can be interpreted as a special case of the field in three spatial dimensions. By equation (2-59), all plane harmonic wave contributions to the space-time wave field are characterized by wavevectors having components $(k_1,0,0)$. As the wavevector has been shown to be directed perpendicular to the phase plane of the plane harmonic wave, it follows that the phase planes of all the harmonic wave contributions to $p(\vec{x},t)$ in equation (2-60) are perpendicular to the x_1 axis. Thus, the phases of the individual harmonic wave components in the integrand of equation (2-60) can be interpreted as descriptions of the kinematics of phase planes oriented perpendicular to the x_1 axis, or as the kinematics of the phase point defined by the intersection of the phase plane with the x_1 axis.

The definitions and kinematic interpretations of section 2.1.1 can be applied to the wave field in one spatial dimension by requiring k_2 and k_3 to be zero. These relations and definitions show that all harmonic components comprising the wave field in one spatial dimension are independent of x_2 and x_3 and propagate in the direction parallel to the x_1 axis and opposite to the direction of k_1.

2.4 REFERENCES

1. Van Nostrand's Scientific Encyclopedia, third edition, D. Van Nostrand Co., Inc., Princeton, NJ, 1958, p. 1795.

2. C. Truesdell and R. Toupin, "The Classical Field Theories," Encyclopedia of Physics, vol. III/1, Springer Verlag, Berlin, 1960, pp. 498-502.

3. P. M. Morse, Vibration and Sound, second edition, McGraw-Hill Book Co., New York, 1948, p. 225.

4. A. P. Dowling and J. E. Ffowcs Williams, Sound and Sources of Sound, Ellis Horwood, Ltd., Chichester, UK, 1983, p. 27.

5. M. J. Lighthill, Introduction to Fourier Analysis and Generalised Functions, University Press at Cambridge, Cambridge, UK, 1958, pp. 8-9.

6. I. N. Sneddon, Fourier Transforms, McGraw-Hill Book Co., New York, 1951, pp. 43-45.

7. A. Papoulis, The Fourier Integral and Its Applications, McGraw-Hill Book Co., New York, 1962.

8. Dowling and Ffowcs Williams, op. cit., p. 29.

9. Lighthill, op. cit., p. 16.

CHAPTER 3

SPACE- AND TIME-INVARIANT LINEAR SYSTEMS

In the first chapter, wavevector-frequency analysis was defined as the description of space-time fields or systems in terms of their wavevector-frequency characteristics. The second chapter treated the description and interpretation of space-time fields in the wavevector-frequency domain. The characterization and interpretation of the response of systems in the wavevector-frequency domain will be the topic of the next five chapters.

The systems approach presented in these chapters parallels, in many aspects, the linear system theory developed by electrical engineers for the analysis of systems and fields that depend only on time. This approach was adopted because it provides a fundamental and consistent method of addressing a wide variety of problems, including those in acoustics.

This chapter reviews the basic concepts of systems theory and demonstrates the rationale for the wavevector-frequency analysis of one class of space-time systems: the space- and time-invariant system.

3.1 SYSTEMS AND THEIR CLASSIFICATIONS

The definition of a system that suits the purpose of this text is a combination of those found in The American Heritage Dictionary of the English Language[1] and Brogan's Modern Control Theory.[2] With suitable apologies to both sources, we define a system as an aggregation or assemblage of interacting elements combined by man or nature to form an integral entity.

The key word in this definition is "elements." If, for example, the elements are taken to be su essive differential lengths of a string under tension, then some finite length of interest of the string can be considered to constitute a system. On the other hand, a finite length of string under tension would be an element of the system called the violin. Clearly, the

above definition of a system is sufficiently flexible to accommodate an infinite variety of components, interactions, and processes.

Systems theory is concerned with the interactions and behavior of the various elements of the system resulting from certain conditions or excitations imposed on the system. Therefore, the statement of a systems problem requires three definitions: (1) the definition of the elements and interactions comprising the system, (2) the definition of the conditions or inputs imposed on the system (usually called the input), and (3) the definition of the specific interaction or behavior of interest in the system, i.e., the system output. By this systems approach, a wide variety of problems can be reduced to the conceptually simple form depicted in figure 3-1.

In systems theory, a distinction is made between the physical system and the mathematical model of that system. The physical system is that assemblage of interacting devices, components, mechanisms, processes, etc., that have been selected for scrutiny. However, owing to cost considerations, the study of the behavior of the physical system under a given input is often conducted by means of an experimental or mathematical model of the system. Systems theory is concerned with the study and solution of these models of systems rather than the physical form of the system. Mathematical systems theory, or the study of mathematical models of systems, is the emphasis of these next few chapters.

The mathematical modeling of systems is an acquired skill, and a detailed discussion of the construction of mathematical models of systems is beyond the scope of this text. However, the mathematical form of the system model, including the forms of the input and consequent output, has a considerable impact on both the relative difficulty of predicting the output

Figure 3-1. Conceptual Form of a Systems Problem

of the system for a given input and on the mathematical techniques required for that prediction. As a result, system models are usually classified according to the mathematical characteristics of the system model and its input. Table 3-1 lists the major characteristics used to classify mathematical models of space-time systems and their inputs.

Table 3-1. Major Classifications of Systems

	Mathematical Properties	
System Model	Linear Deterministic Time Invariant Continuous Time Space Invariant Spatially Distributed	Nonlinear Stochastic Time Varying Discrete Time Space Varying Spatially Discrete
Input	Free Deterministic	Forced Stochastic

In general, all of the factors in table 3-1 must be taken into account in the classification of the mathematical model of the system and its input. However, the order of the listing has no significance.

In this table, a linear system is one in which the equations governing all model elements are linear. If one or more elemental equations are nonlinear, the system is nonlinear.

Systems models that contain parameters which vary in some random fashion, and can be described only in terms of their statistical or average properties, are called stochastic systems. Otherwise, they are considered deterministic.

If the parameters of the mathematical model do not vary with time, the system is time invariant. If the mathematical model of the system is defined for all time, it is a continuous-time model. On the other hand, a model that treats the system only at discrete time intervals is a discrete-time model.

A space-invariant system is one in which the parameters of the mathematical model are independent of the spatial coordinates of the model. A mathematical model that describes the physical system continuously over space is a spatially distributed model, whereas one that treats the system only at discrete points in space is a spatially discrete model. Lumped parameter systems are a special case of spatially discrete systems.

Continuous space-time systems are modeled by partial differential equations, whereas discrete systems are modeled by ordinary differential equations or finite difference equations.

A system is said to be free if there are no external inputs to the system. In this case, the behavior of the system is completely determined by the system itself and its initial conditions. A forced system is one subject to external inputs. If either the external input or the initial conditions are subject to random variations, the input or initial conditions are considered stochastic.

3.2 CLASSIFICATION OF ACOUSTIC SYSTEMS

The systems of interest in this book are those associated with linear acoustics. Further, because (1) the subject of this text is wavevector-frequency analysis and (2) the wavevector and frequency are the respective Fourier conjugates of the spatial vector and time variables, our focus is on those acoustic systems that are continuous in time and spatially distributed.

Our purpose of teaching the fundamentals of wavevector-frequency analysis is best served by restricting attention to the deterministic, time-invariant mathematical models that describe the bulk of acoustic systems. Therefore, we will not attempt to address the acoustics of stochastic and time-varying media.

Infinite, spatially invariant models of systems are often employed in acoustics because they are relatively easy to solve and offer insight regarding the relative importance of the various physical processes influencing the system output. However, in many acoustics problems, the

effects of the spatial limitations and boundary conditions on the system output are the focus of the modeling effort. Such space-bounded models fall in the class of space-varying systems. Clearly, both space-varying and space-invariant acoustic systems must be addressed.

Although stochastic systems will not be treated in this text, considerable interest and history exists in the response of acoustic systems to stochastic inputs. Therefore, all forms of inputs will be considered.

In summary, the acoustic systems treated here will be limited to those that are linear, deterministic, time-invariant and continuous, and spatially distributed. However, all classifications of inputs will be treated.

This chapter treats the response of space- and time-invariant linear systems to deterministic inputs and initial conditions. Chapter 4 addresses the response of space-varying (but time-invariant) systems to deterministic inputs and initial conditions. Chapter 5 reviews some coupled systems of interest in structural acoustics. Chapter 6 develops the statistical concepts and descriptors required for the treatment of the response of systems to stochastic inputs or initial conditions, and chapter 7 deals with the response of systems to such random excitation.

3.3 FREE RESPONSE OF SPACE- AND TIME-INVARIANT LINEAR SYSTEMS

Spatially distributed, continuous-time systems in linear acoustics are modeled by linear partial differential equations in which the independent variables are spatial coordinates and time. If attention is further restricted to systems that are invariant in space and time, the coefficients of the various terms of these linear partial differential equations are constants.

In free systems, the absence of external inputs is reflected in the partial differential equations that model the system by the absence of inhomogeneous terms. Thus, the mathematical models of free space-time-invariant linear systems are homogeneous partial differential equations with constant coefficients.

The output of a free system exists for all time and is sustained by natural interactions within the system. In the absence of external inputs, the initiation of the free response cannot be addressed. However, by specific knowledge of the output at any given time, the output can be determined for all time.

The outputs of free systems with losses cannot be described in the wavevector-frequency domain. The amplitudes of such outputs decrease monotonically with increasing time, and Fourier transforms of such outputs, over all time, do not exist.

The outputs of lossless, free space-time-invariant linear systems, however, can be described equivalently in the space-time domain or the wavevector-frequency domain. This equivalence of description and the techniques for solution in the wavevector-frequency domain can be demonstrated by some illustrative examples.

3.3.1 The Infinite String

A classical problem in linear acoustics is the free vibration of a uniform, infinitely long string, resulting from some specified initial displacement and velocity distribution. Here, the system is the string, free from external input, and the desired information (i.e., the output) is the space-time displacement field, w(x,t), of the string. The mass per unit length (ϵ) and the tension (T) of the string are constant over the length of the string. The mathematical model describing the displacement of the string is given[3] by the following linear partial differential equation with constant coefficients:

$$\frac{\partial^2 w}{\partial x^2} - \frac{1}{c_s^2}\frac{\partial^2 w}{\partial t^2} = 0 \qquad (3\text{-}1)$$

for all x and t, where $c_s^2 = T/\epsilon$.

If w(x,t) is written as the wavenumber-frequency transform

$$w(x,t) = (2\pi)^{-2} \iint_{-\infty}^{\infty} W(k,\omega) \exp\{i(kx + \omega t)\}\, dk\, d\omega \;, \tag{3-2}$$

then it follows from equation (3-1) that $W(k,\omega)$ must satisfy

$$[(\omega/c_s)^2 - k^2] W(k,\omega) = 0 \tag{3-3}$$

for all k and ω. Equation (3-3) states that $W(k,\omega)$ can have a nonzero solution only along the two lines defined by $|k| = |\omega/c_s|$, which are depicted in figure 3-2. Because of this restriction on the wavenumber content

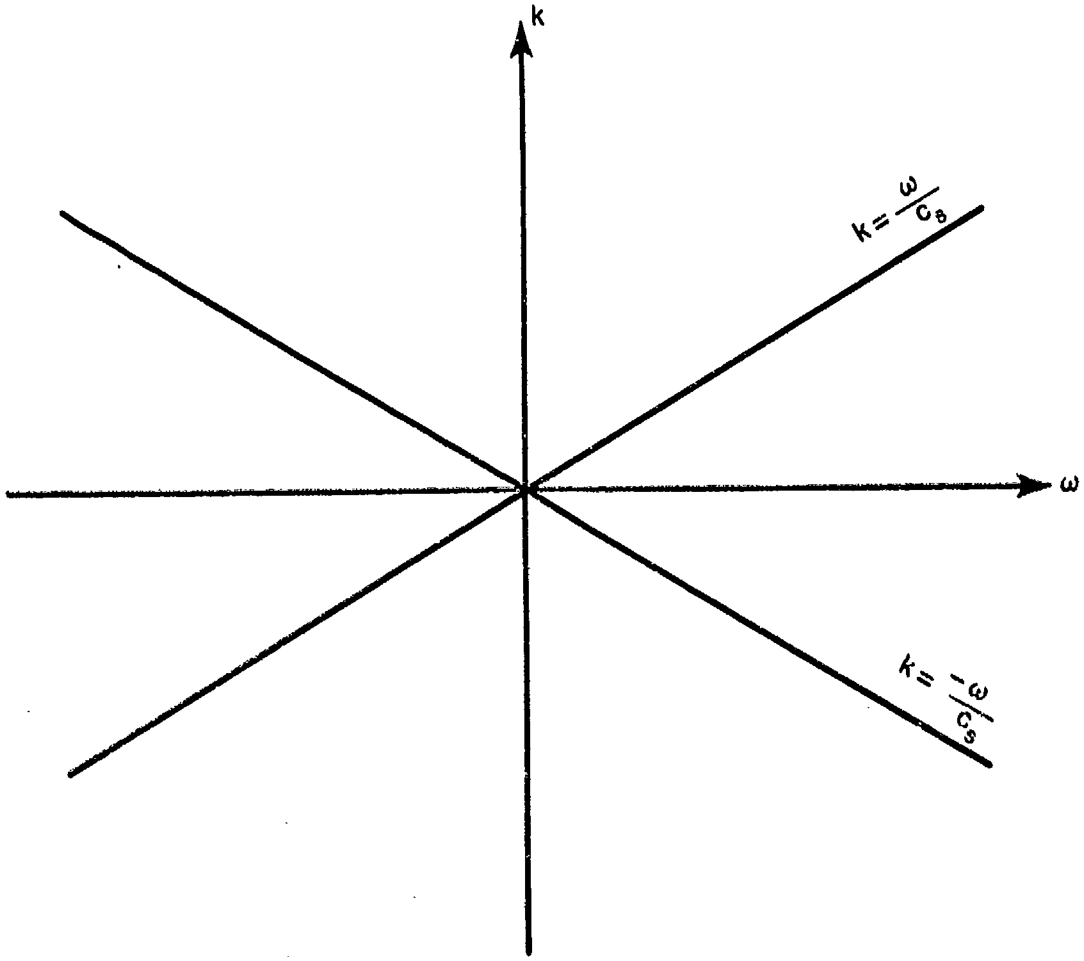

Figure 3-2. Locus of Wavevectors Characterizing Free Waves of an Infinite String as a Function of Frequency

of $W(k,\omega)$ at any frequency, the wavenumber

$$k_s = |\omega/c_s| \tag{3-4}$$

is called the free wavenumber of the string.

It is apparent, by equations (3-2) and (3-3), that if a particular wavenumber component, say k', is present in $W(k,\omega)$, its contributions to $w(x,t)$ can only be complex harmonic waves of the forms $\exp\{ik'(x + c_s t)\}$ and $\exp\{ik'(x - c_s t)\}$. The amplitudes of these harmonic wave components depend, of course, on the exact form of $W(k,\omega)$.

The mathematical form of $W(k,\omega)$ can be deduced by first writing $w(x,t)$ in the form

$$w(x,t) = (2\pi)^{-1} \int_{-\infty}^{\infty} \tilde{W}(k,t)\exp(ikx)\, dk \ . \tag{3-5}$$

Substitution of equation (3-5) into equation (3-1) yields the ordinary differential equation

$$\frac{d^2\tilde{W}(k,t)}{dt^2} + (kc_s)^2\, \tilde{W}(k,t) = 0 \ , \tag{3-6}$$

which has the solution

$$\tilde{W}(k,t) = A(k)\exp(ikc_s t) + B(k)\exp(-ikc_s t) \ . \tag{3-7}$$

By performing the temporal Fourier transformation of equation (3-7), we obtain

$$W(k,\omega) = 2\pi\{A(k)\delta(\omega - kc_s) + B(k)\delta(\omega + kc_s)\} \ . \tag{3-8}$$

Note that this solution to equation (3-3) is consistent, in form, with the solution to equation (2-50) given by equation (2-52). In equation (2-50), ω_0 was tacitly assumed to be a constant and, consequently, A and B in equation (2-52) were constants. In equation (3-3), however, k is a variable.

Therefore, the quantities A and B modifying the delta functions in equation (3-8) must be functions of k.

Equation (3-8) is the form of the general solution for the vibration displacement of the free, infinite, uniform string in the wavenumber-frequency domain. Note that $W(k,\omega)$, the wavenumber-frequency transform of $w(x,t)$, is characterized in the k-ω plane by a weighted distribution of delta functions along the lines $|k| = k_s$. The particular weighting functions, $A(k)$ and $B(k)$, are determined by the initial distribution of displacement and velocity on the string. Before proceeding to the determination of $A(k)$ and $B(k)$ in terms of these initial conditions, it should be noted that, by substituting equation (3-8) into equation (3-2) and performing the required integrations, one obtains

$$w(x,t) = a(x + c_s t) + b(x - c_s t) \ , \tag{3-9}$$

where $a(x)$ and $b(x)$ denote the respective inverse Fourier transforms of $A(k)$ and $B(k)$. Equation (3-9) is the general form of the classical solution for the free vibration of the infinite, uniform string.[4]

Assume that the initial displacement and velocity of the string are given by

$$w(x,0) = w_0(x) \tag{3-10}$$

and

$$\frac{\partial w(x,0)}{\partial t} = v_0(x) \ . \tag{3-11}$$

By equation (3-2), equation (3-9), and the use of the inverse Fourier transform, it is easily shown that

$$A(k) = (1/2)\{W_0(k) + [1/(ikc_s)]V_0(k)\} \tag{3-12}$$

and

$$B(k) = (1/2)\{W_0(k) - [1/(ikc_s)]V_0(k)\} \ . \tag{3-13}$$

where $W_0(k)$ and $V_0(k)$ are the spatial Fourier transforms of $w_0(x)$ and $v_0(x)$, respectively. Thus, by equations (3-8), (3-12), and (3-13), we obtain

$$W(k,\omega) = \pi\{W_0(k)[\delta(\omega - kc_s) + \delta(\omega + kc_s)]$$

$$+ [1/(ikc_s)]V_0(k)[\delta(\omega - kc_s) - \delta(\omega + kc_s)]\} . \qquad (3\text{-}14)$$

Equation (3-14) is the wavenumber-frequency description of the displacement field resulting from the free vibration of an infinite, uniform string with arbitrary initial displacement and velocity conditions. Recall, from section 2.2.1, that this wavenumber-frequency transform defines the amplitudes and initial phases of the harmonic waves comprising the space-time field as a function of the wavenumber and frequency characterizing each wave.

As noted previously, the wavenumber-frequency contributions to the displacement field consist of a weighted distribution of delta functions along the lines $|k| = k_s$. The weighting of the delta functions is completely determined by those wavenumber components comprising the initial displacement and velocity fields of the string.

In free vibration, only waves that result from natural interactions between elements of the string can be propagated. The delta functions of the form $\delta(\omega \pm kc_s)$ in each term of equation (3-14) are the mathematical statements of this restriction. These terms state that only waves characterized by wavenumbers and frequencies in the ratio $|\omega/k| = c_s$ (i.e., those with propagation speed c_s) can be propagated in the string. This restriction, implied by equation (3-3), is illustrated in figure 3-2.

As is evident by both equation (3-14) and figure 3-2, only two frequencies, equal in magnitude and opposite in sign, are associated with each wavenumber component of $W(k,\omega)$. By equation (2-14), this implies that each wavenumber component associated with the initial displacement and velocity fields contributes two harmonic waves to the vibration displacement field of the string: one propagating in the positive x direction and one propagating in the negative x direction. The speeds of propagation of both waves are easily shown (by equations (2-14) and (3-4)) to be independent of both

wavenumber and frequency and to be equal to c_s. The amplitudes and initial phases of these two waves are determined by their respective complex amplitudes, $W_0(k) - V_0(k)/(ikc_s)$ and $W_0(k) + V_0(k)/(ikc_s)$. The space-time displacement field of the vibrating string is the superposition of all such wave pairs dictated by the wavenumber content of the initial displacement and velocity fields.

The space-time field is obtained by substituting equation (3-14) into equation (3-2) and performing the integration on ω. This yields

$$w(x,t) = (4\pi)^{-1} \int_{-\infty}^{\infty} \{[W_0(k) + V_0(k)/(ikc_s)]\exp[ik(x + c_s t)] + [W_0(k) - V_0(k)/(ikc_s)]\exp[ik(x - c_s t)]\} \, dk \; . \tag{3-15}$$

It is easily demonstrated that

$$\frac{\exp(iku)}{ik} = \int_0^u \exp(iky) \, dy + \frac{1}{ik} \; . \tag{3-16}$$

By substitution of the appropriate form of this result in equation (3-15), the integrals over k are immediately recognized as simple inverse Fourier transforms of $W_0(k)$ and $V_0(k)$. It may thereby be shown that equation (3-15) reduces to the form

$$w(x,t) = (1/2)\left\{ w_0(x - c_s t) + w_0(x + c_s t) - \frac{1}{c_s} \int_0^{x-c_s t} v_0(y) \, dy + \frac{1}{c_s} \int_0^{x+c_s t} v_0(y) \, dy \right\} . \tag{3-17}$$

Equation (3-17) is the solution to the vibration of the infinite, uniform string obtained by traditional methods and presented in Morse.[4] That this

space-time solution was obtained by appropriate integration of the wavenumber-frequency description of the vibration field reinforces the assertion that both the space-time and wavenumber-frequency descriptions of a field contain equivalent information.

As a final observation, it should be noted that the solution for the free vibration of the string given by equation (3-17) is valid for all time. The explicit absence of external forces in the free system model precludes any consideration of how the vibratory motion was initiated. The initial conditions are therefore only simultaneous "snapshots" in time of the displacement and velocity fields. However, in the absence of external inputs, these initial conditions provide sufficient information to determine the vibration field prior to, as well as after, the time of the snapshot.

3.3.2 The Infinite Flat Plate

The technique for obtaining the wavenumber-frequency or space-time solution for the free response of space- and time-invariant systems is independent of the number of independent spatial variables required to mathematically model the system. To demonstrate this assertion and to introduce the concept of dispersive waves, we next treat the free transverse vibrations of an infinite, uniform, thin, flat plate.

The space-time field of the displacement of the central plane of the plate, measured normal to that plane, is designated by $w(\underline{x},t)$, where $\underline{x} = [x_1, x_2]$. The free vibration of the thin plate is governed by[5]

$$D\nabla^4 w + \mu \frac{\partial^2 w}{\partial t^2} = 0 \,, \qquad (3\text{-}18)$$

where

$$\nabla^4 = \left[\frac{\partial^2}{\partial x_1^{\,2}} + \frac{\partial^2}{\partial x_2^{\,2}}\right]^2 \qquad (3\text{-}19)$$

and where, for this spatially invariant system, the flexural rigidity (D) and the mass per unit area (μ) of the plate are constants.

If one assumes that the displacement field can be written in the form

$$w(\underline{x},t) = (2\pi)^{-3} \iint_{-\infty}^{\infty} W(\underline{k},\omega)\exp\{i(\underline{k}\cdot\underline{x} + \omega t)\}\, d\underline{k}\, d\omega \ , \tag{3-20}$$

substitution of equation (3-20) into equation (3-18) yields (as the resulting integral must hold for all $\underline{x}$ and t)

$$(k^4 - \frac{\mu}{D}\omega^2)W(\underline{k},\omega) = 0 \ , \tag{3-21}$$

where $k^4 = (k_1^2 + k_2^2)^2$.

Equation (3-21) states that $W(\underline{k},\omega)$ must be zero except at those wavevectors having magnitudes equal to the fourth root of $\mu\omega^2/D$. Therefore, as we found in the case of the free vibration of the infinite string, only those waves that result from natural interactions between the elements of the infinite plate can contribute to its free vibration. By equation (3-21), only waves associated with wavevectors of specific magnitudes can contribute to the motion of the plate at each frequency. This wavevector magnitude, called the free wavenumber of the plate, is designated by k_p and given by

$$k_p = \sqrt[4]{\mu\omega^2/D} \ . \tag{3-22}$$

From equation (3-22) and the above discussion, it is apparent that the locus of all wavevectors contributing to the vibration of the plate at any given frequency must fall on a circle of radius k_p in the $\underline{k}$ plane and that the radius of that circle increases according to the square root of the magnitude of the frequency. However, according to equation (2-14), this implies that the phase speed (i.e., the magnitude of the phase velocity) of the waves comprising the free motion of the plate is a function of frequency and is given by

$$c_p = \sqrt[4]{D\omega^2/\mu} \ . \tag{3-23}$$

The quantity c_p, which is referred to as the free wave speed of the plate, is seen to increase with the square root of the magnitude of the frequency. This is in contrast to the free waves in the infinite string, which had a constant phase speed. Waves characterized by a phase speed that varies with frequency are called dispersive waves.

By equations (3-4) and (3-22), it is evident that the dispersive nature of a wave is reflected in the frequency dependence of the free wavenumber. That is, for the nondispersive waves in the uniform string, the free wavenumber is linearly related to the frequency, as indicated by equation (3-4). For the dispersive waves of the flat plate, the free wavenumber varies nonlinearly with frequency, as evidenced by equation (3-22).

The difference in the wavenumber-frequency characteristics of free waves in dispersive and nondispersive systems is illustrated in figure 3-3. Here, the free wavenumbers of the string (k_s) and the flat plate (k_p) are shown as a function of frequency. The nonlinear behavior of the (dispersive) free wavenumber of the plate with frequency is easily seen in contrast with the linear behavior associated with the (nondispersive) free wavenumber of the string.

Returning now to equation (3-21), the mathematical form of $W(\underline{k},\omega)$ can be determined by an extension of equations (2-50) and (2-51) or by assuming a form for $w(\underline{x},t)$ similar to that assumed for the displacement field of the string in equation (3-5). That is, in the latter approach, we assume

$$w(\underline{x},t) = (2\pi)^{-2} \int_{-\infty}^{\infty} \tilde{W}(\underline{k},t)\exp\{i\underline{k}\cdot\underline{x}\}\, d\underline{k} \ . \qquad (3\text{-}24)$$

Substitution of equation (3-24) into equation (3-18) yields the ordinary differential equation

$$\frac{d^2\tilde{W}(\underline{k},t)}{dt^2} + \frac{Dk^4}{\mu}\tilde{W}(\underline{k},t) = 0 \ . \qquad (3\text{-}25)$$

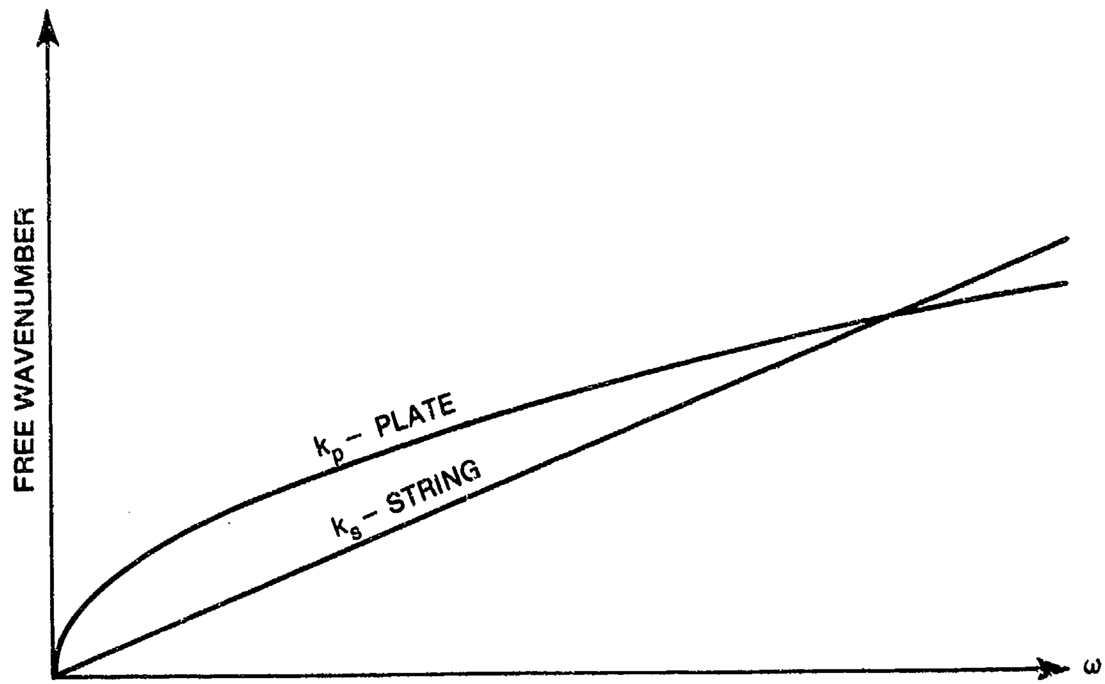

Figure 3-3. Comparison of the Free Wavenumbers of an Infinite Flat Plate and an Infinite String

which has the general solution

$$\tilde{W}(\underline{k},t) = A(\underline{k})\exp\{i\sqrt{D/\mu}\, k^2 t\} + B(\underline{k})\exp\{-i\sqrt{D/\mu}\, k^2 t\}\ , \qquad (3\text{-}26)$$

where A and B are arbitrary functions of $\underline{k}$ and $k^2 = k_1{}^2 + k_2{}^2$. By taking the temporal Fourier transform of equation (3-26), we obtain

$$W(\underline{k},\omega) = 2\pi[A(\underline{k})\delta\{\omega - \sqrt{D/\mu}\, k^2\} + B(\underline{k})\delta\{\omega + \sqrt{D/\mu}\, k^2\}]\ , \qquad (3\text{-}27)$$

and by equation (3-20),

$$w(\underline{x},t) = (2\pi)^{-2} \iint_{-\infty}^{\infty} \Big[A(\underline{k})\exp\{i[\underline{k}\cdot\underline{x} + \sqrt{D/\mu}\, k^2 t]\}$$

$$+ B(\underline{k})\exp\{i[\underline{k}\cdot\underline{x} - \sqrt{D/\mu}\, k^2 t]\}\Big]\, d\underline{k}\ . \qquad (3\text{-}28)$$

As was the case in the vibrating string, the functions $A(\underline{k})$ and $B(\underline{k})$ are determined by the initial conditions of the plate. If the initial

displacement and velocity fields of the plate are given by

$$w(\underline{x},0) = w_0(\underline{x}) \tag{3-29}$$

and

$$\frac{dw(\underline{x},0)}{dt} = v_0(\underline{x}) \ , \tag{3-30}$$

then, by equation (3-28) and the definition of the Fourier transform, it is easily shown that

$$W(\underline{k},\omega) = \pi W_0(\underline{k})\{\delta[\omega - \sqrt{D/\mu}\,k^2] + \delta[\omega + \sqrt{D/\mu}\,k^2]\}$$

$$+ \frac{\pi V_0(\underline{k})}{i\sqrt{D/\mu}\,k^2}\{\delta[\omega - \sqrt{D/\mu}\,k^2] - \delta[\omega + \sqrt{D/\mu}\,k^2]\} \ , \tag{3-31}$$

where $W_0(\underline{k})$ and $V_0(\underline{k})$ are the respective spatial Fourier transforms of $w_0(\underline{x})$ and $v_0(\underline{x})$. Equation (3-31) is the wavevector-frequency description of the displacement field resulting from the free vibration of the infinite plate.

The physical interpretation of equation (3-31) parallels that of the somewhat similar mathematical form obtained, in equation (3-14), for the wavenumber-frequency description of the free vibration of the infinite string. That is, we first recall, from chapter 2, that $W(\underline{k},\omega)$ defines the amplitudes and initial phases of all the harmonic waves comprising the vibration field as a function of the wavevectors and frequencies characterizing each wave.

By equation (3-31), it is apparent that the wavevector content of the displacement field is completely determined by those wavevectors comprising the initial displacement and velocity fields: that is, those defined by $W_0(\underline{k})$ and $V_0(\underline{k})$. Further, only two frequencies, equal in magnitude and opposite in sign, are associated with each wavevector component of the initial displacement or velocity fields. The magnitudes of these frequencies are proportional to the squared magnitude of the wavevector. Thus, by equations

(2-14) and (3-20), each wavevector component of the initial displacement or velocity contributes two harmonic waves to the space-time displacement field of the plate; one wave propagates in the direction of the wavevector associated with that component and the other propagates opposite to that direction. The speeds of propagation of both components are equal and, by equations (3-22) and (3-23), proportional to the magnitude of the wavevector characterizing the component. The amplitudes and initial phases of these two waves are specified, respectively, by $W_0(\underline{k}) \pm iV_0(\underline{k})/[\sqrt{D/\mu}\, k^2]$. The space-time displacement field associated with the free vibration of the infinite plate is the superposition of all such wave pairs dictated by the wavevector content of the initial displacement and velocity fields.

As an illustrative example, consider the free vibration of the infinite thin plate resulting from the initial conditions

$$w_0(\underline{x}) = \alpha \sin(k_{10}x_1)$$

and (3-32)

$$v_0(\underline{x}) = 0 ,$$

where α is the (real) amplitude of the initial displacement and k_{10} is a constant wavenumber in the k_1 direction. It follows, by taking the spatial Fourier transforms of $w_0(\underline{x})$ and $v_0(\underline{x})$, that

$$W_0(\underline{k}) = (2\pi^2\alpha/i)\delta(k_2)\{\delta(k_1 - k_{10}) - \delta(k_1 + k_{10})\}$$

and (3-33)

$$V_0(\underline{k}) = 0 .$$

Therefore, only two wavevector components, with amplitudes equal in magnitude and opposite in phase, are present in the initial displacement and velocity. By substituting equation (3-33) into equation (3-31), we obtain

$$W(\underline{k},\omega) = (2\pi^3\alpha/i)\delta(k_2)\{\delta(k_1 - k_{10}) - \delta(k_1 + k_{10})\}$$

$$\{\delta[\omega - \sqrt{D/\mu}\, k_{10}^2] + \delta[\omega + \sqrt{D/\mu}\, k_{10}^2]\} . \quad (3\text{-}34)$$

By equation (3-34) and the previous discussion, we see that the free vibration field of the plate is comprised of the sum of four complex harmonic waves. The magnitudes of the (complex) amplitudes of all waves are equal, as are the magnitudes of the wavevectors and frequencies characterizing these waves. By use of equation (2-14), it can be shown that two of these waves propagate in the positive x_1 coordinate direction and the other two propagate in the negative x_1 direction. The speeds of propagation of all waves are equal and can be shown to be $\sqrt{D/\mu}\,|k_{10}|$. Finally, it is easily demonstrated that the wavevector-frequency description of this field has conjugate symmetry in the $\underline{k}$ - ω domain; that is, $W(-\underline{k},-\omega) = W^*(\underline{k},\omega)$. Therefore, by the arguments of section 2.2.1, the space-time displacement field associated with this example of the free vibration of an infinite plate is real.

The space-time displacement field for this example is easily shown to be

$$w(\underline{x},t) = (\alpha/2)\{\sin[k_{10}x_1 + \sqrt{D/\mu}\,k_{10}^2 t] + \sin[k_{10}x_1 - \sqrt{D/\mu}\,k_{10}^2 t]\} \,. \tag{3-35}$$

Equation (3-35) shows that the space-time displacement field is the result of the spatial waveform of the initial displacement field being propagated, at half the initial amplitude, in both the positive and negative x_1 coordinate directions. The speed of propagation in both directions is equal and is that identified above.

3.3.3 Summary of Free Response Characteristics

The free response of the systems described in the above examples exhibits certain wavevector-frequency characteristics that are common to all free space- and time-invariant linear acoustic systems. In this section, we briefly summarize those characteristics.

The wavevector-frequency response of free space- and time-invariant systems defines the specific combination of free waves that comprise the space-time field associated with the system output. Free waves are that restricted set of waves which propagate in a system as a result of only the

natural reactions within the system. Inasmuch as (1) each wavevector-frequency combination defines a specific wave and (2) free waves are a restricted set, it follows that the set of wavevectors and frequencies that can contribute to the free response of a system is a restricted set.

Space- and time-invariant systems are infinite in spatial extent and have uniform properties in both space and time. It is therefore illogical, in the absence of external constraints or conditions, that there should be any preferred direction of propagation of free waves in the system. Recall, by the arguments of chapter 2, that the direction of propagation is determined by the direction of the wavevector and the sign of the frequency. It therefore follows that the wavevectors and frequencies that characterize free waves can only be restricted in their magnitudes.

A mathematical definition of the wavevectors and frequencies that characterize the free waves of a system can always be obtained by a multiple Fourier transformation, in all independent variables, of the partial differential equations governing the response, or output, of the system. The resulting equation relates the magnitudes of the wavevectors and frequencies that constitute free waves. The free wavenumber is defined as the magnitude of those wavevectors that constitute free waves at any particular frequency.

In the absence of external forces or inputs, the only wavevectors that can contribute to the output of the system are those present in the initial conditions. The initial conditions define the complex amplitude of each wavevector component that contributes to the free response of the system at some specified initial time. By knowledge of the wavevector components present in the initial conditions and the combinations of frequencies and wavevectors comprising free waves (by the definition of the free wavenumber), the wavevector-frequency content of the system output can be determined.

The illustrative examples presented above demonstrate a consistent mathematical procedure for obtaining the wavevector-frequency description of the free response of the space- and time-invariant systems encountered in linear acoustics.

3.4 FORCED RESPONSE OF SPACE- AND TIME-INVARIANT LINEAR SYSTEMS

The mathematical models of forced space- and time-invariant linear systems differ from those of their free counterparts only by the addition of the forcing term, or input, that is not a function of the independent, or output, variable. Thus, by the arguments of section 3.3, the mathematical models of these forced systems are inhomogeneous linear partial differential equations with constant coefficients.

This section describes a fundamental and consistent technique for obtaining and interpreting the wavevector-frequency response of forced space- and time-invariant linear acoustic systems.

3.4.1 The Principle of Superposition in Linear Systems

The solution for the forced response of linear systems is based on the principle of superposition for linear equations. Let $L_{\vec{x},t}$ denote any linear partial differential operator of the form

$$L_{\vec{x},t}\{\ \} = \sum_{j=0}^{J} \sum_{l=0}^{L} \sum_{m=0}^{M} \sum_{n=0}^{N} a_{jlmn}(\vec{x},t) \left(\frac{\partial^j}{\partial x_1{}^j}\right)\left(\frac{\partial^l}{\partial x_2{}^l}\right)\left(\frac{\partial^m}{\partial x_3{}^m}\right)\left(\frac{\partial^n}{\partial t^n}\right)\{\ \} , \tag{3-36}$$

where $\vec{x} = (x_1, x_2, x_3)$ and the indices j, l, m, and n denote the order of the partial derivatives in x_1, x_2, x_3, and t, respectively. Mathematical descriptions of linear systems in acoustics are characterized by operators of the form of equation (3-36).

If $p(\vec{x},t)$ denotes the output of a linear system resulting from the input $f(\vec{x},t)$, the inhomogeneous linear partial differential equation that describes this input-output relationship is given by

$$L_{\vec{x},t}\{p(\vec{x},t)\} = f(\vec{x},t) . \tag{3-37}$$

If $p_1(\vec{x},t)$, $p_2(\vec{x},t)$, ..., $p_N(\vec{x},t)$ are the solutions of equation (3-37)

resulting from the separate inputs $f_1(\vec{x},t)$, $f_2(\vec{x},t)$, ..., $f_N(\vec{x},t)$, then it follows that

$$\sum_{n=1}^{N} b_n L_{\vec{x},t}\{p_n(\vec{x},t)\} = \sum_{n=1}^{N} b_n f_n(\vec{x},t) \ , \tag{3-38}$$

where the constants b_n are arbitrary. However, owing to the form of $L_{\vec{x},t}$ shown in equation (3-36), it is easily seen that equation (3-38) can be rewritten in the equivalent form

$$L_{\vec{x},t}\left\{\sum_{n=1}^{N} b_n p_n(\vec{x},t)\right\} = \sum_{n=1}^{N} b_n f_n(\vec{x},t) \ . \tag{3-39}$$

By equations (3-37) and (3-39), it is clear that if the input to a system is a linear combination of the form

$$f(\vec{x},t) = \sum_{n=1}^{N} b_n f_n(\vec{x},t) \ , \tag{3-40}$$

then the output is given by

$$p(\vec{x},t) = \sum_{n=1}^{N} b_n p_n(\vec{x},t) \ . \tag{3-41}$$

Equations (3-40) and (3-41) are a mathematical statement of the principle of superposition for linear systems, which forms the foundation for the treatment of forced linear systems.

For the space- and time-invariant systems of interest in this chapter, the partial differential equations governing the system have constant coefficients. Thus, for space- and time-invariant systems, the coefficients a_{jlmn} in the linear operator of equation (3-36) are constants. However, when a_{jlmn} are constants, it is easily seen that the form of the linear

operator of equation (3-36) is independent of the origins of the spatial and temporal coordinates. That is, if we define

$$\vec{\xi} = \vec{x} - \vec{x}_0$$

and (3-42)

$$\tau = t - t_0 ,$$

where $\vec{x}_0$ and t_0 are arbitrary constants, and if we denote the space- and time-invariant linear operator by ${}_I L_{\vec{x},t}$, it is easily shown that

$$ {}_I L_{\vec{\xi},\tau}\{\ \} = {}_I L_{\vec{x},t}\{\ \} \ . \tag{3-43}$$

It follows, by equations (3-37) and (3-43), that

$$ {}_I L_{\vec{\xi},\tau}\{p(\vec{\xi} + \vec{x}_0,\tau + t_0)\} = f(\vec{\xi} + \vec{x}_0,\tau + t_0) \ , \tag{3-44}$$

from which it must be concluded that the output of a linear space- and time-invariant system resulting from the input $f(\vec{\xi} + \vec{x}_0,\tau + t_0)$ is $p(\vec{\xi} + \vec{x}_0,\tau + t_0)$.

By using these fundamental concepts of linear systems, a logical and consistent approach to obtaining solutions for the forced response of space- and time-invariant linear systems can be developed.

3.4.2 The Green's Function or Space-Time Impulse Response

The Green's function (also descriptively known as the space-time impulse response) of a system is defined as the response of that system at the spatial coordinate $\vec{x}$ and time t to an impulsive input applied at the spatial location $\vec{x}_0$ at time t_0. If we denote the Green's function by $g(\vec{x},t;\vec{x}_0,t_0)$ and assume that the system is governed by a linear inhomogeneous partial differential equation of the form of equation (3-37), it follows that the Green's function is mathematically defined by

$$L_{\vec{x},t}\{g(\vec{x},t;\vec{x}_0,t_0)\} = \delta(\vec{x} - \vec{x}_0)\delta(t - t_0) \ . \tag{3-45}$$

where

$$\delta(\vec{x} - \vec{x}_0) = \delta(x_1 - x_{01})\delta(x_2 - x_{02})\delta(x_3 - x_{03}) \; . \tag{3-46}$$

The argument of the Green's function in equation (3-45) is written in the traditional form and deserves some explanation. The independent variables of the Green's function, $\vec{x}$ and t, define the absolute spatial coordinates and time of observation of the output of the system. The parameters $\vec{x}_0$ and t_0 define the spatial coordinates and time of application of the impulsive input. Clearly, the mathematical form of the Green's function depends on both the observation variables and the input parameters. The inclusion of the input parameters in the argument of the Green's function serves as a reminder of this functional dependence.

In this chapter, our focus is only on space- and time-invariant linear systems. Therefore, by noting the form of the particular f in equation (3-45), we can employ equation (3-44) to obtain

$${}_{I}L_{\vec{x},t}\{g(\vec{x} - \vec{x}_0, t - t_0)\} = \delta(\vec{x} - \vec{x}_0)\delta(t - t_0) \; . \tag{3-47}$$

By equation (3-47), it is clear that, for space- and time-invariant linear systems, the Green's function has the mathematical form

$$g(\vec{x},t;\vec{x}_0,t_0) = g(\vec{x} - \vec{x}_0, t - t_0) \tag{3-48}$$

and thereby depends only on the difference between the variables of observation and the parameters of excitation.

By use of the sampling property of the Dirac delta function (see equation (2-31)), we may express any system input, $f(\vec{x},t)$, as

$$f(\vec{x},t) = \iint_{-\infty}^{\infty} f(\vec{x}_0,t_0)\delta(\vec{x} - \vec{x}_0)\delta(t - t_0)\; d\vec{x}_0\; dt_0 \; , \tag{3-49}$$

where $d\vec{x}_0$ denotes $dx_{01}dx_{02}dx_{03}$. It is easily shown, from equations (3-39), (3-47), and (3-49), that the response of a space- and time-invariant linear

system to an arbitrary input, $f(\vec{x},t)$, is governed by

$$L_{\vec{x},t}\left\{\iint_{-\infty}^{\infty} f(\vec{x}_0,t_0)g(\vec{x} - \vec{x}_0,t - t_0)\, d\vec{x}_0\, dt_0\right\}$$

$$= \iint_{-\infty}^{\infty} f(\vec{x}_0,t_0)\delta(\vec{x} - \vec{x}_0)\delta(t - t_0)\, d\vec{x}_0\, dt_0 = f(\vec{x},t) \ . \qquad (3\text{-}50)$$

It therefore follows, by the definition of equation (3-39), that the output, $p(\vec{x},t)$, of a space- and time-invariant linear system to any input, $f(\vec{x},t)$, is given by

$$p(\vec{x},t) = \iint_{-\infty}^{\infty} f(\vec{x}_0,t_0)g(\vec{x} - \vec{x}_0,t - t_0)\, d\vec{x}_0\, dt_0 \ . \qquad (3\text{-}51)$$

By employing the change of variables of equation (3-42), we may write equation (3-51) in the equivalent form

$$p(\vec{x},t) = \iint_{-\infty}^{\infty} f(\vec{x} - \vec{\xi},t - \tau)g(\vec{\xi},\tau)\, d\vec{\xi}\, d\tau \ . \qquad (3\text{-}52)$$

Equations (3-51) and (3-52) show that, by knowledge of the Green's function of a space- and time-invariant linear system, the output of the system resulting from any input can, in principle, be obtained. The caveat "in principle" is stated because, in some cases, the integrals cannot be evaluated in closed form. However, these integral forms pose no problem for characterization of the output in the wavevector-frequency domain.

Up to this point, we have not addressed the question of the initial conditions used to uniquely define the Green's function. The linear acoustic systems treated in this book are causal systems. A causal system is one that is at rest until acted upon by an external input. Thus, the output of a causal system depends only on inputs that existed in past times; the system

does not respond in anticipation of future inputs. Therefore, for a causal system, it follows that

$$g(\vec{x},t;\vec{x}_0,t_0) = 0 \,, \quad t < t_0 \,,$$

and (3-53)

$$\frac{\partial^n g(\vec{x},t;\vec{x}_0,t_0)}{\partial t^n} = 0 \,, \quad t < t_0 \text{ for all } n \,.$$

Equation (3-53) defines the initial conditions for the causal Green's function.

For causal space- and time-invariant linear systems, it follows from equation (3-53) that

$$g(\vec{x} - \vec{x}_0, t - t_0) = 0 \,, \quad t < t_0 \,,$$

or (3-54)

$$g(\vec{\xi},\tau) = 0 \,, \quad \tau < 0 \,.$$

Therefore, for causal systems, the infinite upper limit of the temporal integral in equation (3-51) can be replaced by t, and the negative infinite lower limit on the temporal integral in equation (3-52) can be replaced by zero. Many texts and papers use these alternative limits in expressing system outputs in terms of Green's functions. However, in this text, we will continue to use infinite temporal limits and rely on those temporal properties of the causal Green's functions indicated by equation (3-54) to effectively limit the range of temporal integration.

It should be emphasized that, for the causal systems treated in this text, equations (3-51) and (3-52) describe the output of a system that is at rest (i.e., has zero output) until an external input is applied.

3.4.3 The Wavevector-Frequency Response

The wavevector-frequency transform of the output of the space- and time-invariant linear system can be related to the wavevector-frequency

transform of the input field by use of equation (3-52). That is, by writing

$$p(\vec{x},t) = (2\pi)^{-4} \iint_{-\infty}^{\infty} P(\vec{k},\omega)\exp\{i(\vec{k}\cdot\vec{x} + \omega t)\}\, d\vec{k}\, d\omega \tag{3-55}$$

and

$$f(\vec{x},t) = (2\pi)^{-4} \iint_{-\infty}^{\infty} F(\vec{k},\omega)\exp\{i(\vec{k}\cdot\vec{x} + \omega t)\}\, d\vec{k}\, d\omega , \tag{3-56}$$

we can rewrite equation (3-52) as

$$(2\pi)^{-4} \iint_{-\infty}^{\infty} \{P(\vec{k},\omega) - F(\vec{k},\omega)G(\vec{k},\omega)\}\exp\{i(\vec{k}\cdot\vec{x} + \omega t)\}\, d\vec{k}\, d\omega = 0 , \tag{3-57}$$

where

$$G(\vec{k},\omega) = \iint_{-\infty}^{\infty} g(\vec{\xi},\tau)\exp\{-i(\vec{k}\cdot\vec{\xi} + \omega\tau)\}\, d\vec{\xi}\, d\tau . \tag{3-58}$$

Inasmuch as equation (3-57) is valid for all space and time, it follows that

$$P(\vec{k},\omega) = F(\vec{k},\omega)G(\vec{k},\omega) . \tag{3-59}$$

This simple linear algebraic relation between the wavevector-frequency transforms of the input and output is in sharp contrast to the four-dimensional convolution required (in equation (3-52)) to specify the space-time output. Indeed, it is interesting to note, by inverse Fourier transformation of equation (3-59) and use of equation (3-52), that

$$(2\pi)^{-4} \iint_{-\infty}^{\infty} \{F(\vec{k},\omega)G(\vec{k},\omega)\}\exp\{i(\vec{k}\cdot\vec{x} + \omega t)\}\, d\vec{k}\, d\omega$$

$$= \iint_{-\infty}^{\infty} f(\vec{x} - \vec{\xi}, t - \tau)g(\vec{\xi},\tau)\, d\vec{\xi}\, d\tau . \tag{3-60}$$

This result is the four-dimensional extension of the convolution theorem expressed by equation (2-54).

The wavevector-frequency transform of the Green's function, $G(k,\omega)$, can be shown to have a simple physical interpretation. Consider the response of a space- and time-invariant linear system to the input

$$f(\vec{x},t) = \exp\{i(\vec{k}_0\cdot\vec{x} + \omega_0 t)\} \tag{3-61}$$

over all $\vec{x}$ and t, where $\vec{k}_0$ and ω_0 are constants. Substitution of equation (3-61) into equation (3-52) yields, by use of equation (3-58),

$$p(\vec{x},t) = G(\vec{k}_0,\omega_0)\exp\{i(\vec{k}_0\cdot\vec{x} + \omega_0 t)\} \ . \tag{3-62}$$

By equations (3-61) and (3-62), $G(\vec{k},\omega)$ is the ratio of the space-time output field of the system to the input field when the input is a complex harmonic plane wave of the form $\exp\{i(\vec{k}\cdot\vec{x} + \omega t)\}$. For that reason, $G(\vec{k},\omega)$ is called the wavevector-frequency response of the system.

Some texts on acoustics[6,7,8] employ the concept of mechanical and acoustic impedance. These impedances, based on a force-voltage analogy between acoustic and electrical systems, relate the force or pressure (as appropriate) input to a system to the consequent velocity output of the system under conditions of harmonic excitation. Many of the papers and reports dealing with the application of wavevector-frequency analysis use an impedance to relate the wavevector-frequency transform of the force or pressure to that of the velocity. Consider, for example, a space- and time-invariant linear system in which the input is a pressure field, $p(\vec{x},t)$, and the output is the velocity field, $v(\vec{x},t)$. The acoustic impedance is defined as

$$Z_a(\vec{k},\omega) = P(\vec{k},\omega)/V(\vec{k},\omega) \ , \tag{3-63}$$

where $P(\vec{k},\omega)$ and $V(\vec{k},\omega)$ are the respective wavevector-frequency transforms of $p(\vec{x},t)$ and $v(\vec{x},t)$. Similarly, if the system input is a force field, say $f(\vec{x},t)$, and the output is a velocity field, the mechanical impedance is

defined by

$$Z_m(\vec{k},\omega) = F(\vec{k},\omega)/V(\vec{k},\omega) \ , \tag{3-64}$$

where $F(\vec{k},\omega)$ is the wavevector transform of $f(\vec{x},t)$.

By comparing the forms of equations (3-63) and (3-64) to that of equation (3-59), it is obvious that the acoustic and mechanical impedances are simply the reciprocals of the wavevector-frequency response in these specialized applications. It follows then, by arguments similar to those employed in equations (3-61) and (3-62), that the acoustic and mechanical impedances are simply the ratio of the space-time pressure or force field, as appropriate, to the resultant velocity field when the pressure or force field is a single complex harmonic plane wave of the form $\exp\{i(\vec{k}\cdot\vec{x} + \omega t)\}$ for all $\vec{x}$ and t.

By the above arguments, the wavevector-frequency description (i.e., transform) of the output of a space- and time-invariant linear system is easily achieved, given the wavevector-frequency response of the system and the wavevector-frequency description of the forcing field. Alternatively, if one knows (by observation or measurement) the wavevector-frequency transform of the output and the wavevector-frequency response of the system, the wavevector-frequency characteristics of the input field can be deduced. Finally, by knowledge of the wavevector-frequency transforms of the input and output fields, the wavevector-frequency response of the system can be deduced.

To illustrate (1) the mathematical techniques for obtaining the wavevector-frequency response and (2) the interpretative advantages of the wavevector-frequency description of systems, we present the following illustrative examples of the forced response of space- and time-invariant linear systems.

3.4.4 The Forced Vibration of a Uniform Infinite String

Consider the displacement, $w(x,t)$, of a uniform, infinitely long string resulting from a force per unit length, $f(x,t)$, applied to the string. The mathematical model of this system is given by

$$T \frac{\partial^2 w}{\partial x^2} - \varepsilon \frac{\partial^2 w}{\partial t^2} = -f(x,t) , \qquad (3\text{-}65)$$

where it will be recalled that T and ε are the respective (constant) tension and mass per unit length of the string. In equation (3-65), f(x,t) is considered positive when applied in the direction of positive w(x,t).

The Green's function for the uniform, infinite string is the solution to equation (3-65) when f(x,t) is replaced by $\delta(x - x_0)\delta(t - t_0)$. As equation (3-65) applies over all space and time, we define $\xi = x - x_0$ and $\tau = t - t_0$ and then write the equation for the Green's function, $g(\xi,\tau)$, as

$$\frac{\partial^2 g}{\partial \xi^2} - \frac{1}{c_s^2}\frac{\partial^2 g}{\partial \tau^2} = \frac{-\delta(\xi)\delta(\tau)}{\varepsilon c_s^2} , \qquad (3\text{-}66)$$

where it will be recalled that $c_s^2 = T/\varepsilon$.

There are a variety of methods for obtaining the solution to equation (3-66). However, because our immediate goal is the determination of the wavenumber-frequency transform, $G(k,\omega)$, of the causal Green's function, we will use Fourier transform techniques to solve this equation.

To obtain the particular solution, denoted by g_p, to equation (3-66), we write

$$g_p(\xi,\tau) = (2\pi)^{-2} \iint_{-\infty}^{\infty} G_p(k,\omega)\exp\{i(k\xi + \omega\tau)\}\, dk\, d\omega . \qquad (3\text{-}67)$$

Then, by using equations (2-38) and (3-67), equation (3-66) can be written in the form

$$(2\pi c_s)^{-2} \iint_{-\infty}^{\infty} \{[\omega^2 - (kc_s)^2]G_p(k,\omega) + 1/\varepsilon\}\exp\{i(k\xi + \omega\tau)\}\, dk\, d\omega = 0 .$$

(3-68)

As equation (3-68) holds for all ξ and τ, it follows that the wavenumber-frequency transform of the particular solution is

$$G_p(k,\omega) = \frac{-1}{\varepsilon[\omega^2 - (kc_s)^2]} . \qquad (3\text{-}69)$$

The wavenumber-frequency transform of the homogeneous solution to equation (3-66), denoted by $G_h(k,\omega)$, is precisely that developed for the free vibration of the string and given by equation (3-8). That is,

$$G_h(k,\omega) = 2\pi\{A(k)\delta(\omega - kc_s) + B(k)\delta(\omega + kc_s)\} . \qquad (3\text{-}70)$$

The wavenumber-frequency transform of the Green's function for the infinite string is the sum of the particular and homogeneous solutions, where the functions A(k) and B(k) are determined by the initial conditions.

The initial condition for the desired causal Green's function is $g(\xi,\tau) = 0$ for $\tau < 0$ for all ξ. If we define

$$\tilde{G}(k,\tau) = \int_{-\infty}^{\infty} g(\xi,\tau)\exp\{-ik\xi\}\, d\xi , \qquad (3\text{-}71)$$

it follows that the initial condition translates to $\tilde{G}(k,\tau) = 0$ for $\tau < 0$ for all k. From equations (3-69) and (3-70), $\tilde{G}(k,\tau)$ can be obtained by the inverse Fourier transformation

$$\tilde{G}(k,\tau) = (2\pi)^{-1} \int_{-\infty}^{\infty} \{G_p(k,\omega) + G_h(k,\omega)\}\exp\{i\omega\tau\}\, d\omega \qquad (3\text{-}72)$$

Let us consider the inverse transforms of G_p and G_h separately.

By a partial fraction expansion of equation (3-69) and use of equation (3-72), the particular portion $\tilde{G}_p(k,\tau)$ of $\tilde{G}(k,\tau)$ may be written

$$\tilde{G}_p(k,\tau) = \frac{1}{4\pi\epsilon kc_s} \int_{-\infty}^{\infty} \left\{\frac{1}{\omega + kc_s} - \frac{1}{\omega - kc_s}\right\} \exp\{i\omega\tau\}\, d\omega \ . \tag{3-73}$$

However,

$$\int_{-\infty}^{\infty} \frac{\exp\{i\omega\tau\}}{\omega + \beta}\, d\omega = \exp\{-i\beta\tau\} \int_{-\infty}^{\infty} \frac{\exp\{i\sigma\tau\}}{\sigma}\, d\sigma \ , \tag{3-74}$$

and Papoulis[9] shows that

$$(2\pi)^{-1} \int_{-\infty}^{\infty} \frac{2\exp\{i\omega\tau\}}{i\omega}\, d\omega = \mathrm{sgn}(\tau) \ . \tag{3-75}$$

The generalized function sgn(τ) in equation (3-75) is defined by

$$\mathrm{sgn}(\tau) = \begin{Bmatrix} 1 \ , & \tau > 0 \\ -1 \ , & \tau < 0 \end{Bmatrix} = 2U(\tau) - 1 \ , \tag{3-76}$$

where $U(\tau)$ is the Heaviside function defined in equation (2-32).

By equations (3-73), (3-74), and (3-75), it is straightforward to show that

$$\tilde{G}_p(k,\tau) = \frac{1}{2\epsilon}\, \mathrm{sgn}(\tau)\, \frac{\sin(kc_s\tau)}{kc_s} \ . \tag{3-77}$$

Further, by equations (3-70) and (3-72), it can be shown that

$$\tilde{G}_h(k,\tau) = A(k)\exp\{ikc_s\tau\} + B(k)\exp\{-ikc_s\tau\} \ . \tag{3-78}$$

Inasmuch as $\tilde{G}(k,\tau) = \tilde{G}_p(k,\tau) + \tilde{G}_h(k,\tau)$ and causality requires that $\tilde{G}(k,\tau) = 0$ for $\tau < 0$ for all k, it follows, by equations (3-77) and (3-78), that

$$A(k) = -B(k) = 1/(4i\epsilon kc_s) \ , \tag{3-79}$$

and thus, by use of equations (3-76), (3-77), (3-78), and (3-79),

$$\tilde{G}(k,\tau) = (1/\varepsilon)U(\tau)\,\frac{\sin(kc_s\tau)}{kc_s}\,. \tag{3-80}$$

Equation (3-80) is the wavenumber transform of the causal Green's function for the infinite, uniform string.

Our interest is in the wavenumber-frequency rather than in the space-time description of the Green's function. However, for the sake of completeness, we note that the space-time description of the causal Green's function can be obtained by the inverse Fourier transformation of equation (3-80). By writing $\sin(kc_s\tau)$ in equation (3-80) in its exponential form and by using equations (3-75) and (3-76), one can show that

$$g(\xi,\tau) = [1/(4\varepsilon c_s)]U(\tau)\{\mathrm{sgn}(\xi + c_s\tau) - \mathrm{sgn}(\xi - c_s\tau)\} = [1/(2\varepsilon c_s)]U(c_s\tau - |\xi|)\,. \tag{3-81}$$

Figure 3-4 depicts the Green's function for the infinite string as a function of ξ at a constant, but arbitrary, value of τ. The Green's function is usually interpreted as the output of the system resulting from an impulsive force. This is not strictly true inasmuch as equation (3-52) shows that the dimensions of the Green's function are not those of the output, or even the output divided by the input. However, if I is defined as a constant of magnitude one and dimensions of force-time, it can be argued (by equations (3-52) and (3-66)) that $Ig(\xi,\tau)$ is the displacement of the string resulting from the impulsive force per unit length $I\delta(x - x_0)\delta(t - t_0)$. Thus, it follows that $g(\xi,\tau)$ is proportional to the displacement resulting from the impulsive excitation.

Note, by figure 3-4, that at τ seconds after the applied impulse, $g(\xi,\tau)$ is constant at all spatial locations less than $|c_s\tau|$ from the point of application of the impulsive force and is zero at all spatial locations greater than $|c_s\tau|$. As time increases, the region of constant displacement increases, linearly with time, symmetrically about the point of excitation.

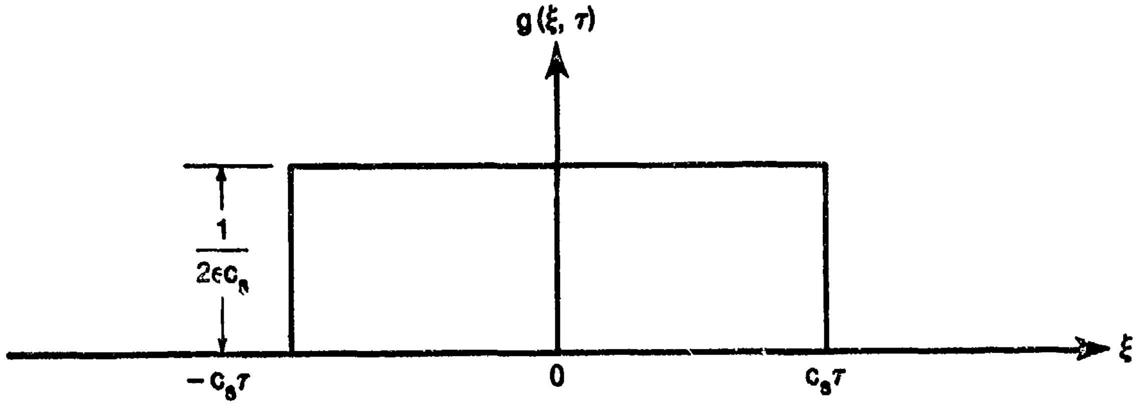

Figure 3-4. The Spatial Dependence of the Green's Function of an Infinite String for a Fixed τ

We now turn our attention to the wavenumber-frequency response of the infinite string. The wavenumber-frequency response, it will be recalled, is defined as the wavenumber-frequency transform of the causal Green's function. By equations (3-69), (3-70), and (3-79), the wavenumber-frequency response of the infinite, uniform string is given by

$$G(k,\omega) = \frac{-1}{\epsilon[\omega^2 - (kc_s)^2]} + \frac{\pi}{2i\epsilon kc_s}\{\delta(\omega - kc_s) - \delta(\omega + kc_s)\} . \qquad (3\text{-}82)$$

Figures 3-5(a) and (b) illustrate the real and imaginary parts, respectively, of $G(k,\omega)$ as a function of k at a fixed, but arbitrary, frequency, ω. Both real and imaginary parts of $G(k,\omega)$ are seen to be even functions of k. Note that the real part of $G(k,\omega)$ is the wavenumber-frequency transform of the particular part of the Green's function, and the imaginary part is the transform of the homogeneous part. Figure 3-5 shows that the wavenumber-frequency response is well-behaved, except at those wavenumbers where $|k| = |\omega/c_s|$. Let us therefore interpret the wavenumber-frequency response in this wavenumber range (i.e., $|k| \neq |\omega/c_s|$) first.

Recall, by equation (3-62), that the wavenumber-frequency response can be interpreted as the ratio of $w(x,t)$ to $f(x,t)$ when $f(x,t)$ is a single complex harmonic wave of the form $\exp\{i(kx + \omega t)\}$ for all x and t. Note, by equation (3-82) and figure 3-5, that when $|k| \neq |\omega/c_s|$, the imaginary part of $G(k,\omega)$ is zero. As the imaginary part corresponds to the homogeneous solution, the

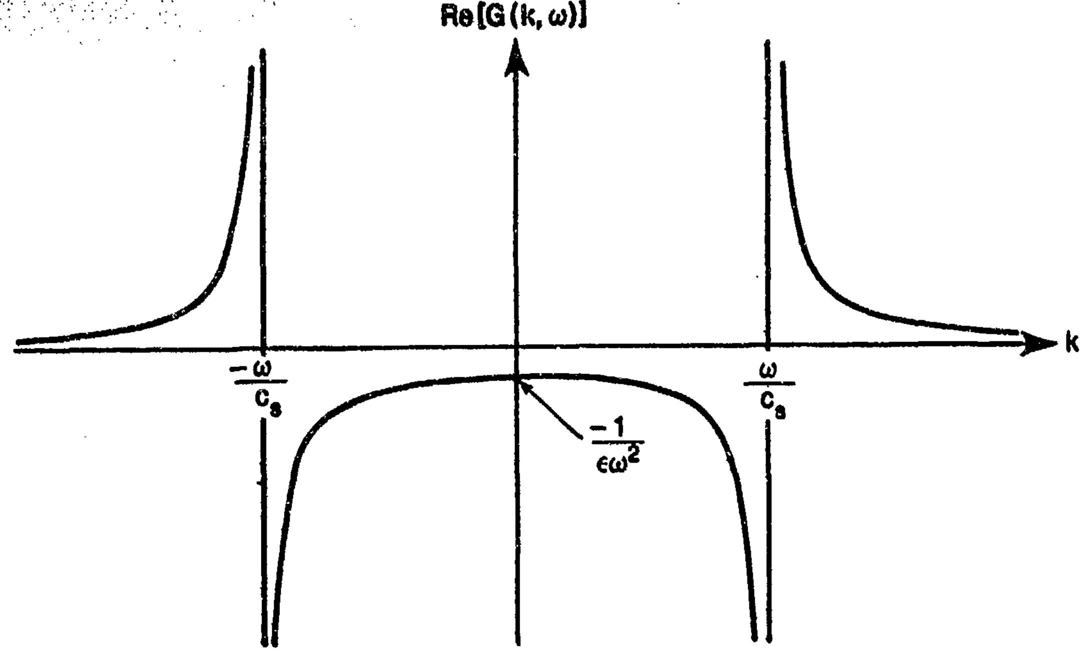

Figure 3-5(a). Real Part of Wavenumber-Frequency Response

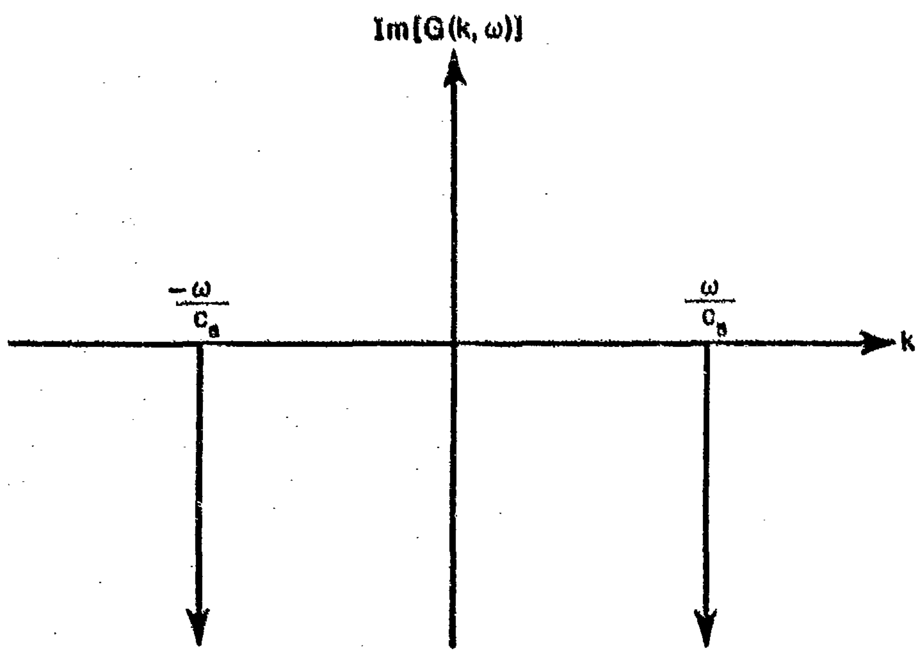

Figure 3-5(b). Imaginary Part of Wavenumber-Frequency Response

Figure 3-5. Real and Imaginary Parts of the Wavenumber-Frequency Response of an Infinite String

wavenumber-frequency response, over the range $|k| \neq |\omega/c_s|$, can be interpreted as the ratio of the particular solution of equation (3-65) to the forcing field $f(x,t) = \exp\{i(kx + \omega t)\}$. This particular solution corresponds to the real part of the wavenumber-frequency response illustrated in figure 3-5(a).

Consider now a fixed (but arbitrary) frequency of the harmonic wave excitation, $f(x,t) = \exp\{i(kx + \omega t)\}$. The particular solution to equation (3-65) is $w(x,t) = G_p(k,\omega)\exp\{i(kx + \omega t)\}$, where G_p, the amplitude of $w(x,t)$, is the real part of $G(k,\omega)$. By substituting this form of solution into equation (3-65), one can see that when the magnitude of the wavenumber of excitation is large compared with the free wavenumber (ω/c_s) of the string, the applied force is primarily balanced by the tensile forces in the string and the displacement, $w(x,t)$, is in phase with the applied force. For a wave in the string of the form $\exp\{i(k\xi + \omega\tau)\}$ and constant amplitude, tensile forces increase with increasing wavenumber magnitude (i.e., decreasing wavelength). Thus, in the wavenumber region $|k| > |\omega/c_s|$, where tensile forces dominate, the response of the string to the constant amplitude applied force must decrease with increasing wavenumber magnitude. For wavenumbers less, in magnitude, than the free wavenumber of the string, similar arguments can be used to show that the applied force is primarily balanced by inertial forces in the string. These inertial forces are independent of wavenumber and act 180 degrees out of phase with both the tensile forces and the local displacement. Thus, in the wavenumber range $|k| < |\omega/c_s|$, where inertial forces dominate, the local displacement is nearly constant and out of phase with the applied force.

When the magnitude of the wavenumber of the applied force is in the neighborhood of, but not at, the free wavenumber of the string, the tensile and inertial forces in the string nearly cancel each other, and the displacement becomes very large. The relative phase between the displacement and the applied force in this wavenumber region is determined by the relative dominance of the tensile and inertial forces.

From the above discussion, the real part of the wavenumber-frequency response defines the amplitude and relative phase of the displacement field

resulting from the unit amplitude harmonic force, $\exp\{i(kx + \omega t)\}$, at all wavenumbers and frequencies of the applied force except those characterized by $k = \omega/c_s$.

At the wavenumber-frequency combinations characterized by $k = \omega/c_s$, equation (3-82) and figure 3-5 show the real part of $G(k,\omega)$ to be undefined and the imaginary part to be a pair of weighted Dirac delta functions. The imaginary part, introduced by the wavenumber-frequency transform of the homogeneous part of the Green's function, characterizes free waves in the string. Recall that these free waves were necessary in order that the Green's function be causal. Regardless of the value of the real part of $G(k,\omega)$ at $k = \omega/c_s$, the delta functions in the imaginary part ensure an infinite displacement of the string when the steady state harmonic wave excitation coincides with a free wave: that is, $f(x,t) = \exp\{ik(x \pm c_s t)\}$ for any k. While this result is consistent with physical intuition, it is not possible, by this example alone, to physically interpret the separate roles of the real and imaginary parts of the wavenumber-frequency response for harmonic excitations coincident with free waves in the string.

With the above background, let us now examine the wavenumber-frequency description (i.e., transform), $W(k,\omega)$, of the space-time displacement field of the string, $w(x,t)$, resulting from an arbitrary force per unit length, $f(x,t)$, applied to the string. By equations (3-59) and (3-82), this wavenumber-frequency transform is given by

$$W(k,\omega) = \frac{-F(k,\omega)}{\epsilon[\omega^2 - (kc_s)^2]} + \frac{\pi F(k,\omega)}{2i\epsilon kc_s}\{\delta(\omega - kc_s) - \delta(\omega + kc_s)\} \; . \quad (3\text{-}83)$$

where $F(k,\omega)$ is the wavenumber-frequency transform of $f(x,t)$.

Recall that $W(k,\omega)$ defines the complex amplitudes of the various harmonic waves of the form $\exp\{i(kx + \omega t)\}$ comprising the displacement field as a function of the wavenumber and frequency characterizing each wave. Equation (3-83) clearly shows that the displacement field is comprised of only those harmonic wave components present in the forcing field.

At all wavenumber-frequency combinations, except those that characterize free waves in the string (i.e., $|k| = |\omega/c_s|$), the amplitudes and initial phases of the wavenumber-frequency components of the displacement field are defined by the product of the wavenumber-frequency transform of the forcing function and the real part of the wavenumber-frequency response of the string. This product is equivalent to a filtering of the forcing function, in both wavenumber and frequency, by the real part of the wavenumber-frequency response. Figure 3-6(a) illustrates how the magnitudes of the various wavenumber components of the forcing function are filtered, at some fixed frequency, by the magnitude of the real part of the wavenumber-frequency response of the string. The product of these magnitudes is the magnitude of the complex amplitude of the harmonic wave components of the displacement field at the corresponding wavenumber and frequency. Figure 3-6(a) clearly shows that, at any frequency, the magnitude of $W(k,\omega)$ will be relatively large at (1) those wavenumbers where $F(k,\omega)$ is large and (2) in the neighborhood of $\pm\omega/c_s$, if $F(k,\omega)$ is nonzero in that wavenumber range.

Figure 3-6(b) illustrates the phase shift applied to the various wavenumber components of the forcing function (at the same fixed frequency) by the wavenumber-frequency response of the string. The initial phase of $W(k,\omega)$ at each wavenumber is determined by applying this phase shift to the phase of $F(k,\omega)$ at the corresponding wavenumber. Note that the phase at $k = \pm\omega/c_s$ is undefined.

It will be recalled that the real part of the wavenumber-frequency response of the string is undefined at all wavenumber-frequency combinations defined by $|k| = |\omega/c_s|$. It follows therefore, by equation (3-59), that $W(k,\omega)$ is undefined at any wavenumber and frequency where $|k| = |\omega/c_s|$ and $F(k,\omega)$ is nonzero.

The above example illustrates a technique for obtaining the wavenumber-frequency response by treating the forced vibration of an infinite, uniform string. This example further shows that, given the wavenumber-frequency transform of the applied force and the wavenumber-frequency response of the string, a description of the harmonic waves comprising the displacement field of the string can be determined and interpreted at all wavenumbers and

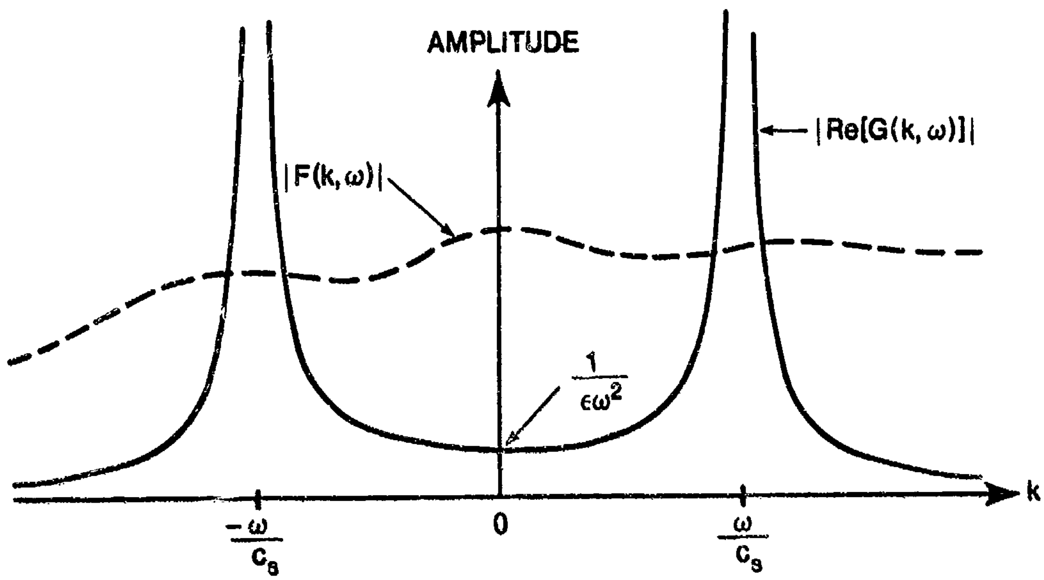

Figure 3-6(a). Filtering of the Magnitude of the Forcing Field by the Magnitude of the Real Part of the Wavenumber-Frequency Response

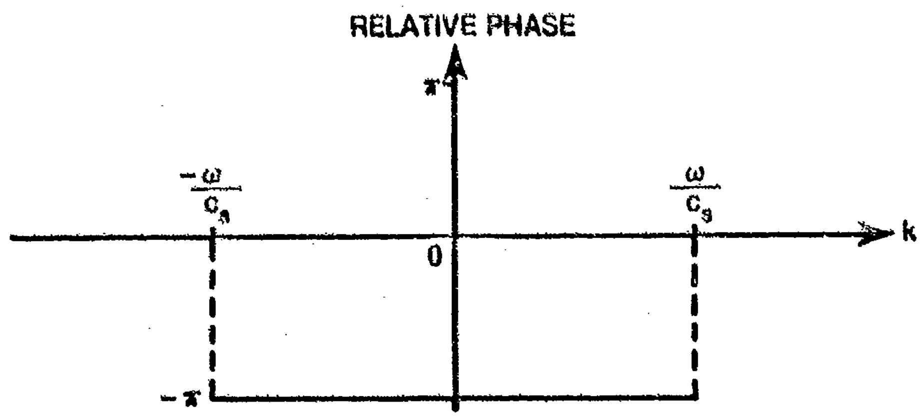

Figure 3-6(b). Phase of W(k,ω) Relative to F(k,ω)

Figure 3-6. Filtering of the Forcing Field by the Wavenumber-Frequency Response of the String

frequencies, except those coincident with free waves in the string, where the wavenumber-frequency response is undefined.

The reason that the wavenumber-frequency response is undefined at $|k| = |\omega/c_s|$ is the absence of any loss mechanism in the mathematical model of the string. As we will show in the next example, the inclusion of losses in the mathematical model permits definition of the harmonic waves comprising the displacement field at all wavenumbers and frequencies.

3.4.5 The Forced Vibration of a Damped, Infinite String

Consider the displacement of a damped, uniform, infinitely long string resulting from a force per unit length, f(x,t), applied to the string. The damping force per unit length opposes the motion of the string and is proportional to the local velocity. To ensure that this damping force is space and time invariant, we assume this proportionality (denoted by r) to be constant. The mathematical model of this system is given by

$$T \frac{\partial^2 w}{\partial x^2} - \epsilon \frac{\partial^2 w}{\partial t^2} - r \frac{\partial w}{\partial t} = -f(x,t) \ , \tag{3-84}$$

where T and ϵ are, respectively, the constant tension and mass per unit length of the string.

The Green's function for the damped string is the solution to equation (3-84) when f(x,t) is replaced by $\delta(x - x_0)\delta(t - t_0)$. As equation (3-84) applies over all space and time, we let $\xi = x - x_0$ and $\tau = t - t_0$ and write the equation for the Green's function as

$$\frac{\partial^2 g}{\partial \xi^2} - \frac{1}{c_s^2} \frac{\partial^2 g}{\partial \tau^2} - \frac{r}{\epsilon c_s^2} \frac{\partial g}{\partial \tau} = \frac{-\delta(\xi)\delta(\tau)}{\epsilon c_s^2} \ , \tag{3-85}$$

where it will be recalled that $c_s^2 = T/\epsilon$.

As we did for the undamped string, we assume the particular solution, g_p, of equation (3-85) can be written in the form

$$g_p(\xi,\tau) = (2\pi)^{-2} \iint_{-\infty}^{\infty} G_p(k,\omega)\exp\{i(k\xi + \omega\tau)\}\, dk\, d\omega \,. \qquad (3\text{-}86)$$

Then, by use of equations (2-38) and (3-86) in equation (3-85), arguments identical to those used between equations (3-67) and (3-69) yield

$$G_p(k,\omega) = \frac{-1}{\epsilon[\omega^2 - (kc_s)^2 - ir\omega/\epsilon]} \,. \qquad (3\text{-}87)$$

In anticipation of applying the initial conditions for the causal Green's function in the same form as we did for the undamped string, we wish to obtain the wavenumber transform of the particular solution $\tilde{G}_p(k,t)$ by the inverse temporal Fourier transformation of equation (3-87). It is straightforward to show, by partial fraction expansion of equation (3-87), that

$$\tilde{G}_p(k,t) = \frac{-1}{4\pi\epsilon\omega_d(k)} \left[\int_{-\infty}^{\infty} \frac{\exp(i\omega\tau)\, d\omega}{\omega - ir/(2\epsilon) - \omega_d(k)} - \int_{-\infty}^{\infty} \frac{\exp(i\omega\tau)\, d\omega}{\omega - ir/(2\epsilon) + \omega_d(k)}\right] , \qquad (3\text{-}88)$$

where

$$\omega_d(k) = \sqrt{[kc_s]^2 - [r/(2\epsilon)]^2} \,. \qquad (3\text{-}89)$$

By reference 10, it can be shown that

$$\int_{-\infty}^{\infty} \frac{\exp(i\omega\tau)\, d\omega}{\omega - ir/(2\epsilon) + \omega_d(k)} = 2\pi i U(\tau)\exp\{-[r/(2\epsilon) + i\omega_d(k)]\tau\} \,. \qquad (3\text{-}90)$$

It follows, by equations (3-88) and (3-90), that

$$\tilde{G}_p(k,\tau) = (1/\epsilon)U(\tau)\exp\{-r\tau/(2\epsilon)\} \frac{\sin\{\omega_d(k)\tau\}}{\omega_d(k)} \,. \qquad (3\text{-}91)$$

Equation (3-91) is the wavenumber transform of the particular solution to equation (3-85).

To obtain the wavenumber transform of the homogeneous solution to equation (3-85), we assume that the homogeneous portion of the Green's function can be written in the form

$$g_h(\xi,\tau) = (2\pi)^{-1} \int_{-\infty}^{\infty} \tilde{G}_h(k,\tau)\exp\{ik\xi\}\, dk \; . \tag{3-92}$$

By substituting equation (3-92) into the homogeneous form of equation (3-85) and by realizing that the resultant integral applies for all ξ, we obtain the ordinary differential equation

$$\frac{d^2\tilde{G}_h}{d\tau^2} + \frac{r}{\epsilon}\frac{d\tilde{G}_h}{d\tau} + (kc_s)^2\,\tilde{G}_h = 0 \; . \tag{3-93}$$

The solution to equation (3-93) is

$$\tilde{G}_h(k,\tau) = \exp\{-r\tau/(2\epsilon)\}\{A(k)\exp[i\omega_d(k)\tau] + B(k)\exp[-i\omega_d(k)\tau]\} \; , \tag{3-94}$$

where $\omega_d(k)$ is given by equation (3-89).

As we argued for the undamped string, the causality condition that $g(\xi,\tau) = 0$ for $\tau < 0$ at all ξ can be translated to the condition that $\tilde{G}(k,\tau) = 0$ for $\tau < 0$ at all k. Therefore, for a causal system, we require that $\tilde{G}_p(k,\tau) + \tilde{G}_h(k,\tau) = 0$ for $\tau < 0$. By equations (3-91) and (3-94), this condition can be satisfied only if $A(k) = B(k) = 0$, from which it follows that $\tilde{G}_h(k,\tau) = 0$ for all k.

Therefore,

$$\tilde{G}(k,\tau) = \tilde{G}_p(k,\tau) = (1/\epsilon)U(\tau)\exp\{-r\tau/(2\epsilon)\}\,\frac{\sin\{\omega_d(k)\tau\}}{\omega_d(k)} \tag{3-95}$$

and

$$G(k,\omega) = G_p(k,\omega) = \frac{-1}{\epsilon[\omega^2 - (kc_s)^2 - ir\omega/\epsilon]} . \tag{3-96}$$

Equation (3-96), which defines the wavenumber-frequency response for the damped string, shows that the causal Green's function is completely defined by the particular solution to equation (3-85). This result is in contrast to the Green's function of the undamped string, where the inclusion of the homogeneous solution was necessary to satisfy causality.

Before examining the properties of the wavenumber-frequency response, it would be interesting to determine the causal Green's function of the damped, infinite string for comparison with the undamped case. By use of equation (3-89), it is evident that $\tilde{G}(k,\tau)$, in equation (3-95), is an even function of k. By use of reference 11 and the properties of the Heaviside function, one can perform the inverse Fourier transform of equation (3-95) to obtain

$$g(\xi,\tau) = [1/(2\epsilon c_s)]U\{c_s\tau - |\xi|\}\exp\{-r\tau/(2\epsilon)\}I_0\left\{[r/(2\epsilon c_s)]\sqrt{(c_s\tau)^2 - \xi^2}\right\} , \tag{3-97}$$

where I_0 is the zero-th order, modified Bessel function of the first kind. Comparison of this result with the causal Green's function of the undamped string, given by equation (3-81), shows that the damping introduces a temporal decay (via the negative exponential) and a spatial decay (via the modified Bessel function) into the causal Green's function.

Figure 3-7 illustrates the spatial dependence of the causal Green's function of the infinite, damped string at a constant time, τ, after application of the impulsive loading. By comparison with figure 3-4, the obvious difference between the Green's functions of the damped and undamped strings is that the Green's function of the damped string decreases with increasing magnitude of ξ in the range $|\xi| < c_s\tau$, whereas that of the undamped string is constant in this range. Another difference, however, is that the amplitude of the Green's function for the undamped string is constant, whereas that for the damped string decreases with increasing τ.

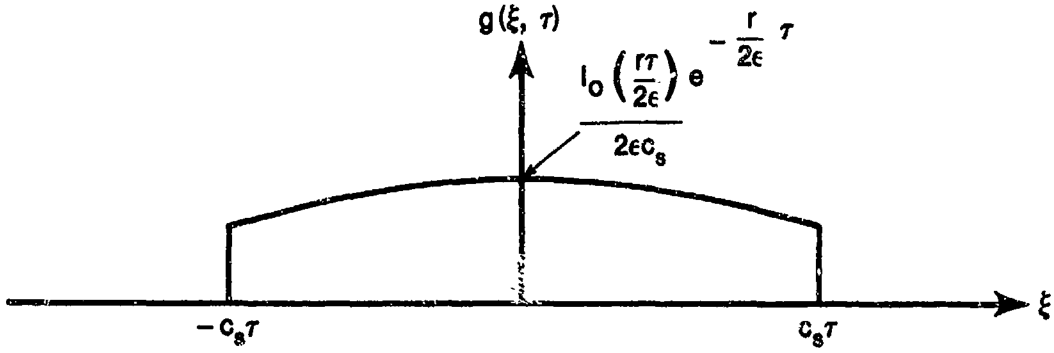

Figure 3-7. Spatial Dependence of the Causal Green's Function for a Damped, Infinite String

Let us now examine the characteristics of the wavenumber-frequency response. By a rearrangement of equation (3-96), we can separate $G(k,\omega)$ for the damped string into its real and imaginary parts as follows:

$$G(k,\omega) = \frac{-\{[\omega^2 - (kc_s)^2] + i[r\omega/\epsilon]\}}{\epsilon\{[\omega^2 - (kc_s)^2]^2 + [r\omega/\epsilon]^2\}} . \qquad (3\text{-}98)$$

Figures 3-8(a) and (b) illustrate the wavenumber dependence of the real and imaginary parts of the wavenumber-frequency response of the damped string at a fixed frequency, ω, for a (constant) damping coefficient, r, such that the ratio $r/(\epsilon\omega) = 0.1$.

Comparison of figure 3-8(a) with figure 3-5(a) shows the real parts of the wavenumber-frequency responses of the damped and undamped strings to be similar, except in the neighborhood of $k = \pm\omega/c_s$, where the response of the damped string remains defined, whereas that of the undamped string is undefined. In these regions of similarity, damping forces are insignificant, so the physical interpretation of the wavenumber-frequency response of the undamped string can be shown to apply to the damped string. At $k = \omega/c_s$, figure 3-8(a) shows the real part of $G(k,\omega)$ to be zero. Recall, from the discussion of the undamped string, that the tensile and inertial forces in the string are in balance at this wavenumber. Thus, in the damped string, the applied force at this wavenumber must be balanced by the forces due to

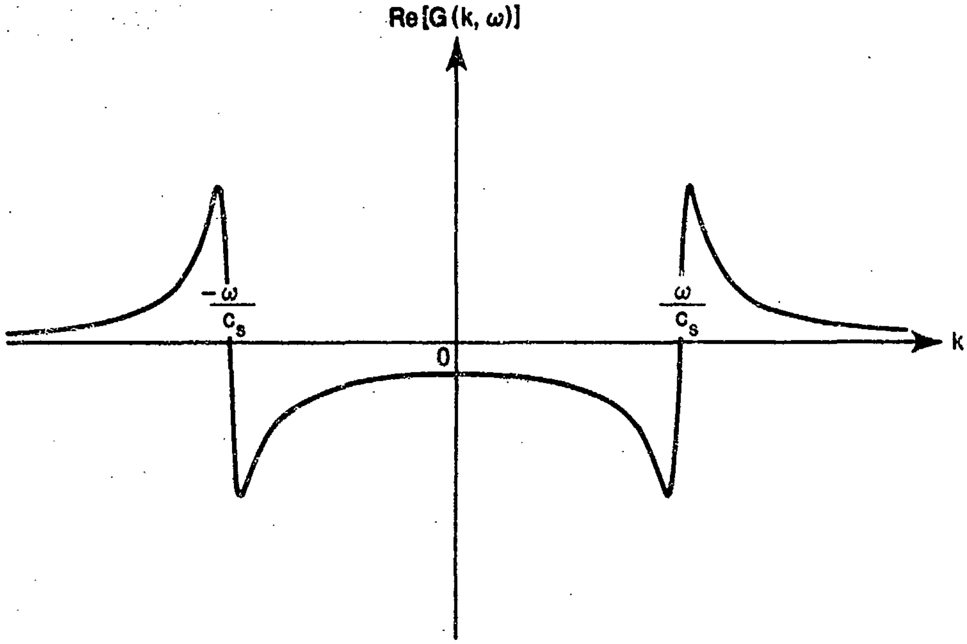

Figure 3-8(a). Real Part of Wavenumber-Frequency Response

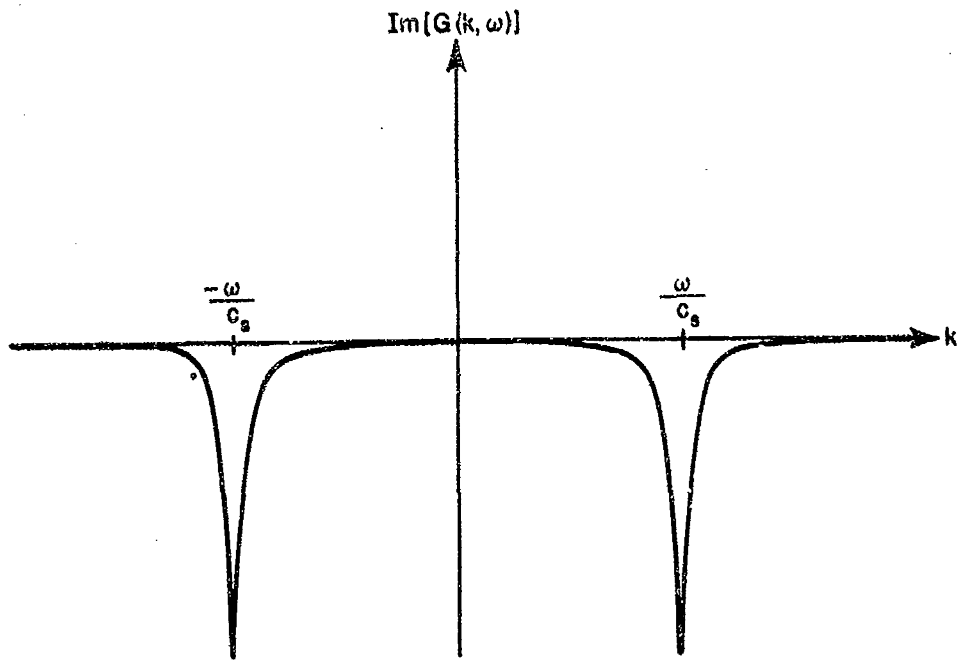

Figure 3-8(b). Imaginary Part of Wavenumber-Frequency Response

Figure 3-8. Real and Imaginary Parts of Wavenumber-Frequency Response of a Damped, Infinite String

damping. By inspection of equation (3-98), these damping forces are reflected in the imaginary part of $G(k,\omega)$.

Recall that the wavenumber-frequency response can be interpreted as the ratio of $w(x,t)$ to $f(x,t)$ when $f(x,t) = \exp\{i(kx + \omega t)\}$ for all x and t. By substitution of a solution of the form $w(x,t) = G(k,\omega)\exp\{i(kx + \omega t)\}$ into equation (3-84), it is easily established that $ir\omega$ is the ratio of the damping force per unit length to the displacement field, $w(x,t)$. Recall, from the example of the undamped string, that $\varepsilon\omega^2$ and $\varepsilon k^2 c_s^2$ are the ratios of the inertial and tensile forces per unit length, respectively, to the displacement field. For the fixed frequency and damping coefficient selected for this example, the ratio of the inertial force to the damping force is 10:1. With this background, the behavior of the imaginary part of $G(k,\omega)$, illustrated in figure 3-8(b), can easily be understood.

In the wavenumber ranges $|k| > |\omega/c_s|$, where tensile forces dominate both inertial and damping forces, equations (3-98) and figure 3-8(b) show the imaginary part of $G(k,\omega)$ to be small and negative. In the wavenumber range $|k| < |\omega/c_s|$, inertial forces dominate tensile forces. However, as stated above, the inertial forces are about 10 times greater than the damping forces, so, according to equation (3-98), the imaginary part of $G(k,\omega)$ is nearly constant and about 10 times smaller than the real part of $G(k,\omega)$ in this wavenumber range. At wavenumbers in the neighborhood of $|\omega/c_s|$, where the tensile and inertial forces nearly balance, the imaginary part of $G(k,\omega)$ is dictated by the ratio of the displacement to the damping force. As the inertial and tensile forces come into balance, the applied force must be balanced by the damping force. For the typically small damping coefficient used in this example, the displacement must be large to produce a force equal to the applied force. Hence, the ratio of the displacement to the damping force per unit length is large in the neighborhood of $|k| = |\omega/c_s|$. This behavior is reflected in the imaginary part of $G(k,\omega)$ depicted in figure 3-8(b).

As a final observation, note that at $|k| = |\omega/c_s|$,

$$G(|\omega/c_s|,\omega) = \mathrm{Im}[G(|\omega/c_s|,\omega)] = -i/(r\omega) , \qquad (3\text{-}99)$$

where Im[] denotes the imaginary part. Thus, as the damping (dictated by r) decreases, the imaginary part of $G(k,\omega)$ tends to infinity at $|k| = |\omega/c_s|$. Further, as the damping coefficient decreases, equation (3-98) can be used to show that the width, in wavenumber, of the negative peaks at $k = \pm\omega/c_s$ in the imaginary part of $G(k,\omega)$ decreases, while the amplitudes of the positive and negative peaks on either side of $k = \pm\omega/c_s$ in the real part of $G(k,\omega)$ increase. Thus, in the limit, as r tends to zero, the real and imaginary parts of $G(k,\omega)$ tend toward those shown for the undamped string. Further, by this limiting process, the behavior of the real part of $G(k,\omega)$ remains interpretable as the damping tends to zero. The lesson here is that undamped systems are best understood and interpreted when they are treated as limiting cases of damped systems.

For the general case of the forced, infinite, damped string, the magnitude and initial phase of each of the various harmonic waves comprising the space-time displacement field can be obtained as a function of the wavenumber and frequency characterizing each wave. We first write

$$\begin{aligned} W(k,\omega) &= |W(k,\omega)| \exp[i\alpha(k,\omega)] \,, \\ F(k,\omega) &= |F(k,\omega)| \exp[i\beta(k,\omega)] \,, \\ G(k,\omega) &= |G(k,\omega)| \exp[i\sigma(k,\omega)] \,, \end{aligned} \tag{3-100}$$

where $F(k,\omega)$ is the wavenumber-frequency transform of the applied forcing field per unit length, $f(x,t)$; $\alpha(k,\omega)$ and $\beta(k,\omega)$ are the initial phases of the harmonic waves comprising $w(x,t)$ and $f(x,t)$, respectively, as a function of the wavenumber and frequency characterizing each wave; and $\sigma(k,\omega)$ is the argument of $G(k,\omega)$. By use of equations (3-59) and (3-100), it follows that the magnitude of $W(k,\omega)$ is equal to the magnitude of $F(k,\omega)$ filtered by the magnitude of $G(k,\omega)$. That is,

$$|W(k,\omega)| = |F(k,\omega)G(k,\omega)| = |F(k,\omega)|\ |G(k,\omega)| \,. \tag{3-101}$$

It also follows that the initial phase, $\alpha(k,\omega)$, of each complex harmonic wave comprising $w(x,t)$ is equal to the initial phase, $\beta(k,\omega)$, of the corresponding wave component of $f(x,t)$ shifted by the argument of $G(k,\omega)$. That is,

$$\alpha(k,\omega) = \beta(k,\omega) + \sigma(k,\omega) \ . \tag{3-102}$$

Figures 3-9(a) and (b) depict the filtering of the magnitude of $F(k,\omega)$ by the magnitude of $G(k,\omega)$ and the phase shift, $\sigma(k,\omega)$, respectively, for the infinite, damped string. By equation (3-101), the magnitude of $W(k,\omega)$ will be large when the product of the magnitudes of $F(k,\omega)$ and $G(k,\omega)$ are large. From figure 3-9(a), the magnitude of $G(k,\omega)$ has relative maxima at $k = \pm\omega/c_s$. Thus, unless $|F(k,\omega)|$ is small in this region, $|W(k,\omega)|$ will exhibit relative maxima at wavenumbers characterizing free waves in the string. Other relative maxima of $|W(k,\omega)|$ can occur, at any frequency, in the neighborhood of those wavenumbers characterizing large relative contributions to $|F(k,\omega)|$. Through this filtering process, the relative amplitudes of the various harmonic waves comprising the displacement field are determined as a function of the wavenumber and frequency characterizing each wave.

Figure 3-9(b) shows that the phase shift applied to each wavenumber component of the forcing field, at a fixed frequency, by the wavenumber-frequency response of the string is (1) small for $|k|$ large in comparison to $|\omega/c_s|$, (2) $-\pi/2$ at $|k| = |\omega/c_s|$, and (3) approximately $-\pi$ for $|k| < |\omega/c_s|$.

As a final comment, it should be noted that the magnitude and phase of $G(k,\omega)$ for the infinite, damped string, shown in figure 3-9, do not exhibit the discontinuities or undefined response in the vicinity of the free wavenumber found (see figure 3-6) in the magnitude and phase of $G(k,\omega)$ for the case of the undamped string. Thus, if one is interested in the response of a system near such resonances, it is clear that some estimate of the damping or loss must be included in the mathematical model of the system.

3.4.6 The Wavevector-Frequency Response of a Damped, Infinite Plate

This final example is included to demonstrate that the mathematical techniques employed to obtain the Green's function (or its informational equivalent, the wavenumber-frequency response) for the systems illustrated above, which depend on only one spatial variable, can be applied to systems requiring two or three independent spatial variables in their mathematical

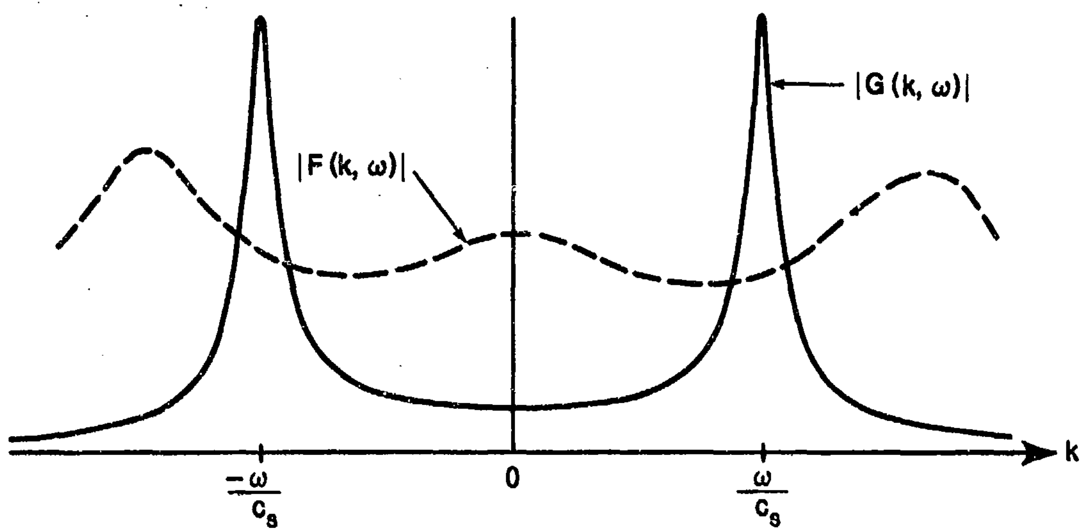

Figure 3-9(a). Filtering of $F(k,\omega)$ by $G(k,\omega)$

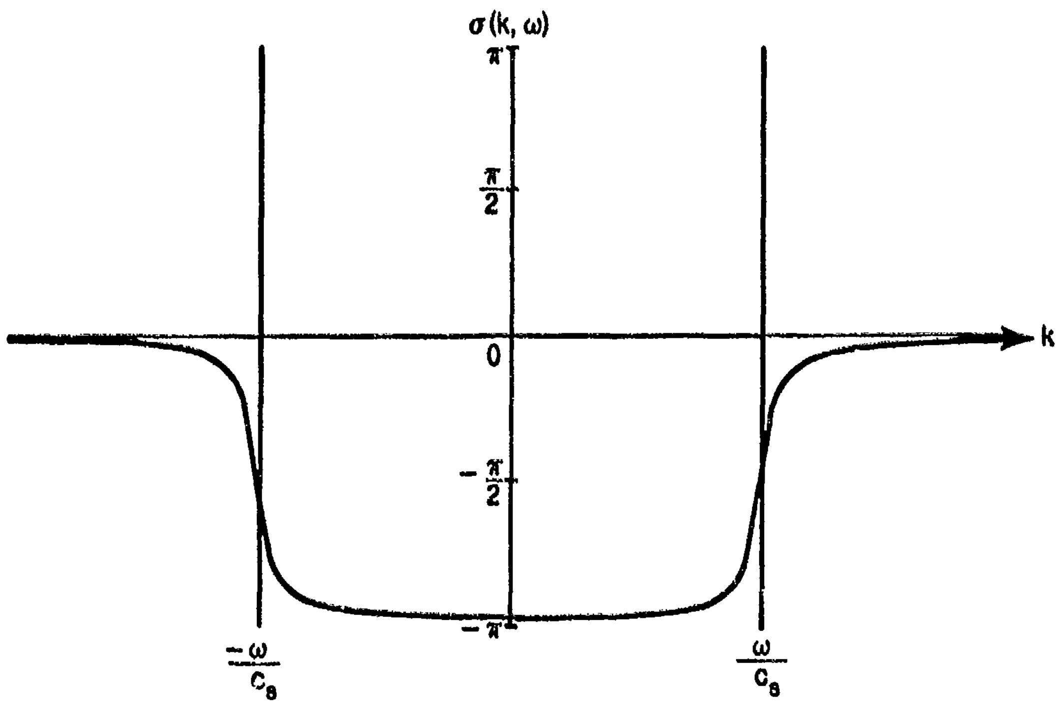

Figure 3-9(b). The Phase Shift, $\sigma(k,\omega)$

Figure 3-9. Filtering and Phase Shift of the Forcing Field by the Wavenumber-Frequency Response of a Damped, Infinite String

model. The specific problem treated here is the wavevector-frequency response of a uniform, infinite, damped plate.

A mathematical model for the forced vibrations of a damped plate is given by Davies.[12] That model, in the notation adopted in section 3.3.2, states that

$$D\nabla^4 w(\underline{x},t) + r\,\frac{\partial w(\underline{x},t)}{\partial t} + \mu\,\frac{\partial^2 w(\underline{x},t)}{\partial t^2} = f(\underline{x},t) \ , \qquad (3\text{-}103)$$

where, for this space- and time-invariant system, the damping coefficient, r, is assumed constant and $f(\underline{x},t)$ is the force per unit area applied to the plate.

The mathematical model for the Green's function is obtained by replacing the applied force per unit area in equation (3-103) by $\delta(\underline{x} - \underline{x}_0)\delta(t - t_0)$, where $\delta(\underline{x} - \underline{x}_0) = \delta(x_1 - x_{01})\delta(x_2 - x_{02})$. However, because the infinite plate system is space- and time-invariant, we can define $\underline{\xi} = \underline{x} - \underline{x}_0 = [x_1 - x_{01}, x_2 - x_{02}]$ and $\tau = t - t_0$ and then write the equation governing the Green's function as

$$D\nabla^4 g(\underline{\xi},\tau) + r\,\frac{\partial g(\underline{\xi},\tau)}{\partial \tau} + \mu\,\frac{\partial^2 g(\underline{\xi},\tau)}{\partial \tau^2} = \delta(\underline{\xi})\delta(\tau) \ . \qquad (3\text{-}104)$$

As we did in the case of the forced vibration of the string, we assume a particular solution, $g_p(\underline{\xi},\tau)$, exists of the form

$$g_p(\underline{\xi},\tau) = (2\pi)^{-3} \iint_{-\infty}^{\infty} G_p(\underline{k},\omega)\exp\{i(\underline{k}\cdot\underline{\xi} + \omega\tau)\}\ d\underline{k}\ d\omega \ . \qquad (3\text{-}105)$$

By equations (3-104), (3-105), and (2-38) and arguments similar to those employed between equations (3-67) and (3-69), it can be shown that

$$G_p(\underline{k},\omega) = \frac{1}{Dk^4 - \mu\omega^2 + ir\omega} \ , \qquad (3\text{-}106)$$

where $k = \sqrt{k_1^2 + k_2^2}$.

We argue here, as we did in the case of the vibration of the string, that the causality condition that $g(\underline{\xi},\tau) = 0$ for $\tau < 0$ at all $\underline{\xi}$ translates, under wavevector transformation, to $\tilde{G}(\underline{k},\tau) = 0$ for $\tau < 0$ at all wavevectors, $\underline{k}$.

By a partial fraction expansion of equation (3-106), the particular part of $\tilde{G}(\underline{k},\tau)$ can be written as

$$\tilde{G}_p(\underline{k},\tau) = \frac{1}{4\pi\mu\omega_d(k)} \left\{ \int_{-\infty}^{\infty} \frac{\exp(i\omega\tau)\, d\omega}{\omega - ir/(2\mu) + \omega_d(k)} - \int_{-\infty}^{\infty} \frac{\exp(i\omega\tau)\, d\omega}{\omega - ir/(2\mu) - \omega_d(k)} \right\} , \tag{3-107}$$

where

$$\omega_d(k) = \sqrt{[Dk^4/\mu] - [r/(2\mu)]^2} \quad . \tag{3-108}$$

Comparison of equation (3-107) with equation (3-88) reveals that the particular part of $\tilde{G}(\underline{k},\tau)$ for the infinite, damped plate has the same mathematical form as the particular part of $\tilde{G}(\underline{k},\tau)$ for the infinite, damped string. It therefore follows, by the arguments of equations (3-90) and (3-91), that

$$\tilde{G}_p(\underline{k},\tau) = (1/\mu)U(\tau)\exp[-r\tau/(2\mu)] \, \frac{\sin\{\omega_d(k)\tau\}}{\omega_d(k)} \, . \tag{3-109}$$

The homogeneous solution, g_h, to equation (3-104) is assumed to exist in the form

$$g_h(\underline{\xi},\tau) = (2\pi)^{-2} \int_{-\infty}^{\infty} \tilde{G}_h(\underline{k},\tau)\exp\{i\underline{k}\cdot\underline{\xi}\}\, d\underline{k} \, . \tag{3-110}$$

By substituting equation (3-110) into the homogeneous form of equation (3-104) and by realizing that the resultant integral applies for all $\underline{\xi}$, we obtain the ordinary differential equation

$$\mu \frac{d^2\tilde{G}_h}{d\tau^2} + r \frac{d\tilde{G}_h}{d\tau} + Dk^4\tilde{G}_h = 0 \ . \qquad (3\text{-}111)$$

The solution to equation (3-111) is easily shown to be

$$\tilde{G}_h(\underline{k},\tau) = \exp\{-r\tau/(2\mu)\}\{A(\underline{k})\exp[i\omega_d(k)\tau] + B(\underline{k})\exp[-i\omega_d(k)\tau]\} \ , \qquad (3\text{-}112)$$

where $\omega_d(k)$ is given by equation (3-108).

By the arguments given previously, the functions $A(\underline{k})$ and $B(\underline{k})$ are selected to satisfy causality; that is

$$\tilde{G}(\underline{k},\tau) = \tilde{G}_p(\underline{k},\tau) + \tilde{G}_h(\underline{k},\tau) = 0 \ , \quad \tau < 0 \ , \qquad (3\text{-}113)$$

for all $\underline{k}$. By equations (3-109) and (3-112), it is evident that equation (3-113) can be satisfied only if $A(\underline{k}) = B(\underline{k}) = 0$. It follows that $\tilde{G}_h(k,\tau) = 0$ and therefore

$$G(\underline{k},\omega) = G_p(\underline{k},\omega) = \frac{1}{Dk^4 - \mu\omega^2 + ir\omega} \ . \qquad (3\text{-}114)$$

A significant feature of the wavevector-frequency response of the infinite, damped plate, described by equation (3-114), is that it depends only on the magnitude of the wavevector ($\underline{k}$) and not on its direction. Inasmuch as $G(\underline{k},\omega)$ is the ratio of the space-time displacement field, $w(\underline{x},t)$, to the forcing field, $f(\underline{x},t)$, when the forcing field is given by $\exp\{i(\underline{k}\cdot\underline{x} + \omega t)\}$ for all $\underline{x}$ and t, it follows that $w(\underline{x},t) = G(\underline{k},\omega)\exp\{i(\underline{k}\cdot\underline{x} + \omega t)\}$. Thus, $G(\underline{k},\omega)$ can also be interpreted as the complex amplitude of the wave of displacement of the plate that corresponds, in wavevector and frequency, to the wave that excites the plate in motion. By the arguments of chapter 2, knowledge of the frequency and wavevector magnitude determines the wavelength and period of a (complex) plane harmonic wave. The direction of propagation is determined by the direction of the wavevector and the sign of the frequency. Therefore, the dependence of $G(\underline{k},\omega)$ on only the magnitude of the wavevector can be

interpreted as a reflection of the spatial invariance, or isotropy, of the plate. That is, for a unit amplitude, harmonic wave excitation of the plate, the amplitude of the resultant displacement of the plate depends only on the wavelength and frequency of the excitation and is independent of the direction of propagation of the harmonic wave excitation.

Figures 3-10(a) and (b) illustrate the magnitude and phase of the wavevector-frequency response of the damped, infinite plate as a function of wavevector magnitude, k, at an arbitrary, fixed, positive frequency. At this frequency, the (constant) damping coefficient was taken to be $r = 0.1\ \mu\omega$.

The behavior of the magnitude and phase of $G(\underline{k},\omega)$ with k, depicted in figure 3-10, is easily understood by recalling that for the harmonic wave excitation $\exp\{i(\underline{k}\cdot\underline{x} + \omega t)\}$, the displacement field is given by $w(\underline{x},t) = G(\underline{k},\omega)\exp\{i(\underline{k}\cdot\underline{x} + \omega t)\}$. Substitution of these displacement and excitation fields into equation (3-103) reveals that for $k < k_p(\omega) = \sqrt[4]{\mu\omega^2/D}$, the excitation is primarily balanced by the inertial forces in the plate and $G(\underline{k},\omega) = w(\underline{x},t)/f(\underline{x},t) \approx 1/(-\mu\omega^2)$. Thus, in this wavenumber range, the magnitude of G is nearly constant with k, and the displacement is nearly 180 degrees out of phase with the applied force.

In the wavenumber range $k > k_p(\omega)$, the applied force is primarily balanced by the forces associated with the bending stiffness of the plate, given by $Dk^4 w(\underline{x},t)$. Thus, in this wavenumber range, it follows that $G(\underline{k},\omega) \approx w(\underline{x},t)/f(\underline{x},t) \approx 1/(Dk^4)$. Here, therefore, the magnitude of G decreases with increasing wavevector magnitude as k^{-4}, and, as depicted in figure 3-10(b), the displacement is nearly in phase with the applied force.

In the neighborhood of $|\underline{k}| = k_p(\omega)$, the forces associated with bending stiffness and inertia nearly cancel each other, and the applied forces are primarily balanced by the damping force, given by $ir\omega w(\underline{x},t)$. The damping coefficient, r, was chosen such that, at the fixed frequency of this example, the damping force was one-tenth of the inertial force. Thus, at $|\underline{k}| = k_p(\omega)$, the magnitude of G is about 10 times greater than it is in the wavenumber range $|\underline{k}| < k_p(\omega)$, where inertial forces dominate. The initial phase of $w(\underline{x},t)$, at $|\underline{k}| = k_p(\omega)$, is seen to lag that of the harmonic excitation by 90 degrees

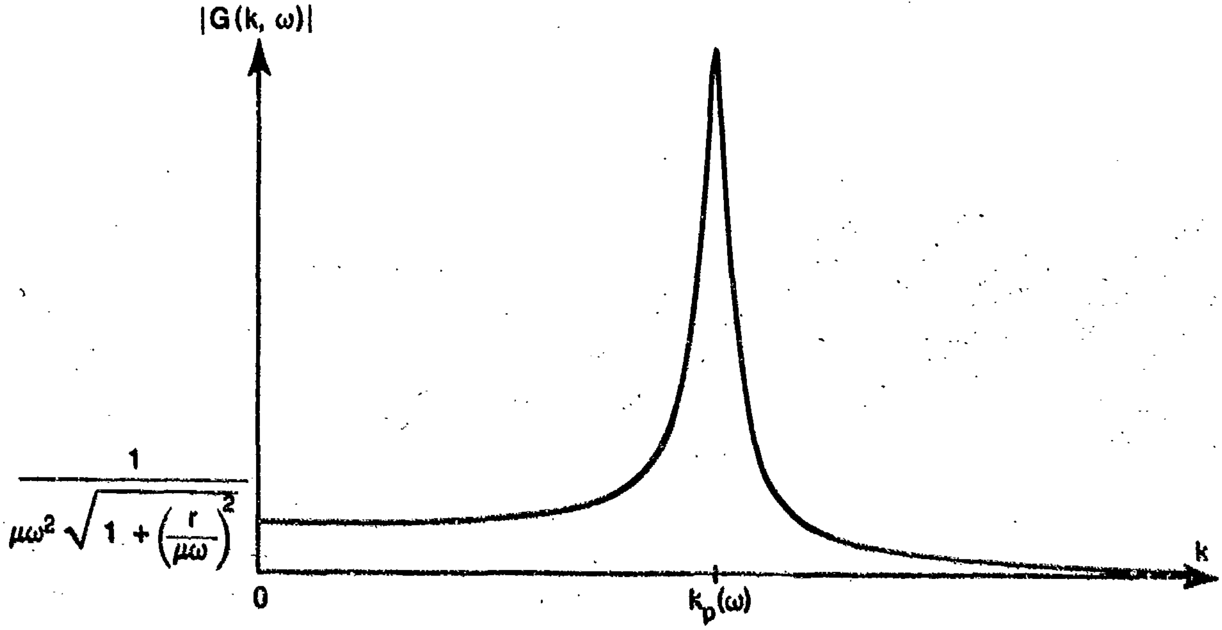

Figure 3-10(a). Magnitude of Wavevector-Frequency Response

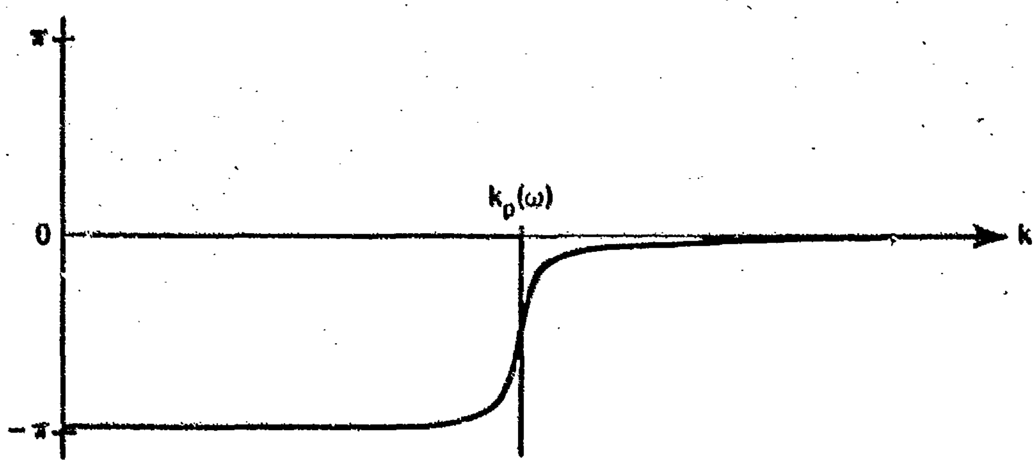

Figure 3-10(b). Phase of Wavevector-Frequency Response

Figure 3-10. Magnitude and Phase of the Wavevector-Frequency Response of a Damped, Infinite Plate

In figure 3-10, we plotted the magnitude and phase of the wavevector-frequency response as a function of k (i.e., the magnitude of the wavevector, $\underline{k}$) at an arbitrary frequency for purposes of graphical convenience. However, if one wished to use the relation $W(\underline{k},\omega) = F(\underline{k},\omega)G(\underline{k},\omega)$ to determine $W(\underline{k},\omega)$ for an arbitrary excitation of the plate, $F(\underline{k},\omega)$, it must be realized that both the magnitude and phase of $G(\underline{k},\omega)$ are circularly symmetric functions in the (k_1,k_2) plane. To illustrate this circular pattern of the wavevector-frequency response in the $\underline{k}$ plane, figure 3-11 shows the locus of the maximum magnitude of $G(\underline{k},\omega)$ for the damped, infinite plate in the $\underline{k}$ plane at an arbitrary, fixed frequency. As shown in figure 3-10(a) and illustrated in figure 3-11, the magnitude of $G(\underline{k},\omega)$ has a maximum at those wavevectors having magnitudes equal to the free wavenumber of the plate at the frequency of interest: that is, at $k = \sqrt{k_1^2 + k_2^2} = k_p(\omega)$, where $k_p(\omega) = \sqrt[4]{\mu\omega^2/D}$.

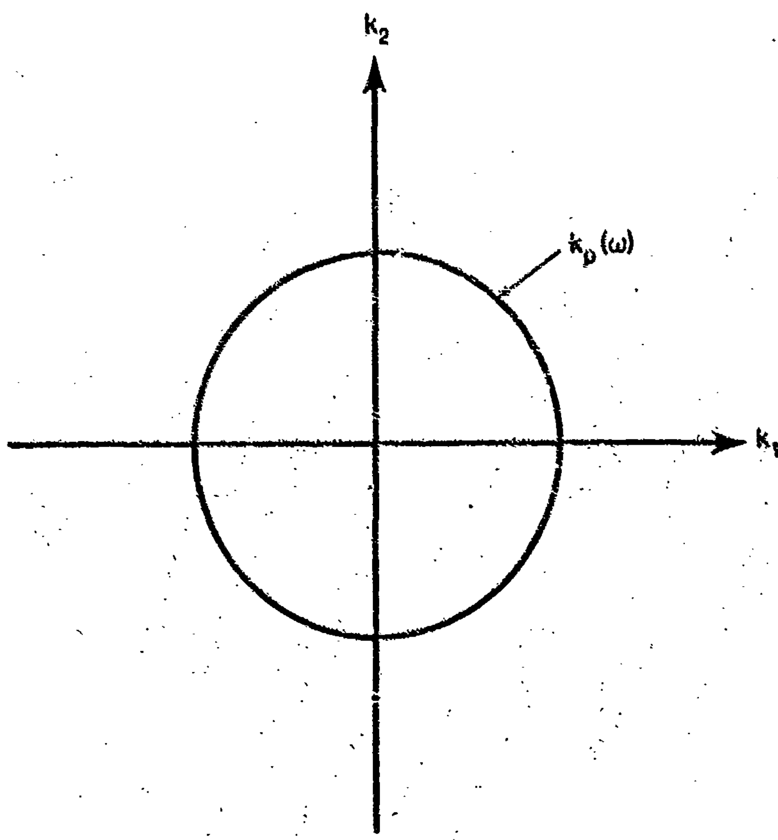

Figure 3-11. Locus of the Maximum Magnitude of $G(\underline{k},\omega)$
for a Damped, Infinite Plate

3.4.7 Summary of the Forced Response of Space- and Time-Invariant Linear Systems

The approach to the forced response of linear systems taken in this text is that of linear superposition by use of the Green's function. The Green's function is defined as the response of the linear system, in space and time, to an impulsive loading applied at any arbitrary location in space and at any arbitrary time. Inasmuch as (1) any input can be expressed as a weighted integral (summation) of impulses (i.e., Dirac delta functions) in space and time and (2) any summation of solutions to the linear differential equation describing a system also constitutes a solution to that equation, it then follows that the response of the system to an arbitrary input can be expressed as an integral of the Green's function weighted by the space-time excitation field.

For space- and time-invariant systems, the coefficients of the linear differential equations governing the system are constants. As a consequence, the Green's functions of linear space- and time-invariant systems depend only on the spatial separation vector, $\vec{\xi}$, and the temporal difference, τ, between the coordinates of observation, $(\vec{x},t)$, and excitation, $(\vec{x} - \vec{\xi}, t - \tau)$. As a result, the relation between the output field, $p(\vec{x},t)$, the input field, $f(\vec{x},t)$, and the Green's function, $g(\vec{\xi},\tau)$, is the convolution given by equation (3-52). This useful result states that, given the Green's function of a space- and time-invariant linear system, the output field of that system resulting from any input field can, in principle, be predicted.

By a Fourier transformation of the Green's function solution on all space and time variables, a simple algebraic expression is obtained that relates the wavevector-frequency transform of the output field to the product of the transforms of the input field and the Green's function. This relation is given by equation (3-59). By this equation, the amplitudes and initial phases of each plane harmonic wave component of the output field can be obtained, given the wavevector-frequency transform of the Green's function, $G(\vec{k},\omega)$, and the amplitudes and initial phases of the corresponding wave components of the input. The wavevector-frequency transform of the Green's function is called the wavenumber-frequency response of the system because it can be shown to be

equal to the ratio of the space-time output field to the space-time input field when that input field is the single complex harmonic plane wave $\exp\{i(\vec{k}\cdot\vec{x} + \omega t)\}$ for all $\vec{x}$ and t.

Systems of practical interest in acoustics are causal systems. That is, they respond only to past inputs and do not respond in anticipation of future inputs. Therefore, in deriving the Greens' function or its informational equivalent, the wavevector-frequency response, it is important to ensure that the Green's function satisfies conditions of causality specified by equation (3-53).

To illustrate the mathematical techniques for obtaining causal Green's functions or wavevector-frequency responses and to demonstrate how the wavevector-frequency description of forced space- and time-invariant systems can be physically interpreted, illustrative examples are presented in sections 3.4.4, 3.4.5, and 3.4.6.

3.5 REFERENCES

1. The American Heritage Dictionary of the English Language, Houghton Mifflin Co., Boston, MA, 1976, p. 1306.

2. W. L. Brogan, Modern Control Theory, Quantum Publishers, Inc., New York, 1974, p. 1.

3. P. M. Morse, Vibration and Sound, second edition, McGraw-Hill Book Co., New York, 1948, pp. 81-83.

4. Ibid., pp. 71-76.

5. M. C. Junger and D. Feit, Sound, Structures, and Their Interactions, MIT Press, Cambridge, MA, 1972, p. 148.

6. Morse, op. cit., pp. 29, 237.

7. Junger and Feit, op. cit., pp. 143-150.

8. A. P. Dowling and J. E. Ffowcs-Williams, Sound and Sources of Sound, Ellis-Horwood, Ltd., Chichester, UK, 1983, p. 306.

9. A. Papoulis, The Fourier Integral and Its Applications, McGraw-Hill Book Co., New York, 1962, pp. 36-37.

10. A. Erdelyi et al., Tables of Integral Transforms -- Volume I, McGraw-Hill Book Co., New York, 1954, p. 118, equation 3.2(3).

11. Ibid., p. 26, equation 1.7(30).

12. H. G. Davies, "Sound From Turbulent-Boundary-Layer-Excited Panels," Journal of the Acoustical Society of America, vol. 49, no. 3, March 1970, pp. 878-889.

CHAPTER 4
SPACE-VARYING LINEAR SYSTEMS

4.1 INTRODUCTION

The spatially distributed, continuous time systems of linear acoustics are mathematically modeled by partial differential equations of the form of equation (3-37): that is, by

$$L_{\vec{x},t}\{p(\vec{x},t)\} = f(\vec{x},t) \ . \tag{4-1}$$

Here $f(\vec{x},t)$ is the system input, $p(\vec{x},t)$ is the system output, and $L_{\vec{x},t}\{\ \}$ is the partial differential operator defined (see equation (3-36)) by

$$L_{\vec{x},t}\{\ \} = \sum_{j=0}^{J} \sum_{l=0}^{L} \sum_{m=0}^{M} \sum_{n=0}^{N} a_{jlmn}(\vec{x},t) \left(\frac{\partial^j}{\partial x_1{}^j}\right)\left(\frac{\partial^l}{\partial x_2{}^l}\right)\left(\frac{\partial^m}{\partial x_3{}^m}\right)\left(\frac{\partial^n}{\partial t^n}\right)\{\ \} . \tag{4-2}$$

The space- and time-invariant linear systems treated in chapter 3 were defined as systems having constant properties, or parameters, over all space and time. In the mathematical model of acoustic systems specified by equations (4-1) and (4-2), system parameters are reflected in the coefficients, $a_{jlmn}(\vec{x},t)$, of the partial differential operator, $L_{\vec{x},t}\{\}$. Thus, for space- and time-invariant linear systems, we required that

$$a_{jlmn}(\vec{x},t) = a_{jlmn} = \text{constant} \tag{4-3}$$

for all $\vec{x}$ and t. By defining ${}_I L_{\vec{x},t}\{\}$ as that form of $L_{\vec{x},t}\{\}$ in which the parameters $a_{jlmn}(\vec{x},t)$ are constants over all space and time (that is,

$${}_I L_{\vec{x},t}\{\ \} = \sum_{j=0}^{J} \sum_{l=0}^{L} \sum_{m=0}^{M} \sum_{n=0}^{N} a_{jlmn} \left(\frac{\partial^j}{\partial x_1{}^j}\right)\left(\frac{\partial^l}{\partial x_2{}^l}\right)\left(\frac{\partial^m}{\partial x_3{}^m}\right)\left(\frac{\partial^n}{\partial t^{\,n}}\right)\{\ \} \tag{4-4}$$

for all $\vec{x}$ and t), it follows that space- and time-invariant linear acoustic systems can be mathematically modeled by

$$ {}_{I}L_{\vec{x},t}\{p(\vec{x},t)\} = f(\vec{x},t) \tag{4-5}$$

for all $\vec{x}$ and t.

In this chapter, we explore the wavenumber-frequency analysis of space-varying, but time-invariant, linear acoustic systems. Space-varying, time-invariant systems are those in which the parameters of the system vary in space, but not in time. As we argued above, the system parameters are reflected in the general mathematical model of the linear acoustic system (equations (4-1) and (4-2)) by the coefficients $a_{jlmn}(\vec{x},t)$ contained in the linear partial differential operator, $L_{\vec{x},t}\{\ \}$. Therefore, if the coefficients a_{jlmn} in equation (4-2) describe the variation of the system parameters over all space and are constant in time (that is,

$$a_{jlmn}(\vec{x},t) = b_{jlmn}(\vec{x}) \tag{4-6}$$

for all $\vec{x}$ and t), we can define the space-varying, time-invariant linear partial differential operator, ${}_{It}L_{\vec{x},t}\{\ \}$, by

$$ {}_{It}L_{\vec{x},t}\{\ \} = \sum_{j=0}^{J} \sum_{l=0}^{L} \sum_{m=0}^{M} \sum_{n=0}^{N} b_{jlmn}(\vec{x}) \left(\frac{\partial^j}{\partial x_1{}^j}\right)\left(\frac{\partial^l}{\partial x_2{}^l}\right)\left(\frac{\partial^m}{\partial x_3{}^m}\right)\left(\frac{\partial^n}{\partial t^n}\right)\{\ \} \tag{4-7}$$

for all space and time. If ${}_{It}L_{\vec{x},t}\{\ \}$ is substituted for $L_{\vec{x},t}\{\ \}$ in equation (4-1), it follows that space-varying, time-invariant systems in linear acoustics are mathematically modeled by

$$ {}_{It}L_{\vec{x},t}\{p(\vec{x},t)\} = f(\vec{x},t) \tag{4-8}$$

for all $\vec{x}$ and t.

The mathematical form of equation (4-8) is an n-th order linear partial differential equation with nonconstant coefficients. Finite (or closed) form solutions cannot be obtained for most ordinary linear differential equations

greater than first order with nonconstant coefficients.[1] Therefore, our exploration of space-varying, time-invariant acoustic systems cannot be general. Rather, the primary emphasis in this chapter will be to obtain wavevector-frequency descriptions of space-varying versions of some of the physical systems treated in chapter 3. Comparison of the wavevector-frequency descriptions of the outputs of space-varying and space-invariant versions of the system will then be used to illustrate the effects of the spatial variation. Another objective of this chapter is to develop and interpret wavevector-frequency descriptions of certain space-varying fields that arise in structural-acoustics.

Space-varying systems result from only two characteristics of the physical system: (1) boundaries and (2) nonuniformities in the spatial properties between elements of the system. Space-varying systems can therefore be classified according to the source of the spatial variation. Bounded systems are referred to as space limited, whereas unbounded systems are infinite. Systems are termed spatially uniform or nonuniform, depending on the respective absence or presence of spatial nonuniformities in properties over the physical extent of the system. By use of these definitions, it follows that space-varying systems can be classified into three categories: (1) uniform, space limited, (2) nonuniform, space limited, and (3) nonuniform, infinite. Uniform, infinite systems are, of course, space invariant.

Of the three categories of space-varying systems, the one most commonly encountered, and best understood, in acoustic applications is the uniform, space-limited system. Consequently, the primary focus in this chapter will be on the wavevector-frequency characteristics of uniform, space-limited acoustic systems.

As we did for space- and time-invariant systems, we will first present some illustrative examples of free, space-varying systems and then explore the forced response.

4.2 FREE RESPONSE OF SPACE-VARYING, TIME-INVARIANT SYSTEMS

Recall that free systems are systems free of externally imposed inputs, characterized by $f(\vec{x},t)$ in equation (4-8). Thus, free, space-varying,

time-invariant acoustic systems are modeled by equations of the form

$$\mathrm{It}\,L_{\vec{x},t}\{p(\vec{x},t)\} = 0 \ . \tag{4-9}$$

Recall further, from the previous chapter, that free systems with losses cannot be described in the wavevector-frequency domain. Therefore, the illustrative examples presented below will be confined to lossless systems.

4.2.1 The Finite String With Fixed Ends

Consider the free vibration of a string of length L, fixed at $x = 0$ and $x = L$ such that no motion occurs at the ends. The tension, T, and mass per unit length, ϵ, are constant over the length of the string, $0 < x < L$, and are taken to be zero outside this interval. The equation governing the displacement field of the string, $w(x,t)$, can then be written as

$$b(x)\left\{T\,\frac{\partial^2 w}{\partial x^2} - \epsilon\,\frac{\partial^2 w}{\partial t^2}\right\} = 0 \tag{4-10}$$

for all x and t. The spatially varying coefficient, $b(x)$, that modifies T and ϵ is defined by

$$b(x) = U(x) - U(x - L) = \begin{cases} 1 \ , & 0 < x < L \ , \\ 0 \ , & \text{otherwise} \ , \end{cases} \tag{4-11}$$

where $U(x)$ denotes the Heaviside function.

The requirement that the ends of the string be motionless translates into the boundary conditions

$$w(0,t) = w(L,t) = 0 \tag{4-12}$$

for all t. To complete the statement of the free vibration problem, we assume (as we did in the case of the uniform, infinite string) that the initial displacement and velocity fields of the string are given by

$$w(x,0) = w_0(x) \tag{4-13}$$

and

$$\frac{\partial w(x,0)}{\partial t} = v_0(x) \ . \tag{4-14}$$

Equation (4-10) is equivalent to the mathematical statement

$$\frac{\partial^2 w}{\partial x^2} - \frac{1}{c_s^{\ 2}} \frac{\partial^2 w}{\partial t^2} = 0 \tag{4-15}$$

for $0 < x < L$ and all t. Recall that $c_s^{\ 2} = T/\epsilon$. The space-limited nature of this equation precludes a solution by the Fourier transform technique used for the free vibration of the infinite string in chapter 3. That is, although we may write the vibration field in the form

$$w(x,t) = (2\pi)^{-1} \int_{-\infty}^{\infty} \tilde{W}(k,t)\exp(ikx)\,dk \ , \tag{4-16}$$

substitution of this form into equation (4-15) yields

$$(2\pi)^{-1} \int_{-\infty}^{\infty} \left[\frac{d^2\tilde{W}(k,t)}{dt^2} + (kc_s)^2\,\tilde{W}(k,t)\right] \exp(ikx)\,dk = 0 \ , \tag{4-17}$$

which is valid only over the spatial range $0 < x < L$. Thus, we cannot argue, as we did for the case of the free, infinite string, that

$$\frac{d^2\tilde{W}(k,t)}{dt^2} + (kc_s)^2\,\tilde{W}(k,t) = 0 \ , \tag{4-18}$$

because equation (4-18) is a valid conclusion from equation (4-17) only when equation (4-17) holds for all x.

From the argument presented above, it is evident that the wavenumber-frequency description of the vibration field of the free, space-limited string cannot be obtained by direct application of Fourier transforms to the partial differential equation governing the motion of the string. However, the free

vibration of the finite-length string, fixed at its ends, is a classic problem in acoustics, and the space-time description of the displacement field for this system is derived in most standard texts on acoustics. Our approach, therefore, to obtaining a wavenumber-frequency description of the free vibration of the finite, fixed-end string is simply to perform a double Fourier transform of the classical solution for the space-time displacement field.

The space-time displacement field of the free, finite string with fixed ends is generally obtained (see reference 2, for example) by a separation of variables approach. This approach leads to a description of the displacement field, $w(x,t)$, in terms of a complete set of orthogonal functions, called normal modes, in the variable x. Associated with each normal mode is a natural frequency. The details of this solution procedure for the space-time field of the finite string are well documented (see references 2 and 3, for example) and will not be further reviewed here.

From reference 3, the space-time displacement field of the finite string that satisfies the fixed-end boundary conditions of equation (4-12) and the arbitrary initial conditions specified by equations (4-13) and (4-14) is given by

$$w(x,t) = \sum_{n=1}^{\infty} \left\{ C_n \cos(\omega_n t) + D_n \sin(\omega_n t) \right\} \alpha_n(x) \tag{4-19}$$

for $0 \le x \le L$ and for all time. Here, the normal modes, denoted by $\alpha_n(x)$ and given by

$$\alpha_n(x) = \sin(n\pi x/L) \ , \tag{4-20}$$

form a complete set of orthogonal functions over the spatial interval $0 \le x \le L$. The orthogonality condition is given by

$$\int_0^L \alpha_m(x)\alpha_n(x)\, dx = (L/2)\delta_{mn} \ . \tag{4-21}$$

where δ_{mn} is the Kronecker delta. The modal natural frequencies, ω_n, are given by

$$\omega_n = n\pi c_s/L \ . \tag{4-22}$$

The modal coefficients, C_n and D_n, in equation (4-19) are determined by the modal content of the initial displacement and velocity. That is,

$$C_n = (2/L) \int_0^L w_0(x)\alpha_n(x)\, dx \tag{4-23}$$

and

$$D_n = 2/(n\pi c_s) \int_0^L v_0(x)\alpha_n(x)\, dx \ . \tag{4-24}$$

As is evident, by equation (4-19), the space-time displacement field of the free, finite, fixed-end string is expressed as a weighted sum of natural modes of vibration of the string, where each natural mode of vibration is characterized by a specific spatial pattern of displacement, $\alpha_n(x)$, and a specific frequency of vibration, ω_n. The amplitude and initial phase of each modal contribution to the displacement field is determined (see equations (4-23) and (4-24)) by the initial displacement and velocity fields of the string.

The wavenumber-frequency description, $W(k,\omega)$, of the displacement field is defined as the double Fourier transform of the space-time displacement field, $w(x,t)$, over all space and time. That is,

$$W(k,\omega) = \int_{-\infty}^{\infty}\int_{-\infty}^{\infty} w(x,t)\exp\{-i(kx + \omega t)\}\, dx\, dt \ . \tag{4-25}$$

Equation (4-19) defines the space-time displacement field of the fixed-end, finite string only over the spatial interval $0 \leq x \leq L$. Outside this spatial

interval, the string does not exist, so the displacement in the regions $x < 0$ and $x > L$ is not defined. However, it is evident, by equation (4-25), that the wavenumber content of $W(k,\omega)$ depends on the displacement field outside, as well as inside, the spatial interval $0 \leq x \leq L$. Inasmuch as our interest is in the wavenumber-frequency description of the displacement field of the string in the interval $0 \leq x \leq L$, we want to avoid contaminating that description with wavenumber-frequency components arising from any assumed displacement field exterior to this spatial interval. Such contamination is avoided by requiring that $w(x,t) = 0$ for $x < 0$ and $x > L$.

For mathematical convenience, we define the space-time field $w_\infty(x,t)$ as the extension of the mathematical form of equation (4-19) over all x and t. That is,

$$w_\infty(x,t) = \sum_{n=1}^{\infty} \left\{C_n \cos(\omega_n t) + D_n \sin(\omega_n t)\right\} \alpha_n(x) \tag{4-26}$$

for all x and t. By use of equations (4-11) and (4-26), we can then express the desired space-time displacement field as

$$w(x,t) = b(x) w_\infty(x,t) \tag{4-27}$$

for all x and t. It is easily verified that the displacement field defined by equation (4-27) is equivalent to that of equation (4-19) in the spatial interval $0 \leq x \leq L$ and is zero elsewhere.

By equations (4-25) and (4-27), the wavenumber-frequency transform of the space-time displacement field of the free, finite string with fixed-end conditions can be written in the form

$$W(k,\omega) = \int_{-\infty}^{\infty} \int_{-\infty}^{\infty} b(x) w_\infty(x,t) \exp\{-i(kx + \omega t)\}\, dx\, dt \ . \tag{4-28}$$

By (1) substitution of equation (4-26) into equation (4-28), (2) expression of the $\cos(\omega_n t)$ and $\sin(\omega_n t)$ in their exponential forms, and (3) use of

equation (2-38), it is straightforward to show that

$$W(k,\omega) = \pi \sum_{n=1}^{\infty} \{(C_n - iD_n)\delta(\omega - \omega_n) + (C_n + iD_n)\delta(\omega + \omega_n)\}I_n(k) \ , \tag{4-29}$$

where $I_n(k)$ is the spatial Fourier transform of the n-th normal mode, space limited by b(x). That is,

$$I_n(k) = \int_{-\infty}^{\infty} b(x)\alpha_n(x)\exp(-ikx)\ dx \ . \tag{4-30}$$

By expressing the normal mode, defined by equation (4-20), in exponential form, we can write $I_n(k)$ as

$$I_n(k) = \frac{1}{2i}\{B(k - n\pi/L) - B(k + n\pi/L)\} \ , \tag{4-31}$$

where B(k), the Fourier transform of b(x), is easily shown to be

$$B(k) = L\ \exp(-ikL/2)\ \frac{\sin(kL/2)}{(kL/2)} \ . \tag{4-32}$$

Equation (4-29) shows $W(k,\omega)$ for the free, finite string with fixed ends to be a discrete function of ω, with Dirac delta functions at all positive and negative integer multiples of $\pi c_s/L$. At each ω_n, the delta function in ω is multiplied by the wavenumber transform of the corresponding space-limited, n-th normal mode and a weighting factor appropriate to the particular ω_n. The wavenumber transform of the n-th normal mode can be seen, by equations (4-31) and (4-32), to be continuous functions of k for all n. Thus, the wavenumber-frequency transform of the displacement field of the free, finite string with fixed ends is discrete in ω, but continuous in k.

As stated above, the continuous behavior of $W(k,\omega)$ in k, at each ω_n, results from $I_n(k)$, the wavenumber transform of the n-th normal mode, space limited by b(x). By equations (4-31) and (4-32), it is evident that $I_n(k)$

is, in general, a complex quantity and therefore influences both the magnitude and phase of $W(k,\omega)$. Figure 4-1 illustrates the magnitude and phase of $I_6(k)$: that is, $I_n(k)$ for the 6-th normal mode of the fixed-end, finite string.

The magnitude of $I_6(k)$, shown in figure 4-1(a) over the wavenumber range $-12\pi/L \le k \le 12\pi/L$, defines the magnitudes of the (complex) amplitudes of the waves of the form $\exp(ikx)$ that comprise the spatial field defined by $b(x)\alpha_6(x)$. By equations (4-11) and (4-20) and use of the exponential form for $\sin(n\pi x/L)$, it can be shown that

$$b(x)\alpha_6(x) = \begin{cases} 0 \, , & -\infty < x < 0 \, , \\ (1/2i)\{\exp(i6\pi x/L) - \exp(-i6\pi x/L)\} \, , & 0 \le x \le L \, , \\ 0 \, , & L < x < \infty \, . \end{cases} \quad (4\text{-}33)$$

By the form of equation (4-33), it is not surprising that the largest contributions to the wavenumber transform of $b(x)\alpha_6(x)$ occur at the wavenumbers $\pm 6\pi/L$. Indeed, it can easily be shown that the Fourier transform of $\alpha_6(x)$ alone, over all space, is the weighted pair of Dirac delta functions, $\delta(k - 6\pi/L)$ and $\delta(k + 6\pi/L)$. It therefore follows that all wavenumber contributions to $I_6(k)$, other than those at $\pm 6\pi/L$, result from the restriction, mathematically imposed by $b(x)$, that the displacement field be equal to zero outside the spatial interval $0 \le x \le L$.

Figure 4-1(b) depicts the phase of $I_6(k)$. Physically, this phase can be interpreted as the phase, at $x = 0$, of the various spatial waves of the form $\exp(ikx)$ that comprise the space-limited, 6-th normal mode as a function of the wavenumber (k) characterizing the spatial waveform. The phase is presented modulo 2π in figure 4-1(b), so all discontinuities of magnitude 2π are merely scale adjustments. The phase discontinuities of magnitude π result from the sign changes in $I_6(k)$ associated with the terms of the form $\sin(kL/2)/(kL/2)$ in $B(k - 6\pi/L)$ and $B(k + 6\pi/L)$. These discontinuities occur at all integer multiples of $2\pi/L$, except $\pm 6\pi/L$. In between such discontinuities, the phase decreases linearly (with slope $-L/2$) with increasing k.

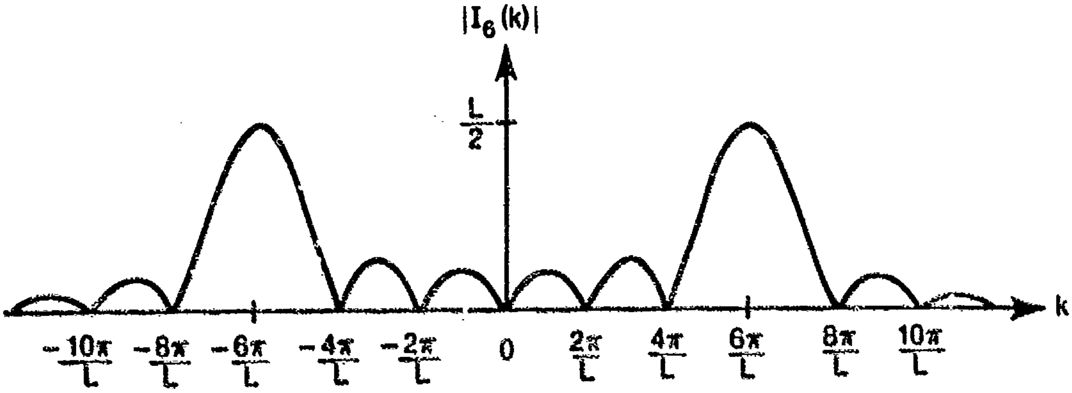

Figure 4-1(a). Magnitude of $I_6(k)$

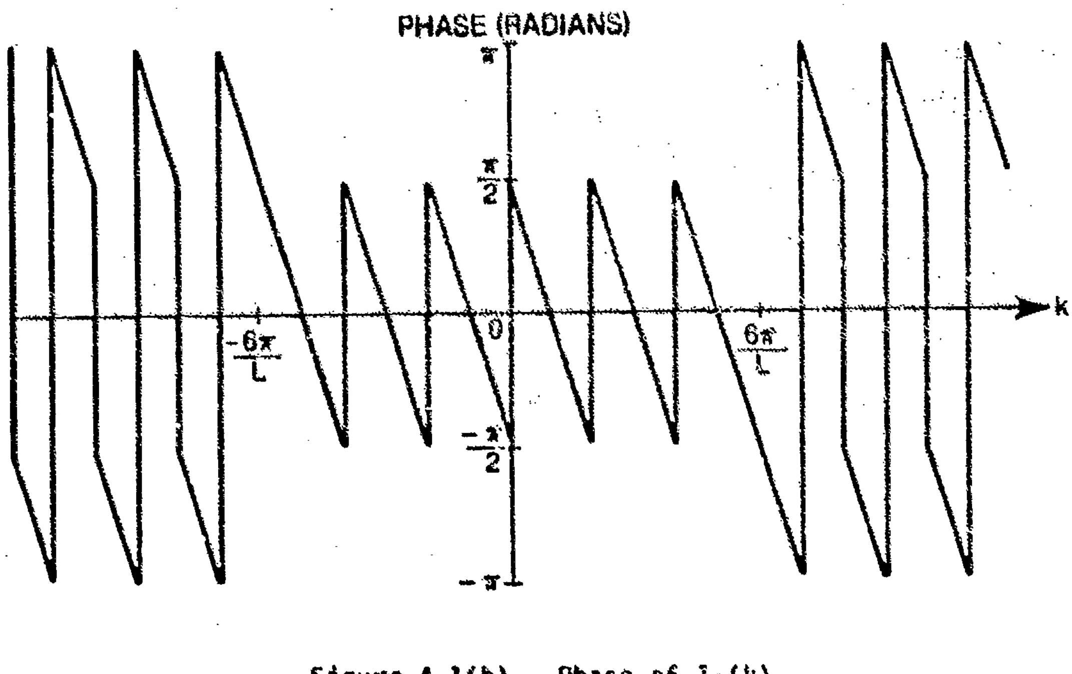

Figure 4-1(b). Phase of $I_6(k)$

Figure 4-1. Magnitude and Phase of $I_n(k)$ for the 6th Mode of the Free, Finite, Fixed-End String

Owing to the discrete nature of $W(k,\omega)$ with frequency, it can be argued, from equation (4-29), that the magnitude of $W(k,\omega)$ can be written as

$$|W(k,\omega)| = \pi \sum_{n=1}^{\infty} \{|C_n - iD_n|\ |I_n(k)|\ \delta(\omega - \omega_n)$$

$$+ |C_n + iD_n|\ |I_n(k)|\ \delta(\omega + \omega_n)\} , \qquad (4\text{-}34)$$

where $|\ |$ denotes the absolute value. Inasmuch as C_n and D_n are real constants, it is evident that the wavenumber dependence of $|W(k,\omega)|$ at each modal natural frequency, ω_n, is dictated by $|I_n(k)|$. To illustrate this wavenumber dependence, figure 4-2 presents, in a waterfall-type display, the magnitude of $I_n(k)$ as a function of k at each of the modal natural frequencies in the range $-6\pi c_s/L \leq \omega_n \leq 6\pi c_s/L$. Superposed on this plot are the free wavenumbers, $k = \omega/c_s$, of the infinite, uniform string treated in section 3.3.1 of chapter 3.

By figure 4-2, it is evident that the largest (in magnitude) contribution to $W(k,\omega)$ at each natural frequency (with the exception of $w_{\pm 1}$) occurs at $k \approx \omega_n/c_s$. These contributions are associated with the maxima of $|B(k - n\pi/L) - B(k + n\pi/L)|$, which, by equation (4-31), dictate the wavenumber dependence of $|I_n(k)|$. It should be noted that, although the maximum of $B(k - n\pi/L)$ occurs at $n\pi/L$, the maximum of $|B(k - n\pi/L) - B(k + n\pi/L)|$ is shifted away from $k = n\pi/L$, owing to the interaction between the main lobe of $B(k - n\pi/L)$ and the side lobe of $B(k + n\pi/L)$. The same argument applies to the maximum of $I_n(k)$ at $k = -n\pi/L$. For large values of n, and therefore high modal frequencies, this wavenumber shift is small. However, for the lower order modes, this shift is significant. Indeed, at the first modal frequency (i.e., $n = 1$), the main lobes of $B(k - \pi/L)$ and $B(k + \pi/L)$ interact to produce a single maximum at $k = 0$ rather than the expected pair of maxima at $k = \pm\pi/L$.

To the extent that (1) figure 4-2 illustrates, to within a frequency-dependent scale factor, the wavenumber-frequency characteristics of the magnitude of $W(k,\omega)$ associated with the free vibration of a finite,

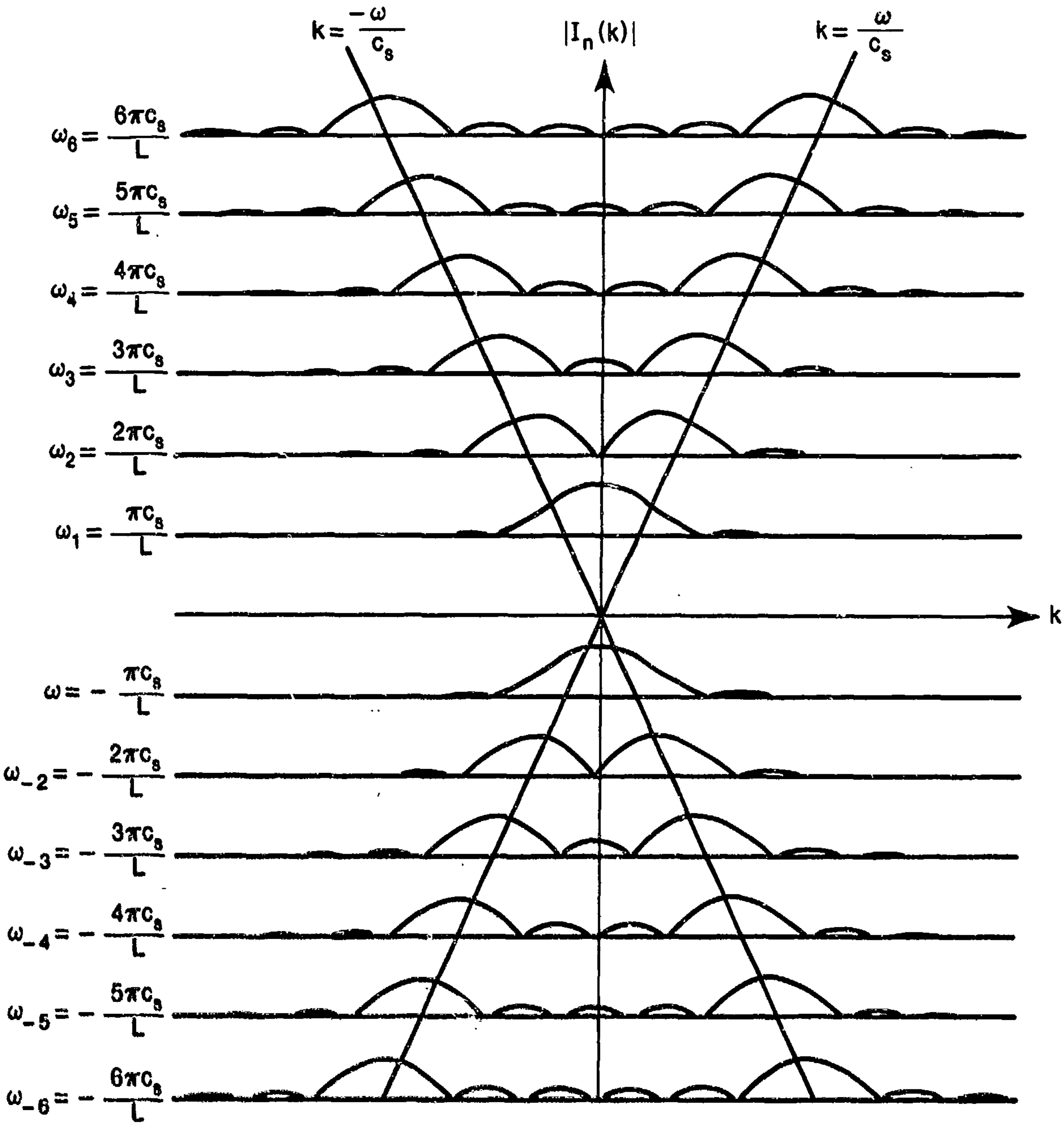

Figure 4-2. $|I_n(k)|$ as a Function of k at Each of the Modal Natural Frequencies in the Range $-6\pi c_s/L \leq \omega_n \leq 6\pi c_s/L$

fixed-end string and (2) only wavenumber-frequency combinations that lie on the lines $k = \pm\omega/c_s$ can contribute to the free vibration of the uniform, infinite string (see chapter 3), figure 4-2 illustrates the two essential differences in the wavenumber-frequency characteristics of the vibration field between the space- and time-invariant string and the space-limited, but time-invariant, string.

The first difference is that the wavenumber-frequency transform of the free vibration field of the infinite (space-invariant) string is a continuous function of frequency along the lines $k = \pm\omega/c_s$, whereas that of the finite (space-limited) string is a discrete function of ω. The reason for this difference can be traced to the boundary conditions. The infinite string, owing to the absence of boundaries, can support the propagation of any wavenumber component introduced by the initial conditions at the frequencies $\omega = \pm kc_s$. The fixed-end, finite string, owing to the boundary condition that $w(0,t) = w(L,t) = 0$, can support propagation, over the spatial interval $0 \leq x \leq L$, of only that discrete set of wavenumber components associated with the normal modes of the string: that is, by equation (4-20), $k = \pm n\pi/L$. According to the differential equation for the free motion of the finite string (equation (4-15)), the string will support propagation of these discrete wavenumber components only at the corresponding set of discrete frequencies, $\omega = \omega_{\pm n} = \pm n\pi c_s/L$.

The second difference in the wavenumber-frequency transforms of the fields of the finite and infinite, uniform strings is that, at any given frequency, the wavenumber content is discrete for the infinite string, but distributed for the finite string. As discussed above, the string, in free vibration, will only support propagation of waves characterized by $k = \pm\omega/c_s$. As shown in chapter 3, the wavenumber-frequency transform of the displacement field of the infinite string consists, at any frequency, of a weighted pair of Dirac delta functions in k: one at $k = +\omega/c_s$ and one at $k = -\omega/c_s$. It is also evident, by equations (4-19), (4-20), and (4-22), that only the wavenumber-frequency combinations related by $k_n = \omega_n/c_s$ (where $k_n = n\pi/L$) satisfy the governing equation for the displacement field of the free, finite string. However, owing to the finite length of the string, we imposed the restriction that the displacement field, $w(x,t)$, be zero outside the physical extent of the string (i.e., $x < 0$ and $x > L$). It was this restriction that introduced, at each natural frequency (ω_n), wavenumber components other than ω_n/c_s in $W(k,\omega)$. Such additional wavenumber components will be present in any space-limited system if the space-time output field of the system is restricted to be zero outside the physical bounds of the system.

Before leaving the example of the free vibrations of the fixed-end, finite string, it is instructive to consider the relationship between the wavenumber

transform of the initial displacement and velocity fields and the modal coefficients C_n and D_n. By writing

$$w_0(x) = 1/(2\pi) \int_{-\infty}^{\infty} W_0(k)\exp(ikx)\, dk \tag{4-35}$$

and

$$v_0(x) = 1/(2\pi) \int_{-\infty}^{\infty} V_0(k)\exp(ikx)\, dk \tag{4-36}$$

and substituting these expressions into equations (4-23) and (4-24), we can show, by use of equation (4-30), that

$$C_n = 1/(\pi L) \int_{-\infty}^{\infty} W_0(k)I_n^*(k)\, dk \tag{4-37}$$

and

$$D_n = 1/(n\pi^2 c_s) \int_{-\infty}^{\infty} V_0(k)I_n^*(k)\, dk\ , \tag{4-38}$$

where the asterisk denotes the complex conjugate. Equations (4-37) and (4-38) show that the modal coefficients, C_n and D_n, are proportional to the integral, over all wavenumbers, of the wavenumber transforms of the respective initial displacement and velocity fields filtered by $I_n^*(k)$, the conjugate of the Fourier transform of the space-limited, n-th normal mode.

Owing to the restriction that $w(x,t)$ is zero outside the spatial interval $0 \le x \le L$, neither $W_0(k)$ nor $V_0(k)$ can consist of only a single wavenumber contribution of the form $\delta(k - k_0)$. However, it is interesting to note, by equations (4-37) and (4-38), that each such delta function contribution to W_0 or V_0 produces an infinite number of nonzero modal coefficients, C_n or D_n.

If $W_0(k)$ is proportional to $I_M(k)$, where M is a fixed, positive integer, it is straightforward to show, by equations (4-37), (2-38), and (4-21), that

$$C_n = A\delta_{nM} \ , \tag{4-39}$$

where A is the constant of proportionality. Thus, when $W_0(k)$ is proportional to $I_M(k)$, only the modal coefficient C_M contributes to the wavenumber-frequency transform. In a similar fashion, it can be shown that when $V_0(k)$ is proportional to $I_M(k)$, all D_n's, except D_M, are zero. These results stem from the orthogonality of the normal modes over the interval $0 \leq x \leq L$. That is, by the inverse Fourier transformation of equation (4-30),

$$b(x)\alpha_n(x) = 1/(2\pi) \int_{-\infty}^{\infty} I_n(k)\exp(ikx)\ dk \ . \tag{4-40}$$

It then follows, by equation (4-21), that the orthogonality condition can be expressed in terms of $I_n(k)$ in the form

$$1/(2\pi) \int_{-\infty}^{\infty} I_m(k)I_n{}^*(k)\ dk = (L/2)\delta_{mn} \ . \tag{4-41}$$

The orthogonality condition, as expressed by equation (4-41), can be used to aid the interpretation of the wavenumber filtering of $W_0(k)$ and $V_0(k)$ by $I_n(k)$ in equations (4-37) and (4-38). By use of equations (4-13), (4-14), (4-26), (4-27), and (4-30), it is straightforward to show that

$$W_0(k) = \sum_{n=1}^{\infty} C_n I_n(k) \tag{4-42}$$

and

$$V_0(k) = \sum_{n=1}^{\infty} \omega_n D_n I_n(k) \ . \tag{4-43}$$

By equations (4-42) and (4-43), it is seen that the wavenumber description of the initial conditions can be expressed as a weighted summation of the

wavenumber transforms of the various normal modes. Further, the modal coefficients, C_n and D_n, are the same as those used in the space-time domain to describe w(x,t). Substitution of equations (4-42) and (4-43) into equations (4-37) and (4-38), respectively, yields

$$C_n = 1/(\pi L) \int_{-\infty}^{\infty} \sum_{m=1}^{\infty} C_m I_m(k) I_n^*(k)\, dk \tag{4-44}$$

and

$$D_n = 1/(\pi L \omega_n) \int_{-\infty}^{\infty} \sum_{m=1}^{\infty} \omega_m D_m I_m(k) I_n^*(k)\, dk \ . \tag{4-45}$$

Note that the integrations in equations (4-44) and (4-45) are simply a restatement of the orthogonality condition of equation (4-41). Application of this orthogonality condition to equations (4-44) and (4-45) yields identities for C_n and D_n.

It is clear from the above arguments that the wavenumber description of the initial conditions can be viewed as weighted superpositions of the wavenumber transforms of the space-limited, normal modes of the finite string. The coefficients that weight this superposition are the same coefficients that weight the normal modes in the space-time description of the displacement field, w(x,t).

It should be emphasized that the space-time description of the free vibration field of the fixed-end, finite string given by equation (4-19) applies for all time. In a fashion similar to that observed for the free vibration of the infinite string, the "snapshot" in time of the initial displacement and velocity fields of the finite string determines the modal coefficients C_n and D_n. By equation (4-19), it is evident that, given the normal modes and modal natural frequencies of the finite string, specification of these modal coefficients provides sufficient information to determine the space-time displacement field for all time.

4.2.2 The Finite, Simply Supported Plate

As an example of a space-limited system in two spatial dimensions, $\underline{x} = (x_1, x_2)$, we next treat the free vibrations of the simply supported plate illustrated in figure 4-3. Here, the flexural rigidity, D, and the mass per unit area, μ, of the plate are constant over the physical extent of the plate and are taken to be zero elsewhere. By defining the two-dimensional space-limiting function, $\beta(\underline{x})$, to be

$$\beta(\underline{x}) = \{U(x_1) - U(x_1 - L_1)\}\{U(x_2) - U(x_2 - L_2)\} = \begin{cases} 1 , & 0 < x_1 < L_1 \text{ and} \\ & 0 < x_2 < L_2 , \\ 0 , & \text{otherwise} , \end{cases} \tag{4-46}$$

the equation governing the displacement field, $w(\underline{x},t)$, can be written as

$$\beta(\underline{x})\left\{D\nabla^4 w(\underline{x},t) + \mu \frac{\partial^2 w(\underline{x},t)}{\partial t^2}\right\} = 0 \tag{4-47}$$

for all $\underline{x}$ and t.

The simply supported boundary conditions require that the displacement and the moment be zero at the boundaries of the plate. Mathematically, the zero displacement condition requires that

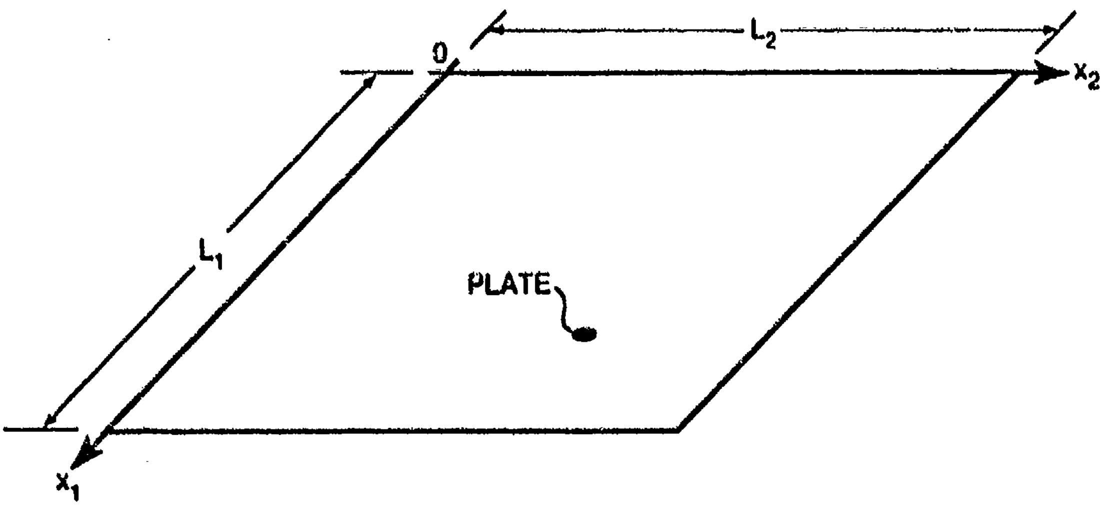

Figure 4-3. Geometry of Simply Supported Plate

$$w(0,x_2,t) = w(L_1,x_2,t) = w(x_1,0,t) = w(x_1,L_2,t) = 0 \tag{4-48}$$

for $0 \le x_1 \le L_1$, $0 \le x_2 \le L_2$, and all t. The zero-moment boundary conditions can be shown[4] to translate to the mathematical statements

$$\frac{\partial^2 w(0,x_2,t)}{\partial x_1^{\,2}} = \frac{\partial^2 w(L_1,x_2,t)}{\partial x_1^{\,2}} = \frac{\partial^2 w(x_1,0,t)}{\partial x_2^{\,2}} = \frac{\partial^2 w(x_1,L_2,t)}{\partial x_2^{\,2}} = 0 \tag{4-49}$$

for $0 \le x_1 \le L_1$, $0 \le x_2 \le L_2$, and all t.

For initial conditions, we again assume that

$$w(\underline{x},0) = w_0(\underline{x}) \tag{4-50}$$

and

$$\frac{\partial w(\underline{x},0)}{\partial t} = v_0(\underline{x}) \ . \tag{4-51}$$

The free vibration of the finite, simply supported plate, like the space-limited string, cannot easily be solved by direct application of Fourier transforms. However, it is easily solved by a separation of variables approach in the space-time domain. The details of this solution procedure are presented in standard texts (see Meirovitch,[5] for example) and will not be reviewed here. The separation of variables solution for the displacement field associated with free vibration of the simply supported plate is

$$w(\underline{x},t) = \sum_{m=1}^{\infty} \sum_{n=1}^{\infty} \{A_{mn} \cos(\omega_{mn} t) + B_{mn} \sin(\omega_{mn} t)\} \alpha_{mn}(\underline{x}) \tag{4-52}$$

over $0 \le x_1 \le L_1$ and $0 \le x_2 \le L_2$ for all t. In equation (4-52), $\alpha_{mn}(\underline{x})$, the normal modes of the plate defined by

$$\alpha_{mn}(\underline{x}) = \sin(m\pi x_1/L_1)\sin(n\pi x_2/L_2) \ , \tag{4-53}$$

form a complete set of orthogonal functions, over the spatial area $0 \le x_1 \le L_1$ and $0 \le x_2 \le L_2$, that individually satisfy the boundary

conditions of equations (4-48) and (4-49). The orthogonality condition is given by

$$\int_0^{L_1}\int_0^{L_2} \alpha_{mn}(\underline{x})\alpha_{qs}(\underline{x})\, d\underline{x} = (L_1 L_2/4)\delta_{mq}\delta_{ns} \ . \tag{4-54}$$

The modal natural frequencies of the simply supported plate, denoted by ω_{mn}, are given by

$$\omega_{mn} = (D/\mu)^{1/2}\{(m\pi/L_1)^2 + (n\pi/L_2)^2\} \ . \tag{4-55}$$

By use of equations (4-50), (4-51), and (4-52), the orthogonality condition (equation (4-54)) can be used to show that the modal coefficients, A_{mn} and B_{mn}, are related to the initial conditions by

$$A_{mn} = \frac{4}{L_1 L_2}\int_0^{L_1}\int_0^{L_2} w_0(\underline{x})\alpha_{mn}(\underline{x})\, d\underline{x} \tag{4-56}$$

and

$$B_{mn} = \frac{4}{L_1 L_2 \omega_{mn}}\int_0^{L_1}\int_0^{L_2} v_0(\underline{x})\alpha_{mn}(\underline{x})\, d\underline{x} \ . \tag{4-57}$$

To complete the specification of the displacement field of the free, simply supported plate over all space, we define (as we did for the finite string) the displacement field, $w(\underline{x},t)$, to be zero outside the physical extent of the plate: that is, outside the spatial region $0 \leq x_1 \leq L_1$ and $0 \leq x_2 \leq L_2$. By defining w_∞ to be the extension of the displacement field of equation (4-52) over all $\underline{x}$ (that is,

$$w_\infty(\underline{x},t) = \sum_{m=1}^{\infty}\sum_{n=1}^{\infty} \{A_{mn}\cos(\omega_{mn}t) + B_{mn}\sin(\omega_{mn}t)\}\alpha_{mn}(\underline{x}) \tag{4-58}$$

for all $\underline{x}$ and $\underline{t}$), we can then use equations (4-46) and (4-58) to express the requisite displacement field over all space and time as

$$w(\underline{x},t) = B(\underline{x})w_{\infty}(\underline{x},t) \ . \tag{4-59}$$

The wavevector-frequency description, $W(\underline{k},\omega)$, of the displacement field is obtained by the following multiple Fourier transform of the space-time field, $w(\underline{x},t)$:

$$W(\underline{k},\omega) = \int_{-\infty}^{\infty}\int_{-\infty}^{\infty} w(\underline{x},t)\exp\{-i(\underline{k}\cdot\underline{x} + \omega t)\} \, d\underline{x} \, dt \ . \tag{4-60}$$

By substituting equation (4-59) into equation (4-60), it is straightforward to show that

$$W(\underline{k},\omega) = \pi \sum_{m=1}^{\infty}\sum_{n=1}^{\infty} \{(A_{mn} - iB_{mn})\delta(\omega - \omega_{mn}) + (A_{mn} + iB_{mn})\delta(\omega + \omega_{mn})\}I_{mn}(\underline{k}) \ , \tag{4-61}$$

where

$$I_{mn}(\underline{k}) = \int_{-\infty}^{\infty}\int_{-\infty}^{\infty} B(\underline{x})\alpha_{mn}(\underline{x})\exp(-i\underline{k}\cdot\underline{x}) \, d\underline{x} \ . \tag{4-62}$$

By defining the Fourier transform of $B(\underline{x})$ as

$$B(\underline{k}) = \int_{-\infty}^{\infty}\int_{-\infty}^{\infty} B(\underline{x})\exp(-i\underline{k}\cdot\underline{x}) \, d\underline{x}$$

$$= L_1L_2 \exp\{-i(k_1L_1/2 + k_2L_2/2)\}\left[\frac{\sin(k_1L_1/2)}{(k_1L_1/2)}\right]\left[\frac{\sin(k_2L_2/2)}{(k_2L_2/2)}\right] , \tag{4-63}$$

it follows, from equation (4-62), that $I_{mn}(\underline{k})$ can be expressed as

$$I_{mn}(\underline{k}) = (1/4)\{B(k_1 - m\pi/L_1, k_2 + n\pi/L_2) + B(k_1 + m\pi/L_1, k_2 - n\pi/L_2)$$

$$- B(k_1 - m\pi/L_1, k_2 - n\pi/L_2) - B(k_1 + m\pi/L_1, k_2 + n\pi/L_2)\} \ . \tag{4-64}$$

By equations (4-61) through (4-64), it is evident that the wavevector-frequency transform of the displacement field of the simply supported plate is discrete in frequency and continuous in both wavevector components, k_1 and k_2. The discrete frequency components occur as Dirac delta functions at $\pm\omega_{mn}$, where ω_{mn} are the modal natural frequencies of the plate. At each modal natural frequency, the wavevector dependence of $W(\underline{k},\omega)$ is dictated by the product of (1) a complex constant, which depends only on the (real) modal coefficients, and (2) $I_{mn}(\underline{k})$, the wavevector transform of the corresponding space-limited, natural mode of the plate. Note that at $\omega = -\omega_{mn}$, the constant that modifies $I_{mn}(\underline{k})$ is the complex conjugate of the constant that modifies $I_{mn}(\underline{k})$ at $\omega = +\omega_{mn}$.

To aid in the physical interpretation of the wavevector-frequency field given by equation (4-61), it is useful to employ the inverse Fourier transformation of equation (2-56) on equation (4-61) to obtain the following description of the space-time field of the simply supported plate:

$$w(\underline{x},t) = \frac{1}{8\pi^2}\sum_{m=1}^{\infty}\sum_{n=1}^{\infty}\int_{-\infty}^{\infty}\{(A_{mn} - iB_{mn})I_{mn}(\underline{k})\exp[i(\underline{k}\cdot\underline{x} + \omega_{mn}t)]$$

$$+ (A_{mn} + iB_{mn})I_{mn}(\underline{k})\exp[i(\underline{k}\cdot\underline{x} - \omega_{mn}t)]\}\, d\underline{k} \quad . \tag{4-65}$$

By equation (4-65), it is seen that the space-time displacement field of the simply supported plate is comprised of a superposition of complex harmonic waves of the forms $\exp[i(\underline{k}\cdot\underline{x} + \omega_{mn}t)]$ and $\exp[i(\underline{k}\cdot\underline{x} - \omega_{mn}t)]$ over all wavevectors, $\underline{k}$, and over all discrete natural frequencies, ω_{mn}, of the plate. At each natural frequency, the magnitudes of the complex amplitudes and the initial phases of all harmonic wave components of the form $\exp[i(\underline{k}\cdot\underline{x} + \omega_{mn}t)]$ are specified by the product $(A_{mn} - iB_{mn})I_{mn}(\underline{k})$, and the magnitudes and initial phases of harmonic wave components of the form $\exp[i(\underline{k}\cdot\underline{x} - \omega_{mn}t)]$ are specified by the product $(A_{mn} + iB_{mn})I_{mn}(\underline{k})$. Note, by equation (4-61), that these are the same products that specify the wavevector dependence of $W(\underline{k},\omega)$ at the discrete frequencies $+\omega_{mn}$ and $-\omega_{mn}$, respectively.

From equation (4-65), it is obvious that the magnitudes of the complex amplitudes of the harmonic waves of the forms $\exp[i(\underline{k}\cdot\underline{x} + \omega_{mn}t)]$ and

$\exp[i(\underline{k}\cdot\underline{x} - \omega_{mn}t)]$ are equal at any specified wavevector and natural frequency and are given by

$$\frac{|(A_{mn} - iB_{mn})I_{mn}(\underline{k})|}{8\pi^2} = \frac{|(A_{mn} + iB_{mn})I_{mn}(\underline{k})|}{8\pi^2} = \frac{(A_{mn}{}^2 + B_{mn}{}^2)^{1/2}\,|I_{mn}(\underline{k})|}{8\pi^2} . \tag{4-66}$$

Note also, from equation (4-61), that because $W(\underline{k},\omega)$ is discrete in ω, the magnitude of $W(\underline{k},\omega)$ is given by

$$|W(\underline{k},\omega)| = \pi \sum_{m=1}^{\infty} \sum_{n=1}^{\infty} (A_{mn}{}^2 + B_{mn}{}^2)^{1/2}\,|I_{mn}(\underline{k})|\{\delta(\omega - \omega_{mn}) + \delta(\omega + \omega_{mn})\} . \tag{4-67}$$

By comparison of equations (4-66) and (4-67), it is clear that the wavevector dependence of $|W(\underline{k},\omega)|$ at $\omega = \pm\omega_{mn}$ is, within a factor of $8\pi^3$, equal to the magnitudes of the complex amplitudes of the harmonic wave components $\exp[i(\underline{k}\cdot\underline{x} + \omega_{mn}t)]$ and $\exp[i(\underline{k}\cdot\underline{x} - \omega_{mn}t)]$ that contribute to the space-time displacement field at $\omega = \pm\omega_{mn}$.

Recall that A_{mn} and B_{mn} are constants that depend on the initial displacement and velocity conditions of the plate. It is therefore evident, from equation (4-67), that the wavevector dependence of $|W(\underline{k},\omega)|$ at the discrete frequencies $\omega = \pm\omega_{mn}$ is specified, to within a multiplicative constant, by $|I_{mn}(\underline{k})|$. To illustrate this wavevector dependence, figure 4-4 presents the magnitude of $I_{mn}(\underline{k})$ as a function of k_1 and k_2 for the 6-6th (i.e., m = 6, n = 6) natural mode of a simply supported plate.

By inspection of figure 4-4, it is evident that $|I_{66}(\underline{k})|$ is characterized by four primary maxima located at the wavevectors $(6\pi/L_1, 6\pi/L_2)$, $(6\pi/L_1, -6\pi/L_2)$, $(-6\pi/L_1, 6\pi/L_2)$, and $(-6\pi/L_1, -6\pi/L_2)$. From equation (4-64), it can be established that the amplitudes of these primary maxima are identical and equal to $L_1L_2/4$. Figure 4-4 also shows secondary maxima that occur at odd multiples of π/L_1 along the lines $k_2 = \pm 6\pi/L_2$ and at odd multiples of π/L_2 along the lines $k_1 = \pm 6\pi/L_1$. The amplitudes of

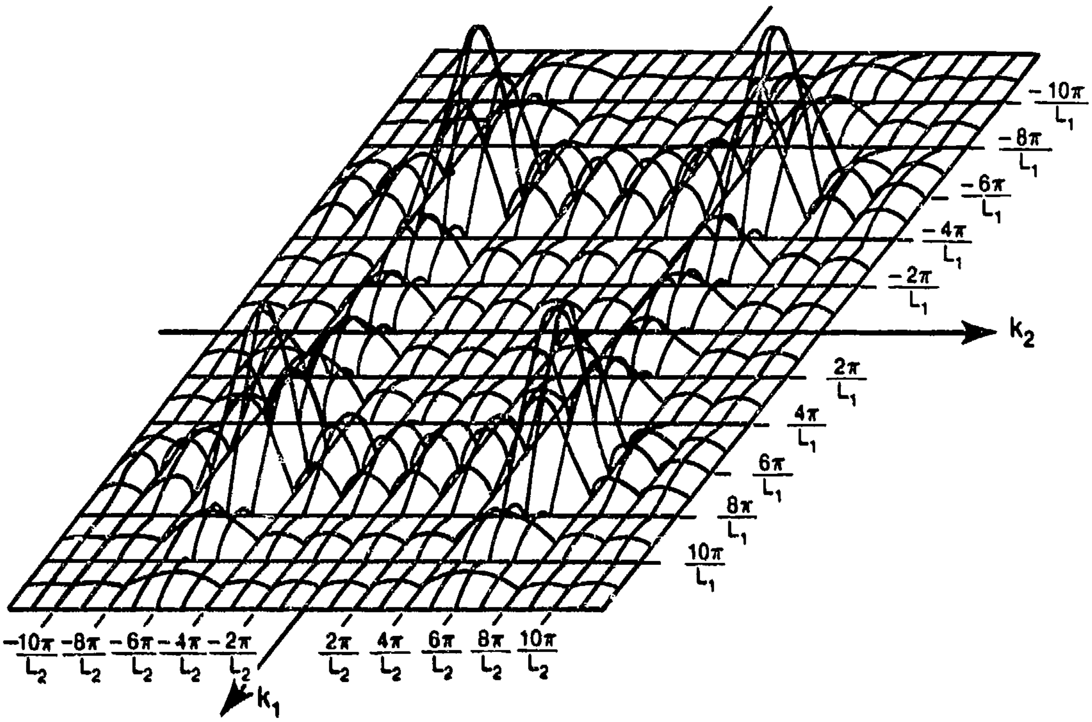

Figure 4-4. Magnitude of $I_{mn}(\underline{k})$ Versus k_1 and k_2 for the 6-6th Mode of a Simply Supported Plate

these secondary maxima can be shown, by equation (4-64), to be less than one-fifth the amplitude of the primary maxima.

It should be emphasized that $|I_{66}(\underline{k})|$ defines the relative magnitude of $|W(\underline{k},\omega)|$ as a function of $\underline{k}$ only at the discrete frequencies $\pm\omega_{66}$. By equation (4-66), $|I_{66}(\underline{k})|$ also defines, as a function of $\underline{k}$, the relative magnitudes of the complex amplitudes of the harmonic waves $\exp[i(\underline{k}\cdot\underline{x} + \omega_{66}t)]$ and $\exp[i(\underline{k}\cdot\underline{x} - \omega_{66}t)]$ that contribute to the space-time displacement field of the plate at the frequencies $\pm\omega_{66}$. By figure 4-4 and the above arguments, it is clear that, although $|I_{66}(\underline{k})|$ is distributed in $\underline{k}$, the wavevector contributions occurring at the wavevectors $(\pm 6\pi/L_1, \pm 6\pi/L_2)$ are significantly larger than those occurring at any other wavevector. Further, the magnitudes of the wavevectors characterizing these primary maxima are equal. If we denote the magnitudes of the wavevectors associated with the primary maxima of $|I_{66}(\underline{k})|$ by k_{66}, it is evident that

$$k_{66} = \{(6\pi/L_1)^2 + (6\pi/L_2)^2\}^{1/2} . \qquad (4\text{-}68)$$

By use of equations (4-55) and (4-68), it is evident that the magnitudes of the wavevectors associated with the four primary maxima of $|I_{66}(\underline{k})|$ are characterized by

$$k_{66} = \sqrt[4]{\mu\omega_{66}^{2}/D} \ . \tag{4-69}$$

In chapter 3, the wavenumber characterizing the free vibrations (i.e., the free wavenumber) of a space- and time-invariant plate at any frequency was defined by

$$k_p(\omega) = \sqrt[4]{\mu\omega^{2}/D} \ . \tag{4-70}$$

By comparison of equations (4-69) and (4-70), it is evident that the magnitudes of the wavevectors associated with the four primary maxima of $|I_{66}(\underline{k})|$ correspond to the free wavenumber of the plate at the natural frequency, ω_{66}, associated with the 6-6th natural mode of the simply supported plate.

The above observations regarding determination of the relative wavevector dependence of $|W(\underline{k},\omega)|$ at the discrete frequencies $\pm\omega_{66}$ by examination of the wavevector characteristics of the magnitude of $I_{66}(\underline{k})$ can be extended to any of the natural frequencies, ω_{mn}. That is, the relative wavevector dependence of $|W(\underline{k},\omega)|$ at ω_{mn} is determined by the magnitude of $I_{mn}(\underline{k})$ for arbitrary values of m and n. Further, from equations (4-63) and (4-64), it is straightforward to show that, for all m and n except unity, $|I_{mn}(\underline{k})|$ is characterized by four primary maxima of amplitude $L_1L_2/4$ occurring at the wavevectors $(m\pi/L_1, n\pi/L_2)$, $(-m\pi/L_1, n\pi/L_2)$, $(m\pi/L_1, -n\pi/L_2)$, and $(-m\pi/L_1, -n\pi/L_2)$. The magnitudes of these four wavevectors are equal and given by

$$k_{mn} = \sqrt[4]{\mu\omega_{mn}^{2}/D} = k_p(\omega_{mn}) \ . \tag{4-71}$$

For $m = 1$, the two associated primary maxima at $k_1 = \pm\pi/L_1$ interact, thereby producing a single, broader maximum at $k_1 = 0$. Similar arguments apply in k_2 for $n = 1$.

The initial phases of the harmonic waves of the form $\exp[i(\underline{k}\cdot\underline{x} + \omega_{mn}t)]$ and $\exp[i(\underline{k}\cdot\underline{x} - \omega_{mn}t)]$ that contribute to the space-time field of the freely vibrating, simply supported plate at each ω_{mn} are seen, from equation (4-65), to be determined by the arguments of the complex products $(A_{mn} - iB_{mn})\, I_{mn}(\underline{k})$ and $(A_{mn} + iB_{mn})I_{mn}(\underline{k})$, respectively. By equation (4-61), these are the same products that specify the wavevector dependence of $W(\underline{k},\omega)$ at the discrete frequencies $\pm\omega_{mn}$. As the argument of a product is the sum of the arguments of the terms comprising the product, we can gain some insight into the initial phase by examining the individual arguments of $(A_{mn} \pm iB_{mn})$ and $I_{mn}(\underline{k})$.

At any discrete frequency ω_{mn}, the modal coefficients A_{mn} and B_{mn} are real constants. Thus, if we denote the argument of $A_{mn} - iB_{mn}$ by θ_{mn}, the terms $A_{mn} - iB_{mn}$ and $A_{mn} + iB_{mn}$ contribute constant initial phase shifts of θ_{mn} and $-\theta_{mn}$ to the respective harmonic waves $\exp[i(\underline{k}\cdot\underline{x} + \omega_{mn}t)]$ and $\exp[i(\underline{k}\cdot\underline{x} - \omega_{mn}t)]$ that contribute to the space-time field, $w(\underline{x},t)$, at the frequency ω_{mn}.

By equations (4-63) and (4-64), it is clear that the argument of $I_{mn}(\underline{k})$ is a complicated function of $\underline{k}$. However, after some tedious manipulation, it can be shown that

$$\arg\{I_{mn}(\underline{k})\} = -\{k_1L_1/2 + k_2L_2/2 + (m + n)\pi/2\} + j(\underline{k})\pi \ , \qquad (4\text{-}72)$$

where $j(\underline{k})$ is a function that is zero or one, depending on the sign (as a function of $\underline{k}$) of the summation of terms of the form $\{\sin(k_1L_1/2) \sin(k_2L_2/2)\}/\{(k_1L_1/2)(k_2L_2/2)\}$ that arise in $I_{mn}(\underline{k})$ from various combinations of $B(k_1 \pm m\pi/L_1, k_2 \pm n\pi/L_2)$. By equation (4-72), it is seen that, in between the jumps of $\pm\pi$ dictated by $j(\underline{k})$, the argument of $I_{mn}(\underline{k})$ is a linear function of k_1 and k_2. Further, at each discrete frequency, ω_{mn}, the argument has a constant component that depends on $m + n$.

The argument of $I_{mn}(\underline{k})$ described by equation (4-72) is much too complicated to illustrate as a function of k_1 and k_2. However, at ω_{66}, the k_1 dependence of $\arg\{I_{66}(\underline{k})\}$ along the lines $k_2 = \pm 6\pi/L_2$ can be shown to be identical to the argument of $I_6(k)$ for the fixed-end, finite string shown in figure 4-1(b).

By the above arguments, the initial phases, at $\underline{x} = (0,0)$, of the harmonic waves of the form $\exp[i(\underline{k}\cdot\underline{x} + \omega_{mn}t)]$ and $\exp[i(\underline{k}\cdot\underline{x} - \omega_{mn}t)]$ that contribute to $w(\underline{x},t)$ at $\omega = \omega_{mn}$ are given by $\theta_{mn} + \arg\{I_{mn}(\underline{k})\}$ and $-\theta_{mn} + \arg\{I_{mn}(\underline{k})\}$, respectively.

By definition of $W_0(\underline{k})$ and $V_0(\underline{k})$ as the wavevector transforms of the initial displacement and velocity fields, $w_0(\underline{x})$ and $v_0(\underline{x})$, respectively, equations (4-56), (4-57), and (4-62) can be used to show that the modal coefficients are related to $W_0(\underline{k})$ and $V_0(\underline{k})$ by

$$A_{mn} = \frac{1}{\pi^2 L_1 L_2} \int_{-\infty}^{\infty}\int_{-\infty}^{\infty} W_0(\underline{k}) I_{mn}^*(\underline{k})\, d\underline{k} \tag{4-73}$$

and

$$B_{mn} = \frac{1}{\pi^2 L_1 L_2 \omega_{mn}} \int_{-\infty}^{\infty}\int_{-\infty}^{\infty} V_0(\underline{k}) I_{mn}^*(\underline{k})\, d\underline{k} \; . \tag{4-74}$$

Equations (4-73) and (4-74) show that the modal coefficients, A_{mn} and B_{mn}, are proportional to respective integrals of the wavevector descriptions of the initial displacement and velocity fields filtered by the conjugate of the wavevector transform of the space-limited, mn-th normal mode.

The restriction that $w(\underline{x},t)$, and thereby $v(\underline{x},t)$, be zero outside the physical extent of the plate precludes $W_0(\underline{k})$ or $V_0(\underline{k})$ from consisting of a single wavevector contribution of the form $\delta(\underline{k} - \underline{k}_0)$, because such a form corresponds to a space-time field of the form $\exp(i\underline{k}\cdot\underline{x})$ over all $\underline{x}$. Rather, by Fourier transformation of equations (4-50), (4-51), and (4-52), over all $\underline{x}$, it is straightforward to show that

$$W_0(\underline{k}) = \sum_{m=1}^{\infty}\sum_{n=1}^{\infty} A_{mn} I_{mn}(\underline{k}) \tag{4-75}$$

and

$$V_0(\underline{k}) = \sum_{m=1}^{\infty} \sum_{n=1}^{\infty} \omega_{mn} B_{mn} I_{mn}(\underline{k}) \; . \tag{4-76}$$

Thus, it is evident that $W_0(\underline{k})$ and $V_0(\underline{k})$ can be expressed as a weighted superposition of the wavevector transforms of the space-limited, normal modes. Recall that these transforms are continuous in $\underline{k}$. Note also that the weighting coefficients, A_{mn} and B_{mn}, are those used to express $w(\underline{x},t)$ in the space-time domain.

The inverse Fourier transform of equation (4-62) is

$$B(\underline{x})\alpha_{mn}(\underline{x}) = \frac{1}{(2\pi)^2} \int_{-\infty}^{\infty} I_{mn}(\underline{k}) \exp(i\underline{k}\cdot\underline{x}) \, d\underline{k} \; . \tag{4-77}$$

By equations (4-54) and (4-77), the orthogonality condition on $\alpha_{mn}(\underline{x})$ can be translated into the following orthogonality condition on $I_{mn}(\underline{k})$:

$$\frac{1}{(2\pi)^2} \int_{-\infty}^{\infty} I_{mn}(\underline{k}) I_{qs}^{*}(\underline{k}) \, d\underline{k} = \frac{L_1 L_2}{4} \delta_{mq} \delta_{ns} \; . \tag{4-78}$$

By equation (4-78), it is evident that $I_{mn}(\underline{k})$, where m and n are integers between one and infinity, constitute a complete set of orthogonal functions over the interval $(-\infty,-\infty) < \underline{k} < (\infty,\infty)$. This set of functions is the Fourier conjugate of the complete orthogonal set formed by the normal modes, $\alpha_{mn}(\underline{x})$. If equations (4-75) and (4-76) are multiplied by $I_{qs}(\underline{k})$ and integrated over all $\underline{k}$, the orthogonality condition of equation (4-78) can be used to verify the relationships of equations (4-73) and (4-74) between the modal coefficients, A_{mn} and B_{mn}, and the wavevector transforms, $W_0(\underline{k})$ and $V_0(\underline{k})$, of the initial conditions.

4.2.3 Summary of Free Wave Characteristics of Space-Limited Systems

The free responses of the space-limited, time-invariant linear systems treated in the above examples exhibit certain common wavevector-frequency

characteristics. This section highlights certain of these common wavevector-frequency characteristics and compares them to the characteristics of the space- and time-invariant systems treated in chapter 3.

The wavevector-frequency description of the free response of space-limited, time-invariant linear systems cannot, in the majority of cases, be easily obtained by direct application of Fourier transforms to the governing equations. Rather, most free, space-limited systems best lend themselves to solution in the space-time domain, where the solution is expressed as a weighted superposition of the normal modes of the system. Each normal mode defines an allowed spatial pattern of free response of the structure. Corresponding to each normal mode is a modal natural frequency, which defines the only frequency at which the system will support the free response defined by the normal mode. The wavevector-frequency description of the response field of a free, space-limited system is obtained by appropriate Fourier transformation of the space-time solution.

The above procedure is in contrast to that employed in chapter 3 to obtain the wavevector-frequency description of the free response of space- and time-invariant linear systems. For these systems, the wavevector-frequency description was obtained by direct transformation of the governing partial differential equations into the wavevector-time domain. The resultant ordinary differential equation in time was solved for the temporal characteristics of the field. Subsequent temporal Fourier transformation of this wavevector-time field led to the desired wavevector-frequency description.

Recall that the wavevector-frequency description (or transform) of the response of a system defines the specific combination of harmonic plane waves that comprise the space-time output field of the system. The space-time field of the free, space-limited system is comprised of a superposition of harmonic waves over an infinite set of discrete frequencies and over all wavevectors at each of the discrete frequencies. The set of discrete frequencies is comprised of all positive and negative values of the (positive) modal natural frequencies of the system. At each discrete frequency, the relative amplitudes and phases of the harmonic waves contributing to the space-time response field are determined by the wavevector transform of the space-limited, normal mode

corresponding to that discrete frequency. Thus, the wavevector-frequency description of the free response of a space-limited system is discrete in frequency, but continuous in the wavevector domain. The continuous nature of the wavevector-frequency description in the wavevector domain at each discrete frequency can be traced to the requirement that the response of the system be zero outside the physical extent of the system.

In contrast, the space-time fields of the free, space- and time-invariant systems treated in chapter 3 were comprised of a superposition of harmonic waves over the restricted set of wavevector and frequency combinations that can propagate as free waves in the system. The wavevector-frequency description (or transform) of the response field of a free, space- and time-invariant system is therefore characterized by nonzero values only along those surfaces or lines, in the wavevector-frequency domain, on which the wavevector-frequency combination corresponds to an allowable free wave of the system.

Owing to the absence of external forces in free systems, the wavevectors contributing to the free response of both the space-limited and space-invariant systems are completely determined by those wavevectors present in the initial conditions. In the space-limited system, the wavevector transforms of the initial space-time fields, filtered by the modal wavevector response, determine the modal coefficients and, thereby, the complex amplitudes of the various wavevector components at each modal natural frequency. In the space-invariant system, knowledge of the wavevector content of the initial fields and the wavevector-frequency combinations comprising free waves in the system is sufficient to completely define the wavevector-frequency description of the free response field.

4.3 FORCED RESPONSE OF SPACE-VARYING, TIME-INVARIANT SYSTEMS

The forced response of space-varying, but time-invariant, linear acoustic systems is governed by mathematical models of the form of equation (4-8): that is,

$$_{It}L_{\vec{x},t}\{p(\vec{x},t)\} = f(\vec{x},t)$$

for all $\vec{x}$ and t. Recall that the space-varying nature of the system is specified by the coefficients $b_{jlmn}(\vec{x})$ in the space-varying, time-invariant linear operator, ${}_{It}L_{\vec{x},t}\{\ \}$, defined by equation (4-7).

In this section, we examine the input-output relationships for space-varying, time-invariant linear systems and present two examples of the forced response of space-limited systems that arise in structural acoustics.

The general input-output relationships for space-varying, time-invariant linear systems are developed from the same basic concepts as those used in chapter 3 to treat space- and time-invariant systems. These concepts are (1) the principle of superposition for linear systems and (2) the Green's function, or impulse response.

The principle of superposition for a general space- and time-varying linear system is described by equations (3-36) through (3-41) in section 3.4.1 of chapter 3. Inasmuch as the space-varying, time-invariant linear systems of interest in this chapter are a subset of space- and time-varying linear systems, the principle of superposition described by these equations applies to space-varying, time-invariant linear systems.

For space-varying, time-invariant linear systems, the coefficients, $b_{jlmn}(\vec{x})$, of the linear operator, ${}_{It}L_{\vec{x},t}\{\ \}$, are independent of time, but are functions of the spatial vector, $\vec{x}$. Thus, the form of the linear operator ${}_{It}L_{\vec{x},t}\{\ \}$ is invariant with a change in the temporal origin, but not with a change in the origin of the spatial coordinates. That is, by defining $\tau = t - \theta$, where θ is a constant, equation (4-8) can be written

$${}_{It}L_{\vec{x},\tau+\theta}\{p(\vec{x},\tau + \theta)\} = f(\vec{x},\tau + \theta) \ . \tag{4-79}$$

However, it is easily shown, by equation (4-7), that

$${}_{It}L_{\vec{x},\tau+\theta}\{\ \} = {}_{It}L_{\vec{x},\tau}\{\ \} \ . \tag{4-80}$$

It therefore follows, from equations (4-79) and (4-80), that

$$ {}_{It}L_{\vec{x},\tau}\{p(\vec{x},\tau + \theta)\} = f(\vec{x},\tau + \theta) \ . \qquad (4\text{-}81) $$

We can conclude, by comparison of equations (4-8) and (4-81), that the output of a space-varying, time-invariant linear system resulting from the input $f(\vec{x},\tau + \theta)$ is $p(\vec{x},\tau + \theta)$.

It also follows from equation (4-8) that if $\vec{\xi} = \vec{x} - \vec{z}$, where $\vec{z}$ is a constant, then

$$ {}_{It}L_{\vec{\xi}+\vec{z},t}\{p(\vec{\xi} + \vec{z},t)\} = f(\vec{\xi} + \vec{z},t) \ . \qquad (4\text{-}82) $$

However, it is clear from equation (4-7) that

$$ {}_{It}L_{\vec{\xi}+\vec{z},t}\{\ \} \neq {}_{It}L_{\vec{\xi},t}\{\ \} \ . \qquad (4\text{-}83) $$

Therefore, the response of a space-varying linear system to the input $f(\vec{\xi} + \vec{z},t)$ is not equal to $p(\vec{\xi} + \vec{z},t)$.

By applying these concepts of superposition to the Green's function, or space-time impulse response, of space-varying, time-invariant linear systems, we can obtain general expressions for the input-output relations for such systems.

4.3.1 Green's Functions For Space-Varying, Time-Invariant Systems

The complete mathematical description of a system requires not only the specification of a mathematical model governing the system, but specification of the response at the spatial and temporal limits, or boundaries, of the system as well. Recall, from section 4.1, that there are three categories of space-varying systems: (1) uniform, space limited, (2) nonuniform, space limited, and (3) nonuniform, infinite. One primary difference between space-limited and infinite systems is the way the response of these systems is specified at the spatial limits of the system.

For systems of infinite spatial (or temporal) extent, the response of the system at the spatial (or temporal) limits is specified on the basis of

physical realizability, or causality. This requirement for causal response in such systems is satisfied by selecting appropriate combinations of the homogeneous and particular solutions to the partial differential equations governing the behavior of the system. All systems treated in this text are time invariant, and their temporal response characteristics are uniquely determined by causal arguments. For spatially infinite, time-invariant systems, causality conditions are applied to both the spatial and temporal response characteristics to define a unique system response.

In space-limited, time-invariant systems, the response of the system at its spatial limits, or boundaries, is specified as a part of the definition of the system. The response of such space-time systems is then uniquely defined by the governing partial differential equation, augmented by the specification of the required response at the spatial boundaries of the system (and, of course, the conditions for temporal causality). The requirement of a specific response at the spatial boundaries of a system usually implies the existence of external inputs acting on the boundaries of the system. The spatial boundary conditions can therefore be interpreted as an equation, supplementary to that governing the behavior of the system, that defines those external inputs (additional to those applied interior to the boundaries) required to achieve the specified response on the spatial boundaries of the system.

As a consequence of the different forms for specification of the responses of infinite and space-limited systems at their spatial limits, different mathematical procedures are required to formulate the respective input-output relationships for these space-varying systems. It is therefore convenient to treat the Green's function solutions for infinite and space-limited versions of space-varying systems separately.

As a prelude to the development of these Green's function solutions, certain remarks are in order regarding the role and treatment of such solutions in this text.

With regard to the role, the Green's function solution for a linear system relates the output of the system to the input and the Green's function in an integral form. This solution is general in the sense that, given the Green's

function for the linear system of interest, the output field resulting from any input field can be predicted. By appropriate Fourier transformation of the Green's function solution, the wavevector-frequency description (or transform) of the output field can be related to the wavevector-frequency description of the input field and the wavevector-frequency response of the system (i.e., the wavevector-frequency transform of the Green's function). This transformed relationship has the same generality as the Green's function solution. Thus, the role of Green's function solutions in the wavevector-frequency analysis of acoustic systems is to provide the basis from which general input-output relationships can be written in the wavevector-frequency domain for various classes of linear acoustic systems.

Let us now address the treatment of the Green's function in this text. The concept of Green's functions is a simple one. However, any rigorous development of the theory of Green's functions for a general linear space-time system requires mathematically complex and, consequently, lengthy arguments. Morse and Feshbach[6] devote over 100 pages to Green's functions, Courant and Hilbert[7] treat this subject in about 40 pages, and Greenberg[8] devotes an entire book to the development of a consistent theory of Green's functions. While these references vary somewhat in the generality and rigor of their respective treatments of Green's functions, they serve to illustrate the futility of attempting to present a comprehensive treatment of Green's functions in a few pages. Inasmuch as the focus of this book is the wavevector-frequency analysis of acoustic systems, we must conclude that a rigorous treatment of Green's functions is beyond the scope of this text. Consequently, we rely on somewhat heuristic arguments for the development of Green's function solutions of linear systems. For a more thorough treatment of such solutions, the reader is encouraged to consult the references cited above.

With apologies to the reader for this lengthy prelude, we now address the Green's function solution for infinite versions of space-varying linear systems.

4.3.1.1 The Green's Function for Infinite, Nonuniform, Time-Invariant Linear Systems. An infinite, nonuniform, time-invariant linear system is one in which (1) at least one of the coefficients, $b_{jlmn}(\vec{x})$, of the linear

operator ${}_{It}L_{\vec{x},t}\{\ \}$, defined by equation (4-7), varies with $\vec{x}$ and (2) at least one of these coefficients, at any $\vec{x}$, is nonzero. These conditions ensure a continuous system over all space that has space-varying properties. An example of an infinite, nonuniform linear system is an infinitely long, uniformly tensioned string having a mass per unit length that varies (but remains positive) over the length of the string.

Subject to the above restriction on the coefficients $b_{jlmn}(\vec{x})$, the output, $p(\vec{x},t)$, of the infinite, nonuniform, time-invariant linear system resulting from the input, $f(\vec{x},t)$, is governed by equation (4-8). Solutions to this equation are restricted to those that are casual in space and time.

Recall that the Green's function, $g(\vec{x},t;\vec{x}_0,t_0)$, is defined as the response of the system at the spatial position $\vec{x}$ and time t to an impulsive input applied at the spatial location $\vec{x}_0$ and time t_0. Therefore, the Green's function for the infinite, nonuniform, time-invariant linear system is defined by that combination of particular and homogeneous solutions to

$$ {}_{It}L_{\vec{x},t}\{g(\vec{x},t;\vec{x}_0,t_0)\} = \delta(\vec{x} - \vec{x}_0)\delta(t - t_0) \tag{4-84} $$

that are physically realizable, or causal, over all space and time.

The condition for temporal causality is that the output, or response, cannot anticipate the input in time. Therefore, for the Green's function to be causal, we require that

$$ g(\vec{x},t;\vec{x}_0,t_0) = 0, \quad t < t_0 \ . $$

and (4-85)

$$ \frac{\partial^n g(\vec{x},t;\vec{x}_0,t_0)}{\partial t^n} = 0, \quad t < t_0, \quad \text{for all } n. $$

Spatial causality, for the infinite, nonuniform linear acoustic systems of interest in this text, requires that the Green's function characterizes a response to the impulsive input that either (1) propagates away from the

spatial location of the impulsive input or (2) decays in amplitude with increasing distance from the location of the input.

By noting the temporal form of the input in equation (4-84), we can take advantage of the time invariance of the system, in the form of equation (4-81), to write

$$\mathrm{It}\,L_{\vec{x},t}\{g(\vec{x},\vec{x}_0,t - t_0)\} = \delta(\vec{x} - \vec{x}_0)\delta(t - t_0) \ . \qquad (4\text{-}86)$$

Thus, by comparison of equations (4-84) and (4-86), the Green's function for the infinite, nonuniform, time-invariant linear system has the mathematical form

$$g(\vec{x},t;\vec{x}_0,t_0) = g(\vec{x},\vec{x}_0,t - t_0) \ . \qquad (4\text{-}87)$$

Clearly, for this category of space-varying system, the Green's function depends on the two independent variables $\vec{x}$ and $t - t_0$ and on the parameter $\vec{x}_0$.

Let us assume that the causal Green's function defined by equation (4-86) is known. By use of the sampling property of the Dirac delta function (see equation (2-31)), we may then express the system input, $f(\vec{x},t)$, of equation (4-8) as an integral (i.e., summation) of the product of a weighting function and the delta functions that define the input for the Green's function. That is,

$$f(\vec{x},t) = \int_{-\infty}^{\infty}\int_{-\infty}^{\infty} f(\vec{x}_0,t_0)\delta(\vec{x} - \vec{x}_0)\delta(t - t_0)\ d\vec{x}_0\ dt_0 \ . \qquad (4\text{-}88)$$

By equations (4-87) and (4-88), the principle of superposition for linear systems (see equations (3-39)-(3-41)) can be used to argue that

$$\mathrm{It}\,L_{\vec{x},t}\int_{-\infty}^{\infty}\int_{-\infty}^{\infty}\{f(\vec{x}_0,t_0)g(\vec{x},\vec{x}_0,t - t_0)\}\ d\vec{x}_0\ dt_0$$

$$= \int_{-\infty}^{\infty}\int_{-\infty}^{\infty} f(\vec{x}_0,t_0)\delta(\vec{x} - \vec{x}_0)\delta(t - t_0)\ d\vec{x}_0\ dt_0 = f(\vec{x},t) \ . \qquad (4\text{-}89)$$

By comparison of equations (4-8) and (4-89), it is evident that the causal response of an infinite, nonuniform, time-invariant linear system to an arbitrary input, $f(\vec{x},t)$, is given by

$$p(\vec{x},t) = \int_{-\infty}^{\infty}\int_{-\infty}^{\infty} f(\vec{x}_0,t_0)g(\vec{x},\vec{x}_0,t - t_0)\, d\vec{x}_0\, dt_0 \; . \tag{4-90}$$

By employing the change of temporal variable $\tau = t_0 - t_0$, equation (4-90) may be written in the equivalent form

$$p(\vec{x},t) = \int_{-\infty}^{\infty}\int_{-\infty}^{\infty} f(\vec{x}_0,t - \tau)g(\vec{x},\vec{x}_0,\tau)\, d\vec{x}_0\, d\tau \; . \tag{4-91}$$

Equation (4-90) or (4-91) is the Green's function solution for the infinite, nonuniform type of space-varying, time-invariant linear system.

4.3.1.2 <u>The Green's Function for Space-Limited, Time-Invariant Linear Systems.</u> A space-limited system, as the name implies, is one which exists over some limited portion of space. If, within this limited portion of space, the properties vary with space, the space-limited system is defined to be nonuniform. If the properties are constant over the limited portion of space occupied by the system, the space-limited system is said to be uniform.

Our treatment of Green's function solutions to space-limited systems is based on the approach of Ffowcs-Williams et al.[9] to such systems.

Consider a space-limited system that exists within the volume, V_0, bounded by the surface, S_0. We define the space-limiting function, $s(\vec{x})$, to be

$$s(\vec{x}) = U\{\sigma(\vec{x})\} \; , \tag{4-92}$$

where U is the Heaviside function defined by equation (2-32) and $\sigma(\vec{x})$ is a function having the properties

$$\sigma(\vec{x}) > 0 \text{ inside } V_0 ,$$

$$\sigma(\vec{x}) < 0 \text{ outside } V_0 , \tag{4-93}$$

$$\sigma(\vec{x}) = 0 \text{ on } S_0 .$$

Thus, $s(\vec{x})$ defines a function that is one for $\vec{x}$ in V_0 and zero for $\vec{x}$ outside V_0. By use of this space-limiting function, the governing equation for any space-limited system can be written in the form of equation (4-8).

Recall that the system parameters (or properties) are reflected in the space-varying, time-invariant linear operator ${}_{It}L_{\vec{x},t}\{\ \}$ by the coefficients $b_{jlmn}(\vec{x})$. For space-limited systems, such system properties do not pertain outside of the spatial extent, V_0, of the system and can therefore be set to zero for $\vec{x}$ outside V_0. The same argument can be applied to the system input: that is, any input acting outside of V_0 is not acting on the space-limited system and can therefore be set to zero. Thus, for space-limited systems,

$$b_{jlmn}(\vec{x}) = s(\vec{x})B_{jlmn}(\vec{x}) \tag{4-94}$$

and

$$f(\vec{x},t) = s(\vec{x})q(\vec{x},t) , \tag{4-95}$$

where $B_{jlmn}(\vec{x})$ defines the parameters of the system inside V_0 and $q(\vec{x},t)$ specifies the input to the system inside V_0. Outside V_0, $B_{jlmn}(\vec{x})$ and $q(\vec{x},t)$ can be specified arbitrarily. Note that, for a uniform space-limited system, $B_{jlmn}(\vec{x})$ is not a function of $\vec{x}$. With $B_{jlmn}(\vec{x})$ and $f(\vec{x},t)$ defined by equations (4-94) and (4-95), equation (4-8) describes a space-limited, time-invariant linear system.

We must now address a notational problem. Let us designate the space-varying, time-invariant linear operator (of the form of equation (4-7)), having coefficients $b_{jlmn}(\vec{x})$, by ${}_{It,b}L_{\vec{x},t}\{\ \}$ and an identical operator, having the coefficients $b_{jlmn}(\vec{x})$ replaced by $B_{jlmn}(\vec{x})$, by ${}_{It,B}L_{\vec{x},t}\{\ \}$.

That is,

$$
{}_{It,b}L_{\vec{x},t}\{\ \} = \sum_{j=0}^{J}\sum_{l=0}^{L}\sum_{m=0}^{M}\sum_{n=0}^{N} b_{jlmn}(\vec{x}) \left(\frac{\partial^j}{\partial x_1{}^j}\right)\left(\frac{\partial^l}{\partial x_2{}^l}\right)\left(\frac{\partial^m}{\partial x_3{}^m}\right)\left(\frac{\partial^n}{\partial t^n}\right)\{\ \} \qquad (4\text{-}96)
$$

and

$$
{}_{It,\beta}L_{\vec{x},t}\{\ \} = \sum_{j=0}^{J}\sum_{l=0}^{L}\sum_{m=0}^{M}\sum_{n=0}^{N} \beta_{jlmn}(\vec{x}) \left(\frac{\partial^j}{\partial x_1{}^j}\right)\left(\frac{\partial^l}{\partial x_2{}^l}\right)\left(\frac{\partial^m}{\partial x_3{}^m}\right)\left(\frac{\partial^n}{\partial t^n}\right)\{\ \} . \qquad (4\text{-}97)
$$

In this notation, the additional presubscript identifies the coefficients of the space-varying linear operator. By use of the notation of equation (4-96), equation (4-8) becomes

$$
{}_{It,b}L_{\vec{x},t}\{p(\vec{x},t)\} = f(\vec{x},t) . \qquad (4\text{-}98)
$$

For the forced, space-limited, time-invariant linear system, use of equations (4-94), (4-95), and (4-97) allows us to rewrite equation (4-98) in the mathematically equivalent form

$$
s(\vec{x})\,{}_{It,\beta}L_{\vec{x},t}\{p(\vec{x},t)\} = s(\vec{x})q(\vec{x},t) . \qquad (4\text{-}99)
$$

Equation (4-99) is the typical form of the governing equation for forced, space-limited, time-invariant linear systems. To complete the specification of the space-limited problem, the output, $p(\vec{x},t)$, is subject to certain restrictions (i.e., boundary conditions) on the boundary S_0.

Inasmuch as the system is space-limited to within V_0, the desired output of the system is also space limited and is nonzero only within V_0 and on S_0. This desired output can be achieved by transferring the space-limiting function, $s(\vec{x})$, inside the linear operator. For the terms in the linear operator containing no spatial derivatives, this transfer presents no problem. For example,

$$
s(\vec{x})\beta_{0001}(\vec{x}) \frac{\partial p(\vec{x},t)}{\partial t} = \beta_{0001}(\vec{x}) \frac{\partial\{s(\vec{x})p(\vec{x},t)\}}{\partial t} . \qquad (4\text{-}100)
$$

However, in the transfer of $s(\vec{x})$ inside the linear operator, each spatial derivative generates an additional term. For example, it is easily verified, by use of equations (4-92) and (2-32), that

$$s(\vec{x})\beta_{1000}(\vec{x}) \frac{\partial p(\vec{x},t)}{\partial x_1} = \beta_{1000}(\vec{x})\frac{\partial\{s(\vec{x})p(\vec{x},t)\}}{\partial x_1}$$

$$- \beta_{1000}(\vec{x})p(\vec{x},t)\delta\{\sigma(\vec{x})\} \frac{\partial\sigma(x)}{\partial x_1} . \qquad (4\text{-}101)$$

It follows that higher spatial derivatives will generate not only terms involving products of $p(\vec{x},t)\delta\{\sigma(\vec{x})\}$, but also additional terms involving products of various order spatial derivatives of $p(\vec{x},t)$ and $\delta\{\sigma(\vec{x})\}$.

The above arguments demonstrate that transferring $s(\vec{x})$ inside the linear operator gives rise to additional terms involving products of $p(\vec{x})$ or its spatial derivatives with $\delta\{\sigma(\vec{x})\}$ or its derivatives. Inasmuch as the Dirac delta function and its derivatives are zero everywhere except at the zeros of the argument of the delta function, these additional terms can be interpreted as additional inputs concentrated at those spatial locations where $\sigma(\vec{x}) = 0$. However, by equation (4-93), these locations are on the bounding surface of the system. Thus, the additional terms correspond to inputs, additional to $q(\vec{x},t)$, that act on the boundary, S_0, of the system.

If we denote the collection of these products of $p(\vec{x})$ or its spatial derivatives with $\delta\{\sigma(\vec{x})\}$ or its derivatives by $\Sigma Q\{p(\vec{x},t),\delta(\sigma)\}$, it can be shown, by arguments similar to those of equation (4-101), that equation (4-99) can be written in the form

$$_{It,\beta}L_{\vec{x},t}\{s(\vec{x})p(\vec{x},t)\} = s(\vec{x})q(\vec{x},t) + \Sigma Q\{p(\vec{x},t),\delta(\sigma)\} \qquad (4\text{-}102)$$

for all $\vec{x}$ and t.

Equation (4-102) is the governing equation for the generalized function $s(\vec{x})p(\vec{x},t)$ that is valid for all space and time. The field described by this generalized function is equal to $p(\vec{x},t)$ in the volume of interest, V_0, and is zero elsewhere. The boundary conditions, in terms of appropriate

specification of $p(\vec{x},t)$ and its spatial derivatives on S_0, are the weighting functions of the additional inputs described in $\Sigma Q\{p(\vec{x},t),\delta(\sigma)\}$. Thus, by absorbing the space-limiting function inside the linear operator, we have transformed a finite space problem with boundary conditions to an infinite space problem with additional inputs concentrated on the boundary.

The Green's function for the space-limited, time-invariant linear system, as defined by equation (4-102), must satisfy

$$It,\beta L_{\vec{x},t}\{g(\vec{x},\vec{x}_0,t - t_0)\} = \delta(\vec{x} - \vec{x}_0)\delta(t - t_0) \qquad (4\text{-}103)$$

over all $\vec{x}$ and t for $\vec{x}_0$ in V_0 or on S_0. For $\vec{x}_0$ outside V_0 and S_0, the right-hand side can be replaced by any distribution of sources. The Green's function must satisfy temporal causality and must also satisfy some appropriate number of spatial constraints or conditions in order that it be a unique solution to equation (4-103). For the moment, we leave these spatial conditions unspecified.

We note that the input to equation (4-102) can be expressed as a weighted superposition of the inputs to equation (4-103). That is,

$$s(\vec{x})q(\vec{x},t) + \Sigma Q\{p(\vec{x},t),\delta[\sigma(\vec{x})]\}$$

$$= \int_{-\infty}^{\infty}\int_{-\infty}^{\infty} \delta(\vec{x} - \vec{x}_0)\delta(t - t_0)[s(\vec{x}_0)q(\vec{x}_0,t_0) + \Sigma Q\{p(\vec{x}_0,t_0),\delta[\sigma(\vec{x}_0)]\}]\, d\vec{x}_0\, dt_0 \,.$$

(4-104)

By assuming that a temporally causal form of the Green's function is known and by once again employing the principle of superposition for linear systems (see section 3.4.1), it follows that

$$It,\beta L_{\vec{x},t}\left\{\int_{-\infty}^{\infty}\int_{-\infty}^{\infty} g(\vec{x},\vec{x}_0,t - t_0)[s(\vec{x}_0)q(\vec{x}_0,t_0) + \Sigma Q\{p(\vec{x}_0,t_0),\delta[\sigma(\vec{x}_0)]\}]\, d\vec{x}_0\, dt_0\right\}$$

$$= s(\vec{x})q(\vec{x},t) + \Sigma Q\{p(\vec{x},t),\delta[\sigma(\vec{x})]\} \,. \qquad (4\text{-}105)$$

By comparison of equations (4-102) and (4-105), it is evident that

$$s(\vec{x})p(\vec{x},t) = \int_{-\infty}^{\infty}\int_{-\infty}^{\infty} g(\vec{x},\vec{x}_0,t - t_0)[s(\vec{x}_0)q(\vec{x}_0,t_0)$$

$$+ \Sigma Q\{p(\vec{x}_0,t_0),\delta[\sigma(\vec{x}_0)]\}]\, d\vec{x}_0\, dt_0 \ . \qquad (4\text{-}106)$$

Because we assumed a temporally causal Green's function, the output field $s(\vec{x})p(\vec{x},t)$ also satisfies temporal causality. However, we have not yet identified the spatial conditions, or constraints, used to uniquely specify the Green's function. The fact of the matter is that equation (4-106) is a valid representation of the space-limited output for any set of spatial constraints sufficient to provide a unique specification of the Green's function. That is not to say, however, that one can obtain a solution to equation (4-106) for the space-limited output field for an arbitrary choice of spatial constraints on the Green's function. Rather, in applying the Green's function approach to space-limited systems, there is an element of art in specifying the spatial constraints on the Green's function.

Note that the first term in the integrand of equation (4-106) is simply the contribution to the output from the inputs within V_0. The second term in the integrand represents the contributions to the output from the additional inputs on the bounding surface, S_0, of the system. The goal, in selecting the spatial constraints that uniquely specify the Green's function, is to obtain the simplest, solvable mathematical form of equation (4-106). For systems with inputs in V_0, it is desirable to specify the spatial constraints such that the terms related to the additional surface inputs vanish. Such a choice leads to what Ffowcs-Williams[9] calls the "exact Green's function." If inputs are applied only to the system boundaries (i.e., $q(\vec{x}) = 0$ in V_0), then it is desirable to choose spatial constraints that minimize the mathematical complexity of the integral containing the surface inputs. The art of specifying such spatial constraints for space-limited systems can best be illustrated by an example.

Consider the acoustic pressure $p(\vec{x},t)$ in the semi-infinite space $x_3 \geq 0$ resulting from source type inputs, $q(\vec{x},t)$, in the space $x_3 \geq 0$. At the boundary $x_3 = 0$, either $p(\underline{x},0,t)$ or $\partial p(\underline{x},0,t)/\partial x_3$, where $\underline{x} = (x_1,x_2)$, is specified.

In the form of equation (4-99), the governing equation can be written

$$U(x_3)\left\{\nabla^2 p(\vec{x},t) - \frac{1}{c^2}\frac{\partial^2 p(\vec{x},t)}{\partial t^2}\right\} = -U(x_3)q(\vec{x},t) \ , \qquad (4\text{-}107)$$

where U( ) denotes the Heaviside function. It is easily verified, by use of equation (2-32), that

$$\nabla^2\{U(x_3)p(\vec{x},t)\} = U(x_3)\nabla^2 p(\vec{x},t) + \delta(x_3)\frac{\partial p(\vec{x},t)}{\partial x_3} + \frac{\partial}{\partial x_3}\{p(\vec{x},t)\delta(x_3)\} \ . \qquad (4\text{-}108)$$

Thus, equation (4-107) can be rewritten in the form of equation (4-102) as

$$\nabla^2\{U(x_3)p(\vec{x},t)\} - \frac{1}{c^2}\frac{\partial^2\{U(x_3)p(\vec{x},t)\}}{\partial t^2}$$

$$= -U(x_3)q(\vec{x},t) + \delta(x_3)\frac{\partial p(\vec{x},t)}{\partial x_3} + \frac{\partial}{\partial x_3}\{p(\vec{x},t)\delta(x_3)\} \ . \qquad (4\text{-}109)$$

The Green's function is defined as the solution to

$$\nabla^2 g(\vec{x},\vec{x}_0,t - t_0) - \frac{1}{c^2}\frac{\partial^2 g(\vec{x},\vec{x}_0,t - t_0)}{\partial t^2} = -\delta(\vec{x} - \vec{x}_0)\delta(t - t_0) \qquad (4\text{-}110)$$

that satisfies temporal and spatial causality. It then follows, by equations (4-104), (4-106), (4-109), and (4-110), that

$$U(x_3)p(\vec{x},t) = \int_{-\infty}^{\infty}\int_{-\infty}^{\infty} g(\vec{x},\vec{x}_0,t - t_0)\left\{U(x_{30})q(\vec{x}_0,t_0) - \delta(x_{30})\frac{\partial p(\vec{x}_0,t_0)}{\partial x_{30}}\right.$$

$$\left. - \frac{\partial}{\partial x_{30}}[p(\vec{x}_0,t_0)\delta(x_{30})]\right\} d\vec{x}_0 \, dt_0 \ . \qquad (4\text{-}111)$$

where $\vec{x}_0 = [x_{10},x_{20},x_{30}]$.

By integrating the terms containing $\delta(x_{30})$ on x_{30} (the first term directly and the second term by parts), we obtain

$$U(x_3)p(\vec{x},t) = \int_{-\infty}^{\infty}\int_{-\infty}^{\infty} g(\vec{x},\vec{x}_0,t - t_0)U(x_{30})q(\vec{x}_0,t_0)\, d\vec{x}_0\, dt_0$$

$$+ \int_{-\infty}^{\infty}\int_{-\infty}^{\infty}\left\{p(\underline{x}_0,0,t_0)\, \frac{\partial g(\vec{x};\underline{x}_0,0;t - t_0)}{\partial x_{30}}\right.$$

$$\left. - g(\vec{x};\underline{x}_0,0;t - t_0)\, \frac{\partial p(\underline{x}_0,0,t_0)}{\partial x_{30}}\right\} d\underline{x}_0\, dt_0 \; . \qquad (4\text{-}112)$$

where $\underline{x}_0$ denotes $[x_{10},x_{20}]$. Note, by equation (4-112), that the space-limited field $U(x_3)p(\vec{x},t)$ is expressed as the sum of a volume integral and a surface integral. The volume integral represents the contribution to the field from all inputs within the space $x_3 > 0$. The surface integral represents the contributions associated with those inputs on the surface $x_3 = 0$ required to produce the desired boundary conditions.

For specific types of inputs and boundary conditions in this acoustic half space, we can use equation (4-112) to illustrate the rationale for selecting spatial constraints on the Green's function.

Consider first the case where the input, $q(\vec{x},t)$, is nonzero. If the pressure field at the boundary $x_3 = 0$ is specified to be $p(\underline{x},0,t) = 0$ for all $\underline{x}$ and t, it is immediately evident, by equation (4-112), that if we subject the Green's function to the spatial restriction $g(\vec{x};\underline{x}_0,0;t - t_0) = 0$ for all $\vec{x}$, $\underline{x}_0$, and $t - t_0$, then the surface integral vanishes and the space-limited pressure field is given by

$$U(x_3)p(\vec{x},t) = \int_{-\infty}^{\infty}\int_{-\infty}^{\infty} g(\vec{x},\vec{x}_0,t - t_0)U(x_{30})q(\vec{x}_0,t_0)\, d\vec{x}_0\, dt_0 \; . \qquad (4\text{-}113)$$

Because the spatial restriction on the Green's function causes the surface integral to vanish, this Green's function is, by definition, exact. Spatial restrictions leading to an exact Green's function can also be defined when $\partial p(\vec{x},t)/\partial x_3 = 0$ at the boundary $x_3 = 0$ for all $\underline{x}$ and t. That is, by equation (4-112), it is evident that if we apply the restriction $\partial g(\vec{x};\underline{x}_0,0;\ t - t_0)/\ \partial x_{30} = 0$ to the Green's function for all $\vec{x}$, $\underline{x}_0$, and $t - t_0$, then the surface integral vanishes and the space-limited pressure field is given in the form of equation (4-113).

Consider now the case where the input, $q(\vec{x},t)$, is equal to zero for all $\vec{x}$ and t. If either $p(\vec{x},t)$ or $\partial p(\vec{x})\partial x_3$ is specified to be zero on the boundary $x_3 = 0$, then it follows, from equation (4-113) and the uniqueness of $U(x_3)p(\vec{x},t)$, that the output pressure field is zero for all space and time. Thus, when $q(\vec{x},t) = 0$, the system has a nonzero response only if $p(\vec{x},t)$ or $\partial p(\vec{x},t)/\partial x_3$ is specified to be nonzero at $x_3 = 0$. If $p(\vec{x},t)$ is specified to be $p_0(\underline{x},t)$ at $x_3 = 0$, it follows from equation (4-112) that the simplest mathematical expression for the space-limited output results when we require that $g(\vec{x};\underline{x},0;t - t_0) = 0$ for all $\vec{x}$, $\underline{x}_0$, and $t - t_0$. In this case, the space-limited output field is related to the specified pressure at the boundary by

$$U(x_3)p(\vec{x},t) = \int_{-\infty}^{\infty}\int_{-\infty}^{\infty} p_0(\underline{x}_0,t_0)\ \frac{\partial g(\vec{x};\underline{x}_0,0;t - t_0)}{\partial x_{30}}\ d\underline{x}_0\ dt_0\ . \qquad (4\text{-}114)$$

By similar arguments, a spatial constraint can be applied to the Green's function to reduce equation (4-112) to a single integral when $\partial p/\partial x_3$ is specified to be nonzero at $x_3 = 0$. The specification of this constraint is left as an exercise for the reader.

The above examples illustrate the manner by which spatial constraints on the Green's function can be selected to simplify the mathematical form of the solution for one particular type of space-limited system. It should be emphasized that the results of these examples cannot be extended to other systems because the additional inputs generated at the boundaries by incorporating the space-limiting function inside the linear operator depend on the form of the linear operator governing the system.

For an arbitrary, space-limited, time-invariant linear system, the general Green's function solution is given by equation (4-106). However, without knowledge of (1) the form of the governing partial differential equation, (2) the definition of the space-limiting function, and (3) the boundary conditions for the particular system of interest, the specific mathematical form for the additional inputs on the bounding surfaces cannot be defined.

4.3.2 The Wavevector-Frequency Response of Space-Varying Systems

By appropriate Fourier transformations of the Green's function solutions for the forced response of space-varying systems, the wavevector-frequency transform of the output field can be related to the corresponding transform of the input field.

Owing to the differences in the mathematical forms of the Green's function solutions between the infinite, nonuniform and the space-limited types of space-varying systems, it is convenient to treat the wavevector-frequency responses of these two types of systems separately. We will start with the infinite, nonuniform type.

4.3.2.1 Wavevector-Frequency Response of Infinite, Nonuniform, Time-Invariant Linear Systems. The space-time output field for an infinite, nonuniform, time-invariant linear system is related to the space-time input field and the Green's function by equation (4-91). We first express the space-time input field as the superposition of harmonic plane waves in the form of equation (2-47). That is,

$$f(\vec{x},t) = (2\pi)^{-4} \int_{-\infty}^{\infty}\int_{-\infty}^{\infty} F(\vec{\alpha},\Omega)\exp\{i(\vec{\alpha}\cdot\vec{x} + \Omega t)\}\, d\vec{\alpha}\, d\Omega \ , \qquad (4\text{-}115)$$

where $\vec{\alpha}$ and Ω denote, respectively, the wavevector and frequency components of the input field. Substitution of equation (4-115) into equation (4-91) yields

$$p(\vec{x},t) = (2\pi)^{-4} \int_{-\infty}^{\infty}\int_{-\infty}^{\infty}\int_{-\infty}^{\infty}\int_{-\infty}^{\infty} g(\vec{x},\vec{x}_0,\tau)F(\vec{\alpha},\Omega)$$

$$\exp\{i[\vec{\alpha}\cdot\vec{x}_0 + \Omega(t - \tau)]\}\, d\vec{x}_0\, d\tau\, d\vec{\alpha}\, d\omega \ . \qquad (4\text{-}116)$$

If we define the wavevector-frequency transform of the output field by

$$P(\vec{k},\omega) = \int_{-\infty}^{\infty}\int_{-\infty}^{\infty} p(\vec{x},t)\exp\{i(\vec{k}\cdot\vec{x} + \omega t)\}\, d\vec{x}\, dt \;, \tag{4-117}$$

it follows, from equations (4-116) and (2-38), that

$$P(\vec{k},\omega) = (2\pi)^{-3} \int_{-\infty}^{\infty} G(\vec{k},-\vec{\alpha},\omega)F(\vec{\alpha},\omega)\, d\vec{\alpha} \;, \tag{4-118}$$

where $-\vec{\alpha}$ denotes the vector $(-\alpha_1,-\alpha_2,-\alpha_3)$ and $G(\vec{k},\vec{\alpha},\omega)$ is the two-wavevector-frequency response of the system, defined by

$$G(\vec{k},\vec{\alpha},\omega) = \int_{-\infty}^{\infty}\int_{-\infty}^{\infty}\int_{-\infty}^{\infty} g(\vec{x},\vec{x}_0,\tau)\exp\{-i(\vec{k}\cdot\vec{x} + \vec{\alpha}\cdot\vec{x}_0 + \omega\tau)\}\, d\vec{x}\, d\vec{x}_0\, d\tau \;. \tag{4-119}$$

Equation (4-118) relates the wavevector-frequency description, or transform, of the output of an infinite, nonuniform, time-invariant linear system to the corresponding description of the input and the two-wavevector-frequency response of the system. Note that for this space-varying system, the wavevector-frequency transform of the output field is expressed in terms of an integral of the wavevector-frequency transform of the input field and the two-wavevector-frequency response of the system. This is in contrast to the algebraic relationship obtained in the wavevector-frequency domain for the space- and time-invariant systems (see section 3.4.3). Further, for the infinite, nonuniform system, the wavevector-frequency response of the system is seen to be a function of two wavevector variables, whereas the wavevector-frequency response of the space-invariant system was a function of a single wavevector. This, of course, is a consequence of the separate dependence of the Green's function for the space-varying system on $\vec{x}$ and $\vec{x}_0$, whereas the Green's function for the space-invariant system depended only on the difference between $\vec{x}$ and $\vec{x}_0$.

To obtain a physical interpretation of the two-wavevector-frequency response of the infinite, nonuniform, space-varying system, consider the output

field resulting from the single harmonic plane wave input field described by

$$f(\vec{x},t) = \exp\{i(\vec{k}_0 \cdot \vec{x} + \omega_0 t)\} \ . \tag{4-120}$$

The wavevector-frequency transform of the input field is then given by

$$F(\vec{k},\omega) = (2\pi)^4 \delta(\vec{k} - \vec{k}_0)\delta(\omega - \omega_0) \ , \tag{4-121}$$

so, by equation (4-118),

$$P(\vec{k},\omega) = 2\pi G(\vec{k},-\vec{k}_0,\omega_0)\delta(\omega - \omega_0) \ . \tag{4-122}$$

However, inasmuch as

$$p(\vec{x},t) = (2\pi)^{-4} \int_{-\infty}^{\infty}\int_{-\infty}^{\infty} P(\vec{k},\omega)\exp\{i(\vec{k}\cdot\vec{x} + \omega t)\} \ d\vec{k} \ d\omega \ , \tag{4-123}$$

$P(\vec{k},\omega)$ represents the amplitudes and initial phases of the various harmonic plane waves comprising the output field. It therefore follows, by equations (4-120)-(4-123), that $2\pi G(\vec{k},-\vec{k}_0,\omega_0)$ represents the amplitude and initial phase of the harmonic plane wave component of the output field characterized by the wavevector $\vec{k}$ and frequency ω_0 resulting from excitation of the space-varying system by the harmonic plane wave characterized by the wavevector $\vec{k}_0$ and the frequency ω_0. Thus, for infinite, nonuniform, space-varying systems, the two-wavevector-frequency response, $G(\vec{k},\vec{\alpha},\omega)$, defines, at each frequency, the response of the system at the wavevector $\vec{k}$ resulting from excitation of the system at the wavevector $-\vec{\alpha}$.

The conversion, by the infinite, nonuniform, space-varying system, of one wavevector component of the input field into different wavevector components of the output field is called wavevector conversion. Recall that, in space- and time-invariant systems (see equation (3-59)), each wavevector component of the input produces, at any frequency, only the corresponding wavevector component in the output field. Therefore, wavevector conversion does not occur in space-invariant systems. We can therefore conclude that wavevector

conversion is a characteristic of space-varying systems that results from the space-varying properties of the system.

Given knowledge of the wavevector-frequency transform of the input field and the two-wavevector-frequency response of an infinite, nonuniform system, one can (in theory) predict the wavevector-frequency transform of the output field from equation (4-118). Further, as illustrated by equations (4-120)-(4-122), one can determine the two-wavevector-frequency response of the system, $G(\vec{k},\vec{\alpha},\omega)$, as a function of $\vec{k}$ at any desired wavevector, $\vec{\alpha}$, and frequency, ω, by exciting the system by a single plane harmonic wave characterized by the wavevector $-\vec{\alpha}$ and frequency ω and observing the output as a function of $\vec{k}$. However, it is evident from equation (4-118) that, given knowledge of the wavevector-frequency transform of the output field and the two-wavevector-frequency response of the system, one is faced with the solution of an integral equation to determine the wavevector-frequency transform of the input field.

4.3.2.2. <u>Wavevector-Frequency Response of Space-Limited, Time-Invariant Linear Systems</u>. The space-time output field of a space-limited system is related to the space-time input field, the boundary conditions, and the Green's function by equation (4-106). For brevity, let us designate the space-limited input and output fields by

$$f(\vec{x},t) = s(\vec{x})q(\vec{x},t) \tag{4-124}$$

and

$$o(\vec{x},t) = s(\vec{x})p(\vec{x},t) \ , \tag{4-125}$$

respectively. By substituting equations (4-124) and (4-125) into equation (4-106), we obtain

$$o(\vec{x},t) = \int_{-\infty}^{\infty}\int_{-\infty}^{\infty} g(\vec{x},\vec{x}_0,t - t_0)[f(\vec{x}_0,t_0) + \Sigma Q\{p(\vec{x}_0,t_0),\delta[\sigma(\vec{x}_0)]\}]\, d\vec{x}_0\, dt_0 \ . \tag{4-126}$$

We will deal with the wavevector-frequency response of space-limited systems by considering three special cases of equation (4-126).

We first consider the case in which the boundary conditions imposed on the system are such that it is possible to define an exact Green's function. Recall that an exact Green's function is one defined in such a fashion that

$$\int_{-\infty}^{\infty}\int_{-\infty}^{\infty} g(\vec{x},\vec{x}_0,t - t_0)[\Sigma Q\{p(\vec{x}_0,t_0),\delta[\sigma(\vec{x}_0)]\}]\, d\vec{x}_0\, dt_0 = 0 \ , \qquad (4\text{-}127)$$

and therefore the output of the space-limited system is given by

$$o(\vec{x},t) = \int_{-\infty}^{\infty}\int_{-\infty}^{\infty} g(\vec{x},\vec{x}_0,t - t_0)f(\vec{x}_0,t_0)\, d\vec{x}_0\, dt_0 \ . \qquad (4\text{-}128)$$

By following the same arguments used for the infinite, nonuniform space-varying system, it is straightforward to show that the wavevector-frequency transform of the space-limited output field, $O(\vec{k},\omega)$, is related to the wavevector-frequency transform of the space-limited input field, $F(\vec{k},\omega)$, by

$$O(\vec{k},\omega) = (2\pi)^{-3} \int_{-\infty}^{\infty} G(\vec{k},-\vec{\alpha},\omega)F(\vec{\alpha},\omega)\, d\vec{\alpha} \ , \qquad (4\text{-}129)$$

where $G(\vec{k},\vec{\alpha},\omega)$ is the two-wavevector-frequency response of the space-limited system and is mathematically defined by equation (4-119).

The form of equation (4-129) is exactly the same as equation (4-118), and the interpretations of this result and of the two-wavevector-frequency response of the space-limited system are identical to those given for the infinite, nonuniform system.

For the second case, consider a space-limited system with boundary conditions and Green's function specified such that

$$\int_{-\infty}^{\infty}\int_{-\infty}^{\infty} g(\vec{x},\vec{x}_0,t - t_0)[\Sigma Q\{p(\vec{x}_0,t_0),\delta[\sigma(\vec{x}_0)]\}]\, d\vec{x}_0\, dt_0 \neq 0 \, , \tag{4-130}$$

but such that the product of the Green's function and the additional forces imposed by the boundary constraints is known. Separate knowledge of this product and the Green's function is equivalent to knowledge of $\Sigma Q\{p(\vec{x}_0,t_0),\delta[\sigma(\vec{x}_0)]\}$. Thus, for this case, we assume that the distribution of inputs at the boundary is known and is designated by $f_s(\vec{x},t)$. That is,

$$f_s(\vec{x},t) = \Sigma Q\{p(\vec{x},t),\delta[\sigma(\vec{x})]\} \, . \tag{4-131}$$

By using the notation of equations (4-124), (4-125), and (4-131) for the space-limited inputs within the boundaries, the space-limited output, and the distribution of inputs on the boundary, respectively, equation (4-126) can be rewritten as

$$o(\vec{x},t) = \int_{-\infty}^{\infty}\int_{-\infty}^{\infty} g(\vec{x},\vec{x}_0,t - t_0)[f(\vec{x}_0,t_0) + f_s(\vec{x}_0,t_0)]\, d\vec{x}_0\, dt_0 \, . \tag{4-132}$$

It follows, by arguments similar to those used above, that the wavevector-frequency transform of the space-limited output is given by

$$O(\vec{k},\omega) = (2\pi)^{-3} \int_{-\infty}^{\infty} G(\vec{k},-\vec{\alpha},\omega)\{F(\vec{\alpha},\omega) + F_s(\vec{\alpha},\omega)\}\, d\vec{\alpha} \, , \tag{4-133}$$

where $F_s(\vec{\alpha},\omega)$ denotes the wavevector-frequency transform $f_s(\vec{x},t)$. Note that, with the exception of the presence of the additional input term associated with the boundary forces, the form of equation (4-133) is identical to that of equation (4-129).

As an example of a space-limited system with known boundary inputs, consider the semi-infinite acoustic system described in section 4.3.1.2, where

the source inputs, $q(\vec{x},t)$, in the space $x_3 > 0$ and the normal derivative of the pressure field at $x_3 = 0$ are specified. The general Green's function solution for this problem is given by equation (4-112). For notational simplicity, we define

$$o(\vec{x},t) = U(x_3)p(\vec{x},t)$$

and (4-134)

$$f(\vec{x},t) = U(x_3)q(\vec{x},t) .$$

Also, we specify the normal derivative of the pressure at $x_3 = 0$ to be

$$\frac{\partial p(\underline{x},0,t)}{\partial x_3} = a(\underline{x},t) , \tag{4-135}$$

where $a(\underline{x},t)$ is a known function of $\underline{x}$ and t.

For this example, the Green's function is uniquely specified by requiring that the solution to equation (4-110) be restricted by

$$\frac{\partial g(\vec{x};\underline{x}_0,0;t - t_0)}{\partial x_{30}} = 0 . \tag{4-136}$$

Thus, by use of equations (4-112) and (4-134)-(4-136), the space-limited pressure field is given by

$$o(\vec{x},t) = \int_{-\infty}^{\infty}\int_{-\infty}^{\infty} g(\vec{x},\vec{x}_0,t - t_0)f(\vec{x}_0,t_0)\, d\vec{x}_0\, dt_0$$

$$- \int_{-\infty}^{\infty}\int_{-\infty}^{\infty} g(\vec{x};\underline{x}_0,0;t - t_0)a(\underline{x}_0,t_0)\, d\underline{x}_0\, dt_0 . \tag{4-137}$$

By use of the inverse of equation (4-119), that is,

$$g(\vec{x},\vec{x}_0,\tau) = (2\pi)^{-7} \int_{-\infty}^{\infty}\int_{-\infty}^{\infty}\int_{-\infty}^{\infty} G(\vec{k},\vec{\alpha},\omega)\exp\{i(\vec{k}\cdot\vec{x} + \vec{\alpha}\cdot\vec{x}_0 + \omega\tau)\}\ d\vec{k}\ d\vec{\alpha}\ d\omega \ , \tag{4-138}$$

the wavevector-frequency transform of the space-limited pressure field, $O(\vec{k},\omega)$, can be related to the wavevector-frequency transforms of the space-limited source distribution and the specified pressure gradient on the boundary, $F(\vec{k},\omega)$ and $A(\underline{k},\omega)$, respectively, by

$$O(\vec{k},\omega) = (2\pi)^{-3} \int_{-\infty}^{\infty}\int_{-\infty}^{\infty} G(\vec{k},-\vec{\alpha},\omega)\{F(\vec{\alpha},\omega) - A(\underline{\alpha},\omega)\}\ d\vec{\alpha} \ . \tag{4-139}$$

Clearly, equation (4-139) has the mathematical form of equation (4-133) with $F_s(\vec{\alpha},\omega)$ independent of α_3.

As the final case of space-limited systems, consider a system with boundary conditions and Green's function specified such that

$$\int_{-\infty}^{\infty}\int_{-\infty}^{\infty} g(\vec{x},\vec{x}_0,t - t_0)[\Sigma Q\{p(\vec{x}_0,t_0),\delta[\sigma(\vec{x}_0)]\}]\ d\vec{x}_0\ dt_0 \neq 0 \ , \tag{4-140}$$

but such that some terms resulting from the product of the Green's function and the additional inputs associated with the boundary constraints are not known. This situation can arise when, regardless of the restrictions imposed on the Green's function at the spatial limits of the system, the specified boundary conditions do not provide the information required for the integrand of equation (4-140) to be completely known.

In this case, the Green's function $g(\vec{x},\vec{x}_0,t - t_0)$, the space-limiting function $s(\vec{x})$, and the external input field $q(\vec{x},t)$ are known. Thus, the first product in the integrand of equation (4-126) is known. In principle, the integration of this first term can be performed, yielding a known function of $\vec{x}$ and t. If we denote this known function by $h(\vec{x},t)$, that is,

$$h(\vec{x},t) = \int_{-\infty}^{\infty}\int_{-\infty}^{\infty} g(\vec{x},\vec{x}_0,t - t_0)s(\vec{x}_0)q(\vec{x}_0,t_0)\, d\vec{x}_0\, dt_0 \ , \qquad (4\text{-}141)$$

then equation (4-106) can be rewritten as

$$s(\vec{x})p(\vec{x},t) = h(\vec{x},t) + \int_{-\infty}^{\infty}\int_{-\infty}^{\infty} g(\vec{x},\vec{x}_0,t - t_0)\Sigma Q\{p(\vec{x}_0,t_0),\delta[\sigma(\vec{x}_0)]\}\, d\vec{x}_0\, dt_0 \ . \qquad (4\text{-}142)$$

Because $\delta[\sigma(\vec{x}_0)]$ is the derivative of the known function $s(\vec{x})$, the only unknown in equation (4-142) is the output field, $p(\vec{x},t)$, over all $\vec{x}$ and t. However, as $p(\vec{x},t)$ appears on both the left-hand side and in the integrand on the right-hand side, equation (4-142) represents an integral equation for the unrestricted output field, $p(\vec{x},t)$.

The treatment of such integral equations is beyond the scope of this text. Therefore, no attempt will be made to define or describe the wavevector-frequency characteristics of space-limited systems for which the output is specified by integral equations. The reader interested in such systems is encouraged to consult such standard texts as Morse and Feshbach[10] or Courant and Hilbert.[11] However, it should be emphasized that, in this text, we restrict our attention to space-limited systems for which the integrand of equation (4-126) is known. For such systems, the input-output relationships in the wavevector-frequency domain are given by equation (4-129) or (4-133), as appropriate.

Before we leave the subject of wavevector-frequency response of space-limited systems, a couple of observations are in order regarding the two-wavevector-frequency response, $G(\vec{k},\vec{\alpha},\omega)$, of space-limited systems.

First, recall that the physical interpretation of the two-wavevector-frequency response for space-limited systems is the same as that for the infinite, nonuniform type of space-varying system: that is, $G(\vec{k},\vec{\alpha},\omega)$ represents the response of the system at the wavevector $\vec{k}$ and frequency ω resulting from excitation of the system by a unit amplitude input at the

wavevector $-\vec{\alpha}$ and frequency ω. Recall further that, for the infinite, nonuniform system, it was (theoretically) possible, owing to the infinite extent of the system, to excite the system by an input characterized by a single wavevector and frequency component (i.e., a harmonic plane wave characterized by wavevector $-\vec{\alpha}$ and frequency ω). The resultant system output, in this case, defines the two-wavevector-frequency response of the system, $G(\vec{k},\vec{\alpha},\omega)$, over all wavevectors $\vec{k}$ for those (fixed) input parameters, $\vec{\alpha}$ and ω. It would be desirable to employ such a procedure to determine samplings of the two-wavevector-frequency response of the space-limited systems that one invariably encounters in practice. However, owing to the space-limited nature of the system, no such single wavevector-frequency excitation is possible. That is, for $F(\vec{k},\omega)$ to be a single wavevector-frequency component, $f(\vec{x},t)$ must be a harmonic plane wave, existing over all $\vec{x}$ and t. However, by equations (4-92) and (4-124), $f(\vec{x},t)$ is zero outside the spatial limits of the system, so excitation of a space-limited system by a single harmonic wave is impossible. Therefore, for space-limited systems, it is impractical to attempt direct measurement of the two-wavevector-frequency response of the system. Rather, common practice is to obtain spatial samples of the impulse response (or Green's function) as a function of time or frequency and, by discrete Fourier transformation of these spatial samples, obtain an estimate of the two-wavevector-frequency response.

The second observation regarding the two-wavevector-frequency response has to do with a distinction in terminology. Recall that the two-wavevector-frequency response defines the conversion, by the space-varying system, of each wavevector component of the input, at any frequency, to all wavevector components of the output at that same frequency. This wavevector conversion can result from either the space-varying properties of the system or from the boundaries of the system. In acoustics, it is common practice to refer to the wavevector conversion associated with system boundaries or abrupt discontinuities in system properties as wavevector scattering.

4.3.2.3 Summary of Wavevector-Frequency Response Characteristics of Space-Varying Systems. The space-varying systems treated in this text are limited to those in which all inputs (i.e., both external and boundary associated) to the system are known. We omit consideration of space-limited systems in which the output can only be specified as an integral equation.

For space-varying systems with known inputs, the relation between the wavevector-frequency descriptions of the input and output fields, $F(\vec{k},\omega)$ and $O(\vec{k},\omega)$, respectively, has the general mathematical form

$$O(\vec{k},\omega) = (2\pi)^{-3} \int_{-\infty}^{\infty} G(\vec{k},-\vec{\alpha},\omega)F(\vec{\alpha},\omega)\, d\vec{\alpha} \ . \tag{4-143}$$

Here, $G(\vec{k},\vec{\alpha},\omega)$ is the two-wavevector-frequency response of the system and defines the response of the system at the wavevector $\vec{k}$ and frequency ω resulting from a unit amplitude, plane wave input characterized by the wavevector $-\vec{\alpha}$ and frequency ω. Thus, the two-wavevector-frequency response is a metric of the conversion (or scattering), by the space-varying system, of each wavevector component $(-\vec{\alpha})$ of the input field, at any frequency, into the various wavevector components $(\vec{k})$ of the output field at that same frequency.

For nonuniform, infinite systems, $F(\vec{k},\omega)$ and $O(\vec{k},\omega)$, in equation (4-143), represent the wavevector-frequency transforms of the respective input and output space-time fields. These fields are infinite in spatial extent.

For space-limited systems, $O(\vec{k},\omega)$ represents the wavevector-frequency transform of the space-limited output field and, for systems with boundary conditions yielding an exact Green's function, $F(\vec{k},\omega)$ represents the wavevector-frequency transform of the space-limited input field. However, for systems having boundary conditions incompatible with the specification of an exact Green's function, $F(\vec{k},\omega)$ represents the wavevector-frequency transform of the sum of the space-limited input field and the additional space-time input field imposed by the constraints at the system boundaries.

4.3.3 Illustrative Examples of the Wavevector-Frequency Response of Space-Varying Systems

In this section, we present the wavenumber-frequency response of two space-limited systems having application to structural acoustics. These systems are (1) the acoustic field in an infinite half space resulting from excitation at the boundary and (2) the forced vibration of a simply supported, flat plate.

We first treat the problem of the acoustic half space.

4.3.3.1 The Pressure Field in an Acoustic Half Space Excited at the Boundary. A common problem in structural acoustics is the prediction of the acoustic field resulting from some specified displacement or velocity field at the boundary of the acoustic medium. Perhaps the most common version of this problem is the acoustic field produced in an infinite half space as a result of a known displacement field at the boundary of the half space.

Consider the acoustic half space depicted in figure 4-5. The half-space $x_3 > 0$ is occupied by a fluid of density ρ and speed of sound c. The space $x_3 < 0$ is vacuous. The displacement field on the plane $x_3 = 0$ is specified to be $w(\underline{x},t)$, where $\underline{x}$ denotes the two-dimensional vector (x_1,x_2). The consequent pressure field, $p(\vec{x},t)$, in the space $x_3 > 0$ is desired. The pressure in the space $x_3 < 0$ is, of course, zero.

The pressure in the half-space $x_3 > 0$ is governed by the homogeneous wave equation

$$\nabla^2 p(\vec{x},t) - \frac{1}{c^2}\frac{\partial^2 p(\vec{x},t)}{\partial t^2} = 0\ , \quad x_3 > 0\ , \tag{4-144}$$

for all $\underline{x}$ and t. The linearized momentum equation for the acoustic fluid requires that, at the boundary $x_3 = 0$,

$$\frac{\partial p(\underline{x},0,t)}{\partial x_3} = -\rho\frac{\partial^2 w(\underline{x},t)}{\partial t^2}\ . \tag{4-145}$$

In addition, the pressure field must satisfy the causal condition that (because motion at the plane $x_3 = 0$ is responsible for the pressure field in the space $x_3 > 0$) the pressure must propagate away, or decay with increasing distance, from the boundary.

A Green's function solution for this space-limited acoustic field could be obtained by recognizing this system as a special case of the illustrative

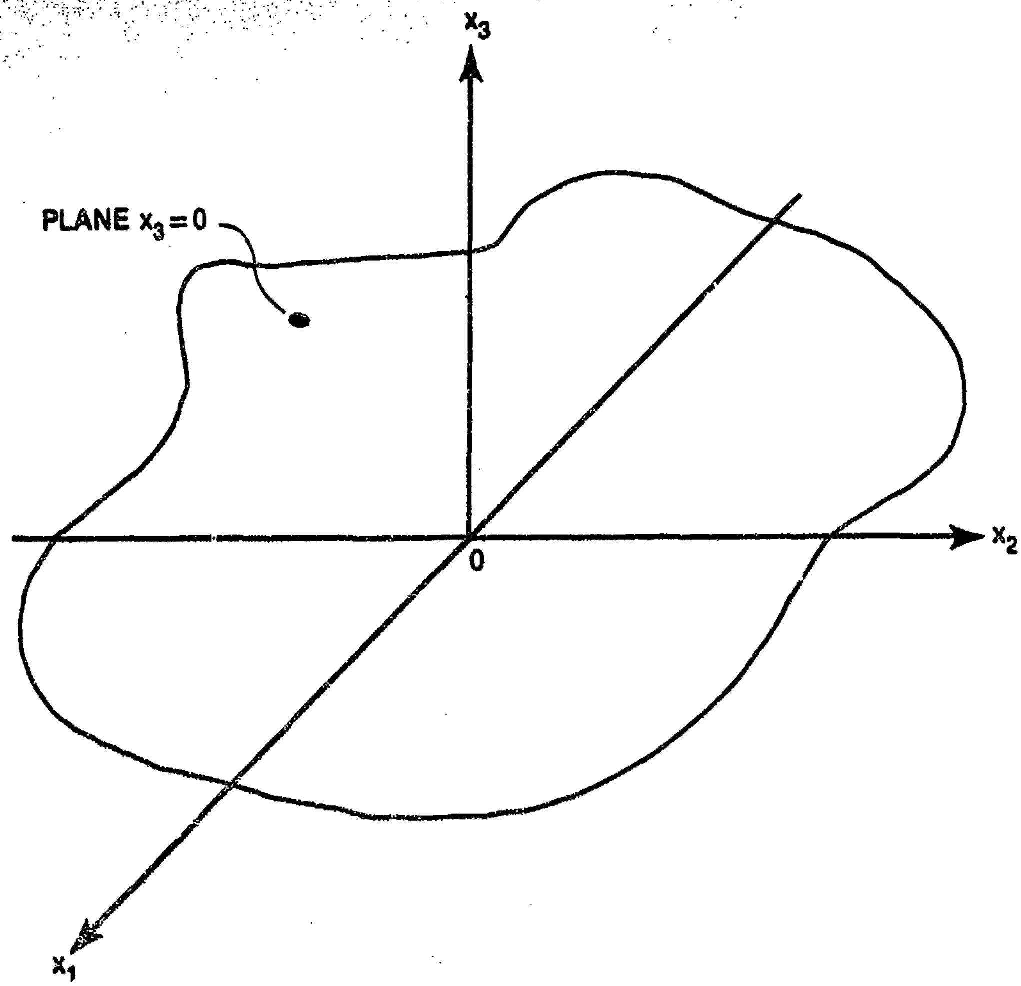

Figure 4-5. Geometry of the Acoustic Half Space

example presented in section 4.3.2.2, equations (4-134)-(4-139). In this special case, $q(\vec{x},t)$ in equation (4-134) is equal to zero inasmuch as there are no sources in the space $x_3 > 0$, and the boundary condition of equation (4-135) is replaced by that of equation (4-145). The Green's function is governed by equation (4-110) for $x_{30} \geq 0$. For $x_{30} < 0$, the Green's function is governed by a similar inhomogeneous wave equation, but with an initially unspecified distribution of sources on the right-hand side. This distribution of sources is then uniquely defined by requiring the Green's function to satisfy spatial and temporal causality and the restriction of equation (4-136).

A more direct and commonly used approach to this acoustic half-space problem is to solve the homogeneous wave equation (equation (4-144)) subject

to the boundary condition of equation (4-145). The wavevector-frequency description of the space-limited pressure field can then be obtained by appropriate Fourier transformation of the space-time field. This is the approach that will be presented here.

In light of the emphasis placed on Green's function solutions to space-varying systems in the previous sections, the reader is justified in asking why this direct, rather than the Green's function, approach is being adopted. The answer is that while the Green's function approach is most useful for developing the general mathematical forms of the input-output relationships for various types of systems and for introducing certain system concepts, it is not necessarily the simplest mathematical approach for obtaining a solution to a specific system. For the problem at hand, it is mathematically simpler to solve the homogeneous wave equation, subject to a boundary condition, than to solve the inhomogeneous wave equation, subject to a constraint on the input field. Whichever approach is taken, however, uniqueness demands that the solutions be mathematically equivalent.

With apologies for this lengthy preface, let us proceed with the solution for the problem of the acoustic half space, driven at the boundary.

The acoustic half space is invariant in time and in the two-dimensional spatial vector $\underline{x}$. Therefore, we assume that the pressure field can be written in the form

$$p(\underline{x},x_3,t) = (2\pi)^{-3} \int_{-\infty}^{\infty}\int_{-\infty}^{\infty} P(\underline{k},x_3,\omega)\exp\{i(\underline{k}\cdot\underline{x} + \omega t)\}\ d\underline{k}\ d\omega\ , \quad x_3 > 0\ , \tag{4-146}$$

where $\underline{k}$ denotes the two-dimensional wavevector (k_1,k_2). Substitution of equation (4-146) into (4-144) yields

$$\int_{-\infty}^{\infty}\int_{-\infty}^{\infty} \left[\frac{d^2P(\underline{k},x_3,\omega)}{dx_3^{\ 2}} + (k_0^{\ 2} - k^2)P(\underline{k},x_3,\omega)\right]\exp\{i(\underline{k}\cdot\underline{x} + \omega t)\}\ d\underline{k}\ d\omega = 0 \tag{4-147}$$

for $x_3 > 0$ and for all $\underline{x}$ and t. In equation (4-147), k_0 denotes the acoustic wavenumber, ω/c, and k denotes $\sqrt{k_1^2 + k_2^2}$, the magnitude of the two-dimensional wavevector, $\underline{k}$. Inasmuch as equation (4-147) is valid for any choice of $\underline{x}$ or t, it follows that

$$\frac{d^2P(\underline{k},x_3,\omega)}{dx_3^2} + (k_0^2 - k^2)P(\underline{k},x_3,\omega) = 0 \ , \quad x_3 > 0 \ , \tag{4-148}$$

for all $\underline{k}$ and ω. The general solution of equation (4-148) is

$$P(\underline{k},x_3,\omega) = A(\underline{k},\omega)\exp\left\{i\sqrt{k_0^2 - k^2}\, x_3\right\} + B(\underline{k},\omega)\exp\left\{-i\sqrt{k_0^2 - k^2}\, x_3\right\} \ , \quad x_3 > 0 \ . \tag{4-149}$$

Substitution of equation (4-149) into equation (4-146) yields the following expression for the pressure field in the half-space $x_3 > 0$:

$$p(\underline{x},x_3,t) = (2\pi)^{-3} \int_{-\infty}^{\infty}\int_{-\infty}^{\infty} \left[A(\underline{k},\omega)\exp\left\{i[\underline{k}\cdot\underline{x} + \sqrt{k_0^2 - k^2}\, x_3 + \omega t]\right\}\right.$$

$$\left. + B(\underline{k},\omega)\exp\left\{i[\underline{k}\cdot\underline{x} - \sqrt{k_0^2 - k^2}\, x_3 + \omega t]\right\}\right] d\underline{k}\, d\omega \ . \tag{4-150}$$

The functions $A(\underline{k},\omega)$ and $B(\underline{k},\omega)$ in equations (4-149) and (4-150) are determined by application of (1) the causality, or radiation, condition that requires the pressure field to be comprised of waves which either propagate away, or decrease in amplitude with increasing distance, from the boundary $x_3 = 0$ and (2) the boundary condition of equation (4-145). Let us first examine the radiation condition.

At any fixed frequency, ω, wave components of the pressure field described by equation (4-150) that propagate away from $x_3 = 0$ in the positive x_3 direction are those characterized by the exponential forms

$$\exp\left\{i\left[\sqrt{k_0^2 - k^2}\, x_3 + \omega t\right]\right\} \ , \quad \omega < 0 \ ,$$

and

$$\exp\left\{i\left[-\sqrt{k_0^2 - k^2}\, x_3 + \omega t\right]\right\} , \quad \omega \geq 0 ,$$

when $k \leq |k_0|$. It is also obvious, by inspection of equation (4-150), that waves which decay in amplitude with increasing distance in the positive x_3 direction from the boundary $x_3 = 0$ must be characterized by the exponential form

$$\exp\left\{-\sqrt{k^2 - k_0^2}\, x_3\right\} = \exp\left\{i\sqrt{k_0^2 - k^2}\, x_3\right\} , \quad k > |k_0| .$$

For the pressure field described by equation (4-150) to be comprised only of waves consistent with these exponential forms, we require that

$$A(\underline{k},\omega) = 0 , \quad k \leq |k_0| \text{ and } \omega > 0 ,$$

$$B(\underline{k},\omega) = 0 , \quad k \leq |k_0| \text{ and } \omega < 0 , \tag{4-151}$$

$$B(\underline{k},\omega) = 0 , \quad k > |k_0| \text{ for all } \omega .$$

By defining

$$P_1(\underline{k},\omega) = \begin{Bmatrix} B(\underline{k},\omega) , & \omega \geq 0 \\ A(\underline{k},\omega) , & \omega < 0 \end{Bmatrix} , \quad k \leq |k_0| , \tag{4-152}$$

and

$$P_2(\underline{k},\omega) = A(\underline{k},\omega) , \quad k > |k_0| \text{ for all } \omega , \tag{4-153}$$

we can express equation (4-150) in a form that satisfies the causality (or radiation) condition. That form is

$$p(\underline{x},x_3,t) = \frac{1}{(2\pi)^3}\int_{-\infty}^{\infty}\left[\int_{k\le|k_0|} P_1(\underline{k},\omega)\exp\left\{i\left[\underline{k}\cdot\underline{x} - k_0x_3\sqrt{1 - k^2/k_0^2}\,\right]\right\}d\underline{k}\right.$$

$$\left. + \int_{k>|k_0|} P_2(\underline{k},\omega)\exp\left\{-\sqrt{k^2 - k_0^2}\,x_3\right\}\exp\{i\underline{k}\cdot\underline{x}\}\,d\underline{k}\right]\exp\{i\omega t\}\,d\omega\,. \tag{4-154}$$

We now employ the boundary condition of equation (4-145) to determine $P_1(\underline{k},\omega)$ and $P_2(\underline{k},\omega)$. This is most easily accomplished by first writing $w(\underline{x},t)$ in the form

$$w(\underline{x},t) = (2\pi)^{-3}\int_{-\infty}^{\infty}\int_{-\infty}^{\infty} W(\underline{k},\omega)\exp\{i(\underline{k}\cdot\underline{x} + \omega t)\}\,d\underline{k}\,d\omega\,. \tag{4-155}$$

Then, by use of equations (4-154) and (4-155) in equation (4-145), we obtain

$$\int_{-\infty}^{\infty}\left\{\int_{k\le|k_0|}\left[\rho\omega^2W(\underline{k},\omega) + ik_0\sqrt{1 - k^2/k_0^2}\,P_1(\underline{k},\omega)\right]\exp\{i(\underline{k}\cdot\underline{x} + \omega t)\}\,d\underline{k}\right.$$

$$\left. + \int_{k>|k_0|}\left[\rho\omega^2W(\underline{k},\omega) + \sqrt{k^2 - k_0^2}\,P_2(\underline{k},\omega)\right]\exp\{i(\underline{k}\cdot\underline{x} + \omega t)\}\,d\underline{k}\right\}d\omega = 0\,, \tag{4-156}$$

which is valid for all $\underline{x}$ and t. It therefore follows that

$$P_1(\underline{k},\omega) = \frac{i\rho\omega^2W(\underline{k},\omega)}{k_0\sqrt{1 - k^2/k_0^2}}$$

and (4-157)

$$P_2(\underline{k},\omega) = \frac{-\rho\omega^2W(\underline{k},\omega)}{\sqrt{k^2 - k_0^2}}\,.$$

Substitution of equations (4-157) into equation (4-154) yields the following expression for the space-time pressure field in the half-space $x_3 \geq 0$:

$$p(\underline{x},x_3,t) = \frac{1}{(2\pi)^3} \int_{-\infty}^{\infty} \left[\int_{k \leq |k_0|} \frac{i\rho\omega^2 W(\underline{k},\omega)}{k_0\sqrt{1 - k^2/k_0^2}} \right.$$

$$\exp\left\{i[\underline{k}\cdot\underline{x} - k_0 x_3 \sqrt{1 - k^2/k_0^2} + \omega t]\right\} d\underline{k}$$

$$\left. - \int_{k>|k_0|} \frac{\rho\omega^2 W(\underline{k},\omega)}{\sqrt{k^2 - k_0^2}} \exp\left\{-\sqrt{k^2 - k_0^2}\, x_3\right\} \exp\{i\underline{k}\cdot\underline{x} + \omega t\}\, d\underline{k} \right] d\omega \; . \tag{4-158}$$

The pressure in the half-space $x_3 < 0$, it will be recalled, is zero because that space is vacuous.

Comparison of equation (4-158) with equation (4-146) reveals that $P(\underline{k},x_3,\omega)$ can be described in the half-space $x_3 \geq 0$ by

$$P(\underline{k},x_3,\omega) = \begin{cases} \dfrac{i\rho\omega^2 W(\underline{k},\omega)}{k_0\sqrt{1 - k^2/k_0^2}} \exp\left\{-ik_0 x_3 \sqrt{1 - k^2/k_0^2}\right\}, & k \leq |k_0| \\[2ex] \dfrac{-\rho\omega^2 W(\underline{k},\omega)}{\sqrt{k^2 - k_0^2}} \exp\left\{-\sqrt{k^2 - k_0^2}\, x_3\right\} . & k > |k_0| \; . \end{cases} \tag{4-159}$$

Of course, $P(\underline{k},x_3,\omega)$ is equal to 0 for $x_3 < 0$.

The complete wavevector-frequency transform of the pressure field in the half space is obtained by Fourier transformation of $\tilde{P}(\underline{k},x_3,\omega)$ on the x_3 variable. This complete wavevector-frequency transform of the pressure field, denoted by $P(\underline{k},k_3,\omega)$, can be defined from equation (4-159) by use of the Heaviside function. That is,

$$\tilde{P}(\underline{k},k_3,\omega) = \begin{cases} \dfrac{i\rho\omega^2 W(\underline{k},\omega)}{k_0\sqrt{1 - k^2/k_0^2}} \displaystyle\int_{-\infty}^{\infty} U(x_3)\exp\left\{-i\left[k_3 + k_0\sqrt{1 - k^2/k_0^2}\right]x_3\right\} dx_3 \ , & k \le |k_0| \ , \\ \dfrac{-\rho\omega^2 W(\underline{k},\omega)}{\sqrt{k^2 - k_0^2}} \displaystyle\int_{-\infty}^{\infty} U(x_3)\exp\left\{-i\left[k_3 - i\sqrt{k^2 - k_0^2}\right]x_3\right\} dx_3 \ , & k > |k_0| \ . \end{cases} \tag{4-160}$$

The Fourier transform applicable to the wavenumber range $k \le |k_0|$ can be recognized as a Fourier transform of the Heaviside function $U(x_3)$. Papoulis[12] shows that

$$\int_{-\infty}^{\infty} U(x)\exp(-ikx)\, dx = \pi\delta(k) + 1/(ik) \ . \tag{4-161}$$

The transform applicable to the wavenumber range $k > |k_0|$ can be evaluated by simple integration so, by use of equation (4-161), it is straightforward to show that the complete wavevector-frequency transform of the pressure field in the half space is given by

$$\tilde{P}(\underline{k},k_3,\omega) = \begin{cases} \dfrac{\rho\omega^2 W(\underline{k},\omega)}{k_0\sqrt{1 - k^2/k_0^2}} \left\{ i\pi\delta\left[k_3 + k_0\sqrt{1 - k^2/k_0^2}\right] + \dfrac{1}{k_3 + k_0\sqrt{1 - k^2/k_0^2}} \right\} , & k \le |k_0| \ , \\ \dfrac{-\rho\omega^2 W(\underline{k},\omega)}{k^2 - k_0^2 + ik_3\sqrt{k^2 - k_0^2}} \ , & k > |k_0| \ . \end{cases} \tag{4-162}$$

Equations (4-159) and (4-162) represent two alternative forms by which a wavevector-frequency description of the pressure field can be related to the wavevector-frequency description of the displacement field at the boundary $x_3 = 0$. Equation (4-159) expresses the complex amplitudes of those waves of the form $\exp\{i(\underline{k}\cdot\underline{x} + \omega t)\}$ that comprise the pressure field on any surface of

constant x_3, in the range $0 \leq x_3 < \infty$, as a function of the complex amplitude of the corresponding wave component of the displacement field on the boundary. Equation (4-162) expresses the complex amplitudes of plane wave components of the form $\exp\{i(\underline{k}\cdot\underline{x} + k_3x_3 + \omega t)\}$ that comprise the pressure field as a function of the complex amplitudes of the surface waves of the form $\exp\{i(\underline{k}\cdot\underline{x} + \omega t)\}$ that comprise the displacement field at the boundary. Before exploring the wavevector properties of these descriptions of the half-space pressure field, it is instructive to examine certain physical interpretations of these results.

Consider first the pressure field in the half-space $x_3 \geq 0$ resulting from an impulsive displacement, in space and time, at the boundary $x_3 = 0$. Let the pressure field resulting from this impulsive displacement field be denoted by $h(\underline{x},\underline{x}_0,x_3,t,t_0)$: that is,

$$p(\underline{x},x_3,t) = h(\underline{x},\underline{x}_0,x_3,t,t_0)$$

when

$$w(\underline{x},t) = \delta(\underline{x} - \underline{x}_0)\delta(t - t_0) \quad . \tag{4-163}$$

By equations (4-155) and (4-158), it follows that, for $x_3 \geq 0$,

$$\begin{aligned} h(\underline{x},\underline{x}_0,x_3,t,t_0) = (2\pi)^{-3} \int_{-\infty}^{\infty} \Bigg[\int_{k \leq |k_0|} & \frac{i\rho\omega^2}{k_0\sqrt{1 - k^2/k_0^2}} \\ & \exp\left\{i\left[\underline{k}\cdot(\underline{x} - \underline{x}_0) - k_0x_3\sqrt{1 - k^2/k_0^2} + \omega(t - t_0)\right]\right\} d\underline{k} \\ - \int_{k > |k_0|} & \frac{\rho\omega^2}{\sqrt{k^2 - k_0^2}} \exp\left\{-\sqrt{k^2 - k_0^2}\, x_3\right\} \\ & \exp\{i[\underline{k}\cdot(\underline{x} - \underline{x}_0) + \omega(t - t_0)]\}\, d\underline{k} \Bigg] d\omega \quad . \end{aligned} \tag{4-164}$$

For $x_3 < 0$, $h(\underline{x},\underline{x}_0,x_3,t,t_0)$ is equal to 0. By the form of the exponents in equation (4-164), it is evident that

$$h(\underline{x},\underline{x}_0,x_3,t,t_0) = h(\underline{x} - \underline{x}_0,x_3,t - t_0) \ . \qquad (4\text{-}165)$$

This form of the impulse response is consistent with the invariance of the acoustic half-space system in the $\underline{x}$ and t variables and with the space-limited nature of the system in the x_3 coordinate.

By writing $W(\underline{k},\omega)$ in equation (4-158) as the multiple Fourier transform of $w(\underline{x}_0,t_0)$ and interchanging the order of integration, it is easily shown, by use of equation (4-164), that the pressure field in the half space is related to the displacement field at the boundary and the impulse response by

$$p(\underline{x},x_3,t) = \int_{-\infty}^{\infty}\int_{-\infty}^{\infty} h(\underline{x} - \underline{x}_0,x_3,t - t_0)w(\underline{x}_0,t_0)\ d\underline{x}_0\ dt_0 \ . \qquad (4\text{-}166)$$

It is straightforward to show, from equation (4-166), that

$$P(\underline{k},x_3,\omega) = H(\underline{k},x_3,\omega)W(\underline{k},\omega) \qquad (4\text{-}167)$$

and

$$\tilde{P}(\underline{k},k_3,\omega) = \tilde{H}(\underline{k},k_3,\omega)W(\underline{k},\omega) \ , \qquad (4\text{-}168)$$

where H and $\tilde{H}$ denote the two- and three-wavenumber-frequency transforms, respectively, of the impulse response, h. By comparison of equation (4-167) with equation (4-159), it is evident that, for $x_3 \geq 0$,

$$H(\underline{k},x_3,\omega) = \begin{cases} \dfrac{i\rho\omega^2}{k_0\sqrt{1 - k^2/k_0^2}} \exp\left\{-ik_0\sqrt{1 - k^2/k_0^2}\ x_3\right\}, & k \leq |k_0| \ , \\[2ex] \dfrac{-\rho\omega^2}{\sqrt{k^2 - k_0^2}} \exp\left\{-\sqrt{k^2 - k_0^2}\ x_3\right\}, & k > |k_0| \ . \end{cases}$$

(4-169)

and $H(\underline{k},x_3,\omega) = 0$ for $x_3 < 0$. Similarly, comparison of equation (4-168) with equation (4-162) reveals that

$$\tilde{H}(\underline{k},k_3,\omega) = \begin{cases} \dfrac{\rho\omega^2}{k_0\sqrt{1 - k^2/k_0^2}}\left\{i\pi\delta\left[k_3 + k_0\sqrt{1 - k^2/k_0^2}\right] + \dfrac{1}{k_3 + k_0\sqrt{1 - k^2/k_0^2}}\right\}, & k \le |k_0| , \\ \\ \dfrac{-\rho\omega^2}{k^2 - k_0^2 + ik_3\sqrt{k^2 - k_0^2}} , & k > |k_0| . \end{cases} \tag{4-170}$$

The quantity H can be interpreted, from equations (4-146) and (4-167), as the wavevector-frequency response of the acoustic half space to displacement at the boundary $x_3 = 0$. That is, by arguments similar to those used in section 3.4.3, $H(\underline{k},x_3,\omega)$ can be shown to represent the ratio of the space-time pressure field to the space-time displacement field at $x_3 = 0$ when that displacement field is a complex wave of the form $\exp\{i(\underline{k}\cdot\underline{x} + \omega t)\}$. $\tilde{H}(\underline{k},k_3,\omega)$, the Fourier transform of $H(\underline{k},x_3,\omega)$ on the variable x_3, is simply the ratio of the complex amplitudes of the plane wave components of the form $\exp\{i(\underline{k}\cdot\underline{x} + k_3x_3 + \omega t)\}$ that comprise the pressure field to the complex amplitudes, at corresponding values of $\underline{k}$ and ω, of the waves of the form $\exp\{i(\underline{k}\cdot\underline{x} + \omega t)\}$ that comprise the displacement field at $x_3 = 0$.

One might be reasonably curious as to the relationship between the impulse response, $h(\underline{x} - \underline{x}_0,x_3,t - t_0)$, and the Green's function, $g(\tilde{x},\tilde{x}_0,t - t_0)$, for the semi-infinite acoustic system presented as an illustrative example in section 4.3.2.2 (see equation (4-137)). To specialize this illustrative example to the problem of the acoustic half space driven at the boundary, we first note that, inasmuch as the half space is driven only at the boundary, no sources are present in the space $x_3 > 0$, and thereby $q(\tilde{x},t) = 0$. By equation (4-134), this implies that $f(\tilde{x},t) = 0$. Further, from the boundary condition for the acoustic half space (equation (4-145)), it follows that $a(\underline{x},t)$ in equation (4-135) is given by

$$a(\underline{x},t) = -\rho \frac{\partial^2 w(\underline{x},t)}{\partial t^2} . \qquad (4\text{-}171)$$

With these conditions applied to equation (4-137), the Green's function solution for the acoustic half space driven at the boundary can be written

$$o(\vec{x},t) = \int_{-\infty}^{\infty}\int_{-\infty}^{\infty} g(\underline{x},x_3;\underline{x}_0,0;t - t_0)\ \rho \frac{\partial^2 w(\underline{x}_0,t_0)}{\partial t_0{}^2}\, d\underline{x}_0\, dt_0 . \qquad (4\text{-}172)$$

By recognizing that the acoustic half-space system is invariant in the two-dimensional spatial vector, $\underline{x}$, and by using equation (4-134), it follows that equation (4-172) has the form

$$U(x_3)p(\vec{x},t) = \int_{-\infty}^{\infty}\int_{-\infty}^{\infty} g(\underline{x} - \underline{x}_0;x_3,0;t - t_0)\ \rho \frac{\partial^2 w(\underline{x}_0,t_0)}{\partial t_0{}^2}\, d\underline{x}_0\, dt_0 .$$

(4-173)

As the only x_3 variation in the integrand of equation (4-173) is that associated with the Green's function, it follows that the Green's function must be of the mathematical form

$$g(\underline{x} - \underline{x}_0;x_3,0;t - t_0) = U(x_3)g'(\underline{x} - \underline{x}_0;x_3,0;t - t_0) , \qquad (4\text{-}174)$$

where g' is a function equal to g in the half-space $x_3 \geq 0$, but of arbitrary specification in the space $x_3 < 0$.

The product of the fluid density (ρ) and the second derivative of the boundary displacement (w) with respect to time in the integrand of equation (4-173) can be interpreted as the inertial force of each unit volume of fluid at the boundary. It follows that the Green's function, $g(\underline{x} - \underline{x}_0;x_3,0;t - t_0)$, can be interpreted as the pressure field resulting from an impulsive inertial force applied to a unit volume of fluid at the boundary $x_3 = 0$. This interpretation is in contrast to that of the impulse response $h(\underline{x} - \underline{x}_0;x_3;t - t_0)$, defined by equation (4-163), which represents the pressure field resulting from an impulsive displacement at the boundary.

It is straightforward to show, from equations (4-155) and (4-173), that

$$U(x_3)P(\underline{k},x_3,\omega) = -G(\underline{k};x_3,0;\omega)\{\rho\omega^2 W(\underline{k},\omega)\} \ . \tag{4-175}$$

Further, by comparison of equations (4-167) and (4-175), it is evident that

$$G(\underline{k};x_3,0;\omega) = -H(\underline{k},x_3,\omega)/[\rho\omega^2] \ . \tag{4-176}$$

Clearly then, the wavevector-frequency response associated with the Green's function is related to the wavevector-frequency response associated with the impulse response, $h(\underline{x} - \underline{x}_0;x_3;t - t_0)$. By substitution of equation (4-169) in equation (4-176), an expression for the Green's function, $g(\underline{x} - \underline{x}_0;x_3,0;t - t_0)$, can be obtained in terms of an inverse Fourier transform. This procedure is left as an exercise for the interested reader.

If we denote the three-wavenumber-frequency transform of the Green's function by $\tilde{G}(\underline{k};k_3,0;\omega)$, it follows from equation (4-176) that

$$\tilde{G}(\underline{k};k_3,0;\omega) = -\tilde{H}(\underline{k},k_3,\omega)/[\rho\omega^2] \ . \tag{4-177}$$

As a final note on the Green's function, it follows from equations (4-134) and (4-175) that

$$O(\underline{k},k_3,\omega) = -\tilde{G}(\underline{k};k_3,0;\omega)\{\rho\omega^2 W(\underline{k},\omega)\} \ . \tag{4-178}$$

By comparison of equation (4-178) with equation (4-139) (with $F(\vec{\alpha},\omega)$ set to zero as no sources are present in the space $x_3 > 0$ and with $A(\underline{\alpha},\omega) = \rho\omega^2 W(\underline{\alpha},\omega)$), there appears to be a difference in the two solutions. However, owing to the invariance of the acoustic half-space system in the two-dimensional spatial vector $\underline{x}$ and in time, it may be shown that $G(\vec{k},-\vec{\alpha},\omega)$ in equation (4-139) takes the form

$$G(\vec{k},-\vec{\alpha},\omega) = (2\pi)^2 \delta(\underline{\alpha} - \underline{k})\check{G}(\underline{k},k_3;\alpha_3,\omega) \ , \tag{4-179}$$

where $\overset{\nabla}{G}$ is the multiple Fourier transform of $g(\underline{x} - \underline{x}_0;x_3,x_{30};t - t_0)$ on the variables $\underline{x} - \underline{x}_0$, x_3, x_{30}, and $t - t_0$. By substituting equation (4-179) into equation (4-139) and performing the integration on $\underline{\alpha}$, we obtain

$$O(\underline{k},k_3,\omega) = -\rho\omega^2 W(\underline{k},\omega)\left\{\frac{1}{2\pi}\int_{-\infty}^{\infty}\overset{\nabla}{G}(\underline{k},k_3;\alpha_3;\omega)\,d\alpha_3\right\} . \qquad (4-180)$$

However, the integral in equation (4-180) can easily be shown to be equal to $\tilde{G}(\underline{k};k_3,0;\omega)$. Thus, the result of equation (4-178) is not in conflict with, but rather a consequence of, equation (4-139).

In some of the literature dealing with structural acoustics (see, for example, reference 13), the pressure field in the acoustic half space is expressed in terms of the spectral surface impedance of the acoustic medium. The spectral surface impedance, Z_s, is defined as the ratio of the wavevector-frequency transform of the pressure field at the boundary $x_3 = 0$ to the wavevector-frequency transform of the normal velocity of the boundary. The wavevector-frequency transform of the pressure field at the boundary is specified by equation (4-159), evaluated at $x_3 = 0$. The normal velocity at the boundary, $v(\underline{x},t)$, is the temporal derivative of the displacement field, $w(\underline{x},t)$. By use of equation (4-155), it is easily shown that the wavevector-frequency transform of the velocity field, $V(\underline{k},\omega)$, is related to the wavevector-frequency transform of the displacement field by $V(\underline{k},\omega) = i\omega W(\underline{k},\omega)$. It therefore follows that the spectral surface impedance is given by

$$Z_s(\underline{k},\omega) = P(\underline{k},0,\omega)/V(\underline{k},\omega) = P(\underline{k},0,\omega)/[i\omega W(\underline{k},\omega)] . \qquad (4-181)$$

A concept often used in conjunction with the spectral surface impedance in acoustics is that of the spectral transfer function. The spectral transfer function of the pressure field in the half space, denoted by $T(\underline{k},x_3,\omega)$, is the ratio of the wavevector-frequency transform of the pressure field at a distance x_3 from the boundary to the wavevector-frequency transform of the pressure field at the boundary. That is,

$$T(\underline{k},x_3,\omega) = \frac{P(\underline{k},x_3,\omega)}{P(\underline{k},0,\omega)} . \qquad (4-182)$$

It follows, by equations (4-181) and (4-182), that the wavevector-frequency transform of the pressure field in the half space is related to the spectral surface impedance and the spectral transfer function by

$$P(\underline{k},x_3,\omega) = Z_s(\underline{k},\omega)T(\underline{k},x_3,\omega)V(\underline{k},\omega) \ . \qquad (4\text{-}183)$$

By comparison of equation (4-167) with equation (4-181), the spectral surface impedance is related to the wavevector-frequency response, $H(\underline{k},x_3,\omega)$, by

$$Z_s(\underline{k},\omega) = H(\underline{k},0,\omega)/(i\omega) \ . \qquad (4\text{-}184)$$

Further, by equations (4-167) and (4-182), the spectral transfer function is related to the wavevector-frequency response by

$$T(\underline{k},x_3,\omega) = \frac{H(\underline{k},x_3,\omega)}{H(\underline{k},0,\omega)} \ . \qquad (4\text{-}185)$$

By the above arguments, it is evident that the wavevector-frequency transform of the pressure field in the half space can be expressed in terms of several different, but related, descriptors. These various descriptors relate the wavevector-frequency description of the pressure field to wavevector-frequency descriptions of different physical characterizations of the excitation applied at the boundary. The selection of any particular descriptor for the wavevector-frequency analysis of acoustic fields is usually made for reasons of mathematical convenience or personal preference.

Figure 4-6 illustrates the magnitude and phase of the wavevector-frequency response, $H(\underline{k},x_3,\omega)$, of the acoustic half space for an arbitrary, but positive, frequency at three values of the dimensionless spatial variable k_0x_3. Recall, by equation (4-166), that $H(\underline{k},x_3,\omega)\exp\{i(\underline{k}\cdot\underline{x} + \omega t)\}$ is the pressure field that results from the displacement field $\exp\{i(\underline{k}\cdot\underline{x} + \omega t)\}$ applied at the boundary, $x_3 = 0$.

To aid in the interpretation of figure 4-6, it should first be noted, from equation (4-169), that the argument (or phase) of $H(\underline{k},x_3,\omega)$ is given by

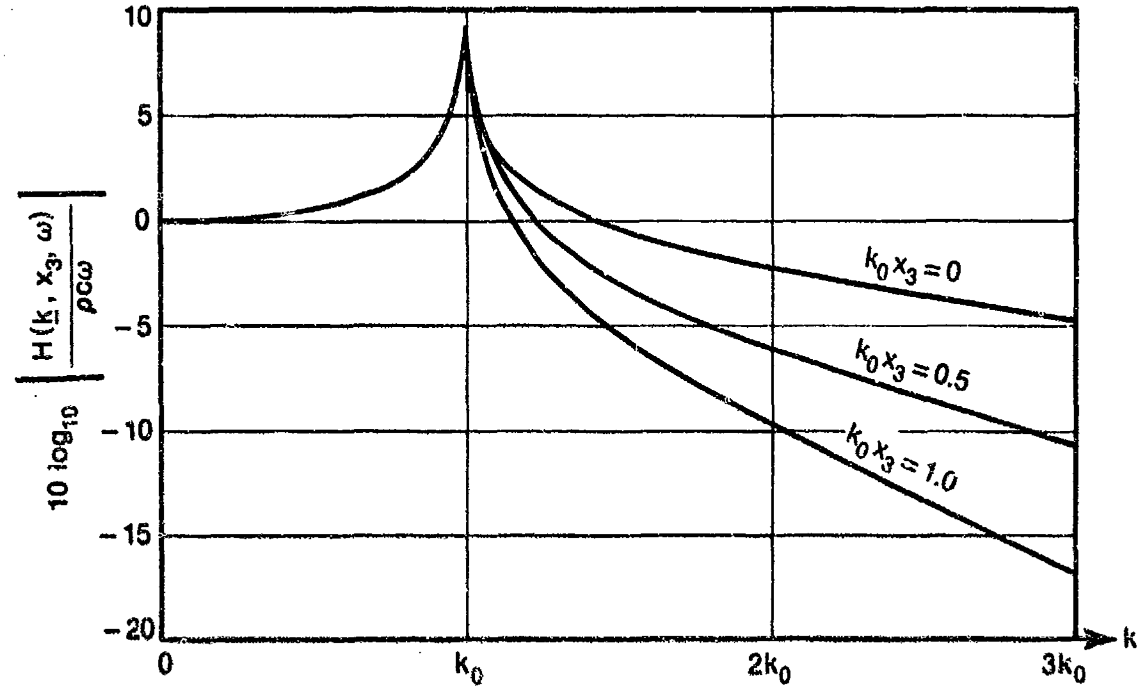

Figure 4-6(a). Magnitude of $H(\underline{k},x_3,\omega)$ as a Function of k

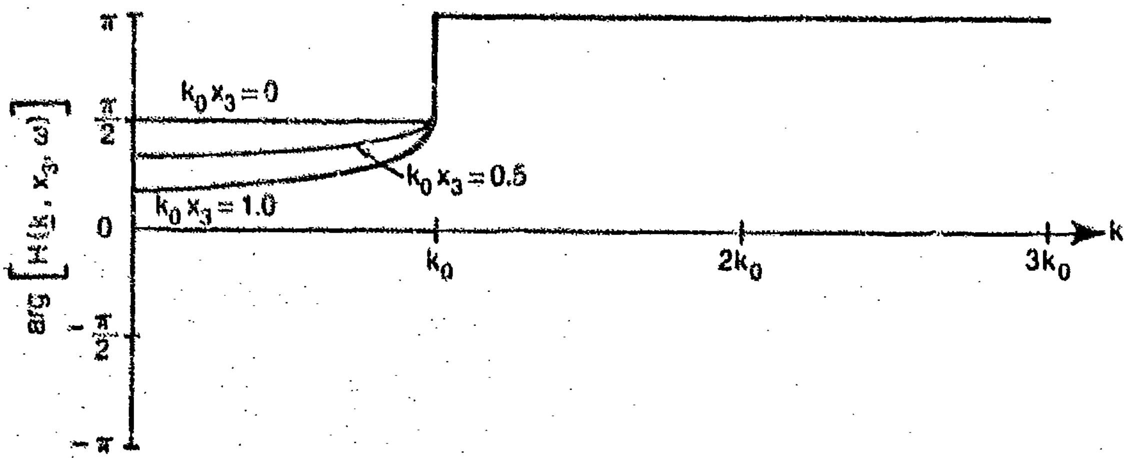

Figure 4-6(b). Phase of $H(\underline{k},x_3,\omega)$ as a Function of k

Figure 4-6. Magnitude and Phase of $H(\underline{k},x_3,\omega)$ as a Function of k

$$\arg\{H(\underline{k},x_3,\omega)\} = \begin{cases} \mathrm{sgn}(\omega)\,\frac{\pi}{2} - k_0\sqrt{1 - k^2/k_0^2}\;x_3\,, & k \le |k_0|\,, \\ \pi\,, & k > |k_0|\,. \end{cases} \quad (4\text{-}186)$$

Therefore, it follows that the pressure field resulting from the displacement field $\exp\{i(\underline{k}\cdot\underline{x} + \omega t)\}$ applied at the boundary can be written

$$p(\underline{x},x_3,t) = \begin{cases} |H(\underline{k},x_3,\omega)|\;\exp\left\{i\left[\underline{k}\cdot\underline{x} - k_0x_3\sqrt{1 - k^2/k_0^2} + \omega t + (\pi/2)\mathrm{sgn}(\omega)\right]\right\}\,, \\ \qquad\qquad\qquad\qquad\qquad\qquad\qquad\qquad\qquad k \le |k_0|\,, \\ |H(\underline{k},x_3,\omega)|\;\exp\{i(\underline{k}\cdot\underline{x} + \omega t) + \pi\}\,, \qquad\qquad k > |k_0|\,. \end{cases}$$

(4-187)

By equation (4-187), it is evident that, if the magnitude of the wavevector, $\underline{k}$, characterizing the displacement field, $\exp\{i(\underline{k}\cdot\underline{x} + \omega t)\}$, is less than or equal to the magnitude of the acoustic wavenumber, $k_0 = \omega/c$, of the fluid medium, the pressure field in the half space is a plane wave of amplitude $|H(\underline{k},x_3,\omega)|$, which is characterized by the wavevector $\underline{k}$ in the plane of the boundary and by the wavevector $-k_0\sqrt{1 - k^2/k_0^2}$ in the x_3 coordinate direction. Therefore, on a plane parallel to the boundary, this wave propagates in the same direction and with the same phase speed as the displacement wave at the boundary. In the x_3 coordinate direction, the wave propagates away from the boundary at an angle θ to the plane of the boundary. The angle θ is given by

$$\theta = \arctan\left[\frac{|k_0|\sqrt{1 - k^2/k_0^2}}{k}\right]. \quad (4\text{-}188)$$

The phase speed, c_3, of the wave in the positive x_3 direction is given by

$$c_3 = \frac{c}{\sqrt{1 - k^2/k_0^2}}\,. \quad (4\text{-}189)$$

When the magnitude of the wavevector characterizing the displacement of the boundary is greater than the magnitude of k_0, equation (4-187) reveals that the pressure field in the half space, at any positive value of x_3, is characterized by a wave of the same form as that applied at the boundary: that

is, by $\exp\{i(\underline{k}\cdot\underline{x} + \omega t)\}$. However, the pressure wave is 180 degrees out of phase with the displacement wave. The amplitude of the pressure wave is specified by $|H(\underline{k},x_3,\omega)|$ and, according to equation (4-169), decreases exponentially with increasing distance (x_3) from the boundary. As the pressure wave is characterized, on any plane of constant and positive x_3, by the same wavevector and frequency as the displacement wave at the boundary, the wave propagates on that plane in the same direction and with the same phase speed as does the wave on the boundary. These waves that propagate parallel to the boundary, but decrease exponentially in amplitude with distance from the boundary, are called evanescent waves.

Figure 4-6(a) presents the magnitude of $H(\underline{k},x_3,\omega)$ normalized by $\rho c\omega$, the value of $H(\underline{k},x_3,\omega)$ at $\underline{k} = (0,0)$, as a function k (the magnitude of $\underline{k}$). From the above discussion, the magnitude of $H(\underline{k},x_3,\omega)$ represents (1) the amplitudes of the acoustic waves that propagate in x_3 in the wavenumber range $k \leq |k_0|$ and (2) the amplitudes of the evanescent waves that only propagate along surfaces of constant (and positive) x_3 in the wavenumber range $k > |k_0|$. The normalized magnitude of $H(\underline{k},x_3,\omega)$ is presented for three values of the normalized coordinate k_0x_3: 0, 0.5, and 1.

Note first that, because the acoustic half-space system is space invariant in the two-dimensional vector variable $\underline{x}$, the wavevector-frequency response, $H(\underline{k},x_3,\omega)$, is a function of only the magnitude of the two-dimensional wavevector $\underline{k}$. That is, owing to the spatial invariance in $\underline{x}$, the response of the half space to a wave of the form $\exp\{i(\underline{k}\cdot\underline{x} + \omega t)\}$at the boundary is independent of the direction of propagation of the applied wave.

Note further that, in the wavenumber range $k \leq |k_0|$, the magnitude of $H(\underline{k},x_3,\omega)$, and thereby the amplitude of the acoustic wave radiated into the half space, is independent of the variable x_3. However, as is evident by figure 4-6(a), the amplitude of the evanescent waves associated with the wavenumber range $k > |k_0|$ decreases with increasing positive values of x_3 and with increasing values of k.

Note that when the magnitude of the wavevector that characterizes the wave of displacement, $\exp\{i(\underline{k}\cdot\underline{x} + \omega t)\}$, at the boundary is equal to $|k_0|$, the

magnitude of $H(\underline{k},x_3,\omega)$, and thereby the amplitude of the radiated pressure field in the half space, becomes infinite. However, if the pressure field had infinite amplitude at the boundary, a force of infinite amplitude would be required to initiate any displacement of the boundary. Thus, the infinite value of $|H(\underline{k},x_3,\omega)|$ at $k = |k_0|$ is best interpreted as a statement that the surface impedance of the acoustic half space becomes infinite at $k = |k_0|$, and thus no wave of displacement (or, more properly, velocity) characterized by such a wavevector magnitude can be excited at the surface.

Figure 4-6(b) illustrates the argument, or phase, of $H(\underline{k},x_3,\omega)$ as a function of the magnitude of the wavevector characterizing the wave of displacement, $\exp\{i(\underline{k}\cdot\underline{x} + \omega t)\}$, on the bounding surface, $x_3 = 0$. In the wavenumber range $k \leq |k_0|$, where acoustic propagation occurs in the x_3 coordinate direction, equation (4-186) shows the phase to depend on both the magnitude of the wavevector of excitation, k, and the distance from the boundary, x_3. Figure 4-6(b) illustrates the wavenumber dependency for k_0x_3 equal to 0, 0.5, and 1. For wavevectors of excitation greater, in magnitude, than $|k_0|$, the phase of $H(\underline{k},x_3,\omega)$ is independent of k and equal to π.

The wavevector characteristics of $\tilde{H}(\underline{k},k_3,\omega)$, the complete wavevector-frequency transform of $h(\underline{x} - \underline{x}_0,x_3,t - t_0)$ defined by equation (4-170), are difficult to illustrate in graphical form. However, they can be described and interpreted.

Recall that $\tilde{H}(\underline{k},k_3,\omega)$ is the ratio of the complex amplitudes of waves of the form $\exp\{i(\underline{k}\cdot\underline{x} + k_3x_3 + \omega t)\}$ that comprise the pressure field in the space $x_3 \geq 0$ to the complex amplitudes, at corresponding wavevectors ($\underline{k}$) and frequencies (ω), of waves of the form $\exp\{i(\underline{k}\cdot\underline{x} + \omega t)\}$ that comprise the displacement field on the boundary. We have established that a wavevector component, $\underline{k}$, of the displacement field produces a plane wave of pressure in the half-space $x_3 > 0$ when $|\underline{k}| \leq |k_0|$. The propagation of that plane wave in $\underline{x}$ is characterized, for all x_3, by the wavevector, $\underline{k}$, and frequency, ω, of the displacement field. The propagation in the x_3 coordinate direction, however, is determined by the allowable waves (i.e., the free waves) in the acoustic medium and the radiation condition that waves in the acoustic half

space must propagate in the positive x_3 direction (i.e., away from the boundary).

It is straightforward to establish, by arguments similar to those used in section 3.3, that free waves in an infinite acoustic medium are governed, in the wavevector-frequency domain, by

$$[k_1{}^2 + k_2{}^2 + k_3{}^2 - (\omega/c)^2]P(\underline{k},k_3,\omega) = [k^2 + k_3{}^2 - k_0{}^2]P(\underline{k},k_3,\omega) = 0 \ . \tag{4-190}$$

For fixed values of k_1, k_2, and ω, it follows that the wavevector-frequency description of allowable free waves in an infinite acoustic medium is of the form

$$P(\underline{k},k_3,\omega) = A(\underline{k},\omega)\delta\left\{k_3 - k_0\sqrt{1 - k^2/k_0{}^2}\right\} + B(\underline{k},\omega)\delta\left\{k_3 + k_0\sqrt{1 - k^2/k_0{}^2}\right\}. \tag{4-191}$$

The first term on the right-hand side corresponds to a wave propagating in the negative x_3 direction, and the second term corresponds to a wave propagating in the positive x_3 direction.

Note that, for $k \leq |k_0|$, the first term on the right-hand side of equation (4-170) is of the form of the second term on the right-hand side of equation (4-191) and therefore corresponds to a free acoustic wave propagating in the positive x_3 direction in an infinite acoustic medium. The values of k and ω associated with this wave are dictated by the wavevector-frequency component of interest in the displacement field. The amplitude of this free wave is seen, in equation (4-170), to be a function of the wavenumber and frequency of the boundary excitation.

The acoustic half space, however, is not an infinite acoustic medium; it is space limited in the x_3 coordinate. Therefore, in the wavenumber range $k \leq |k_0|$, the free wave must be augmented by other wave components to eliminate the pressure field in the space $x_3 < 0$. The second term on the right-hand side of that portion of equation (4-170) applicable to the wavenumber range $k \leq |k_0|$ defines these additional wave components. For a

given wavevector-frequency component of the displacement field (and thereby given values of k and ω), it is evident that the largest of these additional components occurs at $k_3 = -\sqrt{k_0^2 - k^2}$.

For a wave component of the displacement field characterized by a wavevector and frequency such that $k > |k_0|$, we have established that the resulting pressure field, on any plane of constant and positive x_3, propagates in the same direction and with the same speed as the displacement field. However, the amplitude of this pressure wave decreases exponentially with increasing x_3. In the wavenumber range $k > |k_0|$, equation (4-170) defines the complex amplitudes of that combination of plane waves of the form $\exp\{i(\underline{k}\cdot\underline{x} + k_3x_3 + \omega t)\}$ that produces such an evanescent wave field for each corresponding wavevector, $\underline{k}$, and frequency, ω, component of the displacement field on the boundary. In this wavenumber range, it is easily established from equation (4-170) that the magnitude of $\tilde{H}(\underline{k},k_3,\omega)$ is inversely proportional to $k^2 + k_3^2 - k_0^2$ and is therefore largest when the magnitude of the wavevector $\tilde{k} = (k_1,k_2,k_3)$ is greater than, but in the neighborhood of, $|k_0|$: that is, when

$$\sqrt{k^2 + k_3^2} = \sqrt{k_1^2 + k_2^2 + k_3^2} \approx |k_0| \ .$$

While it is not obvious how the distribution of plane waves in equation (4-170) produces a pressure field that decays in amplitude with increasing positive values of x_3 when $k > |k_0|$, it should be noted that, in the complex k_3 plane, $\tilde{H}(\underline{k},k_3,\omega)$ is characterized by a simple pole on the positive, imaginary k_3 axis. By the Cauchy integral theorem,[14] this pole corresponds, under Fourier transformation of $\tilde{H}$ on k_3, to the exponential decay noted in $H(\underline{k},x_3,\omega)$ for positive x_3 and to zero for negative x_3.

To summarize, we have presented two alternative wavevector-frequency descriptions of the pressure field produced in an acoustic half space by a prescribed displacement field at the boundary. This acoustic system is space invariant in the two-dimensional space $\underline{x} = (x_1,x_2)$, but is space limited in x_3.

One wavevector-frequency description is the Fourier transform of the pressure field on only those variables over which the system is invariant:

that is, the spatial vector variable $\underline{x}$ and time. In this case, the wavevector-frequency transform of the pressure field, $P(\underline{k},x_3,\omega)$, was shown to be equal to the product of the corresponding transform of the displacement field at the boundary, $W(\underline{k},\omega)$, and the wavevector-frequency response of the acoustic half space, $H(\underline{k},x_3,\omega)$. This wavevector-frequency response was shown to be related to the spectral surface impedance, $Z(\underline{k},\omega)$, and to the corresponding wavevector-frequency transform of the Green's function, $G(\underline{k};x_3,0,\omega)$. The magnitude of the wavevector-frequency response (and that of these related descriptors of the system response) was shown to be greatest, for all $x_3 \geq 0$, at those wavevectors equal, in magnitude, to the free wavevector, k_0, of the acoustic medium.

The second wavevector-frequency description of the pressure field, $\tilde{P}(\underline{k},k_3,\omega)$, was formed by Fourier transformation of the space-time pressure field on all independent variables (i.e., on $\underline{x}$, x_3, and t). This transform of the pressure field was shown to be equal to the product of the wavevector-frequency transform of the boundary displacement field, $W(\underline{k},\omega)$, and the Fourier transform of the wavevector-frequency response, $H(\underline{k},x_3,\omega)$, of the acoustic half space on the spatial variable x_3. This complete wavevector-frequency transform of the displacement impulse response, $h(\underline{x} - \underline{x}_0,x_3,t - t_0)$, was denoted by $\tilde{H}(\underline{k},k_3,\omega)$ and was shown to represent the ratio of the complex amplitudes of the plane wave components of the form $\exp\{i(\underline{k}\cdot\underline{x} + k_3x_3 + \omega t)\}$ comprising the pressure field to the complex amplitudes, at corresponding values of $\underline{k}$ and ω, of the waves of the form $\exp\{i(\underline{k}\cdot\underline{x} + \omega t)\}$ comprising the displacement field at the boundary. It was shown that this complete wavevector-frequency response, $\tilde{H}(\underline{k},k_3,\omega)$, was characterized by discrete wavevector contributions (i.e., delta functions) on the hemisphere defined by $k^2 + k_3^2 = k_1^2 + k_2^2 + k_3^2 = k_0^2$, $k_3 \leq 0$. Further, the magnitude of $\tilde{H}(\underline{k},k_3,\omega)$ was shown to approach infinity when the magnitude of the wavevector $\vec{k} = (k_1,k_2,k_3)$ approached the magnitude of the free wavenumber of the acoustic medium, k_0.

The point to be stressed is that the magnitude of the wavevector-frequency response, in either the two- or three-dimensional wavevector form, of this boundary-excited, space-varying acoustic system is greatest at wavevectors equal, in magnitude, to that of the free wavenumber of the acoustic medium.

Recall, from chapter 3, that the magnitude of the wavevector-frequency response of space- and time-invariant systems was also found to be greatest at wavevectors equal, in magnitude, to that of the free wavenumber of the system.

4.3.3.2 <u>The Forced Vibration of a Simply Supported Plate</u>. The free vibration of a simply supported plate was treated in section 4.2.2 to illustrate the wavevector-frequency properties of a free system, space limited in two dimensions. Here, to illustrate the wavevector-frequency properties of a forced system that is space limited in two dimensions, we investigate the forced vibration of the simply supported plate.

In this example, the simply supported plate illustrated in figure 4-3 is subjected to a force per unit area, $f(\underline{x},t)$, that is considered positive when it acts in the direction of positive displacement, $w(\underline{x},t)$, of the plate. To simplify temporal causality arguments, the plate is subjected to a damping force per unit area equal to $r\partial w/\partial t$, which opposes motion of the plate. By using the notation of section 4.2.2, the displacement field of the plate resulting from the externally applied forcing field is governed, over $0 < x_1 < L_1$, $0 < x_2 < L_2$, and all t, by

$$B(\underline{x})\left[D^4 w(\underline{x},t) + r\,\frac{\partial w(\underline{x},t)}{\partial t} + \mu\,\frac{\partial^2 w(\underline{x},t)}{\partial t^2}\right] = B(\underline{x})f(\underline{x},t)\ , \qquad (4\text{-}192)$$

where $B(\underline{x})$ is the two-dimensional space-limiting function defined by equation (4-45). The displacement field in the space outside the physical extent of the plate is assumed to be zero. At the boundaries of the plate, the displacement field must satisfy the simply supported conditions specified by equations (4-48) and (4-49).

The simply supported plate is a causal, time-invariant system, and it was established in section 4.2.2 that the normal modes of the plate, $\alpha_{mn}(\underline{x})$, defined by equation (4-53) individually satisfy the simply supported boundary conditions. We therefore assume that the displacement field can be expressed in the form

$$w(\underline{x},t) = (2\pi)^{-1}\int_{-\infty}^{\infty}\sum_{m=1}^{\infty}\sum_{n=1}^{\infty} A_{mn}(\omega)\alpha_{mn}(\underline{x})\exp(i\omega t)\,d\omega \qquad (4\text{-}193)$$

over $0 \leq x_1 \leq L_1$ and $0 \leq x_2 \leq L_2$ for all t. We also assume the forcing field, $f(\underline{x},t)$, can be expressed by

$$f(\underline{x},t) = (2\pi)^{-1} \int_{-\infty}^{\infty} \sum_{q=1}^{\infty} \sum_{s=1}^{\infty} B_{qs}(\omega)\alpha_{qs}(\underline{x})\exp(i\omega t)\, d\omega \tag{4-194}$$

over $0 \leq x_1 \leq L_1$ and $0 \leq x_2 \leq L_2$ for all t. Substitution of equations (4-193) and (4-194) into equation (4-192) yields

$$\int_{-\infty}^{\infty}\left[\sum_{m=1}^{\infty} \sum_{n=1}^{\infty} \{D[(m\pi/L_1)^2 + (n\pi/L_2)^2]^2 + ir\omega - \mu\omega^2\}A_{mn}(\omega)\beta(\underline{x})\alpha_{mn}(\underline{x}) - \sum_{q=1}^{\infty} \sum_{s=1}^{\infty} B_{qs}(\omega)\beta(\underline{x})\alpha_{qs}(\underline{x})\right]\exp(i\omega t)\, d\omega = 0 \,. \tag{4-195}$$

As equation (4-195) is valid for all t, it follows that

$$\sum_{m=1}^{\infty} \sum_{n=1}^{\infty} \{D[(m\pi/L_1)^2 + (n\pi/L_2)^2]^2 + ir\omega - \mu\omega^2\}A_{mn}(\omega)\beta(\underline{x})\alpha_{mn}(\underline{x}) - \sum_{q=1}^{\infty} \sum_{s=1}^{\infty} B_{qs}(\omega)\beta(\underline{x})\alpha_{qs}(\underline{x}) = 0 \,. \tag{4-196}$$

By multiplying equation (4-196) by $\alpha_{uv}(\underline{x})$ and integrating over all $\underline{x}$, we can use the orthogonality condition of equation (4-54) to show that

$$A_{mn}(\omega) = \frac{B_{mn}(\omega)}{D[(m\pi/L_1)^2 + (n\pi/L_2)^2]^2 + ir\omega - \mu\omega^2} \,. \tag{4-197}$$

However, from equation (4-194) and the orthogonality condition of equation (4-54), it can be shown that

$$B_{mn}(\omega) = (4/L_1L_2) \int_{-\infty}^{\infty}\int_{-\infty}^{\infty} f(\underline{x},t)\beta(\underline{x})\alpha_{mn}(\underline{x})\exp(-i\omega t)\, d\underline{x}\, dt \,. \tag{4-198}$$

Therefore, by equations (4-193), (4-197), and (4-198), it follows that

$$w(\underline{x},t) = \frac{2}{\pi L_1 L_2} \int_{-\infty}^{\infty} \sum_{m=1}^{\infty} \sum_{n=1}^{\infty} \left\{ \frac{\int_{-\infty}^{\infty}\int_{-\infty}^{\infty} f(\underline{z},\Theta)B(\underline{z})\alpha_{mn}(\underline{z})\exp(-i\omega\Theta)d\underline{z}d\Theta}{D[(m\pi/L_1)^2 + (n\pi/L_2)^2]^2 + ir\omega - \mu\omega^2} \right\}$$

$$\alpha_{mn}(\underline{x})\exp(i\omega t)\,d\omega \qquad (4\text{-}199)$$

over $0 \leq x_1 \leq L_1$ and $0 \leq x_2 \leq L_2$ for all t. Recall that $w(\underline{x},t) = 0$ for $\underline{x}$ outside $0 \leq x_1 \leq L_1$ or $0 \leq x_2 \leq L_2$.

To obtain a single expression for the displacement field, valid over all space and time, it is convenient to define the field $w_\infty(\underline{x},t)$ as the extension of equation (4-199) over all space. That is,

$$w_\infty(\underline{x},t) = \frac{2}{\pi L_1 L_2} \int_{-\infty}^{\infty} \sum_{m=1}^{\infty} \sum_{n=1}^{\infty} \left\{ \frac{\int_{-\infty}^{\infty}\int_{-\infty}^{\infty} f(\underline{z},\Theta)B(\underline{z})\alpha_{mn}(\underline{z})\exp(-i\omega\Theta)d\underline{z}d\Theta}{D[(m\pi/L_1)^2 + (n\pi/L_2)^2]^2 + ir\omega - \mu\omega^2} \right\}$$

$$\alpha_{mn}(\underline{x})\exp(i\omega t)\,d\omega \qquad (4\text{-}200)$$

for all $\underline{x}$ and t. The displacement field that, for all time, satisfies equation (4-192) in the space $0 \leq x_1 \leq L_1$ and $0 \leq x_2 \leq L_2$, the boundary conditions of equations (4-48) and (4-49), and the requirement of zero displacement for $\underline{x}$ outside $0 \leq x_1 \leq L_1$ or $0 \leq x_2 \leq L_2$ can then be written

$$w(\underline{x},t) = B(\underline{x})w_\infty(\underline{x},t) \ . \qquad (4\text{-}201)$$

By definition, the Green's function for the simply supported plate is a solution to equation (4-192) when $f(\underline{x},t)$ is an impulse in time and space. That is, the Green's function is governed by

$$B(\underline{x})\left\{D^4 g(\underline{x},\underline{x}_0,t,t_0) + r\,\frac{\partial g(\underline{x},\underline{x}_0,t,t_0)}{\partial t} + \mu\,\frac{\partial^2 g(\underline{x},\underline{x}_0,t,t_0)}{\partial t^2}\right\}$$

$$= B(\underline{x})\delta(\underline{x} - \underline{x}_0)\delta(t - t_0) \ . \qquad (4\text{-}202)$$

To complete the specification of the Green's function, suitable spatial and temporal constraints must be applied to the solutions to equation (4-202).

If we require that the Green's function satisfy the simply supported conditions at the boundaries of the plate, that is,

$$g(0,x_2;\underline{x}_0;t,t_0) = g(L_1,x_2;\underline{x}_0;t,t_0) = g(x_1,0;\underline{x}_0;t,t_0) = g(x_1,L_2;\underline{x}_0;t,t_0) = 0 \tag{4-203}$$

and

$$\frac{\partial^2 g(0,x_2;\underline{x}_0;t,t_0)}{\partial x_1^{\,2}} = \frac{\partial^2 g(L_1,x_2;\underline{x}_0;t,t_0)}{\partial x_1^{\,2}}$$

$$= \frac{\partial^2 g(x_1,0;\underline{x}_0;t,t_0)}{\partial x_2^{\,2}} = \frac{\partial^2 g(x_1,L_2;\underline{x}_0;t,t_0)}{\partial x_2^{\,2}} = 0 \;, \tag{4-204}$$

then the form of the Green's function can be obtained from equations (4-200) and (4-201) by replacing $f(\underline{x},t)$ by $\delta(\underline{x} - \underline{x}_0)\delta(t - t_0)$. That form is easily shown to be

$$g(\underline{x},\underline{x}_0,t - t_0) = \frac{2}{\pi L_1 L_2} \int_{-\infty}^{\infty} \sum_{m=1}^{\infty} \sum_{n=1}^{\infty} \left\{\frac{\beta(\underline{x})\alpha_{mn}(\underline{x})\beta(\underline{x}_0)\alpha_{mn}(\underline{x}_0)}{D[(m\pi/L_1)^2 + (n\pi/L_2)^2]^2 + ir\omega - \mu\omega^2}\right\}$$

$$\exp\{i\omega(t - t_0)\}\, d\omega \;. \tag{4-205}$$

Note that, owing to the time invariance of this plate system, the Green's function depends only on the time difference between excitation and observation.

With regard to temporal dependence, equations (4-200) and (4-201), and thereby equation (4-205), assume only that the response of the system is such that the temporal transform of the displacement field exists. However, the Green's function must satisfy the temporal constraint that the response cannot anticipate the input. Mathematically, this means

$$\frac{\partial^n g(\underline{x},\underline{x}_0,t - t_0)}{\partial t^n} = 0, \quad \text{for } t < t_0 , \tag{4-206}$$

for all n. By inspection of equation (4-205), the frequency dependence of each term in the summation is of the form

$$S_{mn}(\omega) = \frac{-1}{\mu\left\{\omega^2 - \omega_{mn}^{\;2} - ir\omega/\mu\right\}} , \tag{4-207}$$

where ω_{mn} is the modal natural frequency defined by equation (4-55). Equation (4-207) is of the same mathematical form as equation (3-87). Consequently, by arguments similar to those presented in equations (3-88)-(3-91), it can be shown that the temporal dependence of each term in the summation of equation (4-205) is given by

$$s_{mn}(t) = (1/\mu)U(t - t_0)\exp\{-r(t - t_0)/(2\mu)\} \frac{\sin\{{}_d\omega_{mn}(t - t_0)\}}{{}_d\omega_{mn}} , \tag{4-208}$$

where ${}_d\omega_{mn}$ is the damped modal natural frequency of the simply supported plate, defined by

$${}_d\omega_{mn} = \sqrt{\omega_{mn}^{\;2} - (r/2\mu)^2} . \tag{4-209}$$

It is evident that $s_{mn}(t)$ and all its temporal derivatives are identically zero for $t < t_0$, regardless of the values of m and n. It follows, inasmuch as each term of the summation comprising $g(\underline{x},\underline{x}_0,t - t_0)$ has the temporal dependence specified by equation (4-208), that the Green's function of equation (4-205) satisfies the causal condition of equation (4-206).

By multiplying equation (4-205) by $f(\underline{x}_0,t_0)$ and integrating over all $\underline{x}_0$ and t_0, it is evident, by comparing the result with equations (4-200) and (4-201), that

$$w(\underline{x},t) = \int_{-\infty}^{\infty}\int_{-\infty}^{\infty} g(\underline{x},\underline{x}_0,t - t_0)f(\underline{x}_0,t_0)\, d\underline{x}_0\, dt_0 . \tag{4-210}$$

Note that this Green's function solution for the simply supported plate, a system space limited in two dimensions, contains no line integrals representing additional inputs associated with boundary forces. Thus, by the arguments of section 4.3.1.2, the Green's function specified by equation (4-205) is exact.

A note is also in order regarding the forcing function $f(\underline{x},t)$. As used in equations (4-198)-(4-200) and in equation (4-210), $f(\underline{x},t)$ is a function defined over all $\underline{x}$ and t that is equal to the force per unit area applied over the surface of the plate in the spatial range $0 < x_1 < L_1$ and $0 < x_2 < L_2$. Outside this spatial range, $f(\underline{x},t)$ can be arbitrarily specified, inasmuch as forces applied outside the physical extent of the plate do not affect any displacement of the plate.

If we write

$$g(\underline{x},\underline{x}_0,\tau) = (2\pi)^{-5} \int_{-\infty}^{\infty}\int_{-\infty}^{\infty}\int_{-\infty}^{\infty} G(\underline{k},\underline{\alpha},\omega)\exp\{i(\underline{k}\cdot\underline{x} + \underline{\alpha}\cdot\underline{x}_0 + \omega\tau)\}\, d\underline{k}\, d\underline{\alpha}\, d\omega, \quad (4\text{-}211)$$

then it follows from equations (4-210) and (4-211) that the wavevector-frequency transform of the displacement field, $W(\underline{k},\omega)$, is related to the wavevector-frequency transform of the forcing field, $F(\underline{k},\omega)$, by

$$W(\underline{k},\omega) = (2\pi)^{-2} \int_{-\infty}^{\infty} G(\underline{k},-\underline{\alpha},\omega)F(\underline{\alpha},\omega)\, d\underline{\alpha} \; . \quad (4\text{-}212)$$

If we denote the magnitude of the wavevector $\underline{k}_{mn} = (m\pi/L_1, n\pi/L_2)$ associated with the mn-th mode of the plate by

$$k_{mn} = \sqrt{(m\pi/L_1)^2 + (n\pi/L_2)^2} \quad (4\text{-}213)$$

and make use of the definitions of equations (4-62) and (4-70), it is straightforward to show, from equation (4-205), that

$$G(\underline{k},\underline{\alpha},\omega) = \frac{4}{DL_1L_2} \sum_{m=1}^{\infty} \sum_{n=1}^{\infty} \frac{I_{mn}(\underline{k})I_{mn}(\underline{\alpha})}{k_{mn}^4 - k_p^4(\omega) + i r\omega/D} \; . \quad (4\text{-}214)$$

Therefore, by equations (4-212) and (4-214), it follows that

$$W(\underline{k},\omega) = \frac{1}{\pi^2 D L_1 L_2} \sum_{m=1}^{\infty} \sum_{n=1}^{\infty} \left\{ \frac{I_{mn}(\underline{k})}{k_{mn}^4 - k_p^4(\omega) + ir\omega/D} \right\} \int_{-\infty}^{\infty} I_{mn}^*(\underline{\alpha}) F(\underline{\alpha},\omega)\, d\underline{\alpha} \,. \quad (4\text{-}215)$$

If we make use of the definitions of $I_{mn}(\underline{k})$ and $F(\underline{k},\omega)$, it is straightforward to show that

$$\int_{-\infty}^{\infty} I_{mn}(\underline{\mu}) F(\underline{\mu},\omega)\, d\underline{\mu} = \pi^2 L_1 L_2 B_{mn}(\omega) \,, \quad (4\text{-}216)$$

where $B_{mn}(\omega)$ is the frequency-dependent modal force defined by equation (4-198). Therefore, we can rewrite equation (4-215) as

$$W(\underline{k},\omega) = \frac{1}{D} \sum_{m=1}^{\infty} \sum_{n=1}^{\infty} \frac{B_{mn}(\omega) I_{mn}(\underline{k})}{k_{mn}^4 - k_p^4(\omega) + ir\omega/D} \,. \quad (4\text{-}217)$$

Equations (4-214) and (4-217) (or (4-215)) define, respectively, the two-wavevector-frequency response, $G(\underline{k},\underline{\alpha},\omega)$, and the wavevector-frequency transform, $W(\underline{k},\omega)$, of the displacement field for the forced simply supported plate.

A noteworthy feature of equations (4-214) and (4-217) is that the description of this space-limited field in the wavevector domain does not offer an advantage in mathematical simplicity over the description in the spatial domain. That is, by equations (4-198)-(4-201),

$$w(\underline{x},t) = \frac{1}{2\pi D} \int_{-\infty}^{\infty} \sum_{m=1}^{\infty} \sum_{n=1}^{\infty} \left\{ \frac{B_{mn}(\omega) B(\underline{x}) \alpha_{mn}(\underline{x})}{k_{mn}^4 - k_p^4(\omega) + ir\omega/D} \right\} \exp(i\omega t)\, d\omega \,. \quad (4\text{-}218)$$

Comparison of equation (4-217) with equation (4-218) reveals that, while the transformation from the temporal domain to the frequency domain has resulted in a mathematical simplification by elimination of an integral, both the spatial and wavevector characteristics of the field are expressed as doubly infinite summations of modal functions characteristic of the respective

domains. Similar arguments apply to the Green's function (see equation (4-205)) and its wavevector-frequency transform, $G(\underline{k},\underline{\alpha},\omega)$, defined by equation (4-214). Thus, the prediction of the wavevector characteristics of the space-limited displacement field of a simply supported plate is a mathematical task equally difficult to that of predicting the spatial characteristics.

The mathematical complexity of the expressions for $W(\underline{k},\omega)$ and $G(\underline{k},\underline{\alpha},\omega)$ preclude us from attempting any detailed analysis of the wavevector-frequency characteristics of the forced motion of the simply supported plate. However, by examination of equations (4-214) and (4-217), we can identify significant contributions to $W(\underline{k},\omega)$ and $G(\underline{k},\underline{\alpha},\omega)$ and thereby gain insight into the general nature of these wavevector-frequency descriptions.

We first note, from equation (4-212), that $G(\underline{k},\underline{\alpha},\omega)$ defines the complex amplitudes of waves of the form $\exp\{i(\underline{k}\cdot\underline{x} + \omega t)\}$ that comprise the displacement field of the plate as a result of excitation of the plate by the wave $(2\pi)^{-1} \exp\{i(-\underline{\alpha}\cdot\underline{x} + \omega t)\}$. Similarly, equation (4-215) or (4-217) relates the complex amplitudes, $W(\underline{k},\omega)$, of the waves of the form $\exp\{i(\underline{k}\cdot\underline{x} + \omega t)\}$ that comprise the displacement field of the plate to, respectively, the complex amplitudes, $F(\underline{\alpha},\omega)$, of the waves of the form $\exp\{i(\underline{\alpha}\cdot\underline{x} + \omega t)\}$ or the frequency-dependent modal forces, $B_{mn}(\omega)$, that comprise the forcing field of the plate.

By inspection of equations (4-214) and (4-217), it is evident that, at any fixed frequency, ω_0, the dependence of both $G(\underline{k},\underline{\alpha},\omega_0)$ and $W(\underline{k},\omega_0)$ on the wavevector $\underline{k}$ is specified by a weighted superposition of wavevector transforms of the space-limited natural modes, $I_{mn}(\underline{k})$, over all mode numbers, m and n. Two separate functions weight $I_{mn}(\underline{k})$ at each value of m and n. One weighting function, the term

$$\left\{k_{mn}^4 - k_p^4(\omega_0) + i r\omega_0/D\right\}^{-1} ,$$

specifies the response of the mn-th mode of the plate at the frequency ω_0. The other weighting function is the frequency-dependent modal force, $B_{mn}(\omega_0)$, acting on the plate. In equation (4-214), this modal force is frequency independent and is given by $I_{mn}(\underline{\alpha})$, where $-\underline{\alpha}$ is the fixed, but

arbitrary, wavevector characterizing the (single) complex wave that forces the motion of the plate. It is important to note that $I_{mn}(\underline{k})$ and the two weighting functions are, in general, complex.

Clearly, the relation between the wavevector-frequency characteristics of the displacement field and those of the forcing field is not a mathematically simple one. However, we can gain some insight into the wavevector-frequency characteristics of the displacement field by identifying those terms in the summations of equations (4-214) and (4-217) that provide the largest, in magnitude, wavevector contributions to the displacement field at some fixed, but arbitrary, frequency ω_0. We will perform this identification for $W(\underline{k},\omega)$, described by equation (4-217). The general wavevector-frequency characteristics of $G(\underline{k},\underline{\alpha},\omega)$ can then be examined as a special case of $W(\underline{k},\omega)$.

From our investigation of the free vibration of the simply supported plate (section 4.2.2), we know that the magnitude of $I_{mn}(\underline{k})$ has four equal primary maxima at the wavevectors $\underline{k} = (\pm m\pi/L_1, \pm n\pi/L_2)$ and has secondary maxima at the wavevectors $\underline{k} = \{\pm[m \pm (2p + 1)]\pi/L_1, \pm[n \pm (2q + 1)]\pi/L_2\}$ for all integers p and q equal to or greater than one. The magnitudes of these secondary maxima decrease with increasing wavevector distance, $\underline{\epsilon}$, from the primary maxima approximately as $(|\epsilon_1|\,|\epsilon_2|)^{-1}$ and are therefore considerably smaller than the magnitudes at $\underline{k} = (\pm m\pi/L_1, \pm n\pi/L_2)$. The reader can refresh his memory regarding the wavevector characteristics of $|I_{mn}(\underline{k})|$ by referring to figure 4-4. It follows, by the above arguments, that the largest, in magnitude, wavevector contributions to $W(\underline{k},\omega_0)$ from each mn-th term in the summation of equation (4-215) occur at the four wavevectors $\underline{k} = (\pm m\pi/L_1, \pm n\pi/L_2)$. These wavevectors associated with the primary maxima of $I_{mn}(\underline{k})$ are referred to as the modal wavevectors, and their magnitudes, k_{mn}, as modal wavenumbers (see equation (4-213)).

By equation (4-64), it can be shown that the magnitudes of the four primary maxima of $I_{mn}(\underline{k})$ are equal and independent of the mode numbers m and n. Therefore, from equation (4-217), it is evident that (1) the largest, in magnitude, wavevector contributions to $W(\underline{k},\omega_0)$ from each mode occur at the wavevectors $\underline{k} = (\pm m\pi/L_1, \pm n\pi/L_2)$ and (2) the magnitudes of the contributions at each of these modal wavevectors are determined by the magnitudes of the

weightings applied to these modes: that is, by the magnitude of the product of $B_{mn}(\omega_0)$ and $\{k_{mn}^4 - k_p^4(\omega_0) + ir\omega_0/D\}^{-1}$. In the absence of specific knowledge of the modal forces, $B_{mn}(\omega_0)$, the complete set of modal wavevectors must be considered as sites of potentially large contributions to $W(\underline{k},\omega_0)$. Figure 4-7 illustrates the wavevector locations of this set of modal wavevectors.

Also illustrated in figure 4-7 is a circle of radius equal to the free wavenumber of the plate, $k_p(\omega_0)$, at the frequency ω_0. A coincidence of the magnitude of a modal wavevector, say k_{MN}, with $k_p(\omega_0)$ defines a resonance of the MN-th mode plate. By equation (4-71), this resonance occurs at the frequency $\omega_0 = \omega_{MN}$. At resonance, the magnitude of the weighting function that specifies the response of the mn-th mode of the plate at the frequency ω_0, i.e., $\{k_{mn}^4 - k_p^4(\omega_0) + ir\omega_0/D\}^{-1}$, reaches its maximum value. That is, at the frequency ω_{MN} where the MN-th mode is resonant, the magnitude of the MN-th modal contribution to $W(\underline{k},\omega_{MN})$ is weighted by

$$\frac{|B_{MN}(\omega_{MN})|}{|\{k_{MN}^4 - k_p^4(\omega_{MN}) + ir\omega_{MN}/D\}|} = \frac{|B_{MN}(\omega_{MN})|}{|(r\omega_{MN}/D)|} . \qquad (4\text{-}219)$$

By contrast, the magnitude of a nonresonant (say PQ-th) modal contribution to $W(\underline{k},\omega_{MN})$ is weighted by

$$\frac{|B_{PQ}(\omega_{MN})|}{|\{k_{PQ}^4 - k_p^4(\omega_{MN}) + ir\omega_{MN}/D\}|} .$$

Clearly, for equal magnitudes of excitation of the resonant MN-th and the nonresonant PQ-th modes (i.e., $|B_{MN}(\omega_{MN})| = |B_{PQ}(\omega_{MN})|$), the ratio of the magnitude of the weighting applied to the MN-th modal contribution to $W(\underline{k},\omega_{MN})$ to that applied to the PQ-th contribution is

$$\frac{|\{k_{PQ}^4 - k_p^4(\omega_{MN}) + ir\omega_{MN}/D\}|}{|(r\omega_{MN}/D)|} > 1 . \qquad (4\text{-}220)$$

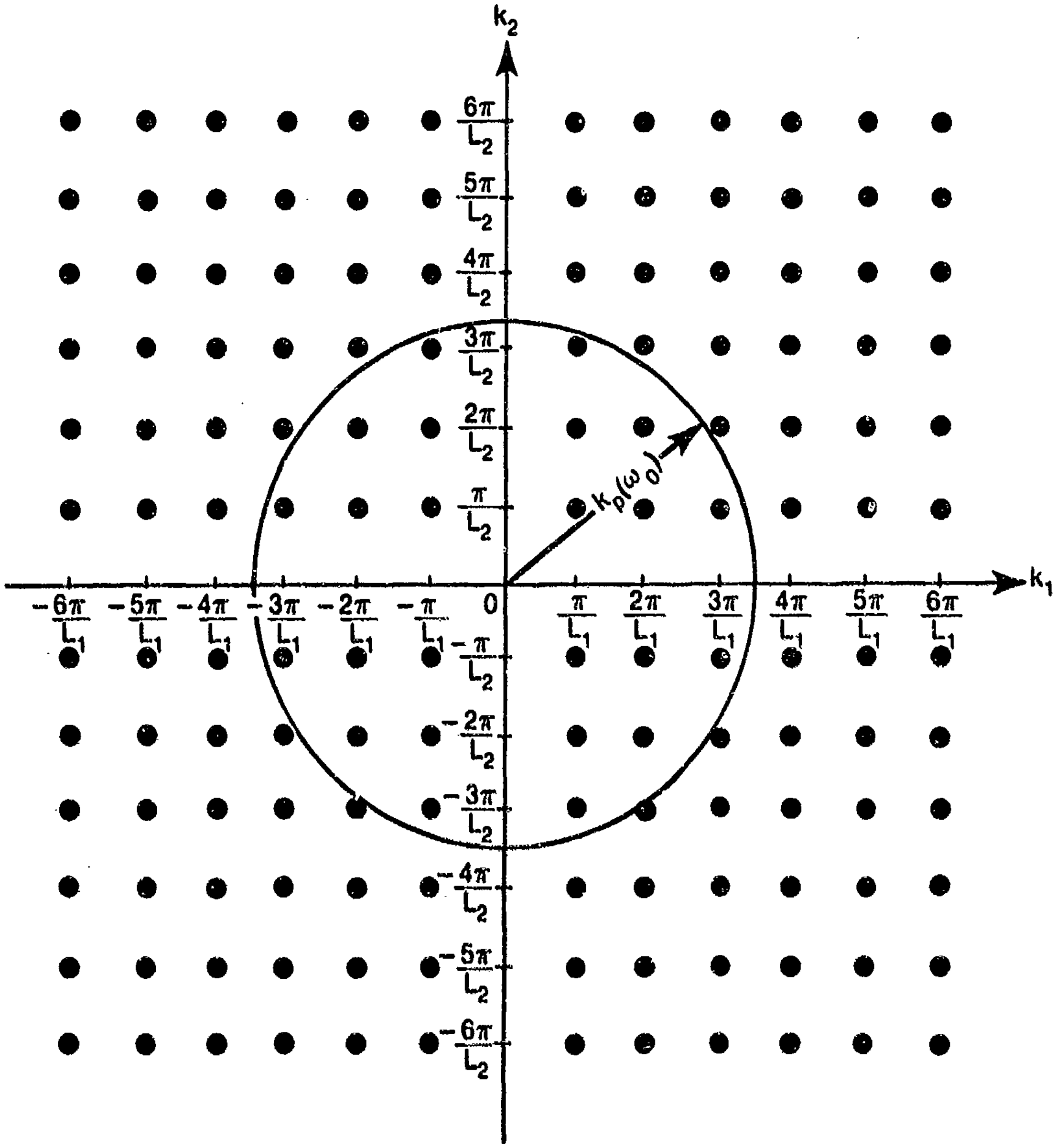

Figure 4-7. Wavevector Locations of Potentially Large Contributions to the Magnitude of $W(\underline{k},\omega)$

Thus, in figure 4-7, the modes characterized by modal wavevectors on or near the circle defining the free wavenumber of the plate (i.e., those where $k_{mn} \approx k_p(\omega_{MN})$) respond more strongly to modal forces than do those modes characterized by modal wavevectors well inside or outside that circle. By equation (4-220), the magnitude of the relative response of resonant to nonresonant modes depends on both the damping and the relative magnitudes of the modal and free wavenumbers.

Let us now examine how knowledge of the magnitudes of the maximum wavevector contributions from the various terms in the summation of equation (4-217) can be used to gain insight into the wavevector characteristics of $W(\underline{k},\omega)$ at a fixed, but arbitrary, frequency, ω_0. We assume that the plate properties and dimensions are known and, therefore, that the modal natural frequencies, modal wavevectors, and the damping are known quantities. We also assume that the modal forces are known. We know, from basic vibration theory, that the response of the plate will be greatest at the modal natural frequencies of the plate. Therefore, the characteristics of $W(\underline{k},\omega)$ at these natural frequencies are of primary interest. Let us therefore examine the characteristics of $W(\underline{k},\omega_{MN})$, where ω_{MN} is the natural frequency of the MN-th mode of the plate.

By equation (4-71) and (4-217),

$$W(\underline{k},\omega_{MN}) = \frac{1}{D}\sum_{m=1}^{\infty}\sum_{n=1}^{\infty}\frac{B_{mn}(\omega_{MN})I_{mn}(\underline{k})}{k_{mn}{}^4 - k_{MN}{}^4 + ir\omega_{MN}/D} . \tag{4-221}$$

By our previous arguments, we know that the maximum, in magnitude, wavevector contributions to $W(\underline{k},\omega_{MN})$ from each term occur at the mn-th modal wavevectors, $\underline{k} = (\pm m\pi/L_1, \pm n\pi/L_2)$. Further, we know that $\{k_{mn}{}^4 - k_{MN}{}^4 + ir\omega_{MN}/D\}^{-1}$ is a maximum when $k_{mn} = k_{MN}$, or when $m = M$ and $n = N$. Thus, ignoring the relative magnitudes of the modal forces, we would expect significant contributions to $W(\underline{k},\omega_{MN})$ at the modal wavevectors $\underline{k} = (\pm M\pi/L_1, \pm N\pi/L_2)$. On the other hand, if we assume that one modal force, say B_{PQ}, is much larger than the others, we might also expect significant contributions to $W(\underline{k},\omega_{MN})$ at the modal wavevectors $\underline{k} = (\pm P\pi/L_1, \pm Q\pi/L_2)$. Let us first look at the relative magnitudes of the modal contributions to $W(\underline{k},\omega_{MN})$ at the wavevector $\underline{k} = (M\pi/L_1, N\pi/L_2)$.

The magnitude of the contribution from the MN-th modal term is

$$\frac{|B_{MN}(\omega_{MN})|\ |I_{MN}(M\pi/L_1, N\pi/L_2)|}{|r\omega_{MN}/D|} ,$$

and the magnitudes of the contributions from the nonreasonant terms are

$$\frac{|B_{mn}(\omega_{MN})| \; |I_{mn}(M\pi/L_1, N\pi/L_2)|}{|k_{mn}^4 - k_{MN}^4 + ir\omega_{MN}/D|} .$$

The largest nonresonant contributions will be those from modes adjacent to the resonant mode and from the mode with the large modal force, the PQ-th mode. If we assume that the closest nonresonant mode is the M-1, N-th mode, it can be established from equations (4-63) and (4-64) that

$$|I_{M-1,N}(M\pi/L_1, N\pi/L_2)| \approx (2/\pi)\,|I_{MN}(M\pi/L_1, N\pi/L_2)| . \qquad (4\text{-}222)$$

Therefore, the ratio of the magnitude of the resonant modal contribution to that of an adjacent, nonresonant mode is given by

$$\frac{\pi |B_{MN}(\omega_{MN})| \; |k_{M-1,N}^4 - k_{MN}^4 + ir\omega_{MN}/D|}{2 |B_{M-1,N}(\omega_{MN})| \; |r\omega_{MN}/D|} .$$

For modal forces of comparable magnitudes, large wavevector separations between adjacent modes, and small damping, this ratio can be large (say of the order of 10). Conversely, for small modal separations, large damping, and comparable modal forces, this ratio is just slightly greater than 1. If the M-1,N-th mode were subjected to a much larger modal force than the MN-th mode, this ratio could be less than 1.

Consider now the magnitude of the contribution from the PQ-th mode (where the modal force is significantly larger than other modal forces) to $W(M\pi/L_1, N\pi/L_2, \omega_{MN})$. Because we have already looked at the contributions of adjacent modes, we will assume that the PQ-th mode is somewhat removed from the resonant MN-th mode. The magnitude of the contribution from the PQ-th mode to $W(M\pi/L_1, N\pi/L_2, \omega_{MN})$ is given by

$$\frac{|B_{PQ}(\omega_{MN})| \; |I_{PQ}(M\pi/L_1, N\pi/L_2)|}{|k_{PQ}^4 - k_{MN}^4 + ir\omega_{MN}/D|} .$$

However, for |M-P| and |N-Q| greater than 2, we can show that

$$|I_{PQ}(M\pi/L_1, N\pi/L_2)| \le \frac{|I_{PQ}(P\pi/L_1, Q\pi/L_2)|}{|M - P| \; |N - Q|} = \frac{|I_{MN}(M\pi/L_1, N\pi/L_2)|}{|M - P| \; |N - Q|} .$$

Thus, the ratio of the magnitude of the resonant MN-th modal contribution to $W(M\pi/L_1,N\pi/L_2,\omega_{MN})$ to the magnitude of the PQ-th modal contribution can be shown to be equal to or greater than

$$\frac{|B_{MN}(\omega_{MN})|\ |M-P|\ |N-Q|\ |k_{PQ}{}^4 - k_{MN}{}^4 + ir\omega_{MN}/D|}{|B_{PQ}(\omega_{MN})|\ |r\omega_{MN}/D|} .$$

Because we have assumed that $|M-P|$ and $|N-Q|$ are both greater than 2, it follows that, when the modal separations are sufficiently large and the damping sufficiently small that

$$\frac{|k_{PQ}{}^4 - k_{MN}{}^4 + ir\omega_{MN}/D|}{|r\omega_{MN}/D|} \approx 10 ,$$

the magnitude of the PQ-th modal force must be nearly two orders of magnitude greater than that of the MN-th modal force in order for the magnitude of the PQ-th modal contribution to be of the order of the magnitude of the MN-th modal contribution.

By the above arguments, it follows that, for sufficiently large modal separations, sufficiently small damping, and modal forces that exhibit large variations in magnitude only at modes well removed from resonance, the magnitude of the resonant MN-th modal contribution to $W(M\pi/L_1,N\pi/L_2,\omega_{MN})$ is at least an order of magnitude greater than the magnitudes of each of the other modal contributions. It is also easily verified that the phases of the various modal contributions vary with the mode numbers m and n. Therefore, if we envision each modal contribution as a vector, it is reasonable to argue that the sum of one large vector (the MN-th contribution) with many small vectors of random direction (the nonresonant modal contributions) results in a vector nearly equal to the original large vector. By this argument, it follows that, under the above restrictions,

$$|W(M\pi/L_1,N\pi/L_2,\omega_{MN})| \approx \frac{|B_{MN}(\omega_{MN})|\ |I_{MN}(M\pi/L_1,N\pi/L_2)|}{D|r\omega_{MN}/D|} . \qquad (4\text{-}223)$$

This estimate is also valid at the other three wavevectors associated with the MN-th mode: that is, at $\underline{k} = (-M\pi/L_1, N\pi/L_2)$, $\underline{k} = (M\pi/L_1, -N\pi/L_2)$, and $\underline{k} = (-M\pi/L_1, -N\pi/L_2)$.

As we relax the restrictions on modal separation, damping, and variations in modal forces, the contributions from some of the nonresonant modes increase, and the estimate of the magnitude of $W(\underline{k}, \omega_{MN})$ at the resonance wavevectors by the maximum magnitude of the MN-th modal term becomes a poorer one. Inasmuch as the magnitude of a sum is less than or equal to the sum of the magnitudes, the estimate of the magnitude of $W(M\pi/L_1, N\pi/L_2, \omega_{MN})$ under these relaxed conditions will likely decrease from its true value. However, for reasonable relaxations of these conditions, it is likely that $W(\underline{k}, \omega_{MN})$ will still exhibit relative maxima in the neighborhoods of $\underline{k} = (\pm M\pi/L_1, \pm N\pi/L_2)$.

Arguments similar to the above may be applied to estimate the magnitude of $W(\underline{k}, \omega_{MN})$ at the modal wavevector $\underline{k} = (P\pi/L_1, Q\pi/L_2)$ associated with the modal force that was assumed large in comparison with the others. By such arguments, it can be demonstrated that, at $\underline{k} = (P\pi/L_1, Q\pi/L_2)$ and $\omega = \omega_{MN}$, the ratio of the magnitude of the PQ-th modal contribution to that of the MN-th contribution is given by

$$\frac{|B_{PQ}(\omega_{MN})|\,|M - P|\,|N - Q|\,|r\omega_{MN}/D|}{|B_{MN}(\omega_{MN})|\,|k_{PQ}^{\,4} - k_{MN}^{\,4} + ir\omega_{MN}/D|} .$$

If we again assume values of damping and modal wavevector separations such that

$$\frac{|k_{PQ}^{\,4} - k_{MN}^{\,4} + ir\omega_{MN}/D|}{|r\omega_{MN}/D|} \approx 10 ,$$

then, because we have assumed that $|M-P|$ and $|N-Q|$ are both greater than 2, it follows that the ratio of the magnitude of the PQ-th contribution to that of the MN-th contribution is of the order $|B_{PQ}(\omega_{MN})| / |B_{MN}(\omega_{MN})|$. Thus, if $|B_{PQ}(\omega_{MN})|$ is an order of magnitude larger than $|B_{MN}(\omega_{MN})|$, then, by the arguments presented previously, the magnitude of $W(P\pi/L_1, Q\pi/L_2, \omega_{MN})$

can be approximated by

$$|W(P\pi/L_1, Q\pi/L_2, \omega_{MN})| \approx \frac{|I_{PQ}(P\pi/L_1, Q\pi/L_2)|\, |B_{PQ}(\omega_{MN})|}{D|k_{PQ}{}^4 - k_{MN}{}^4 + ir\omega_{MN}/D|} . \qquad (4\text{-}224)$$

It is interesting to compare this estimate with the estimate of the magnitude of $W(\pm M\pi/L_1, \pm N\pi/L_2, \omega_{MN})$ obtained previously under similar assumptions of damping, modal separations, and relative magnitudes of modal forces. By equations (4-223) and (4-224), we can show

$$\frac{|W(M\pi/L_1, N\pi/L_2, \omega_{MN})|}{|W(P\pi/L_1, Q\pi/L_2, \omega_{MN})|} \approx \frac{|B_{MN}(\omega_{MN})|\, |k_{PQ}{}^4 - k_{MN}{}^4 + ir\omega_{MN}/D|}{|B_{PQ}(\omega_{MN})|\, |\omega_{MN}/D|} . \qquad (4\text{-}225)$$

For the small damping, large modal separations and relative magnitudes of modal forces used to obtain equations (4-223) and (4-224), this ratio is of the order of unity. Thus, we can conclude that the magnitude of $W(\underline{k},\omega)$ at the resonance frequency ω_{MN} is characterized by equally large contributions at the four wavevectors $\underline{k} = (\pm M\pi/L_1, \pm N\pi/L_2)$ associated with the resonance of the MN-th mode and at the four wavevectors $\underline{k} = (\pm P\pi/L_1, \pm Q\pi/L_2)$ associated with the modal response of the strongly driven PQ-th mode.

The reader should be reminded once again that the above approximations, and thereby the above conclusions, are strictly valid only for small damping, large modal separations, and the ratios of modal force magnitudes used for their derivations. However, it is likely that, under reasonable relaxations of these restrictions, the magnitude of $W(\underline{k},\omega)$ at a resonance frequency ω_{MN} will be relatively large in the neighborhoods of those modal wavevectors associated with resonances and in the neighborhoods of those modal wavevectors associated with relatively large modal forces. Indeed, it seems reasonable to expect that, at any frequency, the magnitude of the $W(\underline{k},\omega)$ will be relatively large in the neighborhoods of the (four) modal wavevectors associated with each resonant or near-resonant mode and in the neighborhoods of the modal wavevectors associated with relatively large modal forces. The exact wavevector locations of these relative maxima of $|W(\underline{k},\omega)|$ will depend on the relative separation between the modal wavevectors associated with the

resonant and near-resonant modes and on the exact distribution of modal forces. To the degree that such an extension of the highly specialized example presented above is a valid one, the plot of the modal wavevectors and the radius of the free wavenumber shown in figure 4-7 can be a useful tool for identifying potentially large wavevector contributions to $W(\underline{k},\omega)$.

As stated previously, the two-wavevector-frequency response, $G(\underline{k},\underline{\alpha},\omega)$, can be treated as a special case of the wavevector-frequency description of the forced displacement field, $W(\underline{k},\omega)$, of the simply supported plate. That is, $G(\underline{k},\underline{\alpha},\omega)$ is the wavevector-frequency transform of the displacement field when the space-time forcing field is the single complex wave given by $(1/2\pi)\exp\{-i(\underline{\alpha}\cdot\underline{x} - \omega t)\}$. As can be seen, by comparison of equations (4-214) and (4-217), the modal forces associated with this forcing field are $I_{mn}(\underline{\alpha})$, independent of the frequency characterizing the forcing wave.

By applying arguments similar to those used to investigate the wavevector behavior of $W(\underline{k},\omega)$, the most significant wavevector-frequency characteristics of $G(\underline{k},\underline{\alpha},\omega)$ can be deduced. Inasmuch as the procedure used to identify these characteristics is identical to that employed previously, we will omit the details of this deduction process. However, the reader is encouraged to perform such a detailed analysis to gain familiarity and confidence with this predictive technique.

Consider first the response of the plate to the wave $\exp\{-i(P\pi x_1/L_1 + Q\pi x_2/L_2 - \omega_{MN}t)\}$; thus, $\underline{\alpha} = (P\pi/L_1, Q\pi/L_2)$, one of the four modal wavevectors of the PQ-th mode of the plate, and $\omega = \omega_{MN}$, the natural frequency of the MN-th mode. It is straightforward to show that for small damping, large modal separations, and $|P-M|$ and $|Q-N|$ greater than 2, the largest contributions to $|G(\underline{k};P\pi/L_1,Q\pi/L_2;\omega_{MN})|$ occur at the four wavevectors, $\underline{k} = (\pm M\pi/L_1, \pm N\pi/L_2)$, associated with the resonant MN-th mode and at the four wavevectors, $\underline{k} = (\pm P\pi/L_1, \pm Q\pi/L_2)$, associated with the mode that includes the wavevector of excitation. The relative magnitudes of the contributions at the resonant modal wavevectors and at the modal wavevectors associated with the input depend on the exact values of the damping, the modal separation, and the differences $|P-M|$ and $|Q-N|$. It should be recognized that $G(\underline{k},\omega)$ is zero in this example when $\omega \neq \omega_{MN}$.

It is easily shown that if the plate is forced at resonance, i.e., by $\exp\{-i(M\pi x_1/L_1 + N\pi x_2/L_2 - \omega_{MN}t)\}$, $|G(\underline{k};M\pi/L_1,N\pi/L_2;\omega_{MN})|$ is characterized by only four large contributions: one at each of the modal wavevectors $\underline{k} = (\pm M\pi/L_1,\pm N\pi/L_2)$.

By extending these results to arbitrary wavevectors and frequencies of excitation, it appears that the magnitude of $G(\underline{k},\underline{\alpha},\omega)$, at the frequency of excitation, will be relatively large in the neighborhoods of the four modal wavevectors associated with each resonant or near-resonant mode and in the neighborhoods of those modal wavevectors that have a member close in amplitude and direction to the wavevector characterizing the wave input to the plate. The exact wavevector locations of these relative maxima of $|G(\underline{k},\underline{\alpha},\omega)|$ will depend on the relative separation between the modal wavevectors associated with the resonant and near-resonant modes and on the wavevector characterizing the single wave excitation of the plate.

By the arguments presented above, we have demonstrated two important features of the wavevector-frequency response of the space-limited plate. The first is that the plate responds most strongly, at any given frequency, to those wave components of the input field that are characterized by wavevectors closest, in magnitude, to the free wavenumber of the plate. The second is that any single wavevector-frequency component of excitation to the plate produces, at the frequency of excitation, a strong response at not only those modal wavevectors with members most nearly coinciding with the wavevector of excitation, but also at those modal wavevectors close, in magnitude, to the free wavenumber of the plate. These resonant components of the plate motion are a consequence of the reflections (or wavevector scattering) of the forced waves at the boundaries of the plate.

4.3.3.3 Observations From Illustrative Examples. The two relatively simple examples of space-limited systems presented above provide ample evidence that the analysis and interpretation of the wavevector-frequency characteristics of space-limited systems is a considerably more complex task than that of analyzing and interpreting space-invariant systems in the wavevector-frequency domain.

By use of these examples, we have shown that the wavevector-frequency response of space-limited systems has two characteristics in common with the wavevector-frequency response of space-invariant systems. The first characteristic is that both space-limited and space-invariant systems respond most strongly, at any frequency, to wavevector components of excitation equal, in magnitude, to the free wavevector of the system. The second common characteristic is that the magnitudes of the wavevector-frequency transform of the output field of both space-limited and space-invariant systems exhibit, at any given frequency, relative maxima in the neighborhoods of those wavevectors characterizing relatively large inputs to the system.

However, the example of the simply supported plate illustrates a characteristic of the wavevector-frequency response of space-limited systems not encountered in space-invariant systems. That characteristic is wavevector scattering (or conversion). Recall that in space- (and time-) invariant systems, a single wavevector-frequency component of input produces only a single wavevector-frequency component of response, with that response component occurring at the wavevector and frequency characterizing the input. In the space-limited system of the simply supported plate, we found that a single wavevector-frequency component of input produced, at any frequency, a continuum of wavevector components in the output as a result of reflection, or scattering, of the input wave from the boundaries of the plate. The largest (in magnitude) components in the output field occurred at the (four) modal wavevectors associated with each resonant (or near-resonant) mode at that frequency and at the modal wavevectors with members nearly equal to the wavevector of excitation. The most important feature of this wavevector scattering is the excitation of wavevector components close, in magnitude, to that of the free wavenumber of the plate by inputs characterized by wavevectors far removed, in their magnitudes, from the free wavenumber.

4.4 REFERENCES

1. L. M. Kells, Elementary Differential Equations, McGraw-Hill Book Co., New York, 1954, p. 124.

2. W. T. Thompson, Vibration Theory and Applications, Prentice-Hall, Inc., Englewood Hills, NJ, 1965, pp. 264-268.

3. P. M. Morse, Vibration and Sound, second edition, McGraw-Hill Book Co., New York, 1948, pp. 83-87.

4. L. Meirovitch, Analytical Methods in Vibrations, The Macmillan Co., New York, 1967, pp. 179-185.

5. Ibid., pp. 184-185.

6. P. M. Morse and H. Feshbach, Methods of Theoretical Physics, Part I, McGraw-Hill Book Co., New York, 1953, pp. 791-895.

7. R. Courant and D. Hilbert, Methods of Mathematical-Physics, Interscience Publishers, Inc., New York, 1952, pp. 351-388.

8. M. D. Greenberg, Applications of Green's Functions in Science and Engineering, Prentice-Hall, Inc., Englewood Hills, NJ, 1971.

9. J. Ffowcs-Williams et al., Modern Methods for Flow Noise Analysis, Volume I, Unpublished Course Notes, Department of Mathematics, Imperial College, London, 1969, chapter 4.

10. Morse and Feshbach, op. cit., pp. 896-997.

11. Courant and Hilbert, op. cit., pp. 112-163.

12. A. Papoulis, The Fourier Integral and Its Applications, McGraw-Hill Book Co., New York, 1962, p. 38.

13. G. Maidanik, "Surface Impedance Discontinuities as Wavevector Converters," Journal of the Acoustical Society of America, vol. 46, no. 5, November 1969, pp. 1062-1073.

14. R. V. Churchill, Introduction to Complex Variables and Applications, McGraw-Hill Book Co., New York, 1948, p. 90.

CHAPTER 5
COUPLED LINEAR SYSTEMS

The spatially distributed, time-invariant linear systems treated in the previous two chapters have consisted of a single physical component, such as a string, a plate, or an acoustic fluid. However, in such specialized fields as structural acoustics, musical acoustics, architectural acoustics, and noise, the systems of practical interest are comprised of multiple interacting physical components. This chapter addresses the response of spatially distributed, time-invariant linear systems comprised of more than one physical component.

5.1 FUNDAMENTAL CONCEPTS OF COUPLED SYSTEMS

In section 3.1 of chapter 3, we defined a system as "an aggregation or assemblage of interacting elements combined by man or nature to form an integral entity." In a spatially distributed system comprised of a single physical component, the "interacting elements" of the system are differential lengths, areas, or volumes (as appropriate) of the physical component under scrutiny. For a spatially distributed system comprised of multiple interacting physical components, the "interacting elements" of the composite system are the individual physical components of the system. Thus, we see that for a spatially distributed single component system, the elements of the system are of microscopic spatial scale, whereas for a spatially distributed multicomponent system, the elements of the composite system are of macroscopic scale. This difference in spatial scale, though initially somewhat confusing, is simply a consequence of defining a system in terms of "interacting elements."

The macroscopic spatial scale of the elements of a system comprised of multiple physical components does present a dilemma. It has been demonstrated, by the illustrative examples of the preceding chapters, that the spatial scale of the interacting elements of a system corresponds to the

spatial detail to which the system and its response can be described. Further, by definition, the wavevector-frequency description of the response of a system requires knowledge of the system response over all space and time. Clearly then, the macroscopic spatial scales associated with the various physical components of a multicomponent system are not compatible with a wavevector-frequency description of that system.

The solution to this dilemma is really quite simple. We define each physical component (or interacting element) of the multicomponent system to be a subsystem. Each subsystem is now a single component system and is comprised of elements having spatial scales of differential order. The various subsystems are then coupled in accordance with the interactions between the various physical components (or macroscopic elements) of the composite system.

By these arguments, a spatially distributed system comprised of several (say N) interacting physical components can be interpreted as an assemblage of N-coupled subsystems, where each subsystem represents a single physical component of the composite system, and the couplings between the subsystems are chosen to reflect the appropriate interactions between the physical components of the composite system. The title of this chapter, Coupled Linear Systems, was chosen to reflect this interpretation of, and approach to, spatially distributed, time-invariant multicomponent linear systems.

5.1.1 The Causes and Effects of Coupling

Consider a system comprised of several interacting physical components. For an interaction to exist between any two of the various physical components, those components must be either in physical contact, physically connected through one or more of the other components of the system, or subject to some physical field that induces mutual forces between the two components. In the interpretation of a multicomponent system as an assemblage of coupled single component subsystems, the interactions between the various physical components of the composite system define the couplings between the various subsystems. The specific nature of the coupling between any two subsystems can be determined only by examining the physics of the particular interaction between the corresponding components of the composite system.

However, certain characteristics of the coupling between subsystems and, in some cases, of the physical subsystems themselves can be deduced from the specific form of the interaction between them.

Consider the situation in which the interaction between two components of the composite system results from physical contact between the components. The line or surface of physical contact between the two components establishes a spatial boundary common to both components. It therefore follows that the coupling between the physical subsystems corresponding to these components occurs at the boundaries of the subsystems. It further follows that the physical subsystems corresponding to these components are space limited.

Arguments similar to the above apply when the interaction between two components of a composite system results from an interconnection of these components via one or more of the other components of the composite system. That is, the lines or surfaces of physical contact between the components of interest and the interconnecting component(s) establish spatial boundaries for both components of interest, thereby spatially limiting the corresponding physical subsystems. In addition, the coupling between these physical subsystems acts at these boundaries.

Two components of a composite system can interact through the presence of some field of physical origin (an electromagnetic field, for example) between the components. Such fields can produce interactive forces between components at the atomic or molecular level in the absence of any physical contact between the components. It follows that, in the presence of such interactions between components, the coupling between the associated physical subsystems acts not only at the boundaries of the subsystems, but can act between any of the (differential scale) elements of the two subsystems. All physical subsystems associated with a multicomponent system are, of course, space limited inasmuch as two components cannot simultaneously occupy all of space.

5.1.2 Classification of Coupled Systems

From the above discussion, it would appear that, inasmuch as each of the various physical subsystems associated with a given multicomponent system is

space limited, all coupled systems are space limited. However, the reader should recall (from chapter 3) that a distinction is made between a physical system and the mathematical model of a system and that a system (or subsystem) is classified on the basis of the mathematical model. Thus, while it is true that all physical subsystems associated with a multicomponent system are space limited, it does not necessarily follow that the mathematical model of each subsystem is space limited. If, for example, one physical component of a multicomponent system was a large flat plate, it might prove useful or convenient to mathematically model the plate subsystem as a flat plate of infinite extent. As demonstrated in chapter 3, the mathematical model of the infinite flat plate is linear and space invariant. Clearly then, the mathematical models of all subsystems associated with a multicomponent system need not be space limited.

If we interpret a multicomponent system as an assemblage of coupled subsystems, it follows that the mathematical model of a multicomponent system is formulated by appropriately coupling the assemblage of mathematical models corresponding to these subsystems. By the arguments presented above, the mathematical models of these subsystems can be either space invariant or space limited, as appropriate. The question to be addressed in this section is, given such an assemblage of coupled space-invariant and space-limited subsystems, how does one determine the classification of the mathematical model of the resultant coupled system?

The answer to this question is again quite simple: the classification of the mathematical model of a multicomponent system (or any system, for that matter) is determined by examination of the mathematical form of relationship between the input and output of the system. Recall, first, that all systems (and subsystems) treated in this text are linear and time invariant. For space-invariant forms of such systems, we showed in chapter 3 that the relationship between the space-time descriptions of the input and output fields was of the mathematical form of equation (3-52). The associated relationship between the wavevector-frequency descriptions of the input and output fields of a space-invariant system was shown to have the simpler mathematical form given by equation (3-59). In chapter 4, corresponding relationships were developed between the input and output fields of

space-varying systems in both the space-time and wavevector-frequency domains. The respective mathematical forms of these relationships are given in equations (4-128) and (4-129). Thus, to establish the appropriate classification of a multicomponent system, it is only necessary to determine whether the input-output relationship for the composite system, in either the space-time or wavevector-frequency domain, has the mathematical form corresponding to a space-varying or space-invariant system.

Although the mathematical form of the input-output relationship is the unambiguous indicator of the classification of a multicomponent system, it can be demonstrated, for a wide assortment of coupled systems, that the presence of a single space-varying subsystem renders the associated composite system space varying. The reader is encouraged to test this assertion for various coupled combinations of space-varying and space-invariant subsystems. This exercise will, in addition to lending credence to the above assertion, demonstrate the advantage, in mathematical simplicity, of formulating such input-output relationships in the wavevector-frequency domain rather than in the space-time domain.

Recall, from chapter 3, that the specification of a systems problem requires definition of the input to, and output from, the system, as well as the definition of the interacting elements comprising the system. Given these definitions, a mathematical model of the system can be formulated. In a multicomponent system, an input can be applied to any one, or several, of the physical components comprising the system. Further, the output can alternatively be defined to be the response of any component, or the interaction between any components, of the composite system. Clearly, given a specific assemblage of interacting physical components and a specific input, many multi-element systems problems can be specified merely by redefinition of the output. However, it must be realized that each redefinition of the output results in a modification of the mathematical model of the composite system and, potentially, in the classification of that system.

5.1.3 The Coupled System of the Fluid-Loaded Plate

To add perspective to some of the concepts discussed above, it is convenient to introduce, at this point, a relatively simple spatially

distributed, time-invariant linear multicomponent system that will be used in this chapter as an illustrative example. This example is the forced vibration of a large flat plate with an acoustic fluid on one side and a vacuum on the other. The physical system consists of two interacting elements: the plate and the acoustic fluid. The vacuum, being an absence of matter, plays no part in the dynamic motion of the plate. The plate is excited into motion by a distribution of force per unit area, $f(\underline{x},t)$, applied on the vacuum side of the plate. We wish to determine the resultant displacement field, $w(\underline{x},t)$, of the plate.

The geometry of this system is illustrated in figure 5-1. Here, the central (or neutral) plane of the large flat plate is taken to be coincident with the plane defined by $x_3 = 0$. The half space defined by $x_3 > 0$ is occupied by an acoustic fluid of density ρ and speed of sound c. The half-space $x_3 < 0$ is vacuous. The force per unit area, $f(\underline{x},t)$, applied to the vacuous side of the plate and the displacement of the plate, $w(\underline{x},t)$, are taken to be positive in the positive x_3 direction.

The first step in the formulation of a mathematical model of the system is to interpret the two interacting elements of the composite plate-fluid system as two appropriately coupled single component subsystems. If we assume that the large flat plate can be considered to be thin and of infinite extent, it follows that the respective interacting elements of these two subsystems are (1) the differential area segments comprising the infinite plate and (2) the differential volume segments of the acoustic fluid occupying the half-space $x_3 > 0$. To complete the specification of these two coupled single component subsystems, we need to define (1) the inputs to each subsystem, (2) the outputs from each subsystem, and (3) the nature of the coupling between subsystems. This definition process is facilitated by examining the sequence of physical processes that occur in the infinite plate and acoustic half space subsequent to the excitation of the plate by the externally applied input, $f(\underline{x},t)$.

This sequence of physical processes, which is illustrated in figure 5-2, proceeds as follows. The externally applied input, $f(\underline{x},t)$, excites a vibration displacement field, $w(\underline{x},t)$, in the infinite plate. Because the

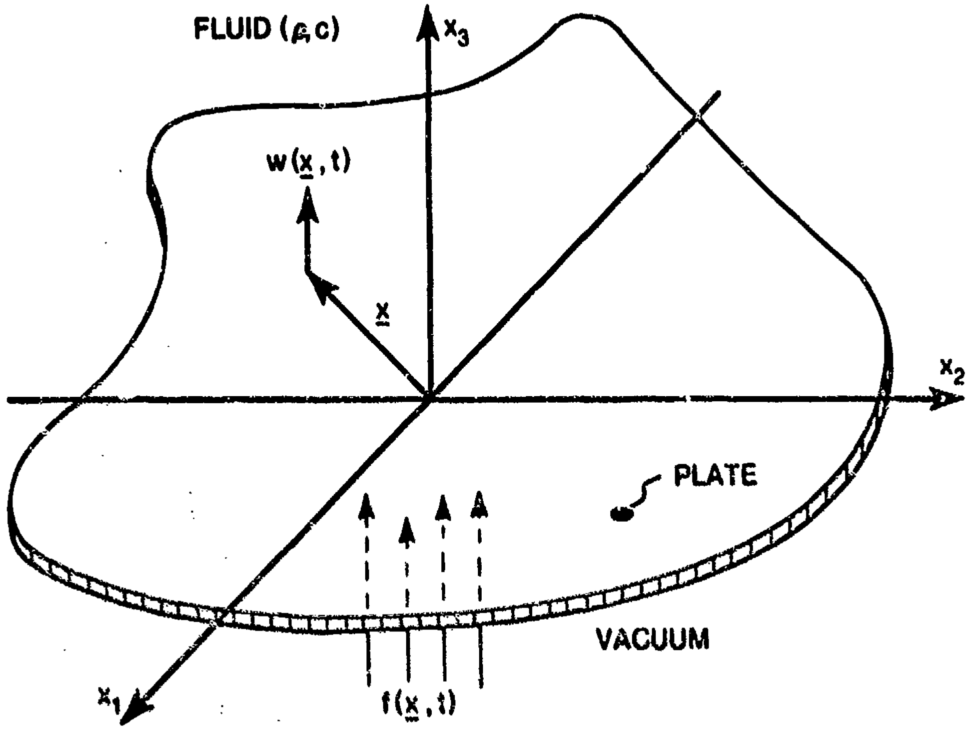

Figure 5-1. Geometry of Fluid-Loaded Plate

plate and fluid are in contact at the top surface of the plate, the displacement field of the plate is imposed on the fluid at this boundary, thereby exciting a pressure field, $p(\underline{x},x_3,t)$, in the acoustic half space. This pressure field, acting on the top surface of the plate, produces an additional input field, $p(\underline{x},0,t)$, to the plate that acts opposite in direction to the external input, $f(\underline{x},t)$. We have assumed here that, with respect to the acoustic half space, the plate is of infinitesimal thickness. Further, we have applied the law of conservation of mass (or continuity), which requires that the displacement field of the plate and the component of the displacement field of the fluid normal to the plane of the plate be equal at the plate-fluid interface ($x_3 = 0$).

By means of the above arguments and figure 5-2, we can completely specify the subsystems associated with the infinite plate and the acoustic half-space components of the composite plate-fluid system and the coupling between them. The elements of the infinite plate subsystem are subjected to two inputs: the externally imposed input, $f(\underline{x},t)$, and the oppositely directed pressure field, $p(\underline{x},0,t)$, that is induced in the acoustic half space and acts on the upper

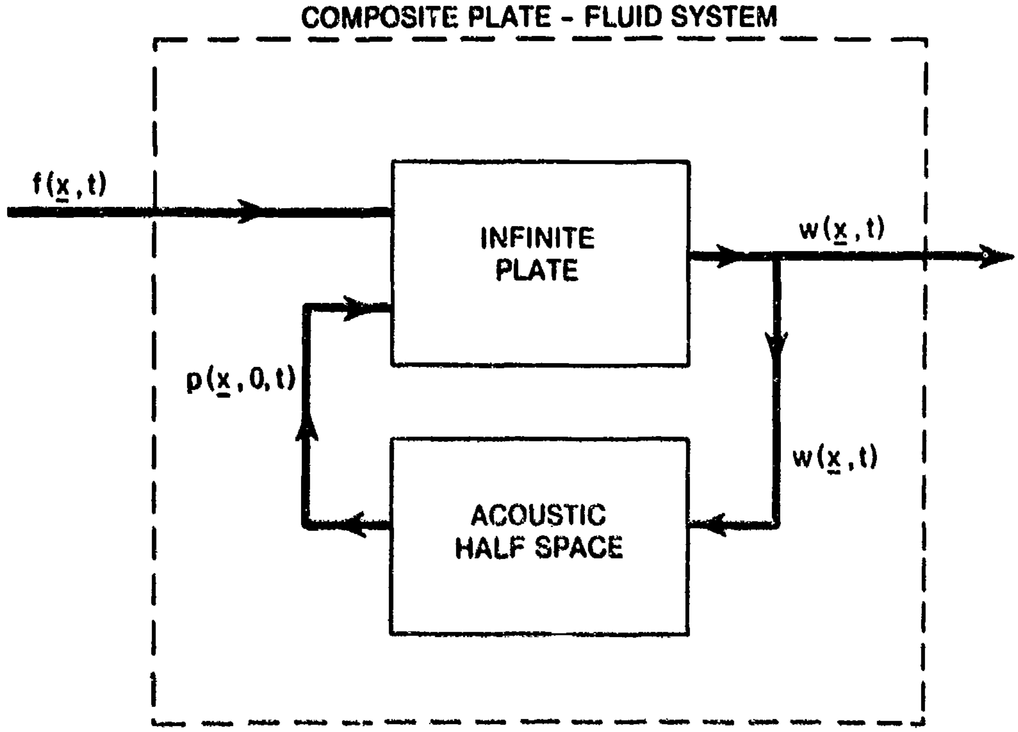

Figure 5-2. Schematic Diagram of the Fluid-Loaded Infinite Plate System

surface of the plate. The only output of consequence from the infinite plate is the vibratory displacement field of the plate, $w(\underline{x},t)$. With the exception of the additional input of the pressure field from the half space, the infinite plate subsystem is identical to the infinite plate system treated in chapter 3 as an illustrative example of a forced, linear, space- and time-invariant system.

Contrary to the impression conveyed by figure 5-2, no inputs (or sources) are applied to all elements of the acoustic half space. Rather, the connection of the output of the infinite plate subsystem to the acoustic half-space subsystem in figure 5-2 indicates that the half-space subsystem is coupled to the infinite plate subsystem via the displacement field of the plate. In this coupling, the displacement of each element of the plate (measured normal to the plane of the plate) is imposed on the contacting element of the acoustic half space over the planar boundary of the half space, $x_3 = 0$, prescribed by the plate. The pressure field in the half space results solely from this imposition of the displacement field of the plate on the boundary of the half space. The quantity of interest, or output, from the

acoustic half-space subsystem is the acoustic pressure field over the planar surface, $x_3 = 0$, that defines the plate-fluid interface. The subsystem associated with the acoustic fluid component of the composite plate-fluid system is a special case of the linear, time-invariant, space-limited acoustic half-space system treated in section 4.3.3.1 of chapter 4.

In identifying the subsystem associated with the acoustic fluid as a special case of the space-limited acoustic half-space system treated in section 4.3.3.1, the words "special case" must be emphasized. The system treated in section 4.3.3.1 was that of the pressure field produced in the acoustic half-space $x_3 \geq 0$ as a result of a prescribed displacement field applied to the boundary of the half space at $x_3 = 0$. This system was shown to be space invariant in the x_1 and x_2 coordinate directions but, owing to the boundary at $x_3 = 0$. space limited in the x_3 coordinate direction. Consequently, this acoustic half-space system was classified as a space-limited system. The subsystem associated with the acoustic fluid component of the composite plate-fluid system is a special case of the half-space system treated in section 4.3.3.1, because the output of this subsystem is the pressure field over the two-dimensional surface defined by $x_3 = 0$, a subset of the three-dimensional half-space $x_3 \geq 0$. However, inasmuch as the pressure field over the plane $x_3 = 0$ (or, for that matter, any plane of constant x_3) is independent of x_3, it is space invariant. Consequently, as can be demonstrated by comparison of the mathematical forms of the input-output relationships of equations (4-159) (at $x_3 = 0$) and (3-59), the subsystem associated with the acoustic fluid component of the composite plate-fluid system is space invariant.

By the use of figure 5-2 and the above arguments, we have defined the coupled plate and acoustic fluid subsystems that will be used to mathematically model the composite system of the fluid-loaded plate. Both subsystems have been argued to be linear, time invariant, and space invariant. It therefore follows that the mathematical model of the composite plate-fluid system is also linear, time invariant, and space invariant.

By reference to figure 5-2, it is evident that the plate and acoustic fluid subsystems are mutually coupled. That is, the acoustic fluid subsystem

is coupled to the plate subsystem through the common displacement field at the interface of these two systems. In addition, the plate subsystem is coupled to the acoustic fluid subsystem by means of the pressure field exerted, by the fluid, on the upper surface of the plate. Because of this mutual coupling, the composite plate-fluid system is a form of feedback system. That is, the output of the composite system (the displacement field of the plate) is fed back through the acoustic fluid subsystem to produce a pressure field that augments the input to the composite system, $f(\underline{x},t)$, in exciting the infinite plate subsystem.

Recall (see figure 5-2) that the input to the composite plate-fluid system described above is the force per unit area, $f(\underline{x},t)$, applied to the infinite plate subsystem and the output was defined to be the displacement field of the plate, $w(\underline{x},t)$. If we redefine the output of the composite system to be the pressure field, $p(\underline{x},x_3,t)$, throughout the acoustic half-space $x_3 \geq 0$ rather than the displacement field of the plate, we specify a new composite system that has the same physical elements (or components) and the same interactions between components as the composite system used to predict the displacement field. The redefinition of the output, therefore, has no effect on the definition of the interacting elements of the two subsystems associated with the plate and acoustic fluid components of the composite system.

To complete the specification of the coupled subsystems associated with this new composite system, we again trace the sequence of physical processes occurring subsequent to the excitation of the plate to define the inputs, outputs, and couplings associated with these subsystems. A schematic diagram of these processes is shown in figure 5-3.

A comparison of figures 5-2 and 5-3 reveals that the primary difference between the coupled subsystems that define the mathematical model for the displacement of the plate and those that define the mathematical model for the pressure field in the half space is the subsystem associated with the acoustic half space. As shown in figure 5-3, the output of the acoustic half-space subsystem is the pressure field over the entire half space. This output, in addition to being defined as the output of the composite plate-fluid system, is spatially filtered such that the pressure field at the surface of the plate

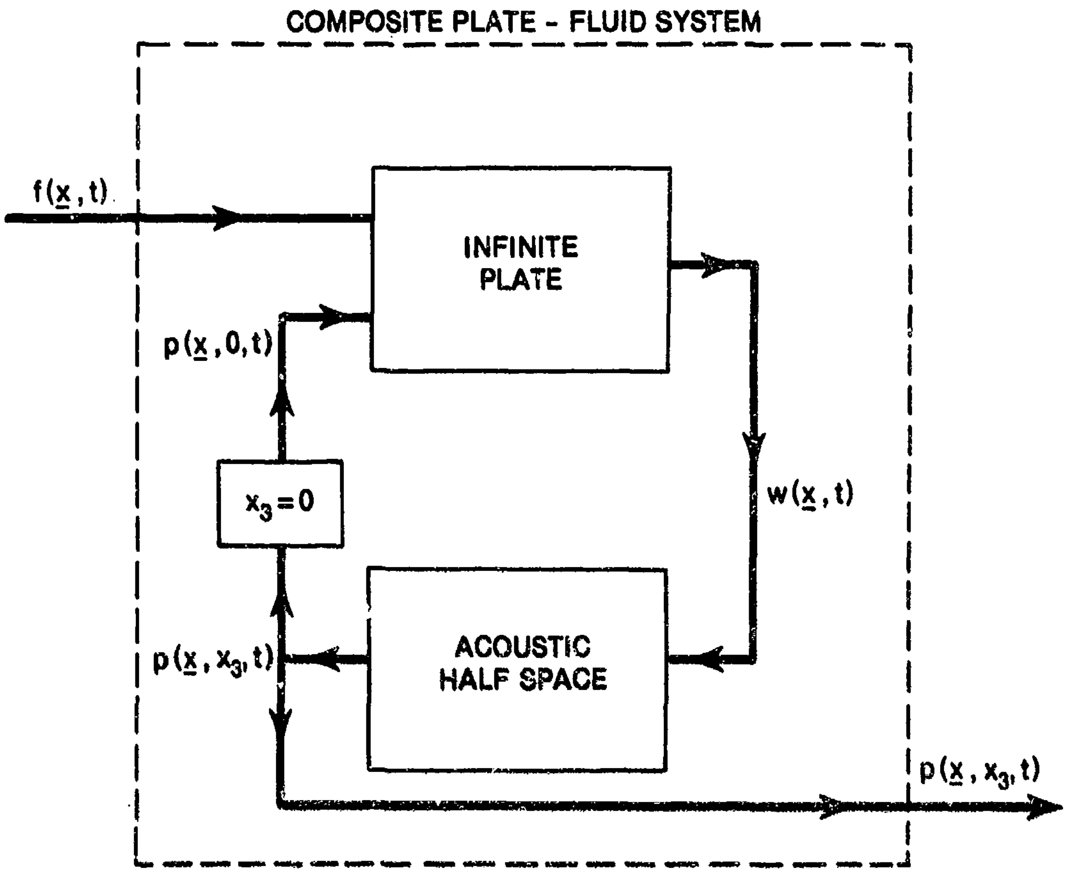

Figure 5-3. Schematic Systems Diagram for the Pressure Field Produced by the Forced Vibration of an Infinite Flat Plate

(i.e., at $x_3 = 0$) acts as an additional input to the plate. For the coupled system shown in figure 5-2, this spatial filtering was incorporated in the acoustic half-space subsystem so that the output of that subsystem was the pressure field at the surface of the plate, $p(\underline{x},0,t)$.

By the above arguments, it is evident that the redefinition of the output of the composite plate-fluid system from the displacement field of the plate to the pressure field over the entire acoustic half space requires a redefinition of the acoustic half-space subsystem, but not of the infinite plate subsystem or the couplings between the subsystems. This redefined acoustic half-space subsystem is exactly that linear, time-invariant, space-limited,acoustic half-space system treated in section 4.3.3.1 of chapter 4. Inasmuch as one of the two coupled subsystems that forms the basis of the mathematical model for the pressure field produced by the forced

vibration of an infinite, flat plate is space varying, it follows that the redefined composite system is space varying.

The above examples demonstrate that changing the definition of the output from a specific assemblage of interacting physical components can effect a change in (1) the specification and classification of one or more of the single component subsystems used to mathematically model the multicomponent system and (2) the classification of the multicomponent system itself.

5.2 THE FREE RESPONSE OF COUPLED SYSTEMS

By definition, the free response of a multicomponent system is the self-sustained output of that system in the absence of any externally applied input. Recall that, in the absence of any input to the system, the initiation of the output field of the system cannot be addressed but, given certain knowledge of the output at any specific time, the output can be determined for all time.

Because the mathematical model of a multicomponent system is formulated by interpreting that composite system as an assemblage of coupled subsystems, the determination of the free response of the composite system is equivalent to determining the free response of the corresponding assemblage of coupled subsystems. The title of this section emphasizes this equivalence.

In this section, we demonstrate, by example, the procedure for formulating a mathematical model of, and obtaining a solution for, the free response of a multicomponent system. The multicomponent system addressed in this illustrative example is the displacement field of a free infinite plate subjected to fluid loading on one side. By comparing the free displacement field of the fluid-loaded plate to that of the plate in vacuo, we also examine the effects of the fluid loading on the free waves of the plate.

5.2.1. The Free Response of an Infinite Plate With Fluid Loading on One Side

The physical system and the corresponding assemblage of coupled subsystems associated with the forced vibration of a thin, infinite, flat plate with an

acoustic fluid on one side and a vacuum on the other were presented and discussed in section 5.1.3. The physical system of interest in this section is the response of that same plate, fluid loaded on one side, in the absence of the externally applied forcing field, $f(\underline{x},t)$. Thus, it follows that a mathematical model for the free displacement field of this fluid-loaded plate can be formulated from that assemblage of coupled subsystems illustrated in figure 5-2 with the forcing function, $f(\underline{x},t)$, set equal to zero.

By reference to figure 5-2, it is evident that, in the absence of an externally applied forcing field, the infinite plate subsystem represents the displacement field of the plate forced by the pressure field, $p(\underline{x},0,t)$, applied to the upper surface of the plate. The resulting displacement field of the plate is the output of the composite plate-fluid system, as well as that of the infinite plate subsystem. The forced response of a damped, infinite plate is treated in section 3.4.6. However, recall from section 3.3 that the outputs of free systems having losses cannot be described in the wavevector-frequency domain. To circumvent this difficulty, we assume the plate to be undamped. With this assumption and the recollection that the pressure field $p(\underline{x},0,t)$ is applied in the negative x_3 direction, it follows from equation (3-103) that the displacement field output from the infinite plate subsystem is governed by

$$D\nabla^4 w(\underline{x},t) + \mu \frac{\partial^2 w(\underline{x},t)}{\partial t^2} = -p(\underline{x},0,t) \qquad (5\text{-}1)$$

for all $\underline{x}$ and t. Recall that D denotes the flexural rigidity of the plate and μ represents the mass per unit area of the plate. In this text, our interest is confined to those displacement and pressure fields that can be expressed in the forms

$$w(\underline{x},t) = (2\pi)^{-3} \iint_{-\infty}^{\infty} W(\underline{k},\omega)\exp\{i(\underline{k}\cdot\underline{x} + \omega t)\}\, d\underline{k}\, d\omega \qquad (5\text{-}2)$$

and

$$p(\underline{x},0,t) = (2\pi)^{-3} \iint_{-\infty}^{\infty} P(\underline{k},0,\omega)\exp\{i(\underline{k}\cdot\underline{x} + \omega t)\}\, d\underline{k}\, d\omega\ . \qquad (5\text{-}3)$$

By using equations (5-2) and (5-3) in equation (5-1) and by recalling that equation (5-1) applies for all $\underline{x}$ and t, it follows that the wavevector-frequency descriptions of the input and output fields of the infinite plate subsystem are related by

$$W(\underline{k},\omega) = \frac{-P(\underline{k},0,\omega)}{\{Dk^4 - \mu\omega^2\}} , \tag{5-4}$$

where $k = |\underline{k}| = \sqrt{k_1^{\ 2} + k_2^{\ 2}}$. This relationship has the mathematical form shown, in equation (3-59), to be characteristic of space and time-invariant linear systems. Thus, we conclude that the infinite plate subsystem is space and time invariant.

As was stated in section 5.1.3, the subsystem associated with the acoustic fluid is a special case of the space-limited acoustic half-space system treated in section 4.3.3.1. By reference to equations (4-144) and (4-145) of section 4.3.3.1, it is evident that the output, $p(\underline{x},0,t)$, of the acoustic half-space subsystem is governed by

$$\nabla^2 p(\underline{x},x_3,t) + \frac{\partial^2 p(\underline{x},x_3,t)}{\partial x_3^{\ 2}} - \frac{1}{c^2}\frac{\partial^2 p(\underline{x},x_3,t)}{\partial t^2} = 0 , \quad x_3 > 0 , \tag{5-5}$$

and

$$\frac{\partial p(\underline{x},0,t)}{\partial x_3} = -\rho \frac{\partial^2 w(\underline{x},t)}{\partial t^2} \tag{5-6}$$

for all $\underline{x}$ and t. Here, ∇^2 denotes the two-dimensional Laplacian operator. ρ and c are the respective density and speed of sound in the fluid, and $w(\underline{x},t)$ is the displacement of the fluid at the boundary $x_3 = 0$ in the direction normal to that boundary. Recall, however, from section 5.1.3, that the normal displacement of the fluid at $x_3 = 0$ is imposed by the displacement of the plate. Recall, further, that the pressure field in the half space must satisfy the causality condition that the pressure must either propagate away,

or decay with increasing distance, from the source of excitation of the pressure field: that is, the boundary common to the plate and fluid at $x_3 = 0$.

It is interesting to note, from equations (5-5) and (5-6), that to obtain a solution for the pressure field at $x_3 = 0$, one must first obtain a solution for the pressure throughout the entire half space inasmuch as the boundary condition (equation (5-6)) requires knowledge of the gradient of the pressure normal to the boundary.

The solution to equations (5-5) and (5-6), subject to the causality condition, were developed in section 4.3.3.1. By use of equation (4-159), it is straightforward to show that the wavevector-frequency description of the output field, $P(\underline{k},0,\omega)$, of the subsystem associated with the acoustic fluid is related to the wavevector-frequency description of the displacement field of the plate, $W(\underline{k},\omega)$, imposed at the boundary of the fluid by

$$P(\underline{k},0,\omega) = \begin{cases} \dfrac{i\rho\omega^2 W(\underline{k},\omega)}{k_0\sqrt{1 - k^2/k_0^2}} \,, & k \leq |k_0| \,, \\[2ex] \dfrac{-\rho\omega^2 W(\underline{k},\omega)}{\sqrt{k^2 - k_0^2}} \,, & k > |k_0| \,, \end{cases} \tag{5-7}$$

where it will be recalled that $k_0 = \omega/c$. By reference to section 3.4.3, it can be verified that the input-output relationship described by equation (5-7) has a mathematical form consistent with that of a space- and time-invariant system.

The coupled set of equations (5-4) and (5-7) form the mathematical model, in the wavevector-frequency domain, for the displacement field of the free, infinite plate subjected to fluid loading on one side. By substituting equation (5-7) into equation (5-4), it is easily verified that the wavevector-frequency description of the displacement field of this fluid-loaded plate is governed by

$$\left\{Dk^4 - \mu\omega^2 + \frac{i\rho\omega^2}{k_0\sqrt{1 - k^2/k_0^2}}\right\}W(\underline{k},\omega) = 0\ , \quad k \leq |k_0|\ , \tag{5-8}$$

and

$$\left\{Dk^4 - \mu\omega^2 - \frac{\rho\omega^2}{\sqrt{k^2 - k_0^2}}\right\}W(\underline{k},\omega) = 0\ , \quad k > |k_0|\ . \tag{5-9}$$

By these equations, it is evident that unless

$$\left\{Dk^4 - \mu\omega^2 + \frac{i\rho\omega^2}{k_0\sqrt{1 - k^2/k_0^2}}\right\} = 0\ , \quad k \leq |k_0|\ , \tag{5-10}$$

$W(\underline{k},\omega)$ is zero over the wavevector range $k \leq |k_0|$, and unless

$$\left\{Dk^4 - \mu\omega^2 - \frac{\rho\omega^2}{\sqrt{k^2 - k_0^2}}\right\} = 0\ , \quad k > |k_0|\ , \tag{5-11}$$

$W(\underline{k},\omega)$ is zero over the wavevector range $k > |k_0|$.

In equations (5-2) and (5-3), the components k_1 and k_2 of the wavevector $\underline{k}$ and the frequency ω are restricted to be real. Thus, we seek only those solutions to equations (5-10) and (5-11) for which both k and ω are real. With this restriction, it is evident that equation (5-10) is satisfied only if $k = \omega = 0$. This solution represents a static, rigid body displacement rather than a vibratory motion of the plate and can therefore be ignored. We thus conclude that equation (5-10) has no solutions of consequence to the dynamic motion of the plate in the real wavevector domain $k < |k_0|$, and therefore

$$W(\underline{k},\omega) = 0\ , \ k \leq |k_0|\ . \tag{5-12}$$

Let us now seek the solutions of equation (5-11) for real values of ω and k. To accomplish this, we recall that the symbol $\sqrt{\ }$ denotes the positive

square root of a positive number, and we define the real, positive parameter

$$s = \sqrt{k^2 - k_0^2}\ , \quad k > |k_0|\ . \tag{5-13}$$

By using equation (5-13) and by recalling that $k_0 = \omega/c$, we can rewrite equation (5-11) in the form of the following cubic equation in s:

$$s^3 + \left(\frac{\rho}{\mu}\right)s^2 + \left(\frac{Dk^4}{\mu c^2} - 1\right)k^2 s - \left(\frac{\rho}{\mu}\right)k^2 = 0\ . \tag{5-14}$$

Inasmuch as s is defined to be real and positive, we seek the real, positive roots of equation (5-14). It is well known that a cubic equation with real coefficients has either three real roots or one real root and two conjugate complex roots. It is also known[1] that if s_1, s_2, and s_3 denote the roots of equation (5-14), then

$$s_1 s_2 s_3 = \rho/\mu \tag{5-15}$$

and

$$s_1 + s_2 + s_3 = -\rho/\mu\ . \tag{5-16}$$

By equations (5-15) and (5-16), it is easily deduced that there is only one real, positive root of equation (5-14). If we denote that real, positive root by $s_1(k)$, it follows from equation (5-13) that the corresponding (and only) real roots of equation (5-11) are given by

$$\omega = \pm c\sqrt{k^2 - s_1^{\,2}(k)} = \pm\omega_1(k)\ . \tag{5-17}$$

Thus, it is evident that equation (5-11) has two real roots in ω, equal in magnitude and opposite in sign.

It is convenient to use equation (2-14) to define the phase speed, c_p', associated with $\omega_1(k)$ at any wavevector $\underline{k}$ as

$$c_p'(k) = |\omega_1(k)|/|\underline{k}| = |\omega_1(k)|/k \tag{5-18}$$

and then to rewrite equation (5-17) as

$$\omega = \pm kc_p'(k) \ . \tag{5-19}$$

The phase speed $c_p'(k)$ represents the speed of propagation of the free waves in the fluid-loaded infinite plate as a function of the magnitude of the wavevector characterizing that wave. By substitution of equation (5-19) into equation (5-11), it can be shown that the phase speed, $c_p'(k)$, is the positive, real root of

$$Dk^2 - \mu c_p'^2 - \frac{\rho c c_p'^2}{k\sqrt{c^2 - c_p'^2}} = 0 \ , \quad c^2 > c_p'^2 \ . \tag{5-20}$$

By the above arguments, we have established that equation (5-11) has only two real roots in ω. It can further be shown, by equations (5-13), (5-15), and (5-16), that equation (5-11) also has four other complex roots that occur in conjugate pairs. If we denote the product of the factors of equation (5-11) associated with these complex roots by $Q(k,\omega)$, then it follows, by use of equations (5-17) and (5-19), that equation (5-11) can be rewritten in the form

$$Dk^4 - \mu\omega^2 - \frac{\omega^2}{\sqrt{k^2 - k_0^2}} = (\omega^2 - k^2c_p'^2)Q(k,\omega) = 0 \ , \quad k > |k_0| \ . \tag{5-21}$$

Consequently, equation (5-9) can be written

$$(\omega^2 - k^2c_p'^2)Q(k,\omega)W(\underline{k},\omega) = 0 \ , \quad k > |k_0| \ . \tag{5-22}$$

To obtain a solution of equation (5-22) for $W(\underline{k},\omega)$, we argue as follows. By use of equation (2-50) and the arguments presented in section 3.3.1, it can be shown that

$$Q(k,\omega)W(\underline{k},\omega) = A(\underline{k})\delta(\omega - kc_p') + B(\underline{k})\delta(\omega + kc_p') \ , \quad k > |k_0| \ . \tag{5-23}$$

where $A(\underline{k})$ and $B(\underline{k})$ are unspecified functions of the wavevector $\underline{k}$. Therefore, it follows that

$$W(\underline{k},\omega) = \frac{A(\underline{k})}{Q(k,\omega)}\,\delta(\omega - kc_p') + \frac{B(\underline{k})}{Q(k,\omega)}\,\delta(\omega + kc_p')\ , \quad k > |k_0|\ . \tag{5-24}$$

However, by making use of the sampling property of the Dirac delta function and recalling that c_p' is a function of k, we can write

$$\{A(\underline{k})/Q(k,\omega)\}\delta(\omega - kc_p') = \{A(\underline{k})/Q(k,kc_p')\}\delta(\omega - kc_p') = \alpha(\underline{k})\delta(\omega - kc_p') \tag{5-25}$$

and

$$\{B(\underline{k})/Q(k,\omega)\}\delta(\omega + kc_p') = \{B(\underline{k})/Q(k,-kc_p')\}\delta(\omega + kc_p') = \beta(\underline{k})\delta(\omega + kc_p')\ . \tag{5-26}$$

Consequently,

$$W(\underline{k},\omega) = \alpha(\underline{k})\delta(\omega - kc_p') + \beta(\underline{k})\delta(\omega + kc_p')\ , \quad k > |k_0|\ , \tag{5-27}$$

where $\alpha(\underline{k})$ and $\beta(\underline{k})$ are, as yet, unspecified functions of the wavevector $\underline{k}$.

By equations (5-12) and (5-27), we can conclude that the wavevector-frequency description of the displacement field of the fluid-loaded, infinite plate has the mathematical form

$$W(\underline{k},\omega) = \alpha(\underline{k})\delta(\omega - kc_p') + \beta(\underline{k})\delta(\omega + kc_p') \tag{5-28}$$

for all $\underline{k}$ and ω. The unspecified functions $\alpha(\underline{k})$ and $\beta(\underline{k})$ are determined by the initial conditions of the plate motion.

As we did in the case of the in-vacuo infinite plate, let us specify the initial displacement and velocity fields of the plate to be

$$w(\underline{x},0) = w_0(\underline{x}) \tag{5-29}$$

and

$$\frac{\partial w(\underline{x},0)}{\partial t} = v_0(\underline{x})\ . \tag{5-30}$$

By use of equations (5-2), (5-28), (5-29), and (5-30), it is a simple matter to show that

$$W(\underline{k},\omega) = \pi W_0(\underline{k})\{\delta(\omega - kc_p') + \delta(\omega + kc_p')\}$$

$$+ \frac{\pi V_0(\underline{k})}{ikc_p'(k)} \{\delta(\omega - kc_p') - \delta(\omega + kc_p')\} \qquad (5\text{-}31)$$

for all $\underline{k}$ and ω, where $W_0(\underline{k})$ and $V_0(\underline{k})$ are the respective spatial Fourier transforms of $w_0(\underline{x})$ and $v_0(\underline{x})$.

It is instructive to compare the wavevector-frequency description of the displacement field of the freely vibrating infinite plate with fluid loading on one side, given by equation (5-31), with the corresponding description of the free vibration of the infinite plate in vacuo, given by equation (3-31). By use of equations (2-15) and (3-23), it is straightforward to show that the phase speed, c_p, of the in-vacuo plate can be expressed as

$$c_p(k) = k\sqrt{D/\mu} \ . \qquad (5\text{-}32)$$

Consequently, from equation (3-31), the wavevector-frequency description of the displacement field of the freely vibrating infinite plate in vacuo can be written in the form

$$W(\underline{k},\omega) = \pi W_0(\underline{k})\{\delta(\omega - kc_p) + \delta(\omega + kc_p)\} + \frac{\pi V_0(\underline{k})}{ikc_p(k)} \{\delta(\omega - kc_p) - \delta(\omega + kc_p)\} \ . \qquad (5\text{-}33)$$

Comparison of equations (5-31) and (5-33) reveals that the wavevector-frequency descriptions of the free vibration of the infinite, fluid-loaded plate and the infinite plate in vacuo differ only in the propagation speeds of the respective free waves. Therefore, the physical interpretation of equation (3-31) given in section 3.3.2 can be directly applied to equation (5-31) by properly accounting for this difference in phase speeds.

Inasmuch as the phase speed of a free wave in an infinite fluid-loaded plate differs from that in an infinite plate in vacuo, it follows that the

free wavenumber associated with the fluid-loaded plate must differ from that of the in-vacuo plate. Recall that the free wavenumber is defined as the magnitude of a wavevector associated with a free wave. If we denote a free wavenumber of the fluid-loaded plate by k_p', then it follows from equation (5-19) that

$$k_p'(\omega) = |\omega|/c_p' \,. \tag{5-34}$$

By equations (5-19), (5-20), and (5-34), the free wavenumber of the fluid-loaded plate is the real, positive root of

$$Dk_p'^4 - \mu\omega^2 - \frac{\rho\omega^2}{\sqrt{k_p'^2 - k_0^2}} = 0 \,, \quad k_p' > |k_0| \,. \tag{5-35}$$

In section 3.2.2, we showed the free wavenumber of the in-vacuo infinite plate, k_p, to be given by

$$k_p = \sqrt[4]{\mu\omega^2/D} \,. \tag{5-36}$$

In contrast to equation (5-36), equation (5-35) is of such complexity that a solution for k_p' can only be obtained by numerical techniques. However, by use of equation (5-36) and the mathematical form of equation (5-35), we can deduce that (1) k_p' must exceed k_p for all ω and (2) the fluid parameters appear in a term consistent, in form, with an additional mass, or inertial force. Thus, we conclude that the fluid loading acts as an additional mass to the plate, thereby (in accordance with equation (5-36)) increasing the free wavenumber of the plate.

To provide a quantitative example of the effect of fluid loading on the free wavenumber of a plate, figure 5-4 presents a comparison of the free wavenumber (k_p') of an infinite 2.54-cm-thick steel plate with water loading on one side with the free wavenumber (k_p) of the same plate in vacuo over the frequency range 0 to 12 kilohertz (kHz). Also included in this figure, for reference purposes, is the acoustic wavenumber (k_0) of the water.

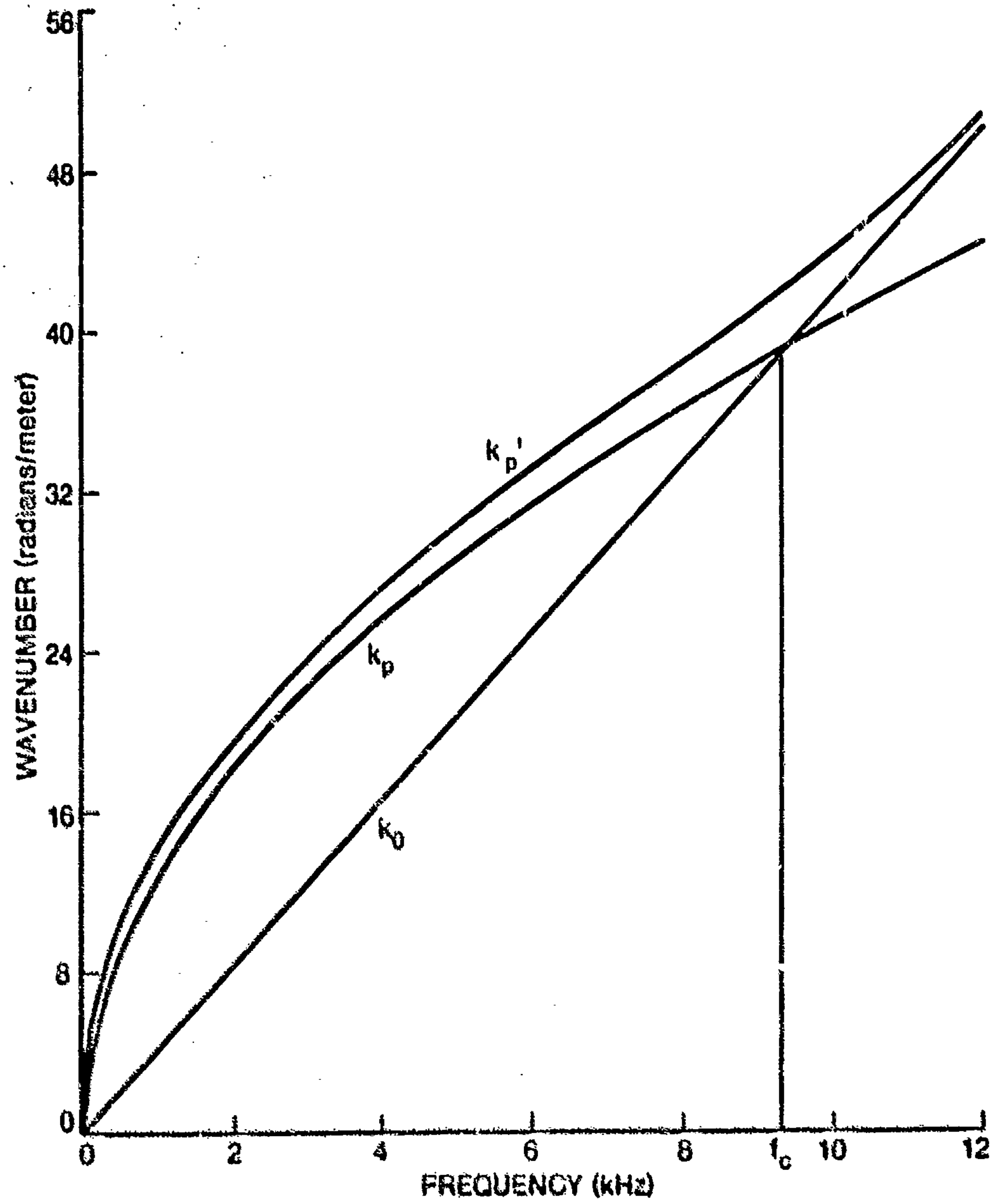

Figure 5-4. Comparison of In-Vacuo and Water-Loaded (One Side) Free Wavenumber of an Infinite 2.54-cm-Thick Steel Plate

Figure 5-4 shows that, in the frequency range where k_p is greater than k_0, the free wavenumber of the water-loaded plate is about 6 percent greater than that of the plate in vacuo. In the frequency range where k_p is less than k_0, the free wavenumber of the water-loaded plate asymptotically approaches k_0, and the ratio of k_p' to k_p increases with increasing frequency. Note that, as required by equation (5-35), k_p' exceeds k_0 at all frequencies.

Because the character of k_p' is similar to that of k_p at frequencies where $k_p > k_0$ and similar to k_0 at frequencies where $k_p < k_0$, the frequency at which $k_p = k_0$ is given the special name "coincidence frequency" and is denoted by f_c. By equation (5-36) and the definition of k_0, it is easily shown that the coincidence frequency is given by

$$f_c = \frac{c^2}{2\pi} \sqrt{\mu/D} \ . \tag{5-37}$$

For the example shown in figure 5-4, the coincidence frequency is about 9.4 kHz.

Junger and Feit[2] show that an "extremely accurate" approximation to k_p' can be obtained at frequencies below the coincidence frequency by replacing the k_p' under the radical in equation (5-35) by the free wavenumber of the in-vacuo infinite plate, k_p. With this substitution, we obtain the following approximation for the free wavenumber of the infinite plate, fluid loaded on one side:

$$k_p'(\omega) \approx k_p \sqrt[4]{1 + \frac{\rho}{\mu\sqrt{k_p^2 - k_0^2}}} \ , \quad f < f_c \ . \tag{5-38}$$

Figure 5-5 compares the free wavenumber computed from equation (5-35) with the approximate value obtained by equation (5-38) for the same 2.54-cm-thick steel plate, water loaded on one side, that was characterized in figure 5-4. As is evident from figure 5-5, equation (5-38) provides an excellent approximation to the free wavenumber of the fluid-loaded plate over the frequency range $f \leq 0.8 \ f_c$.

By applying similar arguments to equation (5-20), it would seem reasonable that a good approximation to $c_p'(k)$ can be obtained, over the wavenumber range where $c_p(k) < c$, by replacing the c_p' under the square root by the phase speed of the in-vacuo plate, c_p. By making this substitution and using equation (5-32), we obtain

$$c_p'(k) \approx c_p(k) / \sqrt{1 + \frac{\rho c}{\mu k \sqrt{c^2 - c_p^2(k)}}} \ , \quad k < k_c \ . \tag{5-39}$$

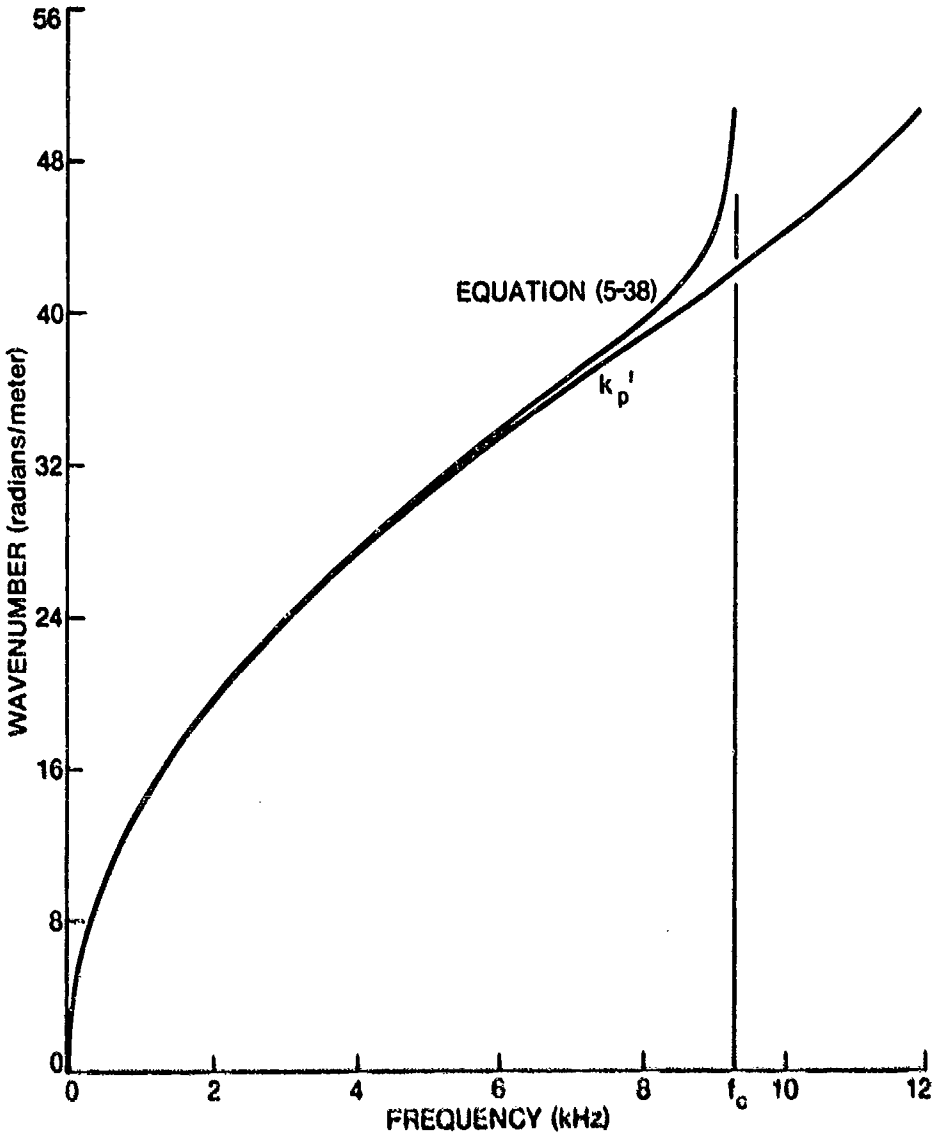

Figure 5-5. Comparison of Exact and Approximate Values of the Free Wavenumber of an Infinite 2.54-cm-Thick Steel Plate, Fluid Loaded on One side

Here, k_c denotes the critical wavenumber, defined as that wavenumber at which $c_p(k) = c$ and, by equation (5-32), given as

$$k_c = c\sqrt{\mu/D} \ . \tag{5-40}$$

Figure 5-6 compares the phase speed of the free wave computed from equation (5-20) with the approximate value computed from equation (5-39) for the 2.54-cm-thick infinite steel plate with water loading on one side. Here again, it is seen that equation (5-39) provides an excellent approximation

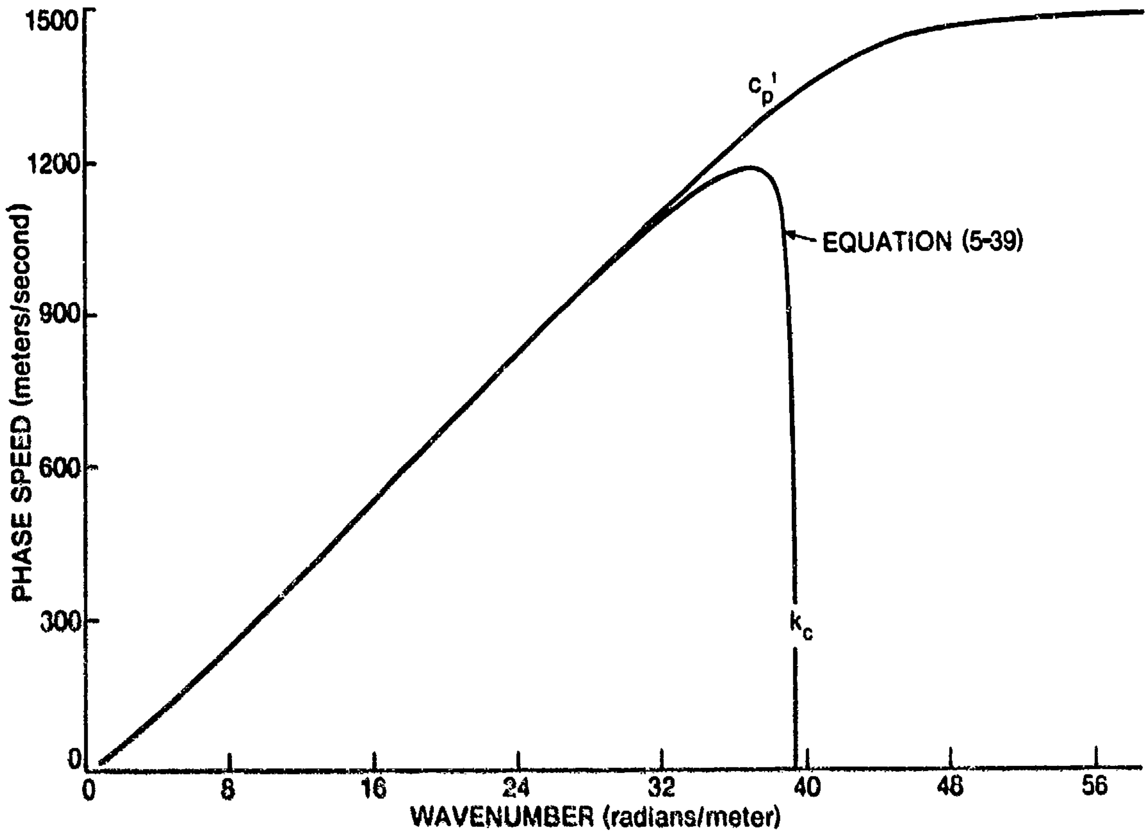

Figure 5-6. Comparison of Exact and Approximate Values of the Propagation Speed of the Free Wave in an Infinite 2.54-cm-Thick Steel Plate, Fluid Loaded on One Side

of the phase speed at wavenumbers less than 80 percent of the critical wavenumber.

As a final observation, it is easily shown, by equations (5-2) and (5-33), that the space-time description of the free vibration of the fluid-loaded infinite plate is given by

$$w(\underline{x},t) = (2\pi)^{-2} \int_{-\infty}^{\infty} \left[\left\{ W_0(\underline{k}) - \frac{iV_0(\underline{k})}{kc_p'(k)} \right\} \exp\{i[\underline{k}\cdot\underline{x} + kc_p'(k)t]\} \right.$$

$$\left. + \left\{ W_0(\underline{k}) + \frac{iV_0(\underline{k})}{kc_p'(k)} \right\} \exp\{i[\underline{k}\cdot\underline{x} - kc_p'(k)t]\} \right] d\underline{k} \qquad (5\text{-}41)$$

for all $\underline{x}$ and t. However, owing to the dependence of c_p' on k, no further simplification of equation (5-41) is possible without specification of $W_0(\underline{k})$ and $V_0(\underline{k})$.

5.3 THE FORCED RESPONSE OF COUPLED SYSTEMS

Different multicomponent systems consist of different assemblages of physical components with different interactions between components and different inputs. By the arguments of section 5.1, such different multicomponent systems can be interpreted as different combinations of single component subsystems with different couplings between, and inputs to, the various subsystems. These coupled systems form the basis for the mathematical models of the corresponding multicomponent systems. Recall that although all systems (or subsystems) treated here are linear and time invariant, they can be either space varying or space invariant, as appropriate. By the arguments of chapters 3 and 4, it follows that the mathematical models of different multicomponent systems consist of different combinations of simultaneous, linear, homogeneous or inhomogeneous partial differential equations with different coupling conditions between equations. The coefficients of the various differential equations are time invariant, but may be either space invariant or space varying, as appropriate.

Clearly, by the above discussion, it is impractical to attempt to develop a general input-output relationship applicable to all multicomponent, or coupled, systems. Rather, the emphasis in this section will be to demonstrate, by example, techniques for formulating and solving mathematical models for the forced response of coupled systems. In the subsections to follow, we will address the forced response of two multicomponent systems: (1) the infinite plate subjected to fluid loading on one side and (2) the finite, simply supported plate subjected to fluid loading on one side. The forced response of these systems can then be compared with the forced response of the corresponding plates in vacuo to determine the effects of fluid loading on the forced response of infinite and finite plates.

5.3.1 <u>The Forced Response of an Infinite Plate With Fluid Loading on One Side</u>

This illustrative example is the forced version of the coupled system described and discussed in section 5.1.3. The geometry of the physical system is illustrated in figure 5-1, and the schematic diagram of the corresponding assemblage of coupled subsystems is illustrated in figure 5-2.

Let us first consider the subsystem associated with the infinite plate. By reference to figures 5-1 and 5-2, it is evident that the plate is subjected to two forcing fields: (1) the externally applied input, $f(\underline{x},t)$, and (2) the oppositely directed pressure field, $p(\underline{x},0,t)$, acting over the upper surface of the plate. The output of this subsystem, the displacement field, $w(\underline{x},t)$, of the plate, is also the output of the composite plate-fluid system. By equation (3-103), the response of an infinite plate (having flexural rigidity D, mass per unit area μ, and viscous damping per unit area r) to the forcing fields $f(\underline{x},t)$ and $-p(\underline{x},0,t)$ is governed by

$$D\nabla^4 w(\underline{x},t) + r\,\frac{\partial w(\underline{x},t)}{\partial t} + \mu\,\frac{\partial^2 w(\underline{x},t)}{\partial t^2} = f(\underline{x},t) - p(\underline{x},0,t) \qquad (5\text{-}42)$$

over all $\underline{x}$ and t.

Note that, for the treatment of the forced response of this composite system, we have assumed the plate to be damped, whereas in our treatment of the free response of the same composite system, the plate was assumed (for reasons explained in section 5.2.1) to be undamped. The reason for including damping in the model for the forced response of the plate subsystem is that its presence, as explained and illustrated in sections 3.4.4 and 3.4.5, simplifies causality arguments and permits unambiguous definition of the subsystem response over all wavevectors and frequencies.

By assuming that $w(\underline{x},t)$ and $p(\underline{x},0,t)$ exist in the forms of equations (5-2) and (5-3), respectively, and that $f(\underline{x},t)$ can be expressed as

$$f(\underline{x},t) = (2\pi)^{-3}\int_{-\infty}^{\infty} F(\underline{k},\omega)\exp\{i(\underline{k}\cdot\underline{x} + \omega t)\}\,d\underline{k}\,d\omega\,, \qquad (5\text{-}43)$$

it is straightforward to show, from equation (5-42), that the wavevector-frequency descriptions of the input and output fields of the infinite plate subsystem are related by

$$W(\underline{k},\omega) = \frac{F(\underline{k},\omega) - P(\underline{k},0,\omega)}{Dk^4 - \mu\omega^2 + ir\omega}\,, \qquad (5\text{-}44)$$

where $k = \sqrt{k_1^2 + k_2^2}$. This input-output relation has the mathematical form characteristic of a space- and time-invariant linear system.

By inspection of figure 5-2, it is evident that, inasmuch as the input to the coupled plate-fluid system is applied to the plate, the subsystem associated with the acoustic fluid is the same for both the forced and free versions of the composite plate-fluid system. This acoustic half-space subsystem was shown, in section 5.2.1, to be governed by equations (5-5) and (5-6) in the space-time domain and by equation (5-7) in the wavevector-frequency domain.

By the coupled set of equations (5-7) and (5-44), it can be shown that the wavevector-frequency description of the forced response of the infinite plate, fluid loaded on one side, is given by

$$W(\underline{k},\omega) = \begin{cases} \dfrac{F(\underline{k},\omega)}{\left\{[Dk^4 - \mu\omega^2] + i\left[r\omega + \dfrac{\rho\omega^2}{k_0\sqrt{1 - k^2/k_0^2}}\right]\right\}}, & k \le |k_0| , \\[2em] \dfrac{F(\underline{k},\omega)}{\left\{\left[Dk^4 - \mu\omega^2 - \dfrac{\rho\omega^2}{\sqrt{k^2 - k_0^2}}\right] + i[r\omega]\right\}}, & k > |k_0| . \end{cases} \tag{5-45}$$

Note that, over both ranges of wavevector magnitudes, this input-output relationship for the composite plate-fluid system has the algebraic form (see equation (3-59)) characteristic of space- and time-invariant systems. Thus, we conclude that the composite system of the infinite plate, fluid loaded on one side, is a space- and time-invariant linear system.

By recognizing the composite plate-fluid system to be space and time invariant, we can readily deduce, by equations (3-59) and (5-45), that the wavevector-frequency response, $G(\underline{k},\omega)$, of the infinite plate, fluid loaded on one side, is given by

$$G(\underline{k},\omega) = \begin{cases} \dfrac{1}{\left\{[Dk^4 - \mu\omega^2] + i\left[r\omega + \dfrac{\rho\omega^2}{k_0\sqrt{1 - k^2/k_0^2}}\right]\right\}}, & k \le |k_0| , \\ \dfrac{1}{\left\{\left[Dk^4 - \mu\omega^2 - \dfrac{\rho\omega^2}{\sqrt{k^2 - k_0^2}}\right] + i[r\omega]\right\}}, & k > |k_0| . \end{cases} \tag{5-46}$$

Recall that the wavevector-frequency response, $G(\underline{k},\omega)$, is the wavevector-frequency transform of the Green's function, $g(\underline{\xi},\tau)$. It is good practice, at this point, to ensure that $G(\underline{k},\omega)$ is the causal wavevector-frequency response: that is, the wavevector-frequency transform of the causal Green's function. In section 3.4.4, we established that $G(\underline{k},\omega)$ was a causal wavevector-frequency response if $\tilde{G}(\underline{k},\tau)$, the inverse Fourier transformation of $G(\underline{k},\omega)$ on ω, and its temporal derivatives were zero for $\tau < 0$. However, as is often the case in coupled systems, the form of equation (5-46) is of sufficient mathematical complexity that one is quickly discouraged from attempting the inverse Fourier transformation required to obtain $\tilde{G}(\underline{k},\tau)$. Consequently, we are motivated to address the question of the causality of the wavevector-frequency response of the fluid-loaded plate (given by equation (5-46)) by logical, rather than mathematical, arguments.

To this end, we submit the following arguments. The composite plate-fluid system can be interpreted, according to figure 5-2, as two subsystems arranged in a feedback loop. The input-output relationship for the plate subsystem (equation (5-44)) has the form shown (by equation (3-59)) to be characteristic of space- and time-invariant systems. From equations (3-59) and (5-44), it can easily be verified that the wavevector-frequency response of the plate subsystem is identical to that given by equation (3-114), which was shown to characterize the causal Green's function for the infinite plate in vacuo. The input-output relationship for the acoustic half-space subsystem was taken directly from equation (4-159) (with x_3 set to zero). The causality of this input-output relationship was addressed and ensured in its derivation. Inasmuch as (1) the input to the composite system is applied directly to the

plate subsystem, (2) the input-output relationships used to model both the plate and half-space subsystems in the wavevector-frequency domain are causal, (3) the causal output of each of the two subsystems is input directly to the other subsystem in a feedback loop, and (4) the output of the (causal) plate system is defined as the output of the composite plate-fluid system, it follows that the wavevector-frequency response of the composite plate-fluid system, described by equation (5-46), must be causal.

Let us now shift our focus to the response characteristics of the fluid-loaded plate in the wavevector-frequency domain. As explained in section 3.4.6, the wavevector-frequency response can be interpreted as the complex amplitude of the wave of the form $\exp\{i(\underline{k}\cdot\underline{x} + \omega t)\}$ output from a system as the result of excitation of the system by the unit amplitude wave, $\exp\{i(\underline{k}\cdot\underline{x} + \omega t)\}$. Note, by equation (5-46), that the wavevector-frequency response of the fluid-loaded plate, like that of the plate in vacuo (see section 3.4.6), depends only on the magnitude of the wavevector, and not on its direction. As was explained for the case of the infinite plate in vacuo, this independence of $G(\underline{k},\omega)$ on the direction of $\underline{k}$ is a reflection of the spatial invariance of the fluid-loaded infinite plate system. That is, for a unit amplitude harmonic wave excitation of the plate, the complex amplitude of the response of the fluid-loaded infinite plate depends only on the wavelength and frequency of excitation and is independent of the direction of propagation of the harmonic wave excitation.

The effects of the fluid loading on the wavevector-frequency response of an infinite plate can best be illustrated by comparing the response of a fluid-loaded plate with that of the same plate in vacuo. Figures 5-7(a) and (b) compare the magnitude and phase, respectively, of the wavevector-frequency response of an infinite plate, fluid loaded on one side, to that of an identical plate in vacuo as a function of the wavevector magnitude, k, at a fixed frequency, ω.

By figure 5-7(a), it is evident that the fluid loading has a significant effect on the magnitude of the wavevector-frequency response of the infinite plate. However, by use of equations (3-114) and (5-46), the reasons for the differences between the magnitudes of these wavevector-frequency responses can

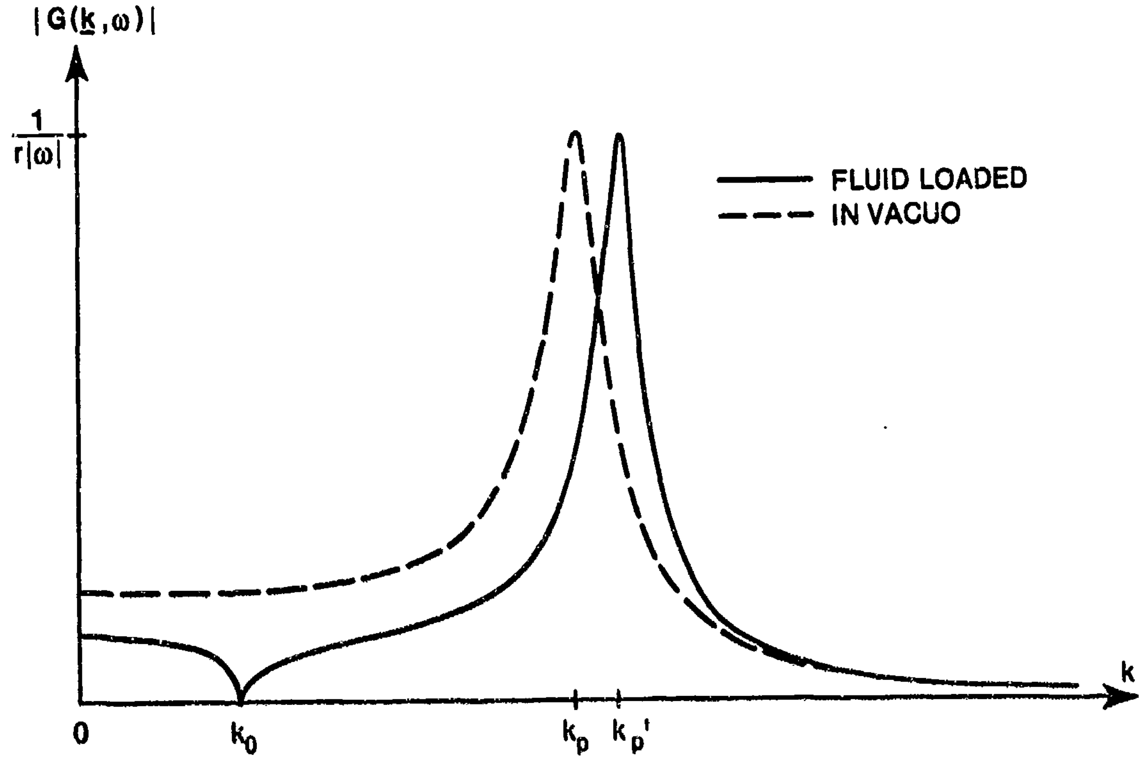

Figure 5-7(a). Comparison of the Magnitudes of the Wavevector-Frequency Responses of Fluid-Loaded and In-Vacuo Infinite Plates

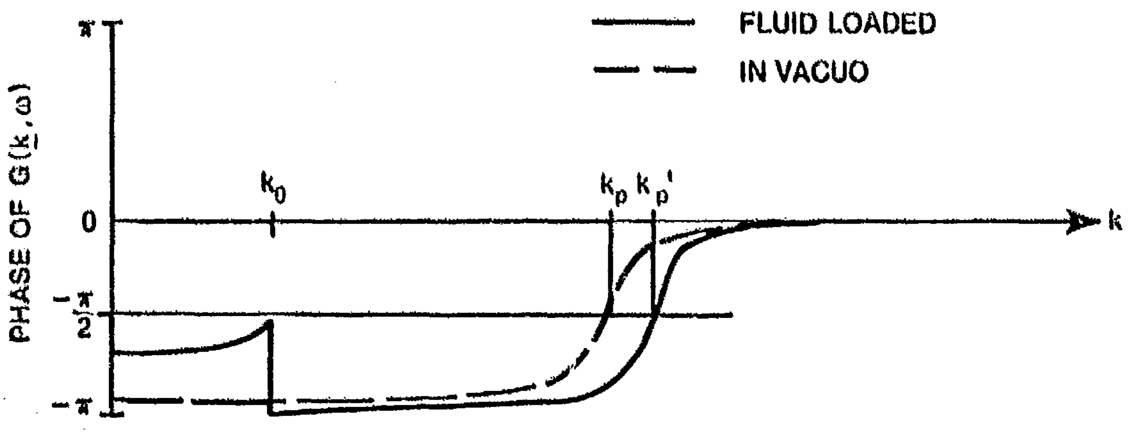

Figure 5-7(b). Comparison of the Phases of the Wavevector-Frequency Responses of Fluid-Loaded and In-Vacuo Infinite Plates

Figure 5-7. Comparison of the Wavevector-Frequency Responses of Fluid-Loaded and In-Vacuo Infinite Plates

easily be understood. Note first that, at wavenumber magnitudes less than the free wavenumber (k_p) of the in-vacuo plate, the magnitude of the wavevector-frequency response of the fluid-loaded plate is less than that of the plate in vacuo. This difference results from the additional damping (at wavevector magnitudes below k_0) or the additional mass (at wavevector magnitudes above k_0) imposed on the plate by the fluid in these respective wavenumber regimes. The amount of this difference in magnitude of response between fluid-loaded and in-vacuo plates in this wavenumber region can be shown, by equations (3-114) and (5-46), to increase as the quantity $\rho c/(\mu\omega)$, the ratio of the specific acoustic impedance of the fluid (ρc) to the inertial impedance of the plate ($\mu\omega$), increases. Thus, if the fluid impedance is small in comparison with the inertial impedance of the plate, the effect of the fluid loading on the magnitude of the wavevector-frequency response of the plate will be small (except at the wavenumber k_0). Conversely, if the specific acoustic impedance is large in comparison with the inertial impedance of the plate, the magnitude of the wavevector-frequency response of the fluid-loaded plate will be significantly lower than that of the plate in vacuo.

At the wavenumber k_0, the response of the fluid-loaded plate is seen to be zero, whereas that of the in-vacuo plate is nonzero. Recall, from section 4.3.3.1, that the impedance of the acoustic half space at the surface $x_3 = 0$ becomes infinite at wavevectors equal, in magnitude, to that of the acoustic wavenumber, $|k_0|$. Inasmuch as the plate motion and the fluid motion must be equal at the interface $x_3 = 0$, it follows that the impedance of the coupled plate-fluid system must also be infinite at wavevectors equal, in magnitude, to $|k_0|$. Consequently, the wavevector-frequency response of the fluid-loaded plate is zero at $k = k_0$. Conversely, equation (3-144) shows the wavevector-frequency response of the in-vacuo plate to be nonzero for all wavenumbers below the free wavenumber, k_p, of the plate.

Resonance in the wavevector-frequency responses of the in-vacuo and fluid-loaded plates occurs, at any fixed frequency, when the wavevector of excitation is equal, in magnitude, to the free wavenumbers, k_p and k_p', of the respective plates. As is evident in figure 5-7(a), the magnitude of the wavevector-frequency response at these resonance wavenumbers is equal to $1/(r|\omega|)$ for both the fluid-loaded and in-vacuo plates. However, because the

free wavenumber of the fluid-loaded plate is greater than that of the plate in vacuo, resonance occurs at a higher wavenumber in the fluid-loaded plate than in the in-vacuo plate.

For wavevector magnitudes large in comparison with the resonance wavenumbers, the wavevector-frequency responses of both the fluid-loaded and in-vacuo plates are governed by the flexural rigidity of the plate (i.e., the term Dk^4 in equations (3-114) and (5-46)). Inasmuch as figure 5-7(a) compares the magnitudes of the wavevector-frequency responses of identical plates, fluid loaded and in vacuo, it is not surprising that the magnitudes of the responses of the two plates are approximately equal at high wavenumbers.

Figure 5-7(b) compares the phases of the wavevector-frequency responses of the fluid-loaded and in-vacuo plates at the fixed frequency ω. As explained in section 3.4.6, the phase of the wavevector-frequency response can be interpreted as the phase of each harmonic wave component of the displacement field relative to that of the corresponding harmonic wave component of the excitation field. At wavevectors less, in magnitude, than the resonance wavenumber, k_p, the response of the in-vacuo plate is dictated primarily by inertial effects (i.e., the term $\mu\omega^2$ in equation (3-114)), and the displacement is nearly out of phase with the applied force. This same argument applies to the fluid-loaded plate for wavevector magnitudes greater than k_0 and less than k_p', where the inertia of the plate is augmented by the inertia associated with the fluid loading. For wavevectors less, in magnitude, than k_0, the fluid acts as additional damping to the plate, thereby reducing the phase lag between output and input relative to that shown for the in-vacuo plate. When the plate is excited by a harmonic wave characterized by a wavevector nearly equal (but less) in magnitude to that of the acoustic wavenumber, the damping force associated with the fluid loading becomes extremely large, and the displacement lags the applied force by 90 degrees. At resonance, the harmonic waves of displacement of both the fluid-loaded and in-vacuo plates lag the associated waves of applied force by 90 degrees. For harmonic wave excitations characterized by wavevectors larger, in magnitude, than the resonance wavenumber, the responses of both the fluid-loaded and in-vacuo plates are governed by the flexural rigidity of the plates (i.e., the term Dk^4 in the respective wavevector-frequency responses).

and the resulting wave of displacement is nearly in phase with the excitation.

The above example illustrates that the fluid-loaded plate responds most strongly to harmonic wave components of excitation that are characterized by wavevectors equal, in magnitude, to the free wavenumber of the fluid-loaded plate at the frequency of excitation. This behavior parallels that observed (in section 3.4.6) for the in-vacuo plate.

5.3.2 The Forced Response of a Finite, Simply Supported Plate With Fluid Loading on One Side

In this section, we develop the wavevector-frequency description of the forced displacement field of a finite, simply supported plate subjected to fluid loading on one side. The composite plate-fluid system of interest is illustrated in figure 5-8. Here, a thin plate (with flexural rigidity D, mass per unit area μ, damping coefficient per unit area r, and dimensions L_1 by L_2) is simply supported in a rigid baffle of infinite extent. The space above the plate and baffle, $x_3 > 0$, is occupied by an acoustic fluid having a density ρ and a speed of sound c. The space $x_3 < 0$ is vacuous. The plate is excited into motion by a force per unit area, $f(\underline{x},t)$, applied to the bottom surface of the plate. We wish to determine the displacement field of the plate resulting from this externally applied excitation.

A schematic diagram of this composite system is illustrated in figure 5-9. The baffled, simply supported plate is excited into motion by the externally applied forcing field, $f(\underline{x},t)$. The resulting displacement field, $w(\underline{x},t)$, is imposed on the fluid in the acoustic half space at the plate-fluid interface ($x_3 = 0$), thereby exciting a pressure field, $p(\underline{x},x_3,t)$, throughout the acoustic half space, $x_3 > 0$. This pressure field, acting over the top surface of the plate, produces an additional input field, $p(\underline{x},0,t)$, over the upper surface of the plate and baffle that acts opposite in direction to the externally applied forcing field. The output of this composite system is the displacement field of the plate, $w(\underline{x},t)$.

By figure 5-9, it is evident that the composite system of the fluid-loaded, simply supported plate can be interpreted as two coupled subsystems:

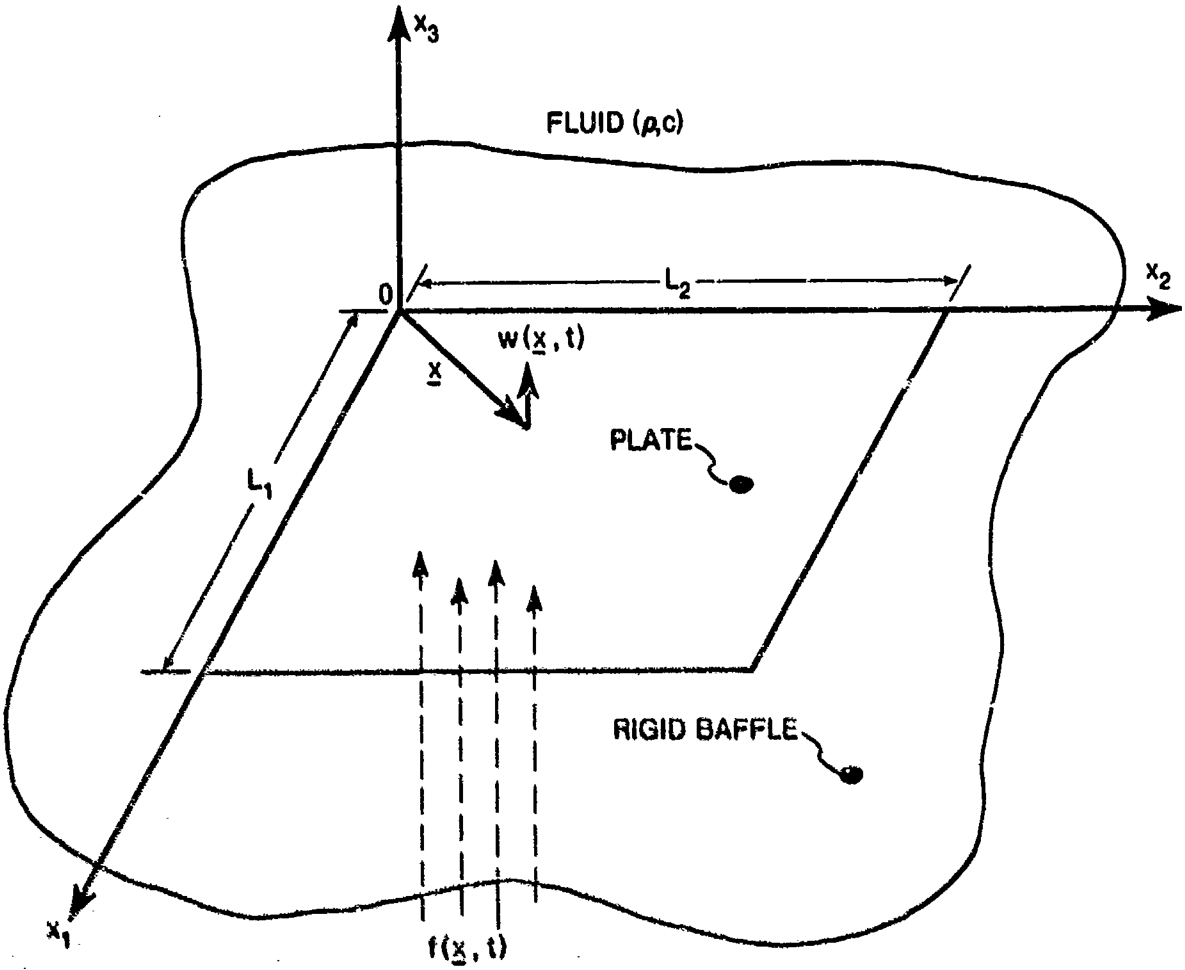

Figure 5-8. Geometry of the Finite, Simply Supported Plate With Fluid Loading on One Side

one subsystem represents the simply supported plate and the surrounding baffle and the second subsystem represents the acoustic half space. The couplings between these systems are identical to those occurring in the fluid-loaded infinite plate, which were described and discussed in section 5.1.3.

The reader might be justifiably curious as to why the simply supported plate and the surrounding rigid baffle are treated as a single subsystem. The answer is that, by including the rigid baffle in the subsystem associated with the simply supported plate, the input-output relationship for the plate-baffle subsystem can be directly obtained from that of the forced response of the simply supported plate, which was treated in section 4.3.3.2. That is, because the baffle is assumed to be rigid (i.e., of infinite impedance for all

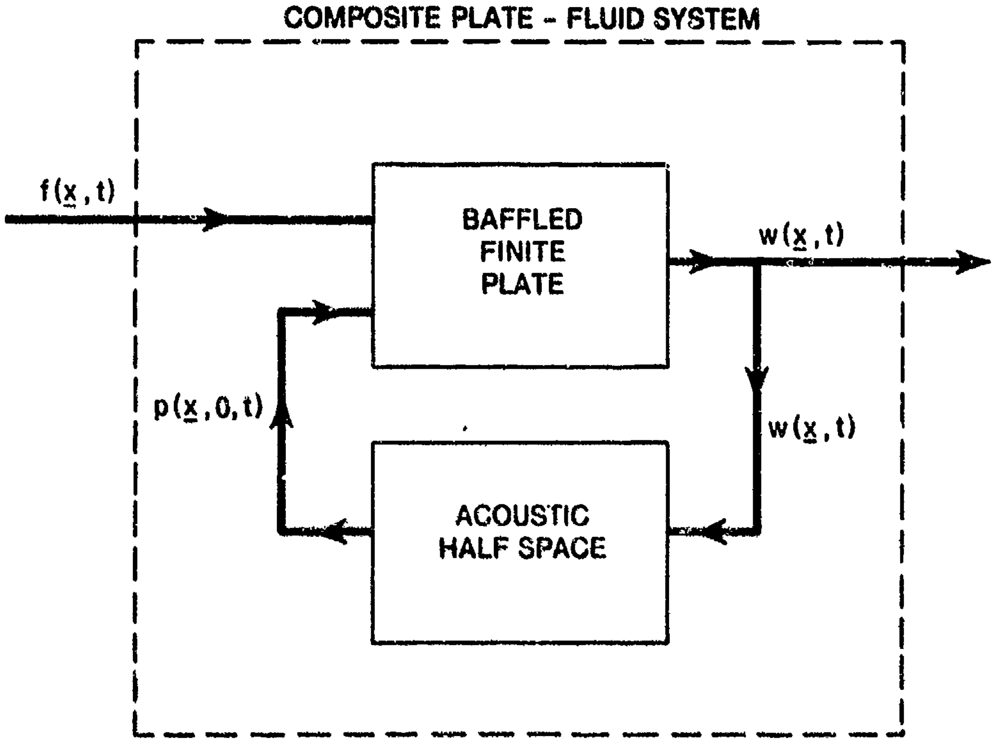

Figure 5-9. Schematic Diagram of Fluid-Loaded, Simply Supported Plate System

wavevectors and frequencies), the displacement, $w(\underline{x},t)$, normal to the plane of the plate and baffle is then known to be zero for all $\underline{x}$ outside the boundaries of the plate: that is, outside $0 < x_1 < L_1$ and $0 < x_2 < L_2$. This is exactly the displacement field that was assumed to exist outside the confines of the simply supported plate in the forced system treated in section 4.3.3.2. Thus, the motivation for including the rigid baffle in the subsystem associated with the simply supported plate was to enable us to use the relationships developed in section 4.3.3.2 to model this subsystem.

By reference to equation (4-210) of section 4.3.3.2, the displacement field output from the subsystem associated with the baffled, simply supported plate as a result of the forcing fields $f(\underline{x},t)$ and $-p(\underline{x},0,t)$ can be written as

$$w(\underline{x},t) = \int_{-\infty}^{\infty}\int_{-\infty}^{\infty} g(\underline{x},\underline{x}_0,t - t_0)\{f(\underline{x}_0,t_0) - p(\underline{x}_0,0,t_0)\}\, d\underline{x}_0\, dt_0 \qquad (5\text{-}47)$$

for all $\underline{x}$ and t. Here, $g(\underline{x},\underline{x}_0,t - t_0)$ is the exact and causal Green's function for the baffled, simply supported plate, which was shown, by equation (4-205), to be given by

$$g(\underline{x},\underline{x}_0,t - t_0) = \frac{2}{\pi L_1 L_2} \int_{-\infty}^{\infty} \sum_{m=1}^{\infty} \sum_{n=1}^{\infty} \left\{ \frac{\beta(\underline{x})\alpha_{mn}(\underline{x})\beta(\underline{x}_0)\alpha_{mn}(\underline{x}_0)}{D[(m\pi/L_1)^2 + (n\pi/L_2)^2]^2 + ir\omega - \mu\omega^2} \right\}$$

$$\exp\{i\omega(t - t_0)\}\ d\omega\ , \tag{5-48}$$

where $\alpha_{mn}(\underline{x})$ are the normal modes of the simply supported plate defined by

$$\alpha_{mn}(\underline{x}) = \sin(m\pi x_1/L_1)\sin(n\pi x_2/L_2) \tag{5-49}$$

and $\beta(\underline{x})$ is the two-dimensional space-limiting function defined by

$$\beta(\underline{x}) = \{U(x_1) - U(x_1 - L_1)\}\{U(x_2) - U(x_2 - L_2)\}\ . \tag{5-50}$$

It should also be recalled (from section 4.3.3.2) that, in equation (5-47), $f(\underline{x},t)$ is equal to the force per unit area applied to the under surface of the plate in the spatial range $0 < x_1 < L_1$ and $0 < x_2 < L_2$, but can be arbitrarily specified outside this range inasmuch as forces outside the physical extent of the plate act only on the baffle, which is rigid.

It is straightforward to show, from equation (5-47), that the wavevector-frequency transform, $W(\underline{k},\omega)$, of the space-time displacement field is related to the wavevector-frequency descriptions of the forcing and surface pressure fields, $F(\underline{k},\omega)$ and $P(\underline{k},0,\omega)$, by

$$W(\underline{k},\omega) = (2\pi)^{-2} \int_{-\infty}^{\infty} G(\underline{k},-\underline{\sigma},\omega)\{F(\underline{\sigma},\omega) - P(\underline{\sigma},0,\omega)\}\ d\underline{\sigma}\ . \tag{5-51}$$

Here, $G(\underline{k},\underline{\sigma},\omega)$ is the two-wavevector-frequency response of the system (i.e., the multiple Fourier transform of $g(\underline{x},\underline{x}_0,\tau)$ on the variables $\underline{x}$, $\underline{x}_0$, and τ), which is given by

$$G(\underline{k},\underline{\sigma},\omega) = \frac{4}{L_1 L_2} \sum_{m=1}^{\infty} \sum_{n=1}^{\infty} \frac{I_{mn}(\underline{k})I_{mn}(\underline{\sigma})}{Dk_{mn}^4 - \mu\omega^2 + ir\omega}\ , \tag{5-52}$$

where

$$k_{mn} = \sqrt{(m\pi/L_1)^2 + (n\pi/L_2)^2} \tag{5-53}$$

and

$$I_{mn}(\underline{k}) = \int_{-\infty}^{\infty} \beta(\underline{x})\alpha_{mn}(\underline{x})\exp(-i\underline{k}\cdot\underline{x})\ d\underline{x}\ . \tag{5-54}$$

Equation (5-51), with equation (5-52), defines the relationship between the wavevector-frequency descriptions of the input and the output fields for the subsystem associated with the baffled, simply supported plate. This input-output relationship has the mathematical form shown, in section 4.3.2, to be characteristic of a space-varying, time-invariant system.

The subsystem associated with the acoustic half space is identical to that used in the coupled system that represents the fluid-loaded infinite plate in sections 5.2.1 and 5.3.1. The causal relationship between the wavevector-frequency descriptions of the boundary displacement and the resulting surface pressure was given by equation (5-7). As was argued previously, this relationship has the mathematical form characteristic of a space- and time-invariant system.

The composite system of the fluid-loaded, simply supported plate surrounded by an infinite rigid baffle is mathematically modeled by the coupled set of equations (5-7) and (5-51). By substitution of equation (5-7) into equation (5-51), it can be shown that the wavevector-frequency description of the forced displacement of the baffled, simply supported plate, fluid loaded on one side, is governed by

$$W(\underline{k},\omega) = (2\pi)^{-2}\left[\int_{-\infty}^{\infty} G(\underline{k},-\underline{\sigma},\omega)\ F(\underline{\sigma},\omega)\ d\underline{\sigma} - i\rho c\omega \int_{|\underline{\sigma}|\le|k_0|} \frac{G(\underline{k},-\underline{\sigma},\omega)W(\underline{\sigma},\omega)}{\sqrt{1-\sigma^2/k_0^{\ 2}}}\, d\underline{\sigma}\right.$$

$$\left. + \rho\omega^2 \int_{|\underline{\sigma}|>|k_0|} \frac{G(\underline{k},-\underline{\sigma},\omega)W(\underline{\sigma},\omega)}{\sqrt{\sigma^2 - k_0^{\ 2}}}\, d\underline{\sigma}\right] . \tag{5-55}$$

where $\sigma^2 = \sqrt{\sigma_1{}^2 + \sigma_2{}^2}$. Note, by equation (5-55), that the input-output relationship for the fluid-loaded, baffled, simply supported plate in the wavevector-frequency domain is expressed in the form of an integral equation for $W(\underline{k},\omega)$. This mathematical form of input-output relationship was shown, in section 4.3.1.2, to be characteristic of space-limited, time-invariant linear systems.

The solution of the integral equation (5-55) for $W(\underline{k},\omega)$, subject to the constraints imposed by the simply supported boundary conditions and the surrounding rigid baffle, presents a formidable mathematical challenge. However, a conceptually simple (although computationally inefficient) approach to obtaining a solution for $W(\underline{k},\omega)$ is to assume that the space-time displacement and forcing fields can be expressed as a weighted superposition of the in-vacuo normal modes of the simply supported plate. That is, assume that the $w(\underline{x},t)$ and $f(\underline{x},t)$ can be expressed as

$$w(\underline{x},t) = \frac{1}{2\pi} \int_{-\infty}^{\infty} \sum_{m=1}^{\infty} \sum_{n=1}^{\infty} \overset{\nabla}{W}_{mn}(\omega)\beta(\underline{x})\alpha_{mn}(\underline{x})\exp(i\omega t)\, d\omega \tag{5-56}$$

and

$$f(\underline{x},t) = \frac{1}{2\pi} \int_{-\infty}^{\infty} \sum_{m=1}^{\infty} \sum_{n=1}^{\infty} \overset{\nabla}{F}_{mn}(\omega)\beta(\underline{x})\alpha_{mn}(\underline{x})\exp(i\omega t)\, d\omega \, . \tag{5-57}$$

As expressed in the form of equation (5-56), the displacement field of the baffled, fluid-loaded plate satisfies the simply supported boundary conditions and the requirement that the displacement be zero over the surface of the rigid baffle. The form of equation (5-57) reflects the fact that the externally applied forcing field acts only over the surface of the plate.

By assuming that the space-time displacement and forcing fields exist in the forms of equations (5-56) and (5-57), it follows (by use of equation (5-54)) that $W(\underline{k},\omega)$ and $F(\underline{k},\omega)$ can be written in the form

$$W(\underline{k},\omega) = \sum_{m=1}^{\infty} \sum_{n=1}^{\infty} \check{W}_{mn}(\omega) I_{mn}(\underline{k}) \tag{5-58}$$

and

$$F(\underline{k},\omega) = \sum_{m=1}^{\infty} \sum_{n=1}^{\infty} \check{F}_{mn}(\omega) I_{mn}(\underline{k}) \ . \tag{5-59}$$

By substituting equations (5-52), (5-58), and (5-59) into equation (5-55), we obtain the following relationship between the frequency-dependent modal coefficients of the displacement and forcing fields:

$$\begin{aligned}
&\sum_{m=1}^{\infty} \sum_{n=1}^{\infty} \check{W}_{mn}(\omega) I_{mn}(\underline{k}) \\
&= \frac{1}{\pi^2 L_1 L_2} \Bigg\{ \sum_{p=1}^{\infty} \sum_{q=1}^{\infty} \sum_{u=1}^{\infty} \sum_{v=1}^{\infty} \frac{\check{F}_{pq}(\omega) I_{uv}(\underline{k})}{D k_{uv}^4 - \mu\omega^2 + i r\omega} \int_{-\infty}^{\infty} I_{pq}(\underline{\sigma}) I^*_{uv}(\underline{\sigma}) \, d\underline{\sigma} \\
&\quad - i\rho c\omega \sum_{m=1}^{\infty} \sum_{n=1}^{\infty} \sum_{u=1}^{\infty} \sum_{v=1}^{\infty} \frac{\check{W}_{mn}(\omega) I_{uv}(\underline{k})}{D k_{uv}^4 - \mu\omega^2 + i r\omega} \int_{|\underline{\sigma}| \le |k_0|} \frac{I_{mn}(\underline{\sigma}) I^*_{uv}(\underline{\sigma})}{\sqrt{1 - \sigma^2/k_0^2}} \, d\underline{\sigma} \\
&\quad + \rho\omega^2 \sum_{m=1}^{\infty} \sum_{n=1}^{\infty} \sum_{u=1}^{\infty} \sum_{v=1}^{\infty} \frac{\check{W}_{mn}(\omega) I_{uv}(\underline{k})}{D k_{uv}^4 - \mu\omega^2 + i r\omega} \int_{|\underline{\sigma}| > |k_0|} \frac{I_{mn}(\underline{\sigma}) I^*_{uv}(\underline{\sigma})}{\sqrt{\sigma^2 - k_0^2}} \, d\underline{\sigma} \Bigg\} \ .
\end{aligned} \tag{5-60}$$

By multiplying equation (5-60) by $I^*_{ij}(\underline{k})$ and integrating over all $\underline{k}$, we can employ the orthogonality condition (derived in section 4.2.2)

$$\int_{-\infty}^{\infty} I_{mn}(\underline{k}) I^*_{qs}(\underline{k}) \, d\underline{k} = \pi^2 L_1 L_2 \delta_{mq} \delta_{ns} \tag{5-61}$$

to show that

$$\overset{\nabla}{W}_{ij}(\omega) = \frac{\overset{\nabla}{F}_{ij}(\omega)}{Dk_{ij}^{4} - \mu\omega^2 + ir\omega}$$

$$- i \frac{\rho c\omega}{\pi^2 L_1 L_2} \sum_{m=1}^{\infty} \sum_{n=1}^{\infty} \frac{\overset{\nabla}{W}_{mn}(\omega)}{Dk_{ij}^{4} - \mu\omega^2 + ir\omega} \int_{|\underline{\sigma}|\le|k_0|} \frac{I_{mn}(\underline{\sigma}) I^*_{ij}(\underline{\sigma})}{\sqrt{1 - \sigma^2/k_0^2}} \, d\underline{\sigma}$$

$$+ \frac{\rho\omega^2}{\pi^2 L_1 L_2} \sum_{m=1}^{\infty} \sum_{n=1}^{\infty} \frac{\overset{\nabla}{W}_{mn}(\omega)}{Dk_{ij}^{4} - \mu\omega^2 + ir\omega} \int_{|\underline{\sigma}|>|k_0|} \frac{I_{mn}(\underline{\sigma}) I^*_{ij}(\underline{\sigma})}{\sqrt{\sigma^2 - k_0^2}} \, d\underline{\sigma} \, . \tag{5-62}$$

If we then define

$$r_{mnqs}(\omega) = \frac{\rho c}{\pi^2 L_1 L_2} \int_{|\underline{\sigma}|\le|k_0|} \frac{I^*_{mn}(\underline{\sigma}) I_{qs}(\underline{\sigma})}{\sqrt{1 - \sigma^2/k_0^2}} \, d\underline{\sigma} \tag{5-63}$$

and

$$\mu_{mnqs}(\omega) = \frac{\rho}{\pi^2 L_1 L_2} \int_{|\underline{\sigma}|>|k_0|} \frac{I^*_{mn}(\underline{\sigma}) I_{qs}(\underline{\sigma})}{\sqrt{\sigma^2 - k_0^2}} \, d\underline{\sigma} \, , \tag{5-64}$$

equation (5-62) can be written

$$\left\{Dk_{mn}^{4} - \mu\omega^2 + ir\omega\right\}\overset{\nabla}{W}_{mn}(\omega) + \sum_{q=1}^{\infty} \sum_{s=1}^{\infty} [-\omega^2 \mu_{mnqs}(\omega) + i\omega r_{mnqs}(\omega)]\overset{\nabla}{W}_{qs}(\omega) = \overset{\nabla}{F}_{mn}(\omega) \, . \tag{5-65}$$

By recalling that the free wavenumber of the space- and time-invariant plate in vacuo is defined by

$$k_p(\omega) = \sqrt[4]{\mu\omega^2/D} \, , \tag{5-66}$$

we can rewrite equation (5-65) in the form

$$\sum_{q=1}^{\infty}\sum_{s=1}^{\infty}\left\{\delta_{mq}\delta_{ns}k_{qs}{}^{4}-k_{p}{}^{4}\left[\delta_{mq}\delta_{ns}+\frac{\mu_{mnqs}(\omega)}{\mu}\right]\right.$$

$$\left.+\,i\,\frac{r\omega}{D}\left[\delta_{mq}\delta_{ns}+\frac{r_{mnqs}(\omega)}{r}\right]\right\}\overset{\nabla}{W}_{qs}(\omega)=\frac{\overset{\nabla}{F}_{mn}(\omega)}{D}\,. \tag{5-67}$$

Equation (5-67) represents a doubly infinite set of coupled equations for the frequency-dependent modal coefficients of the plate displacement, $\overset{\nabla}{W}_{mn}(\omega)$, in terms of the frequency-dependent modal coefficients of the external forcing field, $\overset{\nabla}{F}_{mn}(\omega)$. Owing to the coupled nature of these equations, a single modal component of the forcing field excites many modal components of displacement. This behavior is in sharp contrast to that observed in the forced response of the simply supported plate in vacuo (see equation (4-197) of section 4.3.3.2), where each modal component of the forcing field excited only the corresponding modal component of displacement. Clearly then, the coupling between a single modal component of force and the infinite set of modal coefficients of the displacement results from the fluid loading of the plate.

The fluid loading of the plate is applied by the pressure field (that is induced throughout the acoustic half space by the motion of the plate) acting on the upper surface of the plate. By equation (4-146) of section 4.3.3.1, the space-time description of the pressure field over the surface $x_3 = 0$ can be expressed as

$$p(\underline{x},0,t) = (2\pi)^{-3}\int_{-\infty}^{\infty}\int_{-\infty}^{\infty} P(\underline{k},0,\omega)\exp\{i(\underline{k}\cdot\underline{x}+\omega t)\}\,d\underline{k}\;d\omega \tag{5-68}$$

for all $\underline{x}$ and t. However, over the surface of the plate, $0 \le x_1 \le L_1$ and $0 \le x_2 \le L_2$, $p(\underline{x},0,t)$ can be expressed in the form

$$p(\underline{x},0,t) = (2\pi)^{-1}\int_{-\infty}^{\infty}\sum_{m=1}^{\infty}\sum_{n=1}^{\infty}\overset{\nabla}{P}_{mn}(\omega)\alpha_{mn}(\underline{x})\exp(i\omega t)\,d\omega\,,\qquad \begin{matrix}0 \le x_1 \le L_1\,,\\ 0 \le x_2 \le L_2\,.\end{matrix} \tag{5-69}$$

By use of equations (5-7), (5-58), (5-68), and (5-69), it follows that

$$\sum_{u=1}^{\infty} \sum_{v=1}^{\infty} \overset{\nabla}{P}_{uv}(\omega)\alpha_{uv}(\underline{x})$$

$$= (2\pi)^{-2} \sum_{q=1}^{\infty} \sum_{s=1}^{\infty} \left\{ \int_{|\underline{k}| \leq |k_0|} \frac{i\rho c\omega \overset{\nabla}{W}_{qs}(\omega) I_{qs}(\underline{k})}{\sqrt{1 - k^2/k_0^{\,2}}} \exp[i(\underline{k}\cdot\underline{x})]\, d\underline{k} \right.$$

$$\left. - \int_{|\underline{k}| > |k_0|} \frac{\rho\omega^2 \overset{\nabla}{W}_{qs}(\omega) I_{qs}(\underline{k})}{\sqrt{k^2 - k_0^{\,2}}} \exp[i(\underline{k}\cdot\underline{x})]\, d\underline{k} \right\} \tag{5-70}$$

for $0 \leq x_1 \leq L_1$ and $0 \leq x_2 \leq L_2$. By multiplying equation (5-70) by $\alpha_{mn}(\underline{x})$ and integrating over $0 \leq x_1 \leq L_1$ and $0 \leq x_2 \leq L_2$, we can use equations (4-54), (5-54), (5-63), and (5-64) to show that

$$\overset{\nabla}{P}_{mn}(\omega) = \sum_{q=1}^{\infty} \sum_{s=1}^{\infty} \{i\omega r_{mnqs}(\omega) - \omega^2 \mu_{mnqs}(\omega)\} \overset{\nabla}{W}_{qs}(\omega) \ . \tag{5-71}$$

Equation (5-71), which defines the complex, frequency-dependent amplitude of the mn-th modal component of the pressure field acting over the upper surface of the plate, clearly shows that a single modal component of the displacement field, $\overset{\nabla}{W}_{qs}(\omega)$, produces an infinite number of modal components of pressure on the upper surface of the plate. These modal components of pressure, in turn, excite the corresponding modes of displacement of the plate. This phenomenon is known as modal coupling.

The presence and degree of modal coupling is dictated, in both equations (5-67) and (5-71), by the frequency-dependent quantities r_{mnqs} and μ_{mnqs}, defined by equations (5-63) and (5-64), respectively. It is desirable to interpret the roles of these quantities on the physics of the plate motion.

It is easily shown, by use of equations (5-54), (5-63), and (5-64), that r_{mnqs} and μ_{mnqs} are real quantities. Further, by equation (5-71), it is

evident that the combination of terms

$$\{i\omega r_{mnqs}(\omega) - \omega^2 \mu_{mnqs}(\omega)\}\overset{\nabla}{W}_{qs}(\omega)$$

can be interpreted, at any given frequency, as the contribution to the mn-th modal component of the pressure acting over the upper surface of the plate resulting from the qs-th modal component of the displacement field of the plate. More specifically, it can be shown by use of equation (5-56) that $i\omega\overset{\nabla}{W}_{qs}(\omega)$ can be interpreted as the complex frequency-dependent amplitude of the qs-th modal component of the normal velocity field of the plate. Therefore, because r_{mnqs} is real, the term $i\omega r_{mnqs}(\omega)\overset{\nabla}{W}_{qs}(\omega)$ describes a contribution to the mn-th modal component of pressure that is proportional to the qs-th modal component of the velocity field of the plate. Inasmuch as forces per unit area that are proportional to velocity are normally associated with losses (e.g., damping) to the system, the term r_{mnqs} can be interpreted as additional damping per unit area of the plate resulting from the coupling between mn-th and qs-th in-vacuo modes of the plate caused by the presence of the fluid. This interpretation is supported by equation (5-63), which shows that $r_{mnqs}(\omega)$ is proportional to an integral over the supersonic (i.e., $|\underline{\alpha}| \leq |k_0|$) wavevector components of the acoustic half space. Recall, from section 4.3.3.1, that these supersonic wavevector components are associated with waves that propagate away from the boundary (the plate-baffle surface) and, thereby, represent a loss mechanism to the plate.

By similar reasoning, the term $-\omega^2\overset{\nabla}{W}_{qs}(\omega)$ can be interpreted as the complex amplitude of the qs-th modal component of the acceleration field of the plate in a direction normal to its surface. Because μ_{mnqs} is real, the term $-\omega^2\mu_{mnqs}(\omega)\overset{\nabla}{W}_{qs}(\omega)$ represents a contribution to the mn-th modal component of the pressure acting over the upper surface of the plate that is proportional to the qs-th modal component of the acceleration field of the plate. Because forces per unit area that are proportional to acceleration are associated with the inertia (or mass) of the system, the term μ_{mnqs} can be interpreted as an additional mass imposed on the plate as a result of the coupling of the mn-th and qs-th modes caused by the presence of the fluid. As seen by equation (5-64), this additional mass is proportional to an integral of the subsonic (i.e., $|\underline{\alpha}| > |k_0|$) wavevector components of the acoustic

half space. These subsonic components were shown, in section 4.3.3.1, to be associated with waves that did not propagate away from the boundary, but decayed in amplitude with increasing distance from the boundary, (i.e., the plate). As these waves do not propagate away from the plate, they do not represent a loss mechanism to the plate. Rather they can only represent reactive forces (i.e., inertia or stiffness) on the plate. Davies[3] argued that the terms containing μ_{mnqs} lead to additional virtual mass of the plate. Therefore, μ_{mnqs} is interpreted as additional mass to the plate rather than additional stiffness.

By the above arguments, we conclude that the modal coupling, introduced by the physical coupling between the plate and the fluid, has the effect of adding mass and damping to the simply supported plate. The reader will recall that the effects of fluid loading on the space-invariant, infinite plate were to increase the apparent mass and damping of the plate. Thus, we see that the effects of fluid loading are similar between finite, simply supported plates and infinite, space-invariant plates.

If we define

$$A_{mnqs}(\omega) = \delta_{mq}\delta_{ns}k_{qs}^4 - k_p^4\left[\delta_{mq}\delta_{ns} + \frac{\mu_{mnqs}(\omega)}{\mu}\right]$$

$$+ i\,\frac{r\omega}{D}\left[\delta_{mq}\delta_{ns} + \frac{r_{mnqs}(\omega)}{r}\right], \tag{5-72}$$

then equation (5-67) can be rewritten as

$$\sum_{q=1}^{\infty}\sum_{s=1}^{\infty} A_{mnqs}(\omega)\overset{\nabla}{W}_{qs}(\omega) = \frac{\overset{\nabla}{F}_{mn}(\omega)}{D}\,. \tag{5-73}$$

In principle, although not necessarily in practice, a four-dimensional, frequency-dependent matrix, $B_{mnqs}(\omega)$, can be found that satisfies the relationship

$$\sum_{q=1}^{\infty}\sum_{s=1}^{\infty} B_{ijmn}(\omega)A_{mnqs}(\omega) = \delta_{iq}\delta_{js}\,. \tag{5-74}$$

That is, the matrix $B_{mnqs}(\omega)$ is the inverse of the matrix $A_{mnqs}(\omega)$ at the frequency ω. By use of equations (5-73) and (5-74), it follows that $\overset{\nabla}{W}_{mn}(\omega)$ has the form

$$\overset{\nabla}{W}_{mn}(\omega) = \sum_{q=1}^{\infty} \sum_{s=1}^{\infty} B_{mnqs}(\omega) \frac{\overset{\nabla}{F}_{qs}(\omega)}{D} . \tag{5-75}$$

Therefore, by equation (5-58), the wavevector-frequency description of the displacement field of the baffled, simply supported plate, fluid loaded on one side, has the form

$$W(\underline{k},\omega) = \sum_{m=1}^{\infty} \sum_{n=1}^{\infty} \sum_{q=1}^{\infty} \sum_{s=1}^{\infty} B_{mnqs}(\omega) \frac{\overset{\nabla}{F}_{qs}(\omega)}{D} I_{mn}(\underline{k}) . \tag{5-76}$$

Equation (5-76) shows that, at any fixed frequency ω, the wavevector dependence of the displacement field of the baffled, fluid-loaded, simply supported plate is specified by a weighted summation of the wavevector transforms of the space-limited natural modes of the in-vacuo plate, $I_{mn}(\underline{k})$, over all mode numbers, m and n. By reference to equation (4-217) of section 4.3.3.2, it is evident that the wavevector dependence of the displacement field of the in-vacuo, simply supported plate is also specified by a weighted summation of $I_{mn}(\underline{k})$ over all m and n. However, a comparison of equations (4-217) and (5-76) shows that the modal weights applied to $I_{mn}(\underline{k})$ are considerably more complicated for the fluid-loaded plate than for the in-vacuo plate. Determination of the modal weights, $\overset{\nabla}{W}_{mn}(\omega)$, for the fluid-loaded, simply supported plate requires, by equation (5-75), knowledge of $B_{mnqs}(\omega)$, the inverse of $A_{mnqs}(\omega)$. Inasmuch as the mode numbers, m and n, range from 1 to infinity, it is evident that $B_{mnqs}(\omega)$ cannot be determined exactly. Therefore, only approximate solutions can be obtained for the wavevector-frequency (or space-time, for that matter) characteristics of the baffled, simply supported, fluid-loaded plate. A variety of such approximate solutions are presented by Junger and Feit[4] and Davies.[5] The majority of these approximate solutions require arguments too complex and lengthy to be presented here. However, to provide some insight into the response characteristics of the baffled, fluid-loaded, simply supported plate, we will

present one, somewhat simplistic, example of an approximate solution: the example of a light fluid loading.

Light fluid loading is defined as that situation in which the modal amplitude of the pressure, $\overset{\nabla}{P}_{mn}(\omega)$, defined by equation (5-71), is small in comparison with the externally applied modal force, $\overset{\nabla}{F}_{mn}(\omega)$. Thus, in the case of light fluid loading, the forces resulting from modal coupling are small, and each modal component of the applied force is primarily balanced by the modal forces associated with the stiffness and inertia of the plate. Under these assumptions, equation (5-65) can be rewritten

$$\left\{Dk_{mn}{}^{4} - [\mu + \mu_{mnmn}(\omega)]\omega^{2} + i[r + r_{mnmn}(\omega)]\omega\right\}\overset{\nabla}{W}_{mn}(\omega) + \epsilon_{mn}(\omega) = \overset{\nabla}{F}_{mn}(\omega) \ , \tag{5-77}$$

where $\epsilon_{mn}(\omega)$ denotes the contribution to the modal pressure resulting from the sum of the crosscoupled terms (i.e., $q \neq m$ and $s \neq n$) in equation (5-71). That is,

$$\epsilon_{mn}(\omega) = \sum_{\substack{q=1\\ q\neq m}}^{\infty} \sum_{\substack{s=1\\ s\neq n}}^{\infty} [-\omega^{2}\mu_{mnqs}(\omega) + i\omega r_{mnqs}(\omega)]\, \overset{\nabla}{W}_{qs}(\omega) \ . \tag{5-78}$$

We now assume that $\epsilon_{mn}(\omega)$ is of the same order of magnitude as the modal pressure, $\overset{\nabla}{P}_{mn}(\omega)$, and is therefore sufficiently small, in comparison with the externally applied modal force, $\overset{\nabla}{F}_{mn}(\omega)$, to be neglected. Under this assumption, it follows that the modal amplitudes, $\overset{\nabla}{W}_{mn}(\omega)$, can be approximated by

$$\overset{\nabla}{W}_{mn}(\omega) \approx \frac{\overset{\nabla}{F}_{mn}(\omega)}{\{Dk_{mn}{}^{4} - [\mu + \mu_{mnmn}(\omega)]\omega^{2} + i[r + r_{mnmn}(\omega)]\omega\}} \ . \tag{5-79}$$

It therefore follows that the wavevector-frequency description of the displacement field of the baffled, lightly fluid-loaded, simply supported plate can be approximated by

$$W(\underline{k},\omega) = \sum_{m=1}^{\infty} \sum_{n=1}^{\infty} \frac{\overset{\nabla}{F}_{mn}(\omega) I_{mn}(\underline{k})}{\{Dk_{mn}{}^4 - [\mu + \mu_{mnmn}(\omega)]\omega^2 + i[r + r_{mnmn}(\omega)]\omega\}} . \qquad (5\text{-}80)$$

Comparison of equation (5-80) with equation (4-217) of section 4.3.3.2 shows that the wavevector-frequency description of the displacement field of the lightly fluid-loaded, simply supported plate has a mathematical form similar to that of the simply supported plate in vacuo. Indeed, this comparison reveals that the effect of the light fluid loading is to increase the apparent mass and damping of the plate. The additional mass and damping are modally dependent quantities, which, in this first order approximation, result only from the autocoupled ($m = q$ and $n = s$) modal contributions to the pressure field at the surface of the plate.

The similarity in the mathematical forms of equations (5-80) and (4-217) implies a similarity between the wavevector-frequency characteristics of in-vacuo and lightly fluid-loaded, simply supported plates. By arguments presented in section 4.3.3.2, certain wavevector-frequency characteristics of the forced response of the in-vacuo, simply supported plate were deduced from equation (4-217). By taking proper account of the differences in inertia and damping between equations (4-127) and (5-80), a similar set of wavevector-frequency characteristics can be inferred for the forced response of the lightly fluid-loaded, simply supported plate.

Recall that at any resonance frequency, ω_{MN}, the magnitude of the wavevector-frequency response of the simply supported plate in vacuo was argued to be relatively large in the neighborhoods of those modal wavevectors associated with the resonance (i.e., where $|\underline{k}| = k_{MN}$) and in the neighborhoods of those modal wavevectors associated with relatively large modal forces. By similarity arguments, it follows that, at any resonance frequency of the lightly fluid-loaded, simply supported plate, ω_{MN}', the magnitude of the wavevector-frequency response will be relatively large in the neighborhoods of those modal wavevectors associated with the resonance (i.e., where $|\underline{k}| = k_{MN}$) and in the neighborhoods of those modal wavevectors associated with relatively large modal forces. Here, ω_{MN}' is the natural frequency of the MN-th mode of the lightly fluid-loaded plate, which is

defined as that frequency at which

$$Dk_{MN}^4 - [\mu + \mu_{MNMN}(\omega)]\omega^2 = 0 \ . \tag{5-81}$$

In contrast, the MN-th modal natural frequency of the in-vacuo plate was defined as that frequency satisfying

$$Dk_{MN}^4 - \mu\omega^2 = 0 \ . \tag{5-82}$$

Thus, we see that lightly fluid-loaded and in-vacuo simply supported plates have similar wavevector-frequency characteristics at resonance. However, owing to the additional apparent mass associated with the fluid loading, the resonance frequencies of the lightly fluid-loaded plate differ from those of the plate in vacuo.

In section 4.3.3.2, we argued that, at a nonresonance frequency ω_0, the in-vacuo plate responded most strongly to those modal forces characterized by modal wavenumbers, k_{mn}, nearest to the free wavenumber, $k_p(\omega_0)$, of the in-vacuo plate: that is, those modal forces characterized by modal numbers, m and n, such that

$$k_{mn} = \sqrt{(m\pi/L_1)^2 + (n\pi/L_2)^2} \approx k_p(\omega_0) \ . \tag{5-83}$$

By similarity arguments, the lightly fluid-loaded plate also responds most strongly at a nonresonance frequency to modal forces characterized by modal wavenumbers, k_{mn}, nearest to the free wavenumber of the lightly fluid-loaded plate, $\tilde{k}_p(\omega_0)$, which (by equation (5-80)) can be approximated by

$$\tilde{k}_p(\omega_0) = \sqrt[4]{[\mu + \mu_{mnmn}(\omega_0)]\omega_0^2/D} \ . \tag{5-84}$$

Thus, off resonance, both the in-vacuo and lightly fluid-loaded plate respond most strongly to modal forces characterized by modal wavenumbers nearest to the free wavenumbers of the respective plates. However, owing to the additional mass associated with the fluid loading, the free wavenumber of the lightly fluid-loaded plate differs from that of the plate in vacuo.

It was demonstrated in section 4.3.3.2 that excitation of the in-vacuo simply supported plate by a single wavevector-frequency component of the externally applied forcing field produced a response, at the frequency of excitation, that was comprised of a weighted distribution of wavevectors. This conversion of a single wavevector component of the input into multiple wavevector components of response was attributed to wavevector scattering at the boundaries of the plate. This mechanism for wavevector conversion is, of course, also present in the lightly fluid-loaded, simply supported plate. However, as was shown above, fluid loading provides an additional mechanism for wavevector conversion in the simply supported plate: that is, modal coupling. Whereas only autocoupling of modes is assumed in the light fluid-loading approximation, it should be recognized that the forces associated with crosscoupled modes can be significant for heavier fluid loadings.

5.4 CONCLUDING REMARKS

In this chapter, we have demonstrated that spatially distributed, multicomponent linear systems can be interpreted as an assemblage of coupled subsystems, where each subsystem represents a single physical component of the composite system and the couplings between subsystems reflect appropriate interactions between the corresponding physical components. By use of this interpretation, we argued that the mathematical model of a multicomponent system is formulated by appropriately coupling the assemblage of mathematical models of the subsystems associated with the composite system. To demonstrate this procedure for the formulation and solution of mathematical models of multicomponent systems, we treated the free and forced vibrations of an infinite plate with fluid loading on one side and the forced vibration of a baffled, simply supported plate with fluid loading on one side as illustrative examples.

These illustrative examples reveal that a primary effect of the fluid loading, common to both the infinite and simply supported plates, is to increase the apparent mass and damping of the plate. The increase in apparent mass, though frequency dependent, causes the free wavenumber of the fluid-loaded plate to be greater, at any frequency, than that of the same plate

in vacuo. Inasmuch as the free wavenumber defines the resonance characteristics of the plate in the wavevector-frequency domain, it follows that the fluid loading alters the resonance behavior of infinite and space-limited plates. In the case of the simply supported plate, it was shown that the fluid loading provides a means for wavevector conversion supplemental to the scattering mechanism associated with reflections at the boundaries of the in-vacuo plate. This additional means of wavevector conversion is modal coupling, whereby a single modal component of displacement of the plate produces a pressure field at the surface of the plate that is comprised of many modal components. These modal components of the pressure field act as additional modal forces on the plate and produce corresponding modal responses of the plate.

The response of multicomponent systems comprised of structural and fluid components is the focus of structural acoustics. The response of interest (i.e., output) in such systems can be either the vibratory field of the structure or the acoustic pressure field produced by the vibration of the structure. The illustrative examples for this chapter are a subset of perhaps the most exhaustively studied class of problems in structural acoustics: the vibration of, and radiation from, plates in contact with an acoustic fluid. Owing to space limitations and the desire to provide a simple and consistent set of illustrative examples of coupled systems, the examples presented here focus only on the vibratory displacement fields of the simplest space-invariant and space-limited forms of plate-fluid systems: that is, the infinite and simply supported fluid-loaded plates. Space limitations also restricted the detail to which the effects of fluid-loading were examined. To supplement the treatment of coupled plate-fluid systems provided here and to demonstrate the variety of plate-fluid systems addressed in the literature, we close this chapter with a brief listing of references. These references can be used as a springboard by the interested reader to further expand his sources of information.

The vibration and pressure fields associated with uniform, infinite plates under various forms of excitations constitute the most extensively studied class of coupled systems in structural acoustics. Examples of these systems are treated in such standard texts as Junger and Feit[6] and Morse and

Ingard.[7] However, as late as 1979, there was continuing interest[8,9,10] (and some confusion) regarding the free waves of fluid-loaded plates. The vibration and acoustic fields associated with fluid-loaded infinite plates are usually obtained by asymptotic methods. Examples of such approaches are presented by Morse and Ingard[11] and by Crighton.[12,13]

The vibration and acoustic fields of the simply supported, rectangular plate are treated by Junger and Feit.[14] However, for a detailed treatment of the modal coupling terms (i.e., μ_{mnqs} and r_{mnqs}) and high and low frequency approximate solutions of the displacement and radiated fields of fluid-loaded, simply supported plates, the reader is referred to Davies.[15] In addition, Maidanik[16] devised a method for classifying the various modes of simply supported plates in terms of their radiation efficiencies. Crighton and Innes[13] apply asymptotic methods to obtain approximate solutions for the vibration and radiation fields of certain other examples of fluid-loaded, space-limited plates.

Finally, the vibration and acoustic radiation fields of beam-stiffened, fluid-loaded plates have received much attention over the past 25 years. This work has progressed from the consideration of the vibration and acoustic fields of a single beam attached to a plate,[17,18] through the treatment of the vibration and pressure fields associated with periodically stiffened, fluid-loaded plates,[19] to the prediction of the vibratory and radiated fields of a plate with any number of supports.[20,21]

The above references illustrate the variety of coupled plate-fluid systems encountered in structural acoustics and provide a starting point for readers interested in such systems.

5.5 REFERENCES

1. M. Abramowitz and I. Stegun, Handbook of Mathematical Functions, National Bureau of Standards, Applied Mathematics Series No. 55, Washington, DC, 1967, p. 17.

2. M. C. Junger and D. Feit, Sound, Structures, and Their Interaction, second edition, MIT Press, Cambridge, MA, 1986, pp. 236-239.

3. H. G. Davies, Acoustic Radiation From Fluid-Loaded Rectangular Plates, MIT Report No. 71476-1, December 1969, pp. 20-27.

4. Junger and Feit, op. cit., pp. 264-272.

5. Davies, op. cit., pp. 28-63.

6. Junger and Feit, op. cit., pp. 235-264.

7. P. M. Morse and K. U. Ingard, Theoretical Acoustics, McGraw-Hill Book Co., New York, 1968, pp. 624-642.

8. A. D. Stewart, "Acoustic Radiation From Submerged Plates. I. Influence of Leaky Wave Poles," Journal of the Acoustical Society of America, vol. 59, no. 5, May 1976, pp. 1160-1169.

9. D. G. Crighton, "The Free and Forced Waves on a Fluid-Loaded Elastic Plate," Journal of Sound and Vibration, vol. 63, no. 2, March 1979, pp. 225-235.

10. W. A. Strawderman, S-H Ko, and A. H. Nuttall, "The Real Roots of the Fluid-Loaded Plate," Journal of the Acoustical Society of America, vol. 66, no. 2, August 1979, pp. 579-585.

11. Morse and Ingard, op. cit., pp. 627-633.

12. Crighton, op. cit.

13. D. G. Crighton and D. Innes, "Low Frequency Acoustic Radiation and Vibration Response of Locally Excited Fluid-Loaded Structures," Journal of Sound and Vibration, vol. 91, no. 2, November 1983, pp. 293-314.

14. Junger and Feit, op. cit., pp. 264-272.

15. Davies, op. cit.

16. G. Maidanik, "Response of Ribbed Panels to Reverberant Acoustic Fields," Journal of the Acoustical Society of America, vol. 34, no. 6, June 1962, pp. 809-826.

17. R. H. Lyon, "Sound Radiation From a Beam Attached to a Plate," Journal of the Acoustical Society of America, vol. 34, no. 9, September 1962, pp. 1265-1268.

18. G. Maidanik, A. J. Tucker, and W. H. Vogel, "Transmission of Free Waves Across a Rib on a Panel," Journal of Sound and Vibration, vol. 49, no. 4, December 1976, pp. 445-452.

19. V. N. Evseev, "Sound Radiation From a Plate With Periodic Inhomogeneities," Soviet Physics Acoustics, vol. 19, no. 3, November-December 1973, pp. 226-229.

20. J. M. Garrelick and G-F Lin, "Effect of the Number of Frames on the Sound Radiated by Fluid-Loaded, Frame-Stiffened Plates," Journal of the Acoustical Society of America, vol. 58, no. 2, August 1978, pp. 499-500.

21. D. Crighton, T. Eisler, and G. Maidanik, "Influence of Fluid Loading on the Transmission Across, Radiation From, and Reflection By Ribs on a Panel," David Taylor Naval Ship Research and Development Center, Technical Memorandum TM-1902-78-52, November 1978.

CHAPTER 6

RANDOM SPACE-TIME FIELDS

In the previous chapters, we have presented examples of various classes of linear systems excited by deterministic input fields -- that is, input fields that can be explicitly described over all space and time for all repetitions, or realizations, of the experiment or computation. In many problems of practical interest in acoustics, however, the system of interest is excited by a field that behaves unpredictably, in both space and time, from one experiment, or observation, to another. Such fields are called random space-time fields, and can be described only in terms of their statistical properties.

In this chapter, we define the statistical metrics used to characterize random space-time fields. In addition, we define various classes of random space-time fields, and show how the classification of the field affects the functional form of the statistical metric.

The random space-time fields encountered in acoustics fall into a category that statisticians call random, or stochastic, processes. Inasmuch as these space-time fields describe real physical quantities, we will limit our attention to real random processes. Random processes are rigorously treated in texts dealing with the mathematical theory of probability and statistics (see, for example, reference 1), and are somewhat less rigorously treated in engineering texts (such as references 2, 3 and 4). The intent of this chapter is to define those statistical metrics and concepts used in wavevector-frequency analysis of linear acoustic systems. The most cursory examination of any of references 1 through 4 will demonstrate the futility of attempting either a complete or rigorous treatment of stochastic processes in a single chapter. Therefore, to accommodate both the intent and spatial restrictions of this chapter, we must assume that the reader has some familiarity with the theory of probability and statistics. Moreover, we must disclaim any pretense of rigor in our presentation of statistical definitions and concepts. For

comprehensive or rigorous treatments of the statistical concepts and metrics presented here, the reader is encouraged to consult the above cited (or equivalent) references. Readers unfamiliar with probability and statistics will find the first chapter of Random Vibration by Crandall and Mark[5] to be a helpful introduction to random processes and statistical concepts.

6.1 REVIEW OF BASIC CONCEPTS

Probability and statistics are mathematical theories developed to describe and predict certain average properties of experimental outcomes that vary randomly over repeated trials. The concept of repeated experiments or observations is central to the definition of randomness. Consider, for example, an experiment in which the pressure, $p(\underline{x}_0,t)$, at the spatial location $\underline{x}_0$ on a planar surface is measured as a function of time between $0 \leq t \leq T$. Assume that the time history of $p(\underline{x}_0,t)$ illustrated in figure 6-1 is the result of one trial of this experiment. This time history has no apparent pattern, and one is tempted to say that the pressure varies randomly in time. However, if the experiment is repeated many times, either on the same system or on a series of identical (within the control of the experimenter) systems, and if the time histories of the input pressure at $\underline{x}_0$ are identical for all repetitions of the experiment, the pressure field, $p(\underline{x}_0,t)$, is said to be deterministic over the interval $0 \leq t \leq T$ inasmuch as the result of one experiment defines the results of all repetitions of the experiment. If, however, each repetition of the experiment produces a different time history of the pressure at $\underline{x}_0$ over the time interval $0 \leq t \leq T$, the pressure field, $p(\underline{x}_0,t)$, is said to be random in that time interval.

The fields of interest in acoustics are wave fields, which vary in both space and time. To facilitate the application of the theory of probability and statistics to the random space-time fields occurring in acoustics, it is desirable to review certain definitions and concepts. To illustrate these definitions and concepts, we will use (here, and throughout this chapter) the pressure field, $p(\underline{x},t)$, on a planar surface. The reader should realize, however, that the arguments, definitions, and concepts illustrated by this surface pressure field apply equally to displacement, acceleration, or other

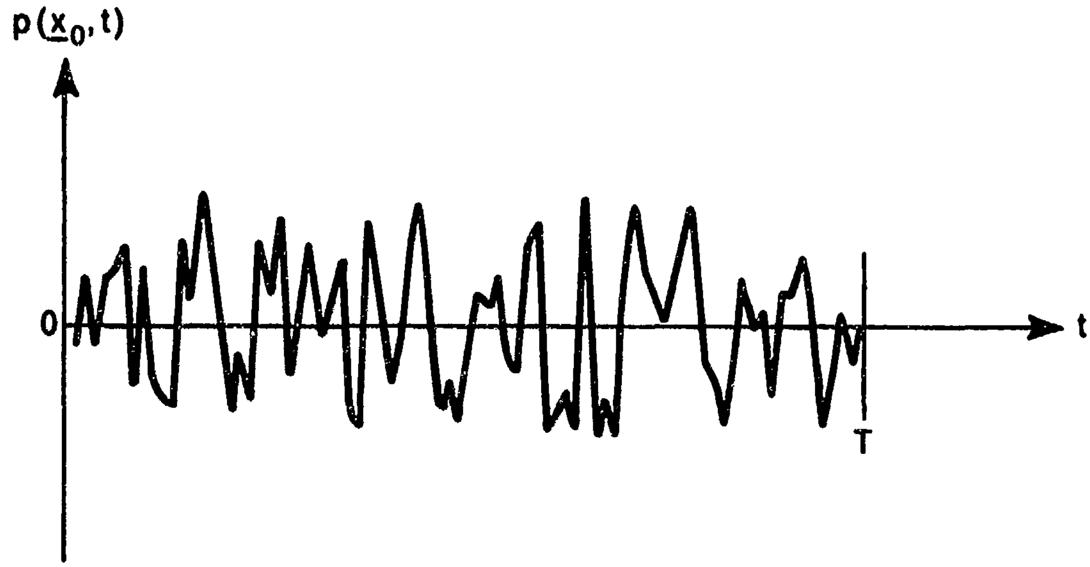

Figure 6-1. Time History of $p(\underline{x}_0,t)$

space-time fields of interest in acoustics.

6.1.1 Fundamental Definitions

An outcome of an experiment is a predefined result of one trial of an experiment. In an experiment of drawing one card from a deck of 52 cards, the outcome could be defined as the particular card drawn. Thus, the outcome of one trial of this experiment might be the king of clubs. In an experiment designed to measure the pressure field on a planar surface, the outcome might be defined as the pressure at the spatial location $\underline{x}_1$ and time t_1. The important characteristic of an outcome is that it is a single data point associated with one trial of the experiment.

A random variable is a function, or rule of correspondence, for assigning numbers to all possible outcomes of an experiment. In the experiment of drawing a single card from a deck, there are 52 possible outcomes, and one might define the random variable by assigning the numbers 1 to 13 to the ace through king of clubs, 14 to 26 to the ace through king of diamonds, and so forth, such that all possible outcomes are assigned the numbers 1 through 52. In engineering experiments, the assignation (or definition) of a random

variable to all possible outcomes of an experiment is a trivial exercise inasmuch as the outcomes of such experiments are generally expressed in numerical terms. For example, we may desire all possible outcomes of the various trials of measuring the surface pressure at the location $\underline{x}_1$ and time t_1 to be expressed in units of micropascals. In this case, the random variable is the function, or rule, by which the repeated measurements of $p(\underline{x}_1, t_1)$ are converted to numbers with units of micropascals.

The value of the random variable associated with a particular outcome of the experiment is the number assigned to a particular outcome. The range of the random variable is defined as the set of values that the random variable assigns within the ensemble (or collection) of all possible outcomes of the experiment. Note, for example, that for the card experiment described above, the range of the random variable is the discrete set of numbers 1 to 52. In repeated measurements of the surface pressure at $\underline{x}_1$ and t_1, the value of pressure (in units of micropascals) may assume any value between $-\infty$ and $+\infty$. Thus, the range of the random variable is the continuous set of all numbers between minus and plus infinity.

Although there is a distinction between a random variable (the rule of correspondence between outcomes and numbers) and the value of a random variable (a number), this distinction is commonly ignored, and the terms "value of a random variable" and "random variable" are often used synonymously.

Attendant with the concept of assigning numbers to all possible outcomes of an experiment by definition of a random variable is the concept of the relative frequency of occurrence, or probability density, of each possible value of the random variable over a very large number of repetitions (or trials) of the experiment. The probability density (or, more precisely, the probability density function) of a random variable is a central concept in the mathematical theory of probability and statistics because all statistical metrics are defined in terms of appropriate probability density functions.

The probability density function of a random variable is usually defined in terms of the distribution function of that random variable. The distribution function of the (value of the) random variable v, which we denote

by $F_v(\alpha)$, is the continuous function defined by

$$F_v(\alpha) = \text{Prob}[v \leq \alpha] \tag{6-1}$$

over all values of α. Here, the subscript v indicates that the distribution function applies to the random variable v, and Prob[ ] denotes the probability that the statement within the braces is true. Papoulis[6] shows that the distribution function of a random variable (say v) has the following properties:

(a) $F_v(-\infty) = 0$ and $F_v(+\infty) = 1$

and

(b) $F_v(\alpha)$ is a nondecreasing function of α; that is,

$$F_v(\alpha_1) \leq F_v(\alpha_2) \text{ for } \alpha_1 \leq \alpha_2 .$$

By equation (1), it follows that if $\alpha_2 > \alpha_1$,

$$F_v(\alpha_2) - F_v(\alpha_1) = \text{Prob}[v \leq \alpha_2] - \text{Prob}[v \leq \alpha_1] = \text{Prob}[\alpha_1 < v \leq \alpha_2] . \tag{6-2}$$

An example of a distribution function of the random variable v is illustrated in figure 6-2.

The probability density function of a random variable is defined[7] as the derivative of the distribution function of that random variable. Thus, for the random variable v, the probability density function of v, designated by f_v, is defined by

$$f_v(\alpha) = \frac{dF_v(\alpha)}{d\alpha} . \tag{6-3}$$

By equation (6-3) and the properties of the distribution function listed above, it is evident that the probability density function has the following properties:

(a) $f_v(\alpha) \geq 0$ (because $F_v(\alpha)$ is a nondecreasing function of α),

(b) $$\int_{-\infty}^{\infty} f_v(\alpha)\, d\alpha = 1 \text{ (because } F_v(\infty) = 1 \text{ and } F_v(-\infty) = 0) ,$$

(c) $$\int_{-\infty}^{b} f_v(\alpha)\, d\alpha = F_v(b) = \text{Prob}[v \leq b], \text{ and}$$

(d) $$\int_{a}^{b} f_v(\alpha)\, d\alpha = F_v(b) - F_v(a) = \text{Prob}[a < v \leq b].$$

The probability density function associated with the distribution function of figure 6-2 is illustrated in figure 6-3.

Unless the probability density of a random variable is given or can be physically or intuitively deduced, it must be estimated from measured data. To illustrate how the probability density might be estimated and to lay a foundation for future arguments, it is useful at this point to examine the interpretation of the probability density in terms of the relative frequency of occurrence of the values of a random variable. Consider an experiment in which values of the random variable, v, have been assigned to all possible outcomes. The experiment is repeated N times, and we wish to estimate the probability density function of v from the resultant data. By statement (d) of the properties of the probability density function and by use of the mean value theorem for integrals, it is straightforward to show that

$$\int_{a-\Delta a/2}^{a+\Delta a/2} f_v(\alpha)\, d\alpha = \text{Prob}[a - \Delta a/2 < v \leq a + \Delta a/2] \approx f_v(a)\, \Delta a \,. \qquad (6\text{-}4)$$

Let us divide the range of the value of the random variable into equal, nonoverlapping increments, $\Delta\alpha$, centered at the values $\alpha_m = m\Delta\alpha$, where $-\infty \leq m \leq \infty$. If we then denote the number of times the value of the random variable

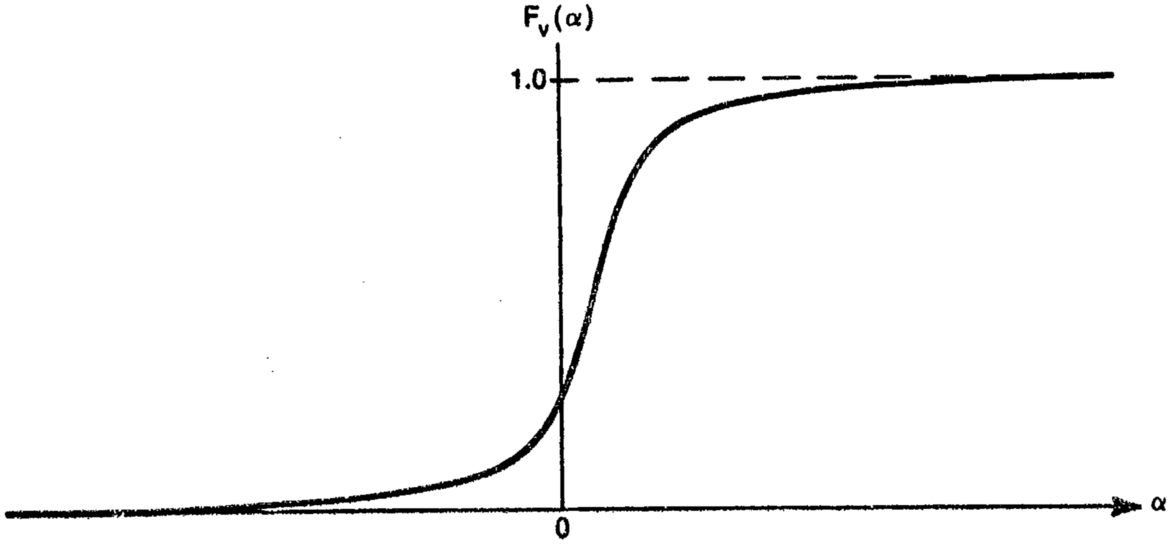

Figure 6-2. Example of a Distribution Function for a Random Variable, v

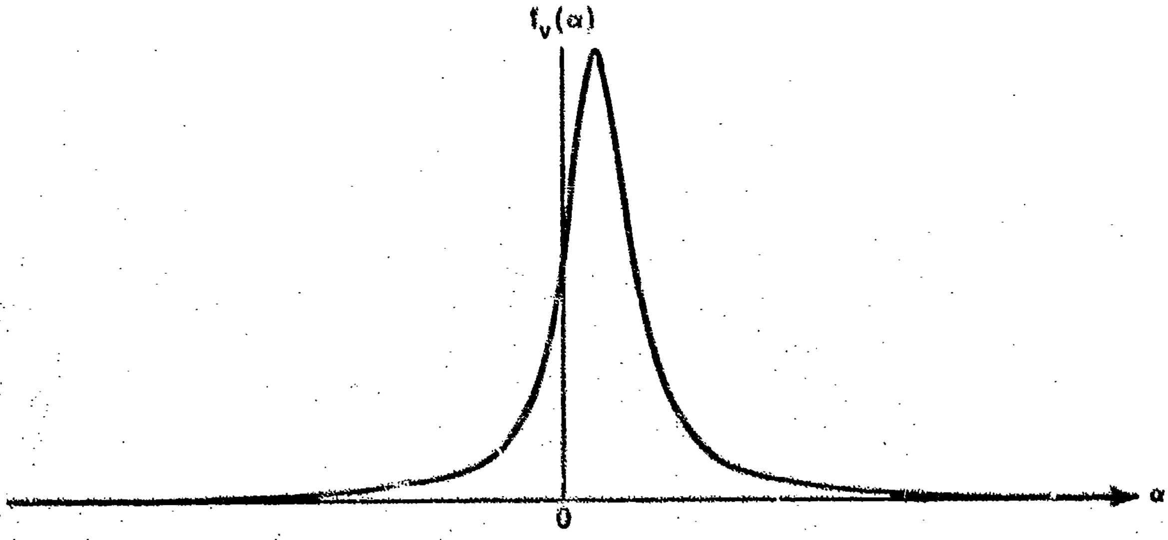

Figure 6-3. Probability Density Function Associated With the Distribution Function of Figure 6-2

occurs within any given increment $\alpha_m - \Delta\alpha/2$ to $\alpha_m + \Delta\alpha/2$ by $n(\alpha_m)$, the probability that v is greater than $\alpha_m - \Delta\alpha/2$ and less than or equal to $\alpha_m + \Delta\alpha/2$ can be estimated by

$$\text{Prob}[\alpha_m - \Delta\alpha/2 < v \leq \alpha_m + \Delta\alpha/2] \approx \frac{n(\alpha_m)}{N} . \tag{6-5}$$

It follows from equation (6-4) that an estimate of the value of the probability density function at α_m, which we denote by $\tilde{f}_v(\alpha_m)$, is given by

$$\tilde{f}_v(\alpha_m) = \frac{n(\alpha_m)}{N\Delta a} . \tag{6-6}$$

By repeating this process at increments of $\Delta\alpha$, an estimate of the entire probability density function of the random variable v can be obtained. As one might expect, for a fixed $\Delta\alpha$, the quality of the estimate improves as the number of repetitions, N, increases.

6.1.2 Metrics of a Single Random Variable

A special set of statistical metrics of a random variable are called moments. The j-th moment of a random variable (say v) is defined by

$$E[v^j] = \int_{-\infty}^{\infty} \alpha^j f_v(\alpha)\, d\alpha , \tag{6-7}$$

where E[ ] denotes the average, or "expected value," of the argument. The most commonly used metrics are the first (j=1) moment, which is called the mean of the random variable v, and the second (j=2) moment, which is called the mean square value of v. For brevity, we will denote the mean and mean square values of the random variable v by $\langle v \rangle$ and $\langle v^2 \rangle$. Another set of moments are the central moments, defined by

$$E[(v - \langle v \rangle)^j] = \int_{-\infty}^{\infty} (\alpha - \langle v \rangle)^j f_v(\alpha)\, d\alpha . \tag{6-8}$$

It is easily verified, from equations (6-7) and (6-8), that the first (i.e., j=1) central moment is zero. The second (j=2) central moment is called the variance of v, and is denoted by the symbol σ^2. Note, by equations (6-7) and (6-8), that

$$\sigma^2 = \langle v^2 \rangle - \langle v \rangle^2 . \tag{6-9}$$

Moments can also be written for functions of a random variable. For example, let y be defined as an ordinary function of the variable x; that is, y = g(x). Then, the random variable w, defined by w = g(v), is a function of the random variable v. The function g(v) maps all values of the random variable v into corresponding values of the random variable w. We denote the values of v by α and the corresponding values of w by β. By equation (6-7), the j-th moment of the random variable w is defined by

$$E[w^j] = \int_{-\infty}^{\infty} \beta^j f_w(\beta)\, d\beta . \tag{6-10}$$

Recalling that β is simply the value of $g(\alpha)$, Papoulis[8] demonstrates that equation (6-10) can be rewritten in terms of the probability density of the random variable v. That is,

$$E[w^j] = E[g^j(v)] = \int_{-\infty}^{\infty} g^j(\alpha) f_v(\alpha)\, d\alpha . \tag{6-11}$$

Although we will not do so here, expressions similar to equation (6-8) may be written for central moments of a function of a random variable.

To provide a simple mathematical interpretation of the mean of a random variable and a foundation for future arguments, consider again an experiment in which values of the random variable, v, have been assigned to all possible outcomes. The experiment is repeated N times, and the value of the random variable obtained from the j-th trial (or repetition) of the experiment is designated by $\alpha(j)$. We wish to estimate the mean value (or first moment) of

the random variable from the resultant data. By using equation (6-6) to approximate $f_v(\alpha)d\alpha$ in equation (6-7) and by replacing the integral over α by a summation over all indices, m, of $\alpha_m = m\Delta\alpha$, we can approximate the mean value of v by

$$E[v] \approx \sum_{m=-\infty}^{\infty} \alpha_m \frac{n(\alpha_m)}{N} . \tag{6-12}$$

For a large number of trials (N) and a small increment ($\Delta\alpha$), the sum of the values of the random variable (ordered by increments of range) must approach, in value, the sum of the values of the random variable ordered by trial sequence. That is, for large N and small $\Delta\alpha$,

$$\sum_{m=-\infty}^{\infty} \alpha_m n(\alpha_m) \approx \sum_{j=1}^{N} \alpha(j) . \tag{6-13}$$

Therefore, the mean value of v can be approximated by the arithmetic average of the ensemble of trial values, $\alpha(j)$, of the random variable, v. That is,

$$E(v) \approx \frac{1}{N} \sum_{j=1}^{N} \alpha(j) . \tag{6-14}$$

It follows that the mean, or expected value, of any random variable or function of a random variable can be interpreted as the arithmetic average, over an infinite number of trials, of the observed values of that random variable or function.

6.1.3 Random Processes

The definitions and concepts presented above provide a foundation for the introduction of random processes. The clearest and most concise definition of a random process that I have found appears in a set of unpublished lecture notes by Kneipfer[9] for a graduate level course in Random Signals and Noise.

Kneipfer defines a random process as an indexed collection of random variables. To put this definition in perspective, consider again the pressure field on a planar surface. We define an experiment in which the pressure is observed continuously over the circular area $|\underline{x}| \leq R$ and $0 \leq t \leq T$. Over repeated experiments, the pressure at any predefined spatial location and time is observed to vary from trial to trial. Note that a single trial of this experiment requires definition of an infinite number of outcomes, one corresponding to the observed pressure at each spatial location and time within the specified limits. It is convenient to write the set of random variables defined for each of the outcomes of a single trial of the experiment in the form $p(\underline{x},t)$. Expressed in this fashion, $\underline{x}$ and t are indices that identify the random variable associated with each defined outcome of a single experiment. Thus, $p(\underline{x}_1,t_1)$ and $p(\underline{x}_2,t_2)$ specify the value of the random variables associated with the outcomes of a single trial at the spatial location $\underline{x}_1$ and time t_1 and at the spatial location $\underline{x}_2$ and time t_2, respectively.

The specification of $p(\underline{x},t)$ over $|\underline{x}| \leq R$ and $0 \leq t \leq T$ from a single trial of the experiment is called a sample function of the random process. The collection, or ensemble, of all possible sample functions of the experiment constitutes a random, or stochastic, process.

A random process indexed by three parameters (i.e., two spatial coordinates and time) is difficult to illustrate. Therefore, let us consider the simpler random process comprised of all possible sample functions of the pressure at $\underline{x} = \underline{x}_1$ over the time interval $0 \leq t \leq T$. Here, each sample function, denoted by $p_\beta(\underline{x}_1,t)$, consists of the values of the infinity of random variables associated with the continuous range, zero to T, of the index t for the β-th realization of the experiment. Figure 6-4 illustrates a few of the sample functions of this process at increments of $m\beta_0$, where m is an integer. However, it should be realized that there are a continuous infinity of possible sample functions, and therefore the parameter β can assume any value between $-\infty$ and ∞.

Recall that the average properties of a random variable were expressed in terms of the probability density function of that random variable. The

statistical metrics of random processes are also described in terms of probability density functions. However, inasmuch as a random process is an indexed collection of random variables, the average properties of a single random variable are insufficient to characterize the average properties of a random process. Rather, the statistical metrics of random processes are averages of various products of the different random variables comprising the process. The mathematical formulation of the average properties of random processes is based on the joint probability density function of two or more random variables.

6.1.4 Joint Metrics of Multiple Random Variables

The joint probability density function, like the probability density function for a single random variable, is defined in terms of a distribution function. For illustration, consider two random variables that have the values v and w, respectively. The joint distribution function of the (values of the) random variables v and w, denoted by $F_{vw}(\alpha,\beta)$, is the function defined by

$$F_{vw}(\alpha,\beta) = \mathrm{Prob}[v \le \alpha, w \le \beta] \tag{6-15}$$

over all values of α and β. Here, the subscripts v and w indicate that the distribution function pertains to the random variables v and w. According to reference 10, the joint distribution function is a nondecreasing function of α and β, and has the following properties:

(a) $F_{vw}(-\infty,\beta) = F_{vw}(\alpha,-\infty) = 0$,

(b) $F_{vw}(\infty,\infty) = 1$,

(c) $F_{vw}(\alpha,\infty) = F_v(\alpha)$,

(d) $F_{vw}(\infty,\beta) = F_w(\beta)$.

The joint probability density function of the (values of the) random variables v and w, which we denote by f_{vw}, is defined[11] by

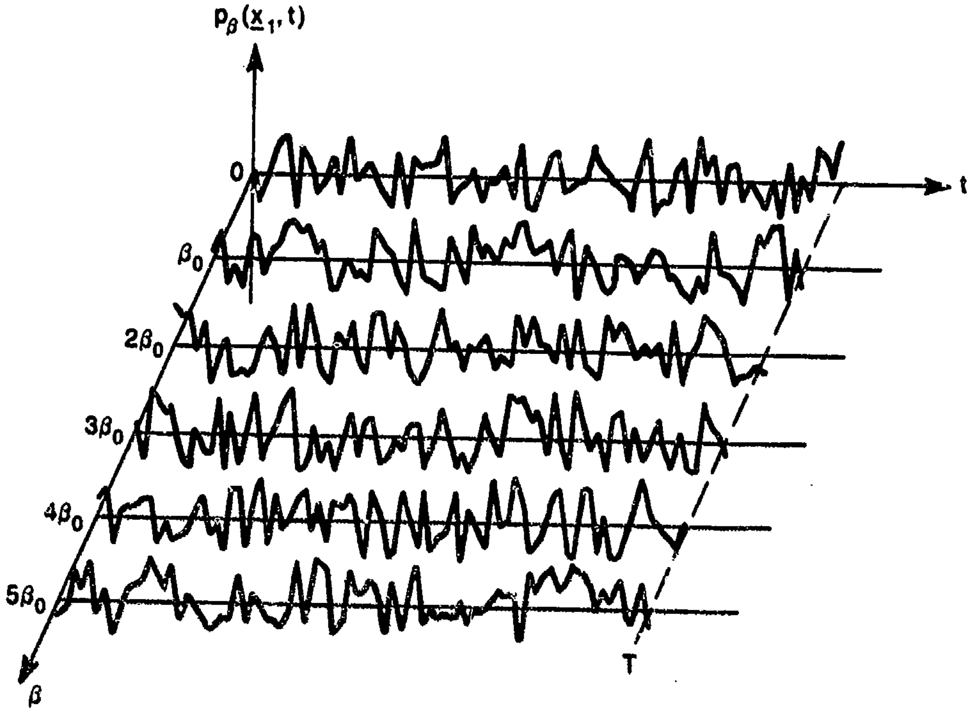

Figure 6-4. Sample Functions of the Random Process $p_\beta(\underline{x}_1,t)$ at Equal Increments of β

$$f_{vw}(\alpha,\beta) = \frac{\partial^2 F_{vw}(\alpha,\beta)}{\partial\alpha\,\partial\beta} . \tag{6-15}$$

The joint probability density function has the following properties:

(a) $f_{vw}(\alpha,\beta) \geq 0$,

(b) $\displaystyle\int_{-\infty}^{\infty}\int_{-\infty}^{\infty} f_{vw}(\alpha,\beta)\, d\alpha\, d\beta = F_{vw}(\infty,\infty) = 1$,

(c) $\displaystyle\int_{-\infty}^{a}\int_{-\infty}^{b} f_{vw}(\alpha,\beta)\, d\alpha\, d\beta = F_{vw}(a,b) = \text{Prob}[v \leq a, w \leq b]$,

(d) $\displaystyle\int_{a}^{b}\int_{c}^{d} f_{vw}(\alpha,\beta)\, d\alpha\, d\beta = F_{vw}(b,d) - F_{vw}(b,c) - F_{vw}(a,d) + F_{vw}(a,c)$

$$= \text{Prob}[a < v \leq b, c < w \leq d] .$$

The joint probability density function of a random process can be estimated from measured data in a fashion similar to that described previously for estimating the probability density function of a random variable. That is, by the property (d) of the joint probability density shown above and the mean value theorem of integrals, it is easily shown that

$$\int_{a-\Delta a/2}^{a+\Delta a/2} \int_{b-\Delta b/2}^{b+\Delta b/2} f_{vw}(\alpha,\beta)\, d\alpha\, d\beta =$$

$$\text{Prob}[a - \Delta a/2 < v \leq a + \Delta a/2, b - \Delta b/2 < w \leq b + \Delta b/2] \approx f_{vw}(a,b)\, \Delta a\, \Delta b \ . \tag{6-17}$$

Thus, if v and w are values of two random variables assigned to the sample functions of a random process and if N trials of the experiment are conducted, one can estimate the joint probability density function at $\alpha_i = i\Delta\alpha$ and $\beta_j = j\Delta\beta$ by determining the number of times, $n(\alpha_i,\beta_j)$, that $\alpha_i - \Delta\alpha/2 < v \leq \alpha_i + \Delta\alpha/2$ and $\beta_j - \Delta\beta/2 < w \leq \beta_j - \Delta\beta/2$. That is, by arguments similar to those used between equations (6-4) and (6-6), an estimate, $\tilde{f}_{vw}(\alpha_i,\beta_j)$, of the joint probability density function of the random variables v and w can be shown to be given by

$$\tilde{f}_{vw}(\alpha_i,\beta_j) \approx \frac{n(\alpha_i,\beta_j)}{N\, \Delta\alpha\, \Delta\beta} \ . \tag{6-18}$$

As was noted for the case of a single random variable, for fixed values of $\Delta\alpha$ and $\Delta\beta$, the quality of the estimate of the joint probability density improves as the number of trials, N, increases.

The statistical metrics for two random variables of a random process are called joint moments. The m,n-th joint moment of the random variables, v and w, is defined by

$$E[v^m w^n] = \int_{-\infty}^{\infty} \int_{-\infty}^{\infty} \alpha^m \beta^n f_{vw}(\alpha,\beta)\, d\alpha\, d\beta \ , \tag{6-19}$$

where, again, E[ ] denotes the mean, or expected value, of the argument. The most commonly used joint moment is the 1,1 moment, which is called the

correlation. We will denote the correlation of the random variables v and w by Q_{vw} and note, for future reference, that

$$Q_{vw} = E[vw] = \int_{-\infty}^{\infty}\int_{-\infty}^{\infty} \alpha\beta f_{vw}(\alpha,\beta)\, d\alpha\, d\beta \ . \qquad (6\text{-}20)$$

The two random variables, v and w, are said to be uncorrelated if E[vw] = E[v]E[w].

Central moments are also defined for two random variables. The mn-th central moment for the random variables v and w is defined by

$$E[(v - \langle v\rangle)^m (w - \langle w\rangle)^n] = \int_{-\infty}^{\infty}\int_{-\infty}^{\infty} (\alpha - \langle v\rangle)^m (\beta - \langle w\rangle)^n f_{vw}(\alpha,\beta)\, d\alpha\, d\beta \ . \qquad (6\text{-}21)$$

The 1,1 central moment is called the covariance.

It is useful, for future reference, to provide a simple mathematical interpretation of the correlation. Consider an experiment in which the values, v and w, of two random variables of a random process have been assigned to all possibilities of their respective outcomes. The experiment is repeated N times, and the product of v and w obtained from the m-th trial is designated by $\alpha\beta(m)$. The number of times, $n(\alpha_i,\beta_j)$, that the product $\alpha\beta$ occurs in each incremental area $\Delta\alpha\Delta\beta$ centered at $\alpha_i = i\Delta\alpha$ and $\beta_j = j\Delta\beta$ is noted and recorded. If we use equation (6-18) to approximate $f_{vw}(\alpha,\beta)$ in equation (6-20) and if we replace the integrals over α and β by appropriate summations over the indices of α_i and β_j, the correlation can be approximated by

$$Q_{vw} = \sum_{i=-\infty}^{\infty}\sum_{j=-\infty}^{\infty} \alpha_i\beta_j \frac{n(\alpha_i,\beta_j)}{N} \ . \qquad (6\text{-}22)$$

However, for a large number of trials (N) and small incremental areas ($\Delta\alpha\Delta\beta$) of range, the sum of the values of the product $\alpha\beta$ ordered by increments of

range must approach, in value, the sum of the values of $\alpha\beta$ ordered by trial sequence. That is,

$$\sum_{i=-\infty}^{\infty} \sum_{j=-\infty}^{\infty} \alpha_i \beta_j n(\alpha_i, \beta_j) \approx \sum_{m=1}^{N} \alpha\beta(m) \ . \tag{6-23}$$

Thus, it follows that the correlation of the random variables v and w can be approximated by, and interpreted as, the arithmetic average of the trial values of the product $\alpha\beta(m)$ over a large number of trials. That is,

$$Q_{vw} \approx \frac{1}{N} \sum_{m=1}^{N} \alpha\beta(m) \ . \tag{6-24}$$

The concepts presented above for two random variables can be extended to any number of random variables. Let the values of N random variables be denoted by v_i, $1 \leq i \leq N$. The joint distribution function of these N random variables is

$$F_{v_1 v_2 \ldots v_N}(\alpha_1, \alpha_2, \ldots \alpha_N) = \mathrm{Prob}[v_1 \leq \alpha_1, v_2 \leq \alpha_2, \ldots v_N \leq \alpha_N] \ . \tag{6-25}$$

The associated joint probability density function is defined by

$$f_{v_1 v_2 \ldots v_N}(\alpha_1, \alpha_2, \ldots \alpha_N) = \frac{\partial^N F_{v_1 v_2 \ldots v_N}(\alpha_1, \alpha_2, \ldots \alpha_N)}{\partial\alpha_1 \ \partial\alpha_2 \ldots \partial\alpha_N} \ , \tag{6-26}$$

and the joint moments are given by

$$E[v_1{}^a, v_2{}^b, \ldots v_N{}^n] = \int_{-\infty}^{\infty} \int_{-\infty}^{\infty} \cdots \int_{-\infty}^{\infty} \alpha_1{}^a \alpha_2{}^b \ldots \alpha_N{}^n$$

$$f_{v_1 v_2 \ldots v_N}(\alpha_1, \alpha_2, \ldots \alpha_N) \ d\alpha_1 \ d\alpha_2 \ldots d\alpha_N \ . \tag{6-27}$$

With the above concepts and definitions, we are now prepared to address the description of a random space-time field, or process, in the space-time domain.

6.2 DESCRIPTORS OF RANDOM SPACE-TIME FIELDS IN THE SPACE-TIME DOMAIN

Consider again the pressure field on a planar surface. We define an experiment in which the outcomes are the infinite set of pressures at each spatial location, $\underline{x}$, and time, t. Over repeated experiments, the pressure at any predefined spatial location and time is observed to vary from trial to trial. We define an infinite set of random variables that assigns values, $p(\underline{x},t)$, to the pressure at each spatial location and time. By this procedure, $p(\underline{x},t)$ constitutes a random process in which the spatial vector, $\underline{x}$, and the time, t, are the indices of (the values of) the infinite set of random variables. We will refer to random processes in which the values of the predefined set of random variables are indexed by spatial and temporal coordinates as random space-time fields.

In section 6.1.4, we defined various joint metrics of multiple random variables. However, as explained above, the random process, $p(\underline{x},t)$, comprises an infinite number of random variables. A complete statistical characterization of this random process requires specification of all possible moments of all combinations of all random variables. Clearly, such a complete characterization is practically impossible. Indeed, specification of even the simplest statistical metric (i.e., the mean value) of all the random variables constituting this random process requires a triply infinite, three-dimensional array of numbers. These realizations prompt two questions. The first is "What statistical metric(s) do we use to characterize a random process?" The second is "Can we describe these metrics in a mathematically economical form?" We will address these questions in reverse order.

6.2.1 Mathematical Form for Descriptors of a Random Process

A mathematically economical description of the statistics of random processes is facilitated by using the indices of the collection of random variables constituting the random process to index the collection of single or

joint moments formed from that collection of random variables. To illustrate, consider the single random variable, $p(\underline{x}_1,t_1)$, of the random process $p(\underline{x},t)$. We can write the distribution function of $p(\underline{x}_1,t_1)$ in the following functional form:

$$F_p(\alpha:\underline{x}_1,t_1) \equiv F_{p(\underline{x}_1,t_1)}(\alpha) = \mathrm{Prob}[p(\underline{x}_1,t_1) \leq \alpha] \ . \tag{6-28}$$

Here, $\equiv$ signifies definition, the subscript p on F indicates that the random variable is a member of the random process $p(\underline{x},t)$, and the arguments of F_p following the colon specify the indices that identify the particular random variable to which the distribution function applies. By this notation, we are reminded that a change in either index, $\underline{x}_1$ or t_1, specifies a distribution function of a different random variable. Further, if $F_p(\alpha:\underline{x}_1,t_1)$ is known for all possible values of α, $\underline{x}_1$, and t_1, the distribution functions of all possible random variables associated with the random process $p(\underline{x},t)$ can be expressed as a single function.

Assume that $F_p(\alpha:\underline{x}_1,t_1)$ is known for all $\underline{x}_1$ and t_1. It then follows, by equations (6-3) and (6-28), that the probability density function of any random variable of the random process $p(\underline{x},t)$ can be expressed in the functional form

$$f_p(\alpha:\underline{x}_1,t_1) \equiv \frac{dF_p(\alpha:\underline{x}_1,t_1)}{d\alpha} = \frac{dF_{p(\underline{x}_1,t_1)}(\alpha)}{d\alpha} = f_{p(\underline{x}_1,t_1)}(\alpha) \tag{6-29}$$

Here, the subscript and the arguments following the colon in f_p have the same significance as described above for the distribution function.

By use of equations (6-7) and (6-29), the j-th moment of $p(\underline{x}_1,t_1)$ can be written

$$E[p^j(\underline{x}_1,t_1)] = \int_{-\infty}^{\infty} \alpha^j f_p(\alpha:\underline{x}_1,t_1)\, d\alpha \ . \tag{6-30}$$

Thus, given the probability density function, $f_p(\alpha:\underline{x}_1,t_1)$, for all α, $\underline{x}_1$, and t_1, $E[p^j(\underline{x}_1,t_1)]$ specifies, in a single function, the j-th moment of all random

variables of the random process, $p(\underline{x},t)$. In similar fashion, the j-th central moment of any random variable of the random process, $p(\underline{x},t)$, can be written as

$$E\{[p(\underline{x}_1,t_1) - \langle p(\underline{x}_1,t_1)\rangle]^j\} = \int_{-\infty}^{\infty} [\alpha - \langle p(\underline{x}_1,t_1)\rangle]^j f_p(\alpha:\underline{x}_1,t_1)\, d\alpha \ , \qquad (6\text{-}31)$$

where $\langle p(\underline{x}_1,t_1)\rangle$ is the mean of the random variable $p(\underline{x}_1,t_1)$.

The joint moments of the random variables constituting a random process can also be economically stated by indexing these joint moments with the indices of the random variables associated with that moment. To illustrate, consider the two random variables, $p(\underline{x}_1,t_1)$ and $p(\underline{x}_2,t_2)$, associated with the random process $p(\underline{x},t)$. The spatial locations of these two points of observation are illustrated in figure 6-5. We can express the joint distribution function of these random variables in the following functional form:

$$\hat{F}_{pp}(\alpha,\beta:\underline{x}_1,t_1;\underline{x}_2,t_2) \equiv F_{p(\underline{x}_1,t_1)p(\underline{x}_2,t_2)}(\alpha,\beta)$$

$$= \mathrm{Prob}[p(\underline{x}_1,t_1) \le \alpha, p(\underline{x}_2,t_2) \le \beta] \ . \qquad (6\text{-}32)$$

Here, the subscripts pp on $\hat{F}$ indicate that both random variables are members of the random process $p(\underline{x},t)$, and the arguments following the colon in $\hat{F}_{pp}$ specify the indices that identify the two random variables to which the distribution function applies. By this notation, we are again reminded that a change in either set of indices (i.e., $\underline{x}_1,t_1$ or $\underline{x}_2,t_2$) specifies a distribution function of a different set of random variables. Clearly, if $\hat{F}_{pp}(\alpha,\beta:\underline{x}_1,t_1;\underline{x}_2,t_2)$ is known for all α, β, $\underline{x}_1$, $\underline{x}_2$, t_1, and t_2, the joint distributions of any two random variables associated with the random process, $p(\underline{x},t)$, can specified by a single function.

Assume that $\hat{F}_{pp}(\alpha,\beta:\underline{x}_1,t_1;\underline{x}_2,t_2)$ is known for all α, β, $\underline{x}_1$, $\underline{x}_2$, t_1, and t_2. It then follows, from equations (6-16) and (6-32), that the joint probability density function of any two random variables associated with the random process $p(\underline{x},t)$ can be written in the form

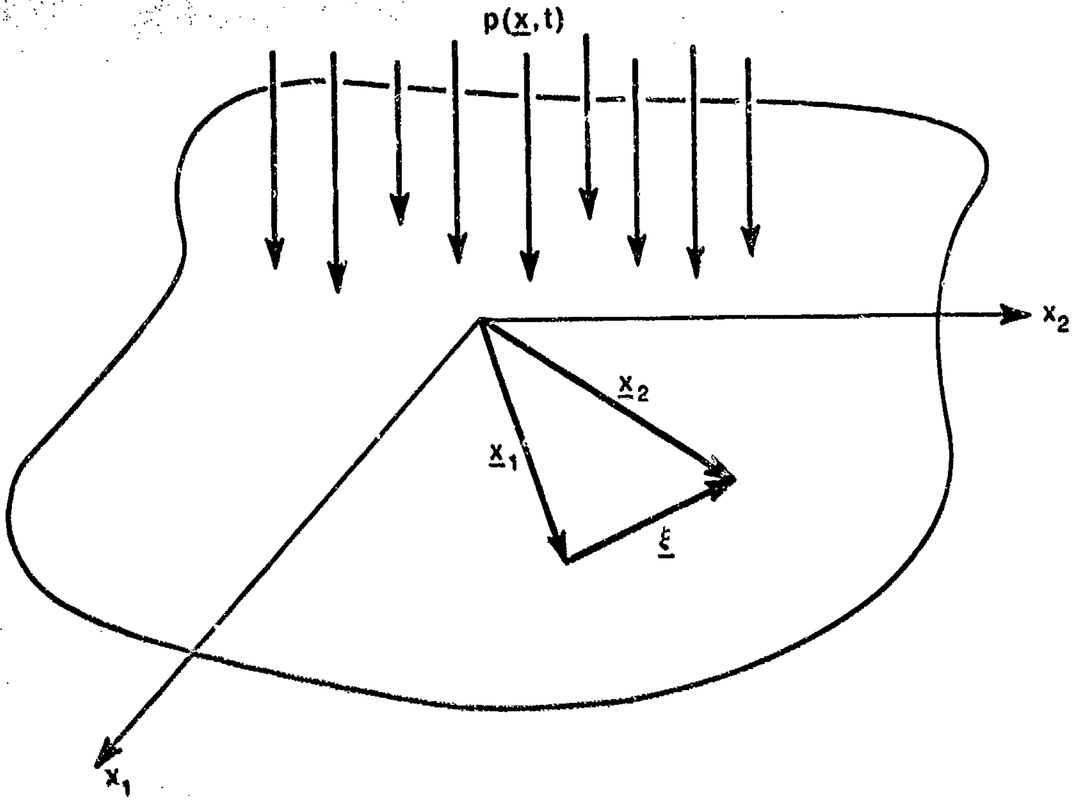

Figure 6-5. Geometry of Pressure Field on a Planar Surface

$$\hat{f}_{pp}(\alpha,\beta:\underline{x}_1,t_1;\underline{x}_2,t_2) \equiv \frac{\partial^2 \hat{F}_{pp}(\alpha,\beta:\underline{x}_1,t_1;\underline{x}_2,t_2)}{\partial\alpha\,\partial\beta}$$

$$= \frac{\partial^2 F_{p(\underline{x}_1,t_1)p(\underline{x}_2,t_2)}(\alpha,\beta)}{\partial\alpha\,\partial\beta} = f_{p(\underline{x}_1,t_1)p(\underline{x}_2,t_2)}(\alpha,\beta) \; . \qquad (6\text{-}33)$$

By use of equations (6-19) and (6-33), the mn-th joint moment of the random variables $p(\underline{x}_1,t_1)$ and $p(\underline{x}_2,t_2)$ can be expressed in the indexed form

$$E[p^m(\underline{x}_1,t_1)p^n(\underline{x}_2,t_2)] = \int_{-\infty}^{\infty}\int_{-\infty}^{\infty} \alpha^m\beta^n\hat{f}_{pp}(\alpha,\beta:\underline{x}_1,t_1;\underline{x}_2,t_2)\,d\alpha\,d\beta$$

$$= \int_{-\infty}^{\infty}\int_{-\infty}^{\infty} \alpha^m\beta^n f_{p(\underline{x}_1,t_1)p(\underline{x}_2,t_2)}(\alpha,\beta)\,d\alpha\,d\beta \; . \qquad (6\text{-}34)$$

If the joint probability density function, $\hat{f}_{pp}(\alpha,\beta:\underline{x}_1,t_1;\underline{x}_2,t_2)$, is known for all $\underline{x}_1,t_1$, $\underline{x}_2$, and t_2, then the joint moments of all pairs of random variables in the random process $p(\underline{x},t)$ are known. The function of $\underline{x}_1$, t_1, $\underline{x}_2$, and t_2 resulting from the 1-1 joint moments (i.e., correlations) of all random variables of the process is called the autocorrelation function of the random process, and is designated by $\hat{Q}_{pp}(\underline{x}_1,t_1,\underline{x}_2,t_2)$. That is,

$$\hat{Q}_{pp}(\underline{x}_1,t_1,\underline{x}_2,t_2) \equiv E[p(\underline{x}_1,t_1)p(\underline{x}_2,t_2)]$$

$$= \int_{-\infty}^{\infty}\int_{-\infty}^{\infty} \alpha\beta\hat{f}_{pp}(\alpha,\beta:\underline{x}_1,t_1;\underline{x}_2,t_2)\, d\alpha\, d\beta \ . \qquad (6\text{-}35)$$

The prefix "auto" to the term "correlation function" denotes that both random variables are members of the same random process.

Although we will not do so here, the indexing process illustrated above can be applied to equations (6-25) through (6-27) to obtain similar functional forms for the joint moments of any number of the random variables belonging to the random process $p(\underline{x},t)$.

As a final note, it should be recognized that one can index the joint metrics of the random variables associated with the random process $p(\underline{x},t)$ by variables other than $\underline{x}_1$, t_1, $\underline{x}_2$, and t_2. To illustrate, we will express the joint metrics of equations (6-32) through (6-35) in terms of an alternative set of indices that will prove useful in later sections. Note, from figure 6-5, that

$$\underline{x}_2 = \underline{x}_1 + \underline{\xi} \ . \qquad (6\text{-}36)$$

If we define

$$\tau = t_2 - t_1 \ , \qquad (6\text{-}37)$$

we can express the joint distribution function, the joint probability density function, and the autocorrelation function of the random process $p(\underline{x},t)$ as a

function of the indices $\underline{x}_1$, $\underline{\xi}$, t_1, and τ rather than $\underline{x}_1$, $\underline{x}_2$, t_1, and t_2. That is, the joint distribution function can be expressed in the form

$$F_{pp}(\alpha,\beta:\underline{x}_1,\underline{\xi},t_1,\tau) \equiv F_{p(\underline{x}_1,t_1)p(\underline{x}+\underline{\xi},t_1+\tau)}(\alpha,\beta)$$

$$= \text{Prob}[p(\underline{x}_1,t_1) \leq \alpha, p(\underline{x}_1+\underline{\xi},t_1+\tau) \leq \beta] \ . \qquad (6\text{-}38)$$

To distinguish this functional form of the joint distribution function from that of equation (6-32), we have omitted the caret over F_{pp}. Note also that the indices that identify the random variables (following the colon in the argument list of F_{pp}) are listed in a different order in equation (6-38) than in equation (6-32). This reordering is intended to serve as a reminder that $\underline{\xi}$ and τ are relative rather than absolute spatial and temporal variables, respectively.

Given $F_{pp}(\alpha,\beta:\underline{x}_1,\underline{\xi},t_1,\tau)$ for all α, β, $\underline{x}_1$, $\underline{\xi}$, t_1, and τ, it follows from equations (6-16) and (6-38) that the joint probability density function of any two of the random variables of the random process $p(\underline{x},t)$ is defined by

$$f_{pp}(\alpha,\beta:\underline{x}_1,\underline{\xi},t_1,\tau) \equiv \frac{\partial F_{pp}(\alpha,\beta:\underline{x}_1,\underline{\xi},t_1,\tau)}{\partial\alpha\ \partial\beta} \ . \qquad (6\text{-}39)$$

By equations (6-19) and (6-39), the m,n-th joint moment of any two random variables associated with $p(\underline{x},t)$ is given by

$$E[p^m(\underline{x}_1,t_1)p^n(\underline{x}_1+\underline{\xi},t_1+\tau)] = \int_{-\infty}^{\infty}\int_{-\infty}^{\infty} \alpha^m\beta^n f_{pp}(\alpha,\beta:\underline{x}_1,\underline{\xi},t_1,\tau)\ d\alpha\ d\beta \ . \qquad (6\text{-}40)$$

Thus, the autocorrelation function of $p(\underline{x},t)$ can be written as

$$Q_{pp}(\underline{x}_1,\underline{\xi},t_1,\tau) \equiv E[p(\underline{x}_1,t_1)p(\underline{x}_1+\underline{\xi},t_1+\tau)]$$

$$= \int_{-\infty}^{\infty}\int_{-\infty}^{\infty} \alpha\beta f_{pp}(\alpha,\beta:\underline{x}_1,\underline{\xi},t_1,\tau)\ d\alpha\ d\beta \ . \qquad (6\text{-}41)$$

By the above arguments, it is evident that the infinite set of numbers resulting from the application of any single or joint metric to all random variables of a random process can be expressed as a single function of the indices of the random process.

6.2.2 Metrics of Random Processes in the Space-Time Domain

As stated previously, a complete statistical description of a random process requires specification of all possible moments of all combinations of the random variables contributing to the random process. However, for reasons that are, historically, both logical and practical, we will characterize random processes in the space-time domain by just two statistical metrics. Those metrics are the mean and the autocorrelation functions of the process.

The logic for the characterization of a random process by only the mean and autocorrelation functions is based on three concepts that are central to the theory of signal processing. These three concepts are (1) the Gaussian (or normal) random process, (2) the linear system, and (3) the central limit theorem. A complete explanation of these concepts and logic is well beyond the scope of this chapter. However, to lend credibility to the idea that a random process can be characterized by its mean and autocorrelation functions, we offer a brief review of the relevant aspects of these concepts and the consequent logical arguments.

A Gaussian (also called "normal") random process is defined[12] as a random process in which all single and joint probability density functions of the constituent random variables are Gaussian. The central feature of a Gaussian random process is[13] that all its statistical moments are completely defined by knowledge of its mean and autocorrelation functions.

In chapters 3 and 4 (see equations (3-51), (4-91), (4-128), and (4-132)), we demonstrated that the output field, $o(\underline{x},t)$, of any time-invariant linear system is related to the input field, say $p(\underline{x},t)$, and the Green's function, $g(\underline{x},\underline{x}_0,t - t_0)$, of the system by

$$o(\underline{x},t) = \int_{-\infty}^{\infty}\int_{-\infty}^{\infty} g(\underline{x},\underline{x}_0,t - t_0)p(\underline{x}_0,t_0)\, d\underline{x}_0\, dt_0 . \qquad (6\text{-}42)$$

By equation (3-43) and the principle of superposition for linear systems (see section 3.4.1 of chapter 3), we can deduce certain characteristics of the output field of a deterministic linear system excited by a random process. That is, if the input field, $p(\underline{x},t)$, is a random process, the output field at any spatial location $\underline{x}$ and time t can be interpreted (by the principle of superposition) as a weighted summation of all the random variables that constitute $p(\underline{x},t)$. As location, $\underline{x}$, and time, t, of the output are varied, the weighting, $g(\underline{x},\underline{x}_0,t - t_0)$, applied to the various random variables associated with $p(\underline{x},t)$ is altered. Inasmuch as a weighted sum of random variables is a random variable, we conclude that the output field, $o(\underline{x},t)$, of a deterministic, time-invariant linear system excited by a random process is, itself, a random process comprising random variables that are various weighted sums of those random variables constituting the input field.

The essence of the central limit theorem is[14] that, under fairly general conditions, the probability distribution of a sum of statistically independent random variables tends to become Gaussian as the number of random variables approaches infinity. This result holds regardless of the probability distribution of the random variables contributing to the sum as long as that distribution has a finite mean and variance. Further, under certain conditions, the probability density of a sum of random variables will tend to become Gaussian even when the requirement of statistical independence of the random variables is relaxed.[15] However, it should be noted that the limiting distribution of an infinite sum of random variables is not always Gaussian, and therefore each individual case must be examined to determine whether or not such a theorem applies.

If the central limit theorem applies to the weighted sum of random variables that constitutes the output field of a linear system excited by a random process, then the output field of the linear system is a Gaussian random process, and is completely characterized by its mean and autocorrelation functions. Further, as will be illustrated in the next chapter,

the mean and autocorrelation functions of the random process output from a linear system are determined from the autocorrelation function of the process input to the system and the Green's function of the system. Therefore, when the central limit theorem applies to the random process output from a given linear system, knowledge of the autocorrelation function of the input field is sufficient to completely specify the statistics of the output field.

If it is determined that the central limit theorem does not apply to the weighted sum of random variables constituting the output field, then the output process is not Gaussian, and the mean and autocorrelation functions do not constitute a complete characterization of the statistics of the output field. It is at this point that the aforementioned practical reasoning comes into play. That reasoning is as follows:

(1) Inasmuch as it is clearly impractical to attempt to measure or predict the infinity of single and joint moments required for a complete statistical characterization of the output, one must decide which set of moments constitutes a practicable description of the statistics of the output field.

(2) A practicable (though admittedly incomplete) description is provided by the mean and autocorrelation functions.

Here again, the mean and autocorrelation functions of the output process of a given linear system are determined by the autocorrelation function of the random process input to the system.

6.3 CLASSIFICATION OF RANDOM SPACE-TIME FIELDS

As shown in section 6.2.1, the autocorrelation function of the random space-time field (i.e., random process) $p(\underline{x},t)$ is a function of the indices that identify the two random variables being correlated. For example, we showed in equation (6-35) that the autocorrelation of the random variables $p(\underline{x}_1,t_1)$ and $p(\underline{x}_2,t_2)$ is defined by

$$\hat{Q}_{pp}(\underline{x}_1,t_1,\underline{x}_2,t_2) \equiv E[p(\underline{x}_1,t_1)p(\underline{x}_2,t_2)] \; . \tag{6-43}$$

The functional form of equation (6-43) clearly indicates that the value of the correlation, $\hat{Q}_{pp}$, depends on the indices, $\underline{x}_1$, t_1, $\underline{x}_2$, and t_2, that identify which two random variables of the random process, $p(\underline{x},t)$, are being correlated. We also showed in section 6.2.1 that equation (6-43) was not a unique functional form for the autocorrelation function of the random process $p(\underline{x},t)$. That is, we showed (see equation (6-41)) that the autocorrelation function of $p(\underline{x},t)$ could also be expressed as

$$Q_{pp}(\underline{x}_1,\underline{\xi},t_1,\tau) \equiv E[p(\underline{x}_1,t_1)p(\underline{x}_1 + \underline{\xi},t_1 + \tau)] \ , \tag{6-44}$$

where (see figure 6-5 and equations (6-36) and (6-37)) $\underline{\xi} = \underline{x}_2 - \underline{x}_1$ and $\tau = t_2 - t_1$. Other functional forms for the autocorrelation function are limited only by one's imagination and the requirement that the arguments unambiguously identify the random variables to which the value of the correlation applies. For example, two valid alternative functional forms are

$$\bar{Q}_{pp}(\underline{x}_1,\underline{x}_2,t_1,\tau) \equiv E[p(\underline{x}_1,t_1)p(\underline{x}_2,t_1 + \tau)] \tag{6-45}$$

and

$$\tilde{Q}_{pp}(\underline{\tilde{x}},\underline{\xi},t_1,\tau) \equiv E[p(\underline{\tilde{x}} - \underline{\xi}/2,t_1)p(\underline{\tilde{x}} + \underline{\xi}/2,t_1 + \tau)] \ , \tag{6-46}$$

where

$$\underline{\tilde{x}} = (\underline{x}_1 + \underline{x}_2)/2 \ . \tag{6-47}$$

Although the functional forms of equations (6-43) through (6-46) are different, it should be noted that for any two specific random variables, say $p(\underline{x}_1,t_1)$ and $p(\underline{x}_2,t_2)$, of the random space-time field, all functional forms of the autocorrelation function yield the same value. That is, for fixed values of $\underline{x}_1$, $\underline{x}_2$, t_1, and t_2, and thereby for fixed values of $\underline{\tilde{x}}$, $\underline{\xi}$, and τ,

$$\begin{aligned} \hat{Q}_{pp}(\underline{x}_1,t_1,\underline{x}_2,t_2) &= Q_{pp}(\underline{x}_1,\underline{\xi},t_1,\tau) \\ &= \bar{Q}_{pp}(\underline{x}_1,\underline{x}_2,t_1,\tau) = \tilde{Q}_{pp}(\underline{\tilde{x}},\underline{\xi},t_1,\tau) \ . \end{aligned} \tag{6-48}$$

Equations (6-43) through (6-46) represent alternative forms of the autocorrelation function for a general random space-time field (i.e., random

process). We will now define certain classes of random space-time fields and examine how the class of the field affects the form of the mean and correlation functions.

6.3.1 Stationary Fields

A random space-time field (or process) is said[16] to be stationary in the strict sense if its statistics are unaffected by the choice of the temporal origin. Thus, the random process $p(\underline{x},t)$ is stationary in the strict sense if all single and joint moments of the random variables associated with $p(\underline{x},t)$ are equal to the corresponding single and joint moments of $p(\underline{x},t+\theta)$ for all choices of θ. This implies that

$$\langle p(\underline{x}_1,t_1)\rangle = \langle p(\underline{x}_1,t_1+\theta)\rangle \tag{6-49}$$

for any choice of $\underline{x}_1$, t_1, and θ. Clearly, by equation (6-49), the mean of a strictly stationary random space-time field must be independent of time. Further, if $p(\underline{x},t)$ is stationary in the strict sense, it follows from equation (6-44) that

$$Q_{pp}(\underline{x}_1,\underline{\xi},t_1,\tau) = Q_{pp}(\underline{x}_1,\underline{\xi},t_1+\theta,\tau) \tag{6-50}$$

for any choice of $\underline{x}_1,\underline{\xi}$, t_1, τ, and θ. This can only be so if the autocorrelation function is independent of the origin of the time variable, t_1. Thus, for a strictly stationary random space-time field,

$$Q_{pp}(\underline{x}_1,\underline{\xi},t_1,\tau) = Q_{pp}(\underline{x}_1,\underline{\xi},\tau)\ . \tag{6-51}$$

Although we will not do so here, it can be demonstrated that if the random space-time field, $p(\underline{x},t)$, is strictly stationary, all joint moments of the random variables associated with $p(\underline{x},t)$ are independent of the absolute times of observation (i.e., times referenced to a specific temporal origin) but depend on the time differences between observations.

A random space-time field is said[17] to be weakly stationary (or stationary in the wide sense) if its mean value is independent of time and its

autocorrelation function depends only on the spatial coordinates of, and the time difference $(t_2 - t_1)$ between, observations. Thus, the mean of a weakly stationary random space-time field is a function of only the spatial coordinate, $\underline{x}$, and has the functional form of equation (6-49). By review of equations (6-43) through (6-46), it is evident that the autocorrelation function of a weakly stationary random space-time field, $p(\underline{x},t)$, can be defined by any of the following alternative functional forms:

$$Q_{pp}(\underline{x}_1,\underline{\xi},\tau) = E[p(\underline{x}_1,t_1)p(\underline{x}_1 + \underline{\xi},t_1 + \tau)] \ , \tag{6-52}$$

$$\bar{Q}_{pp}(\underline{x}_1,\underline{x}_2,\tau) = E[p(\underline{x}_1,t_1)p(\underline{x}_2,t_1 + \tau)] \ , \tag{6-53}$$

or

$$\tilde{Q}_{pp}(\tilde{\underline{x}},\underline{\xi},\tau) = E[p(\tilde{\underline{x}} - \underline{\xi}/2,t_1)p(\tilde{\underline{x}} + \underline{\xi}/2,t_1 + \tau)] \ . \tag{6-54}$$

Note, by comparison of equations (6-44)-(6-46) with equations (6-52)-(6-54), that the autocorrelation function of a stationary field is characterized by a single temporal variable (the difference between the temporal indices of the random variables being correlated), whereas the autocorrelation function of a nonstationary field is characterized by two temporal variables (or indices).

Clearly, a random space-time field that is stationary in the strict sense is also weakly stationary; however, the converse is not necessarily true.

By use of figure 6-5 and a change of the temporal variable in equations (6-52)-(6-54), it is straightforward to show that the various forms of the autocorrelation function of a stationary random space-time field have the following symmetry properties:

$$Q_{pp}(\underline{x}_1,\underline{\xi},\tau) = Q_{pp}(\underline{x}_2,-\underline{\xi},-\tau) \ , \tag{6-55}$$

where $\underline{x}_2 = \underline{x}_1 + \underline{\xi}$,

$$\bar{Q}_{pp}(\underline{x}_1,\underline{x}_2,\tau) = \bar{Q}_{pp}(\underline{x}_2,\underline{x}_1,-\tau) \ , \tag{6-56}$$

or

$$\tilde{Q}_{pp}(\tilde{\underline{x}},\underline{\xi},\tau) = \tilde{Q}_{pp}(\tilde{\underline{x}},-\underline{\xi},-\tau) \ . \tag{6-57}$$

AUTHOR'S COMMENT

Throughout the remainder of this book, we shall restrict our attention to random space-time fields that are, at least, weakly stationary. The reasons for this restriction are as follows:

- The assumption of stationarity affords considerable mathematical simplification in the analysis of linear systems excited by random space-time fields.
- Many of the random space-time fields occurring in nature have statistics that are, over practical times of observation, weakly stationary.
- In laboratory environments, the random space-time field of interest can often be rendered weakly stationary by means of experimental controls.

6.3.2 Ergodic Random Processes

Ergodic random processes are a subclass of strictly stationary random processes in which any statistical metric obtained by an ensemble average is equal to the corresponding metric obtained from the temporal average of a representative sample function.[18] To illustrate, let $p_\beta(\underline{x},t)$ designate the β-th sample function from the continuum of all possible sample functions of the stationary random space-time field, $p(\underline{x},t)$. If the random process $p(\underline{x},t)$ is ergodic, then the mean and correlation functions are given by

$$E[p(\underline{x}_1,t_1)] = E[p(\underline{x}_1,t_2)] = \lim_{T\to\infty} \frac{1}{2T}\int_{-T}^{T} p_\beta(\underline{x}_1,t)\, dt \qquad (6\text{-}58)$$

and

$$Q_{pp}(\underline{x}_1,\underline{\xi},\tau) = E[p(\underline{x}_1,t_1)p(\underline{x}_1+\underline{\xi},t_1+\tau)]$$

$$= \lim_{T\to\infty} \frac{1}{2T}\int_{-T}^{T} p_\beta(\underline{x}_1,t)p_\beta(\underline{x}_1+\underline{\xi},t+\tau)\, dt \qquad (6\text{-}59)$$

so long as the β-th sample function is representative of the entire random process. Inasmuch as ergodic random processes are, by definition, stationary in the strict sense, it follows that higher order moments of ergodic processes are also specified by a temporal average of appropriate products from some representative sample function. The formulation of such higher order moments is left as an exercise for the reader.

It should be noted that an ergodic random process must be strictly stationary, but a strictly stationary process is not necessarily ergodic. It should be further noted that the correlation function of an ergodic random process can be expressed in any of the functional forms of equations (6-52)-(6-54) and that it maintains the symmetry properties shown for these functional forms in equations (6-55)-(6-57).

6.3.3 Homogeneous Random Processes

Homogeneous random processes are introduced in the description of the statistics of turbulent flow and, consequently, are often encountered in treatises of flow-induced noise and structural acoustics. To paraphrase Smol'yakov and Trachenko,[19] a homogeneous random process is another name for a process that is spatially stationary. Indeed, in the literature of flow noise and structural acoustics, the reader will sometimes find the homogeneous random process described as spatially stationary.

Because the above definition of a homogeneous random process prescribes characteristics of the process, in the spatial domain, that parallel those of a stationary process in the time domain, we define a random space-time field (or process) to be homogeneous in the strict sense if its statistics are unaffected by the choice of the spatial origin. Thus, the random process $p(\underline{x},t)$ is homogeneous in the strict sense if all single and joint moments of the random variables associated with $p(\underline{x},t)$ are equal to the corresponding single and joint moments of $p(\underline{x} + \underline{\varepsilon},t)$ for all choices of $\underline{\varepsilon}$. This implies that

$$\langle p(\underline{x}_1,t_1)\rangle = \langle p(\underline{x}_1 + \underline{\varepsilon},t_1)\rangle \qquad (6\text{-}60)$$

for any choice of $\underline{x}_1$, t_1, and $\underline{\varepsilon}$. Clearly, the mean of a strictly homogeneous random space-time field is a function only of time. Further, by arguments parallel to those of equations (6-50) and (6-51), it can be demonstrated that, when $p(\underline{x},t)$ is homogeneous in the strict sense,

$$Q_{pp}(\underline{x}_1,\underline{\xi},t_1,\tau) = Q_{pp}(\underline{\xi},t_1,\tau) \tag{6-61}$$

and that all other joint moments of the random variables associated with $p(\underline{x},t)$ are independent of the absolute spatial coordinates (i.e., spatial vectors referenced to a specific spatial origin), but depend on the spatial separation vectors between observations.

We will define a random space-time field to be weakly homogeneous (or homogeneous in the wide sense) if its mean value is independent of any spatial variable and its autocorrelation function depends only on the times of, and the spatial separation vector $(\underline{x}_2 - \underline{x}_1)$ between, observations. Thus, the mean of a weakly homogeneous random space-time field is a function of only the temporal coordinate, t, and has the functional form of equation (6-60). By examination of equations (6-43) through (6-46), it is evident that an appropriate functional form for the autocorrelation function of a weakly homogeneous random space-time field, $p(\underline{x},t)$, is

$$Q_{pp}(\underline{\xi},t_1,\tau) = E[p(\underline{x}_1,t_1)p(\underline{x}_1 + \underline{\xi},t_1 + \tau)] \ . \tag{6-62}$$

Recall that, in this text, we characterize random space-time fields by only the mean and autocorrelation functions. Thus, the homogeneity of the fields treated in this book can be only established in the weak sense. Recall further that we are restricting our attention to random space-time fields that are, at least, stationary in the weak sense. Thus, all homogeneous random processes treated in this text will be assumed to be, at least, weakly stationary.

For a real random space-time field, $p(\underline{x},t)$, that is both weakly stationary and homogeneous, it can easily be established, by equations (6-49) and (6-60), that the mean of the field is a constant. That is, inasmuch as the mean of $p(\underline{x},t)$ must be independent of the choices of both the spatial and temporal

origins, we require

$$<p(\underline{x}_1,t_1)> = <p(\underline{x}_1 + \underline{\varepsilon},t_1)> = <p(\underline{x}_1,t_1 + \theta)> = <p(\underline{x}_1 + \underline{\varepsilon},t_1 + \theta)> \quad (6\text{-}63)$$

for any choice of $\underline{x}_1$, $\underline{\varepsilon}$, t_1, and θ. This can be so only if

$$<p(\underline{x},t)> = \text{constant} . \quad (6\text{-}64)$$

Further, inasmuch as the autocorrelation of a weakly stationary field is independent of the absolute time of observation and that of a weakly homogeneous field is independent of the absolute spatial location of observation, it follows that the autocorrelation of a weakly stationary and weakly homogeneous field, $p(\underline{x},t)$, must have the functional form

$$Q_{pp}(\underline{\xi},\tau) = E[p(\underline{x}_1,t_1)p(\underline{x}_1 + \underline{\xi},t_1 + \tau)] . \quad (6\text{-}65)$$

Note, by equation (6-65), that

$$\begin{aligned} Q_{pp}(\underline{\xi},\tau) &= E[p(\underline{x}_1,t_1)p(\underline{x}_1 + \underline{\xi},t_1 + \tau)] \\ &= E[p(\underline{x}_1 + \underline{\xi},t_1 + \tau)p(\underline{x}_1,t_1)] = Q_{pp}(-\underline{\xi},-\tau) . \end{aligned} \quad (6\text{-}66)$$

Clearly then, the autocorrelation function of a real homogeneous, stationary field has the symmetry property

$$Q_{pp}(\underline{\xi},\tau) = Q_{pp}(-\underline{\xi},-\tau) . \quad (6\text{-}67)$$

We stated previously that the mathematical analysis of linear systems excited by random space-time fields is simplified if the statistics of the excitation field are stationary. An additional simplification is afforded if the excitation field is also homogeneous. Unfortunately, as we will show in the next chapter, we cannot restrict our attention to fields that are both homogeneous and stationary because, in some linear systems, a homogeneous and stationary input field can produce an output field that, while stationary, is nonhomogeneous.

6.4 SUMMARY OF THE SPACE-TIME CHARACTERIZATION OF RANDOM FIELDS

Because of the lengthy development of the descriptors and classification of random space-time fields presented in sections 6.2 and 6.3, it seems appropriate to briefly summarize the more significant results, assumptions, and decisions presented in those sections.

For logical and practical reasons (see section 6.2.2), a random space-time field is characterized in the space-time domain by two statistical metrics: the mean and autocorrelation functions.

There are four major classes of space-time fields:

- nonstationary and nonhomogeneous
- stationary and nonhomogeneous
- nonstationary and homogeneous
- stationary and homogeneous.

There are two degrees of both stationarity and homogeneity. These degrees are termed strict and weak.

A space-time field is strictly stationary if all single and joint moments of the field are independent of the temporal origin (i.e., independent of absolute time).

A space-time field is defined as weakly stationary if its mean is independent of time and its autocorrelation function depends on the spatial locations of, and the time difference between, observations of the random variables being correlated. If either the mean or correlation function depends on the absolute time (or choice of time origin) of observation, the field is said to be nonstationary.

A space-time field is strictly homogeneous if all single and joint moments of the field are independent of the choice of the spatial origin (i.e., independent of the absolute spatial coordinates).

A space-time field is weakly homogeneous if its mean is independent of any spatial coordinate and its autocorrelation function depends on the times of, and the spatial separation vector ($\underline{\xi}$) between, observations of the random variables being correlated. If either the mean or correlation function depends on the absolute spatial location (choice of spatial origin) of observation, the field is nonhomogeneous.

An important subclass of stationary processes is the ergodic random process. An ergodic random process is one in which any statistical metric obtained by averaging the ensemble of all possible sample functions is equal to the corresponding metric obtained from the temporal average of a single representative sample function.

Inasmuch as random space-time fields are characterized, in this text, by the mean and autocorrelation functions, it must be realized that the functional forms of these metrics can only establish whether a field is stationary or homogeneous in the weak sense.

For reasons outlined in section 6.3.1, we will restrict our attention, in the remainder of this book, to fields that are, at least, weakly stationary. Within this restriction, we will deal with only two classes of fields: the stationary, nonhomogeneous field and the stationary, homogeneous field.

A real stationary, nonhomogeneous field, say $p(\underline{x},t)$, is characterized by (1) a mean that is a function only of the spatial variable, $\underline{x}$, and (2) an autocorrelation that is a function of the spatial coordinates of, and the temporal difference between, the two random variables being correlated. For such a field, the value (μ_p) of the mean has the functional form

$$\mu_p(\underline{x}) = \langle p(\underline{x},t)\rangle = E[p(\underline{x},t)] \ , \qquad (6\text{-}68)$$

and the autocorrelation can be expressed in one of the following alternative functional forms:

$$Q_{pp}(\underline{x}_1,\underline{\xi},\tau) = E[p(\underline{x}_1,t_1)p(\underline{x}_1 + \underline{\xi},t_1 + \tau)] \ , \qquad (6\text{-}69)$$

$$\tilde{Q}_{pp}(\underline{x}_1,\underline{x}_2,\tau) = E[p(\underline{x}_1,t_1)p(\underline{x}_2,t_1 + \tau)] \ . \qquad (6\text{-}70)$$

or

$$\tilde{Q}_{pp}(\tilde{\underline{x}},\underline{\xi},\tau) = E[p(\tilde{\underline{x}} - \underline{\xi}/2,t_1)p(\tilde{\underline{x}} + \underline{\xi}/2,t_1 + \tau)] \ . \tag{6-71}$$

If the real random space-time field, $p(\underline{x},t)$, is stationary and homogeneous, it is statistically characterized by (1) a constant mean value and (2) an autocorrelation that is a function only of the differences between the spatial locations and times of observation of the two random variables being correlated. Thus, the mean and autocorrelation functions of the stationary, homogeneous field, $p(\underline{x},t)$, have the functional forms

$$\langle p(\underline{x},t)\rangle = \text{constant} \tag{6-72}$$

and

$$Q_{pp}(\underline{\xi},\tau) = E[p(\underline{x}_1,t_1)p(\underline{x}_1 + \underline{\xi},t_1 + \tau)] \ , \tag{6-73}$$

respectively.

Because all physical fields are real, we will confine our attention to real random space-time fields. Thus, for both the homogeneous and nonhomogeneous, stationary fields treated in this text, the mean and autocorrelation functions are real functions of the appropriate space and time variables. Further, as was demonstrated in sections 6.3.1 and 6.3.3, the autocorrelation functions of stationary fields have certain symmetry properties. The alternative functional forms for the autocorrelation function of a nonhomogeneous, stationary field have the following symmetries:

$$Q_{pp}(\underline{x}_1,\underline{\xi},\tau) = Q_{pp}(\underline{x}_2,-\underline{\xi},-\tau) \ , \tag{6-74}$$

where $\underline{x}_2 = \underline{x}_1 + \underline{\xi}$,

$$\tilde{Q}_{pp}(\underline{x}_1,\underline{x}_2,\tau) = \tilde{Q}_{pp}(\underline{x}_2,\underline{x}_1,-\tau) \ , \tag{6-75}$$

and

$$\tilde{Q}_{pp}(\tilde{\underline{x}},\underline{\xi},\tau) = \tilde{Q}_{pp}(\tilde{\underline{x}},-\underline{\xi},-\tau) \ . \tag{6-76}$$

The autocorrelation function of a stationary, homogeneous field was shown to have the following symmetry:

$$Q_{pp}(\underline{\xi},\tau) = Q_{pp}(-\underline{\xi},-\tau) \quad . \tag{6-77}$$

Let us now turn our attention to the characterization of random space-time fields in the wavevector-frequency domain.

6.5 DESCRIPTORS OF RANDOM SPACE-TIME FIELDS IN THE WAVEVECTOR-FREQUENCY DOMAIN

In chapter 2, we demonstrated that the wavevector-frequency description (i.e., transform) of a wave field was informationally equivalent to the space-time description of that field. In this section, we again employ multidimensional Fourier transforms to develop alternative descriptions of the statistics of random space-time fields that are informationally equivalent to the mean and autocorrelation functions. These alternative descriptions of random space-time fields are generically called wavevector-frequency spectra.

Recall that we restrict our attention, in this text, to random space-time fields that are statistically stationary. Therefore, we need to define wavevector-frequency spectra for only two classes of random space-time fields: the stationary, homogeneous field and the stationary, nonhomogeneous field. Let us first define the wavevector-frequency spectrum for the simpler of these fields, the stationary, homogeneous field.

6.5.1 Wavevector-Frequency Spectrum of a Stationary, Homogeneous Random Space-Time Field

The wavevector-frequency spectrum of the stationary, homogeneous random space-time field, $p(\underline{x},t)$, is defined as the multiple Fourier transform of the autocorrelation function, $Q_{pp}(\underline{\xi},\tau)$, on the spatial separation vector, $\underline{\xi}$, and time difference, τ. That is,

$$\Phi_p(\underline{k},\omega) \equiv \int_{-\infty}^{\infty} \int_{-\infty}^{\infty} Q_{pp}(\underline{\xi},\tau)\exp[-i(\underline{k}\cdot\underline{\xi} + \omega\tau)]\, d\underline{\xi}\, d\tau \quad . \tag{6-78}$$

Here, Φ_p denotes the wavevector-frequency spectrum of the stationary,

homogeneous field $p(\underline{x},t)$, the wavevector $\underline{k}$ is the Fourier conjugate variable of the spatial separation vector $\underline{\xi}$, and the circular frequency ω is the conjugate variable of the time difference τ. Inasmuch as the wavevector-frequency spectrum is defined as the (multiple) Fourier transform of the autocorrelation function Q_{pp}, the use of the single subscript p on the wavevector-frequency spectrum (i.e., Φ_p) is sufficient to unambiguously specify the random space-time field being characterized in the wavevector-frequency domain.

The Fourier inverse of equation (6-78) is

$$Q_{pp}(\underline{\xi},\tau) \equiv \frac{1}{(2\pi)^3} \int_{-\infty}^{\infty} \int_{-\infty}^{\infty} \Phi_p(\underline{k},\omega) \exp[i(\underline{k}\cdot\underline{\xi} + \omega\tau)]\, d\underline{k}\, d\omega \ . \qquad (6\text{-}79)$$

By equations (6-78) and (6-79), it is clear that the wavevector-frequency spectrum and autocorrelation function of a stationary, homogeneous field form a multidimensional Fourier transform pair.

Recall that, in this text, all random space-time fields represent real physical quantities. Thus, the autocorrelation function, $Q_{pp}(\underline{\xi},\tau)$, is a real function of $\underline{\xi}$ and τ. Consequently,

$$Q_{pp}(\underline{\xi},\tau) = Q^{*}_{pp}(\underline{\xi},\tau) \ , \qquad (6\text{-}80)$$

where the asterisk denotes the complex conjugate. It therefore follows, by equation (6-78), that

$$\Phi_p(\underline{k},\omega) = \Phi^{*}_p(-\underline{k},-\omega) \ . \qquad (6\text{-}81)$$

Moreover, we showed in section 6.3.3 that the autocorrelation function of the stationary, homogeneous field, $p(\underline{x},t)$, had the symmetry property

$$Q_{pp}(\underline{\xi},\tau) = Q_{pp}(-\underline{\xi},-\tau) \ . \qquad (6\text{-}82)$$

However, inasmuch as Q_{pp} is a real quantity, it follows that

$$Q_{pp}(\underline{\xi},\tau) = Q^{*}_{pp}(-\underline{\xi},-\tau) \ , \tag{6-83}$$

and therefore, by equation (6-78),

$$\Phi_p(\underline{k},\omega) = \Phi^{*}_p(\underline{k},\omega) \ . \tag{6-84}$$

Clearly, by equation (6-84), the wavevector-frequency spectrum of a stationary, homogeneous field is a real function of $\underline{k}$ and ω. Further, by equations (6-81) and (6-84), that spectrum has the symmetry property

$$\Phi_p(\underline{k},\omega) = \Phi_p(-\underline{k},-\omega) \ . \tag{6-85}$$

Throughout this chapter, we have consistently used the pressure field, $p(\underline{x},t)$, on a planar surface to develop and illustrate the statistical metrics of a random space-time field. This planar space-time field is a function of the two spatial coordinates, x_1 and x_2, that specify the location on the surface of the plane and of time, t. It should be realized, however, that the description of the statistics of random fields in one and three spatial dimensions can be developed by arguments parallel to those used for the planar field. That is, let $p(x,t)$ denote a stationary, homogeneous field that is a function of only one spatial variable, x, and time. The autocorrelation function of $p(x,t)$ is defined by

$$Q_{pp}(\xi,\tau) = E\{p(x,t)p(x+\xi,t+\tau)\} \ , \tag{6-86}$$

and the wavevector-frequency spectrum and autocorrelation functions are related by the Fourier transform pair

$$\Phi_p(k,\omega) \equiv \int_{-\infty}^{\infty}\int_{-\infty}^{\infty} Q_{pp}(\xi,\tau)\exp[-i(k\xi+\omega\tau)]\ d\xi\ d\tau \tag{6-87}$$

and

$$Q_{pp}(\xi,\tau) \equiv \frac{1}{(2\pi)^2}\int_{-\infty}^{\infty}\int_{-\infty}^{\infty} \Phi_p(k,\omega)\exp[i(k\xi+\omega\tau)]\ dk\ d\omega \ . \tag{6-88}$$

Similarly, if $p(\vec{x},t)$ denotes a stationary, homogeneous field that is a function of the three-dimensional spatial vector $\vec{x}$ and time, then the correlation function is defined by

$$Q_{pp}(\vec{\xi},\tau) = E\{p(\vec{x},t)p(\vec{x} + \vec{\xi},t + \tau)\} , \tag{6-89}$$

and the wavevector-frequency spectrum and autocorrelation function form the Fourier transform pair

$$\Phi_p(\vec{k},\omega) \equiv \int_{-\infty}^{\infty} \int_{-\infty}^{\infty} Q_{pp}(\vec{\xi},\tau)\exp[-i(\vec{k}\cdot\vec{\xi} + \omega\tau)]\, d\vec{\xi}\, d\tau \tag{6-90}$$

and

$$Q_{pp}(\vec{\xi},\tau) \equiv \frac{1}{(2\pi)^4} \int_{-\infty}^{\infty} \int_{-\infty}^{\infty} \Phi_p(\vec{k},\omega)\exp[i(\vec{k}\cdot\vec{\xi} + \omega\tau)]\, d\vec{k}\, d\omega . \tag{6-91}$$

Note, from equations (6-87), (6-88), (6-90), and (6-91), that, inasmuch as the wavevector is the Fourier conjugate of the spatial separation vector, it has the same dimensionality as the spatial separation vector.

It is also straightforward to show that, regardless of the spatial dimensionality of the random space-time field, the wavevector-frequency spectra of real stationary, homogeneous fields are real and have a symmetry, in the appropriate wavevector dimensions, similar to that shown in equation (6-85).

To illustrate certain features of the wavevector-frequency spectrum of a stationary, homogeneous space-time field, consider the field

$$p(\underline{x},t) = \langle p\rangle + s(\underline{x},t) , \tag{6-92}$$

where $\langle p\rangle$ is the mean of the field $p(\underline{x},t)$ and $s(\underline{x},t)$ is a zero-mean stationary, homogeneous field that characterizes the fluctuations of $p(\underline{x},t)$ about the mean. Inasmuch as the mean of an ensemble of sums is the sum of the

ensemble of means, it is easily established that the autocorrelation function of the field $p(\underline{x},t)$ is given by

$$Q_{pp}(\underline{\xi},\tau) = \langle p\rangle^2 + Q_{ss}(\underline{\xi},\tau) \ . \qquad (6\text{-}93)$$

By equations (6-78) and (6-93) and by use of equation (2-38), it is straightforward to show that the wavevector-frequency spectrum of $p(\underline{x},t)$ has the form

$$\Phi_p(\underline{k},\omega) = (2\pi)^3\langle p\rangle^2\delta(\underline{k})\delta(\omega) + \Phi_s(\underline{k},\omega) \ . \qquad (6\text{-}94)$$

Clearly, the wavevector-frequency spectrum of a stationary, homogeneous field comprises the sum of two spectra. One spectrum, $\Phi_s(\underline{k},\omega)$, characterizes the statistics of $s(\underline{x},t)$, the zero-mean fluctuating component of $p(\underline{x},t)$, in the wavevector-frequency domain. The other spectrum, the Dirac delta function located at $\underline{k} = (0,0)$ and $\omega = 0$, is weighted by a number proportional to $\langle p\rangle^2$, the square of the mean of $p(\underline{x},t)$. Inasmuch as $s(\underline{x},t)$ has zero mean, $\Phi_s(\underline{k},\omega)$ cannot contain a discrete (i.e., Dirac delta function) spectral component at $\underline{k} = (0,0)$ and $\omega = 0$. Moreover, because $\Phi_s(\underline{k},\omega) = \Phi_s(-\underline{k},-\omega)$, the wavevector-frequency spectrum of $s(\underline{x},t)$ must be a continuous function of $\underline{k}$ and ω at $\underline{k} = (0,0)$ and $\omega = 0$. Therefore, the magnitude of the mean, $|\langle p\rangle|$, of a stationary, homogeneous random space-time field, $p(\underline{x},t)$, can be deduced from the discrete spectral component of $\Phi_p(\underline{k},\omega)$ that occurs at $\underline{k} = (0,0)$ and $\omega = 0$. However, the sign of the mean can be determined only by knowledge of $\langle p\rangle$. The remaining spectral contributions to $\Phi_p(\underline{k},\omega)$ characterize, in the wavevector-frequency domain, the statistics of the fluctuations of $p(\underline{x},t)$ about the mean.

Note, by equation (6-79), that

$$Q_{pp}(\underline{0},0) = \langle p^2\rangle = \frac{1}{(2\pi)^3}\int_{-\infty}^{\infty}\int_{-\infty}^{\infty}\Phi_p(\underline{k},\omega)\, d\underline{k}\, d\omega \ , \qquad (6\text{-}95)$$

where $\langle p^2\rangle = \langle p^2(\underline{x},t)\rangle$ = constant for a stationary, homogeneous field. This relationship clearly indicates that the wavevector-frequency spectrum, $\Phi_p(\underline{k},\omega)$, can be interpreted as a metric of the relative contributions of

ensemble of means, it is easily established that the autocorrelation function of the field $p(\underline{x},t)$ is given by

$$Q_{pp}(\underline{\xi},\tau) = \langle p\rangle^2 + Q_{ss}(\underline{\xi},\tau) \ . \tag{6-93}$$

By equations (6-78) and (6-93) and by use of equation (2-38), it is straightforward to show that the wavevector-frequency spectrum of $p(\underline{x},t)$ has the form

$$\Phi_p(\underline{k},\omega) = (2\pi)^3\langle p\rangle^2\delta(\underline{k})\delta(\omega) + \Phi_s(\underline{k},\omega) \ . \tag{6-94}$$

Clearly, the wavevector-frequency spectrum of a stationary, homogeneous field comprises the sum of two spectra. One spectrum, $\Phi_s(\underline{k},\omega)$, characterizes the statistics of $s(\underline{x},t)$, the zero-mean fluctuating component of $p(\underline{x},t)$, in the wavevector-frequency domain. The other spectrum, the Dirac delta function located at $\underline{k} = (0,0)$ and $\omega = 0$, is weighted by a number proportional to $\langle p\rangle^2$, the square of the mean of $p(\underline{x},t)$. Inasmuch as $s(\underline{x},t)$ has zero mean, $\Phi_s(\underline{k},\omega)$ cannot contain a discrete (i.e., Dirac delta function) spectral component at $\underline{k} = (0,0)$ and $\omega = 0$. Moreover, because $\Phi_s(\underline{k},\omega) = \Phi_s(-\underline{k},-\omega)$, the wavevector-frequency spectrum of $s(\underline{x},t)$ must be a continuous function of $\underline{k}$ and ω at $\underline{k} = (0,0)$ and $\omega = 0$. Therefore, the magnitude of the mean, $|\langle p\rangle|$, of a stationary, homogeneous random space-time field, $p(\underline{x},t)$, can be deduced from the discrete spectral component of $\Phi_p(\underline{k},\omega)$ that occurs at $\underline{k} = (0,0)$ and $\omega = 0$. However, the sign of the mean can be determined only by knowledge of $\langle p\rangle$. The remaining spectral contributions to $\Phi_p(\underline{k},\omega)$ characterize, in the wavevector-frequency domain, the statistics of the fluctuations of $p(\underline{x},t)$ about the mean.

Note, by equation (6-79), that

$$Q_{pp}(\underline{0},0) = \langle p^2\rangle = \frac{1}{(2\pi)^3}\int_{-\infty}^{\infty}\int_{-\infty}^{\infty}\Phi_p(\underline{k},\omega)\, d\underline{k}\, d\omega \ , \tag{6-95}$$

where $\langle p^2\rangle = \langle p^2(\underline{x},t)\rangle$ = constant for a stationary, homogeneous field. This relationship clearly indicates that the wavevector-frequency spectrum, $\Phi_p(\underline{k},\omega)$, can be interpreted as a metric of the relative contributions of

various wavevector-frequency components to the mean square value, $\langle p^2 \rangle$, of the random space-time field. Specifically, $(2\pi)^{-3} \Phi_p(\underline{k},\omega) d\underline{k}\, d\omega$ is the contribution to $\langle p^2 \rangle$ from wavevectors in the range $\underline{k}$ to $\underline{k} + d\underline{k}$ and frequencies in the range ω to $\omega + d\omega$.

By equations (6-93) and (6-95), it follows that

$$\frac{1}{(2\pi)^3} \int_{-\infty}^{\infty} \int_{-\infty}^{\infty} \Phi_p(\underline{k},\omega)\, d\underline{k}\, d\omega = \langle p \rangle^2 + Q_{ss}(\underline{0},0) \ . \tag{6-96}$$

By equations (6-94) and (6-96), it is also evident that

$$Q_{ss}(\underline{0},0) = \langle s^2 \rangle = \frac{1}{(2\pi)^3} \int_{-\infty}^{\infty} \int_{-\infty}^{\infty} \Phi_s(\underline{k},\omega)\, d\underline{k}\, d\omega \ , \tag{6-97}$$

where $\langle s^2 \rangle$ denotes $\langle s^2(\underline{x},t) \rangle$, which, for a stationary, homogeneous field, is a constant.

As a specific example, consider the field in one spatial dimension described by

$$p(x,t) = P_0 + P_1 \sin(k_0 x + \omega_0 t + \theta) \ , \tag{6-98}$$

where the initial phase, θ, is a random variable equally probable between $-\pi$ and π. Thus, the probability density of θ is given by

$$f_\theta(\alpha) = \begin{cases} 1/(2\pi), & -\pi \le \alpha \le \pi \ , \\ 0, & \text{otherwise.} \end{cases} \tag{6-99}$$

By reference to chapter 2, we recognize the random process $p(x,t)$ to be an ensemble of real one-dimensional plane waves characterized by a mean P_0, an amplitude P_1 about the mean, a wavenumber k_0, and frequency ω_0, with initial phases distributed uniformly between $-\pi$ and π.

Clearly, the product $p(x,t)p(x + \xi, t + \tau)$ is a function of the random variable θ. Consequently, by equations (6-44) and (6-11), the autocorrelation function of $p(x,t)$ is given by

$$Q_{pp}(x,\xi,t,\tau) = \int_{-\infty}^{\infty} \{p(x,t;\alpha)p(x + \xi, t + \tau;\alpha)\} f_\theta(\alpha)\, d\alpha$$

$$= \frac{1}{2\pi} \int_{-\pi}^{\pi} \{P_0 + P_1 \sin[k_0 x + \omega_0 t + \alpha]\}\{P_0 + P_1 \sin[k_0(x + \xi) + \omega_0(t + \tau) + \alpha]\}\, d\alpha \,. \tag{6-100}$$

The integration of equation (6-100) is easily performed to yield

$$Q_{pp}(x,\xi,t,\tau) = Q_{pp}(\xi,\tau) = P_0^2 + (P_1^2/2)\cos[k_0\xi + \omega_0\tau] \,. \tag{6-101}$$

The functional form of this autocorrelation clearly indicates that $p(x,t)$ is a stationary, homogeneous field. Further, equation (6-101) shows that the autocorrelation function comprises two terms. The first term, P_0^2, is the square of the mean of the field, and the second term, $(P_1^2/2)\cos[k_0\xi + \omega_0\tau]$, is the autocorrelation of the zero-mean fluctuating component of the field. Note that (1) the amplitude of this second term is the mean square value of the fluctuating component of the field and (2) the wavenumber and frequency characterizing the argument of the cosine are identical to those characterizing the zero-mean wave component of $p(x,t)$.

It follows, by equations (6-78) and (6-101), that the wavevector-frequency spectrum of $p(x,t)$ is given by

$$\Phi_p(k,\omega) = (2\pi)^2 P_0^2 \delta(k)\delta(\omega)$$

$$+ (2\pi)^2 (P_1^2/4)\{\delta(k - k_0)\delta(\omega - \omega_0) + \delta(k + k_0)\delta(\omega + \omega_0)\} \,. \tag{6-102}$$

This spectrum, as illustrated in figure 6-6, consists of three discrete wavevector-frequency components. The discrete spectral component (i.e., Dirac

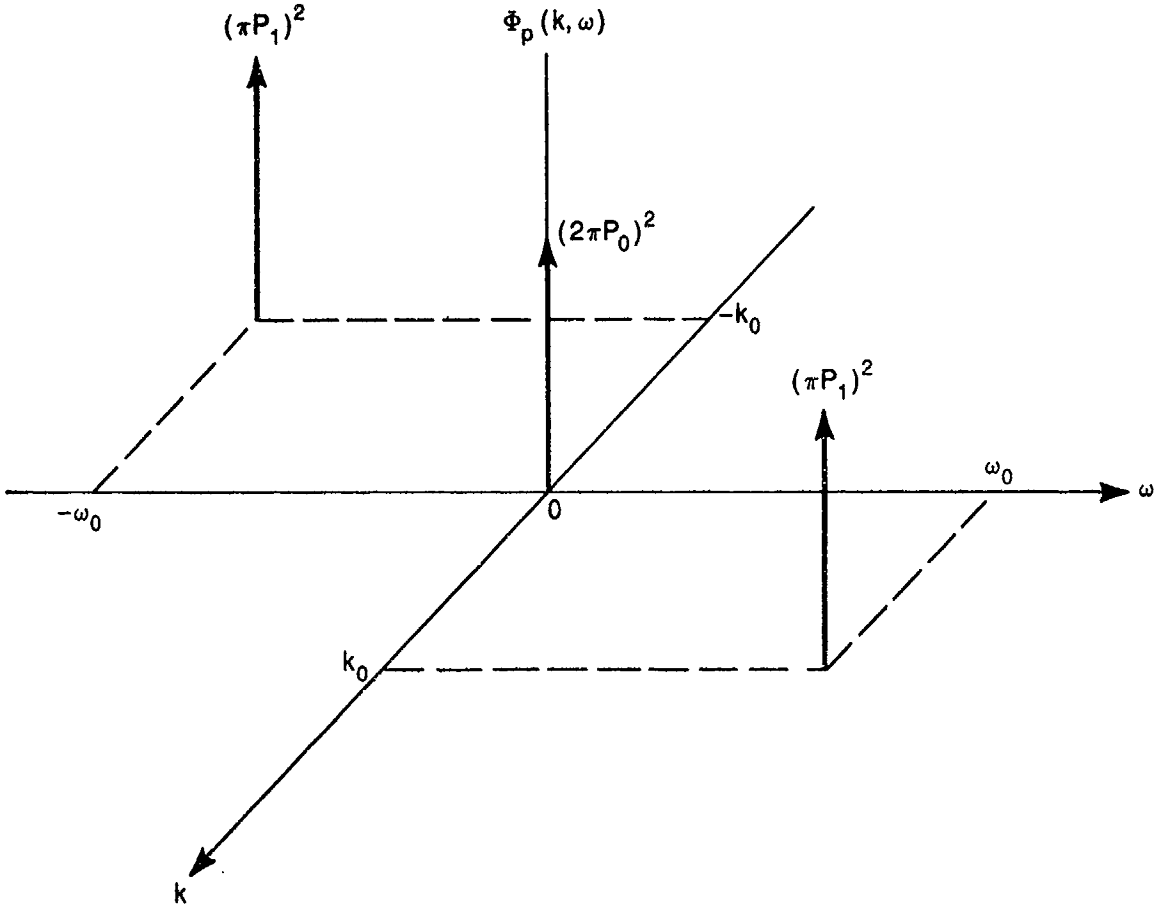

Figure 6-6. Wavevector-Frequency Spectrum of a Plane Wave With a Nonzero Mean and Random Phase

delta function) at $k = \omega = 0$ reflects the presence of a nonzero mean, and the amplitude (or weighting) of this component is seen to be proportional to the square of the mean value, P_0, of the wave field. The pair of equal amplitude, discrete spectral components at (k_0, ω_0) and $(-k_0, -\omega_0)$ characterize the statistics of the zero-mean propagating component of the field. The locations of these discrete components in the wavevector-frequency domain correspond to the wavevector-frequency combinations that characterize the propagation of the wave in the space-time domain, and the amplitudes of these components are proportional to the square of the amplitude of the zero-mean propagating component of p(x,t). Also, it is easily established that the combination of the waves associated with these two weighted discrete spectral components forms the term $(P_1^2/2)\cos[k_0\xi + \omega_0\tau]$ in equation (6-101) that characterizes the correlation function of the zero-mean contribution to the field p(x,t).

It is evident, by inspection of equation (6-102), that

$$\Phi_p(k,\omega) = \Phi_p(-k,-\omega) \ , \tag{6-103}$$

and therefore knowledge of the wavevector-frequency spectrum over all k and $0 \leq \omega < \infty$ is sufficient to define the spectrum over all k and ω. Note further, from equations (6-98), (6-99), (6-101), and (6-102), that

$$\frac{1}{(2\pi)^2} \int_{-\infty}^{\infty} \int_{-\infty}^{\infty} \Phi_p(k,\omega) \, dk \, d\omega = Q_{pp}(0,0) = P_0^2 + P_1^2/2 = \langle p^2 \rangle \ . \tag{6-104}$$

Let us now turn our attention to the wavevector-frequency spectra of stationary, nonhomogeneous fields.

6.5.2 Wavevector-Frequency Spectra of Stationary, Nonhomogeneous Random Space-Time Fields

Recall that the wavevector-frequency spectrum of a stationary, homogeneous field was defined as the multiple Fourier transform of the autocorrelation function, $Q_{pp}(\underline{\xi},\tau)$, on the spatial separation vector, $\underline{\xi}$, and the time difference, τ. The wavevector-frequency spectra of stationary, nonhomogeneous fields are also defined by multiple Fourier transforms of the autocorrelation function. However, a brief review of section 6.4 will remind the reader that (1) the autocorrelation function of a stationary, nonhomogeneous field is a function of two spatial vector variables, whereas the autocorrelation function of a stationary, homogeneous field is a function of a single spatial vector variable and (2) the autocorrelation of a stationary, nonhomogeneous field can be expressed in several functional forms, whereas the autocorrelation of a stationary, homogeneous field is characterized by a single functional form. The presence of the additional spatial variable in the autocorrelation function of the nonhomogeneous field permits some flexibility in the definition of a wavevector-frequency spectrum for a stationary, nonhomogeneous field. Moreover, the existence of alternative functional forms for the autocorrelation of a nonhomogeneous field implies the existence of alternative functional forms for any definition of the wavevector-frequency spectrum of such fields.

By the above arguments, it is evident that there is no unique characterization of the statistics of a stationary, nonhomogeneous field in the wavevector-frequency domain. In the sections to follow, we will define and examine three different wavevector-frequency spectra for characterizing the statistics of stationary, nonhomogeneous fields. These forms are analogous, in the wavevector domain, to those proposed by Bendat and Piersol[20] for describing the statistics of nonstationary processes in the frequency domain.

6.5.2.1 <u>The Space-Varying Wavevector-Frequency Spectrum</u>. The space-varying wavevector-frequency spectrum is defined as the multiple Fourier transform of the autocorrelation function on the second of its spatial vector variables and on the time difference, τ. Thus, from the alternative functional forms of the autocorrelation function defined by equations (6-69), (6-70), and (6-71), we can define three alternative functional forms of the space-varying wavevector-frequency spectrum. These are

$$K_{pp}(\underline{x}_1,\underline{k},\omega) \equiv \int_{-\infty}^{\infty}\int_{-\infty}^{\infty} Q_{pp}(\underline{x}_1,\underline{\xi},\tau)\exp[-i(\underline{k}\cdot\underline{\xi} + \omega\tau)]\, d\underline{\xi}\, d\tau \ , \tag{6-105}$$

$$\bar{K}_{pp}(\underline{x}_1,\underline{\beta},\omega) \equiv \int_{-\infty}^{\infty}\int_{-\infty}^{\infty} \bar{Q}_{pp}(\underline{x}_1,\underline{x}_2,\tau)\exp[-i(\underline{\beta}\cdot\underline{x}_2 + \omega\tau)]\, d\underline{x}_2\, d\tau \ , \tag{6-106}$$

and

$$\tilde{K}_{pp}(\tilde{\underline{x}},\underline{k},\omega) \equiv \int_{-\infty}^{\infty}\int_{-\infty}^{\infty} \tilde{Q}_{pp}(\tilde{\underline{x}},\underline{\xi},\tau)\exp[-i(\underline{k}\cdot\underline{\xi} + \omega\tau)]\, d\underline{\xi}\, d\tau \ . \tag{6-107}$$

Here, the various K_{pp}'s denote alternative forms of the space-varying wavevector-frequency spectra and, consistent with the stationary, homogeneous form of the wavevector-frequency spectrum, the wavevector $\underline{k}$ denotes the Fourier conjugate variable of the spatial separation vector $\underline{\xi}$, and ω is the conjugate variable of the time difference τ. The wavevector $\underline{\beta}$, in equation (6-106), denotes the Fourier conjugate variable of the spatial vector $\underline{x}_2$.

It is straightforward to establish the following inverse relationships:

$$Q_{pp}(\underline{x}_1,\underline{\xi},\tau) = (2\pi)^{-3} \int_{-\infty}^{\infty} \int_{-\infty}^{\infty} K_{pp}(\underline{x}_1,\underline{k},\omega) \exp[i(\underline{k}\cdot\underline{\xi} + \omega\tau)]\, d\underline{k}\, d\omega \ , \tag{6-108}$$

$$\bar{Q}_{pp}(\underline{x}_1,\underline{x}_2,\tau) = (2\pi)^{-3} \int_{-\infty}^{\infty} \int_{-\infty}^{\infty} \bar{K}_{pp}(\underline{x}_1,\underline{\beta},\omega) \exp[i(\underline{\beta}\cdot\underline{x}_2 + \omega\tau)]\, d\underline{\beta}\, d\omega \ , \tag{6-109}$$

and

$$\tilde{Q}_{pp}(\tilde{\underline{x}},\underline{\xi},\tau) = (2\pi)^{-3} \int_{-\infty}^{\infty} \int_{-\infty}^{\infty} \tilde{K}_{pp}(\tilde{\underline{x}},\underline{k},\omega) \exp[i(\underline{k}\cdot\underline{\xi} + \omega\tau)]\, d\underline{k}\, d\omega \ . \tag{6-110}$$

Recall that the random space-time fields treated in this text are real. It follows, by equations (6-69) through (6-71), that the autocorrelation functions Q_{pp}, $\bar{Q}_{pp}$, and $\tilde{Q}_{pp}$ are real, and therefore

$$Q_{pp}(\underline{x}_1,\underline{\xi},\tau) = Q^*_{pp}(\underline{x}_1,\underline{\xi},\tau) \ , \tag{6-111}$$

$$\bar{Q}_{pp}(\underline{x}_1,\underline{x}_2,\tau) = \bar{Q}^*_{pp}(\underline{x}_1,\underline{x}_2,\tau) \ , \tag{6-112}$$

$$\tilde{Q}_{pp}(\tilde{\underline{x}},\underline{\xi},\tau) = \tilde{Q}^*_{pp}(\tilde{\underline{x}},\underline{\xi},\tau) \ . \tag{6-113}$$

It follows, from equations (6-105), (6-106), and (6-107), that

$$K_{pp}(\underline{x}_1,\underline{k},\omega) = K^*_{pp}(\underline{x}_1,-\underline{k},-\omega) \ , \tag{6-114}$$

$$\bar{K}_{pp}(\underline{x}_1,\underline{\beta},\omega) = \bar{K}^*_{pp}(\underline{x}_1,-\underline{\beta},-\omega) \ , \tag{6-115}$$

$$\tilde{K}_{pp}(\tilde{\underline{x}},\underline{k},\omega) = \tilde{K}^*_{pp}(\tilde{\underline{x}},-\underline{k},-\omega) \ . \tag{6-116}$$

The symmetry properties of the autocorrelation functions of stationary, nonhomogeneous fields are summarized in equations (6-74) to (6-76). Note, by equations (6-76) and (6-113), that

$$\tilde{Q}_{pp}(\tilde{\underline{x}},\underline{\xi},\tau) = \tilde{Q}^*_{pp}(\tilde{\underline{x}},-\underline{\xi},-\tau) \ . \tag{6-117}$$

It therefore follows, by equations (6-107) and (6-116), that

$$\tilde{K}_{pp}(\tilde{\underline{x}},\underline{k},\omega) = \tilde{K}^{*}_{pp}(\tilde{\underline{x}},\underline{k},\omega) = \tilde{K}_{pp}(\tilde{\underline{x}},-\underline{k},-\omega) \ . \qquad (6\text{-}118)$$

Thus, $\tilde{K}_{pp}(\tilde{\underline{x}},\underline{k},\omega)$ is a real function of $\tilde{\underline{x}}$, $\underline{k}$, and ω. Equations (6-74) and (6-75) do not lead to a symmetry similar to that shown in equation (6-117). Therefore, it must be concluded that the space-averaged wavevector-frequency spectra $K_{pp}(\underline{x}_1,\underline{k},\omega)$ and $\bar{K}_{pp}(\underline{x}_1,\underline{\beta},\omega)$ are, in general, complex.

It is straightforward to show, from equations (6-52) through (6-54), that

$$Q_{pp}(\underline{x}_1,\underline{\xi},\tau) = \bar{Q}_{pp}(\underline{x}_1,\underline{x}_1 + \underline{\xi},\tau) = \tilde{Q}_{pp}(\underline{x}_1 + \underline{\xi}/2,\underline{\xi},\tau) \ . \qquad (6\text{-}119)$$

By equations (6-105), (6-106), and (6-19), it follows that K_{pp} and $\bar{K}_{pp}$ are related by

$$K_{pp}(\underline{x}_1,\underline{k},\omega) = \exp(i\underline{k}\cdot\underline{x}_1)\bar{K}_{pp}(\underline{x}_1,\underline{k},\omega) \ . \qquad (6\text{-}120)$$

However, the presence, in equation (6-119), of the argument $\underline{x}_1 + \underline{\xi}/2$ in $\tilde{Q}_{pp}$ precludes such a simple relationship between $\tilde{K}_{pp}$ and K_{pp} or $\bar{K}_{pp}$.

To summarize, we have defined three alternative functional forms of the space-varying wavevector-frequency spectrum. One of these forms, $\tilde{K}_{pp}(\tilde{\underline{x}},\underline{k},\omega)$, is a real function of $\tilde{\underline{x}}$, $\underline{k}$, and ω; the other two functional forms, $K_{pp}(\underline{x}_1,\underline{k},\omega)$ and $\bar{K}_{pp}(\underline{x}_1,\underline{\beta},\omega)$, are complex. The two complex forms are simply related, but neither of these functional forms can be simply related to the form that is real.

Let us now examine another characterization of the statistics of a stationary, nonhomogeneous field in the wavevector-frequency domain: that is, the two wavevector-frequency spectrum.

6.5.2.2 <u>The Two Wavevector-Frequency Spectrum</u>. The two wavevector-frequency spectrum is defined as the Fourier transform of the autocorrelation function

of a stationary, nonhomogeneous field on all spatial and temporal variables of the autocorrelation function. Thus, corresponding to the three alternative functional forms of the autocorrelation function defined by equations (6-69), (6-70), and (6-71), we can define the following three alternative forms of the two wavevector-frequency spectrum:

$$S_{pp}(\underline{\mu},\underline{k},\omega) \equiv \int_{-\infty}^{\infty}\int_{-\infty}^{\infty}\int_{-\infty}^{\infty} Q_{pp}(\underline{x}_1,\underline{\xi},\tau)\exp[-i(\underline{\mu}\cdot\underline{x}_1 + \underline{k}\cdot\underline{\xi} + \omega\tau)]\, d\underline{x}_1\, d\underline{\xi}\, d\tau \ , \tag{6-121}$$

$$\bar{S}_{pp}(\underline{\mu},\underline{\beta},\omega) \equiv \int_{-\infty}^{\infty}\int_{-\infty}^{\infty}\int_{-\infty}^{\infty} \bar{Q}_{pp}(\underline{x}_1,\underline{x}_2,\tau)\exp[-i(\underline{\mu}\cdot\underline{x}_1 + \underline{\beta}\cdot\underline{x}_2 + \omega\tau)]\, d\underline{x}_1\, d\underline{x}_2\, d\tau \ , \tag{6-122}$$

and

$$\tilde{S}_{pp}(\underline{\alpha},\underline{k},\omega) \equiv \int_{-\infty}^{\infty}\int_{-\infty}^{\infty}\int_{-\infty}^{\infty} \tilde{Q}_{pp}(\tilde{\underline{x}},\underline{\xi},\tau)\exp[-i(\underline{\alpha}\cdot\tilde{\underline{x}} + \underline{k}\cdot\underline{\xi} + \omega\tau)]\, d\tilde{\underline{x}}\, d\underline{\xi}\, d\tau \ . \tag{6-123}$$

Here, $\underline{\mu}$ and $\underline{\alpha}$ are the Fourier conjugate variables of the absolute spatial vectors $\underline{x}_1$ and $\tilde{\underline{x}}$, respectively. The Fourier inverses of equations (6-121) through (6-123) are

$$Q_{pp}(\underline{x}_1,\underline{\xi},\tau) = (2\pi)^{-5} \int_{-\infty}^{\infty}\int_{-\infty}^{\infty}\int_{-\infty}^{\infty} S_{pp}(\underline{\mu},\underline{k},\omega)$$

$$\exp[i(\underline{\mu}\cdot\underline{x}_1 + \underline{k}\cdot\underline{\xi} + \omega\tau)]\, d\underline{\mu}\, d\underline{k}\, d\omega \ , \tag{6-124}$$

$$\bar{Q}_{pp}(\underline{x}_1,\underline{x}_2,\tau) = (2\pi)^{-5} \int_{-\infty}^{\infty}\int_{-\infty}^{\infty}\int_{-\infty}^{\infty} \bar{S}_{pp}(\underline{\mu},\underline{\beta},\omega)$$

$$\exp[i(\underline{\mu}\cdot\underline{x}_1 + \underline{\beta}\cdot\underline{x}_2 + \omega\tau)]\, d\underline{\mu}\, d\underline{\beta}\, d\omega \ , \tag{6-125}$$

and

$$\tilde{Q}_{pp}(\tilde{\underline{x}},\underline{\xi},\tau) = (2\pi)^{-5} \int_{-\infty}^{\infty}\int_{-\infty}^{\infty}\int_{-\infty}^{\infty} \tilde{S}_{pp}(\underline{\alpha},\underline{k},\omega)$$

$$\exp[i(\underline{\alpha}\cdot\tilde{\underline{x}} + \underline{k}\cdot\underline{\xi} + \omega\tau)]\ d\underline{\alpha}\ d\underline{k}\ d\omega\ . \qquad (6\text{-}126)$$

By comparison of equations (6-105) through (6-107) with (6-121) through (6-123), it is evident that

$$S_{pp}(\underline{\mu},\underline{k},\omega) = \int_{-\infty}^{\infty} K_{pp}(\underline{x}_1,\underline{k},\omega)\exp[-i(\underline{\mu}\cdot\underline{x}_1)]\ d\underline{x}_1\ , \qquad (6\text{-}127)$$

$$\bar{S}_{pp}(\underline{\mu},\underline{\beta},\omega) = \int_{-\infty}^{\infty} \bar{K}_{pp}(\underline{x}_1,\underline{\beta},\omega)\exp[-i(\underline{\mu}\cdot\underline{x}_1)]\ d\underline{x}_1\ , \qquad (6\text{-}128)$$

and

$$\tilde{S}_{pp}(\underline{\alpha},\underline{k},\omega) = \int_{-\infty}^{\infty} \tilde{K}_{pp}(\tilde{\underline{x}},\underline{k},\omega)\exp[-i(\underline{\alpha}\cdot\tilde{\underline{x}})]\ d\tilde{\underline{x}}\ . \qquad (6\text{-}129)$$

The associated inverse relationships are

$$K_{pp}(\underline{x}_1,\underline{k},\omega) = (2\pi)^{-2} \int_{-\infty}^{\infty} S_{pp}(\underline{\mu},\underline{k},\omega)\exp[i(\underline{\mu}\cdot\underline{x}_1)]\ d\underline{\mu}\ , \qquad (6\text{-}130)$$

$$\bar{K}_{pp}(\underline{x}_1,\underline{\beta},\omega) = (2\pi)^{-2} \int_{-\infty}^{\infty} \bar{S}_{pp}(\underline{\mu},\underline{\beta},\omega)\exp[i(\underline{\mu}\cdot\underline{x}_1)]\ d\underline{\mu}\ , \qquad (6\text{-}131)$$

and

$$\tilde{K}_{pp}(\tilde{\underline{x}},\underline{k},\omega) = (2\pi)^{-2} \int_{-\infty}^{\infty} \tilde{S}_{pp}(\underline{\alpha},\underline{k},\omega)\exp[i(\underline{\alpha}\cdot\tilde{\underline{x}})]\ d\underline{\alpha}\ . \qquad (6\text{-}132)$$

Inasmuch as all forms of the autocorrelation functions are real, it follows from equations (6-121) to (6-123) that

$$S_{pp}(\underline{\mu},\underline{k},\omega) = S^{*}_{pp}(-\underline{\mu},-\underline{k},-\omega) \ , \tag{6-133}$$

$$\bar{S}_{pp}(\underline{\mu},\underline{\beta},\omega) = \bar{S}^{*}_{pp}(-\underline{\mu},-\underline{\beta},-\omega) \ , \tag{6-134}$$

$$\tilde{S}_{pp}(\underline{\alpha},\underline{k},\omega) = \tilde{S}^{*}_{pp}(-\underline{\alpha},-\underline{k},-\omega) \ . \tag{6-135}$$

Moreover, by the symmetry properties of the various forms of the auto-correlation functions summarized in equations (6-74), (6-75), and (6-76), it can easily be shown that

$$S_{pp}(\underline{\mu},\underline{k},\omega) = S_{pp}(\underline{\mu},\underline{\mu} - \underline{k},-\omega) \ , \tag{6-136}$$

$$\bar{S}_{pp}(\underline{\mu},\underline{\beta},\omega) = \bar{S}_{pp}(\underline{\beta},\underline{\mu},-\omega) \ , \tag{6-137}$$

$$\tilde{S}_{pp}(\underline{\alpha},\underline{k},\omega) = \tilde{S}_{pp}(\underline{\alpha},-\underline{k},-\omega) \ . \tag{6-138}$$

By the symmetry properties of equations (6-133) through (6-138), it can be deduced that none of the alternative forms of the two wavevector-frequency spectra are real. Thus, in general, all two wavevector-frequency spectra of stationary, nonhomogeneous fields are complex functions of their wavevector and frequency arguments.

By use of equation (6-119) and equations (6-121) to (6-123), the following relationships between the alternative forms of the two wavevector-frequency spectra can be established:

$$S_{pp}(\underline{\mu},\underline{k},\omega) = \tilde{S}_{pp}(\underline{\mu} - \underline{k},\underline{k},\omega) \ , \tag{6-139}$$

$$S_{pp}(\underline{\mu},\underline{k},\omega) = \tilde{S}_{pp}(\underline{\mu},\underline{k} - \underline{\mu}/2,\omega) \ , \tag{6-140}$$

$$\bar{S}_{pp}(\underline{\mu},\underline{\beta},\omega) = \tilde{S}_{pp}\left(\underline{\mu} + \underline{\beta},\ \frac{\underline{\beta} - \underline{\mu}}{2},\ \omega\right) \ . \tag{6-141}$$

Thus, given any form of the two wavevector-frequency spectrum, all other alternative forms can be deduced.

We now turn attention to the third wavevector-frequency characterization of stationary, nonhomogeneous fields: that is, the space-averaged wavevector-frequency spectrum.

6.5.2.3 The Space-Averaged Wavevector-Frequency Spectrum. The wavevector-frequency spectra described in previous sections have simply been various Fourier transforms of the autocorrelation function of the random space-time field of interest and, therefore, are informationally equivalent to the autocorrelation function. As will become evident shortly, the space-averaged wavevector-frequency spectrum does not preserve, in the wavevector-frequency domain, all of the statistical information characterized by the autocorrelation function in the space-time domain. Nonetheless, the space-averaged wavevector-frequency spectrum is a useful, and perhaps the most widely applied, metric of the statistics of nonhomogeneous fields.

Simply stated, the space-averaged wavevector-frequency spectrum is a statistical metric defined for stationary, nonhomogeneous fields such that its properties parallel those of the wavevector-frequency spectrum of a stationary, homogeneous field. Recall (see equation (6-73)) that the autocorrelation function of a stationary, homogeneous field is a function of only the spatial separation vector $\underline{\xi}$ and the time difference τ. Inspection of the alternative forms of the autocorrelation functions for stationary, nonhomogeneous fields shown in equations (6-69) to (6-71) reveals that two of these forms, designated by Q_{pp} and $\tilde{Q}_{pp}$, are functions of both $\underline{\xi}$ and τ. However, Q_{pp} and $\tilde{Q}_{pp}$ are also functions of the additional variables $\underline{x}_1 = (x_{11},x_{12})$ and $\underline{\tilde{x}} = (\tilde{x}_1,\tilde{x}_2)$, respectively. To eliminate these extra variables, we assume that the following space-averaged autocorrelation functions exist and are not identically zero for all $\underline{\xi}$ and τ:

$$Q^a_{pp}(\underline{\xi},\tau) = \lim_{L\to\infty} \frac{1}{4L^2} \int_{-L}^{L}\int_{-L}^{L} Q_{pp}(\underline{x}_1,\underline{\xi},\tau)\, dx_{11}\, dx_{12} \tag{6-142}$$

and

$$\tilde{Q}^a_{pp}(\underline{\xi},\tau) = \lim_{L\to\infty} \frac{1}{4L^2} \int_{-L}^{L} \int_{-L}^{L} \tilde{Q}_{pp}(\underline{\tilde{x}},\underline{\xi},\tau)\, d\tilde{x}_1\, d\tilde{x}_2 \; . \qquad (6\text{-}143)$$

Here, the superscript "a" designates the space-averaged forms of the auto-correlation functions, and L designates a length measured along either the x_{11}, x_{12}, $\tilde{x}_1$, or $\tilde{x}_2$ axis.

For fixed values of $\underline{\xi}$ and τ, it seems intuitively obvious that $Q^a_{pp}(\underline{\xi},\tau)$ and $\tilde{Q}^a_{pp}(\underline{\xi},\tau)$ should be equal. By use of equation (6-119) in equation (6-142), we obtain

$$Q^a_{pp}(\underline{\xi},\tau) = \lim_{L\to\infty} \frac{1}{4L^2} \int_{-L}^{L} \int_{-L}^{L} \tilde{Q}_{pp}(\underline{x}_1 + \underline{\xi}/2,\underline{\xi},\tau)\, dx_{11}\, dx_{12} \; . \qquad (6\text{-}144)$$

By letting $\underline{\tilde{x}} = \underline{x}_1 + \underline{\xi}/2$, we obtain

$$Q^a_{pp}(\underline{\xi},\tau) = \lim_{L\to\infty} \frac{1}{4L^2} \int_{-L+\xi_2/2}^{L+\xi_2/2} \int_{-L+\xi_1/2}^{L+\xi_1/2} \tilde{Q}_{pp}(\underline{\tilde{x}},\underline{\xi},\tau)\, d\tilde{x}_1\, d\tilde{x}_2 \; . \qquad (6\text{-}145)$$

However, for any fixed $\underline{\xi}$ and τ, the right-hand side of equation (6-145) tends to the same limit, as $L\to\infty$, as does the right-hand side of equation (6-143). Thus, consistent with our intuition, we conclude that

$$Q^a_{pp}(\underline{\xi},\tau) = \tilde{Q}^a_{pp}(\underline{\xi},\tau) \; . \qquad (6\text{-}146)$$

Thus, we need consider only one mathematical form for the space-averaged auto-correlation function. We choose to work from the form given by equation (6-142).

By equations (6-76) and (6-146), it is evident that

$$Q^a_{pp}(\underline{\xi},\tau) = Q^a_{pp}(-\underline{\xi},-\tau) \; . \qquad (6\text{-}147)$$

Further, because the autocorrelation function of a real process is real, it follows that

$$Q^a_{pp}(\underline{\xi},\tau) = Q^{a*}_{pp}(-\underline{\xi},-\tau) \ . \qquad (6\text{-}148)$$

The symmetry properties shown in equations (6-147) and (6-148) are identical to those demonstrated for the autocorrelation function of a stationary, homogeneous field in equations (6-82) and (6-83).

The space-averaged wavevector-frequency spectrum is defined as the Fourier transform of the space-averaged autocorrelation function on the spatial separation vector $\underline{\xi}$ and the time difference τ. Thus, if we denote the space-averaged wavevector-frequency spectrum by $\Phi^a_p(\underline{k},\omega)$, it follows that

$$\Phi^a_p(\underline{k},\omega) \equiv \int_{-\infty}^{\infty}\int_{-\infty}^{\infty} Q^a_{pp}(\underline{\xi},\tau)\exp[-i(\underline{k}\cdot\underline{\xi} + \omega\tau)]\, d\underline{\xi}\, d\tau \ . \qquad (6\text{-}149)$$

The Fourier inverse of equation (6-149) is

$$Q^a_{pp}(\underline{\xi},\tau) = (2\pi)^{-3} \int_{-\infty}^{\infty}\int_{-\infty}^{\infty} \Phi^a_p(\underline{k},\omega)\exp[i(\underline{k}\cdot\underline{\xi} + \omega\tau)]\, d\underline{k}\, d\omega \ . \qquad (6\text{-}150)$$

By the symmetry properties of equations (6-147) and (6-148), it follows from equation (6-149) that

$$\Phi^a_p(\underline{k},\omega) = \Phi^{a*}_p(\underline{k},\omega) \qquad (6\text{-}151)$$

and

$$\Phi^a_p(\underline{k},\omega) = \Phi^a_p(-\underline{k},-\omega) \ . \qquad (6\text{-}152)$$

Thus, the space-averaged wavevector-frequency spectrum is real and has the same symmetry (see equation (6-85)) as the spectrum of a stationary, homogeneous field.

By use of equations (6-105), (6-142), and (6-149), it is easily shown that

$$\Phi_p^a(\underline{k},\omega) = \lim_{L\to\infty} \frac{1}{4L^2} \int_{-L}^{L}\int_{-L}^{L} K_{pp}(\underline{x}_1,\underline{k},\omega)\, dx_{11}\, dx_{12} \ . \tag{6-153}$$

By substituting equation (6-130) into equation (6-153), the space-averaged wavevector spectra can also be written in the form

$$\Phi_p^a(\underline{k},\omega) = \lim_{L\to\infty} \frac{1}{16\pi^2 L^2} \int_{-L}^{L}\int_{-L}^{L}\int_{-\infty}^{\infty} S_{pp}(\underline{\mu},\underline{k},\omega)\exp[i(\underline{\mu}\cdot\underline{x}_1)]\, d\underline{\mu}\, dx_{11}\, dx_{12} \ . \tag{6-154}$$

By performing the integrations over x_{11} and x_{12} in equation (6-154), we obtain

$$\Phi_p^a(\underline{k},\omega) = \lim_{L\to\infty} \frac{1}{(2\pi)^2} \int_{-\infty}^{\infty} S_{pp}(\underline{\mu},\underline{k},\omega)\left[\frac{\sin(\mu_1 L)}{\mu_1 L}\right]\left[\frac{\sin(\mu_2 L)}{\mu_2 L}\right] d\underline{\mu} \ . \tag{6-155}$$

However,

$$\lim_{L\to\infty}\left[\frac{\sin(\alpha L)}{\alpha L}\right] = \begin{cases} 1, & \alpha = 0 \ , \\ 0, & \text{otherwise.} \end{cases} \tag{6-156}$$

Thus, in the limit as $L\to\infty$, the integrand of equation (6-155) is zero everywhere except at the point $\underline{\mu} = (0,0)$. Inasmuch as the area associated with any single point is zero, the integral of this contribution is zero, and thus $\Phi_p^a(\underline{k},\omega) = 0$ for all $\underline{k}$ and ω, unless $S_{pp}(\underline{\mu},\underline{k},\omega)$ contains a spectral contribution of the form $\delta(\underline{\mu})V(\underline{k},\omega)$.

Consider a stationary, nonhomogeneous field characterized by the two wavevector-frequency spectrum

$$S_{pp}(\underline{\mu},\underline{k},\omega) = (2\pi)^2\delta(\underline{\mu})V(\underline{k},\omega) + W_{pp}(\underline{\mu},\underline{k},\omega) \ , \tag{6-157}$$

By use of equations (6-105), (6-142), and (6-149), it is easily shown that

$$\Phi_p^a(\underline{k},\omega) = \lim_{L\to\infty} \frac{1}{4L^2} \int_{-L}^{L}\int_{-L}^{L} K_{pp}(\underline{x}_1,\underline{k},\omega)\, dx_{11}\, dx_{12} \; . \tag{6-153}$$

By substituting equation (6-130) into equation (6-153), the space-averaged wavevector spectra can also be written in the form

$$\Phi_p^a(\underline{k},\omega) = \lim_{L\to\infty} \frac{1}{16\pi^2 L^2} \int_{-L}^{L}\int_{-L}^{L}\int_{-\infty}^{\infty} S_{pp}(\underline{\mu},\underline{k},\omega)\exp[i(\underline{\mu}\cdot\underline{x}_1)]\, d\underline{\mu}\, dx_{11}\, dx_{12} \; . \tag{6-154}$$

By performing the integrations over x_{11} and x_{12} in equation (6-154), we obtain

$$\Phi_p^a(\underline{k},\omega) = \lim_{L\to\infty} \frac{1}{(2\pi)^2} \int_{-\infty}^{\infty} S_{pp}(\underline{\mu},\underline{k},\omega)\left[\frac{\sin(\mu_1 L)}{\mu_1 L}\right]\left[\frac{\sin(\mu_2 L)}{\mu_2 L}\right] d\underline{\mu} \; . \tag{6-155}$$

However,

$$\lim_{L\to\infty}\left[\frac{\sin(\alpha L)}{\alpha L}\right] = \begin{cases} 1, & \alpha = 0 \; , \\ 0, & \text{otherwise.} \end{cases} \tag{6-156}$$

Thus, in the limit as $L\to\infty$, the integrand of equation (6-155) is zero everywhere except at the point $\underline{\mu} = (0,0)$. Inasmuch as the area associated with any single point is zero, the integral of this contribution is zero, and thus $\Phi_p^a(\underline{k},\omega) = 0$ for all $\underline{k}$ and ω, unless $S_{pp}(\underline{\mu},\underline{k},\omega)$ contains a spectral contribution of the form $\delta(\underline{\mu})V(\underline{k},\omega)$.

Consider a stationary, nonhomogeneous field characterized by the two wavevector-frequency spectrum

$$S_{pp}(\underline{\mu},\underline{k},\omega) = (2\pi)^2\delta(\underline{\mu})V(\underline{k},\omega) + W_{pp}(\underline{\mu},\underline{k},\omega) \; , \tag{6-157}$$

where $W_{pp}(\underline{\mu},\underline{k},\omega)$ characterizes a nonhomogeneous field that has no spectral contribution in the form of a Dirac delta function at $\underline{\mu} = (0,0)$, but may have discrete wavevector components at any other value of $\underline{\mu}$. By equations (6-155) and (6-156), the space-averaged wavevector-frequency spectrum is given by

$$\Phi_p^a(\underline{k},\omega) = V(\underline{k},\omega) \ . \tag{6-158}$$

However, it is straightforward to demonstrate (by use of equations (2-38), (6-78), and (6-121)) that the two wavevector-frequency spectrum of a stationary, homogeneous field, characterized by the autocorrelation function $Q_{pp}(\underline{\xi},\tau)$ and the wavevector-frequency spectrum $\Phi_p(\underline{k},\omega)$, is given by

$$S_{pp}(\underline{\mu},\underline{k},\omega) = (2\pi)^2\delta(\underline{\mu})\Phi_p(\underline{k},\omega) \ . \tag{6-159}$$

By comparison of equations (6-157) and (6-159), it is evident that equation (6-157) expresses the two wavevector-frequency spectrum, $S_{pp}(\underline{\mu},\underline{k},\omega)$, of a general nonhomogeneous field as a sum of homogeneous spectral components, represented by the term $(2\pi)^2\delta(\underline{\mu})V(\underline{k},\omega)$, and purely nonhomogeneous spectral components, represented by the term $W_{pp}(\underline{x}_1,\underline{\xi},\omega)$. It follows, by these arguments and equation (6-158), that the space-averaged wavevector-frequency spectrum represents the wavevector-frequency spectrum, as defined by equation (6-78), of the homogeneous constituents of a generally nonhomogeneous field.

To summarize, we have demonstrated that the space-averaged wavevector-frequency spectrum is a metric that characterizes, in the wavevector-frequency domain, the homogeneous components of a stationary, but generally nonhomogeneous, field. This metric is defined as the Fourier transform of the space-averaged autocorrelation function on the spatial separation vector $\underline{\xi}$ and on the time difference τ. The space-averaged wavevector-frequency spectrum has symmetry properties identical to those of the wavevector-frequency spectrum of a stationary, homogeneous field. However, it must be recognized that, by spatially averaging the autocorrelation function (or, alternatively, the space-varying wavevector-frequency spectrum) to obtain the space-averaged spectrum, we have lost all information regarding the nonhomogeneous components of the field. Clearly then, the space-averaged wavevector-frequency spectrum does not provide a complete characterization of

the statistics of a nonhomogeneous field. Rather, it characterizes those statistical components that are common to all absolute spatial locations: that is, the homogeneous components.

6.5.2.4 Properties of the Wavevector-Frequency Spectra of Stationary, Nonhomogeneous Fields. In the previous sections, we have explored only such properties as reality and symmetry of the various forms of wavevector-frequency spectra used to characterize the statistics of stationary, nonhomogeneous fields. In this section, we present and illustrate some additional properties of the wavevector-frequency spectra of nonhomogeneous fields that are of practical utility.

Note first, from equations (6-108) through (6-110), that

$$Q_{pp}(\underline{x}_1,\underline{0},0) = \langle p^2(\underline{x}_1)\rangle = (2\pi)^{-3} \int_{-\infty}^{\infty}\int_{-\infty}^{\infty} K_{pp}(\underline{x}_1,\underline{k},\omega)\, d\underline{k}\, d\omega \ , \qquad (6\text{-}160)$$

$$\bar{Q}_{pp}(\underline{x}_1,\underline{x}_1,0) = \langle p^2(\underline{x}_1)\rangle =$$

$$(2\pi)^{-3} \int_{-\infty}^{\infty}\int_{-\infty}^{\infty} \bar{K}_{pp}(\underline{x}_1,\underline{\beta},\omega)\exp[i(\underline{\beta}\cdot\underline{x}_1)]\, d\underline{\beta}\, d\omega \ , \qquad (6\text{-}161)$$

and

$$\tilde{Q}_{pp}(\tilde{\underline{x}},\underline{0},0) = \langle p^2(\tilde{\underline{x}})\rangle = (2\pi)^{-3} \int_{-\infty}^{\infty}\int_{-\infty}^{\infty} \tilde{K}_{pp}(\tilde{\underline{x}},\underline{k},\omega)\, d\underline{k}\, d\omega \ . \qquad (6\text{-}162)$$

Inasmuch as the space-time fields in this text are assumed to be real, the left-hand sides of equations (6-160) through (6-162) are clearly real and positive. Therefore, each of the integrals of the alternative forms of the space-varying wavevector-frequency spectrum given by equations (6-160), (6-161), and (6-162) is real and positive. It follows, by equation (6-160), that the quantity $(2\pi)^{-3}K_{pp}(\underline{x},\underline{k},\omega)d\underline{k}d\omega$ can be interpreted as the contribution to the mean square value of the pressure, $\langle p^2(\underline{x})\rangle$, at the location $\underline{x}$ from wavevectors in the range $\underline{k}$ to $\underline{k} + d\underline{k}$ and frequencies in the range

ω to $\omega + d\omega$. Similar arguments can be applied to the integrals involving alternative space-varying spectral forms (that is, to equations (6-161) and (6-162)).

By substituting equations (6-130), (6-131), or (6-132), as appropriate, into equations (6-160), (6-161), and (6-162), we can also show that the alternative forms of the two wavevector-frequency spectra have the following integral properties:

$$\langle p^2(\underline{x}_1)\rangle = (2\pi)^{-5} \int_{-\infty}^{\infty}\int_{-\infty}^{\infty}\int_{-\infty}^{\infty} S_{pp}(\underline{\mu},\underline{k},\omega)\exp[i(\underline{\mu}\cdot\underline{x}_1)]\; d\underline{\mu}\; d\underline{k}\; d\omega \;, \tag{6-163}$$

$$\langle p^2(\underline{x}_1)\rangle = (2\pi)^{-5} \int_{-\infty}^{\infty}\int_{-\infty}^{\infty}\int_{-\infty}^{\infty} \bar{S}_{pp}(\underline{\mu},\underline{\beta},\omega)\exp[i(\underline{\mu} + \underline{\beta})\cdot\underline{x}_1]\; d\underline{\mu}\; d\underline{\beta}\; d\omega \;, \tag{6-164}$$

and

$$\langle p^2(\tilde{\underline{x}})\rangle = (2\pi)^{-5} \int_{-\infty}^{\infty}\int_{-\infty}^{\infty}\int_{-\infty}^{\infty} \tilde{S}_{pp}(\underline{\alpha},\underline{k},\omega)\exp[i(\underline{\alpha}\cdot\tilde{\underline{x}})]\; d\underline{\alpha}\; d\underline{k}\; d\omega \;. \tag{6-165}$$

By equations (6-142) and (6-150), it is straightforward to show that

$$Q^a_{pp}(\underline{0},0) = \lim_{L\to\infty} \frac{1}{4L^2} \int_{-L}^{L}\int_{-L}^{L} \langle p^2(\underline{x}_1)\rangle\; dx_{11}\; dx_{12}$$

$$= (2\pi)^{-3} \int_{-\infty}^{\infty}\int_{-\infty}^{\infty} \Phi^a_p(\underline{k},\omega)\; d\underline{k}\; d\omega \;. \tag{6-166}$$

Thus, $(2\pi)^{-3}\Phi^a_p(\underline{k},\omega)d\underline{k}d\omega$ can be interpreted as the contribution to the space-averaged mean square value of the field from wavevectors in the range $\underline{k}$ to $\underline{k} + d\underline{k}$ and frequencies in the range ω to $\omega + d\omega$. The space-averaged mean

square value of a real field is, of course, real and positive. Therefore, the multiple integral of the space-averaged wavevector-frequency spectrum over all wavevectors and frequency is real and positive.

Consider the stationary, nonhomogeneous field of the form

$$p(\underline{x},t) = \langle p(\underline{x})\rangle + s(\underline{x},t) \ . \tag{6-167}$$

Here, $\langle p(\underline{x})\rangle$ is the mean of $p(\underline{x},t)$, and $s(\underline{x},t)$ is a stationary, nonhomogeneous field with zero mean. By equations (6-69) through (6-71) and equation (6-167), it is easily shown that

$$Q_{pp}(\underline{x}_1,\underline{\xi},\tau) = \langle p(\underline{x}_1)\rangle\langle p(\underline{x}_1 + \underline{\xi})\rangle + Q_{ss}(\underline{x}_1,\underline{\xi},\tau) \ , \tag{6-168}$$

$$\bar{Q}_{pp}(\underline{x}_1,\underline{x}_2,\tau) = \langle p(\underline{x}_1)\rangle\langle p(\underline{x}_2)\rangle + \bar{Q}_{ss}(\underline{x}_1,\underline{x}_2,\tau) \ , \tag{6-169}$$

and

$$\tilde{Q}_{pp}(\tilde{\underline{x}},\underline{\xi},\tau) = \langle p(\tilde{\underline{x}} - \underline{\xi}/2)\rangle\langle p(\tilde{\underline{x}} + \underline{\xi}/2)\rangle + \tilde{Q}_{ss}(\tilde{\underline{x}},\underline{\xi},\tau) \ . \tag{6-170}$$

Define

$$P(\underline{k}) = \int_{-\infty}^{\infty} \langle p(\underline{x})\rangle \exp[-i(\underline{k}\cdot\underline{x})]\, d\underline{x} \ . \tag{6-171}$$

Then it is straightforward to show, from equations (6-105) through (6-107), that

$$K_{pp}(\underline{x}_1,\underline{k},\omega) = 2\pi\langle p(\underline{x}_1)\rangle P(\underline{k})\delta(\omega)\exp(i\underline{k}\cdot\underline{x}_1) + K_{ss}(\underline{x}_1,\underline{k},\omega) \ , \tag{6-172}$$

$$\bar{K}_{pp}(\underline{x}_1,\underline{\beta},\omega) = 2\pi\langle p(\underline{x}_1)\rangle P(\underline{\beta})\delta(\omega) + \bar{K}_{ss}(\underline{x}_1,\underline{\beta},\omega) \ , \tag{6-173}$$

and

$$\tilde{K}_{pp}(\tilde{\underline{x}},\underline{k},\omega) = \frac{2\delta(\omega)}{\pi} \int_{-\infty}^{\infty} P(\underline{\varepsilon} - \underline{k})P(\underline{\varepsilon} + \underline{k})\exp(i2\underline{\varepsilon}\cdot\tilde{\underline{x}})\, d\underline{\varepsilon} + \tilde{K}_{ss}(\tilde{\underline{x}},\underline{k},\omega) \ . \tag{6-174}$$

By use of equations (6-127), (6-128), and (6-129), it follows that the alternative forms of the two wavevector-frequency spectra of this field are given by

$$S_{pp}(\underline{\mu},\underline{k},\omega) = 2\pi P(\underline{k})P(\underline{\mu} - \underline{k})\delta(\omega) + S_{ss}(\underline{\mu},\underline{k},\omega) \ , \tag{6-175}$$

$$\bar{S}_{pp}(\underline{\mu},\underline{\beta},\omega) = 2\pi P(\underline{\mu})P(\underline{\beta})\delta(\omega) + \bar{S}_{ss}(\underline{\mu},\underline{\beta},\omega) \ , \tag{6-176}$$

and

$$\tilde{S}_{pp}(\underline{\alpha},\underline{k},\omega) = 2\pi P(\underline{\alpha}/2 - \underline{k})P(\underline{\alpha}/2 + \underline{k})\delta(\omega) + \tilde{S}_{ss}(\underline{\alpha},\underline{k},\omega) \ . \tag{6-177}$$

Note, by equations (6-172) through (6-177), that both the space-varying and two wavevector forms of the wavevector-frequency spectra of a stationary, nonhomogeneous field with nonzero mean are characterized, in a fashion similar to the wavevector-frequency spectrum of a stationary, homogeneous field, by the sum of two spectra. One spectrum is characterized by a Dirac delta function at $\omega = 0$ that is weighted by a quantity related to the mean value of the field. The second spectrum has no singular spectral contribution at $\omega = 0$, and characterizes the statistics of the zero-mean component of the field. Note, by equations (6-172) through (6-177), that the mean value of the field cannot be deduced from the singular spectral contribution at $\omega = 0$. Therefore, as we found in the case of a stationary, homogeneous field, separate knowledge of both the mean value and autocorrelation function, or some form of the wavevector-frequency spectrum, is necessary for a complete specification of the first and second order statistics of a stationary, nonhomogeneous field.

By equations (6-153) and (6-172), the space-averaged wavevector-frequency spectrum of the nonzero mean field specified by equation (6-167) is expressed by

$$\Phi_p^a(\underline{k},\omega) = \lim_{L\to\infty} \frac{1}{4L^2} \int_{-L}^{L}\int_{-L}^{L} \left(2\pi\langle p(\underline{x}_1)\rangle P(\underline{k})\delta(\omega)\exp(i\underline{k}\cdot\underline{x}_1)\right.$$

$$\left. + K_{ss}(\underline{x}_1,\underline{k},\omega)\right) dx_{11}\, dx_{12} \ . \tag{6-178}$$

The integral of the second term in the integrand can be recognized, by equation (6-153), as the space-averaged spectrum of the zero-mean component, $s(\underline{x},t)$, of the field. That is,

$$\Phi_s^a(\underline{k},\omega) = \lim_{L\to\infty} \frac{1}{4L^2} \int_{-L}^{L}\int_{-L}^{L} K_{ss}(\underline{x}_1,\underline{k},\omega)\, dx_{11}\, dx_{12} \ . \tag{6-179}$$

By use of the Fourier inverse of equation (6-171), we can show that

$$\lim_{L\to\infty} \frac{1}{4L^2} \int_{-L}^{L}\int_{-L}^{L} \langle p(\underline{x}_1)\rangle \exp(i\underline{k}\cdot\underline{x}_1)\, dx_{11}\, dx_{12}$$

$$= \lim_{L\to\infty} \frac{1}{(2\pi)^2} \int_{-\infty}^{\infty} P(\underline{\mu}) \left\{\frac{\sin(\mu_1 + k_1)L}{(\mu_1 + k_1)L}\right\} \left\{\frac{\sin(\mu_2 + k_2)L}{(\mu_2 + k_2)L}\right\} d\underline{\mu} \; . \qquad (6\text{-}180)$$

By arguments similar to those presented following equation (6-155), the integral shown by equation (6-180) is zero unless $P(\underline{\mu})$ is comprised of terms of the form $G(\underline{\alpha})\delta(\underline{\mu} - \underline{\alpha})$, where $\underline{\alpha}$ is some fixed wavevector. However, inasmuch as $\langle p(\underline{x})\rangle$ is real, it is evident (see equation (6-171)) that $P(\underline{\mu})$ must equal $P^*(-\underline{\mu})$. Therefore, a more precise statement of the requisite form of $P(\underline{\mu})$ is given by

$$P(\underline{\mu}) = \sum_{n=1}^{N} \{G(\underline{k}_n)\delta(\underline{\mu} - \underline{k}_n) + G^*(\underline{k}_n)\delta(\underline{\mu} + \underline{k}_n)\} \; . \qquad (6\text{-}181)$$

where $\underline{k}_n$ specifies the wavevector associated with the n-th pair of delta functions, and N denotes the number of pairs of delta functions contributing to $P(\underline{\mu})$.

For purposes of illustration, consider the case where $P(\underline{\mu})$ consists of a single pair of delta functions. That is,

$$P(\underline{\mu}) = G(\underline{\alpha})\delta(\underline{\mu} - \underline{\alpha}) + G^*(\underline{\alpha})\delta(\underline{\mu} + \underline{\alpha}) \; . \qquad (6\text{-}182)$$

By the Fourier inverse of equation (6-171), this form of $P(\underline{\mu})$ corresponds to a mean component that varies sinusoidally in space. The amplitude and initial phase of the mean are determined by $G(\underline{\alpha})$, and the spatial periods in the x_1 and x_2 coordinate directions are dictated by the wavenumbers α_1 and α_2, respectively.

With $P(\underline{\mu})$ given by the form of equation (6-182), we can show, by use of equations (6-156), (6-178), (6-179), and (6-180), that if neither α_1 or α_2

equals zero, the space-averaged wavevector-frequency spectrum has the form

$$\Phi^a_{pp}(\underline{k},\omega) = \frac{\delta(\omega)|G(\underline{\alpha})|^2}{2\pi} \{\delta(\underline{k} - \underline{\alpha}) + \delta(\underline{k} + \underline{\alpha})\} + \Phi^a_{ss}(\underline{k},\omega) \ . \tag{6-183}$$

If either α_1 or α_2 is zero, the constant multiplying the first term on the right-hand side of equation (6-183) is modified. The determination of this modification is left as an exercise for the reader.

If $P(\underline{\mu})$ has the form of equation (6-182), it follows from equation (6-175) that the two wavevector-frequency spectrum has the form

$$\begin{aligned} S_{pp}(\underline{\mu},\underline{k},\omega) = 2\pi\delta(\omega)\{&|G(\underline{\alpha})|^2\delta(\underline{\mu})[\delta(\underline{k} - \underline{\alpha}) + \delta(\underline{k} + \underline{\alpha})] \\ &+ G^2(\underline{\alpha})\delta(\underline{\mu} - 2\underline{\alpha})\delta(\underline{k} - \underline{\alpha}) + G^{*2}(\underline{\alpha})\delta(\underline{\mu} + 2\underline{\alpha})\delta(\underline{k} + \underline{\alpha})\} \\ &+ S_{ss}(\underline{\mu},\underline{k},\omega) \ . \end{aligned} \tag{6-184}$$

Note that the first term on the right-hand side of this equation has the functional form $\delta(\underline{\mu})V(\underline{k},\omega)$, which was shown in section 6.5.2.3 to characterize a homogeneous field. Thus, this term reflects, in the two wavevector-frequency domain, the presence of a component in the autocorrelation function of the mean field that is independent of the absolute spatial coordinate, $\underline{x}_1$. It is straightforward to show, by equation (6-155), that it is only this absolute space-independent component of the autocorrelation function of the mean field that contributes to the space-averaged wavevector-frequency spectrum given by equation (6-183).

It is straightforward, but tedious, to demonstrate that the more general form for $P(\underline{\mu})$ given by equation (6-181) produces (1) a space-averaged wavevector-frequency spectrum in which the contribution from the mean component of the field consists of a summation of N terms of the form

$$\frac{\delta(\omega)|G(\underline{k}_n)|^2}{2\pi} \{\delta(\underline{k} - \underline{k}_n) + \delta(\underline{k} + \underline{k}_n)\}$$

and (2) a two wavevector-frequency spectrum containing the sum of N contributions of the form

$$2\pi\delta(\omega)\{|G(\underline{k}_n)|^2\delta(\underline{\mu})[\delta(\underline{k} - \underline{k}_n) + \delta(\underline{k} + \underline{k}_n)]$$

from the mean component of the field. By arguments similar to those applied above, it is evident that, even for this more complex form of $P(\underline{\mu})$, the space-averaged wavevector-frequency spectrum reflects only those contributions to the autocorrelation function of the mean component of the field that are independent of the absolute spatial variable, $\underline{x}_1$.

By equation (6-180) and the subsequent arguments, we must conclude that, if $P(\underline{\mu})$ does not have the form of equation (6-181), then

$$\Phi^a_{pp}(\underline{k},\omega) = \Phi^a_{ss}(\underline{k},\omega) \tag{6-185}$$

As a specific example of a stationary, nonhomogeneous field, consider the field in one spatial dimension given by

$$p(x,t) = \exp(-a|x|)\sin(k_0x + \omega_0t + \theta). \tag{6-186}$$

This field will be recognized as a wave, characterized by the wavenumber k_0 and frequency ω_0, that decays exponentially in amplitude with distance from the origin of space. The rate of decay of the amplitude is dictated by the positive constant a. The initial phase, θ, is assumed to be a random variable that is equally probable between $-\pi$ and π. That is, the probability density of θ is given by

$$f_\theta(\alpha) = \begin{cases} 1/(2\pi), & -\pi \leq \alpha \leq \pi \;, \\ 0, & \text{otherwise}. \end{cases} \tag{6-187}$$

Thus, we recognize $p(x,t) = p(x,t;\theta)$ to be a function of the random variable θ. Therefore, by equations (6-11) and (6-69), the mean and one form of the autocorrelation function of this field can be demonstrated to be given by

$$\langle p(x,t)\rangle = E\{p(x,t)\} = 0 \tag{6-188}$$

and

$$Q_{pp}(x_1,\xi,\tau) = \frac{\exp(-a|x_1|)\exp(-a|x_1 + \xi|)}{2} \cos(k_0\xi + \omega_0\tau) , \quad (6\text{-}189)$$

respectively. Thus, the field has zero mean and is clearly nonhomogeneous inasmuch as the autocorrelation function depends on the absolute spatial location, x_1.

By equations (6-105) and (6-189), we can show the associated form of the space-varying wavevector-frequency spectrum to be given by

$$K_{pp}(x_1,k,\omega) = a\pi \exp(-a|x_1|)\left\{\frac{\exp[i(k - k_0)x_1]}{a^2 + (k - k_0)^2} \delta(\omega - \omega_0) + \frac{\exp[i(k + k_0)x_1]}{a^2 + (k + k_0)^2} \delta(\omega + \omega_0)\right\} . \quad (6\text{-}190)$$

Here, we see that the space-varying wavenumber-frequency spectrum of the exponentially decaying wave field is a complex function characterized by discrete frequency components at $\pm\omega_0$. The weighting of these discrete components is seen to be a complex function of both k and x_1. At the frequency ω_0, the magnitude of the weighting function, at any fixed value of x_1, is a maximum at the wavenumber $k = k_0$, and decreases with the square of $k - k_0$ at wavenumbers well removed from k_0. The phases of the various wavenumber contributions to the spectrum at $\omega = \omega_0$ are seen to be equal to $(k - k_0)x_1$. At $\omega = -\omega_0$, the magnitude of the weighting function is a maximum at $k = -k_0$, and the phases of the wavenumber contributions to the spectrum are given by $(k + k_0)x_1$.

By equations (6-127) and (6-190), it can be shown that the two wavevector-frequency spectrum of the field described by equation (6-186) is given by

$$S_{pp}(\mu,k,\omega) = 2\pi a^2 \left\{\frac{\delta(\omega - \omega_0)}{[a^2 + (k - k_0)^2][a^2 + (\mu - k + k_0)^2]} + \frac{\delta(\omega + \omega_0)}{[a^2 + (k + k_0)^2][a^2 + (\mu - k - k_0)^2]}\right\} . \quad (6\text{-}191)$$

By inspection, the two wavenumber-frequency spectrum is real and, like the space-varying spectrum, is characterized by discrete spectral components at the frequencies $\pm\omega_0$. These discrete components are weighted by functions of μ and k. Indeed, if we define the weighting function

$$W(\mu,k) = \frac{2\pi a^2}{[a^2 + (k - k_0)^2][a^2 + (\mu - k + k_0)^2]} , \tag{6-192}$$

we can write equation (6-191) in the form

$$S_{pp}(\mu,k,\omega) = W(\mu,k)\delta(\omega - \omega_0) + W(-\mu,-k)\delta(\omega + \omega_0) . \tag{6-193}$$

By inspection of equation (6-192), it is evident that $W(\mu,k)$ has relative maxima along the lines $k = k_0$ and $k - \mu = k_0$ and an absolute maximum at the intersection of these lines: that is, at $(\mu,k) = (0,k_0)$. The amplitude and bandwidth of this maximum are inversely proportional to a, the constant that specifies the rate of decay of the amplitude of the wave with distance from the spatial origin. Figure 6-7 illustrates the functional behavior of $W(\mu,k)$.

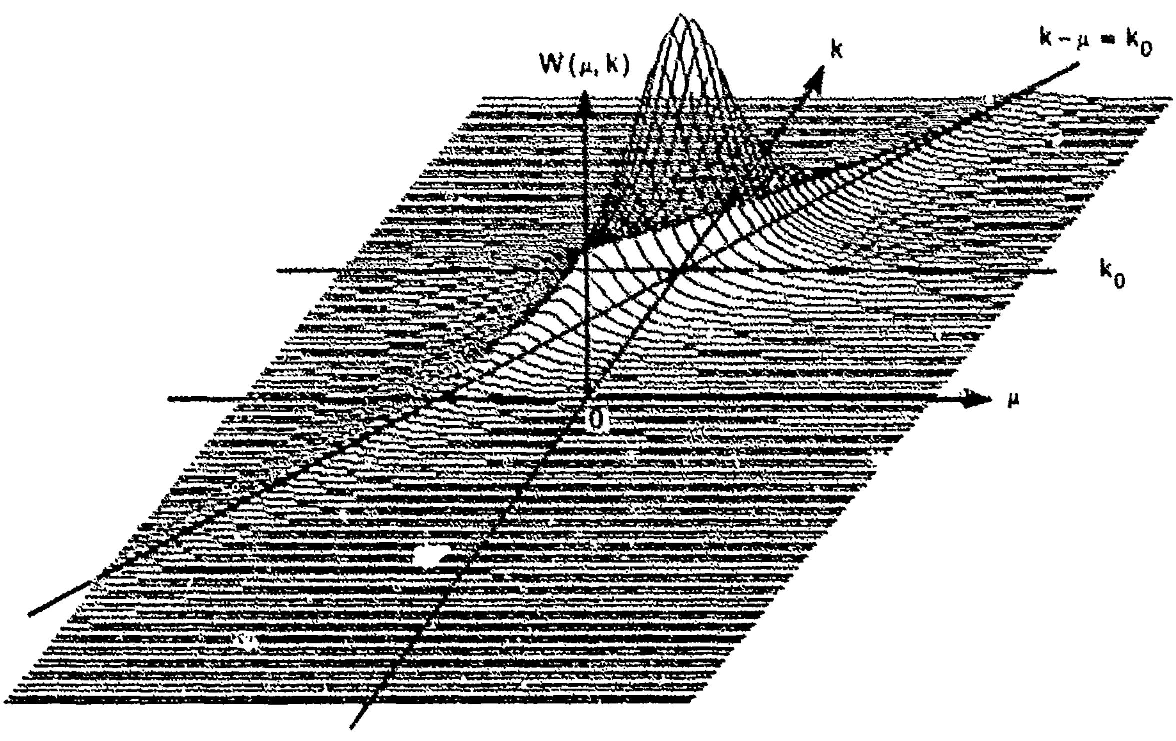

Figure 6-7. Illustration of the Functional Behavior of $W(\mu,k)$

Note that we have presented only one of the alternative forms for the autocorrelation function, the space-varying wavenumber-frequency spectrum, and the two wavenumber-frequency spectrum for this illustrative example. Development of the other forms of these descriptors is left as an exercise for the reader.

For positive and nonzero values of a, the space-averaged wavenumber-frequency spectrum of the exponentially decaying wave field described by equation (6-186) is equal to zero inasmuch as the two wavenumber-frequency spectrum (equation (6-191)) does not contain a term of the form $\delta(\mu)$. Note however, from equation (6-186), that if $a = 0$, the wave field becomes stationary, and the space-averaged spectrum will be nonzero.

6.6 RELATIONSHIP BETWEEN THE WAVEVECTOR-FREQUENCY SPECTRUM AND THE FREQUENCY SPECTRAL DENSITY

The frequency spectral density (or frequency spectrum) is a commonly used descriptor of the statistics of fields that vary only with time. In this section, we will define the frequency spectral density and show how it is related to the various forms of the wavevector-frequency spectrum. Here, as throughout this text, we will restrict our attention to fields that are statistically stationary.

Let $p(t)$ be a time field known to be real and stationary. The autocorrelation of this field, $Q_{pp}(\tau)$, is defined as

$$Q_{pp}(\tau) \equiv E[p(t)p(t + \tau)] \ . \qquad (6\text{-}194)$$

The frequency spectral density, $\phi_p(\omega)$, is defined[21] as the Fourier transform of the autocorrelation function on the time difference, τ. That is,

$$\phi_p(\omega) \equiv \int_{-\infty}^{\infty} Q_{pp}(\tau)\exp(-i\omega\tau)\, d\tau \ . \qquad (6\text{-}195)$$

It is easily shown, by equation (6-194) and the reality of p(t), that

$$Q_{pp}(\tau) = Q_{pp}(-\tau) = Q^{*}_{pp}(\tau) \ . \tag{6-196}$$

It therefore follows, from equation (6-195), that

$$\phi_p(\omega) = \phi_p(-\omega) = \phi^{*}_p(-\omega) \ . \tag{6-197}$$

Therefore, the frequency spectral density is a real and even function of ω.

The Fourier inverse relationship to equation (6-195) is

$$Q_{pp}(\tau) = \frac{1}{2\pi} \int_{-\infty}^{\infty} \phi_p(\omega)\exp(i\omega\tau)\, d\omega \ . \tag{6-198}$$

It therefore follows that

$$\langle p^2 \rangle = E[p^2(t)] = \frac{1}{2\pi} \int_{-\infty}^{\infty} \phi_p(\omega)\, d\omega \ . \tag{6-199}$$

Consider now a space-time field, $p(\underline{x},t)$, that is known to be real and stationary. If the field is homogeneous, we showed previously that the autocorrelation, $Q_{pp}(\underline{\xi},\tau)$, is a real function of both the spatial separation vector, $\underline{\xi}$, and the time difference, τ. However, if $\underline{\xi}$ is fixed at (0,0), $Q_{pp}(\underline{0},\tau)$ is a function only of τ, as required by equation (6-195). Thus, if we substitute $Q_{pp}(\underline{0},\tau)$ for $Q_{pp}(\tau)$ in equation (6-195), it follows that the frequency spectral density is related to the autocorrelation function of a stationary, homogeneous field by

$$\phi_p(\omega) = \int_{-\infty}^{\infty} Q_{pp}(\underline{0},\tau)\exp(-i\omega\tau)\, d\tau \ . \tag{6-200}$$

However, by equation (6-79),

$$Q_{pp}(\underline{0},\tau) = \frac{1}{(2\pi)^3} \int_{-\infty}^{\infty} \int_{-\infty}^{\infty} \Phi_p(\underline{k},\omega)\exp(i\omega\tau)\, d\underline{k}\, d\omega \ . \qquad (6\text{-}201)$$

Therefore, the frequency spectral density is related to the homogeneous form of the wavevector-frequency spectrum by

$$\phi_p(\omega) = \frac{1}{(2\pi)^2} \int_{-\infty}^{\infty} \Phi_p(\underline{k},\omega)\, d\underline{k} \ . \qquad (6\text{-}202)$$

Clearly, by equations (6-201) and (6-202),

$$\langle p^2\rangle = Q_{pp}(\underline{0},0) = \frac{1}{(2\pi)^3} \int_{-\infty}^{\infty} \int_{-\infty}^{\infty} \Phi_p(\underline{k},\omega)\, d\underline{k}\, d\omega = \frac{1}{2\pi} \int_{-\infty}^{\infty} \phi_p(\omega)\, d\omega \ , \qquad (6\text{-}203)$$

in agreement with equation (6-199).

The autocorrelation function, $Q_{pp}(\underline{x},\underline{\xi},\tau)$, of a stationary, nonhomogeneous field is a function of the absolute spatial vector $\underline{x}$, the spatial separation vector $\underline{\xi}$, and the time difference τ. However, for any fixed value of $\underline{x}$, say $\underline{x}_1$, and for $\underline{\xi}$ fixed at (0,0), the autocorrelation function $Q_{pp}(\underline{x}_1,\underline{0},\tau)$ is a function only of τ. By substituting $Q_{pp}(\underline{x}_1,\underline{0},\tau)$ for $Q_{pp}(\tau)$ in equation (6-195), we can show that the frequency spectral density of the field at the spatial location $\underline{x}_1$, which we denote by $\phi_p(\underline{x}_1,\omega)$, is related to the autocorrelation function of a stationary, nonhomogeneous field at the same absolute spatial location by

$$\phi_p(\underline{x}_1,\omega) = \int_{-\infty}^{\infty} Q_{pp}(\underline{x}_1,\underline{0},\tau)\exp(-i\omega\tau)\, d\tau \ . \qquad (6\text{-}204)$$

However, by writing $Q_{pp}(\underline{x}_1,\underline{0},\tau)$ in the form of equation (6-108) and by

performing some simple integrals, we can relate the frequency spectral density at $\underline{x}_1$ to the space-varying wavevector-frequency spectrum at $\underline{x}_1$ by

$$\phi_p(\underline{x}_1,\omega) = \frac{1}{(2\pi)^2} \int_{-\infty}^{\infty} K_{pp}(\underline{x}_1,\underline{k},\omega)\, d\underline{k} \ . \tag{6-205}$$

Alternatively, by writing $Q_{pp}(\underline{x}_1,\underline{0},\tau)$ in the form of equation (6-124), we can show that the frequency spectral density at $\underline{x}_1$ is related to the two wavevector-frequency spectrum of the nonhomogeneous field by

$$\phi_p(\underline{x}_1,\omega) = \frac{1}{(2\pi)^4} \int_{-\infty}^{\infty} \int_{-\infty}^{\infty} S_{pp}(\underline{\mu},\underline{k},\omega)\exp[i\underline{\mu}\cdot\underline{x}_1]\, d\underline{\mu}\, d\underline{k} \ . \tag{6-206}$$

Note, by equation (6-160), that

$$<p^2(\underline{x}_1)> = (2\pi)^{-3} \int_{-\infty}^{\infty} \int_{-\infty}^{\infty} K_{pp}(\underline{x}_1,\underline{k},\omega)\, d\underline{k}\, d\omega \ . \tag{6-207}$$

It follows, by equation (6-205), that

$$<p^2(\underline{x}_1)> = \frac{1}{2\pi} \int_{-\infty}^{\infty} \phi_p(\underline{x}_1,\omega)\, d\omega \ . \tag{6-208}$$

This same result can be obtained from equations (6-163) and (6-206).

Although we will not do so here, it is a simple matter to utilize equation (6-204) to develop relationships between the frequency spectral density and the alternative forms of the space-varying wavevector-frequency spectrum and two wavevector-frequency spectrum.

As a final note, some texts on signal processing define the frequency spectral density in terms of the temporal frequency, f, rather than the

performing some simple integrals, we can relate the frequency spectral density at $\underline{x}_1$ to the space-varying wavevector-frequency spectrum at $\underline{x}_1$ by

$$\phi_p(\underline{x}_1,\omega) = \frac{1}{(2\pi)^2} \int_{-\infty}^{\infty} K_{pp}(\underline{x}_1,\underline{k},\omega)\, d\underline{k} \ . \tag{6-205}$$

Alternatively, by writing $Q_{pp}(\underline{x}_1,\underline{0},\tau)$ in the form of equation (6-124), we can show that the frequency spectral density at $\underline{x}_1$ is related to the two wavevector-frequency spectrum of the nonhomogeneous field by

$$\phi_p(\underline{x}_1,\omega) = \frac{1}{(2\pi)^4} \int_{-\infty}^{\infty} \int_{-\infty}^{\infty} S_{pp}(\underline{\mu},\underline{k},\omega)\exp[i\underline{\mu}\cdot\underline{x}_1]\, d\underline{\mu}\, d\underline{k} \ . \tag{6-206}$$

Note, by equation (6-160), that

$$\langle p^2(\underline{x}_1)\rangle = (2\pi)^{-3} \int_{-\infty}^{\infty} \int_{-\infty}^{\infty} K_{pp}(\underline{x}_1,\underline{k},\omega)\, d\underline{k}\, d\omega \ . \tag{6-207}$$

It follows, by equation (6-205), that

$$\langle p^2(\underline{x}_1)\rangle = \frac{1}{2\pi} \int_{-\infty}^{\infty} \phi_p(\underline{x}_1,\omega)\, d\omega \ . \tag{6-208}$$

This same result can be obtained from equations (6-163) and (6-206).

Although we will not do so here, it is a simple matter to utilize equation (6-204) to develop relationships between the frequency spectral density and the alternative forms of the space-varying wavevector-frequency spectrum and two wavevector-frequency spectrum.

As a final note, some texts on signal processing define the frequency spectral density in terms of the temporal frequency, f, rather than the

circular frequency, ω. For example, Davenport and Root[22] define the frequency spectral density, $\tilde{\phi}_p(f)$, to be the following Fourier transform of the autocorrelation function, $Q_{pp}(\tau)$, of a stationary field:

$$\tilde{\phi}_p(f) \equiv \int_{-\infty}^{\infty} Q_{pp}(\tau)\exp(-i2\pi f\tau)\, d\tau \ . \qquad (6\text{-}209)$$

The inverse transform is given by

$$Q_{pp}(\tau) = \int_{-\infty}^{\infty} \tilde{\phi}_p(f)\exp(i2\pi f\tau)\, df \ . \qquad (6\text{-}210)$$

Recall, by equation (2-7), that the temporal and circular frequencies are related by

$$f = \omega/(2\pi) \ . \qquad (6\text{-}211)$$

It therefore follows, from equations (6-195) and (6-209), that

$$\tilde{\phi}_p(f) = \phi_p(2\pi f) \qquad (6\text{-}212)$$

or, alternatively,

$$\phi_p(\omega) = \tilde{\phi}_p\left(\frac{\omega}{2\pi}\right) \ . \qquad (6\text{-}213)$$

By use of equations (209) and (210), one can parallel the arguments presented previously to obtain relationships between $\tilde{\phi}_p(f)$ and $\Phi_p(\underline{k},\omega)$ or, if appropriate, $\tilde{\phi}_p(\underline{x}_1,f)$ and $K_{pp}(\underline{x}_1,\underline{k},\omega)$ or $S_{pp}(\underline{\mu},\underline{k},\omega)$.

6.7 SUMMARY OF THE WAVEVECTOR-FREQUENCY CHARACTERIZATION OF RANDOM SPACE-TIME FIELDS

Recall that, for the purposes of this text, random space-time fields are characterized in the space-time domain by the mean and autocorrelation functions of the field. By appropriate Fourier transformations of these

space-time statistics, we can define metrics in the wavevector-frequency domain that are informationally equivalent to the mean and autocorrelation functions. The multidimensional Fourier transforms of the autocorrelation functions are generically called wavevector-frequency spectra.

For stationary, homogeneous fields, the wavevector-frequency spectrum, $\Phi_p(\underline{k},\omega)$, is defined as the multiple Fourier transform of the autocorrelation function, $Q_{pp}(\underline{\xi},\tau)$, on the spatial separation vector, $\underline{\xi}$, and the time difference, τ. That is,

$$\Phi_p(\underline{k},\omega) = \int_{-\infty}^{\infty} \int_{-\infty}^{\infty} Q_{pp}(\underline{\xi},\tau)\exp[-i(\underline{k}\cdot\underline{\xi} + \omega\tau)]\, d\underline{\xi}\, d\tau \ . \qquad (6\text{-}214)$$

By use of the symmetry properties of the autocorrelation function, the wavevector-frequency spectrum of a stationary, homogeneous field can be shown to be real and have the symmetry property $\Phi_p(\underline{k},\omega) = \Phi_p(-\underline{k},-\omega)$. For purposes of this text, knowledge of the mean and the wavevector-frequency spectrum yields sufficient information to characterize the statistics of a stationary, homogeneous field.

The autocorrelation of a stationary, nonhomogeneous field is a function of the absolute spatial variable $\underline{x}_1$ as well as the spatial separation vector, $\underline{\xi}$, and the time difference, τ. The presence of this additional variable permits some flexibility in the definition of the wavevector-frequency spectrum. Moreover, the existence of alternative functional forms for the autocorrelation function of a nonhomogeneous field implies the existence of alternative functional forms for the wavevector-frequency spectra.

The space-varying wavevector-frequency spectrum is defined as the multiple Fourier transform of the autocorrelation function on all variables except that variable designating the absolute spatial location. This definition results in three alternative functional forms for the space-varying spectrum: that is, one corresponding to each of the three alternative functional forms of the autocorrelation function listed in equations (6-69) through (6-71). These are

$$K_{pp}(\underline{x}_1,\underline{k},\omega) = \int_{-\infty}^{\infty}\int_{-\infty}^{\infty} Q_{pp}(\underline{x}_1,\underline{\xi},\tau)\exp[-i(\underline{k}\cdot\underline{\xi} + \omega\tau)]\ d\underline{\xi}\ d\tau\ , \qquad (6\text{-}215)$$

$$\bar{K}_{pp}(\underline{x}_1,\underline{\beta},\omega) = \int_{-\infty}^{\infty}\int_{-\infty}^{\infty} \bar{Q}_{pp}(\underline{x}_1,\underline{x}_2,\tau)\exp[-i(\underline{\beta}\cdot\underline{x}_2 + \omega\tau)]\ d\underline{x}_2\ d\tau\ , \qquad (6\text{-}216)$$

and

$$\tilde{K}_{pp}(\tilde{\underline{x}},\underline{k},\omega) = \int_{-\infty}^{\infty}\int_{-\infty}^{\infty} \tilde{Q}_{pp}(\tilde{\underline{x}},\underline{\xi},\tau)\exp[-i(\underline{k}\cdot\underline{\xi} + \omega\tau)]\ d\underline{\xi}\ d\tau\ . \qquad (6\text{-}217)$$

By the symmetry properties of the alternative forms of the autocorrelation functions, it can be shown that $\tilde{K}_{pp}(\tilde{\underline{x}},\underline{k},\omega)$ is real; the other forms of the space-varying wavevector-frequency spectra are, in general, complex. The space-varying wavevector-frequency spectra have the following symmetry properties:

$$K_{pp}(\underline{x}_1,\underline{k},\omega) = K^*_{pp}(\underline{x}_1,-\underline{k},-\omega)\ , \qquad (6\text{-}218)$$

$$\bar{K}_{pp}(\underline{x}_1,\underline{\beta},\omega) = \bar{K}^*_{pp}(\underline{x}_1,-\underline{\beta},-\omega)\ , \qquad (6\text{-}219)$$

$$\tilde{K}_{pp}(\tilde{\underline{x}},\underline{k},\omega) = \tilde{K}_{pp}(\tilde{\underline{x}},-\underline{k},-\omega)\ . \qquad (6\text{-}220)$$

The two wavevector-frequency spectrum is defined as the multiple Fourier transform of the nonhomogeneous autocorrelation function on all spatial and temporal variables. Thus, associated with the three alternative forms of the autocorrelation function for nonhomogeneous fields, we obtain the following three alternative forms of the two wavevector-frequency spectrum:

$$S_{pp}(\underline{\mu},\underline{k},\omega) = \int_{-\infty}^{\infty}\int_{-\infty}^{\infty}\int_{-\infty}^{\infty} Q_{pp}(\underline{x}_1,\underline{\xi},\tau)\exp[-i(\underline{\mu}\cdot\underline{x}_1 + \underline{k}\cdot\underline{\xi} + \omega\tau)]\ d\underline{x}_1\ d\underline{\xi}\ d\tau\ , \qquad (6\text{-}221)$$

$$\bar{S}_{pp}(\underline{\mu},\underline{\beta},\omega) = \int_{-\infty}^{\infty}\int_{-\infty}^{\infty}\int_{-\infty}^{\infty} \bar{Q}_{pp}(\underline{x}_1,\underline{x}_2,\tau)\exp[-i(\underline{\mu}\cdot\underline{x}_1 + \underline{\beta}\cdot\underline{x}_2 + \omega\tau)]\, d\underline{x}_1\, d\underline{x}_2\, d\tau\ , \tag{6-222}$$

and

$$\tilde{S}_{pp}(\underline{\alpha},\underline{k},\omega) = \int_{-\infty}^{\infty}\int_{-\infty}^{\infty}\int_{-\infty}^{\infty} \tilde{Q}_{pp}(\tilde{\underline{x}},\underline{\xi},\tau)\exp[-i(\underline{\alpha}\cdot\tilde{\underline{x}} + \underline{k}\cdot\underline{\xi} + \omega\tau)]\, d\tilde{\underline{x}}\, d\underline{\xi}\, d\tau\ . \tag{6-223}$$

All forms of the two wavevector-frequency spectrum are, in general, complex. Owing to the reality of all forms of the autocorrelation functions, all forms of the two wavevector-frequency spectrum have conjugate symmetry. That is,

$$S_{pp}(\underline{\mu},\underline{k},\omega) = S^*_{pp}(-\underline{\mu},-\underline{k},-\omega)\ , \tag{6-224}$$

$$\bar{S}_{pp}(\underline{\mu},\underline{\beta},\omega) = \bar{S}^*_{pp}(-\underline{\mu},-\underline{\beta},-\omega)\ , \tag{6-225}$$

and

$$\tilde{S}_{pp}(\underline{\alpha},\underline{k},\omega) = \tilde{S}^*_{pp}(-\underline{\alpha},-\underline{k},-\omega)\ . \tag{6-226}$$

Further, from the symmetries of the alternative forms of the autocorrelation functions, the following symmetry properties can be established:

$$S_{pp}(\underline{\mu},\underline{k},\omega) = S_{pp}(\underline{\mu},\underline{\mu} - \underline{k},-\omega)\ , \tag{6-227}$$

$$\bar{S}_{pp}(\underline{\mu},\underline{\beta},\omega) = \bar{S}_{pp}(\underline{\beta},\underline{\mu},-\omega)\ , \tag{6-228}$$

and

$$\tilde{S}_{pp}(\underline{\alpha},\underline{k},\omega) = \tilde{S}_{pp}(\underline{\alpha},-\underline{k},-\omega)\ . \tag{6-229}$$

Finally, the alternative forms of the two wavevector-frequency spectra can be shown to be related by

$$S_{pp}(\underline{\mu},\underline{k},\omega) = \bar{S}_{pp}(\underline{\mu} - \underline{k},\underline{k},\omega) = \tilde{S}_{pp}(\underline{\mu},\underline{k} - \underline{\mu}/2,\omega)\ . \tag{6-230}$$

The space-averaged wavevector-frequency spectrum is defined as the Fourier

transform of the space-averaged autocorrelation function on the spatial separation vector, $\underline{\xi}$, and the time difference, τ. That is,

$$\Phi_p^a(\underline{k},\omega) \equiv \int_{-\infty}^{\infty}\int_{-\infty}^{\infty} Q_{pp}^a(\underline{x}_1,\underline{\xi},\tau)\exp[-i(\underline{k}\cdot\underline{\xi} + \omega\tau)]\, d\underline{\xi}\, d\tau \; , \tag{6-231}$$

where the space-averaged autocorrelation function, $Q_{pp}^a(\underline{k},\omega)$, is defined by

$$Q_{pp}^a(\underline{k},\omega) \equiv \lim_{L\to\infty} \frac{1}{4L^2} \int_{-L}^{L}\int_{-L}^{L} Q_{pp}(\underline{x}_1,\underline{\xi},\tau)\, dx_{11}\, dx_{12} \; . \tag{6-232}$$

The space-averaged spectrum is real and has symmetry properties identical to the wavevector-frequency spectrum of a stationary, homogeneous field. Through the space-averaging process, this spectrum characterizes the statistics of those components of a generally nonhomogeneous field that are independent of absolute spatial position (that is, independent of $\underline{x}_1$). Thus, whereas the space-varying and two wavevector forms of the wavevector-frequency spectrum are informationally equivalent to the autocorrelation function of a random space-time field, the space-averaged spectrum preserves only those statistics that are independent of absolute spatial location within the field.

The frequency spectral density of a stationary time field is defined by

$$\Phi_p(\omega) \equiv \int_{-\infty}^{\infty} Q_{pp}(\tau)\exp(-i\omega\tau)\, d\tau \; , \tag{6-233}$$

where $Q_{pp}(\tau)$ denotes the autocorrelation function of the temporal field. By recognizing that the autocorrelation field of a stationary, homogeneous space-time field is a function only of time when the spatial separation vector, $\underline{\xi}$, is set to zero, it can be shown that the frequency spectral density is related to the wavevector-frequency spectrum, $\Phi_p(\underline{k},\omega)$, of such a field by

$$\phi_p(\omega) = \frac{1}{(2\pi)^2} \int_{-\infty}^{\infty} \Phi_p(\underline{k},\omega)\, d\underline{k} \ . \tag{6-234}$$

Similarly, for any fixed absolute spatial vector location, $\underline{x}_1$, and a zero spatial separation vector, $\underline{\xi}$, the autocorrelation function of a stationary, nonhomogeneous field is a function only of the time difference, τ. It can thus be shown that the frequency spectral density, $\phi_p(\underline{x}_1,\omega)$, of the field at the absolute spatial location $\underline{x}_1$ is related to the space-varying and two wavevector forms of the wavevector-frequency spectrum by

$$\phi_p(\underline{x}_1,\omega) = \frac{1}{(2\pi)^2} \int_{-\infty}^{\infty} K_{pp}(\underline{x}_1,\underline{k},\omega)\, d\underline{k} \tag{6-235}$$

and

$$\phi_p(\underline{x}_1,\omega) = \frac{1}{(2\pi)^4} \int_{-\infty}^{\infty} \int_{-\infty}^{\infty} S_{pp}(\underline{\mu},\underline{k},\omega) \exp[i\underline{\mu}\cdot\underline{x}_1]\, d\underline{\mu}\, d\underline{k} \ , \tag{6-236}$$

respectively. By use of similar reasoning, $\phi_p(\underline{x}_1,\omega)$ can be related to the alternative forms of the wavevector-frequency spectra.

6.8 REFERENCES

1. H. Cramer, Mathematical Methods of Statistics, Princeton University Press, Princeton, New Jersey, 1946.

2. W. B. Davenport and W. L. Root, Random Signals and Noise, McGraw-Hill Book Co., New York, 1958.

3. A. Papoulis, Probability, Random Variables and Stochastic Processes, McGraw-Hill Book Co., New York, 1965.

4. J. S. Bendat and A. G. Piersol, Measurement and Analysis of Random Data, John Wiley and Sons, Inc., New York, 1966.

5. S. H. Crandall and W. D. Mark, Random Vibrations, Academic Press, New York, 1963.

6. Papoulis, op. cit., pp. 92-94.

7. Ibid., p. 94.

8. Ibid., p. 142.

9. R. R. Kneipfer, Unpublished Lecture Notes for a Course in Random Signals and Noise, 1986.

10. Papoulis, op. cit., pp. 166-167.

11. Ibid., p. 167.

12. Davenport and Root, op. cit., p. 154.

13. Papoulis, op. cit., p. 475.

14. Davenport and Root, op. cit., pp. 81-83.

15. Ibid., pp. 83-84.

16. Papoulis, op. cit., p. 300.

17. Ibid., p. 302.

18. Crandall and Mark, op. cit., p. 21.

19. A. V. Smol'yakov and V. M. Trachenko, The Measurement of Turbulent Fluctuations, Springer-Verlag, Berlin, 1983, p. 19.

20. Bendat and Piersol, op. cit., pp. 350-365.

21. Papoulis, op. cit., p. 338.

22. Davenport and Root, op. cit., p. 104.

CHAPTER 7

RESPONSE OF LINEAR SYSTEMS TO RANDOM SPACE-TIME FIELDS

There are two objectives to this chapter. The first is to demonstrate the mathematical techniques for obtaining a statistical description of the output field of a time-invariant linear system excited by an input field that varies randomly in space and time. The second is to demonstrate that, for certain combinations of classes of systems and input field statistics, there are mathematical and, thereby, interpretational advantages to relating the input and output statistics in the wavevector-frequency spectral domain.

Recall that all systems treated in this text are assumed to be time invariant, but can be either space invariant or space varying. Recall further that only stationary random input fields are considered in this text. However, those stationary fields may be either homogeneous or nonhomogeneous. Therefore, we will be concerned, in this chapter, with only four combinations of classes of systems and inputs. Those combinations are (1) a space-invariant system excited by a homogeneous input field, (2) a space-invariant system excited by a nonhomogeneous input field, (3) a space-varying system excited by a homogeneous input field, and (4) a space-varying system excited by a nonhomogeneous input field. These various combinations of systems and excitations will be separately addressed in the sections to follow.

In this treatment, we shall consistently assume that the linear systems have deterministic response characteristics (i.e., Green's functions, wavevector-frequency responses, or impedances). Therefore, the random nature of the output field of any system is a consequence only of the randomness of the input field.

We emphasize one final preliminary note. Throughout the remainder of this text, we will employ only one of the three alternative forms (presented in the previous chapter) for each of the following, informationally equivalent,

metrics of the statistics of stationary, nonhomogeneous fields: (1) the autocorrelation function, (2) the space-varying wavevector-frequency spectrum, and (3) the two wavevector-frequency spectrum. The form of the autocorrelation function will be $Q_{pp}(\underline{x}_1,\underline{\xi},\tau)$, defined by equation (6-69). The space-varying wavevector-frequency will be characterized by $K_{pp}(\underline{x}_1,\underline{k},\omega)$, as defined by equation (6-105), and the two wavevector-frequency spectrum will be characterized by $S_{pp}(\underline{\mu},\underline{k},\omega)$, defined by equation (6-121). Descriptions of system input or output statistics in forms alternative to these can be obtained by using the equivalences developed between alternative forms of these various metrics in chapter 6.

It is both convenient and spatially economical to organize the presentation of the four previously identified combinations of classes of systems and inputs according to system class. We begin with the simpler of the two classes: that is, the space- and time-invariant system.

7.1 RESPONSE OF SPACE- AND TIME-INVARIANT LINEAR SYSTEMS TO RANDOM SPACE-TIME INPUT FIELDS

Consider a space- and time-invariant linear system characterized by the causal Green's function, $g(\underline{\alpha},\theta)$. By equation (3-52) of chapter 3, the output field, $p(\underline{x},t)$, from this system resulting from an input field, $f(\underline{x},t)$, is given by

$$p(\underline{x},t) = \int_{-\infty}^{\infty}\int_{-\infty}^{\infty} g(\underline{\alpha},\theta)f(\underline{x} - \underline{\alpha},t - \theta)\, d\underline{\alpha}\, d\theta \ . \qquad (7\text{-}1)$$

Note here that we have assumed the input and output fields to be functions of the two-dimensional spatial vector, $\underline{x} = (x_1,x_2)$, rather than the three-dimensional vector, $\vec{x} = (x_1,x_2,x_3)$, used in chapter 3. This choice was made for two reasons. The first was to ensure notational consistency of the statistical metrics in this chapter with those presented in chapter 6. The second reason is that, in the majority of practical system problems in acoustics, the input is applied on a boundary of the system (a two-dimensional surface), and the output is also observed over some (two-

dimensional) surface of interest.

By equations (6-44) and (7-1), the autocorrelation function of the output field of a space- and time-invariant system is given by

$$Q_{pp}(\underline{x}_1,\underline{\xi},t,\tau) = E\{p(\underline{x}_1,t)p(\underline{x}_1+\underline{\xi},t+\tau)\}$$

$$= E\left\{\int_{-\infty}^{\infty}\int_{-\infty}^{\infty}\int_{-\infty}^{\infty}\int_{-\infty}^{\infty}[g(\underline{\alpha},\theta_1)f(\underline{x}_1-\underline{\alpha},t-\theta_1)\right.$$

$$\left. g(\underline{\beta},\theta_2)f(\underline{x}_1+\underline{\xi}-\underline{\beta},t+\tau-\theta_2)]\,d\underline{\alpha}\,d\theta_1\,d\underline{\beta}\,d\theta_2\right\}. \qquad (7\text{-}2)$$

If we interpret the expected value, $E\{\}$, as the arithmetic average of the trial values of the product $p(\underline{x}_1,t)p(\underline{x}_1+\underline{\xi},t+\tau)$ over a large number of trials (see equation (6-24)), then we can write the left-hand side of equation (7-2) as

$$Q_{pp}(\underline{x}_1,\underline{\xi},t,\tau) = E\{p(\underline{x}_1,t)p(\underline{x}_1+\underline{\xi},t+\tau)\}$$

$$= \lim_{N\to\infty}\frac{1}{N}\sum_{n=1}^{N}\{p(\underline{x}_1,t)p(\underline{x}_1+\underline{\xi},t+\tau)\}_n = \lim_{N\to\infty}\frac{1}{N}\sum_{n=1}^{N}p_n(\underline{x}_1,t)p_n(\underline{x}_1+\underline{\xi},t+\tau)\ , \qquad (7\text{-}3)$$

where the subscript n denotes the n-th trial value. By applying the same reasoning to the right-hand side of equation (7-2), we can write

$$E\left\{\int_{-\infty}^{\infty}\int_{-\infty}^{\infty}\int_{-\infty}^{\infty}\int_{-\infty}^{\infty}[g(\underline{\alpha},\theta_1)f(\underline{x}_1-\underline{\alpha},t-\theta_1)\right.$$

$$\left. g(\underline{\beta},\theta_2)f(\underline{x}_1+\underline{\xi}-\underline{\beta},t+\tau-\theta_2)]\,d\underline{\alpha}\,d\theta_1\,d\underline{\beta}\,d\theta_2\right\}$$

$$= \lim_{N\to\infty}\frac{1}{N}\sum_{n=1}^{N}\left\{\int_{-\infty}^{\infty}\int_{-\infty}^{\infty}\int_{-\infty}^{\infty}\int_{-\infty}^{\infty}[g(\underline{\alpha},\theta_1)f(\underline{x}_1-\underline{\alpha},t-\theta_1)\right.$$

$$\left. g(\underline{\beta},\theta_2)f(\underline{x}_1+\underline{\xi}-\underline{\beta},t+\tau-\theta_2)]\,d\underline{\alpha}\,d\theta_1\,d\underline{\beta}\,d\theta_2\right\}_n . \qquad (7\text{-}4)$$

By an interchange of the order of summation and integration, equation (7-4) can be rewritten in the form

$$E\left\{\int_{-\infty}^{\infty}\int_{-\infty}^{\infty}\int_{-\infty}^{\infty}\int_{-\infty}^{\infty} [g(\underline{\alpha},\theta_1)f(\underline{x}_1 - \underline{\alpha},t - \theta_1) g(\underline{\beta},\theta_2)f(\underline{x}_1 + \underline{\xi} - \underline{\beta},t + \tau - \theta_2)]\, d\underline{\alpha}\; d\theta_1\; d\underline{\beta}\; d\theta_2\right\}$$

$$= \int_{-\infty}^{\infty}\int_{-\infty}^{\infty}\int_{-\infty}^{\infty}\int_{-\infty}^{\infty}\left[\lim_{N\to\infty}\frac{1}{N}\sum_{n=1}^{N}\{g(\underline{\alpha},\theta_1)f(\underline{x}_1 - \underline{\alpha},t - \theta_1) g(\underline{\beta},\theta_2)f(\underline{x}_1 + \underline{\xi} - \underline{\beta},t + \tau - \theta_2)\}_n\right] d\underline{\alpha}\; d\theta_1\; d\underline{\beta}\; d\theta_2$$

$$= \int_{-\infty}^{\infty}\int_{-\infty}^{\infty}\int_{-\infty}^{\infty}\int_{-\infty}^{\infty}\left[\lim_{N\to\infty}\frac{1}{N}\sum_{n=1}^{N}\{g_n(\underline{\alpha},\theta_1)f_n(\underline{x}_1 - \underline{\alpha},t - \theta_1) g_n(\underline{\beta},\theta_2)f_n(\underline{x}_1 + \underline{\xi} - \underline{\beta},t + \tau - \theta_2)\}\right] d\underline{\alpha}\; d\theta_1\; d\underline{\beta}\; d\theta_2 \; . \qquad (7\text{-}5)$$

Recall, however, that the Green's function of the system is assumed to be deterministic. Thus, for every fixed set of the arguments $\underline{\alpha}$, θ_1, $\underline{\beta}$, and θ_2, the product $g_n(\underline{\alpha},\theta_1)g_n(\underline{\beta},\theta_2)$ is independent of the trial number, n. That is,

$$g_n(\underline{\alpha},\theta_1)g_n(\underline{\beta},\theta_2) = g(\underline{\alpha},\theta_1)g(\underline{\beta},\theta_2) \; . \qquad (7\text{-}6)$$

It therefore follows that

$$E\left\{\int_{-\infty}^{\infty}\int_{-\infty}^{\infty}\int_{-\infty}^{\infty}\int_{-\infty}^{\infty} [g(\underline{\alpha},\theta_1)f(\underline{x}_1 - \underline{\alpha},t - \theta_1) g(\underline{\beta},\theta_2)f(\underline{x}_1 + \underline{\xi} - \underline{\beta},t + \tau - \theta_2)]\, d\underline{\alpha}\; d\theta_1\; d\underline{\beta}\; d\theta_2\right\}$$

$$= \int_{-\infty}^{\infty}\int_{-\infty}^{\infty}\int_{-\infty}^{\infty}\int_{-\infty}^{\infty} g(\underline{\alpha},\theta_1)g(\underline{\beta},\theta_2)$$

$$\left[\lim_{N\to\infty}\frac{1}{N}\sum_{n=1}^{N}\{f_n(\underline{x}_1-\underline{\alpha},t-\theta_1)f_n(\underline{x}_1+\underline{\xi}-\underline{\beta},t+\tau-\theta_2)\}\right] d\underline{\alpha}\, d\theta_1\, d\underline{\beta}\, d\theta_2 \;. \tag{7-7}$$

However, by comparing the form of the summation in equation (7-7) with that of equation (7-3), we recognize that

$$\lim_{N\to\infty}\frac{1}{N}\sum_{n=1}^{N}\{f_n(\underline{x}_1-\underline{\alpha},t-\theta_1)f_n(\underline{x}_1+\underline{\xi}-\underline{\beta},t+\tau-\theta_2)\}$$

$$= \lim_{N\to\infty}\frac{1}{N}\sum_{n=1}^{N}\{f(\underline{x}_1-\underline{\alpha},t-\theta_1)f(\underline{x}_1+\underline{\xi}-\underline{\beta},t+\tau-\theta_2)\}_n$$

$$= E\{f(\underline{x}_1-\underline{\alpha},t-\theta_1)f(\underline{x}_1+\underline{\xi}-\underline{\beta},t+\tau-\theta_2)\}$$

$$= Q_{ff}(\underline{x}_1-\underline{\alpha},\underline{\xi}+\underline{\alpha}-\underline{\beta},t-\theta_1,\tau+\theta_1-\theta_2) \;. \tag{7-8}$$

Therefore, by equations (7-2), (7-7), and (7-8), it follows that the autocorrelation function of the output field of a space- and time-invariant linear system is related to the autocorrelation function of the input field by

$$Q_{pp}(\underline{x}_1,\underline{\xi},t,\tau) = \int_{-\infty}^{\infty}\int_{-\infty}^{\infty}\int_{-\infty}^{\infty}\int_{-\infty}^{\infty} g(\underline{\alpha},\theta_1)g(\underline{\beta},\theta_2)$$

$$Q_{ff}(\underline{x}_1-\underline{\alpha},\underline{\xi}+\underline{\alpha}-\underline{\beta},t-\theta_1,\tau+\theta_1-\theta_2)\, d\underline{\alpha}\, d\theta_1\, d\underline{\beta}\, d\theta_2 \;. \tag{7-9}$$

Note, in equation (7-9), that the arguments of the autocorrelation function of the output field (Q_{pp}) appear on the right-hand side of the equation only in the autocorrelation of the input field (Q_{ff}). We now invoke the previously stated assumption that the input field is statistically stationary. That is, we require

$$Q_{ff}(\underline{x}_1 - \underline{\alpha}, \underline{\xi} + \underline{\alpha} - \underline{\beta}, t - \theta_1, \tau + \theta_1 - \theta_2) = Q_{ff}(\underline{x}_1 - \underline{\alpha}, \underline{\xi} + \underline{\alpha} - \underline{\beta}, \tau + \theta_1 - \theta_2). \tag{7-10}$$

Note that the autocorrelation of the input field is now independent of the absolute temporal variable t. It follows, by the observation above, that the substitution of equation (7-10) into (7-9) will result in an autocorrelation function of the output field (Q_{pp}) that is also independent of the absolute time, t, and is thereby stationary. Thus, for a space- and time-invariant linear system excited by a stationary, but generally nonhomogeneous, input field, we obtain the following relationship between the autocorrelation functions of the input and output fields:

$$Q_{pp}(\underline{x}_1, \underline{\xi}, \tau) = \int_{-\infty}^{\infty}\int_{-\infty}^{\infty}\int_{-\infty}^{\infty}\int_{-\infty}^{\infty} g(\underline{\alpha}, \theta_1) g(\underline{\beta}, \theta_2)$$

$$Q_{ff}(\underline{x}_1 - \underline{\alpha}, \underline{\xi} + \underline{\alpha} - \underline{\beta}, \tau + \theta_1 - \theta_2)\, d\underline{\alpha}\, d\theta_1\, d\underline{\beta}\, d\theta_2 \,. \tag{7-11}$$

Note, by the functional forms of their respective autocorrelation functions, that a nonhomogeneous input to the space- and time-invariant system produces a nonhomogeneous output field.

Before completing the analysis of the space- and time-invariant system excited by a stationary, nonhomogeneous input field, let us first examine the input-output relationships of this system for a stationary, homogeneous input field.

7.1.1 Response of a Space- and Time-Invariant Linear System to a Stationary, Homogeneous Input Field

Recall that a stationary, homogeneous field is characterized by a mean and an autocorrelation function that are independent of both the absolute time and the absolute spatial location of observation. In equation (7-9), the autocorrelation function of the input field appears in the form $Q_{ff}(\underline{x}_1 - \underline{\alpha}, \underline{\xi} + \underline{\alpha} - \underline{\beta}, t - \theta_1, \tau + \theta_1 - \theta_2)$, where $\underline{x}_1 - \underline{\alpha}$ is the absolute spatial variable, $\underline{\xi} + \underline{\alpha} - \underline{\beta}$ is the spatial separation, $t - \theta_1$ is the absolute time, and $\tau + \theta_1 - \theta_2$ is the time difference. Clearly, if the input field

is both stationary and homogeneous, the autocorrelation function of the input field must be independent of the absolute spatial variable $\underline{x}_1 - \underline{\alpha}$ and the absolute temporal variable $t - \theta_1$. That is,

$$Q_{ff}(\underline{x}_1 - \underline{\alpha}, \underline{\xi} + \underline{\alpha} - \underline{\beta}, t - \theta_1, \tau + \theta_1 - \theta_2) = Q_{ff}(\underline{\xi} + \underline{\alpha} - \underline{\beta}, \tau + \theta_1 - \theta_2) \ . \tag{7-12}$$

By substituting this stationary, homogeneous form of the autocorrelation function of the input field into equation (7-9), we obtain the following relationship between the autocorrelation functions of the input and output fields:

$$Q_{pp}(\underline{\xi}, \tau) = \int_{-\infty}^{\infty}\int_{-\infty}^{\infty}\int_{-\infty}^{\infty}\int_{-\infty}^{\infty} g(\underline{\alpha}, \theta_1) g(\underline{\beta}, \theta_2) Q_{ff}(\underline{\xi} + \underline{\alpha} - \underline{\beta}, \tau + \theta_1 - \theta_2) \, d\underline{\alpha} \, d\theta_1 \, d\underline{\beta} \, d\theta_2 \ . \tag{7-13}$$

Note here that the autocorrelation of the output field is also stationary and homogeneous inasmuch as the right-hand side of equation (7-13) is independent of both the absolute spatial location, $\underline{x}_1$, and the absolute time, t, of observation of the output field.

By application of equation (6-78) to equation (7-13), it can easily be shown that the wavevector-frequency spectrum of the output field, $\Phi_p(\underline{k}, \omega)$, is related to the wavevector-frequency spectrum of the input field, $\Phi_f(\underline{k}, \omega)$, by

$$\Phi_p(\underline{k}, \omega) = |G(\underline{k}, \omega)|^2 \Phi_f(\underline{k}, \omega) \ , \tag{7-14}$$

where, it will be recalled from chapter 2, $G(\underline{k}, \omega)$ is the wavevector-frequency response of the space- and time-invariant linear system, and is defined by

$$G(\underline{k}, \omega) = \int_{-\infty}^{\infty}\int_{-\infty}^{\infty} g(\underline{\alpha}, \theta) \exp[-i(\underline{k} \cdot \underline{\alpha} + \omega\theta)] \, d\underline{\alpha} \, d\theta \ . \tag{7-15}$$

Equation (7-13), which relates the statistics of the input and output fields in the space-time domain, shows that the autocorrelation of the output

field is expressed as a multiple convolution of the autocorrelation of the input field with a product of two Green's functions of the system. Equation (7-14), which relates the statistics of the input and output fields in the wavevector-frequency domain, shows the wavevector-frequency spectrum of the output field to be the product of the wavevector-frequency spectrum of the input field with the squared magnitude of the wavevector-frequency response of the system. Clearly, for a space- and time-invariant linear system excited by a stationary, homogeneous input field, the mathematical relationship between the input and output statistics is considerably simpler in the wavevector-frequency domain than in the space-time domain.

Note, from equation (7-14), that if any two of the wavevector-frequency fields are given, the third can be determined by simple algebra. On the other hand, it is evident from equation (7-13) that the determination of either the product of the Green's functions or the autocorrelation of the input field requires solution of an integral equation.

By use of equation (7-14), we can establish an additional property of the wavevector-frequency spectrum of a stationary, homogeneous field. From equation (6-203), the mean square value of the output field, $\langle p^2 \rangle$, can be expressed as

$$\langle p^2 \rangle = \frac{1}{(2\pi)^3} \int_{-\infty}^{\infty} \int_{-\infty}^{\infty} \Phi_p(\underline{k},\omega)\, d\underline{k}\, d\omega \ . \qquad (7\text{-}16)$$

By substitution of equation (7-14) into equation (7-16), we obtain

$$\langle p^2 \rangle = \frac{1}{(2\pi)^3} \int_{-\infty}^{\infty} \int_{-\infty}^{\infty} |G(\underline{k},\omega)|^2 \Phi_f(\underline{k},\omega)\, d\underline{k}\, d\omega \ . \qquad (7\text{-}17)$$

For the real fields considered in this book, $\langle p^2 \rangle$ is a real and positive quantity. Clearly then, the integral of equation (7-17) must be real and positive for any possible combination of space- and time-invariant linear system and stationary, homogeneous input field. Inasmuch as $|G(\underline{k},\omega)|^2$ is real and positive and, by section 6.5.1, $\Phi_f(\underline{k},\omega)$ is real, the reality of this integral is guaranteed. However, for the integral to be positive for

any space- and time-invariant linear system and any stationary, homogeneous input field, the wavevector-frequency spectrum, $\Phi_f(\underline{k},\omega)$, of the stationary, homogeneous input field must be positive for all $\underline{k}$ and ω. Inasmuch as the input field can be any stationary, homogeneous field, we can conclude that the wavevector-frequency spectra of all stationary, homogeneous fields are non-negative as well as real.

We now return our attention to the space- and time-invariant linear system excited by a stationary, but nonhomogeneous, input field.

7.1.2 Response of a Space- and Time-Invariant Linear System to a Stationary, Nonhomogeneous Input Field

The relationship between the autocorrelation functions of the input and output fields of a space- and time-invariant linear system excited by a stationary, nonhomogeneous input field was given by equation (7-11). For reference purposes, this relationship is repeated here:

$$Q_{pp}(\underline{x}_1,\underline{\xi},\tau) = \int_{-\infty}^{\infty}\int_{-\infty}^{\infty}\int_{-\infty}^{\infty}\int_{-\infty}^{\infty} g(\underline{\alpha},\theta_1)g(\underline{\beta},\theta_2)$$

$$Q_{ff}(\underline{x}_1 - \underline{\alpha},\underline{\xi} + \underline{\alpha} - \underline{\beta},\tau + \theta_1 - \theta_2)\, d\underline{\alpha}\, d\theta_1\, d\underline{\beta}\, d\theta_2 \ . \tag{7-18}$$

By application of equation (6-105) to equation (7-18), it can be shown that the space-varying wavevector-frequency spectrum of the output field is related to the space-varying wavevector-frequency spectrum of the input field by

$$K_{pp}(\underline{x}_1,\underline{k},\omega) = \frac{G(\underline{k},\omega)}{(2\pi)^2}\int_{-\infty}^{\infty}\int_{-\infty}^{\infty} G(\underline{\sigma} - \underline{k},-\omega)K_{ff}(\underline{y},\underline{k},\omega)\exp[i\underline{\sigma}\cdot(\underline{x}_1 - \underline{y})]\, d\underline{\sigma}\, d\underline{y} \ . \tag{7-19}$$

Alternatively, by use of equations (6-121) and (7-18), the two wavevector-frequency spectrum of the output field of a space- and time-invariant linear

system can be shown to be related to the two wavevector-frequency spectrum of the input field by

$$S_{pp}(\underline{\mu},\underline{k},\omega) = G(\underline{k},\omega)G(\underline{\mu} - \underline{k},-\omega)S_{ff}(\underline{\mu},\underline{k},\omega) \ . \tag{7-20}$$

Note, from the functional forms of the output statistics described by equations (7-18) to (7-20), that the output field of a space- and time-invariant system subjected to a stationary, nonhomogeneous input field is statistically stationary and nonhomogeneous. Note further that the mathematically simplest form of the input-output relationship results when the statistics of the input and output fields are expressed in terms of the two wavevector-frequency spectrum. Indeed, it is evident from equation (7-20) that the two wavevector-frequency spectrum of either the input or output field is easily predicted, given the two wavevector-frequency spectrum of one field and the wavevector-frequency response of the system. If the two-wavevector spectra of both the input and output fields are known, only the product, $G(\underline{k},\omega)G(\underline{\mu} - \underline{k},-\omega)$, of the wavevector-frequency responses of the system can be determined. However, given this product, the wavevector-frequency response can be specified within a phase factor.

By inspection of the forms of equations (7-18) and (7-19), it is evident that the determination of the space-varying wavevector-frequency spectrum of the output field is a somewhat simpler mathematical task than the determination of the autocorrelation function of the output field. Note, however, that the determination of either the autocorrelation function or space-varying wavevector-frequency spectrum of the input field, given (as appropriate) the autocorrelation or space-varying wavevector-frequency spectrum of the output field and the Green's function or wavevector-frequency response of the system, requires the solution of a formidable-looking integral equation.

Consider now an input field characterized by the two wavevector-frequency spectrum

$$S_{ff}(\underline{\mu},\underline{k},\omega) = (2\pi)^2\delta(\underline{\mu})V(\underline{k},\omega) + W_{ff}(\underline{\mu},\underline{k},\omega) \ . \tag{7-21}$$

where $W_{ff}(\underline{\mu},\underline{k},\omega)$ characterizes a nonhomogeneous field that has no discrete (i.e., Dirac delta function) wavevector contribution at $\underline{\mu}=(0,0)$. As we have shown in chapter 6, this input field is generally nonhomogeneous, and is comprised of spectral components that are independent of the absolute spatial variable $\underline{x}$, represented by the term $(2\pi)^2\delta(\underline{\mu})V(\underline{k},\omega)$, and purely nonhomogeneous spectral components, represented by the term $W_{ff}(\underline{\mu},\underline{k},\omega)$. Substitution of equation (7-21) into (7-20) yields the following expression for the two wavevector-frequency spectrum of the output field resulting from this form of input to a space- and time-invariant linear system:

$$S_{pp}(\underline{\mu},\underline{k},\omega) = G(\underline{k},\omega)G(\underline{\mu}-\underline{k},-\omega)\{(2\pi)^2\delta(\underline{\mu})V(\underline{k},\omega) + W_{ff}(\underline{\mu},\underline{k},\omega)\} \ . \tag{7-22}$$

By application of equation (6-155) to equation (7-22), the space-averaged wavevector-frequency spectrum of the output field is given by

$$\Phi_p^a(\underline{k},\omega) = \lim_{L\to\infty}\frac{1}{(2\pi)^2}\int_{-\infty}^{\infty}\{(2\pi)^2\delta(\underline{\mu})V(\underline{k},\omega) + W_{ff}(\underline{\mu},\underline{k},\omega)\}$$
$$G(\underline{k},\omega)G(\underline{\mu}-\underline{k},-\omega)\left[\frac{\sin(\mu_1L)}{\mu_1L}\right]\left[\frac{\sin(\mu_2L)}{\mu_2L}\right]d\underline{\mu} \ . \tag{7-23}$$

By arguments similar to those employed following equation (6-155), it can be demonstrated that, inasmuch as W_{ff} contains no discrete spectral contribution at $\underline{\mu}=(0,0)$, the integral containing this term is equal to zero. Consequently, by use of equation (6-156), it can be shown that the space-averaged wavevector-frequency spectrum of the output field of a space- and time-invariant linear system, excited by a stationary, nonhomogeneous field characterized by the two wavevector-frequency spectrum of equation (7-21), is given by

$$\Phi_p^a(\underline{k},\omega) = |G(\underline{k},\omega)|^2V(\underline{k},\omega) \ . \tag{7-24}$$

Clearly, by comparison of equations (7-21) and (7-24), the space-averaged wavevector-frequency spectrum reflects the output of the system from only those spectral components of the input field that are independent of the absolute spatial variable, $\underline{x}_1$. The form of equation (7-24) is identical to that of equation (7-14), which relates the wavevector-frequency spectrum of the output field of a space- and time-invariant system to the wavevector-

frequency spectrum of the stationary, homogeneous input field. Further, by use of equation (6-166) and arguments similar to those used following equations (7-16) and (7-17), it is easily established that $V(\underline{k},\omega)$, and thereby $\Phi_p^a(\underline{k},\omega)$, are non-negative for all $\underline{k}$ and ω. It was established in chapter 6 that $\Phi_p^a(\underline{k},\omega)$ is real.

By the arguments of this and the previous section, we have demonstrated that the input-output relationships for space- and time-invariant linear systems excited by random space-time fields have the form of multiple convolutions in the space-time domain, but are reduced to simple algebraic equations when the input and output statistics and the system response are expressed in the wavevector-frequency domain. These simple algebraic forms facilitate both mathematical prediction and physical interpretation of the input, output, or response characteristics of the system.

We now turn our attention to the response of time-invariant, but space-varying, systems to random space-time input fields.

7.2 RESPONSE OF SPACE-VARYING LINEAR SYSTEMS TO RANDOM SPACE-TIME INPUT FIELDS

Consider a time-invariant, space-varying linear system characterized by the causal Green's function, $g(\underline{x},\underline{\alpha},\theta)$. Recall that the space-varying properties of a system result from either spatial variations in system parameters or spatial boundaries of the system. We omit from consideration here, as we did in chapters 4 and 5, space-limited systems in which the output can be specified only in the form of an integral equation. This can be ensured by restricting our treatment of space-limited systems to those characterized by "exact Green's functions," as defined in chapter 4 (see pages 4-42 and 4-50). With this restriction, it can be verified, by inspection of equations (4-91) and (4-128) of chapter 4, that the output field, $o(\underline{x},t)$, from either a spatially nonuniform or space-limited, time-invariant linear system is related to the input field, $f(\underline{x},t)$, by

$$o(\underline{x},t) = \int_{-\infty}^{\infty}\int_{-\infty}^{\infty} g(\underline{x},\underline{\alpha},\theta)f(\underline{\alpha},t-\theta)\, d\underline{\alpha}\; d\theta\, . \tag{7-25}$$

For an infinite, spatially nonuniform system, $f(\underline{x},t)$ and $o(\underline{x},t)$ represent the input and output fields of the system over all space and time. For a space-limited system, $f(\underline{x},t)$ and $o(\underline{x},t)$ represent the space-limited versions of the input and output fields, defined in chapter 4 by equations (4-124) and (4-125).

By equations (6-44) and (7-25), the autocorrelation function of the output field of a time-invariant, space-varying system is given by

$$Q_{oo}(\underline{x}_1,\underline{\xi},t,\tau) = E\{o(\underline{x}_1,t)o(\underline{x}_1 + \underline{\xi},t + \tau)\}$$

$$= E\left\{\int_{-\infty}^{\infty}\int_{-\infty}^{\infty}\int_{-\infty}^{\infty}\int_{-\infty}^{\infty} g(\underline{x}_1,\underline{\alpha},\theta_1)f(\underline{\alpha},t - \theta_1)\right.$$

$$\left. g(\underline{x}_1 + \underline{\xi},\underline{\beta},\theta_2)f(\underline{\beta},t + \tau - \theta_2)\, d\underline{\alpha}\, d\theta_1\, d\underline{\beta}\, d\theta_2\right\} . \quad (7\text{-}26)$$

By arguments identical to those employed in equations (7-4) through (7-9), we can interchange the order of expectation, $E\{\}$, and integration to obtain

$$Q_{oo}(\underline{x}_1,\underline{\xi},t,\tau) = \int_{-\infty}^{\infty}\int_{-\infty}^{\infty}\int_{-\infty}^{\infty}\int_{-\infty}^{\infty} E\{g(\underline{x}_1,\underline{\alpha},\theta_1)f(\underline{\alpha},t - \theta_1)$$

$$g(\underline{x}_1 + \underline{\xi},\underline{\beta},\theta_2)f(\underline{\beta},t + \tau - \theta_2)\}\, d\underline{\alpha}\, d\theta_1\, d\underline{\beta}\, d\theta_2 . \quad (7\text{-}27)$$

Recall, however, that the Green's functions are assumed to be deterministic. Therefore,

$$E\{g(\underline{x}_1,\underline{\alpha},\theta_1)f(\underline{\alpha},t - \theta_1)g(\underline{x}_1 + \underline{\xi},\underline{\beta},\theta_2)f(\underline{\beta},t + \tau - \theta_2)\}$$

$$= g(\underline{x}_1,\underline{\alpha},\theta_1)g(\underline{x}_1 + \underline{\xi},\underline{\beta},\theta_2)E\{f(\underline{\alpha},t - \theta_1)f(\underline{\beta},t + \tau - \theta_2)\}$$

$$= g(\underline{x}_1,\underline{\alpha},\theta_1)g(\underline{x}_1 + \underline{\xi},\underline{\beta},\theta_2)Q_{ff}(\underline{\alpha},\underline{\beta} - \underline{\alpha},t - \theta_1,\tau + \theta_1 - \theta_2) . \quad (7\text{-}28)$$

By substitution of equation (7-28) into equation (7-27), we obtain

$$Q_{oo}(\underline{x}_1,\underline{\xi},t,\tau) = \int_{-\infty}^{\infty}\int_{-\infty}^{\infty}\int_{-\infty}^{\infty}\int_{-\infty}^{\infty} g(\underline{x}_1,\underline{\alpha},\theta_1)g(\underline{x}_1 + \underline{\xi},\underline{\beta},\theta_2)$$

$$Q_{ff}(\underline{\alpha},\underline{\beta} - \underline{\alpha},t - \theta_1,\tau + \theta_1 - \theta_2)\, d\underline{\alpha}\, d\theta_1\, d\underline{\beta}\, d\theta_2 \ . \qquad (7\text{-}29)$$

Inasmuch as we are considering only stationary input fields, we require that

$$Q_{ff}(\underline{\alpha},\underline{\beta} - \underline{\alpha},t - \theta_1,\tau + \theta_1 - \theta_2) = Q_{ff}(\underline{\alpha},\underline{\beta} - \underline{\alpha},\tau + \theta_1 - \theta_2) \ . \qquad (7\text{-}30)$$

By substituting this result into equation (7-29) and by making the change of variable

$$\underline{\varepsilon} = \underline{\beta} - \underline{\alpha} \ , \qquad (7\text{-}31)$$

while holding $\underline{\alpha}$ constant, we obtain the following expression for the auto-correlation function of the output field of a time-invariant, space-varying linear system excited by a stationary, but nonhomogeneous, input field:

$$Q_{oo}(\underline{x}_1,\underline{\xi},\tau) = \int_{-\infty}^{\infty}\int_{-\infty}^{\infty}\int_{-\infty}^{\infty}\int_{-\infty}^{\infty} g(\underline{x}_1,\underline{\alpha},\theta_1)g(\underline{x}_1 + \underline{\xi},\underline{\alpha} + \underline{\varepsilon},\theta_2)$$

$$Q_{ff}(\underline{\alpha},\underline{\varepsilon},\tau + \theta_1 - \theta_2)\, d\underline{\alpha}\, d\theta_1\, d\underline{\varepsilon}\, d\theta_2 \ . \qquad (7\text{-}32)$$

As we did in the case of the space- and time-invariant system, let us examine the input-output relationship of the time-invariant, space-varying system for a stationary, homogeneous input field before completing the analysis for the nonhomogeneous input field.

7.2.1 Response of a Space-Varying Linear System to a Stationary, Homogeneous Input Field

Recall, from chapter 4, that there are three categories of space-varying systems: (1) uniform, space-limited, (2) nonuniform, space-limited, and (3) nonuniform, infinite. In classifying the input field to space-varying systems, it is necessary to distinguish between the classification of the

physical field applied to the system and the classification of the field defined as the input to the system. Specifically, the input field, $f(\underline{x},t)$, of all space-limited systems characterized by exact Green's functions is defined (in section 4.3.1.2) to be

$$f(\underline{x},t) = s(\underline{x})q(\underline{x},t) \ , \tag{7-33}$$

where $q(\underline{x},t)$ is the physical field applied to the system, and $s(\underline{x})$ is the space-limiting function appropriate to that system. If the physical field, $q(\underline{x},t)$, is assumed to be stationary and homogeneous, it is easily shown that the correlation function of the input field, Q_{ff}, has the functional form

$$Q_{ff}(\underline{x}_1,\underline{\xi},\tau) = s(\underline{x}_1)s(\underline{x}_1 + \underline{\xi})Q_{qq}(\underline{\xi},\tau) \ . \tag{7-34}$$

Inasmuch as the space-limiting function is defined to be unity within the system boundaries and zero outside the boundaries, it follows from equation (7-34) that, regardless of the classification of the physical field applied to the system, the defined input field, $f(\underline{x},t)$, of a space-limited system is nonhomogeneous.

In consequence of the above definitions and arguments, it is evident that a stationary, homogeneous input field can be applied to only one category of space-varying systems: that category being the infinite, nonuniform system, for which the input field, $f(\underline{x},t)$, is defined to be equal to the physical field, $q(\underline{x},t)$, applied to the system.

Consider an infinite, nonuniform, time-invariant system excited by a physical field, $q(\underline{x},t)$, that is known to be stationary and homogeneous. Inasmuch as the input field, $f(\underline{x},t)$, to this system is equal to the applied physical field, the autocorrelation function of the input field, Q_{ff}, is also stationary and homogeneous. Thus, the autocorrelation function of the input field in equation (7-32) can be written

$$Q_{ff}(\underline{\alpha},\underline{\varepsilon},\tau + \theta_1 - \theta_2) = Q_{ff}(\underline{\varepsilon},\tau + \theta_1 - \theta_2) = Q_{qq}(\underline{\varepsilon},\tau + \theta_1 - \theta_2) \ , \tag{7-35}$$

where Q_{qq} denotes the autocorrelation function of the physical excitation

field. Substitution of equation (7-35) into equation (7-32) yields the following relationship between the autocorrelation functions of the physical excitation field and the output field for an infinite, nonuniform, time-invariant system subjected to a stationary and homogeneous excitation field:

$$Q_{oo}(\underline{x}_1, \underline{\xi}, \tau) = \int_{-\infty}^{\infty}\int_{-\infty}^{\infty}\int_{-\infty}^{\infty}\int_{-\infty}^{\infty} g(\underline{x}_1, \underline{\alpha}, \theta_1)\, g(\underline{x}_1 + \underline{\xi}, \underline{\alpha} + \underline{\varepsilon}, \theta_2)$$

$$Q_{qq}(\underline{\varepsilon}, \tau + \theta_1 - \theta_2)\; d\underline{\alpha}\; d\theta_1\; d\underline{\varepsilon}\; d\theta_2 \; . \tag{7-36}$$

Note, from the functional form of the autocorrelation function, Q_{oo}, that the output field of this system is stationary, but nonhomogeneous. This nonhomogeneity results, of course, from the spatial nonuniformity of the system properties, as is reflected by the presence of the absolute spatial variable $\underline{x}_1$ in the Green's functions in equation (7-36).

To express this input-output relationship in the wavevector-frequency domain, we first make use of equation (6-79) to write

$$Q_{oo}(\underline{x}_1, \underline{\xi}, \tau) = \frac{1}{(2\pi)^3} \int_{-\infty}^{\infty}\int_{-\infty}^{\infty}\int_{-\infty}^{\infty}\int_{-\infty}^{\infty}\int_{-\infty}^{\infty}\int_{-\infty}^{\infty} g(\underline{x}_1, \underline{\alpha}, \theta_1)\, g(\underline{x}_1 + \underline{\xi}, \underline{\alpha} + \underline{\varepsilon}, \theta_2)$$

$$\Phi_q(\underline{\sigma}, \Omega) \exp\{i[\underline{\sigma}\cdot\underline{\varepsilon} + \Omega(\tau + \theta_1 - \theta_2)]\}\; d\underline{\alpha}\; d\theta_1\; d\underline{\varepsilon}\; d\theta_2\; d\underline{\sigma}\; d\Omega \; , \tag{7-37}$$

where $\Phi_q(\underline{\sigma}, \Omega)$ is the wavevector-frequency spectrum of the physical excitation field. By then applying equation (6-121) to equation (7-37) and performing the resulting simple integrations over τ and Ω, we obtain the following expression for the two-wavevector-frequency spectrum of the output field:

$$S_{oo}(\underline{\mu}, \underline{k}, \omega) = \frac{1}{(2\pi)^2} \int_{-\infty}^{\infty}\int_{-\infty}^{\infty}\int_{-\infty}^{\infty}\int_{-\infty}^{\infty}\int_{-\infty}^{\infty}\int_{-\infty}^{\infty}\int_{-\infty}^{\infty} \Phi_q(\underline{\sigma}, \omega)\, g(\underline{x}_1, \underline{\alpha}, \theta_1)\, g(\underline{x}_1 + \underline{\xi}, \underline{\alpha} + \underline{\varepsilon}, \theta_2)$$

$$\exp\{i[\underline{\sigma}\cdot\underline{\varepsilon} + \omega(\theta_1 - \theta_2)]\} \exp[-i(\underline{\mu}\cdot\underline{x}_1 + \underline{k}\cdot\underline{\xi})]$$

$$d\underline{x}_1\; d\underline{\xi}\; d\underline{\alpha}\; d\theta_1\; d\underline{\varepsilon}\; d\theta_2\; d\underline{\sigma} \; . \tag{7-38}$$

If we now make changes of variables

$$\underline{v} = \underline{x}_1 + \underline{\xi} \, , \tag{7-39}$$

while holding $\underline{x}_1$ constant, and

$$\underline{\gamma} = \underline{\alpha} + \underline{\varepsilon} \, , \tag{7-40}$$

while holding $\underline{\alpha}$ constant, we obtain

$$S_{oo}(\underline{\mu},\underline{k},\omega) = \frac{1}{(2\pi)^2} \int_{-\infty}^{\infty} \{\Phi_q(\underline{\sigma},\omega)$$

$$\int_{-\infty}^{\infty}\int_{-\infty}^{\infty}\int_{-\infty}^{\infty} g(\underline{x}_1,\underline{\alpha},\theta_1)\exp\{-i[(\underline{\mu} - \underline{k})\cdot\underline{x}_1 + \underline{\sigma}\cdot\underline{\alpha} - \omega\theta_1]\} \, d\underline{x}_1 \, d\underline{\alpha} \, d\theta_1$$

$$\int_{-\infty}^{\infty}\int_{-\infty}^{\infty}\int_{-\infty}^{\infty} g(\underline{v},\underline{\gamma},\theta_2)\exp\{-i[\underline{k}\cdot\underline{v} - \underline{\sigma}\cdot\underline{\gamma} + \omega\theta_2]\} \, d\underline{v} \, d\underline{\gamma} \, d\theta_2\} \, d\underline{\sigma} \, . \tag{7-41}$$

However, by equation (4-119), the two wavevector-frequency response of a time-invariant, space-varying system is defined by

$$G(\underline{\mu},\underline{k},\omega) = \int_{-\infty}^{\infty}\int_{-\infty}^{\infty}\int_{-\infty}^{\infty} g(\underline{x},\underline{\alpha},\theta)\exp\{-i[\underline{\mu}\cdot\underline{x} + \underline{k}\cdot\underline{\alpha} + \omega\theta]\} \, d\underline{x} \, d\underline{\alpha} \, d\theta \, . \tag{7-42}$$

It follows, from equations (7-41) and (7-42), that the two wavevector-frequency spectrum of the output field of the infinite, nonuniform system is related to the wavevector-frequency spectrum of the stationary, homogeneous physical excitation field and the two wavevector-frequency response of the system by

$$S_{oo}(\underline{\mu},\underline{k},\omega) = \frac{1}{(2\pi)^2} \int_{-\infty}^{\infty} \Phi_q(\underline{\sigma},\omega)G(\underline{\mu} - \underline{k},\underline{\sigma},-\omega)G(\underline{k},-\underline{\sigma},\omega) \, d\underline{\sigma} \, . \tag{7-43}$$

The space-varying wavevector-frequency spectrum of the output field, obtained by application of equation (6-130) to equation (7-43), is given by

$$K_{oo}(\underline{x}_1,\underline{k},\omega) = \frac{1}{(2\pi)^4} \int_{-\infty}^{\infty} \int_{-\infty}^{\infty} \Phi_q(\underline{\sigma},\omega) G(\underline{\mu} - \underline{k},\underline{\sigma},-\omega)$$

$$G(\underline{k},-\underline{\sigma},\omega) \exp(i\underline{\mu}\cdot\underline{x}_1)\, d\underline{\sigma}\, d\underline{\mu} \ . \qquad (7\text{-}44)$$

Equation (7-37) shows the autocorrelation function of the output of the infinite, nonuniform system to be a multiple convolution of the autocorrelation function of the physical excitation field with the product of the Green's functions of the system. The space-varying wavevector-frequency spectrum of the output field, described by equation (7-44), is expressed as the Fourier transform of an integral of the product of the wavevector-frequency spectrum of the stationary and homogeneous excitation field and a pair of two wavevector-frequency responses of the space-varying system. The two wavevector-frequency spectrum of the output field, as seen by equation (7-43), is expressed as the integral of the product of the wavevector-frequency spectrum of the stationary and homogeneous excitation field and a pair of two wavevector-frequency responses of the space-varying system. By comparison of the mathematical forms of equations (7-37), (7-43), and (7-44), it is evident that, if the number of integrations is taken as a metric of mathematical difficulty, the simplest input-output relationship is equation (7-43), which results from expressing the homogeneous excitation field in the wavevector-frequency domain and the system response and the output field in the two wavevector-frequency domain.

By inspection of equation (7-43), the reader can verify the following observations:

(1) If the wavevector-frequency spectrum of the homogeneous excitation field and the two wavevector-frequency response of the system are specified, the two wavevector-frequency spectrum of the nonhomogeneous output field can, in principle, be predicted.

(2) If the two wavevector-frequency spectrum of the output field and the two wavevector-frequency response of the system are known, the determination of the wavevector-frequency spectrum of the homogeneous physical excitation field requires the solution of an integral equation.

(3) If the product of the two wavevector-frequency responses of the system is the desired result of an experiment, the system must be excited by a stationary, homogeneous field comprised of a single wavevector and single frequency component. By knowledge of the resulting two wavevector-frequency spectrum of the output field, the two wavevector-frequency response of the infinite, nonuniform system can be determined to within a phase factor.

Consider now the space-averaged wavevector-frequency spectrum of the output field of an infinite, nonuniform system excited by a physical field that is stationary and homogeneous. By use of equations (6-153) and (7-44), it can easily be shown that the space-averaged wavevector-frequency spectrum of this output field is related to the wavevector-frequency spectrum of the homogeneous excitation field by

$$\Phi_0^a(\underline{k},\omega) = \frac{1}{(2\pi)^4} \int_{-\infty}^{\infty} \Phi_q(\underline{\alpha},\omega) G(\underline{k},-\underline{\alpha},\omega)$$

$$\left\{ \lim_{L\to\infty} \int_{-\infty}^{\infty} G(\underline{\mu} - \underline{k},\underline{\alpha},-\omega) \left[\frac{\sin(\mu_1 L)}{\mu_1 L}\right]\left[\frac{\sin(\mu_2 L)}{\mu_2 L}\right] d\underline{\mu} \right\} d\underline{\alpha} \ . \qquad (7\text{-}45)$$

By arguments similar to those used in chapter 6, the integral over $\underline{\mu}$ tends to zero as $L\to\infty$ unless the two wavevector-frequency response, $G(\underline{\mu},\underline{k},\omega)$, of the infinite, nonuniform system contains terms of the form $\Gamma(\underline{\alpha},\underline{k},\omega)\delta(\underline{\mu} - \underline{\alpha})$. However, inasmuch as the Green's functions of all systems considered in this text are real, we require that $G(\underline{\mu},\underline{k},\omega) = G^*(-\underline{\mu},-\underline{k},-\omega)$. Therefore, for the space-averaged wavevector-frequency spectrum to be nonzero, $G(\underline{\mu},\underline{k},\omega)$ must be of the form

$$G(\underline{\mu},\underline{k},\omega) = \sum_{n=1}^{N} \{\Gamma(\underline{\alpha}_n,\underline{k},\omega)\delta(\underline{\mu} - \underline{\alpha}_n) + \Gamma^*(\underline{\alpha}_n,-\underline{k},-\omega)\delta(\underline{\mu} + \underline{\alpha}_n)\} , \qquad (7\text{-}46)$$

where $\underline{\alpha}_n$ specifies the fixed wavevector associated with the n-th pair of delta functions and N denotes the number of pairs of delta functions that characterize $G(\underline{\mu},\underline{k},\omega)$.

Substitution of $G(\underline{\mu},\underline{k},\omega)$, in the form of equation (7-46), into equation (7-45) yields (after some lengthy algebra) the following expression for the space-averaged wavevector-frequency spectrum if, for all n, $\underline{\alpha}_n$ are nonzero wavevectors:

$$\Phi_o^a(\underline{k},\omega) = \frac{1}{(2\pi)^4} \sum_{n=1}^{N} \left\{ \delta(\underline{k} - \underline{\alpha}_n) \int_{-\infty}^{\infty} \Phi_q(\underline{\sigma},\omega) |\Gamma(\underline{\alpha}_n,-\underline{\sigma},\omega)|^2 \, d\underline{\sigma} \right.$$

$$\left. + \, \delta(\underline{k} + \underline{\alpha}_n) \int_{-\infty}^{\infty} \Phi_q(\underline{\sigma},\omega) |\Gamma(\underline{\alpha}_n,\underline{\sigma},-\omega)|^2 \, d\underline{\sigma} \right\} . \qquad (7\text{-}47)$$

If one of the wavevectors, say $\underline{\alpha}_J$, is equal to (0,0), then the J-th term of equation (7-47) must be modified. It can easily be demonstrated that this J-th term must be

$$\frac{1}{(2\pi)^4} \delta(\underline{k}) \int_{-\infty}^{\infty} \Phi_q(\underline{\sigma},\omega) \{ |\Gamma(\underline{0},-\underline{\sigma},\omega)|^2 + |\Gamma(\underline{0},\underline{\sigma},-\omega)|^2$$

$$+ \, 2\mathrm{Re}[\Gamma(\underline{0},-\underline{\sigma},\omega)\Gamma(\underline{0},\underline{\sigma},-\omega)]\} \, d\underline{\sigma} ,$$

where Re[] denotes the real part of the argument.

By equation (7-47), it is clear that if the space-averaged wavevector-frequency spectrum of an infinite, nonuniform system excited by a stationary, homogeneous field exists, it is comprised of a set of N discrete wavevector components located at $\underline{k} = \pm\underline{\alpha}_n$, where $1 \leq n \leq N$, that are weighted by functions of $\underline{\alpha}_n$ and ω.

We have seen that the space-averaged wavevector-frequency spectrum of an infinite, nonuniform system subjected to excitation by a stationary, homogeneous field is zero unless the two wavevector-frequency response of the system has the mathematical form of equation (7-46). Let us now examine the form of the space-varying Green's function associated with that two wavevector-frequency response. By equations (4-138) and (7-46), it can be shown that this Green's function must be of the form

$$g(\underline{x},\underline{x}_0,\theta) = \frac{2}{(2\pi)^2} \sum_{n=1}^{N} \mathrm{Re}\{\beta(\underline{\alpha}_n,\underline{x}_0,\theta)\exp(i\underline{\alpha}_n \cdot \underline{x})\} \ , \qquad (7\text{-}48)$$

where

$$\beta(\underline{\alpha}_n,\underline{x}_0,\theta) = \frac{1}{(2\pi)^3} \int_{-\infty}^{\infty} \int_{-\infty}^{\infty} \Gamma(\underline{\alpha}_n,\underline{k},\omega)\exp\{i(\underline{k}\cdot\underline{x}_0 + \omega\theta)\}\, d\underline{k}\, d\omega \ . \qquad (7\text{-}49)$$

Note, by equation (7-48), that the Green's function associated with the two wavevector-frequency response of equation (7-46) characterizes a system whose response to an impulsive loading applied at $\underline{x}_0$ and time zero can be characterized, at any time θ, by a summation of sine waves in $\underline{x}$. Each sine wave component of the output is characterized by a different wavevector, $\underline{\alpha}_n$, and the amplitude and initial phase of each sine wave component are functions of $\underline{\alpha}_n$, $\underline{x}_0$, and θ.

For example, if $N = 1$ in equation (7-46), it follows from equation (7-48) that

$$g(\underline{x},\underline{x}_0,\theta) = \frac{2}{(2\pi)^2} \mathrm{Re}\{\beta(\underline{\alpha}_1,\underline{x}_0,\theta)\exp(i\underline{\alpha}_1 \cdot \underline{x})\} \ . \qquad (7\text{-}50)$$

In this case, for any fixed location of impulsive excitation, $\underline{x}_0$, and time subsequent to the excitation, θ, the system response varies sinusoidally in $\underline{x}$. The wavevector characterizing the sinusoidal variation in the spatial response is $\underline{\alpha}_1$, and the amplitude of the response and phase at $\underline{x} = (0,0)$ is dictated by the magnitude and phase, respectively, of $\beta(\underline{\alpha}_1,\underline{x}_0,\theta)$.

One might legitimately question whether the functional form of the Green's function described by equation (7-48) characterizes the causal response of an infinite model of any physically based nonuniform system. The Green's func-

tions of spatially nonuniform systems require the solutions of differential equations with nonconstant coefficients. The treatment of such equations, and therefore the resolution of this question, is beyond the scope of this text.

We now turn our attention to the response of space-varying systems to stationary, nonhomogeneous fields.

7.2.2 Response of Space-Varying Linear Systems to Stationary, Nonhomogeneous Input Fields

The relationship between the autocorrelation functions of the input and output fields of a space-varying system excited by a stationary, nonhomogeneous input field was given previously in equation (7-32). For ease of reference, we repeat that relationship here:

$$Q_{oo}(\underline{x}_1,\underline{\xi},\tau) = \int_{-\infty}^{\infty}\int_{-\infty}^{\infty}\int_{-\infty}^{\infty}\int_{-\infty}^{\infty} g(\underline{x}_1,\underline{\alpha},\theta_1)g(\underline{x}_1 + \underline{\xi},\underline{\alpha} + \underline{\varepsilon},\theta_2) Q_{ff}(\underline{\alpha},\underline{\varepsilon},\tau + \theta_1 - \theta_2)\, d\underline{\alpha}\, d\theta_1\, d\underline{\varepsilon}\, d\theta_2 \ . \tag{7-51}$$

Note that the autocorrelation functions of both the input and output fields are nonhomogeneous.

Recall, from the previous section, that a distinction is made between the input field, $f(\underline{x},t)$, to the system and the physical field, $q(\underline{x},t)$, that provides the excitation to the system. For space-limited systems, we showed (see equation (7-34)) that, regardless of the classification of the physical excitation field, the input field, defined by $f(\underline{x},t) = s(\underline{x})q(\underline{x},t)$, is always nonhomogeneous owing to the properties of the space-limiting function, $s(\underline{x})$. Thus, by definition of the input field, all space-limited systems are excited by nonhomogeneous input fields, irrespective of the spatial characteristics of the physical excitation field. For infinite, nonuniform systems, however, the input field is equal to the physical excitation field.

In consequence of the above definitions, space-varying systems subjected to stationary, nonhomogeneous input fields comprise all space-limited systems and infinite, nonuniform systems subjected to physical excitation fields that

are stationary and nonhomogeneous.

If one expresses the autocorrelation of the nonhomogeneous input field (Q_{ff}) as the inverse Fourier transform of its two wavevector-frequency spectrum (S_{ff}), it then follows from equations (6-121) and (7-51) that the two wavevector-frequency spectrum of the output field of a space-varying system can be related to the two wavevector-frequency spectrum of the input field by

$$S_{00}(\underline{\mu},\underline{k},\omega) = \frac{1}{(2\pi)^5} \int_{-\infty}^{\infty}\int_{-\infty}^{\infty}\int_{-\infty}^{\infty}\int_{-\infty}^{\infty}\int_{-\infty}^{\infty}\int_{-\infty}^{\infty}\int_{-\infty}^{\infty}\int_{-\infty}^{\infty}\int_{-\infty}^{\infty}\int_{-\infty}^{\infty} S_{ff}(\underline{\beta},\underline{\sigma},\Omega)$$

$$g(\underline{x}_1,\underline{\alpha},\theta_1)\exp\{i[\underline{\beta}\cdot\underline{\alpha} + \underline{\sigma}\cdot\underline{\varepsilon} + \Omega(\tau + \theta_1 - \theta_2)]\}$$

$$g(\underline{x}_1 + \underline{\xi},\underline{\alpha} + \underline{\varepsilon},\theta_2)\exp\{-i(\underline{\mu}\cdot\underline{x}_1 + \underline{k}\cdot\underline{\xi} + \omega\tau)\}$$

$$d\underline{\beta}\ d\underline{\sigma}\ d\Omega\ d\underline{\alpha}\ d\theta_1\ d\underline{\varepsilon}\ d\theta_2\ d\underline{x}_1\ d\underline{\xi}\ d\tau\ . \tag{7-52}$$

If we now define

$$\underline{v} = \underline{x}_1 + \underline{\xi}\ , \tag{7-53}$$

while holding $\underline{x}_1$ constant, and

$$\underline{\gamma} = \underline{\alpha} + \underline{\varepsilon}\ , \tag{7-54}$$

while holding $\underline{\alpha}$ constant, we obtain, after performing the integrations on τ and Ω,

$$S_{00}(\underline{\mu},\underline{k},\omega) = \frac{1}{(2\pi)^4} \int_{-\infty}^{\infty}\int_{-\infty}^{\infty} \{S_{ff}(\underline{\beta},\underline{\sigma},\omega)$$

$$\int_{-\infty}^{\infty}\int_{-\infty}^{\infty}\int_{-\infty}^{\infty} g(\underline{x}_1,\underline{\alpha},\theta_1)\exp\{-i[(\underline{\mu} - \underline{k})\cdot\underline{x}_1 + (\underline{\sigma} - \underline{\beta})\cdot\underline{\alpha} - \omega\theta_1]\}\ d\underline{x}_1\ d\underline{\alpha}\ d\theta_1$$

$$\int_{-\infty}^{\infty}\int_{-\infty}^{\infty}\int_{-\infty}^{\infty} g(\underline{v},\underline{\gamma},\theta_2)\exp\{-i[\underline{k}\cdot\underline{v} - \underline{\sigma}\cdot\underline{\gamma} + \omega\theta_2]\}\ d\underline{v}\ d\underline{\gamma}\ d\theta_2\}\ d\underline{\beta}\ d\underline{\sigma}\ . \tag{7-55}$$

However, by equation (7-42), we recognize the last two multiple integrals to be $G(\underline{\mu} - \underline{k},\underline{\sigma} - \underline{\beta},-\omega)$ and $G(\underline{k},-\underline{\sigma},\omega)$, respectively. Thus, the two wavevector-

frequency spectrum of the output of a space-varying system is related to the two wavevector-frequency spectrum of the nonhomogeneous input field by

$$S_{oo}(\underline{\mu},\underline{k},\omega) = \frac{1}{(2\pi)^4} \int_{-\infty}^{\infty} \int_{-\infty}^{\infty} S_{ff}(\underline{\beta},\underline{\sigma},\omega) G(\underline{\mu} - \underline{k},\underline{\sigma} - \underline{\beta},-\omega) G(\underline{k},-\underline{\sigma},\omega)\, d\underline{\beta}\, d\underline{\sigma}\ . \quad (7\text{-}56)$$

The space-varying wavevector-frequency spectrum of the output field can be related to the space-varying wavevector-frequency spectrum of the input field by applying equation (6-127) to the two wavevector-frequency spectrum of the input field and equation (6-130) to the two wavevector-frequency spectrum of the output field. That is,

$$K_{oo}(\underline{x}_1,\underline{k},\omega) = \frac{1}{(2\pi)^6} \int_{-\infty}^{\infty} \int_{-\infty}^{\infty} \int_{-\infty}^{\infty} \int_{-\infty}^{\infty} K_{ff}(\underline{z},\underline{\sigma},\omega) G(\underline{\mu} - \underline{k},\underline{\sigma} - \underline{\beta},-\omega)$$

$$G(\underline{k},-\underline{\sigma},\omega) \exp\{i(\underline{\mu}\cdot\underline{x}_1 - \underline{\beta}\cdot\underline{z})\}\, d\underline{\mu}\, d\underline{z}\, d\underline{\beta}\, d\underline{\sigma}\ . \quad (7\text{-}57)$$

For a space-varying system subjected to a stationary, nonhomogeneous input field, comparison of the input-output relationships in the space-time (equation (7-51)), space-varying wavevector-frequency (equation (7-57)), and two wavevector-frequency (equation (7-56)) domains reveals, once again, that the simplest mathematical relationship between the statistics of the input and output fields results from expressing the statistics of those fields in the two wavevector-frequency domain.

The space-averaged wavevector-frequency spectrum of the output field from a space-varying system excited by a stationary, nonhomogeneous input field can be obtained by applying equation (6-155) to the two wavevector-frequency spectrum of the output field described by equation (7-56). This yields

$$\Phi_o^a(\underline{k},\omega) = \frac{1}{(2\pi)^6} \int_{-\infty}^{\infty} \int_{-\infty}^{\infty} S_{ff}(\underline{\beta},\underline{\sigma},\omega) G(\underline{k},-\underline{\sigma},\omega)$$

$$\left\{\lim_{L\to\infty} \int_{-\infty}^{\infty} G(\underline{\mu} - \underline{k},\underline{\sigma} - \underline{\beta},-\omega) \left[\frac{\sin(\mu_1 L)}{\mu_1 L}\right]\left[\frac{\sin(\mu_2 L)}{\mu_2 L}\right] d\underline{\mu}\right\} d\underline{\beta}\, d\underline{\sigma}\ . \quad (7\text{-}58)$$

A comparison of equation (7-58) with equation (7-45) reveals that the integral over $\underline{\mu}$ in equation (7-58) is mathematically similar to that in equation (7-45). Therefore, we can employ arguments identical to those applied to equation (7-45) to establish that the space-averaged wavevector-frequency spectrum described by equation (7-58) is identically zero unless the two wavevector-frequency response, $G(\underline{\mu},\underline{k},\omega)$, of the space-varying system has the functional form given by equation (7-46). That is, unless

$$G(\underline{\mu},\underline{k},\omega) = \sum_{n=1}^{N} \{\Gamma(\underline{\alpha}_n,\underline{k},\omega)\delta(\underline{\mu} - \underline{\alpha}_n) + \Gamma^*(\underline{\alpha}_n,-\underline{k},-\omega)\delta(\underline{\mu} + \underline{\alpha}_n)\}, \qquad (7\text{-}59)$$

$\Phi_0^a(\underline{k},\omega) = 0$. If $G(\underline{\mu},\underline{k},\omega)$ is of the form of equation (7-59) (or (7-46)) and $\underline{\alpha}_n \neq (0,0)$ for any n, it can be shown that the space-averaged wavevector-frequency spectrum of the output field of a space-varying system excited by a stationary, nonhomogeneous field is given by

$$\Phi_0^a(\underline{k},\omega) = \frac{1}{(2\pi)^6} \sum_{n=1}^{N} \Bigg\{\delta(\underline{k} - \underline{\alpha}_n) \int_{-\infty}^{\infty}\int_{-\infty}^{\infty} S_{ff}(\underline{\beta},\underline{\sigma},\omega)\Gamma(\underline{\alpha}_n,-\underline{\sigma},\omega)$$

$$\Gamma^*(\underline{\alpha}_n,\underline{\beta} - \underline{\sigma},\omega)\, d\underline{\beta}\, d\underline{\sigma}$$

$$+ \delta(\underline{k} + \underline{\alpha}_n) \int_{-\infty}^{\infty}\int_{-\infty}^{\infty} S_{ff}(\underline{\beta},\underline{\sigma},\omega)\Gamma(\underline{\alpha}_n,\underline{\sigma},-\omega)$$

$$\Gamma^*(\underline{\alpha}_n,\underline{\sigma} - \underline{\beta},-\omega)\, d\underline{\beta}\, d\underline{\sigma}\Bigg\}. \qquad (7\text{-}60)$$

From equation (7-60) and the symmetry property of the two wavevector-frequency spectrum given by equation (6-136), it can be established that

$$\Phi_0^a(\underline{k},\omega) = \Phi_0^{a*}(\underline{k},\omega) . \qquad (7\text{-}61)$$

Therefore, the space-averaged wavevector-frequency spectrum of the output field is real (as it should be).

It is interesting to note that, for both homogeneous and nonhomogeneous input fields, the space-averaged wavevector-frequency spectrum of the output

field of a space-varying system is zero unless the two wavevector-frequency response of the system has the form of equation (7-46). As shown previously, this two wavevector-frequency response implies that the Green's function of the space-varying system must have the mathematical form

$$g(\underline{x},\underline{x}_0,\theta) = \frac{2}{(2\pi)^2} \sum_{n=1}^{N} \mathrm{Re}\{\beta(\underline{\alpha}_n,\underline{x}_0,\theta)\exp(i\underline{\alpha}_n\cdot\underline{x})\} , \qquad (7\text{-}62)$$

where

$$\beta(\underline{\alpha}_n,\underline{x}_0,\theta) = \frac{1}{(2\pi)^3} \int_{-\infty}^{\infty}\int_{-\infty}^{\infty} \Gamma(\underline{\alpha}_n,\underline{k},\omega)\exp\{i(\underline{k}\cdot\underline{x}_0 + \omega\theta)\}\, d\underline{k}\, d\omega . \quad (7\text{-}63)$$

While we do not know, nor do we propose to determine, whether this Green's function represents the causal response of any physically based model of a space-varying system, we can demonstrate that it cannot describe the response of any space-limited system. Note, from equation (7-62), that the Green's function is a sum of waves that vary sinusoidally over all $\underline{x}$. The direction of propagation of the n-th wave component is dictated by $\underline{\alpha}_n$, and the amplitude and initial phase of that component are specified by $\beta(\underline{\alpha}_n,\underline{x}_0,\theta)$. Inasmuch as (1) space-limited systems have zero response outside the spatial bounds of the system and (2) the Green's function of equation (7-62) dictates a sinusoidal response over all $\underline{x}$ for all input locations and times, this Green's function cannot represent a space-limited system. Thus, we conclude that (1) the space-averaged wavevector-frequency spectrum of any space-limited system is identically zero and (2) the space-averaged wavevector-frequency spectrum of an infinite, nonuniform system is zero unless that system has a Green's function of the mathematical form of equation (7-62).

By the arguments presented in this and the previous section, we have demonstrated that the simplest mathematical forms of the input-output relationships for space-varying, time-invariant systems subjected to random space-time input fields result from expressing the statistics of the output field in the form of the two wavevector-frequency spectrum and the statistics of the input field in the form of either the wavevector-frequency spectrum (for homogeneous inputs) or the two wavevector-frequency spectrum (for nonhomogeneous inputs). The space-averaged wavevector-frequency spectrum of

any space-limited system was demonstrated to be identically zero. The space-averaged wavevector-frequency spectra of infinite, nonuniform systems were shown to be zero unless the Green's function had the mathematical form of equation (7-62).

7.3 ILLUSTRATIVE EXAMPLES

In this section, we present analyses of two systems subjected to excitation by random space-time fields. The first system is a uniform flat plate, of infinite extent, excited by the pressure fluctuations associated with homogeneous turbulent flow over the plate. The second system is a finite length string, with fixed ends, excited by a forcing field that is harmonic in space and time, but has a random initial phase. The purpose of these illustrative examples is to demonstrate the utility of the various input-output relationships presented in the previous sections for predicting and analyzing the response of systems subjected to random space-time excitation fields.

7.3.1 The Displacement Field of a Uniform, Infinite Flat Plate Excited By Turbulent Flow

A uniform flat plate of infinite spatial extent is subjected to a turbulent flow field over its upper (i.e., $x_3 > 0$) surface, as illustrated in figure 7-1. The space beneath the lower surface of the plate (i.e., $x_3 < 0$) is vacuous. The pressure fluctuations in the turbulent boundary layer that is formed over the upper surface of the plate apply a force per unit area, $f(\underline{x},t)$, on that surface. This forcing field is random in both space and time. The statistics of this forcing field are assumed to be both stationary and homogeneous. The forcing field excites a displacement field, $w(\underline{x},t)$, in the plate, which, in turn, excites an additional pressure field in the fluid. This pressure field also reacts on the upper surface of the plate. We wish to establish the statistics of the displacement field of the plate resulting from the turbulent flow excitation.

The uniform infinite plate and semi-infinite volume of fluid constitute a coupled system. This particular coupled system was treated in section 5.3.1

of chapter 5, and was determined to be a space- and time-invariant system. Note that the forcing function associated with the turbulent flow is directed opposite to the forcing function illustrated in figure 5-1. However, inasmuch as phase information is not preserved in the wavevector-frequency spectrum, the sign convention of the forcing function is of no consequence to the input-output relationship.

As previously stated, the statistics of the forcing field associated with the turbulent wall pressure are assumed to be stationary and homogeneous. Inasmuch as the infinite plate, fluid loaded on one side, is a space- and time-invariant system, it follows from equation (7-14) that the wavevector-frequency spectrum, $\Phi_w(\underline{k},\omega)$, of the (output) displacement field of the plate is related to the wavevector-frequency spectrum of the forcing field, $\Phi_f(\underline{k},\omega)$, associated with the (input) turbulent pressure field by

$$\Phi_w(\underline{k},\omega) = |G(\underline{k},\omega)|^2 \Phi_f(\underline{k},\omega) , \tag{7-64}$$

where, by equation (5-46), the wavevector-frequency response of the plate, fluid loaded on one side, is given by

$$G(\underline{k},\omega) = \begin{cases} \dfrac{1}{\left\{[Dk^4 - \mu\omega^2] + i\left[r\omega + \dfrac{\rho\omega^2}{k_0\sqrt{(1 - k^2/k_0^2)}}\right]\right\}} , & k \leq |k_0| , \\[2ex] \dfrac{1}{\left\{\left[Dk^4 - \mu\omega^2 - \dfrac{\rho\omega^2}{\sqrt{(k^2 - k_0^2)}}\right] + i[r\omega]\right\}} , & k > |k_0| . \end{cases} \tag{7-65}$$

Here, it will be recalled that D, μ, and r are the flexural rigidity, mass per unit area, and damping force per unit area of the plate, respectively; ρ is the mass density of the fluid; and $k_0 = \omega/c$, where c is the sound speed in the fluid.

The wavevector-frequency response of the infinite plate, fluid loaded on one side, was treated in section 5.3.1 of chapter 5, and the magnitude of this response as a function of the wavenumber of the excitation, at any fixed frequency, is illustrated in figure 5-7(a). By reference to this figure and

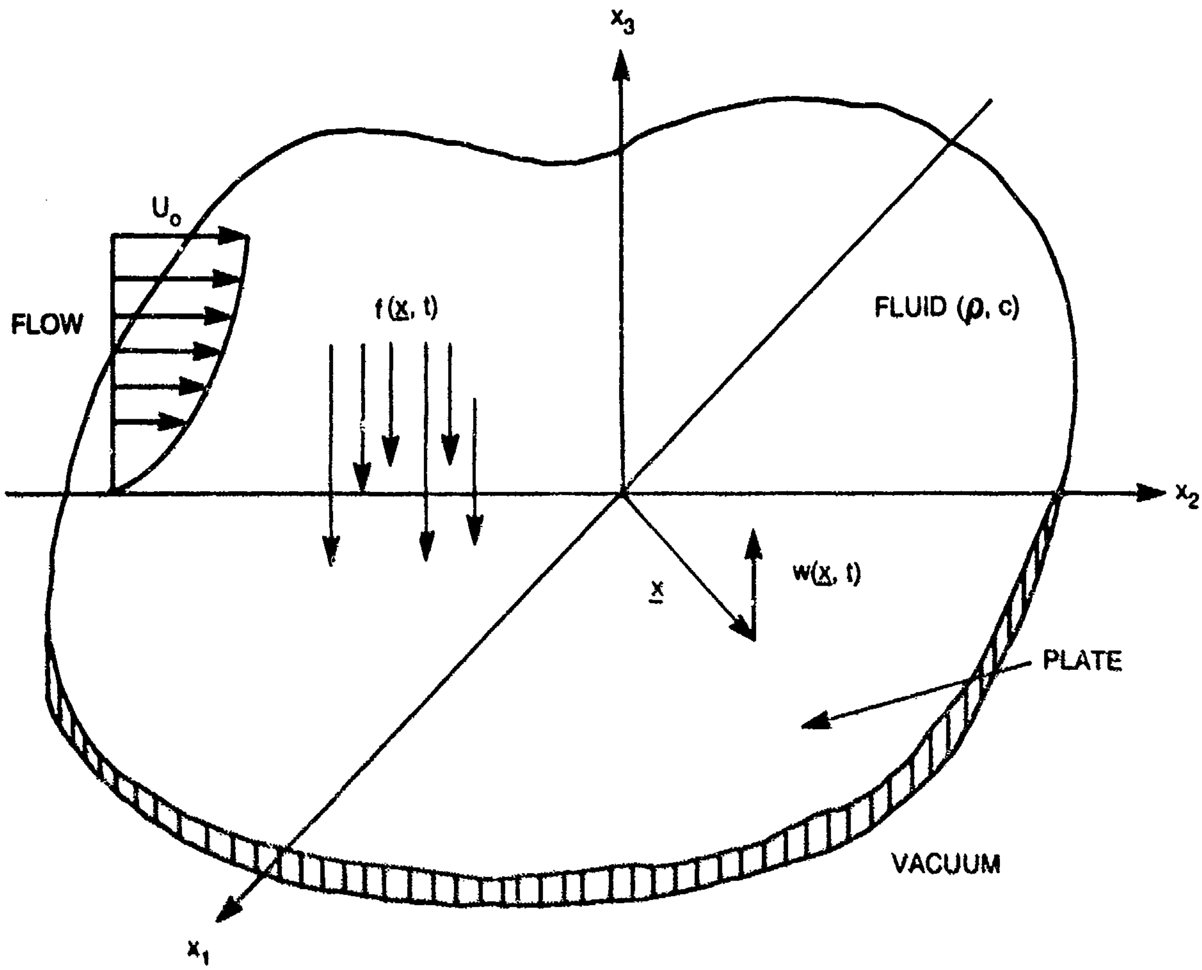

Figure 7-1. Geometry of the Turbulent, Flow-Excited Infinite Flat Plate

section 5.3.1, it will be recalled that, at any given frequency, the response of the fluid-loaded plate to any plane wave component of the excitation is independent of the direction of propagation of that wave component, and depends only on the magnitude of the wavevector that characterizes the plane wave. The fluid-loaded plate responds most strongly, at any frequency, to waves characterized by wavevectors having magnitudes, $|\underline{k}|$, equal to k_p', where k_p' is the free wavenumber of the fluid-loaded plate defined by equation (5-35). Thus, as indicated in figure 5-7(a), $|G(\underline{k},\omega)|$ is characterized, at any given frequency, by a maximum response on the circle defined by $k = |\underline{k}| = k_p'$. For a comprehensive discussion of the wavevector-

frequency response of the fluid-loaded plate, the reader is referred to section 5.3.1 of chapter 5.

To obtain an expression for the wavevector-frequency spectrum of the displacement field of the turbulent, flow-excited plate, it remains to specify a model for the wavevector-frequency spectrum of the forcing field associated with the turbulent wall pressure fluctuations. According to Junger and Feit,[1] the forcing field (i.e., the turbulent pressure fluctuations at the surface of the plate) should be independent of the plate response. Junger and Feit's examples suggest that the force per unit area applied to a flexible plate by an incident pressure wave is equal to the pressure produced on a rigid surface by that incident wave. Thus, we assume the forcing field associated with the turbulent flow to be the pressure produced on a rigid surface by a turbulent flow over that surface.

One of the simpler mathematical models for the second order statistics of turbulent wall pressure fluctuations over a (relatively) rigid surface is the model proposed by Corcos[2] in 1963. The Corcos model assumes that the cross-spectral density (i.e., the temporal Fourier transform of the autocorrelation function) of the turbulent wall pressure field over a rigid surface, $R_{ff}(\underline{\xi},\omega)$, can be written in the separable form

$$R_{ff}(\underline{\xi},\omega) \equiv \int_{-\infty}^{\infty} Q_{ff}(\underline{\xi},\tau)\exp(-i\omega\tau)\, d\tau$$

$$= \phi_f(\omega)A(\omega\xi_1/U_c)B(\omega\xi_2/U_c)\exp(-i\omega\xi_1/U_c) \quad . \qquad (7\text{-}66)$$

where $\phi_f(\omega)$ denotes the frequency spectral density of the pressure, and A and B are (as yet) unspecified functions of the streamwise (ξ_1) and transverse (ξ_2) spatial separations, respectively, and of frequency and the convection speed (U_c) of the turbulent pressure fluctuations. This convection speed usually ranges between $0.6U_0$ to $0.8U_0$, where U_0 is the free stream flow speed.

Curve fits to measured cross-spectral densities of turbulent wall pressure fluctuations reveal that the A and B functions are reasonably approximated by

$$A(\omega\xi_1/U_c) = \exp(-0.1|\omega\xi_1/U_c|) \quad (7\text{-}67)$$

and

$$B(\omega\xi_2/U_c) = \exp(-0.7|\omega\xi_2/U_c|) \; . \quad (7\text{-}68)$$

By equations (6-78) and (7-66), we recognize that

$$\Phi_f(\underline{k},\omega) = \int_{-\infty}^{\infty} R_{ff}(\underline{\xi},\omega)\exp(-i\underline{k}\cdot\underline{\xi})\, d\underline{\xi} \; . \quad (7\text{-}69)$$

Therefore, it can be shown, from equations (7-66) through (7-69), that the wavevector-frequency spectrum of the forcing field of the plate resulting from the turbulent flow is given by

$$\Phi_f(\underline{k},\omega) = \frac{0.28\phi_f(\omega)k_h^{\,2}}{[(0.1k_h)^2 + (k_1 + k_h)^2][(0.7k_h)^2 + k_2^{\,2}]} \; , \quad (7\text{-}70)$$

where k_h is the hydrodynamic wavenumber, defined by

$$k_h = \omega/U_c \; . \quad (7\text{-}71)$$

The wavevector-frequency spectrum of the forcing function associated with the Corcos model of the statistics of the turbulent wall pressure fluctuations is illustrated in figure 7-2. Here, $10\log_{10}$ of the ratio of the wavevector-frequency spectrum (Φ_f) to the frequency spectral density (ϕ_f) is plotted as a function of k_1 and k_2 over the range $-3k_h \leq k_1 \leq 3k_h$ and $-3k_h \leq k_2 \leq 3k_h$. Note that this wavevector-frequency spectrum is characterized by relative maxima, for all values of k_2, at $k_1 = -k_h$. The absolute spectral maximum occurs at $\underline{k} = (-k_h,0)$. To avoid obscuring the shape of this spectrum, the scale of the vertical (i.e., spectral) axis scale is not labeled. However, from equation (7-70), it is easily shown that the difference between the maximum value of $10\log_{10}\{\Phi_f(\underline{k},\omega)/\phi_f(\omega)\}$, which occurs at $\underline{k} = (-k_h,0)$, and the minimum value, which (in figure 7-2) occurs at $\underline{k} = (3k_h,\pm 3k_h)$, is

approximately 45 dB.

By substitution of equations (7-65) and (7-70) into (7-64), we obtain the following expressions for the wavevector-frequency spectrum of the turbulent flow-induced displacement field of a uniform, infinite flat plate:

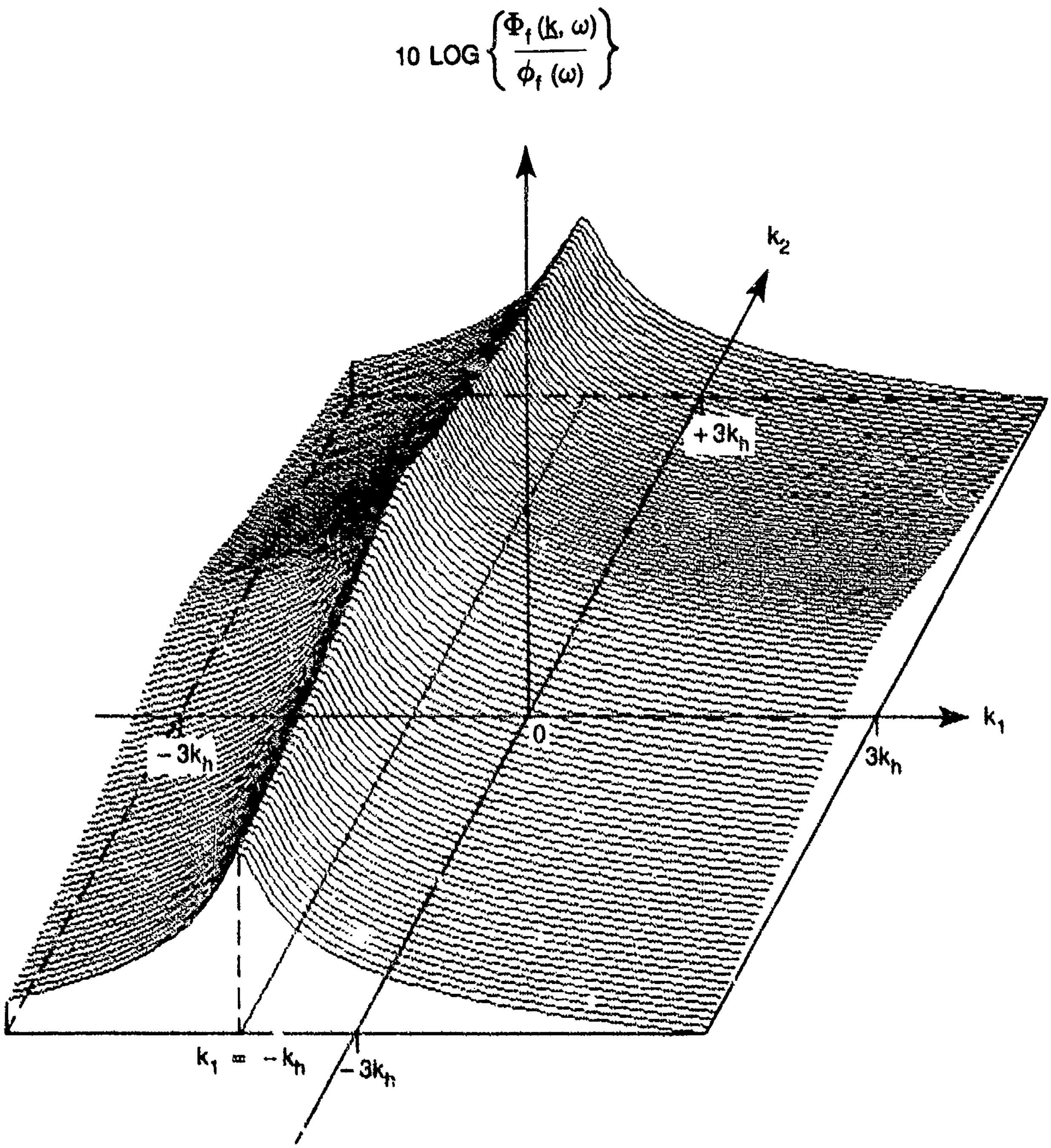

Figure 7-2. Illustration of the Corcos Model of the Wavevector-Frequency Spectrum of the Turbulent Wall Pressure

$$\Phi_w(\underline{k},\omega) = \frac{0.28\phi_f(\omega)}{\left\{[Dk^4 - \mu\omega^2]^2 + \left[r\omega + \dfrac{\rho\omega^2}{k_0\sqrt{(1 - k^2/k_0^2)}}\right]^2\right\}}$$

$$\times \frac{k_h^2}{[(0.1k_h)^2 + (k_1 + k_h)^2][(0.7k_h)^2 + k_2^2]}, \quad k \leq |k_0| , \quad (7\text{-}72)$$

and

$$\Phi_w(\underline{k},\omega) = \frac{0.28\phi_f(\omega)}{\left\{\left[Dk^4 - \mu\omega^2 - \dfrac{\rho\omega^2}{\sqrt{(k^2 - k_0^2)}}\right]^2 + [r\omega]^2\right\}}$$

$$\times \frac{k_h^2}{[(0.1k_h)^2 + (k_1 + k_h)^2][(0.7k_h)^2 + k_2^2]}, \quad k > |k_0| . \quad (7\text{-}73)$$

By inspection of equations (7-72) and (7-73) and use of the discussion of the forced response of the fluid-loaded plate presented in section 5.3.1 of chapter 5, we can establish that, for any given frequency, the wavevector-frequency spectrum of the turbulent flow-induced displacement of the plate is characterized by relative maxima on the circle defined by $|\underline{k}| = k_p{}'$ and in the vicinity of $\underline{k} = (-k_h,0)$. This wavevector-frequency spectrum is difficult to illustrate in three dimensions. However, we can gain some insight to the characteristics of this spectrum by separate examination of its k_1 and k_2 dependence at some fixed frequency.

Figure 7-3 illustrates the k_1 dependence of $\Phi_w(\underline{k},\omega)/\phi_f(\omega)$ at a fixed frequency along the line $k_2 = 0$. For this example, the frequency and the parameters of the plate, flow, and fluid were chosen such that $k_p = 20k_0$ and $k_h = 150k_0$. These parameters are characteristic of a thin steel plate excited by a relatively rapid flow of water. Figure 7-3 shows that, along the k_1 axis, $\Phi_w(k_1,0,\omega)/\phi_f(\omega)$ is characterized by three relative maxima. The two largest spectral contributions occur at $k = \pm k_p{}'$, with the contribution at $-k_p{}'$ being slightly larger. This results from the wavevector-frequency spectrum of the forcing function associated with the turbulent flow being

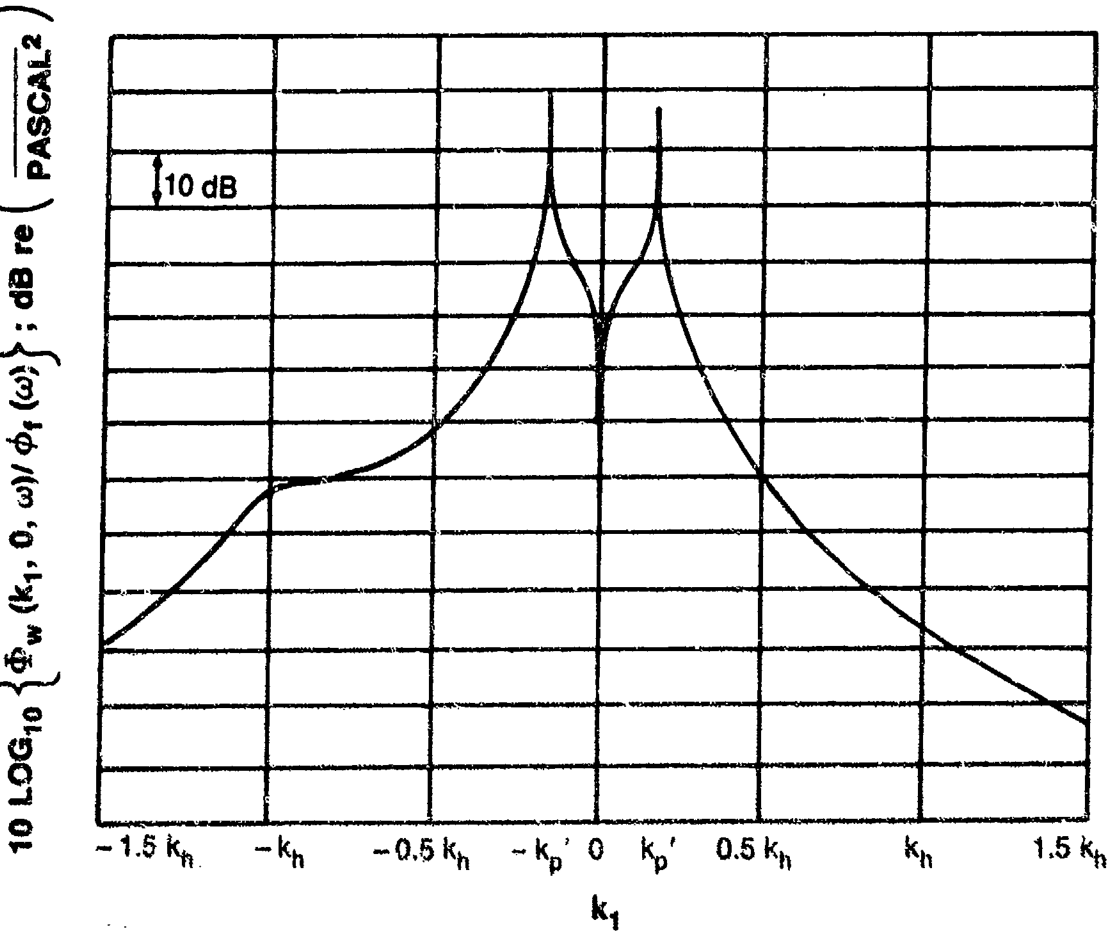

Figure 7-3. Normalized Wavevector Spectrum of the Displacement Field of a Turbulent, Flow-Excited Infinite Plate: k_1 Dependence

greater, for any fixed k_2 and ω, at negative values of k_1 than at positive values of k_1 (see figure 7-2). The third relative maximum occurs near $k_1 = -k_h$, the maximum of the wavevector spectrum of the turbulence excitation. This spectral contribution is seen to be about 70 dB lower than those associated with the resonance (at $k_1 = \pm k_p{}'$) of the fluid-loaded plate. As can be verified by equations (7-64), (7-65), and (7-70), this reduced contribution at the wavenumber associated with the maximum of the spectrum of the turbulence excitation results because $|G(k_1,0,\omega)|^2$ decreases much more rapidly with decreasing k_1 than $\Phi_f(k_1,0,\omega)$ increases with decreasing k_1 over the wavenumber range $-k_h \leq k_1 < -k_p{}'$.

Figure 7-4 illustrates the k_2 dependence of $\Phi_w(\underline{k},\omega)/\phi_f(\omega)$ at a fixed frequency along the line $k_1 = 0$. The frequency and the parameters of

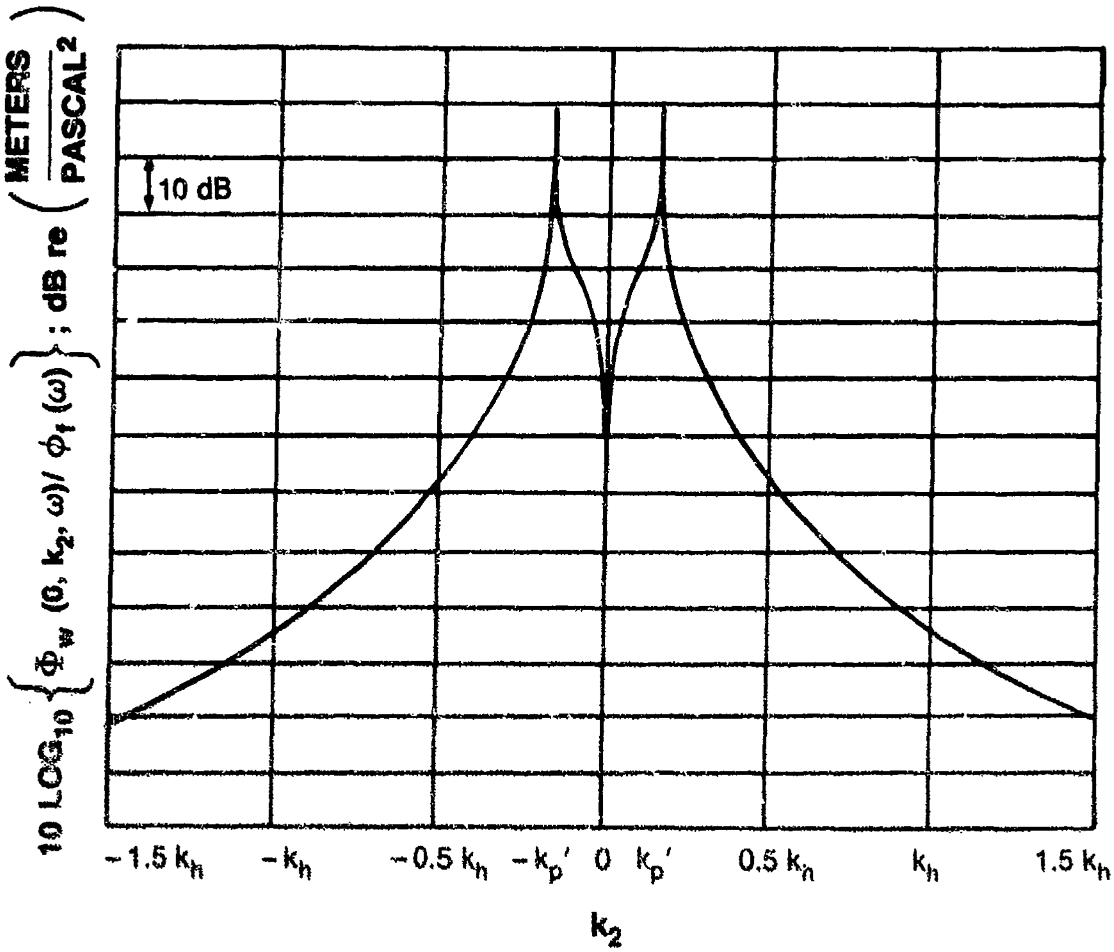

Figure 7-4. Normalized Wavevector Spectrum of the Displacement Field of a Turbulent, Flow-Excited Infinite Plate: k_2 Dependence

the plate and fluid are the same as those used for figure 7-3. Here, we see that, along the k_2 axis, $\Phi_w(0,k_2,\omega)/\phi_f(\omega)$ is characterized by two maxima of equal amplitudes at $k_2 = \pm k_p'$. The equal amplitudes of these maxima are consistent with the even natures of both $\Phi_f(\underline{k},\omega)$ and $|G(\underline{k},\omega)|^2$ in the k_2 variable.

By figures 7-3 and 7-4 and the previously described wavevector-frequency characteristics of $|G(\underline{k},\omega)|$, we conclude that, at any frequency, the dominant contributions to the wavevector-frequency spectrum of the displacement field of the turbulent, flow-excited infinite plate are those in the neighborhood of the circle defined by $k = |\underline{k}| = k_p'$. Consequently, the major contributors to the random space-time displacement field of the turbulent, flow-

excited plate are resonant free waves of the fluid-loaded plate propagating in all directions. However, owing to the slightly larger excitation of waves in the downstream (i.e., negative k_1) direction, the amplitudes of the free waves having downstream velocity components are slightly larger than those having upstream velocity components.

7.3.2 The Displacement Field of a Finite String With Fixed Ends Excited by a Harmonic Wave Field of Unknown Initial Phase

A string of length L, fixed at x = 0 and x = L, is subjected to a force per unit length described by

$$q(x,t) = F_0 \sin(k_0 x + \omega_0 t + \phi) , \qquad (7\text{-}74)$$

over all x and t. Thus, the physical excitation field of the string is a real plane wave characterized by an amplitude F_0, a wavenumber k_0, a frequency ω_0, and an initial phase ϕ. The amplitude, wavenumber, and frequency of this physical forcing field are known, but the initial phase is unpredictable over repeated trials of this experiment. Ignoring the loading effects of the fluid surrounding the string, we wish to predict the second order statistics of the displacement field, w(x,t), of the string that would result from many repetitions of this experiment.

In this problem, the initial phase, ϕ, of the excitation field is a random variable. In the absence of specific knowledge to the contrary, we assume that, in any given trial of the experiment, the value of this random variable is equally probable between $-\pi$ and π. Thus, the probability density function, $f_\phi(\alpha)$, of the initial phase, ϕ, of the physical wave field that excites the string can be written

$$f_\phi(\alpha) = \begin{cases} 1/(2\pi), & -\pi \le \alpha < \pi , \\ \\ 0, & \text{otherwise.} \end{cases} \qquad (7\text{-}75)$$

The physical forcing field, q(x,t), is a function of the random variable, ϕ. By use of equations (6-11) and (7-75), it can be shown that the auto-correlation function of the physical excitation field is given by

$$Q_{qq}(\xi,\tau) = E\{q(x,t)q(x+\xi,t+\tau)\} = \frac{F_0^2}{2}\cos(k_0\xi + \omega_0\tau) \; . \tag{7-76}$$

The fixed-end string is a space-limited system. By the form of equation (7-76), it is evident that the physical excitation field applied to the string is both stationary and homogeneous. Recall, however, that for space-limited systems, the input field is defined to be zero outside the spatial limits of the system. Thus, given that $q(x,t)$ is the physical field applied to the string, and $b(x)$ is the space-limiting function appropriate to that string, then the input field, $f(x,t)$, to the finite, fixed-end string is defined to be

$$f(x,t) = b(x)q(x,t) \; . \tag{7-77}$$

In chapter 4 (see equation (4-11)), we showed that the space-limiting function for the fixed-end string was defined by

$$b(x) = \{U(x) - U(x-L)\} = \begin{cases} 1, & 0 < x < L \; , \\ 0, & \text{otherwise.} \end{cases} \tag{7-78}$$

By equations (6-52) and (7-77), the autocorrelation of the input field to the string is given by

$$Q_{ff}(x,\xi,\tau) = E\{f(x,t)f(x+\xi,t+\tau)\} = E\{b(x)q(x,t)b(x+\xi)q(x+\xi,t+\tau)\} \; . \tag{7-79}$$

However, the space-limiting function is deterministic. Therefore, by equations (7-76) and (7-79), it follows that the autocorrelation function of the input field to the finite, fixed-end string is given by

$$\begin{aligned} Q_{ff}(x,\xi,\tau) &= b(x)b(x+\xi)E\{q(x,t)q(x+\xi,t+\tau)\} = b(x)b(x+\xi)Q_{qq}(\xi,\tau) \\ &= b(x)b(x+\xi)\,\frac{F_0^2}{2}\cos(k_0\xi + \omega_0\tau) \; . \end{aligned} \tag{7-80}$$

Clearly, the input field to the fixed-end string is stationary, but nonhomogeneous.

We know that the finite, fixed-end string is a space-varying system, and we have established that the input field to the string is stationary and nonhomogeneous (even though the physical field applied over all space and time was stationary and homogeneous). By adapting equation (7-56) of section 7.2.2 to the single spatial dimension appropriate to this problem, it follows that the two wavenumber-frequency spectrum of the displacement field of the string, S_{ww}, is related to the two wavenumber-frequency spectrum of the input field, S_{ff}, by

$$S_{ww}(\mu,k,\omega) = \frac{1}{(2\pi)^2} \int_{-\infty}^{\infty} \int_{-\infty}^{\infty} S_{ff}(\beta,\sigma,\omega) G(\mu - k,\sigma - \beta,-\omega) G(k,-\sigma,\omega) \, d\beta \, d\sigma \, , \quad (7\text{-}81)$$

where $G(\mu,k,\omega)$ is the two wavenumber-frequency response of the finite string with fixed ends.

By applying the arguments of section 4.3.1.2 to equation (3-84), we can demonstrate that the forced displacement of a finite, fixed-end, damped string is governed by

$$b(x)\left\{\frac{\partial^2 w}{\partial x^2} - \frac{1}{c_s^2}\frac{\partial^2 w}{\partial t^2} - \frac{r}{T}\frac{\partial w}{\partial t}\right\} = -\frac{b(x)q(x,t)}{T} = -\frac{f(x,t)}{T} \, , \quad (7\text{-}82)$$

for all t within $0 < x < L$. Outside the physical extent of the string, $w(x,t)$ is assumed to be zero. Recall, from section 3.4.5, that T is the tension of the string, c_s is the propagation speed of a free wave on the string, and r is the (constant) coefficient of damping per unit length. By applying techniques similar to those used in section 4.3.3.2 to treat the forced vibration of the simply supported plate, we can show that the Green's function of the finite, fixed-end string is given by

$$g(x,x_0,\theta) = \frac{1}{\pi L T} \int_{-\infty}^{\infty} \sum_{n=1}^{\infty} \frac{b(x_0)\alpha_n(x_0)b(x)\alpha_n(x)\exp(i\Omega\theta)}{[k_s^2(\Omega) - (n\pi/L)^2 - ir\Omega/T]} \, d\Omega \, , \quad (7\text{-}83)$$

where $\alpha_n(x)$ is the n-th normal mode of the finite, fixed-end string, defined by

$$\alpha_n(x) = \sin(n\pi x/L) \ . \tag{7-84}$$

Recall that the two wavenumber-frequency response, $G(\mu,k,\omega)$, is the multiple Fourier transform of the Green's function on the variables x, x_0, and θ. Thus, it follows from equation (7-83) that

$$G(\underline{\mu},\underline{k},\omega) = \frac{2}{LT} \sum_{n=1}^{\infty} \frac{I_n(\mu) I_n(k)}{[k_n^2(\omega) - (n\pi/L)^2 - i r\omega/T]} \ . \tag{7-85}$$

Here, $I_n(k)$ is the Fourier transform of the space-limited n-th mode, $\alpha_n(x)$, of the finite, fixed-end string. That is,

$$I_n(k) = \int_{-\infty}^{\infty} b(x)\alpha_n(x)\exp(-ikx)\ dx \ . \tag{7-86}$$

From equations (6-121) and (7-80), we can show that the two wavevector-frequency spectrum, S_{ff}, of the input field to the string is given by

$$S_{ff}(\mu,k,\omega) = \frac{\pi F_0^2}{2} \ [\delta(\omega - \omega_0)B(\mu - k + k_0)B(k - k_0)$$

$$+ \delta(\omega + \omega_0)B(\mu - k - k_0)B(k - k_0)] \ , \tag{7-87}$$

where B(k) is the spatial Fourier transform of the space-limiting function, b(x). That is,

$$B(k) = \int_{-\infty}^{\infty} b(x)\exp(-ikx)\ dx \ . \tag{7-88}$$

By substitution of equations (7-85) and (7-87) into equation (7-81), and by application of equations (7-86) and (7-88), we can demonstrate that the two

wavevector-frequency spectrum of the displacement field of the string can be written in the form

$$S_{ww}(\mu,k,\omega) = \frac{2\pi F_0^2}{L^2T^2}\,\{V(\mu,k,\omega) + V^*(-\mu,-k,-\omega)\}\ . \qquad (7\text{-}89)$$

Here, $V(\mu,k,\omega)$ is defined by

$$V(\mu,k,\omega) = \delta(\omega - \omega_0)\left\{\sum_{m=1}^{\infty}\sum_{n=1}^{\infty} A_{mn}(k_0)C_{mn}(\omega_0)I_m(\mu - k)I_n(k)\right\}, \qquad (7\text{-}90)$$

where

$$A_{mn}(k_0) = I_m(k_0)I_n^*(k_0) \qquad (7\text{-}91)$$

and

$$C_{mn}(\omega) = \frac{1}{[k_s^2(\omega) - (m\pi/L)^2 + ir\omega/T][k_s^2(\omega) - (n\pi/L)^2 - ir\omega/T]}\ . \qquad (7\text{-}92)$$

Equation (7-89) describes the functional form of the two wavenumber-frequency spectrum of the displacement field of the finite, fixed-end string. Note that this functional form satisfies the conjugate symmetry requirement of equation (6-133): that is, $S_{ww}(\mu,k,\omega) = S_{ww}^*(-\mu,-k,-\omega)$. By inspection of equation (7-90), it is evident that $V(\mu,k,\omega)$ is discrete in frequency, but distributed in the two-wavenumber variables. It is further evident, from equations (7-89) and (7-90), that $V(\mu,k,\omega)$ specifies the wavenumber characteristics of $S_{ww}(\mu,k,\omega)$ over all μ and k at $\omega = \omega_0$ and that $V^*(-\mu,-k,-\omega)$ specifies the wavenumber characteristics of $S_{ww}(\mu,k,\omega)$ over all μ and k at $\omega = -\omega_0$. To determine the two-wavenumber characteristics of $S_{ww}(\mu,k,\omega)$ at these discrete frequcncies, we must determine the two-wavenumber characteristics of $V(\mu,k,\omega)$.

Equation (7-90) shows that the wavenumber dependence of $V(\mu,k,\omega)$ is dictated by a weighted summation of terms of the form $I_m(\mu - k)I_n(k)$ over all positive integer values of m and n. The wavenumber characteristics of $I_n(k)$

were treated in section 4.2.1 of chapter 4, and are well understood. Therefore, the two-wavenumber dependence of any single term, say $I_M(\mu - k)I_N(k)$, in the summation can be easily deduced. However, the two-wavenumber characteristics of the summation of weighted products of $I_m(\mu - k)I_n(k)$ comprising $V(\mu,k,\omega)$ are obscure. To provide some insight into these wavenumber characteristics, we apply arguments similar to those used (in section 4.3.3.2) to analyze the wavevector-frequency characteristics of the forced vibration field of the simply supported plate.

Recall that the frequency, ω_0, and the wavenumber, k_0, that characterize the physical excitation field are known and independent parameters. Note, by equations (7-91) and (7-92), that the modal weighting function $A_{mn}(k_0)$ is a function only of the wavenumber that characterizes the excitation field, and the modal weighting function $C_{mn}(\omega_0)$ depends only on the frequency of the harmonic wave excitation. Let us examine the weighting of the products $I_m(\mu - k)I_n(k)$ as a function of the mode numbers, m and n. We first consider the weighting properties of $A_{mn}(k_0)$.

Recall, from section 4.2.1, that the magnitude of $I_m(k)$ is characterized by two primary maxima, of equal amplitude, at the wavenumbers $k = (\pm m\pi/L)$, and by secondary maxima at $k = \{\pm[m \pm (2p + 1)]\pi/L\}$ for integer values of p equal to or greater than one. However, the ratio of the magnitudes of the secondary to primary maxima is of the order of $|2p + 1|^{-1}$, so the magnitudes of the secondary maxima are considerably smaller than the magnitude of the maxima at $k = (\pm m\pi/L)$. It should also be noted that the amplitudes of the primary maxima of $|I_m(k)|$ are independent of the modal number m. By these properties of $|I_m(k)|$, it is evident that, if the wavenumber, k_0, that characterizes the harmonic excitation field equals either of the wavenumbers characterizing a primary maximum of $|I_M(k_0)|$ (i.e., k_0 equals either $M\pi/L$ or $-M\pi/L$), then $A_{MM}(k_0) \cdot |I_M(M\pi/L)|^2$ will be considerably larger, in magnitude, than any other value of $A_{mn}(k_0)$. If, on the other hand, k_0 does not equal a wavenumber associated with a maximum of $|I_n(k_0)|$ for any choice of m, and therefore falls between the maxima associated with two consecutive modes (say the M and $N = M + 1$ modes), then it can be argued that $A_{MM}(k_0)$, $A_{NN}(k_0)$, $A_{MN}(k_0)$, and $A_{NM}(k_0)$ will be significantly larger, in magnitude, than all other values of $A_{mn}(k_0)$. Thus, it is evident that the magnitude of the weighting function

$A_{mn}(k_0)$ will be relatively large for those combinations of modal numbers (M,N) at which the wavenumber characterizing the plane wave excitation, k_0, closely approximates, in magnitude and direction, one of the wavevectors $(\pm M\pi/L)$ characterizing the maxima of $I_M(k)$ and one of the wavevectors $(\pm N\pi/L)$ characterizing the maxima of $I_N(k)$.

Let us now address the dependence of the weighting coefficient $C_{mn}(\omega_0)$ on the mode numbers, m and n. For the known and fixed frequency (ω_0) of the excitation, it is evident from equation (7-92) that the magnitude of the weighting function $C_{mn}(\omega_0)$ will be relatively large at those combinations of modal numbers (m and n) at which the magnitudes of both $k_s^2(\omega_0) - (m\pi/L)^2$ and $k_s^2(\omega_0) - (n\pi/L)^2$ are smaller than, or comparable to, the magnitude of $r\omega_0/T$. As discussed in section 4.2.1, a modal number associated with a zero value of $k_s^2(\omega_0) - (m\pi/L)^2$ identifies a resonant mode of the plate at the frequency ω_0, and modal numbers associated with values of $k_s^2(\omega_0) - (m\pi/L)^2$ that are comparable, in magnitude, to $r\omega_0/T$ identify near-resonant modes of the plate. For modes well removed from resonance, $|k_s^2(\omega_0) - (m\pi/L)^2|$ becomes large, and the values of $|C_{mn}(\omega_0)|$ associated with combinations of nonresonant mode numbers become small relative to those values associated with resonant and near-resonant modes. Clearly, the magnitudes of weighting coefficient $C_{mn}(\omega_0)$ will be largest for those combinations of mode numbers, m and n, associated with resonant or near-resonant modes at the frequency ω_0: that is, either at that mode number, M, at which $|k_s^2(\omega_0) - (M\pi/L)^2|$ equals zero or at those mode numbers, M and N, at which both $|k_s^2(\omega_0) - (M\pi/L)^2|$ and $|k_s^2(\omega_0) - (N\pi/L)^2|$ are smaller than or comparable to $|r\omega_0/T|$.

According to equation (7 90), $V(\mu,k,\omega)$ is obtained by summing the product $A_{mn}(k_0)C_{mn}(\omega_0)I_m(\mu - k)I_n(k)$ over all integer values of m and n equal to or greater than one. Thus, the two-wavenumber dependence of $V(\mu,k,\omega)$ is dictated by the sum of the weighted products of $I_m(\mu - k)$ and $I_n(k)$. From our discussion of the weighting coefficient $A_{mn}(k_0)$, we know that, for any particular mode, say the M-th, $|I_M(k)|$ has two maxima, of equal amplitude, located at $k = (\pm M\pi/L)$. It therefore follows that the magnitude of the specific product $I_M(\mu - k)I_N(k)$ has four maxima, all of equal amplitude, located at the intersections of $k = (\pm N\pi/L)$ with $\mu - k = (\pm M\pi/L)$. As shown in figure 7-5, these intersections occur at (μ,k) equal to $([M + N]\pi/L, N\pi/L)$, $([M - N]\pi/L, -N\pi/L)$,

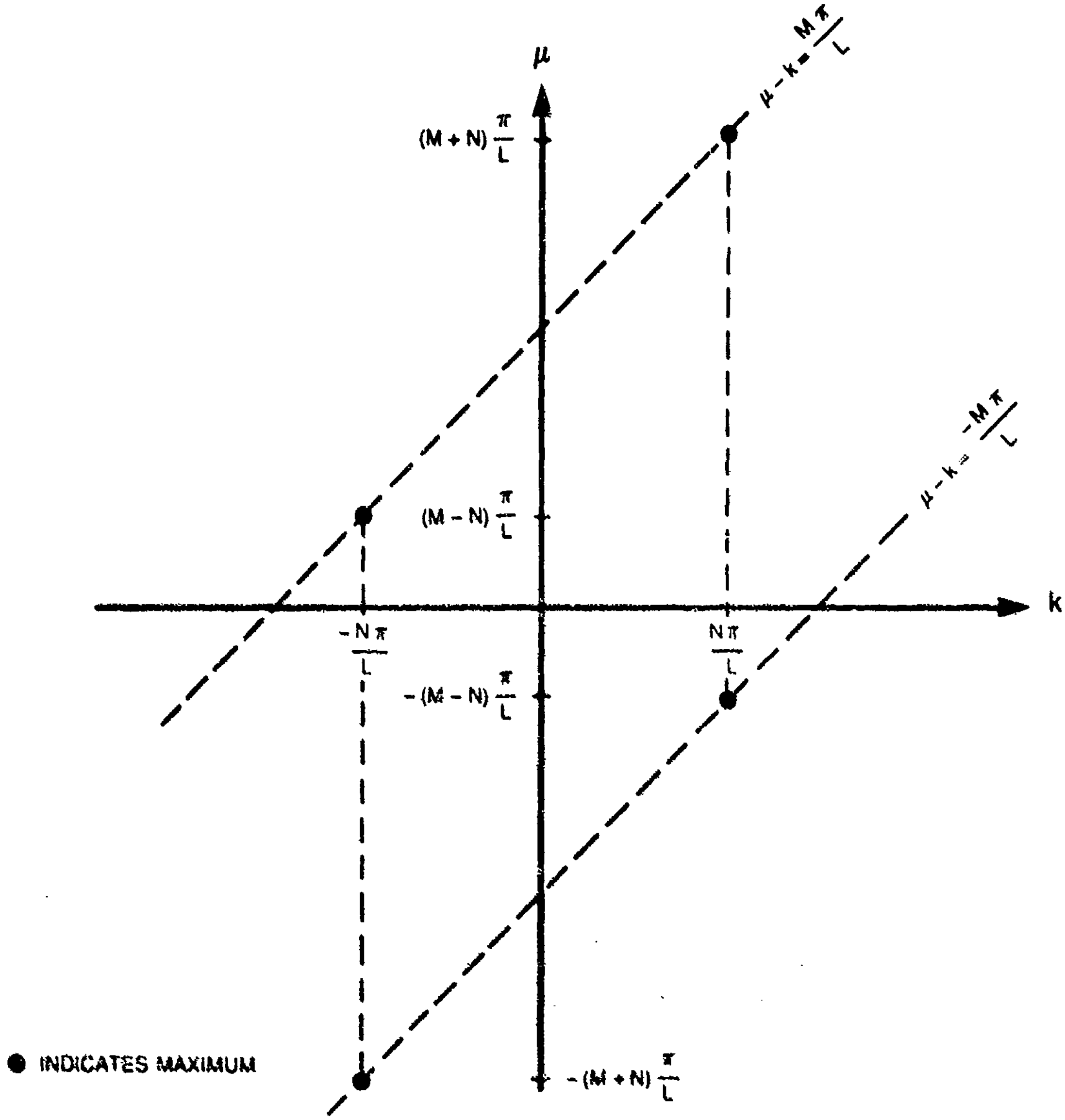

Figure 7-5. Locations of the Primary Maxima of $I_m(\mu - k)I_n(k)$ in the (μ,k) Plane

$(-[M - N]\pi/L, N\pi/L)$, and $(-[M + N]\pi/L, -N\pi/L)$.

The locations of the maxima of $I_M(\mu - k)I_N(k)$ are easily interpreted in terms of the autocorrelation function of the displacement field of the string. By use of equations (7-51), (7-80), and (7-83), or by the inverse Fourier transformation of equation (7-89), it can be shown that the autocorrelation of the displacement field of the fixed-end string excited by a

single wave component (of unknown initial phase) of force per unit length can be described by

$$Q_{ww}(x,\xi,\tau) = \frac{2F_0^2}{L^2T^2}\sum_{m=1}^{\infty}\sum_{n=1}^{\infty} \mathrm{Re}\{A_{mn}(k_0)C_{mn}(\omega_0)\exp(i\omega_0\tau)\}$$

$$b(x)\alpha_m(x)b(x+\xi)\alpha_n(x+\xi) \ . \tag{7-93}$$

It is easily verified (see equation (7-86)) that $I_M(\mu - k)I_N(k)$ is the double Fourier transform of the product of the M- and N-th space-limited modes, $b(x)\alpha_M(x)b(x+\xi)\alpha_N(x+\xi)$, of the fixed-end string on the variables x and ξ. Thus, $I_M(\mu - k)I_N(k)$ identifies, in the two-wavenumber domain, the wave contributions to the autocorrelation function, in both the x and ξ coordinates, from the product of the M- and N-th space-limited modes. It is easily demonstrated that

$$\alpha_M(x)\alpha_N(x+\xi) =$$

$$\frac{1}{4}([\exp\{-i(M - N)\pi x/L\} - \exp\{i(M + N)\pi x/L\}]\exp\{iN\pi\xi/L\}$$

$$+ [\exp\{i(M - N)\pi x/L\} - \exp\{-i(M + N)\pi x/L\}]\exp\{-iN\pi\xi/L\}) \ . \tag{7-94}$$

Recall that, in $S_{ww}(\mu,k,\omega)$, the wavenumber μ reflects the variation of $Q_{ww}(x,\xi,\tau)$ in the absolute spatial variable x, while k reflects the variation of the autocorrelation function in the spatial separation variable ξ. By equations (7-93) and (7-94), it is evident that the product $\alpha_M(x)\alpha_N(x+\xi)$ introduces wavelike contributions to the autocorrelation function that, in the variable ξ, can be expressed as the weighted sum of $\exp(iN\pi\xi/L)$ and $\exp(-iN\pi\xi/L)$. The wavenumbers (k) that characterize these sinusoidal variations in ξ are $N\pi/L$ and $-N\pi/L$, respectively. By equation (7-94), it is evident that the weightings of $\exp(iN\pi\xi/L)$ and $\exp(-iN\pi\xi/L)$ are functions of the absolute spatial variable, x. The weighting of $\exp(iN\pi\xi/L)$ comprises two components that vary sinusoidally in x. These components are characterized by the wavenumbers $-(M - N)\pi/L$ and $(M + N)\pi/L$, respectively. Note, from

figure 7-5, that these are the values of μ that characterize the maxima of $I_M(\mu - k)I_N(k)$ at $k = N\pi/L$. The weighting of $\exp(-iN\pi\xi/L)$ also comprises two-wave components in x, which are characterized by the wavenumbers $-(M + N)\pi/L$ and $(M - N)\pi/L$. The reader can verify that these values of μ specify the locations of the maxima of $I_M(\mu - k)I_N(k)$ at $k = -N\pi/L$. Thus, we conclude that the locations of the maxima of $I_M(\mu - k)I_N(k)$ in the (μ,k) domain correspond to those wavenumbers that characterize the product of the normal modes, $\alpha_M(x)\alpha_N(x + \xi)$, over all x and ξ.

To illustrate how significant wavenumber characteristics of the displacement field of a fixed-end string excited by a wave component (of unknown phase) of force per unit length are deduced from the properties of $A_{mn}(k_0)$, $C_{mn}(\omega_0)$, and $I_m(\mu - k)I_n(k)$, consider the special case in which the wavenumber, k_0, of the applied physical wave is equal to the wavenumber characterizing the Q-th normal mode of the string (i.e., $k_0 = Q\pi/L$) and the frequency of that applied physical wave is equal to the natural frequency of the S-th mode of the string (i.e., $\omega_0 = S\pi c_s/L$). For this example, we also assume that, for any mode m, the damping coefficient (r) is a constant proportion (say ϵ) of the modal critical value (r_{cm}). The critical damping coefficient of the m-th mode can be shown (from equation (7-83)) to be given by $r_{cm} = 2\pi mT/(Lc_s)$.

From equations (4-31), (4-32), and (7-91), it can be shown that

$$|A_{mn}(Q\pi/L)| = \frac{mnL^2}{(Q + m)(Q + n)} \left|\frac{\sin[(Q - m)\pi/2]}{(Q - m)\pi/2}\right|\left|\frac{\sin[(Q - n)\pi/2]}{(Q - n)\pi/2}\right| . \quad (7\text{-}95)$$

Further, under the assumption that $r = \epsilon r_{cm}$ for all mode numbers (m), it follows from equation (7-92) that

$$|C_{mn}(S\pi c_s/L)| = \frac{L^4}{\pi^4\{[(S^2 - m^2)^2 + (2\epsilon Sm)^2][(S^2 - n^2)^2 + (2\epsilon Sn)^2]\}^{1/2}} . \quad (7\text{-}96)$$

From our discussion of the properties of $A_{mn}(k_0)$ and $C_{mn}(\omega_0)$, we know that the maximum value of $|A_{mn}(Q\pi/L)|$ is associated with the modal numbers $m = n = Q$, and that the maximum value of $|C_{mn}(S\pi c_s/L)|$ is associated with the modal numbers

$m = n = S$. Clearly then, we wish to evaluate the relative magnitudes of $|A_{QQ}(Q\pi/L)C_{QQ}(S\pi c_s/L)|$ and $|A_{SS}(Q\pi/L)C_{SS}(S\pi c_s/L)|$. However, by inspection of the forms of equations (7-95) and (7-96), it also appears prudent to consider the relative magnitudes of $|A_{QS}(Q\pi/L)C_{QS}(S\pi c_s/L)|$ and $|A_{SQ}(Q\pi/L)C_{SQ}(S\pi c_s/L)|$, which, it will be noted, are equal.

Under the assumption that ϵ (the ratio of the damping to the modal critical value) is much smaller than $1/\sqrt{2}$ for all modes, we can use equations (7-95) and (7-96) to show that

$$\frac{|A_{SS}(Q\pi/L)C_{SS}(S\pi c_s/L)|}{|A_{QQ}(Q\pi/L)C_{QQ}(S\pi c_s/L)|} = \begin{cases} 4/(\pi\epsilon S)^2, & |Q - S| \text{ odd,} \\ 0, & |Q - S| \text{ even,} \end{cases} \tag{7-97}$$

$$\frac{|A_{SS}(Q\pi/L)C_{SS}(S\pi c_s/L)|}{|A_{QS}(Q\pi/L)C_{QS}(S\pi c_s/L)|} = \begin{cases} 2/(\pi\epsilon S), & |Q - S| \text{ odd,} \\ 0, & |Q - S| \text{ even,} \end{cases} \tag{7-98}$$

and

$$\frac{|A_{QS}(Q\pi/L)C_{QS}(S\pi c_s/L)|}{|A_{QQ}(Q\pi/L)C_{QQ}(S\pi c_s/L)|} = \begin{cases} 2/(\pi\epsilon S), & |Q - S| \text{ odd,} \\ 0, & |Q - S| \text{ even.} \end{cases} \tag{7-99}$$

By these equations, it is evident that the relative magnitudes of the joint modal weightings depends on $|Q - S|$, the magnitude of the difference between the mode number characterizing the wavenumber of excitation (Q) and that characterizing the frequency of the excitation (S).

Consider, first, the case where $|Q - S|$ is odd. Here, the relative magnitudes of the joint modal weightings are seen to depend on the quantity $\pi\epsilon S/2$. For excitation frequencies $(S\pi c_s/L)$ and proportions of critical damping (ϵ) sufficiently small that $\epsilon S < 2/\pi$, it is evident that

$$\begin{aligned} |A_{SS}(Q\pi/L)C_{SS}(S\pi c_s/L)| &> |A_{QS}(Q\pi/L)C_{QS}(S\pi c_s/L)| \\ &> |A_{QQ}(Q\pi/L)C_{QQ}(S\pi c_s/L)| \ . \end{aligned} \tag{7-100}$$

We can therefore expect the two-wavenumber characteristics of $V(\mu,k,S\pi c_s/L)$ will be most strongly affected by the contribution from $I_S(\mu - k)I_S(k)$, with weaker contributions from $I_Q(\mu - k)I_S(k)$ and its complex conjugate

$I_S(\mu - k)I_Q(k)$, and yet weaker contributions from $I_Q(\mu - k)I_Q(k)$. By our previous arguments, therefore, we can expect the magnitude of the two-wavenumber spectrum of the displacement field of the string at the frequency $S\pi c_s/L$ to have the following characteristics:

(1) Four primary maxima, of equal amplitudes, at the two-wavenumber (μ,k) locations associated with the maxima of $|I_S(\mu - k)I_S(k)|$: that is, at $(0,S\pi/L)$, $(2S\pi/L,S\pi/L)$, $(0,-S\pi/L)$, and $(-2S\pi/L,-S\pi/L)$.

(2) Eight secondary maxima of equal, but lower than primary, amplitudes at the two-wavenumber locations associated with the maxima of $|I_Q(\mu - k)I_S(k)|$ and $|I_S(\mu - k)I_Q(k)|$: that is, at $[(S + Q)\pi/L,S\pi/L]$, $[(S - Q)\pi/L,S\pi/L]$, $[(-S + Q)\pi/L,-S\pi/L]$, $[-(S + Q)\pi/L,-S\pi/L]$, and at $[(Q + S)\pi/L,Q\pi/L]$, $[(Q - S)\pi/L,Q\pi/L]$, $[(-Q + S)\pi/L,-Q\pi/L]$, $[-(Q + S)\pi/L,-Q\pi/L]$, respectively.

(3) Four maxima of equal, but lower than secondary, amplitudes at the two-wavenumber locations corresponding to the maxima of $|I_Q(\mu - k)I_Q(k)|$: that is, at $(0,Q\pi/L)$, $(2Q\pi/L,Q\pi/L)$, $(0,-Q\pi/L)$, and $(-2Q\pi/L,-Q\pi/L)$.

Thus, the magnitude of the two-wavenumber spectrum of the displacement field of the string at the frequency $S\pi c_s/L$ can be expected to be characterized by 16 relative maxima. The ratio of the amplitudes of any of the four primary maxima to any of the eight secondary maxima is approximately $2/(\pi\epsilon S)$, and the ratio of the amplitudes of the primary maxima to the tertiary maxima is approximately $4/(\pi\epsilon S)^2$.

For $|Q - S|$ odd and excitation frequencies $(S\pi c_s/L)$, but proportions of critical damping (ϵ) sufficiently large that $\epsilon S > 2/\pi$, the magnitude of the two-wavenumber spectrum of the displacement field of the string at the frequency $S\pi c_s/L$ is characterized by relative maxima at the same two-wavenumber locations identified for the case where $\epsilon S < 2/\pi$. However, for $\epsilon S > 2/\pi$, the order of the primary, secondary, and tertiary maxima is reversed from that presented above. That is, the primary maxima occur at the two-wavenumber locations associated with the maxima of $|I_Q(\mu - k)I_Q(k)|$, and the tertiary maxima occur at the two-wavenumber locations corresponding to maxima

of $|I_S(\mu - k)I_S(k)|$. The wavenumber locations of the eight secondary maxima remain unchanged.

For $|Q - S|$ odd, excitation frequencies $(S\pi c_s/L)$, and proportions of critical damping (ϵ) such that $\epsilon S = 2/\pi$, the magnitude of the two-wavenumber spectrum is characterized by 16 maxima at the two-wavenumber locations identified previously. However, when $\epsilon S = 2/\pi$, all 16 maxima have approximately the same amplitudes.

We now turn attention to wavenumbers $(Q\pi/L)$ and frequencies $(S\pi c_s/L)$ of excitation such that $|Q - S|$ is even and the ratios of the joint modal weightings given by equations (7-97)-(7-99) are zero. These zero values are a reflection of the behavior of the term $I_S(Q\pi/L)$ in $A_{SS}(Q\pi/L)$, $A_{QS}(Q\pi/L)$, and $A_{SQ}(Q\pi/L)$. That is, $I_S(Q\pi/L)$ is equal to zero for $|Q - S|$ even, as can be confirmed by inspection of figure 4-1(a). However, when $|Q - S|$ is even, it can be demonstrated that $I_{S-1}(Q\pi/L)$ and $I_{S+1}(Q\pi/L)$, the wavenumber transforms of the normal modes adjacent to the S-th, are nonzero. Thus, when $|Q - S|$ is even, it can be argued that the largest, in magnitude, joint modal weightings are $|A_{QQ}(Q\pi/L)C_{QQ}(S\pi c_s/L)|$, $|A_{QS+1}(Q\pi/L)C_{QS+1}(S\pi c_s/L)|$ and $|A_{S+1Q}(Q\pi/L)C_{S+1Q}(S\pi c_s/L)|$, $|A_{QS-1}(Q\pi/L)C_{QS-1}(S\pi c_s/L)|$ and $|A_{S-1Q}(Q\pi/L)C_{S-1Q}(S\pi c_s/L)|$, $|A_{S+1S+1}(Q\pi/L)C_{S+1S+1}(S\pi c_s/L)|$ and $|A_{S-1S-1}(Q\pi/L)C_{S-1S-1}(S\pi c_s/L)|$. Thus, it is likely that the magnitude of the two-wavenumber spectrum reflects contributions from the maxima of each of the terms $|I_Q(\mu - k)I_Q(k)|$, $|I_Q(\mu - k)I_{S+1}(k)|$, $|I_Q(\mu - k)I_{S-1}(k)|$, $|I_{S+1}(\mu - k)I_Q(k)|$, $|I_{S-1}(\mu - k)I_Q(k)|$, $|I_{S+1}(\mu - k)I_{S+1}(k)|$, and $|I_{S-1}(\mu - k)I_{S-1}(k)|$.

As shown in figure 4-1(a), the primary lobes of $I_m(k)$ are $4\pi/L$ wide. Thus, as described in section 4.2.1, if one forms the sum of $I_{m-1}(k)$ and $I_{m+1}(k)$, the two sets of primary lobes interact to form a single set of lobes centered at $\pm m\pi/L$. Based on these observations, we argue as follows:

(1) The primary lobes of the weighted sum of $I_Q(\mu - k)I_{S+1}(k)$ and $I_Q(\mu - k)I_{S-1}(k)$ interact in such a fashion that the magnitude of their sum produces maxima in the vicinity of the intersections of $k = \pm S\pi/L$ and $\mu - k = \pm Q\pi/L$: that is, at $[(S + Q)\pi/L, S\pi/L]$,

$[(S - Q)\pi/L, S\pi/L]$, $[(-S + Q)\pi/L, -S\pi/L]$, and $[-(S + Q)\pi/L, -S\pi/L]$.

(2) The primary lobes of the weighted sum of $I_{S-1}(\mu - k)I_Q(k)$ and $I_{S+1}(\mu - k)I_Q(k)$ interact in such a fashion that the magnitude of their sum produces maxima in the vicinity of the intersections of $k = \pm Q\pi/L$ and $\mu - k = \pm S\pi/L$: that is, at $[(Q + S)\pi/L, Q\pi/L]$, $[(Q - S)\pi/L, Q\pi/L]$, $[(-Q + S)\pi/L, -Q\pi/L]$, and $[-(Q + S)\pi/L, -Q\pi/L]$.

(3) The primary lobes of the weighted sum of $I_{S-1}(\mu - k)I_{S-1}(k)$ and $I_{S+1}(\mu - k)I_{S+1}(k)$ interact in such a fashion that the magnitude of their sum produces maxima in the vicinity of the intersections of $k = \pm S\pi/L$ and $\mu - k = \pm S\pi/L$: that is, at $(0, S\pi/L)$, $(2S\pi/L, S\pi/L)$, $(0, -S\pi/L)$, and $(-2S\pi/L, -S\pi/L)$.

(4) The maxima associated with $I_Q(\mu - k)I_Q(k)$ are identical to those discussed previously.

The reader will note that the wavenumber locations of the 16 maxima listed above correspond to the locations of the 16 spectral maxima identified for $|Q - S|$ odd.

On the basis of the above arguments, we contend that, when $|Q - S|$ is even, the two-wavenumber characteristics of the magnitude of the two-wavenumber spectrum of the displacement field of the string at the frequency $S\pi c_s/L$ are similar to those described previously for $|Q - S|$ odd. We further contend that it is reasonable to expect that, when $|Q - S|$ is even, the modal numbers identifying the two-wavenumber locations of the primary, secondary, and tertiary spectral maxima are determined by the value of $2/(\pi\epsilon S)$ in the same fashion as when $|Q - S|$ is even. That is, it will be recalled that the maxima of $|I_m(\mu - k)I_n(k)|$ are located at the intersections of $k = \pm n\pi/L$ and $\mu - k = \pm m\pi/L$. Clearly, knowledge of the modal numbers, m and n, associated with a large weighting, $|A_{mn}(Q\pi/L)C_{mn}(S\pi c_s/L)|$, is sufficient to determine the two-wavenumber locations of the maxima of $|I_m(\mu - k)I_n(k)|$. Thus, when $\epsilon S < 2/\pi$, we can expect (according to equations (7-97)-(7-99)) the locations of the primary maxima to be those associated with the mode numbers S,S; the locations of the secondary maxima to be those associated with the

mode numbers Q,S and S,Q; and the location of the tertiary maxima to be those associated with the mode numbers Q,Q. When $\epsilon S > 2/\pi$, we expect that this ordering would be reversed.

This example of a relatively simple one-dimensional, space-limited system excited by a physical forcing field consisting of a single wave of undetermined phase well illustrates the complexities associated with predicting and interpreting the characteristics of the two wavenumber-frequency spectrum of nonhomogeneous, stationary fields. However, from our analysis of this simple example, we were able to deduce the following characteristics of the two wavenumber-frequency spectrum of the displacement field of the fixed-end string:

(1) Owing to the time invariance of the system and the stationarity of the single wave excitation field, the two wavenumber-frequency spectrum is discrete in frequency, and is characterized by Dirac delta functions at $\omega = \pm S\pi c_S/L$ (the frequencies associated with the wave component of excitation).

(2) The magnitude of the two-wavenumber spectrum at the discrete frequencies $\pm S\pi c_S/L$ is distributed in both μ and k, and is characterized by several relative maxima.

(3) The k (Fourier conjugate of the spatial separation variable ξ) coordinates of these relative maxima are consistent with the wavenumbers, $\pm Q\pi/L$, that characterize the excitation field and the resonant wavenumbers, $\pm S\pi/L$, associated with the frequency of excitation, $S\pi c_S/L$.

(4) The μ (Fourier conjugate of the absolute spatial variable x) coordinates of the relative maxima are specified by the intersection of the lines $\mu - k = \pm Q\pi/L$ and $\mu - k = \pm S\pi/L$ with the lines $k = \pm q\pi/L$ and $k = \pm S\pi/L$. For each value of k, the associated values of μ identify the wavenumbers that characterize the variation of the autocorrelation function of the displacement field in the absolute spatial coordinate, x.

(5) The two-wavenumber coordinates (μ, k) of the various maxima of the magnitude of the two-wavenumber spectrum are specified by ordered pairs of the modal numbers, Q and S. Each ordered pair of mode numbers identifies four relative maxima of equal amplitude. The relative amplitudes of the maxima associated with the various ordered pair of modal numbers are determined by the value of ϵS, the product of the proportion of critical damping in the string, and the modal frequency of excitation.

It should be emphasized that the above observations apply only to the specific example of a fixed-end string excited by a single wave component (of unknown phase) of force per unit length. However, the procedures used for estimating the locations and relative magnitudes of the maxima of the magnitude of the two wavenumber-frequency spectrum can be applied to other space-limited systems. Further, the interpretation of the two-wavenumber characteristics of the spectrum in terms of the autocorrelation function (and vice versa) is applicable to all nonhomogeneous fields.

7.4 REFERENCES

1. M. M. Junger and D. Feit, Sound, Structures, and Their Interaction, (Second Edition), MIT Press, Cambridge, MA, 1986, p. 344.

2. G. M. Corcos, "Resolution of Pressure in Turbulence," Journal of the Acoustical Society of America, vol. 35, February 1963, pp. 192-199.

CHAPTER 8

THE MEASUREMENT PROBLEM

In the previous chapters, we have developed the theory of wavevector-frequency analysis for the various classes of fields and systems encountered in linear acoustics. In short, this theory demonstrates that the mathematical description, and thereby the physical interpretation, of certain classes of systems is greatly simplified by expressing their input-output relationships in the wavevector-frequency, rather than the space-time, domain. It must be recognized, however, that the development of mathematical models of systems is usually motivated by empirical observations. Moreover, such mathematical models can be validated only through agreement with measured data. Therefore, to take practical advantage of the mathematical and interpretational benefits offered by wavevector-frequency analysis, we must be able to obtain desired wavevector-frequency characteristics of space-time fields from measured data. The estimation of such wavevector-frequency characteristics of acoustic fields from measured data is the subject of these next two chapters.

Note that we use the phrase "estimation of the wavevector-frequency characteristics...from measured data" rather than "measurement of the wavevector-frequency characteristics...." Our choice of phrasing can best be justified by an illustrative example. Consider the problem of characterizing a pressure field, $p(\underline{x},t)$, in the wavevector-frequency domain from measured data. If the field is known to be deterministic, it is completely characterized by its wavevector-frequency transform, $P(\underline{k},\omega)$. By definition, however, $P(\underline{k},\omega)$ requires knowledge of the pressure at every point in space over all time. If the pressure field is random, the field is characterized by an appropriate form of wavevector-frequency spectrum. By reference to chapter 6, any form of the wavevector-frequency spectrum requires knowledge of the pressure field over all time and space for all possible realizations of that field. Clearly, these are impossible measurement tasks. In practice, we can measure only samples of the pressure field over some finite limits in space and time. Further, we cannot obtain a true ensemble of any measurement of a

random pressure field inasmuch as we can afford only a limited number of replications of either the experimental apparatus or the measurement. Finally, most pressure measurements are performed with sensors, or transducers, which convert the locally sensed pressure to an electrical signal. Therefore, the value of the pressure must be inferred from the measured electrical signal. In consequence of these practical limitations, we cannot exactly determine any wavevector-frequency descriptor of a space-time field from measured data. Rather, we can obtain only some estimate, or approximation, of it.

It is intuitively obvious that the quality, or accuracy, of the estimate of any descriptor of a field must decrease as the limitations imposed on the measurement of that field increase. It is also obvious that any measurement program is subject to fiscal, temporal, and material constraints. However, within these constraints, the experimenter can control, to some degree, the various limitations he imposes on the measurement. To exercise this control to optimal advantage, the experimenter requires "a priori" knowledge of the consequences of each measurement limitation on the estimate of the desired descriptor.

Limitations on spatial and temporal sampling and the use of transducers are problems common to the measurement of all acoustic fields. This chapter examines the consequences of these common problems on the estimates of various descriptors of space-time fields.

Limitations on replications of apparatus or trials affect only the measurement of random acoustic fields. The estimation of wavevector-frequency spectra of such random fields is the subject of the next chapter.

8.1 SENSORS

Most measurements of acoustic fields are performed by use of sensors or transducers, which convert the local acoustic field variable of interest (pressure, displacement, velocity, etc.) into an electrical variable (voltage or current). In this section, we relate various descriptors of measured space-time fields to the descriptors of the field being measured. For

purposes of illustration, here and throughout this chapter, we will assume the acoustic field of interest to be the pressure field, $p(\underline{x},t)$, at the surface of the planar boundary defined by $x_3 = 0$.

In 1952, Uberoi and Kovasznay[1] theorized that, for a very large class of useful (linear) transducers, the output field from the transducer, $o(\underline{x},t)$, was related to the field being measured, $p(\underline{x},t)$, by

$$o(\underline{x},t) = \int_{-\infty}^{\infty}\int_{-\infty}^{\infty} g(\underline{s} - \underline{x})p(\underline{s},t)\, d\underline{s} \ , \tag{8-1}$$

where $g(\underline{s} - \underline{x})$ is the (assumed instantaneous) output of the transducer located at $\underline{x}$ to an impulsive loading applied at the spatial location $\underline{s}$. In 1969, Strawderman[2] extended this theory to include transducers that do not respond instantaneously in time.

To apply this theory to the measurement of the surface pressure field, consider the planar transducer illustrated in figure 8-1. We assume the transducer to be a linear, time-invariant causal device. As indicated by the figure, the impulse response, $g(\underline{s} - \underline{x}_0, t - t')$, of a transducer centered at $\underline{x}_0$ is defined as the output, $o(\underline{x}_0,t)$, from the transducer at time t resulting from an impulsive loading applied at the spatial location $\underline{s}$ at time t'. By the principle of superposition for linear systems, it follows that the output of a transducer located at $\underline{x}_0$ on the surface $x_3 = 0$ is related to the pressure field, $p(\underline{x},t)$, acting on that surface by

$$o(\underline{x}_0,t) = \int_{-\infty}^{t}\int_{-\infty}^{\infty}\int_{-\infty}^{\infty} g(\underline{s} - \underline{x}_0, t - t')p(\underline{s},t')\, d\underline{s}\, dt' \ . \tag{8-2}$$

However, by defining $\underline{z} = \underline{s} - \underline{x}_0$ and $\theta = t - t'$, and by recalling that the transducer is a causal device, we can rewrite equation (8-2) in the form

$$o(\underline{x}_0,t) = \int_{-\infty}^{\infty}\int_{-\infty}^{\infty}\int_{-\infty}^{\infty} g(\underline{z},\theta)p(\underline{x}_0 + \underline{z}, t - \theta)\, d\underline{z}\, d\theta \ . \tag{8-3}$$

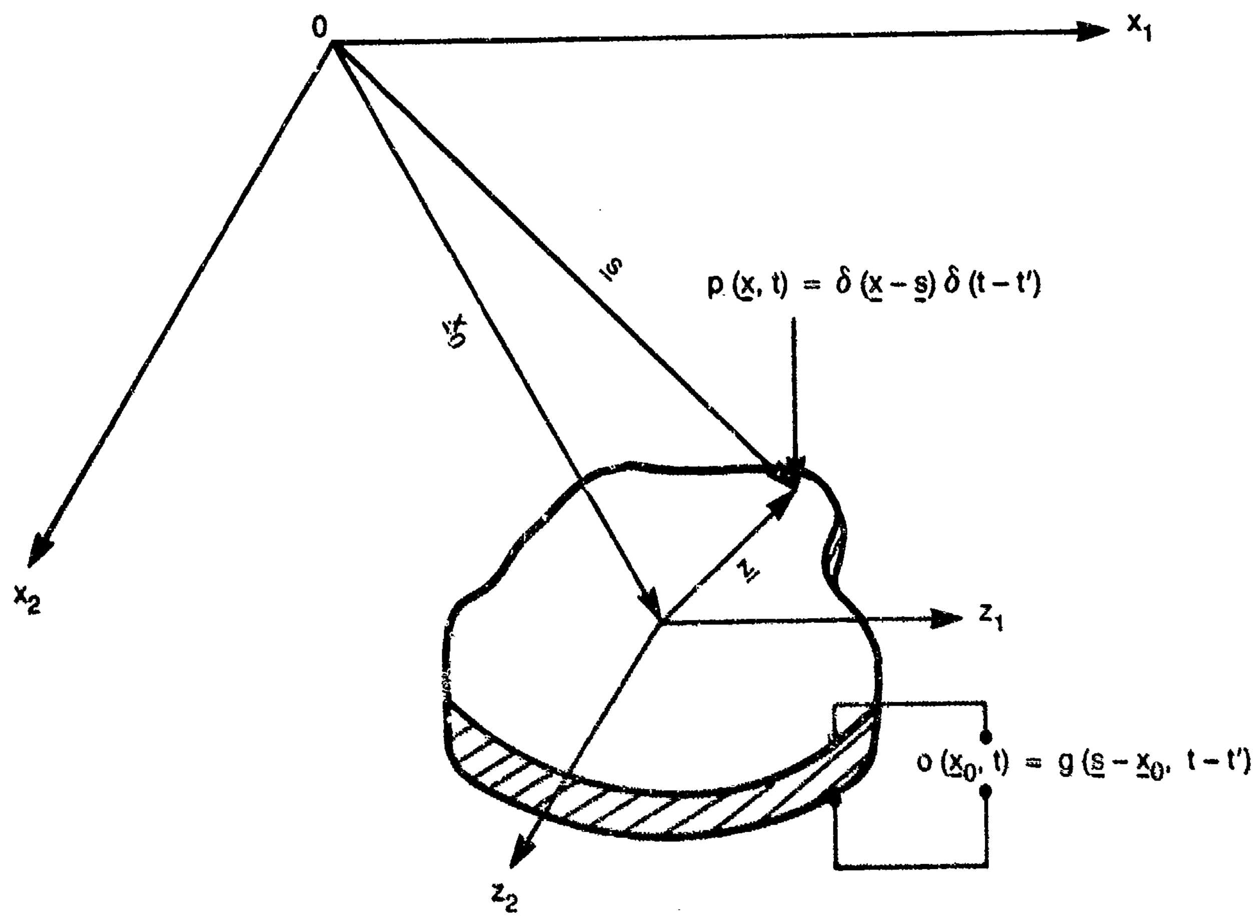

Figure 8-1. Geometry for the Impulse Response of a Planar Transducer

By equation (8-3), it is evident that the output of a transducer located at $\underline{x}_0$ is not simply a scaled replicate of the temporal history of the pressure at $\underline{x} = \underline{x}_0$. Rather, the output, at time t, of a transducer located at $\underline{x}_0$ is a weighted summation of the pressure histories, over all times prior to and including t, at every spatial location over the active surface of the transducer. It is instructive to note that the output of the transducer can only replicate the exact temporal history of the pressure at $\underline{x} = \underline{x}_0$ when $g(\underline{z},\theta) = \delta(\underline{z})\delta(\theta)$. However, this impulse response characterizes a transducer that is infinitesimally small, responds instantaneously in time, and preserves the amplitude of the excitation. Clearly, such a transducer is practically unrealizable.

Having established that the output, $o(\underline{x}_0,t)$, of a transducer located at $\underline{x}_0$ differs from the surface pressure, $p(\underline{x}_0,t)$, at that location, we will

now examine the consequences of transducer selection on estimates of various wavevector-frequency descriptors of the surface pressure field. Our approach to this task is to first develop relationships between the descriptors of the estimated field and those of the pressure field. By use of these relationships, we can then determine how the estimate is affected by the response characteristics of the transducer.

Because we wish to examine only the effects of the transducer on estimates of the various wavevector-frequency descriptors of acoustic fields, we assume that no other limitations are applied to our measurements. Thus, we assume that the surface pressure field, $p(\underline{x},t)$, is measured by identical transducers over all space and time. Consequently, the output of the transducer, $o(\underline{x}_0,t)$, is assumed to be known over all $\underline{x}_0$ and t. We therefore write this field of outputs simply as $o(\underline{x},t)$. By equation (8-3), $o(\underline{x},t)$ is related to the surface pressure field, $p(\underline{x},t)$, by

$$o(\underline{x},t) = \int_{-\infty}^{\infty}\int_{-\infty}^{\infty}\int_{-\infty}^{\infty} g(\underline{z},\theta)p(\underline{x} + \underline{z},t - \theta)\, d\underline{z}\, d\theta \qquad (8\text{-}4)$$

for all $\underline{x}$ and t.

If the surface pressure field is deterministic, it is completely characterized by its wavevector-frequency transform, $P(\underline{k},\omega)$, which is defined by

$$P(\underline{k},\omega) = \int_{-\infty}^{\infty}\int_{-\infty}^{\infty}\int_{-\infty}^{\infty} p(\underline{x},t)\exp\{-i(\underline{k}\cdot\underline{x} + \omega t)\}\, d\underline{x}\, dt\ . \qquad (8\text{-}5)$$

The wavevector-frequency transform of the output field measured by identical transducers is similarly defined by

$$O(\underline{k},\omega) = \int_{-\infty}^{\infty}\int_{-\infty}^{\infty}\int_{-\infty}^{\infty} o(\underline{x},t)\exp\{-i(\underline{k}\cdot\underline{x} + \omega t)\}\, d\underline{x}\, dt\ . \qquad (8\text{-}6)$$

By substituting equation (8-4) into equation (8-6), we can easily show that the wavevector-frequency transform of the output field measured by the

transducer is related to the wavevector-frequency transform of the surface pressure field by

$$O(\underline{k},\omega) = G(-\underline{k},\omega)P(\underline{k},\omega) \ , \tag{8-7}$$

where $G(\underline{k},\omega)$ is the wavevector-frequency response of the transducer, defined by

$$G(\underline{k},\omega) = \int_{-\infty}^{\infty}\int_{-\infty}^{\infty}\int_{-\infty}^{\infty} g(\underline{z},\theta)\exp[-i(\underline{k}\cdot\underline{z} + \omega\theta)]\ d\underline{z}\ d\theta \ . \tag{8-8}$$

By reference to chapter 3, the reader will recognize that equation (8-7) has the mathematical form of the input-output relationship for a space- and time-invariant linear system. The system, in this case, comprises the transducers used to measure the pressure field, and the space and time invariance of the system is a consequence of the assumption that the pressure field is measured over all space by identical transducers.

If the pressure field is random, it is characterized by its autocorrelation function, $Q_{pp}(\underline{x},\underline{\xi},t,\tau)$, or by an appropriate form of the informationally equivalent wavevector-frequency spectrum. By applying the arguments presented in section 7.2 to equation (8-4), we can show that the autocorrelation function of the output field, $Q_{oo}(\underline{x},\underline{\xi},t,\tau)$, measured by identical transducers is related to the autocorrelation function of the pressure field by

$$Q_{oo}(\underline{x},\underline{\xi},t,\tau) = \int_{-\infty}^{\infty}\int_{-\infty}^{\infty}\int_{-\infty}^{\infty}\int_{-\infty}^{\infty}\int_{-\infty}^{\infty}\int_{-\infty}^{\infty} g(\underline{z}_1,\theta_1)g(\underline{z}_2,\theta_2)$$

$$Q_{pp}(\underline{x} + \underline{z}_1,\underline{\xi} + \underline{z}_2 - \underline{z}_1,t - \theta_1,\tau + \theta_1 - \theta_2)\ d\underline{z}_1\ d\underline{z}_2\ d\theta_1\ d\theta_2 \ . \tag{8-9}$$

Recall that, in this text, we limit our attention to stationary pressure fields. Therefore, we require

$$Q_{pp}(\underline{x} + \underline{z}_1,\underline{\xi} + \underline{z}_2 - \underline{z}_1,t - \theta_1,\tau + \theta_1 - \theta_2) = Q_{pp}(\underline{x} + \underline{z}_1,\underline{\xi} + \underline{z}_2 - \underline{z}_1,\tau + \theta_1 - \theta_2) \tag{8-10}$$

By substituting equation (8-10) into equation (8-9), we obtain

$$Q_{oo}(\underline{x},\underline{\xi},\tau) = \int_{-\infty}^{\infty}\int_{-\infty}^{\infty}\int_{-\infty}^{\infty}\int_{-\infty}^{\infty}\int_{-\infty}^{\infty}\int_{-\infty}^{\infty} g(\underline{z}_1,\theta_1)g(\underline{z}_2,\theta_2)$$

$$Q_{pp}(\underline{x} + \underline{z}_1,\underline{\xi} + \underline{z}_2 - \underline{z}_1,\tau + \theta_1 - \theta_2)\, d\underline{z}_1\, d\underline{z}_2\, d\theta_1\, d\theta_2 \ . \quad (8\text{-}11)$$

Note, by the form of its autocorrelation function, that the output field measured by identical transducers is also stationary.

If the pressure field is homogeneous as well as stationary, then

$$Q_{pp}(\underline{x} + \underline{z}_1,\underline{\xi} + \underline{z}_2 - \underline{z}_1,t - \theta_1,\tau + \theta_1 - \theta_2) = Q_{pp}(\underline{\xi} + \underline{z}_2 - \underline{z}_1,\tau + \theta_1 - \theta_2) \ , \quad (8\text{-}12)$$

and (by equation (8-9)) the autocorrelation function of the output field is related to the autocorrelation function of the pressure field by

$$Q_{oo}(\underline{\xi},\tau) = \int_{-\infty}^{\infty}\int_{-\infty}^{\infty}\int_{-\infty}^{\infty}\int_{-\infty}^{\infty}\int_{-\infty}^{\infty}\int_{-\infty}^{\infty} g(\underline{z}_1,\theta_1)g(\underline{z}_2,\theta_2)$$

$$Q_{pp}(\underline{\xi} + \underline{z}_2 - \underline{z}_1,\tau + \theta_1 - \theta_2)\, d\underline{z}_1\, d\underline{z}_2\, d\theta_1\, d\theta_2 \ . \quad (8\text{-}13)$$

Clearly, by the form of its autocorrelation function, the output field measured by the identical transducers is also homogeneous and stationary.

Although equations (8-11) and (8-13) establish relationships between the autocorrelation function of the output field measured by identical transducers and the autocorrelation function of the stationary pressure field being measured for both nonhomogeneous and homogeneous pressure fields, respectively, the mathematical forms of these equations are sufficiently complex that the effects of the transducer on the measured field are obscured. In an attempt to clarify the effect of the transducer on the measured statistics of the field, let us examine the relationship between the wavevector-frequency spectra of the output field measured by identical transducers and the pressure field being measured.

By applying equation (6-121) to equation (8-11) and using the definition of equation (8-8), we can easily show that the two wavevector-frequency spectrum of the stationary, nonhomogeneous output field measured by identical transducers is related to the two wavevector-frequency spectrum of the stationary, nonhomogeneous pressure field being measured by

$$S_{oo}(\underline{\mu},\underline{k},\omega) = G(\underline{k} - \underline{\mu},-\omega)G(-\underline{k},\omega)S_{pp}(\underline{\mu},\underline{k},\omega) \ . \tag{8-14}$$

Here, it is evident that the two wavevector-frequency spectrum of the field measured by identical transducers is a filtered version of the two wavevector-frequency spectrum of the pressure field being measured. The filtering of the two wavevector-frequency spectrum of the pressure field is applied, in both wavevector variables ($\underline{\mu}$ and $\underline{k}$) and in frequency (ω), by the product, $G(\underline{k} - \underline{\mu},-\omega)G(-\underline{k},\omega)$, of wavevector-frequency responses of the identical transducers.

For the stationary and homogeneous pressure field, we employ equations (6-78), (8-8), and (8-13) to demonstrate that the wavevector-frequency spectrum of the field measured by identical sensors is related to the wavevector-frequency spectrum of the pressure field by

$$\Phi_o(\underline{k},\omega) = |G(-\underline{k},\omega)|^2\Phi_p(\underline{k},\omega) \ . \tag{8-15}$$

Here, we see that the wavevector-frequency spectrum of the field measured by identical transducers is equal to the wavevector-frequency spectrum of the pressure field filtered by the squared magnitude of the wavevector-frequency response of the transducer.

By reference to chapter 7, the reader can confirm that equations (8-14) and (8-15) have mathematical forms consistent with the input-output relationships for space- and time-invariant linear systems excited by nonhomogeneous and homogeneous, stationary fields, respectively. As was noted for the deterministic field, the system comprises the identical transducers used to measure the field, and the space and time invariance of this system is a consequence of the assumption that the field of interest is measured by identical transducers. The treatment of fields measured by nonidentical

transducers is beyond the scope of this text.

By equations (8-7), (8-14), and (8-15), it is evident that when a field, either deterministic or random, is measured by identical sensors, the measured field is a filtered version, in both wavevector and frequency, of the field being measured. Thus, in the measurement process, the effect of the transducer is to filter the field being measured, in both the wavevector and frequency domains. As a result of this filtering process, the wavevector and frequency content of the measured field differs from that of the field being measured.

It is also evident, from equations (8-7), (8-14), and (8-15), that if both the wavevector-frequency response of the sensor, $G(-\underline{k},\omega)$, and the appropriate wavevector-frequency descriptor, $O(\underline{k},\omega)$, $S_{oo}(\underline{\mu},\underline{k},\omega)$, or $\Phi_o(\underline{k},\omega)$, of the output field were known, then the corresponding wavevector-frequency descriptor, $P(\underline{k},\omega)$, $S_{pp}(\underline{\mu},\underline{k},\omega)$, or $\Phi_p(\underline{k},\omega)$, of the pressure field can be determined.

Unfortunately, it is a rare instance that the wavevector-frequency response of a sensor is known. In 1965, under the assumption that $g(\underline{z},\theta)$ was of the form $h(\underline{z})\delta(\theta)$, Gilchrist and Strawderman[3] devised a method to measure the spatial response, $h(\underline{z})$, of transducers used to measure the wall pressure fluctuations beneath turbulent boundary layers. By numerical Fourier transformation of $h(\underline{z})$, the wavevector-frequency response of the transducer of the form $G(\underline{k},\omega) = H(\underline{k})$ could be obtained. Alternatively, it can be demonstrated from equations (8-4) and (8-8) that, for any given wavevector and frequency (say $\underline{k}_1$ and ω_1), the wavevector-frequency response of a transducer is equal to the ratio of the measured output, $o(\underline{x}_0,t_0)$, of the transducer at any fixed location, $\underline{x}_0$, and time, t_0, to the local pressure, $p(\underline{x}_0,t_0)$, being measured at the same location and time when that pressure field is a complex harmonic plane wave of the form $\exp[i(-\underline{k}_1\cdot\underline{x} + \omega_1 t)]$. To implement this alternative approach, Powers,[4] in 1980, developed an array of projectors capable of generating relatively pure pressure waves of the form $\cos(k_1 x + \omega_1 t)$ over a limited portion of a planar surface and over a fairly extensive range of k_1 and ω_1. Despite these feasibility demonstrations, however, no commercially available system exists, at this writing.

for directly measuring either the space-time or wavevector-frequency response of transducers.

Inasmuch as (1) the motivation for the measurement of any acoustic field is to determine the space-time or wavevector-frequency characteristics of that acoustic field rather than the output field observed by the sensors, (2) knowledge of the space-time impulse response or wavevector-frequency response of the sensors used in a measurement is required to deduce the desired characteristics of the acoustic field from the output field observed by the sensors, and (3) no commercially available system exists for measuring the requisite response of the sensors employed in the measurement, the experimenter must rely on estimates of the impulse or wavevector-frequency response to deduce the space-time or wavevector-frequency characteristics of the acoustic field of interest. To exercise some degree of control on the quality of the estimate of the space-time or wavevector-frequency characteristics of the acoustic field of interest, estimates of the response characteristics of candidate sensors should be considered an integral part of the planning phase of an experiment. Such estimates can normally be made from information supplied by the sensor manufacturer.

Manufacturers normally publish the sensitivity of their sensors to long-wavelength (effectively zero wavenumber) input fields as a function of frequency. Although standard definitions of sensitivity vary with the type of measuring device (accelerometer, hydrophone, etc.), all definitions of sensitivity are measures of the ratio of the amplitude of the output of the device to the amplitude of the field to be measured when that field is a plane wave characterized by a specific frequency and a wavelength much longer than any dimension of the sensor.

For purposes of illustration, we define the long-wavelength sensitivity, $S(f_1)$, of the planar sensor characterized by equation (8-3) at the frequency f_1 to be the ratio of the amplitude of the output, $o(\underline{x}_0,t)$, of the sensor at some fixed location, $\underline{x}_0$, to the amplitude of the pressure, $p(\underline{x}_0,t)$, at the same location when the pressure field is a (real) plane wave characterized by the frequency f_1 and a wavevector, $\underline{k}_1$, approaching zero magnitude (i.e., of long wavelength). That is, if Amp{} denotes the amplitude of a real waveform,

$$S(f_1) = \frac{\text{Amp}\{o(\underline{x}_0,t)\}}{\text{Amp}\{p(\underline{x}_0,t)\}} \tag{8-16}$$

when

$$p(\underline{x}_0,t) = P(\underline{k}_1,2\pi f_1)\cos(\underline{k}_1 \cdot \underline{x}_0 + 2\pi f_1 t + \alpha) \tag{8-17}$$

and $|\underline{k}_1| \to 0$. Here, $P(\underline{k}_1,2\pi f_1)$ is the (real) amplitude of the plane pressure wave, and α is the phase of the wave at $\underline{x}_0 = (0,0)$ and $t = 0$.

By use of equations (8-3) and (8-8), we can show that the plane pressure wave described by equation (8-17) produces an output from a sensor located at $\underline{x}_0$ that is described by

$$o(\underline{x}_0,t) = P(\underline{k}_1,2\pi f_1)\text{Re}\{G(-\underline{k}_1,2\pi f_1)\exp(\underline{k}_1 \cdot \underline{x}_0 + 2\pi f_1 t + \alpha)\} \; . \tag{8-18}$$

If we express

$$G(\underline{k}_1,2\pi f_1) = |G(\underline{k}_1,2\pi f_1)|\exp\{i\beta(\underline{k}_1,f_1)\} \; , \tag{8-19}$$

where $\beta(\underline{k}_1,f_1)$ denotes the phase of the complex quantity $G(\underline{k}_1,2\pi f_1)$, we can rewrite equation (8-18) in the form

$$o(\underline{x}_0,t) = P(\underline{k}_1,2\pi f_1)|G(-\underline{k}_1,2\pi f_1)|\cos\{\underline{k}_1 \cdot \underline{x}_0 + 2\pi f_1 t + \alpha + \beta(-\underline{k}_1,f_1)\} \; . \tag{8-20}$$

It follows from equations (8-16), (8-17), and (8-20) that, in the limit as $\underline{k}_1 \to (0,0)$,

$$S(f_1) = |G(\underline{0},2\pi f_1)| \; . \tag{8-21}$$

Thus, the sensitivity of the planar sensor at the frequency f_1 is equal to the magnitude of the wavevector-frequency response of that sensor at zero wavevector and frequency f_1.

Most sensors employed in acoustics are resonant devices, and the sensor manufacturer will normally publish measured values of S(f) over a frequency range that extends from as low as practicable to above the first resonance frequency of the sensor. Many sensors, such as small piezoelectric devices, have zero-wavenumber sensitivities similar to that illustrated in figure 8-2.[5] Note here that, between the frequency f_l, located above the low frequency roll-off, and the frequency f_u, located well below the first resonance frequency, f_{res}, of the sensor, the sensitivity of the transducer has an essentially constant value, S_0. For such sensors, it is common practice for the manufacturer to list the constant sensitivity value, S_0, and the applicable frequency limits, f_l and f_u.

Most estimates of the wavevector-frequency response of sensors are made under the assumption that the impulse response, $g(\underline{z},\theta)$, is a separable function of space and time. That is,

$$g(\underline{z},\theta) = h(\underline{z})v(\theta) \quad . \tag{8-22}$$

This assumption is valid only when the highest frequency of interest is well below the first resonance frequency of the transducer. The separable form of the impulse response of the sensor implies a separable form of the wavevector-frequency response of the sensor. That is, by equations (8-8) and (8-22),

$$G(\underline{k},\omega) = H(\underline{k})V(\omega) \quad , \tag{8-23}$$

where

$$H(\underline{k}) = \int_{-\infty}^{\infty}\int_{-\infty}^{\infty} h(\underline{z})\exp(-i\underline{k}\cdot\underline{z})\, d\underline{z} \tag{8-24}$$

and

$$V(\omega) = \int_{-\infty}^{\infty} v(\theta)\exp(-i\omega\theta)\, d\theta \quad . \tag{8-25}$$

By equations (8-21) and (8-23), it is evident that

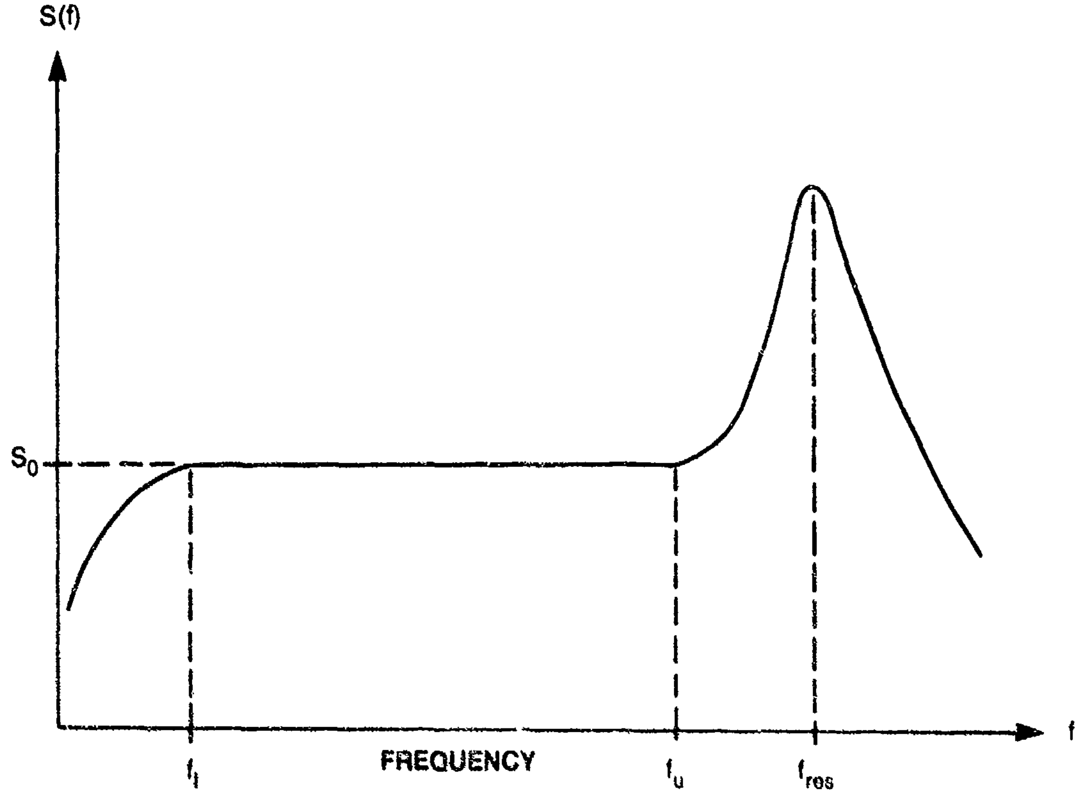

Figure 8-2. Sensitivity of a Small Piezoelectric Sensor

$$|V(2\pi f_1)| = S(f_1)/|H(\underline{0})| \ . \tag{8-26}$$

Note, by equations (8-3), (8-22), (8-24), and (8-25), that if a positive constant pressure, $p(\underline{x},t) = P_0$, is applied to the sensor, then

$$o(\underline{x},t) = P_0 H(\underline{0}) V(0) \ . \tag{8-27}$$

Here, because $h(\underline{z})$ and $v(\theta)$ are real functions, $H(\underline{0})$ and $V(0)$ are also real. If a sensor maintains the sense (sign) of the applied field, $o(\underline{x},t)$ is positive. In this case, $H(\underline{0})$ and $V(0)$ must both be of the same sign, and can both be assumed to be positive. If the sensor does not maintain the sense of the applied field, then $o(\underline{x},t)$, and therefore either $H(\underline{0})$ or $V(0)$, must be negative. We adopt the convention that the polarity of the real function $h(\underline{z})$ is chosen such that $H(0) \geq 0$ and that the sense of the $G(\underline{0},0)$ is reflected in $V(0)$.

Under this convention, $|H(\underline{0})| = H(\underline{0})$. Consequently, it follows from

equation (8-26) that $V(2\pi f_1)$ must be of the form

$$V(2\pi f_1) = \{S(f_1)/H(\underline{0})\}\exp\{i\varepsilon(f_1)\} , \tag{8-28}$$

where $\varepsilon(f_1)$ is the phase of $V(2\pi f_1)$. It therefore follows that

$$G(\underline{k},2\pi f_1) = \frac{H(\underline{k})}{H(\underline{0})} S(f_1)\exp\{i\varepsilon(f_1)\} . \tag{8-29}$$

Let us now address the estimation of $H(\underline{k})$. Vendors normally offer no information regarding the spatial or wavevector response characteristics of their sensors. However, most manufacturers publish the dimensions of their sensors. In the absence of any other information, let us assume that $h(\underline{z})$ is a positive constant over the active surface of the sensor. Thus, if the active surface of the sensor is rectangular, with dimensions L_1 by L_2, we assume that

$$h(\underline{z}) = \begin{cases} A, & |z_1| \le L_1/2 \text{ and } |z_2| \le L_2/2 , \\ 0, & \text{otherwise.} \end{cases} \tag{8-30}$$

For this rectangular sensor, it follows from equation (8-24) that

$$\frac{H(\underline{k})}{H(\underline{0})} = \frac{\sin(k_1L_1/2)}{(k_1L_1/2)} \frac{\sin(k_2L_2/2)}{(k_2L_2/2)} . \tag{8-31}$$

If, on the other hand, the active surface of the sensor is circular and of radius R, we assume that

$$h(\underline{z}) = \begin{cases} A, & |\underline{z}| \le R , \\ 0, & \text{otherwise.} \end{cases} \tag{8-32}$$

By equations (8-24) and (8-31), it can be shown that

$$\frac{H(\underline{k})}{H(\underline{0})} = \frac{2J_1(|\underline{k}|R)}{|\underline{k}|R} . \tag{8-33}$$

The k_1 dependence, at $k_2 = 0$, of the wavevector responses for the rectangular and circular, uniformly weighted planar sensors is illustrated in figures 8-3(a) and 8-3(b), respectively. Note here that the wavevector response of both the rectangular and circular sensors is characterized by a primary response lobe centered at $k_1 = 0$ and that, outside the primary lobe, the envelope of the response decreases as the magnitude of k_1 increases. Similar response characteristics can be shown to hold for the k_2 dependence at $k_1 = 0$. Thus, sensors having spatially uniform responses act as lowpass wavevector filters, admitting wavevector components in the ranges $|k_1| < 2/L_1$ and $|k_2| < 2/L_2$ or $|\underline{k}| < 1/R$, with relatively little attenuation, and effectively attenuating wavevector components in the ranges $|k_1| > 4/L_1$ and $|k_2| > 4/L_2$ or $|\underline{k}| > 3/R$. By recalling that the wavenumber that characterizes a wave is inversely proportional to the wavelength of that wave, we conclude that the spatially uniform sensor responds well to wave components of the pressure field characterized by wavelength components in the x_1 and x_2 directions that are long in comparison with the dimensions of the sensor. On the other hand, wave components of the pressure field characterized by wavelength components comparable to or shorter than the dimensions of the sensor are spatially averaged over the active face of the sensor, thereby reducing the response of the sensor to such components.

By equations (8-29) and (8-31), we obtain the following estimate for the wavevector-frequency response of a planar sensor having a uniform response over a rectangular active surface:

$$G(\underline{k},2\pi f) = \frac{\sin(k_1L_1/2)}{(k_1L_1/2)} \frac{\sin(k_2L_2/2)}{(k_2L_2/2)} S(f)\exp[i\epsilon(f)] \ . \tag{8-34}$$

Similarly, the wavevector-frequency response of a planar sensor with a uniform response over a circular active surface is estimated, from equations (8-29) and (8-33), to be

$$G(\underline{k},2\pi f) = \frac{2J_1(|\underline{k}|R)}{(|\underline{k}|R)} S(f)\exp[i\epsilon(f)] \ . \tag{8-35}$$

Clearly, it is unlikely that any given commercially available sensor will have an impulse response that is spatially uniform. Consequently, it is

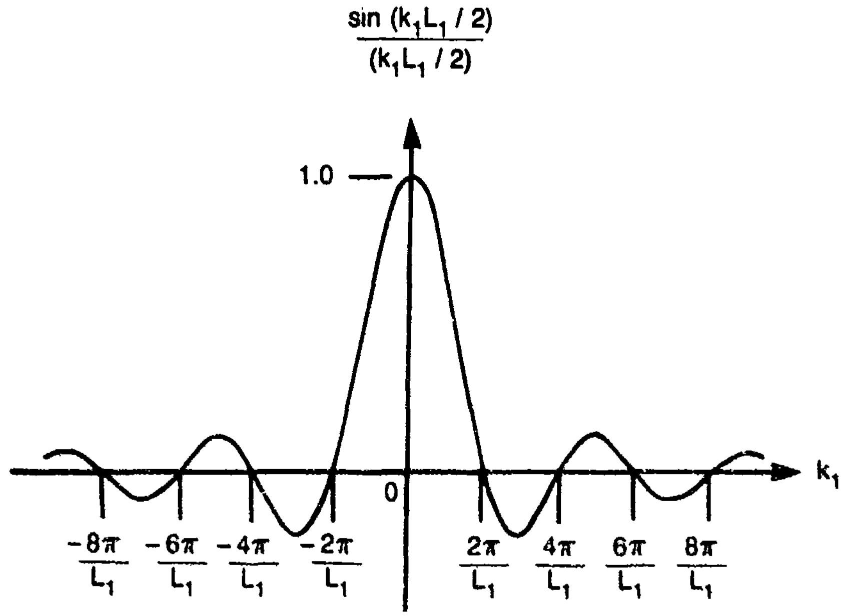

Figure 8-3(a). L_1 by L_2 Rectangular Sensor

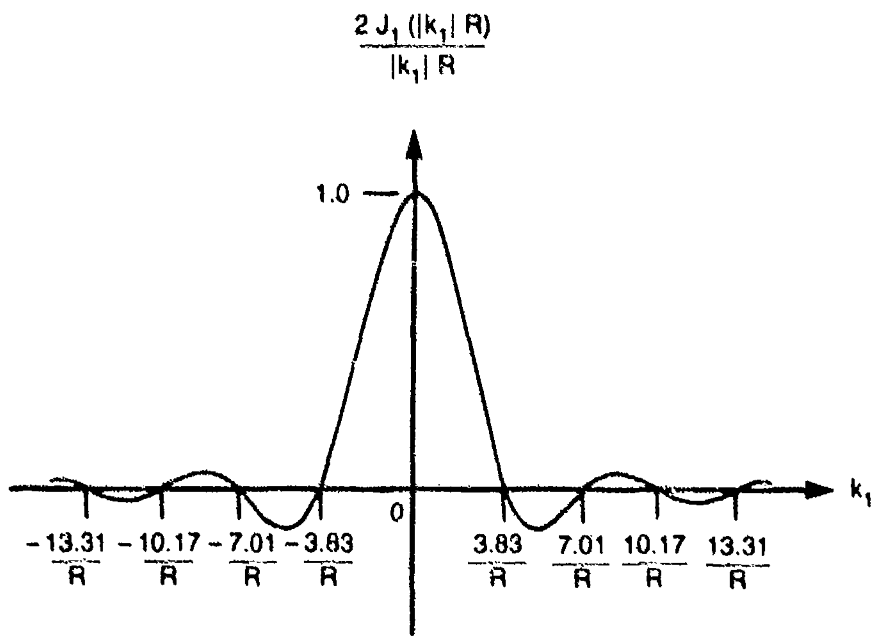

Figure 8-3(b). Circular Sensor of Radius R

Figure 8-3. The k_1 Dependence, at $k_2 = 0$, of $H(\underline{k})/|H(\underline{0})|$ for Uniformly Weighted Rectangular and Circular Sensors

unlikely that the above estimates of $G(\underline{k},2\pi f)$ reflect the actual wavevector-frequency response of such a sensor. However, for any planar sensor with a rectangular active surface, $H(\underline{k})$ can be written in the form

$$H(\underline{k}) = \int_{-L_1}^{L_1}\int_{-L_2}^{L_2} h(z_1,z_2)\exp[-i(k_1z_1 + k_2z_2)]\,dz_1\,dz_2$$

$$= L_1L_2\int_{-1}^{1}\int_{-1}^{1} h(y_1L_1,y_2L_2)\exp[-i(k_1L_1y_1 + k_2L_2y_2)]\,dy_1\,dy_2$$

$$= \tilde{H}(k_1L_1,k_2L_2;L_1,L_2) \quad . \tag{8-36}$$

We can similarly demonstrate that $H(\underline{k})$ for any planar sensor with a circular active face can be written in the form

$$H(\underline{k}) = \tilde{H}(|\underline{k}|R;R) \quad . \tag{8-37}$$

For any real sensor, $h(\underline{z})$ is a real, bounded function over the finite active surface of the sensor. Thus, it follows that $H(\underline{k})$ and its derivatives are finite for all finite $|\underline{k}|$. Consequently, $H(\underline{k})$ and its derivatives are continuous in the neighborhood of $\underline{k} = (0,0)$, so $H(\underline{k})/H(\underline{0})$ tends smoothly to unity as $|\underline{k}|$ approaches zero from any direction. It therefore follows that, for any planar sensor with a rectangular active surface,

$$\frac{H(\underline{k})}{H(\underline{0})} = \frac{\tilde{H}(k_1L_1,k_2L_2;L_1,L_2)}{\tilde{H}(0,0;L_1,L_2)} \approx 1 \tag{8-38}$$

for $|k_1L_1| << 1$ and $|k_2L_2| << 1$. Similarly, for any planar sensor with a circular active surface,

$$\frac{H(\underline{k})}{H(\underline{0})} = \frac{\tilde{H}(|\underline{k}|R;R)}{\tilde{H}(0;R)} \approx 1 \tag{8-39}$$

for $|\underline{k}|R << 1$. Thus, by equations (8-29), (8-38), and (8-39), we conclude that, for planar sensors with rectangular and circular active surfaces,

$$G(\underline{k},2\pi f_1) = S(f_1)\exp[i\epsilon(f_1)] \tag{8-40}$$

if $|k_1L_1| << 1$ and $|k_2L_2| << 1$ or $|\underline{k}|R << 1$, respectively. Note that this low wavenumber behavior of $G(\underline{k},2\pi f_1)$ is consistent with that predicted by equations (8-34) and (8-35).

Equation (8-40) provides a reasonably good estimate of the wavevector-frequency response of any sensor at frequencies well below the first resonance frequency of the sensor and for small products of wavevector magnitudes and sensor dimensions (i.e., for wavelengths much longer than the sensor dimensions). It therefore provides a basis for defining, during the planning phase of an experiment, the sensor characteristics required to ensure that a good estimate of the wavevector-frequency characteristics of the acoustic field of interest can be deduced, over some predefined range of wavevector and frequency, from the output field measured by those sensors. That is, for a deterministic field, substitution of equation (8-40) into equation (8-7) yields the relation

$$O(\underline{k},2\pi f) = S(f)P(\underline{k},2\pi f)\exp[i\epsilon(f)] \tag{8-41}$$

valid for $|k_1|L_1 << 1$ and $|k_2|L_2 << 1$ or $|\underline{k}|R << 1$. Here it is evident that a good estimate of the magnitude of $P(\underline{k},2\pi f)$ can be obtained from the magnitude of $O(\underline{k},2\pi f)$ over some specified range of wavevector and frequency if the sensitivity, $S(f)$, of the candidate sensor is known over the requisite frequency range and the dimensions of that sensor are sufficiently small that $|k_1|L_1 << 1$ and $|k_2|L_2 << 1$ or $|\underline{k}|R << 1$ over the entire wavevector range of interest. Note, however, that unless the phase, $\epsilon(f)$, of the wavevector-frequency response of the sensor is specified or experimentally determined, the phase of $P(\underline{k},2\pi f)$ cannot be determined.

For a stationary, nonhomogeneous pressure field, substitution of equation (8-40) into equation (8-14) yields

$$S_{oo}(\underline{\mu},\underline{k},2\pi f) = S^2(f)S_{pp}(\underline{\mu},\underline{k},2\pi f) \ , \tag{8-42}$$

which is valid within the wavevector ranges $|k_1|L_1 << 1$, $|k_1 - \mu_1|L_1 << 1$,

$|k_2|L_2 \ll 1$, and $|k_2 - \mu_2|L_2 \ll 1$ for rectangular sensors or within $|\underline{k}|R \ll 1$ and $|\underline{k} - \underline{\mu}|R \ll 1$ for circular sensors. Clearly, a good estimate of the two wavevector-frequency spectrum of the pressure field can be obtained from the spectrum of the sensor output field only if (1) the sensitivity of the sensor is known over the requisite frequency range of the measurement and (2) the dimensions of the sensor are sufficiently small to satisfy the above stated criteria over the required wavevector ranges in both $\underline{\mu}$ and $\underline{k}$.

For a stationary, homogeneous pressure field, equations (8-15) and (8-40) reveal that

$$\Phi_0(\underline{k},2\pi f) \approx S^2(f)\Phi_p(\underline{k},2\pi f) \tag{8-43}$$

when $|k_1|L_1 \ll 1$ and $|k_2|L_2 \ll 1$ or $|\underline{k}|R \ll 1$. Thus, to obtain a good estimate of the wavevector-frequency spectrum of the pressure field from the wavevector-frequency spectrum of the sensor output field, the sensitivity of the sensor must be known over the desired frequency range of the estimate and the dimensions of the sensor must be much smaller than any wavelength anticipated in the acoustic pressure field. Note that the spectral estimates of equations (8-42) and (8-43) are independent of $\varepsilon(f)$, the phase of $G(\underline{k},2\pi f)$.

In the event that no available sensor satisfies the above criteria for a good estimate of the desired metric of the acoustic field of interest, the experimenter has little choice but to select, from those available sensors that have sensitivities specified over the requisite frequency range, the sensor having the smallest dimensions. An estimate of the desired metric of the acoustic field can then be obtained by approximating $G(\underline{k},2\pi f)$ by equation (8-34) or (8-35). The quality of the resulting estimate will depend on the difference between the actual spatial response of the sensor and the uniform response assumed in equations (8-34) and (8-35) and on the wavevector range(s) over which the measurements are required.

8.2 EFFECTS OF SAMPLING

In the previous section, we developed relationships between the space-time and wavevector-frequency descriptors of the output field measured by identical

sensors and the corresponding descriptors of the acoustic field being measured. These relationships were predicated on the assumption that the acoustic field of interest was measured by identical sensors over all space and time. However, practical sensors have finite dimensions. Consequently, in practice, the acoustic field cannot be measured at spatial intervals smaller than the dimensions of the (identical) sensors. In addition, modern frequency spectral analyzers utilize computationally efficient fast Fourier transform (FFT) algorithms to perform frequency spectral estimates. The requisite input data for such algorithms are samples of the field of interest taken at regular temporal intervals.

In this section, we explore the consequences of temporal and spatial sampling on the estimation of the space-time and wavevector-frequency characteristics of acoustic fields. We start by examining the effects of temporal sampling.

8.2.1 Temporal Sampling

Consider the output field, $o(\underline{x},t)$, obtained by measurement of a surface pressure field of interest, $p(\underline{x},t)$, with identical sensors over all space and time. We wish to determine how temporal sampling of the output field affects our ability to estimate the characteristics of the pressure field.

Because (1) the motivation for temporal sampling is to accommodate the aforementioned FFT algorithms that facilitate digital signal processing and (2) the requisite inputs to such FFT algorithms are data samples obtained at uniform increments in time, we will restrict attention in this text to uniform temporal sampling.

The concept of uniform temporal sampling is illustrated in figure 8-4. Here, the temporally continuous output, $o(\underline{x}_0,t)$, of the sensor located at $\underline{x}_0$ is sampled at equal increments, T, over all time, with a sampling origin, t_0. As a result of this temporal sampling, our knowledge of $o(\underline{x}_0,t)$ is limited to the data set $o(\underline{x}_0,t_0 + nT)$ for all integer values of n between plus and minus infinity. By synchronous application of the same temporal

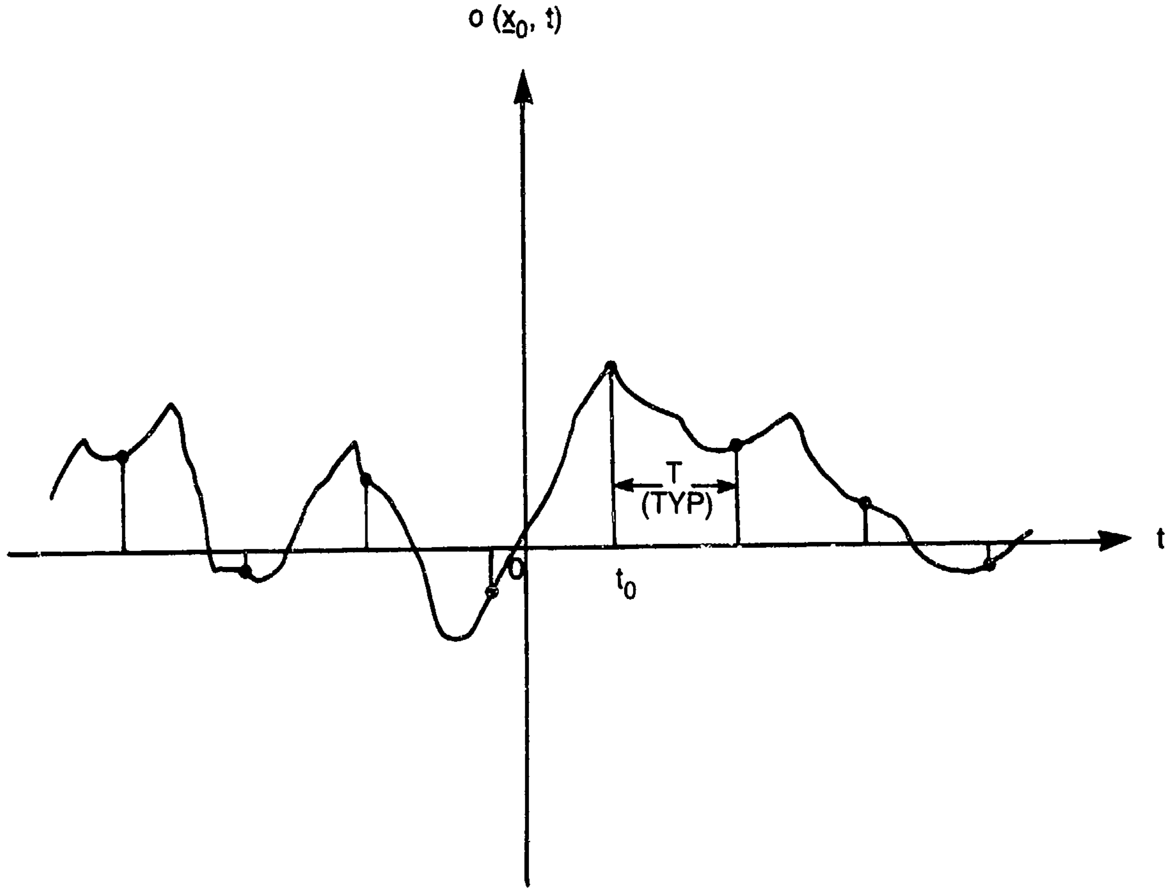

Figure 8-4. Illustration of Temporal Sampling

sampling to the outputs of the (identical) sensors at all other spatial locations, the time-sampled output field from any single trial of the measurement comprises the data set $o(\underline{x},t_0 + nT)$ over all $\underline{x}$ and for all positive and negative integer values of n.

If the surface pressure field and, thereby, the output field are known to be deterministic, they are completely characterized by their respective wavevector-frequency transforms, $P(\underline{k},\omega)$ and $O(\underline{k},\omega)$. By reference to equation (8-6), the determination of $O(\underline{k},\omega)$ requires knowledge of the sensor output field, $o(\underline{x},t)$, over all space and time. However, owing to the temporal sampling, our knowledge of the sensor output field is limited to $o(\underline{x},t_0 + nT)$ for all $\underline{x}$ and for all integer values of n in the range $-\infty \leq n \leq \infty$. Therefore, we cannot exactly determine $O(\underline{k},\omega)$ from the sampled data; we can only obtain some estimate of it.

By examination of equation (8-6), it is evident that the time-sampled sensor output field supports an estimate, $\tilde{O}(\underline{k},\omega)$, of the wavevector-frequency transform of the output field of the form

$$\tilde{O}(\underline{k},\omega) = T \sum_{n=-\infty}^{\infty} \int_{-\infty}^{\infty} \int_{-\infty}^{\infty} o(\underline{x},t_0 + nT)\exp\{-i[\underline{k}\cdot\underline{x} + \omega(t_0 + nT)]\}\ d\underline{x}\ . \quad (8\text{-}44)$$

By employing the sampling property of the Dirac delta function, we can write

$$o(\underline{x},t_0 + nT)\exp\{-i\omega(t_0 + nT)\} = \int_{-\infty}^{\infty} o(\underline{x},\theta)\exp\{-i\omega\theta\}\delta(\theta - t_0 - nT)\ d\theta\ . \quad (8\text{-}45)$$

By substitution of equation (8-45) into (8-44), we can show that

$$\tilde{O}(\underline{k},\omega) = \int_{-\infty}^{\infty} \int_{-\infty}^{\infty} \int_{-\infty}^{\infty} o(\underline{x},\theta)v(\theta - t_0)\exp\{-i(\underline{k}\cdot\underline{x} + \omega\theta)\}\ d\underline{x}\ d\theta\ , \quad (8\text{-}46)$$

where $v(\theta)$ is the temporal sampling function, defined by

$$v(\theta) = T \sum_{n=-\infty}^{\infty} \delta(\theta - nT)\ . \quad (8\text{-}47)$$

It follows, from equation (8-46), that

$$\tilde{O}(\underline{k},\omega) = (2\pi)^{-1} \int_{-\infty}^{\infty} O(\underline{k},\Omega)V(\omega - \Omega)\exp\{-i(\omega - \Omega)t_0\}\ d\Omega\ , \quad (8\text{-}48)$$

where $V(\omega)$ is the Fourier transform of the temporal sampling function, $v(\theta)$. Thus, we see that the estimate of the wavevector-frequency transform of the sensor output field is the convolution of the true wavevector-frequency transform of the sensor output field with a phase-shifted Fourier transform of the temporal sampling function.

Note, by equation (8-47), that $v(\theta)$ is a periodic function of θ, with period T. Therefore, we can express $v(\theta)$ in a Fourier series of the form[6]

$$v(\theta) = \sum_{m=-\infty}^{\infty} C_m \exp\left\{\frac{i2m\pi\theta}{T}\right\} , \tag{8-49}$$

where

$$C_m = T^{-1} \int_{-T/2}^{T/2} v(\theta)\exp\left\{\frac{-i2m\pi\theta}{T}\right\} d\theta . \tag{8-50}$$

By substitution of equation (8-47) into equation (8-50), it is easily verified that $C_m = 1$ for all m. By substitution of this result into equation (8-49), it follows that

$$V(\omega) = \int_{-\infty}^{\infty} \sum_{m=-\infty}^{\infty} \exp\{-i[\omega - (2m\pi/T)]\theta\} \, d\theta = 2\pi \sum_{m=-\infty}^{\infty} \delta(\omega - 2m\pi/T) . \tag{8-51}$$

Thus, we find that the Fourier transform of the temporal sampling function, a periodic train of Dirac delta functions in the time domain, is a periodic train of Dirac delta functions in the frequency domain. Note also that the period, $2\pi/T$, of $V(\omega)$ in ω is inversely proportional to the period, T, of $v(\theta)$ in θ.

By substituting the appropriate form of equation (8-51) into equation (8-48) and performing the requisite integration, we obtain the following relationship between the estimated and true wavevector-frequency transforms of the sensor output field:

$$\tilde{O}(\underline{k},\omega) = \sum_{n=-\infty}^{\infty} O(\underline{k},\omega - 2\pi n/T)\exp(-i2\pi n t_0/T) . \tag{8-52}$$

Note here that the estimated transform of the sensor output field is an infinite sum of frequency and phase-shifted versions of the true wavevector-

frequency transform of the output field. Both the frequency shift and phase shift between successive replications of the true spectrum are uniform and are equal to $2\pi/T$ and $2\pi t_0/T$, respectively.

To illustrate the character of the estimated wavevector-frequency transform, consider a sensor output field that is band limited in frequency, at all wavevectors, to $-\omega_c \leq \omega \leq \omega_c$. The true wavevector-frequency transform, $O(\underline{k},\omega)$, of this field at the wavevector $\underline{k}_0$ is assumed to be the real and even function illustrated in figure 8-5(a). We assume that the sensor output field is sampled at uniform increments, T, over all time and that the sampling origin, t_0, is equal to zero. This choice of temporal origin simplifies illustration of the estimated transform by virtue of eliminating the complex phase term in equation (8-52).

Figure 8-5(b) illustrates the estimated transform, $\tilde{O}(\underline{k}_0,\omega)$, at the wavevector $\underline{k}_0$ for a temporal sampling increment, $T = T_1$, where T_1 is less than π/ω_c. For this choice of sampling increment, the frequency separation, $2\pi/T_1$, between replications of the true transform is greater than the total bandwidth, $2\omega_c$, of the true transform. Consequently, the estimated transform is a periodic function comprising the sum of separated replicates of the true transform at frequency intervals of $2\pi/T_1$. For this choice of sampling, it is evident that

$$\tilde{O}(\underline{k},\omega) = O(\underline{k},\omega), \quad |\omega| \leq \pi/T_1 \ . \tag{8-53a}$$

Figure 8-5(c) illustrates the estimated transform, $\tilde{O}(\underline{k}_0,\omega)$, at the wavevector $\underline{k}_0$ for a temporal sampling increment, $T = T_2$, where T_2 is greater than π/ω_c. For this choice of sampling increment, the frequency separation, $2\pi/T_2$, between replications of the true transform is less than the total bandwidth, $2\omega_c$, of the true transform. As illustrated in figure 8-5(c), this choice of sampling interval produces an overlapping of adjacent periodic replicates of the true spectrum. The regions of overlap are centered at odd multiples of π/T2, and the bandwidth of the overlap is $2(\omega_c - \pi/T_2)$. Note that the estimated transform, $\tilde{O}(\underline{k}_0,\omega)$, formed by the summation of these overlapped replicates of the true transform, is again a periodic function of frequency. However, it is evident that the estimated transform is equal to

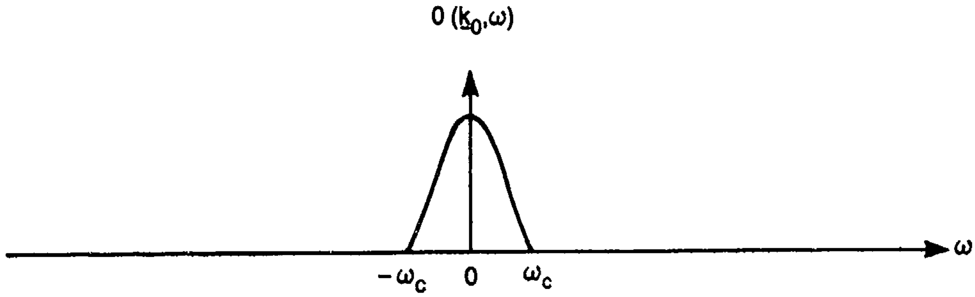

Figure 8-5(a). True Transform of Frequency Band-Limited Output

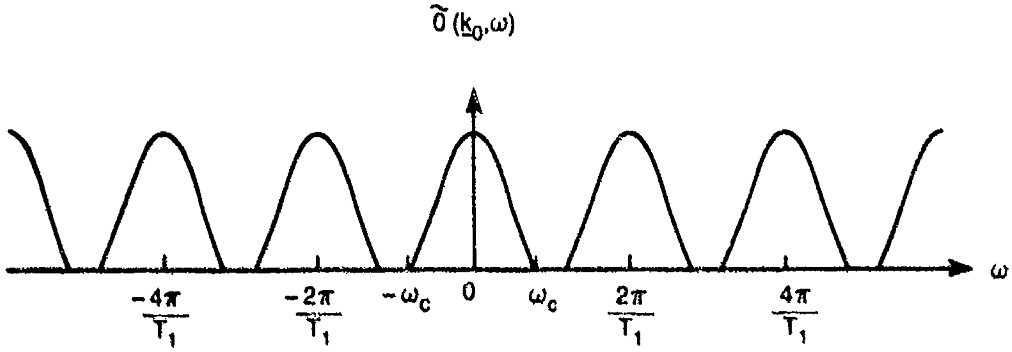

Figure 8-5(b). Estimated Transform of Frequency Band-Limited Output for $T = T_1 < \pi/\omega_c$

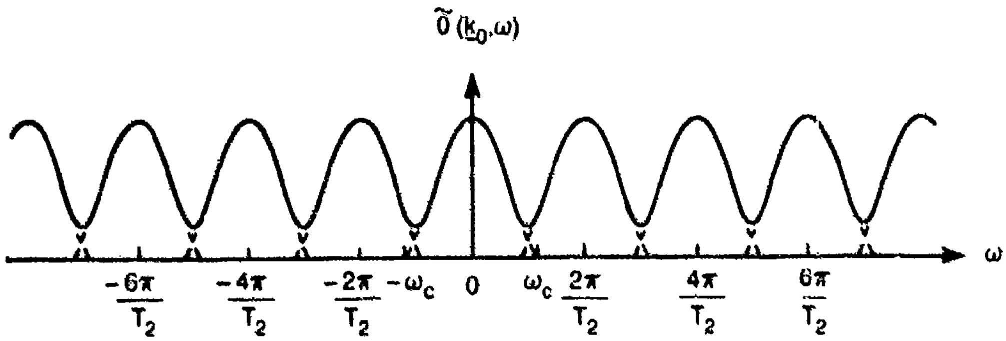

Figure 8-5(c). Estimated Transform of Frequency Band-Limited Output for $T = T_2 > \pi/\omega_c$

Figure 8-5. Comparison of True and Estimated Wavevector-Frequency Transforms of Frequency Band-Limited Output Field

the true transform only in the frequency range $|\omega| \leq (2\pi/T_2) - \omega_c$; the estimate in the range $(2\pi/T_2) - \omega_c < |\omega| \leq \omega_c$ is distorted by the sum of the overlapped contributions. This distortion of the estimated transform that results from the overlapping of the replicates of the true transform is called aliasing.[7]

By the arguments presented above, it is evident that if a deterministic output field, $o(\underline{x},t)$, is sampled synchronously over all space at uniform increments, T, over all time, then the estimate, $\tilde{O}(\underline{k},\omega)$, of the wavevector-frequency transform of the sensor output field obtained by equation (8-44) in the frequency interval $|\omega| \leq \pi/T$ is equal to the true transform, $O(\underline{k},\omega)$, of that field if (1) the true transform is band limited in frequency at all wavevectors and (2) the sampling interval, T, is smaller than one-half the temporal period of any contribution to $O(\underline{k},\omega)$. Mathematically stated,

$$\tilde{O}(\underline{k},\omega) = O(\underline{k},\omega), \quad |\omega| \leq \pi/T , \tag{8-53b}$$

if

$$O(\underline{k},\omega) = 0, \quad |\omega| > \omega_c , \tag{8-54}$$

for all $\underline{k}$, and

$$T < \pi/\omega_c . \tag{8-55}$$

If $O(\underline{k},\omega)$ is not band limited in frequency, the estimate, $\tilde{O}(\underline{k},\omega)$, of the wavevector-frequency transform obtained by equation (8-44) will contain aliased contributions, and will therefore differ from the true transform.

Note that if $O(\underline{k},\omega)$ is band limited in frequency as described by equation (8-54) and the sampling conditions of equation (8-55) are met, then the wavevector-frequency transform of the pressure field being measured can be exactly determined, given the wavevector-frequency response of the sensor. That is, by equations (8-7) and (8-53b),

$$P(\underline{k},\omega) = \frac{O(\underline{k},\omega)}{G(-\underline{k},\omega)} = \begin{cases} \dfrac{\tilde{O}(\underline{k},\omega)}{G(-\underline{k},\omega)} , & |\omega| \leq \pi/T , \\ 0, & \text{otherwise.} \end{cases} \tag{8-56}$$

Given knowledge of $O(\underline{k},\omega)$ or $P(\underline{k},\omega)$, $o(\underline{x},t)$ and $p(\underline{x},t)$ can, of course, be exactly determined by inverse Fourier transformation.

Consider now the problem of estimating the space-time or wavevector-frequency characteristics of a random pressure field, $p(\underline{x},t)$, from knowledge of time samples of the sensor output field, $o(\underline{x},t)$, measured synchronously over all space and over all possible realizations of the experiment. Thus, our knowledge of the output field is limited to $o(\underline{x},t_0 + nT)$ over all $\underline{x}$ and all positive and negative integer values of n for every possible realization of the experiment.

Recall that random space-time fields are characterized in the wavevector-frequency domain by their wavevector-frequency spectra, the multidimensional Fourier transforms of their autocorrelation functions. However, given the ensemble of time-sampled output fields, $o(\underline{x},t_0 + nT)$, and the definition of the autocorrelation function (equation (6-44)), our knowledge of the autocorrelation function of the output field is limited to

$$Q_{oo}(\underline{x},\underline{\xi},t_0 + nT,sT) = E\{o[\underline{x},t_0 + nT]o[\underline{x} + \underline{\xi},t_0 + (n + s)T]\} \qquad (8\text{-}57)$$

over all $\underline{x}$ and $\underline{\xi}$, and over all positive and negative integer values of n and s.

Inasmuch as we restrict our attention in this text to stationary pressure fields and thereby (see equations (8-11) and (8-13)) to stationary sensor output fields, the time-sampled autocorrelation function of equation (8-57) takes the form

$$Q_{oo}(\underline{x},\underline{\xi},t_0 + nT,sT) = Q_{oo}(\underline{x},\underline{\xi},sT) \ . \qquad (8\text{-}58)$$

If the pressure field, and thereby (see equations (8-12) and (8-13)) the sensor output field, is homogeneous as well as stationary, then

$$Q_{oo}(\underline{x},\underline{\xi},t_0 + nT,sT) = Q_{oo}(\underline{\xi},sT) \ . \qquad (8\text{-}59)$$

Consider first the estimation of the wavevector-frequency spectrum of a

homogeneous, stationary output field. From the ensemble of time-sampled output fields, we know $Q_{oo}(\underline{\xi},sT)$ over all $\underline{\xi}$ and over all positive and negative integer values of s. By approximating the temporal integration in equation (6-90) by a summation, we estimate the wavevector-frequency spectrum of the homogeneous, stationary output field by

$$\tilde{\Phi}_o(\underline{k},\omega) = T \sum_{s=-\infty}^{\infty} \int_{-\infty}^{\infty} \int_{-\infty}^{\infty} Q_{oo}(\underline{\xi},sT)\exp\{-i(\underline{k}\cdot\underline{\xi} + \omega sT)\}\, d\underline{\xi} \ . \tag{8-60}$$

By again making use of the sampling property of the Dirac delta function, we can write

$$Q_{oo}(\underline{\xi},sT)\exp(-i\omega sT) = \int_{-\infty}^{\infty} Q_{oo}(\underline{\xi},\theta)\exp(-i\omega\theta)\delta(\theta - sT)\, d\theta \ . \tag{8-61}$$

By substitution of equation (8-61) into equation (8-60) and use of the definition of $v(\theta)$ given in equation (8-47), it follows that the estimate, $\tilde{\Phi}_o(\underline{k},\omega)$, of the wavevector-frequency spectrum is related to the true autocorrelation function, $Q_{oo}(\underline{\xi},\tau)$, of the homogeneous, stationary output field by

$$\tilde{\Phi}_o(\underline{k},\omega) = \int_{-\infty}^{\infty} \int_{-\infty}^{\infty} \int_{-\infty}^{\infty} Q_{oo}(\underline{\xi},\theta)v(\theta)\exp\{-i(\underline{k}\cdot\underline{\xi} + \omega\theta)\}\, d\underline{\xi}\, d\theta \ . \tag{8-62}$$

By use of equation (6-91), it is straightforward to show that the estimated and true wavevector-frequency spectra of the sensor output field are related by the convolution

$$\tilde{\Phi}_o(\underline{k},\omega) = (2\pi)^{-1} \int_{-\infty}^{\infty} \Phi_o(\underline{k},\Omega)V(\omega - \Omega)\, d\Omega \ . \tag{8-63}$$

By substitution of the form of $V(\omega)$ given by equation (8-51) in equation (8-63), it follows that

$$\tilde{\Phi}_0(\underline{k},\omega) = \sum_{n=-\infty}^{\infty} \Phi_0(\underline{k},\omega - 2\pi n/T) \ . \tag{8-64}$$

Thus, the wavevector-frequency spectrum of the stationary, homogeneous field of the sensor output field estimated from the ensemble of time-sampled measurements is seen to be equal to an infinite sum of frequency-shifted replicates of the true wavevector-frequency spectrum of the sensor output field.

Note, by comparison of equation (8-64) with equation (8-52), the similarity in the mathematical relationships between true and estimated wavevector-frequency spectra of a random output field and the true and estimated wavevector-frequency transforms of a deterministic field. Indeed, the only difference between the forms of these expressions is the absence, in equation (8-64), of the uniform phase shift $\exp(-i2\pi n t_0/T)$ between replications. Recall, however, that statistical descriptors, being average quantities, do not preserve absolute phase information, whereas the wavevector-frequency transform preserves both the amplitude and absolute phase of each wavevector-frequency component of a deterministic field.

Owing to the mathematical similarity between equations (8-52) and (8-64), we can apply the analysis and interpretation of equation (8-52) to equation (8-64) to demonstrate that

$$\tilde{\Phi}_0(\underline{k},\omega) = \Phi_0(\underline{k},\omega), \quad |\omega| \leq \pi/T \ , \tag{8-65}$$

if

$$\Phi_0(\underline{k},\omega) = 0, \quad |\omega| > \omega_c \ , \tag{8-66}$$

for all $\underline{k}$, and

$$T \leq \pi/\omega_c \ . \tag{8-67}$$

If $T > \pi\omega_c$ or $\Phi_0(\underline{k},\omega)$ is not frequency band limited for all $\underline{k}$, then the estimate of the wavevector-frequency spectrum provided by equation (8-60) will differ from the true wavevector-frequency spectrum in the frequency range $|\omega| \leq \pi/T$ as a result of aliasing.

Given a wavevector-frequency spectrum of the sensor output field that is band limited as described by equation (8-66), a sampling period satisfying equation (8-67), and knowledge of the wavevector-frequency response, $G(\underline{k},\omega)$, of the identical sensors used to measure the random pressure field, then it follows from equations (8-15) and (8-65) that the true wavevector-frequency spectrum of the homogeneous, stationary pressure field can be recovered from the measured data. That is,

$$\Phi_p(\underline{k},\omega) = \frac{\Phi_0(\underline{k},\omega)}{|G(-\underline{k},\omega)|^2} = \begin{cases} \dfrac{\tilde{\Phi}_0(\underline{k},\omega)}{|G(-\underline{k},\omega)|^2} , & |\omega| \le \pi/T , \\ 0, & \text{otherwise.} \end{cases} \tag{8-68}$$

Arguments similar to those applied to the time-sampled autocorrelation function of the stationary, homogeneous sensor output field can be applied to estimate the two wavevector-frequency spectrum of the stationary, nonhomogeneous sensor output field from the time-sampled autocorrelation function described by equation (8-58). That is, we estimate the two wavevector-frequency spectrum (defined by equation (6-121)) of the sensor output field by

$$\tilde{S}_{00}(\underline{\mu},\underline{k},\omega) = T \sum_{s=-\infty}^{\infty} \int_{-\infty}^{\infty}\int_{-\infty}^{\infty}\int_{-\infty}^{\infty}\int_{-\infty}^{\infty} Q_{00}(\underline{x},\underline{\xi},sT)\exp[-i(\underline{\mu}\cdot\underline{x} + \underline{k}\cdot\underline{\xi} + \omega sT)]\, d\underline{x}\, d\underline{\xi} , \tag{8-69}$$

and use the sampling property of the Dirac delta function to write

$$\tilde{S}_{00}(\underline{\mu},\underline{k},\omega) = \int_{-\infty}^{\infty}\int_{-\infty}^{\infty}\int_{-\infty}^{\infty}\int_{-\infty}^{\infty}\int_{-\infty}^{\infty} Q_{00}(\underline{x},\underline{\xi},\theta)v(\theta)\exp[-i(\underline{\mu}\cdot\underline{x} + \underline{k}\cdot\underline{\xi} + \omega\theta)]\, d\underline{x}\, d\underline{\xi}\, d\theta . \tag{8-70}$$

By employing equations (6-124) and (8-51), it is easily shown that

$$\tilde{S}_{00}(\underline{\mu},\underline{k},\omega) = \sum_{n=-\infty}^{\infty} S_{00}(\underline{\mu},\underline{k},\omega - 2n\pi/T) . \tag{8-71}$$

Here again, we find that the two wavevector-frequency spectrum of the stationary, nonhomogeneous sensor output field estimated from the ensemble of time-sampled measurements is equal to an infinite sum of frequency-shifted replicates of the true two wavevector-frequency spectrum of the sensor output field. By recognizing the mathematical similarity between equation (8-71) and equations (8-52) and (8-64), we can immediately conclude that

$$\tilde{S}_{OO}(\underline{\mu},\underline{k},\omega) = S_{OO}(\underline{\mu},\underline{k},\omega)\ , \quad |\omega| \leq \pi/T\ , \tag{8-72}$$

if

$$S_{OO}(\underline{\mu},\underline{k},\omega) = 0\ , \quad |\omega| > \omega_c\ , \tag{8-73}$$

for all $\underline{\mu}$ and $\underline{k}$, and

$$T < \pi/\omega_c\ . \tag{8-74}$$

If the conditions of either equation (8-73) or (8-74) are not met, the estimate of the two wavevector-frequency spectrum of the sensor output field will differ from the true spectrum of the output field over some, or all, of the frequency range $|\omega| \leq \pi/T$.

If the conditions of equations (8-73) and (8-74) are satisfied, then it follows from equations (8-14) and (8-72) that the true two wavevector-frequency spectrum of the pressure field can be recovered from the ensemble of time-sampled output fields. That is,

$$S_{pp}(\underline{\mu},\underline{k},\omega) = \frac{S_{OO}(\underline{\mu},\underline{k},\omega)}{G(\underline{k}-\underline{\mu},-\omega)G(-\underline{k},\omega)} = \begin{cases} \dfrac{\tilde{S}_{OO}(\underline{\mu},\underline{k},\omega)}{G(\underline{k}-\underline{\mu},-\omega)G(-\underline{k},\omega)}\ , & |\omega| \leq \pi/T\ , \\ 0, & \text{otherwise.} \end{cases} \tag{8-75}$$

Many signal processing texts describe temporal sampling and its effects in terms of the sampling frequency (or rate), $f_s = 1/T$, rather than a sampling period, T. The frequency $f_N = f_s/2 = 1/(2T)$ is defined as the Nyquist frequency.[8] Consider a space-time field that is frequency band limited such that it contains no contributions at frequencies above $f_c = \omega_c/2\pi$. If we specify the Nyquist frequency such that $f_N > f_c$, we thereby realize a

sampling frequency, $f_s = 2f_N$, sufficiently high to ensure an unaliased estimate of the transform or spectrum of the field within $|f| \leq f_N$.

By the analysis and discussion presented in this section, it is abundantly clear that an unaliased estimate of the wavevector-frequency transform or spectrum of a space-time field can be obtained from a uniform temporal sampling of that field, applied synchronously over all space, only if the field is band limited in frequency at all wavevectors. A practical method of ensuring this frequency band limitation is to lowpass filter the output of each sensor in the frequency domain prior to the temporal sampling. By such filtering, contributions to the output of each sensor from frequencies outside the range $-\omega_c \leq \omega \leq \omega_c$ are of negligible magnitude. However, it must be realized that the magnitudes of the various frequency contributions to the lowpass filtered version of the field depend on the specific frequency content of the true field as well as the frequency response characteristics of the candidate lowpass filter. Therefore, the selection of a lowpass filter and subsequent identification of a suitable value of ω_c is, to some degree, a trial and error process.

8.2.2 Spatial Sampling

As implied by previous remarks, temporal sampling is performed as a matter of choice so as to take advantage of the computational speed and efficiency of FFT algorithms in performing temporal Fourier transforms. Spatial sampling, on the other hand, is performed as a matter of necessity because no two (identical) sensors can be located closer than the minimum dimension of the sensor.

In this section, we explore how spatial sampling affects our ability to estimate the space-time or wavevector-frequency characteristics of the pressure field. Although it is not necessary that a field be sampled at uniform intervals in space, most sampling arrays are designed with uniform sensor spacings in order to exploit the advantages of FFT algorithms in performing spatial Fourier transformations of the measured data. For that reason, we will restrict our attention to uniform spatial sampling.

Consider a pressure field, $p(\underline{x},t)$, that is measured, over all time, by the uniformly spaced array of sensors illustrated in figure 8-6. The array is infinite in spatial extent, with uniform spacings d_1 and d_2 between adjacent sensors in the x_1 and x_2 coordinate directions, respectively. The spatial origin of the array is located at $\underline{x}_0 = (x_{01},x_{02})$. In any single trial of the measurement, the use of the array of sensors limits our knowledge of the sensor output field to $o(x_{01} + md_1, x_{02} + nd_2, t)$ over all time for all positive and negative integer values of m and n.

If the pressure field and, consequently, the sensor output field are deterministic, the output field is completely characterized by its wavevector-frequency transform, $O(\underline{k},\omega)$, which is defined by equation (8-6). However, from the limited set of output data measured from the array of sensors, we can form only an estimate, $\tilde{O}(\underline{k},\omega)$, of this wavevector-frequency transform. That estimate is

$$\tilde{O}(\underline{k},\omega) = d_1 d_2 \sum_{m=-\infty}^{\infty} \sum_{n=-\infty}^{\infty} \int_{-\infty}^{\infty} o(x_{01} + md_1, x_{02} + nd_2, t)$$

$$\exp\{-i[k_1(x_{01} + md_1) + k_2(x_{02} + nd_2) + \omega t]\}\, dt \ . \qquad (8\text{-}76)$$

By defining the spatial sampling function, $s(\underline{x})$, as

$$s(\underline{x}) = d_1 d_2 \sum_{m=-\infty}^{\infty} \sum_{n=-\infty}^{\infty} \delta(x_1 - md_1)\delta(x_2 - nd_2) \ , \qquad (8\text{-}77)$$

we can rewrite equation (8-76) in the form

$$\tilde{O}(\underline{k},\omega) = \int_{-\infty}^{\infty}\int_{-\infty}^{\infty}\int_{-\infty}^{\infty} o(\underline{z},t)s(\underline{z} - \underline{x}_0)\exp\{-i(\underline{k}\cdot\underline{z} + \omega t)\}\, d\underline{z}\, dt \ . \qquad (8\text{-}78)$$

By writing $o(\underline{z},t)$ in the form of its inverse Fourier transform, we can show that

$$\tilde{O}(\underline{k},\omega) = (2\pi)^{-2} \int_{-\infty}^{\infty}\int_{-\infty}^{\infty} O(\underline{\mu},\omega)S(\underline{k} - \underline{\mu})\exp\{-i(\underline{k} - \underline{\mu})\cdot\underline{x}_0\}\, d\underline{\mu} \ , \qquad (8\text{-}79)$$

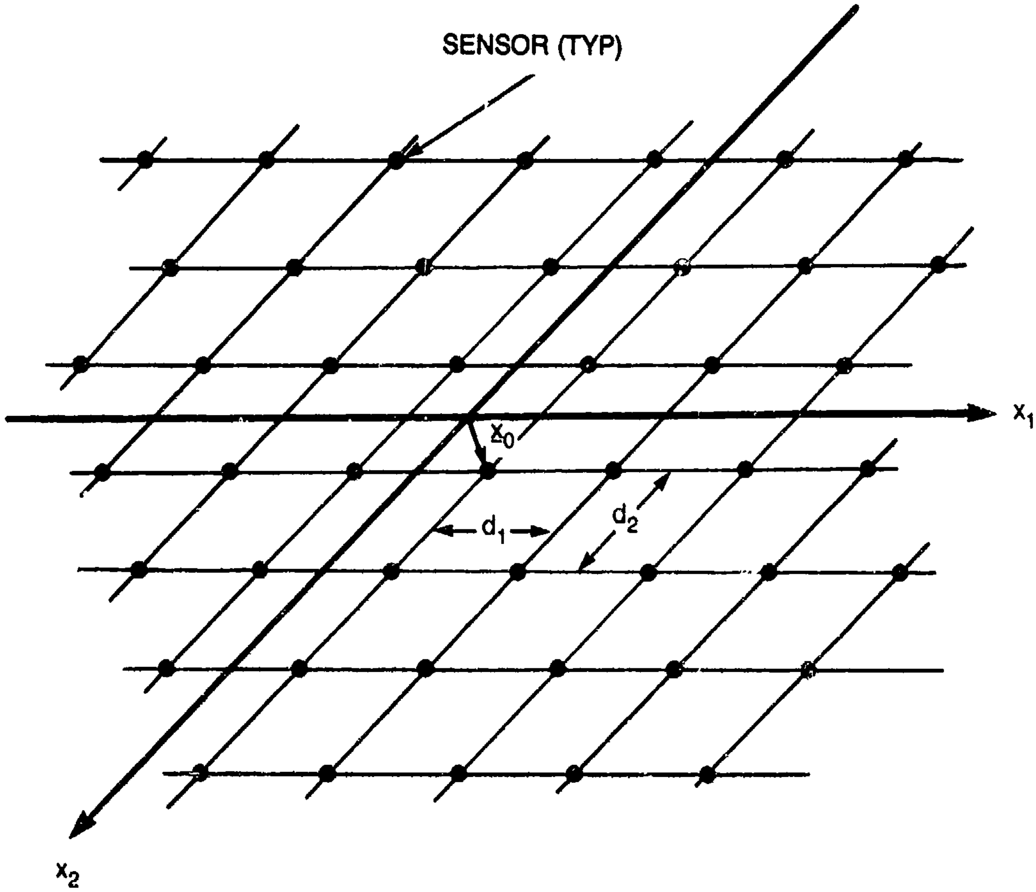

Figure 8-6. Illustration of Uniform Sampling

where $S(\underline{k})$ is the spatial Fourier transform of the spatial sampling function, $s(\underline{x})$.

Note that $s(\underline{x})$ can be written in the separable form

$$s(\underline{x}) = \left\{d_1 \sum_{m=-\infty}^{\infty} \delta(x_1 - md_1)\right\}\left\{d_2 \sum_{n=-\infty}^{\infty} \delta(x_2 - nd_2)\right\} . \tag{8-80}$$

In this form, we recognize $s(\underline{x})$ to be the product of two summations of the form of equation (8-47). We can therefore employ equation (8-51) to show that

$$S(\underline{k}) = (2\pi)^2 \sum_{m=-\infty}^{\infty} \sum_{n=-\infty}^{\infty} \delta(k_1 - 2m\pi/d_1)\delta(k_2 - 2n\pi/d_2) . \tag{8-81}$$

By substituting the appropriate form of equation (8-81) into equation (8-79) and performing the requisite integration, we obtain the following relationship between the estimated and true wavevector-frequency transforms of the sensor output field:

$$\tilde{O}(\underline{k},\omega) = \sum_{m=-\infty}^{\infty} \sum_{n=-\infty}^{\infty} O(k_1 - 2m\pi/d_1, k_2 - 2n\pi/d_2, \omega)$$

$$\exp\{-i(2m\pi x_{01}/d_1 + 2n\pi x_{02}/d_2)\} \ . \qquad (8\text{-}82)$$

Note that the estimate of the wavevector-frequency transform of the sensor output field is equal to a double infinite summation of wavevector and phase-shifted replicates of the true wavevector-frequency transform of the output field. The replicates of the true spectrum occur periodically in both k_1 and k_2, with periods $2\pi/d_1$ and $2\pi/d_2$, respectively. The incremental phase shift between replicates is $2\pi x_{01}/d_1$ in the k_1 coordinate direction and $2\pi x_{02}/d_2$ in the k_2 direction.

To illustrate this replication in the wavevector domain, consider the true wavevector-frequency transform, $O(\underline{k},\omega_0)$, of a sensor output field at the frequency ω_0 illustrated in figure 8-7. As illustrated in the perspective view shown by figure 8-7(a), $O(\underline{k},\omega_0)$ is a real and even function of k_1 and k_2, and is wavevector band limited such that $O(\underline{k},\omega_0)$ is equal to zero for $|k_1| > k_{1c}$ or $|k_2| > k_{2c}$. For future reference, a contour plot of $O(\underline{k},\omega_0)$ is shown in figure 8-7(b).

This wavevector band-limited sensor output field is spatially sampled by an infinite, two-dimensional array of uniformly spaced sensors similar to that illustrated in figure 8-6, but with $\underline{x}_0$ coincident with the spatial origin of the output field: that is, with $\underline{x}_0 = (0,0)$. This choice of $\underline{x}_0$ is made to eliminate the complex phase term in equation (8-82), and thereby simplify the illustration of estimated transforms.

Figure 8-8 illustrates a contour plot of the estimated transform, $\tilde{O}(\underline{k},\omega_0)$, of the wavevector band-limited output field at the frequency ω_0 that results from choosing the uniform spatial sampling intervals, d_1 and

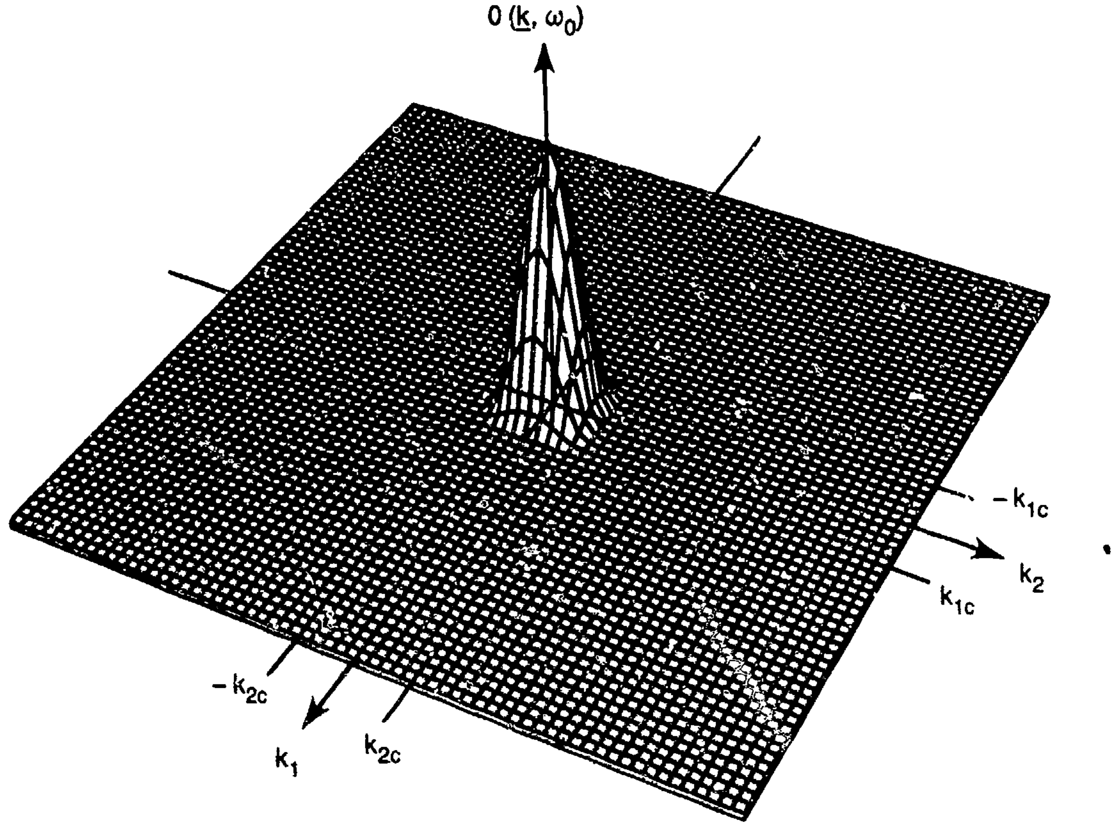

Figure 8-7(a). Perspective View of Wavevector Band-Limited Transform, $O(\underline{k},\omega_0)$

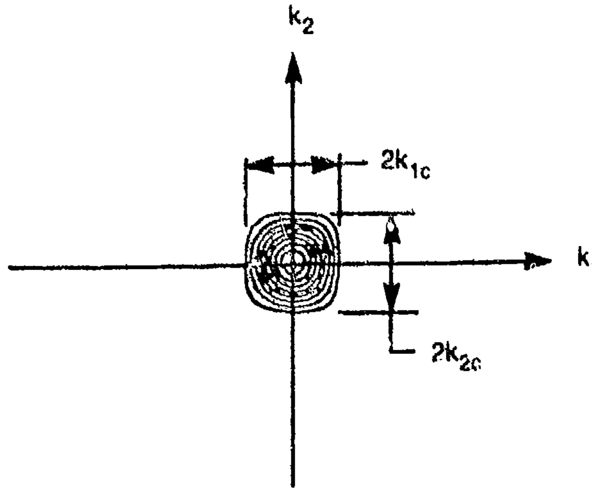

Figure 8-7(b). Contour Plot of Wavevector Band-Limited Transform, $O(\underline{k},\omega_0)$

Figure 8-7. Perspective and Contour Plots of the Wavevector Band-Limited, Wavevector-Frequency Transform, $O(\underline{k},\omega_0)$

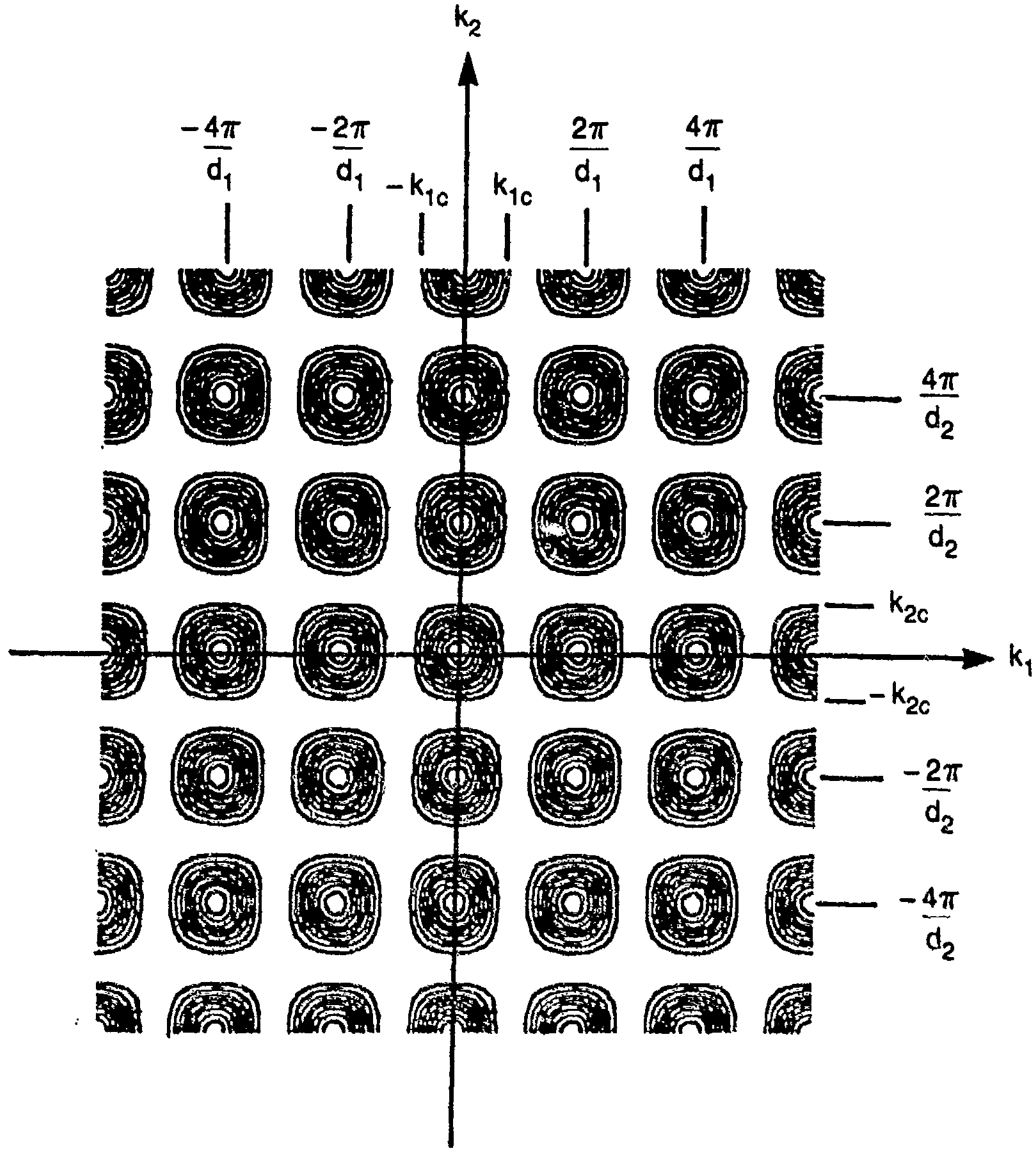

Figure 8-8. Contour Plot of $\tilde{O}(\underline{k},\omega_0)$ for a Wavevector Band-Limited Output Field for $d_1 < \pi/|k_{1c}|$ and $d_2 < \pi/|k_{2c}|$

d_2, such that $d_1 < \pi/k_{1c}$ and $d_2 < \pi/k_{2c}$. For this choice of sampling intervals, the separation between replicates, in both the k_1 and k_2 coordinate directions, is greater than the total bandwidths, $2k_{1c}$ and k_{2c}, of the true transform in the respective wavenumber coordinates. Therefore, the estimated wavevector-frequency transform, at any wavevector, comprises the sum of contributions from a two-dimensional array of separated replicates of the true wavevector band-limited transform. Owing to this separation between the band-limited replicates, it is evident from figure 8-8 that

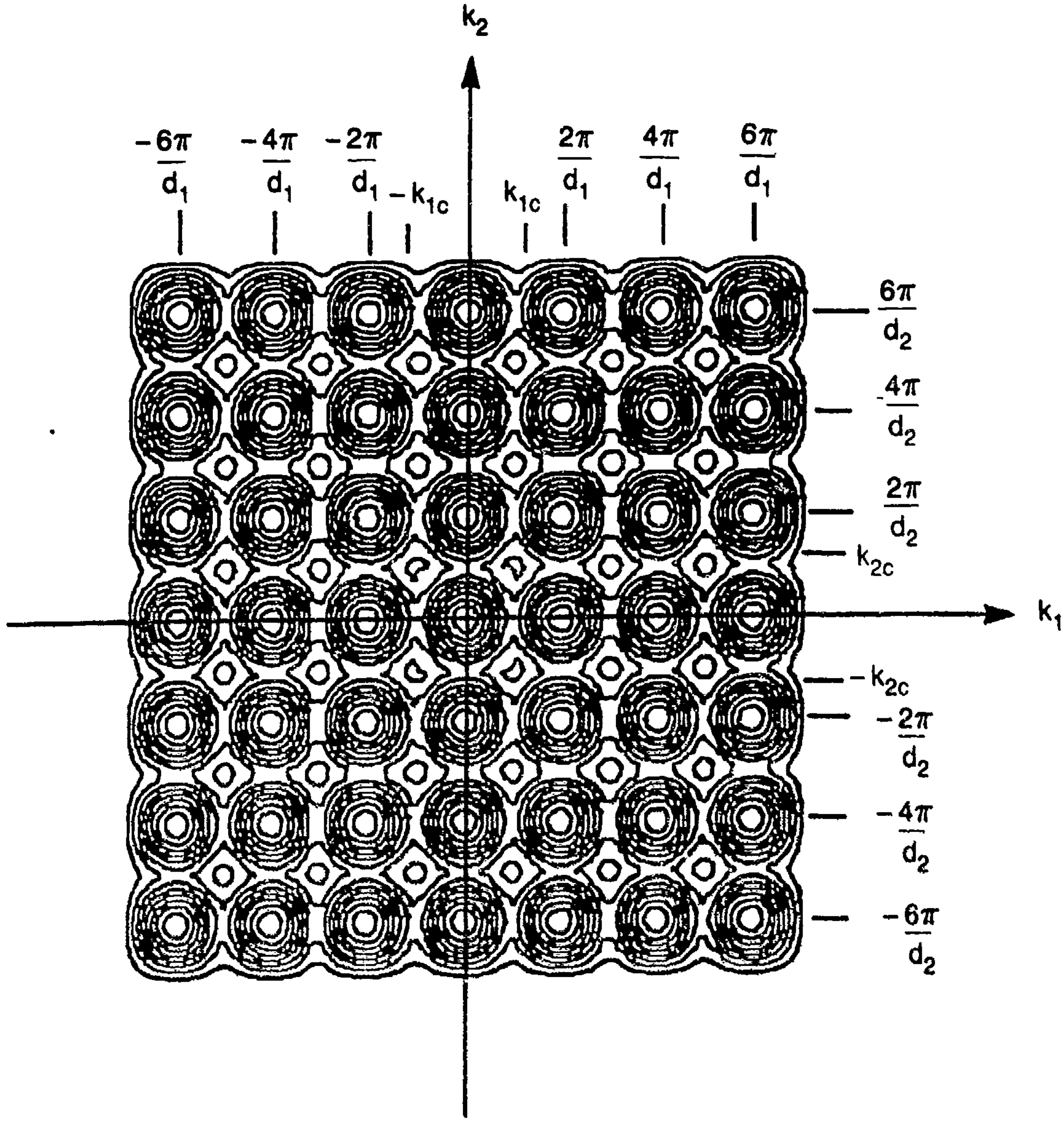

Figure 8-9. Contour Plot of $\tilde{O}(\underline{k},\omega_0)$ For a Wavevector Band-Limited Output Field for $d_1 > \pi/k_{1c}$ and $d_2 > \pi/k_{2c}$

$$\tilde{O}(\underline{k},\omega_0) = O(\underline{k},\omega_0), \quad |k_1| \leq \pi/d_1 \text{ and } |k_2| \leq \pi/d_2 \tag{8-83}$$

when $d_1 < \pi/k_{1c}$ and $d_2 < \pi/k_{2c}$.

Figure 8-9 depicts a contour plot of the estimated transform, $\tilde{O}(\underline{k},\omega_0)$, of the wavevector band-limited output field at the frequency ω_0 that results from choosing spatial sampling intervals such that $d_1 > \pi/k_{1c}$ and $d_2 > \pi/k_{2c}$. Note that this estimated transform is again a periodic function of both k_1 and

k_2. However, the above stated choice of sampling intervals results in wavenumber separations, $2\pi/d_1$ and $2\pi/d_2$, between replicates that are less than the total wavenumber bandwidths, $2k_{c1}$ and $2k_{c2}$, of the true wavevector-frequency transform in the k_1 and k_2 coordinate directions. Thus, as illustrated in figure 8-9, the periodic replicates of the true transform overlap in both the k_1 and k_2 coordinate directions. The regions of overlap are centered at $\underline{k} = [(2m + 1)\pi/d_1, (2n + 1)\pi/d_2]$ for all m and n, and the bandwidths of overlap are $2(k_{1c} - \pi/d_1)$ and $2(k_{2c} - \pi/d_2)$ in the respective k_1 and k_2 coordinate directions. Inasmuch as the estimate of the wavevector-frequency transform, at any wavevector, is the sum of the contributions from all replicates at that wavevector, it is evident that the estimated transform will equal the true transform only within the wavevector range $|k_1| < 2\pi/d_1 - k_{1c}$ and $|k_2| < 2\pi/d_2 - k_{2c}$. The estimate in the wavevector ranges defined by $(2\pi/d_1 - k_{1c}) < |k_1| < \pi/d_1$ and/or $(2\pi/d_2 - k_{2c}) < |k_2| < \pi/d_2$ will differ from the true transform due to contributions from the overlapped replicates (i.e., due to aliasing in the wavevector domain).

By the above examples, it is evident that when a deterministic output field, $o(\underline{x},t)$, is sampled at spatial intervals d_1 and d_2 over the infinite extent of x_1 and x_2, continuously over all time, then, if the true wavevector-frequency transform of the field is wavevector band limited such that

$$O(\underline{k},\omega) = 0, \quad |k_1| > k_{1c} \text{ and } |k_2| > k_{2c} \; , \tag{8-84}$$

the estimate of the transform, $\tilde{O}(\underline{k},\omega)$, is given by

$$\tilde{O}(\underline{k},\omega) = O(\underline{k},\omega), \quad |k_1| \leq \pi/d_1 \text{ and } |k_2| \leq \pi/d_2 \; , \tag{8-85}$$

over all ω provided that the sampling intervals are chosen such that

$$d_1 < \pi/k_{1c} \text{ and } d_2 < \pi/k_{2c} \; . \tag{8-86}$$

If either (1) the true wavevector-frequency transform of the field is not wavevector band limited or (2) the spatial sampling criteria of equation (8-86) are not met, then the estimate of the wavevector-frequency transform

will contain aliased wavevector contributions and will therefore differ from the true transform at some (or possibly all) wavevectors within the range $|k_1| \leq \pi/d_1$ and $|k_2| \leq \pi/d_2$.

If the conditions of equations (8-84) and (8-86) are satisfied, then it follows from equations (8-7) and (8-85) that the wavevector-frequency transform of the pressure field, $P(\underline{k},\omega)$, can be exactly determined from the estimate of the wavevector-frequency transform of the sensor output field, given the wavevector-frequency response of the sensor. That is,

$$P(\underline{k},\omega) = \frac{O(\underline{k},\omega)}{G(-\underline{k},\omega)} = \begin{cases} \dfrac{\tilde{O}(\underline{k},\omega)}{G(-\underline{k},\omega)} , & |k_1| \leq \pi/d_1 \text{ and } |k_2| \leq \pi/d_2 , \\ 0 , & \text{otherwise.} \end{cases} \tag{8-87}$$

Given $O(\underline{k},\omega)$ or $P(\underline{k},\omega)$ over all $\underline{k}$ and ω, then $o(\underline{x},t)$ or $p(\underline{x},t)$ can be obtained by inverse Fourier transformation.

Let us now address the problem of estimating the space-time or wavevector-frequency characteristics of a stationary, random pressure field, $p(\underline{x},t)$, from the ensemble of spatial samples of the sensor output field, $o(x_{01} + md_1, x_{02} + nd_2, t)$, measured (by use of an infinite, two-dimensional array of sensors) over all time for all possible realizations of the random pressure field. From this ensemble of spatially sampled data, our knowledge of the stationary autocorrelation function of the output field is limited to the discrete set of functions

$$Q_{oo}(x_{01} + md_1, x_{02} + nd_2; qd_1, sd_2; \tau) =$$
$$E\{o[x_{01} + md_1, x_{02} + nd_2, t]o[x_{01} + (m + q)d_1, x_{02} + (n + s)d_2, t + \tau]\} \tag{8-88}$$

over all τ for all positive and negative integer values of m, n, q, and s. If the pressure field, and thereby the sensor output field, is homogeneous as well as stationary, our knowledge of the autocorrelation function of the output field is limited to the set of functions $Q_{oo}(qd_1, sd_2, \tau)$ over all τ for all integer values of q and s.

Let us first consider the estimation of the wavevector-frequency spectrum of the stationary and homogeneous sensor output field from the measured samples of the autocorrelation field. We formulate this estimate, which we denote by $\tilde{\Phi}_0(\underline{k},\omega)$, by replacing the spatial integrals in equation (6-90) by appropriate summations. That is,

$$\tilde{\Phi}_0(\underline{k},\omega) = d_1 d_2 \sum_{q=-\infty}^{\infty} \sum_{s=-\infty}^{\infty} \int_{-\infty}^{\infty} Q_{00}(qd_1, sd_2, \tau)$$

$$\exp\{-i(k_1 q d_1 + k_2 s d_2 + \omega\tau)\} \, d\tau \; . \qquad (8\text{-}89)$$

By making use of the sampling function of equation (8-77), we can write equation (8-89) in the form

$$\tilde{\Phi}_0(\underline{k},\omega) = \int_{-\infty}^{\infty}\int_{-\infty}^{\infty}\int_{-\infty}^{\infty} Q_{00}(\underline{\xi},\tau) s(\underline{\xi}) \exp\{-i(\underline{k}\cdot\underline{\xi} + \omega\tau)\} \, d\underline{\xi} \, d\tau \; . \qquad (8\text{-}90)$$

By writing $Q_{00}(\underline{\xi},\tau)$ as the inverse Fourier transform of $\Phi_0(\underline{\mu},\Omega)$, we can show, by making use of equation (8-81), that the relation between the estimated wavevector-frequency spectra of the sensor output field is related to the true spectrum of that field by

$$\tilde{\Phi}_0(\underline{k},\omega) = \sum_{m=-\infty}^{\infty} \sum_{n=-\infty}^{\infty} \Phi_0(k_1 - 2m\pi/d_1, k_2 - 2n\pi/d_2, \omega) \; . \qquad (8\text{-}91)$$

Note that the mathematical form of equation (8-91) is identical to that of equation (8-82) with $\underline{x}_0$ set to zero. Therefore, the arguments and illustrations used to interpret equation (8-82) can be applied to equation (8-91) to show that when the true wavevector-frequency spectrum of the stationary, homogeneous output field is wavevector band limited such that

$$\Phi_0(\underline{k},\omega) = 0, \quad |k_1| > k_{1c} \text{ and } |k_2| > k_{2c} \; . \qquad (8\text{-}92)$$

then the estimate of the spectrum, $\tilde{\Phi}_0(\underline{k},\omega)$, will be equal to the true

spectrum in the wavevector range $|k_1| \leq \pi/d_1$ and $|k_2| \leq \pi/d_2$ if the spatial sampling intervals are chosen such that $d_1 < \pi/k_{1c}$ and $d_2 < \pi/k_{2c}$. That is,

$$\tilde{\Phi}_o(\underline{k},\omega) = \Phi_o(\underline{k},\omega), \quad |k_1| \leq \pi/d_1 \text{ and } |k_2| \leq \pi/d_2 , \tag{8-93}$$

for all ω if the sampling intervals satisfy the restrictions

$$d_1 < \pi/k_{1c} \text{ and } d_2 < \pi/k_{2c} . \tag{8-94}$$

If the true wavevector-frequency spectrum of the homogeneous, stationary output field is not wavevector band limited, or if the true spectrum is band limited but the spatial sampling criteria of equation (8-94) are not satisfied, then the estimate of the wavevector-frequency spectrum will contain aliased wavevector contributions, and will therefore differ from the true spectrum.

Given knowledge that (1) the true wavevector-frequency spectrum of the sensor output field is band limited as described by equation (8-92), (2) the output field is sampled at spatial intervals that satisfy the requirements of equation (8-94), and (3) the wavevector-frequency response, $G(\underline{k},\omega)$, of the identical sensors used to measure the random pressure field is known, then it follows from equations (8-15) and (8-93) that the true wavevector-frequency spectrum of the homogeneous, stationary pressure field can be recovered from the measured data. That is,

$$\Phi_p(\underline{k},\omega) = \frac{\Phi_o(\underline{k},\omega)}{|G(-\underline{k},\omega)|^2} = \begin{cases} \dfrac{\tilde{\Phi}_o(\underline{k},\omega)}{|G(-\underline{k},\omega)|^2} , & |k_1| \leq \pi/d_1 \text{ and } |k_2| \leq \pi/d_2 , \\ 0, & \text{otherwise.} \end{cases} \tag{8-95}$$

Consider now the estimation of the two wavevector-frequency spectrum of the output field from the discrete set of stationary, nonhomogeneous auto-correlation functions specified by equation (8-88) over all time delays, τ, and for all positive and negative integer values of m, n, q, and s. In this case, the estimate of the two wavevector-frequency spectrum of the sensor output field, $\tilde{S}_{oo}(\underline{\mu},\underline{k},\omega)$, is formulated from the discrete set of auto-correlation functions by approximating the spatial integrals in equation

(6-121) by appropriate summations. By this procedure, we obtain

$$\tilde{S}_{oo}(\underline{\mu},\underline{k},\omega) = d_1^2\, d_2^2 \sum_{m=-\infty}^{\infty} \sum_{n=-\infty}^{\infty} \sum_{q=-\infty}^{\infty} \sum_{r=-\infty}^{\infty} \int_{-\infty}^{\infty} Q_{oo}(x_{01} + md_1, x_{02} + nd_2; qd_1, rd_2; \tau)$$

$$\exp\{-i[\mu_1(x_{01} + md_1) + \mu_2(x_{02} + nd_2) + k_1 qd_1 + k_2 rd_2 + \omega\tau]\}\, d\tau\ . \tag{8-96}$$

By making use of the spatial sampling function of equation (8-77), we can rewrite equation (8-96) in the form

$$\tilde{S}_{oo}(\underline{\mu},\underline{k},\omega) = \int_{-\infty}^{\infty}\int_{-\infty}^{\infty}\int_{-\infty}^{\infty}\int_{-\infty}^{\infty}\int_{-\infty}^{\infty} Q_{oo}(\underline{x},\underline{\xi},\tau)s(\underline{x} - \underline{x}_0;m,n)s(\underline{\xi};q,r)$$

$$\exp\{-i(\underline{\mu}\cdot\underline{x} + \underline{k}\cdot\underline{\xi} + \omega\tau)\}\, d\underline{x}\, d\underline{\xi}\, d\tau\ , \tag{8-97}$$

where the indices ";m,n" and ";q,r" are appended to the argument of the sampling function to serve as a reminder that the summation indices of the two sampling functions are different.

By substituting equation (6-124) for $Q_{oo}(\underline{x},\underline{\xi},\tau)$ and performing the resultant integrations, we obtain the following relationship between the estimated and true two wavevector-frequency spectrum of the stationary, nonhomogeneous sensor output field:

$$\tilde{S}_{oo}(\underline{\mu},\underline{k},\omega) = (2\pi)^{-4} \int_{-\infty}^{\infty}\int_{-\infty}^{\infty}\int_{-\infty}^{\infty}\int_{-\infty}^{\infty} S_{oo}(\underline{\alpha},\underline{\beta},\omega)S(\underline{\mu} - \underline{\alpha})S(\underline{k} - \underline{\beta})$$

$$\exp\{-i(\underline{\mu} - \underline{\alpha})\cdot\underline{x}_0\}\, d\underline{\alpha}\, d\underline{\beta}\ . \tag{8-98}$$

By substituting appropriate forms of equation (8-81) for $S(\underline{\mu} - \underline{\alpha})$ and $S(\underline{k} - \underline{\beta})$, we then obtain

$$\tilde{S}_{oo}(\underline{\mu},\underline{k},\omega) =$$

$$\sum_{m=-\infty}^{\infty} \sum_{n=-\infty}^{\infty} \sum_{q=-\infty}^{\infty} \sum_{s=-\infty}^{\infty} S_{oo}(\mu_1 - 2m\pi/d_1, \mu_2 - 2n\pi/d_2; k_1 - 2q\pi/d_1, k_2 - 2s\pi/d_2; \omega)$$

$$\exp\{-i(2m\pi x_{01}/d_1 + 2n\pi x_{02}/d_2)\}\ . \tag{8-99}$$

Here, we see that the estimate of the two wavevector-frequency spectrum of the sensor output field comprises a quadruple infinite sum of periodic replicates of the true two wavevector-frequency spectrum. These replicates occur periodically in μ_1, μ_2, k_1, and k_2, with periods $2\pi/d_1$, $2\pi/d_2$, $2\pi/d_1$, and $2\pi/d_2$, respectively. In addition, the replicates occurring in the μ_1 and μ_2 coordinate directions are phase shifted by $2m\pi x_{01}/d_1$ and $2n\pi x_{02}/d_2$, respectively, where the integers m and n denote the indices of the replicate.

The primary difference between equation (8-99) and equation (8-82) or (8-91) is that the replications of the spectra occur in four, rather than two, wavenumber dimensions. However, inasmuch as $\underline{\mu}$ and $\underline{k}$ are independent wavevector variables, we can apply our previous experience with sums of periodically replicated functions in two-wavenumber dimensions in an iterative fashion to interpret the consequences of spatial sampling on the two wavevector-frequency spectrum of the sensor output field. That is to say, if the two wavevector-frequency spectrum of the stationary, nonhomogeneous pressure field being measured and, by equation (8-14), the stationary, nonhomogeneous sensor output field are wavevector band limited in both $\underline{\mu}$ and $\underline{k}$ such that

$$S_{00}(\underline{\mu},\underline{k},\omega) = 0: \quad |\mu_1| > \mu_{1c},\ |\mu_2| > \mu_{2c},\ |k_1| > k_{1c},\ \text{and } |k_2| > k_{2c}\ . \tag{8-100}$$

then, if the output field is spatially sampled at periodic intervals of d_1 and d_2 over all x_1 and x_2, continuously over all time, we find that

$$\tilde{S}_{00}(\underline{\mu},\underline{k},\omega) = S_{00}(\underline{\mu},\underline{k},\omega): \quad |\mu_1| \le \pi/d_1,\ |\mu_2| \le \pi/d_2,$$
$$|k_1| \le \pi/d_1,\ \text{and } |k_2| \le \pi/d_2 \tag{8-101}$$

for all ω provided the sampling intervals are chosen such that

$$d_1 < \mathrm{MIN}\{\pi/\mu_{1c},\pi/k_{1c}\} \text{ and } d_2 < \mathrm{MIN}\{\pi/\mu_{2c},\pi/k_{2c}\}\ , \tag{8-102}$$

where MIN{} denotes the minimum value of the arguments enclosed by the braces. The restrictions on the spatial sampling intervals must be expressed in the form of such minima inasmuch as the wavenumber interval between

replicates in both the μ_1 and k_1 coordinates is $2\pi/d_1$ and the interval between replicates in both the μ_2 and k_2 coordinates is $2\pi/d_2$. Therefore, to avoid overlap of the replicates (i.e., aliasing) in both the $\underline{\mu}$ and $\underline{k}$ domains, the sampling intervals must be selected to preclude overlap of the larger of the wavenumber bandwidths, μ_{1c} or k_{1c}, in the μ_1 and k_1 coordinate directions, respectively, and the larger of the wavenumber bandwidths, μ_{2c} or k_{2c}, in the μ_2 and k_2 coordinate directions, respectively.

If $S_{oo}(\underline{\mu},\underline{k},\omega)$ is not band limited in both $\underline{\mu}$ and $\underline{k}$, or if $S_{oo}(\underline{\mu},\underline{k},\omega)$ is band limited in $\underline{\mu}$ and $\underline{k}$ but the spatial sampling requirements of equation (8-102) are not satisfied, then aliasing will occur, and the estimate of the two wavevector-frequency spectrum of the sensor output field will differ from the true spectrum in those wavevector regions where the spectral replicates overlap.

Given that $S_{oo}(\underline{\mu},\underline{k},\omega)$ is band limited in $\underline{\mu}$ and $\underline{k}$ and that the spatial sampling requirements of equation (8-102) are satisfied, then it follows, from equations (8-14), (8-100), and (8-101), that the two wavevector-frequency spectrum of the pressure field can be recovered from the estimate of the two wavevector-frequency spectrum of the sensor output field. That is,

$$S_{pp}(\underline{\mu},\underline{k},\omega) = \frac{S_{oo}(\underline{\mu},\underline{k},\omega)}{G(\underline{k}-\underline{\mu},-\omega)G(-\underline{k},\omega)} = \begin{cases} \dfrac{\tilde{S}_{oo}(\underline{\mu},\underline{k},\omega)}{G(\underline{k}-\underline{\mu},-\omega)G(-\underline{k},\omega)}, & \begin{array}{l} |\mu_1| \le \pi/d_1 , \\ |\mu_2| \le \pi/d_2 , \\ |k_1| \le \pi/d_1 , \\ |k_2| \le \pi/d_2 , \end{array} \\ 0, & \text{otherwise.} \end{cases} \quad (8\text{-}103)$$

Given knowledge of $S_{oo}(\underline{\mu},\underline{k},\omega)$ or $S_{pp}(\underline{\mu},\underline{k},\omega)$ over all $\underline{\mu}$, $\underline{k}$, and ω, then $Q_{oo}(\underline{x},\underline{\xi},\tau)$ or $Q_{pp}(\underline{x},\underline{\xi},\tau)$ can be obtained by appropriate inverse Fourier transformation.

We have established that the spatial characteristics of any sensor output field cannot be measured continuously over space. Rather, in any practical experiment, the sensor output field can be measured only at spatial intervals equal to or greater than the dimensions of the sensors employed in the measurement. In this section, we examined the limitations that spatial sampling of the sensor output field imposes on our ability to deduce the

space-time or wavevector-frequency characteristics of the pressure field being measured. In this examination, we assumed that each realization of the sensor output field was sampled at uniform increments, d_1 and d_2, over all x_1 and x_2, respectively, from a sampling origin $\underline{x}_0$. Each spatial sample was assumed to be measured continuously over all time. Under these assumptions, we showed that the true wavevector-frequency transform of a deterministic output field or the true wavevector-frequency spectrum of a stationary and homogeneous output field could be recovered from this ensemble of sample functions of the output field only if (1) the respective true wavevector-frequency transform or spectrum of the output field was wavevector band limited such that $O(\underline{k},\omega)$ or $\Phi_0(\underline{k},\omega)$ was zero for $|k_1| > k_{1c}$ and $|k_2| > k_{2c}$ and (2) the sampling intervals were selected such that $d_1 < \pi/k_{1c}$ and $d_2 < \pi/k_{2c}$. We further showed that the true two wavevector-frequency spectrum of a stationary, nonhomogeneous output field could be recovered from the ensemble of sample functions of the output field only if (1) the true two wavevector-frequency spectrum of that output field was wavevector band limited in both $\underline{\mu}$ and $\underline{k}$ such that $S_{00}(\underline{\mu},\underline{k},\omega)$ was zero for $|\mu_1| > \mu_{1c}$, $|\mu_2| > \mu_{2c}$, $|k_1| > k_{1c}$, and $|k_2| > k_{2c}$ and (2) the sampling intervals were selected such that $d_1 < \mathrm{MIN}\{\pi/\mu_{1c},\pi/k_{1c}\}$ and $d_2 < \mathrm{MIN}\{\pi/\mu_{2c},\pi/k_{2c}\}$. Given the true wavevector-frequency transform or spectrum, as appropriate, of the sensor output field and the wavevector-frequency response of the (identical) sensors, the corresponding wavevector-frequency transform or spectrum of the measured pressure field can be deduced.

Clearly, the true space-time or wavevector-frequency characteristics of a field cannot be recovered from spatial samples of that field unless the wavevector-frequency transform or spectrum of the field is appropriately wavevector band limited. If the wavevector-frequency transform or spectrum of the pressure field being measured is not band limited in the wavevector domain, one can (according to the theory presented in section 8.1) render the wavevector-frequency transform or spectrum of the sensor output field to be wavevector band limited by measuring the pressure field with sensors designed to have wavevector-frequency responses that pass, without attenuation, those wavevector components within the wavevector range of interest and that strongly attenuate wavevector components outside that range. Then, in theory, the true wavevector-frequency transform or spectrum of the sensor output field

can be recovered from the spatial samples of that output field within the wavevector passband of the sensor. Given knowledge of the wavevector-frequency response of the identical sensors and the wavevector-frequency transform or spectrum of the output field within the wavevector passband, the corresponding wavevector-frequency transform or spectrum of the pressure field can be determined within that passband. However, at this writing, we have not demonstrated the ability, with current sensor technology, to design and construct sensors that provide prespecified lowpass characteristics in the wavevector domain.

8.3 EFFECTS OF FINITE SAMPLING CONSTRAINTS

In the previous section, we examined the consequences of temporal and spatial sampling, over infinite limits of time and space, on our ability to estimate the space-time and wavevector-frequency characteristics of acoustic fields. In practice, however, we can obtain temporal or spatial samples of any sensor output field only over a limited portion of time or space. In this section, we examine the consequences of these temporal and spatial sampling constraints on our ability to estimate the space-time and wavevector-frequency characteristics of the acoustic field being measured. We will begin by examining the effects of finite constraints on temporal sampling of the sensor output field.

8.3.1 Finite Temporal Sampling

Assume that the sensor output field, $o(\underline{x},t)$, obtained by measuring the surface pressure field, $p(\underline{x},t)$, with identical sensors, is sampled synchronously over all $\underline{x}$ at uniform increments, T, in time, starting at the time t_0. At each spatial location, N temporal samples are obtained. This sampling is illustrated in figure 8-10 for the spatial location $\underline{x}_0$. As a result of this uniform temporal sampling over a finite interval of time, our knowledge of $o(\underline{x},t)$ from any realization of the measurement is limited to the set of functions $o(\underline{x},t_0 + nT)$ over all $\underline{x}$ for integer values of n between 0 and N - 1.

If the pressure field and, thus, the output field are deterministic, then

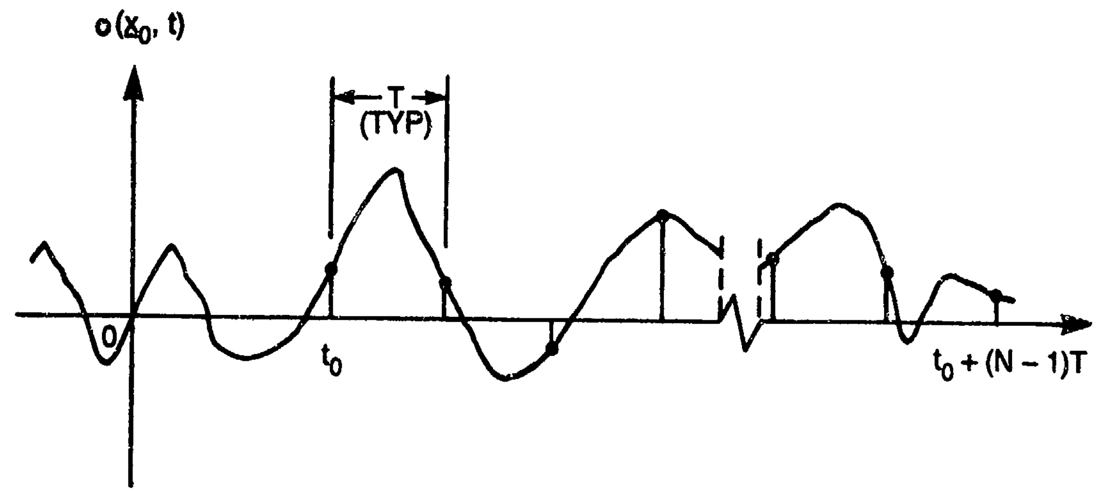

Figure 8-10. Illustration of Finite Temporal Sampling

the output field is completely characterized by its wavevector-frequency transform, $O(\underline{k},\omega)$. However, given only N temporal samples of $o(\underline{x},t)$ at any $\underline{x}$, we can only estimate $O(\underline{k},\omega)$. To obtain this estimate, which we denote by $\tilde{O}(\underline{k},\omega)$, we approximate equation (8-6) by

$$\tilde{O}(\underline{k},\omega) = T \sum_{n=0}^{N-1} \int_{-\infty}^{\infty} \int_{-\infty}^{\infty} o(\underline{x},t_0 + nT)\exp\{-i[\underline{k}\cdot\underline{x} + \omega(t_0 + nT)]\} \, d\underline{x} \; . \qquad (8\text{-}104)$$

By making use of the sampling property of the Dirac delta function, we can rewrite equation (8-104) in the form

$$\tilde{O}(\underline{k},\omega) = \int_{-\infty}^{\infty} \int_{-\infty}^{\infty} \int_{-\infty}^{\infty} o(\underline{x},t) \left\{ T \sum_{n=0}^{N-1} \delta(t - t_0 - nT) \right\} \exp\{-i(\underline{k}\cdot\underline{x} + \omega t)\} \, d\underline{x} \, dt \; . \qquad (8\text{-}105)$$

We define the finite temporal sampling function as

$$v_f(t;N) = T \sum_{n=0}^{N-1} \delta(t - nT) \qquad (8\text{-}106)$$

and write equation (8-105) in the form

$$\tilde{O}(\underline{k},\omega) = \int_{-\infty}^{\infty}\int_{-\infty}^{\infty}\int_{-\infty}^{\infty} o(\underline{x},t)v_f(t - t_0;N)\exp\{-i(\underline{k}\cdot\underline{x} + \omega t)\}\, d\underline{x}\, dt \,. \qquad (8\text{-}107)$$

However, this equation has the form of equation (8-46), which, according to equation (8-48), can be expressed in the form

$$\tilde{O}(\underline{k},\omega) = (2\pi)^{-1} \int_{-\infty}^{\infty} O(\underline{k},\Omega)V_f(\omega - \Omega;N)\exp\{-i(\omega - \Omega)t_0\}\, d\Omega \,, \qquad (8\text{-}108)$$

where $V_f(\omega;N)$, the Fourier transform of $v_f(t;N)$, is given by

$$V_f(\omega;N) = T \sum_{n=0}^{N-1} \exp\{-i\omega nT\} = T \exp\{-i\omega(N - 1)T/2\} \frac{\sin(\omega NT/2)}{\sin(\omega T/2)} \,. \qquad (8\text{-}109)$$

Substitution of equation (8-109) into equation (8-108) yields

$$\tilde{O}(\underline{k},\omega) = \frac{T}{2\pi} \int_{-\infty}^{\infty} O(\underline{k},\Omega) \frac{\sin[(\omega - \Omega)NT/2]}{\sin[(\omega - \Omega)T/2]} \exp\{-i[\omega - \Omega][t_0 + (N - 1)T/2]\}\, d\Omega \,.$$

(8-110)

Note that the mathematical form of equation (8-108) is identical to equation (8-48), which relates the estimated and true transforms for an infinite number of temporal samples of the sensor output field. However, as is evident by comparison of equation (8-109) with equation (8-51), the temporal Fourier transform, $V_f(\omega;N)$, of the finite temporal sampling function, $v_f(t;N)$, is not so mathematically simple as the infinite train of Dirac delta functions that characterize the transform, $V(\omega)$, of the infinite temporal sampling function, $v(t)$. Consequently, for a finite temporal sampling of the sensor output field, the estimate of the wavevector-frequency transform is related to the true transform by the convolution shown in equation (8-110) rather than the simple summation obtained in equation (8-52) for the case of infinite temporal sampling.

One impediment to either the interpretation or computation of the convolution in equation (8-110) is the phase term $\exp\{-i[\omega - \Omega][t_0 + (N-1)T/2]\}$, which varies rapidly with frequency. We can eliminate this phase term by noting that the wavevector-frequency transform, $O[\underline{k},\omega;\tau]$, of $o(\underline{x},t+\tau)$ can be written as

$$O[\underline{k},\omega;\tau] = \int_{-\infty}^{\infty} o(\underline{x},t+\tau)\exp\{-i(\underline{k}\cdot\underline{x} + \omega t)\}\, d\underline{x}\, dt$$

$$= \int_{-\infty}^{\infty} o(\underline{x},\theta)\exp\{-i[\underline{k}\cdot\underline{x} + \omega(\theta - \tau)]\}\, d\underline{x}\, d\theta = O(\underline{k},\omega)\exp\{i\omega\tau\} \ . \tag{8-111}$$

By employing equation (8-111), and by denoting $\tilde{O}(\underline{k},\omega)\exp\{i\omega\tau\}$ as $\tilde{O}[\underline{k},\omega;\tau]$, we can write equation (8-110) in the somewhat simpler form

$$\tilde{O}[\underline{k},\omega;t_0 + (N-1)T/2] = \frac{T}{2\pi}\int_{-\infty}^{\infty} O[\underline{k},\Omega;t_0 + (N-1)T/2]\,\frac{\sin[(\omega - \Omega)NT/2]}{\sin[(\omega - \Omega)T/2]}\, d\Omega \ . \tag{8-112}$$

Here, we see that the estimate, $\tilde{O}[\underline{k},\Omega;t_0 + (N-1)T/2]$, of the wavevector-frequency transform of the temporally shifted sensor output field, $o[\underline{x},t + t_0 + (N-1)T/2]$, is proportional to the convolution of the true wavevector-frequency transform, $O[\underline{k},\Omega;t_0 + (N-1)T/2]$, of that time-shifted sensor output field with the function $\sin(\Omega NT/2)/\sin(\Omega T/2)$.

As illustrated in figure 8-11, $\sin(\Omega NT/2)/\sin(\Omega T/2)$ is a periodic function of Ω, with major acceptance lobes occurring at intervals of $2\pi/T$. These major acceptance lobes have amplitudes N and bandwidths (between zero crossings) of $4\pi/(NT)$. Thus, for a fixed temporal sampling interval, T, the amplitudes of the major acceptance lobes increase, and the bandwidths of these lobes decrease, as the number of temporal samples, N, and thereby the total sampling time, NT, increases. Recall that $V(\omega)$, the transform of the uniform, infinite temporal sampling function, was characterized by an infinite, periodic train of Dirac delta functions. The period of these delta functions in ω was also $2\pi/T$.

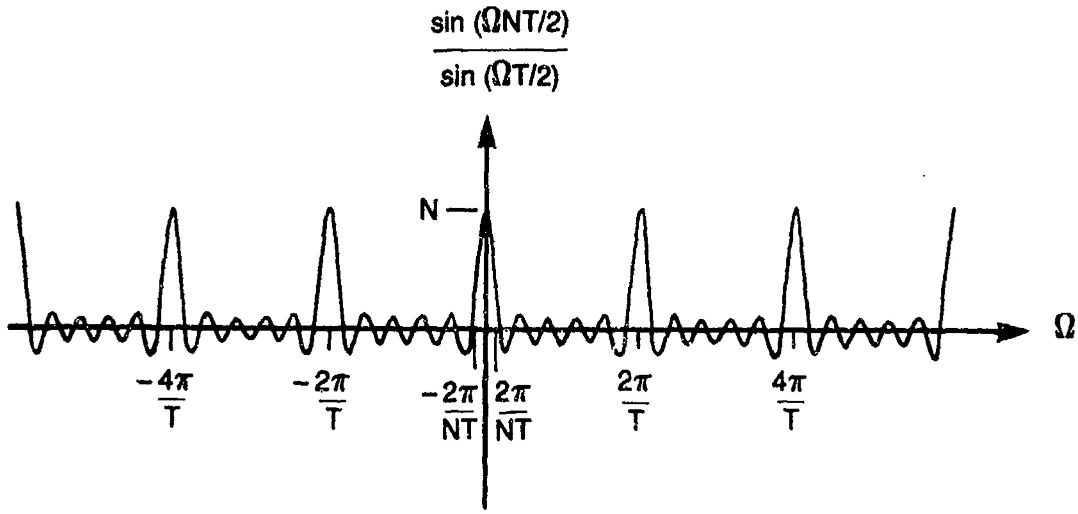

Figure 8-11. The Function $\frac{\sin(\Omega NT/2)}{\sin(\Omega T/2)}$

When the output field was uniformly sampled over all time, the estimate of the wavevector-frequency transform of the output field was obtained by the convolution of the true transform of that field with the periodic train of Dirac delta functions that characterized $V(\omega)$. In that case, we found that if (1) the true transform was band limited in frequency such that $O(\underline{k},\omega) = 0$ for $\omega > \omega_c$ and (2) the period, T, between temporal samples was selected such that $T < \pi/\omega_c$, then the estimate of the transform of the output field comprised an infinite series of periodic, separated replicates of the true transform. The true transform was then deduced from the estimated transform within the frequency range $|\omega| \leq \pi/T$. By reducing the number of temporal samples of the output field from an infinite to a finite number, we reduce our knowledge of the temporal characteristics of that field and, thereby, further restrict our ability to estimate the true space-time or wavevector-frequency characteristics of the output field. Inasmuch as the space-time or wavevector-frequency characteristics of a sensor output field cannot be deduced from an infinite number of uniformly spaced temporal samples of that field unless $O(\underline{k},\omega) = 0$ for $\omega > \omega_c$ and the sampling period is selected such that $T < \pi/\omega_c$, we must anticipate that the space-time or wavevector-frequency characteristics of an output field cannot be deduced from a finite number of temporal samples of that field unless these same frequency band limitations and temporal sampling restrictions are satisfied. Note, however, that, even if these band limitations and sampling restrictions are satisfied, the convolution of equation (8-112) cannot yield, for finite N, an estimate,

$\tilde{O}[\underline{k},\omega;t_0 + (N-1)T/2]$, of the wavevector-frequency transform of the time-shifted output field $o[\underline{x},t + t_0 + (N-1)T/2]$ that comprises periodic, separated replicates of the true transform, $O[\underline{k},\omega;t_0 + (N-1)T/2]$, of that output field.

Unfortunately, even if $O(\underline{k},\omega)$ is band limited in frequency, we cannot exactly solve equation (8-112). However, by investigation of the integrand of equation (8-112), we can gain some insight into how the estimate, $\tilde{O}[\underline{k},\omega;t_0 + (N-1)T/2]$, of the band-limited transform $O[\underline{k},\Omega;t_0 + (N-1)T/2]$ is affected by the number, N, of temporal samples of the output field. Figure 8-12 shows both the (assumed real) transform $O[\underline{k}_0,\Omega;t_0 + (N-1)T/2]$, band limited to frequencies between $-\omega_c \leq \omega \leq \omega_c$, and $\sin[(\omega - \Omega)NT/2]/\sin[(\omega - \Omega)T/2]$ as functions of Ω. The sampling period has been selected such that $T < \pi/\omega_c$.

The convolution in equation (8-112), evaluated at the frequency ω, is simply the integral, over all Ω, of the product of the two functions illustrated in figure 8-12. Note, from this figure, that if $O[\underline{k}_0,\Omega;t_0 + (N-1)T/2]$ is a smoothly varying function of Ω, the value of this integral is dominated by contributions from the products in the vicinity of the major acceptance lobe of $\sin[(\omega - \Omega)NT/2]/\sin[(\omega - \Omega)T/2]$, which is centered at the frequency ω within the band limits, $-\omega_c \leq \Omega \leq \omega_c$, of $O[\underline{k}_0,\Omega;t_0 + (N-1)T/2]$. By expanding $O[\underline{k}_0,\Omega;t_0 + (N-1)T/2]$ in a Taylor series about the frequency ω, we obtain

$$\begin{aligned} O[\underline{k}_0,\Omega;t_0 + (N-1)T/2] &= O[\underline{k}_0,\omega;t_0 + (N-1)T/2] \\ &+ (\Omega - \omega) \left.\frac{\partial O[\underline{k}_0,\Omega;t_0 + (N-1)T/2]}{\partial \Omega}\right|_{\Omega=\omega} \\ &+ \frac{(\Omega - \omega)^2}{2} \left.\frac{\partial^2 O[\underline{k}_0,\Omega;t_0 + (N-1)T/2]}{\partial^2 \Omega}\right|_{\Omega=\omega} + \ldots . \end{aligned} \quad (8\text{-}113)$$

If N is chosen sufficiently large that, within the bandwidth of the major acceptance lobe of $\sin[(\omega - \Omega)NT/2]/\sin[(\omega - \Omega)T/2]$, $O[\underline{k}_0,\Omega;t_0 + (N-1)T/2]$ changes only linearly with frequency, then it follows that equation (8-112) can be approximated, at any value of $\underline{k}$, by

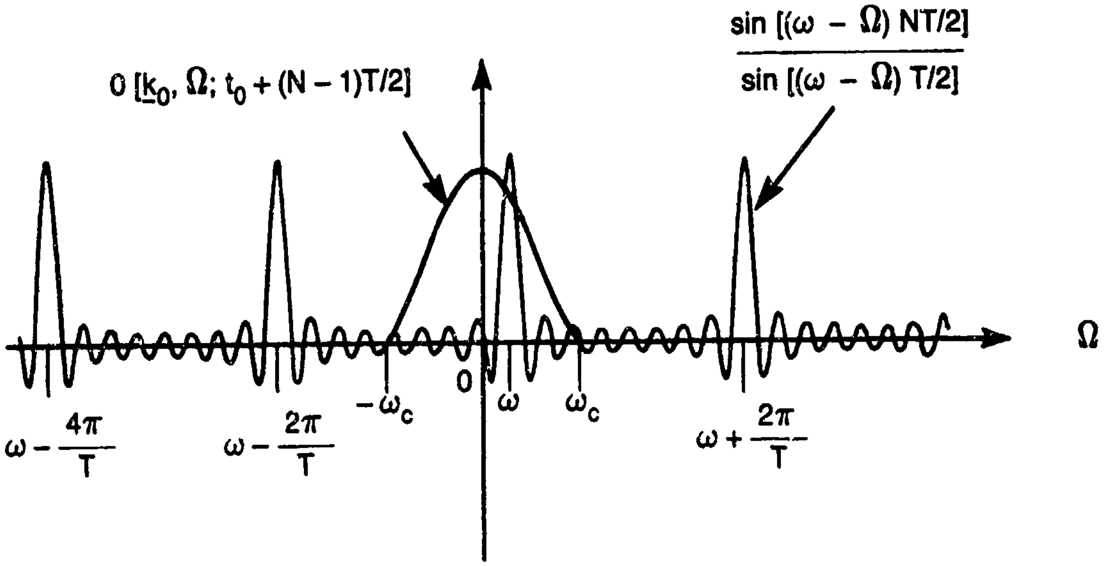

Figure 8-12. Illustration of the Terms Comprising the Integrand of Equation (8-112)

$$\tilde{O}[\underline{k},\omega;t_0 + (N - 1)T/2] \approx \frac{T}{2\pi} \int_{-\omega_c}^{\omega_c} \left\{ O[\underline{k},\omega;t_0 + (N - 1)T/2] + (\Omega - \omega) \cdot \left. \frac{\partial O[\underline{k},\Omega;t_0 + (N - 1)T/2]}{\partial\Omega} \right|_{\Omega=\omega} \right\} \frac{\sin[(\omega - \Omega)NT/2]}{\sin[(\omega - \Omega)T/2]} \, d\Omega \tag{8-114}$$

when $-\omega_c \leq \omega \leq \omega_c$. However, inasmuch as $\sin[(\omega - \Omega)NT/2]/\sin[(\omega - \Omega)T/2]$ is an even function about $\Omega = \omega$ whereas $\Omega - \omega$ is odd, it can be demonstrated that the integral of the second term in equation (8-114) is small in comparison with the integral of the first term. Consequently, a relatively small error results from neglecting the integral of this second term. We assume that a similarly small error is introduced by extending the limits of integration to the range $|\Omega| \leq \pi/T$. Under these assumptions, equation (8-114) takes the form

$$\tilde{O}[\underline{k},\omega;t_0 + (N - 1)T/2] \approx \frac{T}{2\pi} O[\underline{k},\omega;t_0 + (N - 1)T/2] \int_{-\pi/T}^{\pi/T} \frac{\sin[(\omega - \Omega)NT/2]}{\sin[(\omega - \Omega)T/2]} \, d\Omega \, . \tag{8-115}$$

By use of equation (8-109), it can be shown that, if N is odd,

$$\int_{-\pi/T}^{\pi/T} \frac{\sin[(\omega - \Omega)NT/2]}{\sin[(\omega - \Omega)T/2]}\, d\Omega = \frac{2\pi}{T} . \tag{8-116}$$

However, equation (8-116) is also approximately true if N is even, with the degree of approximation improving as N increases. Thus, for N sufficiently large that the bandwidth of the major lobe of $\sin(\omega NT/2)/\sin(\omega T/2)$ is much smaller than the bandwidth of any variation of $O[\underline{k},\omega;t_0 + (N - 1)T/2]$ with frequency, it follows that

$$\tilde{O}[\underline{k},\omega;t_0 + (N - 1)T/2] \approx O[\underline{k},\omega;t_0 + (N - 1)T/2], \quad |\omega| \leq \pi/T . \tag{8-117}$$

By returning our attention to figure 8-12, we note that if the transform is estimated at any of the frequencies $\omega \pm 2\pi n/T$, a major acceptance lobe of $\sin[(\omega - \Omega)NT/2 + nN\pi]/\sin[(\omega - \Omega)T/2 + n\pi]$ will again be centered at $\Omega = \omega$, and the resulting convolution of $O[\underline{k},\Omega;t_0 + (N - 1)T/2]$ with $\sin[(\omega - \Omega)NT/2]/\sin[(\omega - \Omega)T/2]$ is identical to that required to estimate the transform at the frequency ω. Thus, it is evident that, when $O(\underline{k},\omega)$ is band limited such that $O(\underline{k},\Omega) = 0$ for $|\omega| > \omega_c$ and the sampling period is selected such that $T < \pi/\omega_c$, the estimate, $\tilde{O}[\underline{k},\omega;t_0 + (N - 1)T/2]$, of the wavevector-frequency transform of the time-shifted output field, $o[\underline{x},t + t_0 + (N - 1)T/2]$, is a periodic function of frequency. That periodic function of frequency consists of an infinite series of approximations to $O[\underline{k},\omega;t_0 + (N - 1)T/2]$, repeated at intervals of $2\pi/T$. It can be demonstrated, by examination of the major acceptance lobes of $\sin(\omega NT/2)/\sin(\omega T/2)$, that successive approximations are of the same sense (or sign) when N is odd, and are of alternating sense when N is even.

By the above arguments, it is evident that if (1) $O(\underline{k},\omega)$ is band limited such that

$$O(\underline{k},\omega) = 0 , \quad |\omega| > \omega_c , \tag{8-118}$$

(2) the temporal sampling period is chosen such that

$$T < \pi/\omega_c , \tag{8-119}$$

and (3) the number, N, of temporal samples is chosen sufficiently large that

the bandwidth, $4\pi/(NT)$, of the major response lobe of $\sin(\omega NT/2)/\sin(\omega T/2)$ is small compared to the bandwidth of any fluctuation in $O[\underline{k},\omega;t_0 + (N-1)T/2]$ with frequency, then the estimate, $\tilde{O}[\underline{k},\omega;t_0 + (N-1)T/2]$, of the transform $O[\underline{k},\omega;t_0 + (N-1)T/2]$ can be approximated by

$$\tilde{O}[\underline{k},\omega;t_0 + (N-1)T/2] \approx \sum_{n=-\infty}^{\infty} (-1)^{n(N-1)} O[\underline{k},\omega - 2n\pi/T;t_0 + (N-1)T/2] \ , \tag{8-120}$$

and therefore

$$\tilde{O}[\underline{k},\omega;t_0 + (N-1)T/2] \approx O[\underline{k},\omega;t_0 + (N-1)T/2] \ , \quad |\omega| \leq \pi/T \ . \tag{8-121}$$

The quality of these approximations improves as the number, N, of temporal samples increases.

To demonstrate the effect of the number of temporal samples on the quality of the estimate of the wavevector-frequency transform, we assume that, at the wavevector $\underline{k} = \underline{k}_0$, the true transform, $O[\underline{k}_0,\omega;t_0 + (N-1)T/2]$, of the time-shifted output field, $o[\underline{x},t + t_0 + (N-1)T/2]$, is the real, frequency-band-limited function shown in figure 8-13(a). We assume further that the sensor output field $o(\underline{x},t)$ is sampled as illustrated in figure 8-10, with the sampling intervals, T, chosen to be less than π/ω_c to avoid aliasing. Figures 8-13(b) and (c) illustrate estimates, $\tilde{O}[\underline{k},\omega;t_0 + (N-1)T/2]$, of the transform $O[\underline{k}_0,\omega;t_0 + (N-1)T/2]$ for two different choices of the number, N, of temporal samples of the field $o(\underline{x},t)$.

Figure 8-13(b) depicts $\tilde{O}[\underline{k}_0,\omega;t_0 + (N-1)T/2]$ as a function of ω for a choice of N such that the bandwidth, $4\pi/(NT)$, of the major acceptance lobe of $\sin(\Omega NT/2)/\sin(\Omega T/2)$ is about 20 percent of the total frequency bandwidth, $2\omega_c$, of $O(\underline{k}_0,\omega)$. This choice of N is equivalent to requiring the total sampling time, NT, to be about five times greater than the period, $T_c = 2\pi/\omega_c$, associated with the band limit, ω_c, of $O(\underline{k}_0,\omega)$. Figure 8-13(b) shows that, for this choice of N, $\tilde{O}[\underline{k}_0,\omega;t_0 + (N-1)T/2]$ closely approximates an infinite sum of replicates of $O[\underline{k}_0,\omega;t_0 + (N-1)T/2]$, spaced periodically at intervals of $2\pi/T$. Indeed, the only apparent differences between $\tilde{O}[\underline{k}_0,\omega;t_0 + (N-1)T/2]$ and an infinite sum of replicates of $O[\underline{k}_0,\omega;t_0 + (N-1)T/2]$, spaced periodically at intervals of $2\pi/T$, are the slight rounding (or smearing) of the estimate

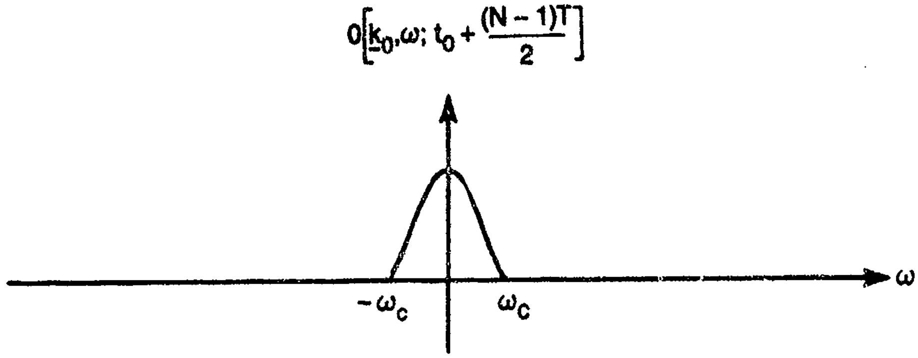

Figure 8-13(a). The True Transform $O[\underline{k}_0, \omega; t_0 + (N - 1)T/2]$

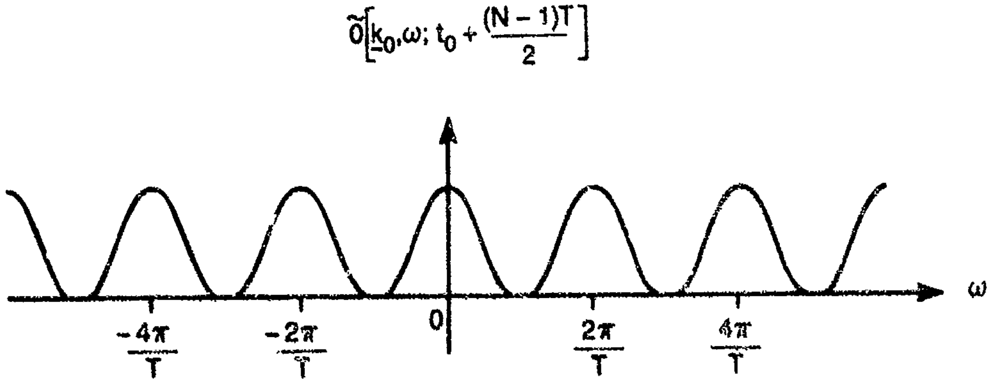

Figure 8-13(b). The Estimated Transform $\tilde{O}[\underline{k}_0, \omega; t_0 + (N - 1)T/2]$ for $NT \gg 2\pi/\omega_c$

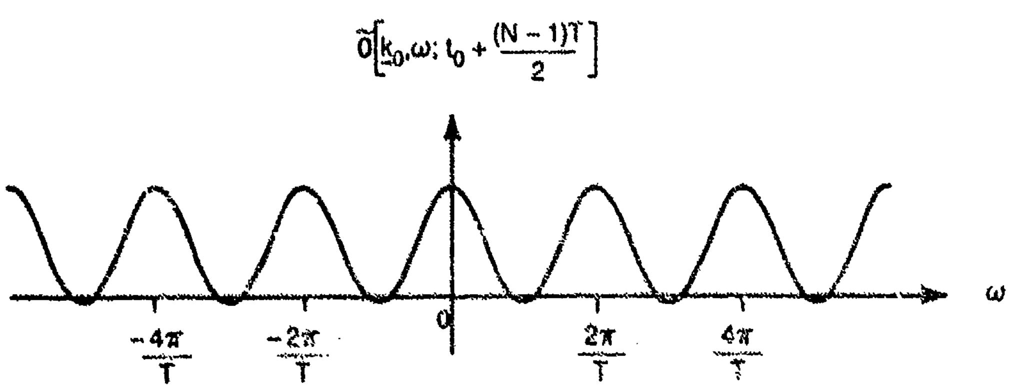

Figure 8-13(c). The Estimated Transform $\tilde{O}[\underline{k}_0, \omega; t_0 + (N - 1)T/2]$ for $NT \approx 4\pi/\omega_c$

Figure 8-13. Comparison of True and Estimated Wavevector-Frequency Transforms of a Frequency Band-Limited Output Field

in the vicinities of the frequencies $2n\pi/T \pm \omega_c$ and the slightly negative value of the estimate in the frequency intervals $2n\pi/T + \omega_c < \omega < 2(n + 1)\pi/T - \omega_c$.

Figure 8-13(c) illustrates $\tilde{O}[\underline{k}_0,\omega;t_0 + (N - 1)T/2]$ as a function of ω for a choice of N such that the bandwidth, $4\pi/(NT)$, of the major acceptance lobe of $\sin(\Omega NT/2)/\sin(\Omega T/2)$ is approximately one-half the total frequency bandwidth, $2\omega_c$, of $O(\underline{k}_0,\omega)$. Here again, we see that $\tilde{O}[\underline{k}_0,\omega;t_0 + (N - 1)T/2]$ is a periodic function of frequency that somewhat resembles an infinite sum of replicates of $O[\underline{k}_0,\omega;t_0 + (N - 1)T/2]$ separated in frequency by $2\pi/T$. However, owing to the relatively small number, N, of temporal samples, the bandwidth of $\sin(\Omega NT/2)/\sin(\Omega T/2)$ is comparable to the bandwidth of $O(\underline{k}_0,\omega)$, so the replicates of $O[\underline{k}_0,\omega;t_0 + (N - 1)T/2]$ are smeared by the convolution process, especially in the vicinity of the frequencies $2n\pi/T \pm \omega_c$ and in the frequency intervals $2n\pi/T + \omega_c < \omega < 2(n + 1)\pi/T - \omega_c$.

Figure 8-13 shows that if $O(\underline{k}_0,\omega)$ is band limited such that $O(\underline{k}_0,\omega) = 0$ for $|\omega| > \omega_c$ and the temporal sampling period is chosen such that $T < \pi/\omega_c$, then the estimate of the transform, $\tilde{O}[\underline{k}_0,\omega;t_0 + (N - 1)T/2]$, formed by the convolution of the true transform, $O[\underline{k}_0,\omega;t_0 + (N - 1)T/2]$, with $\sin(\omega NT/2)/\sin(\omega T/2)$ is a periodic function of frequency. It further illustrates that $\tilde{O}[\underline{k}_0,\omega;t_0 + (N - 1)T/2]$ tends toward a summation of replicates of $O[\underline{k}_0,\omega;t_0 + (N - 1)T/2]$, periodically spaced at frequency intervals $2\pi/T$, as the number of temporal samples, N, of the output field increases. However, it must be emphasized that, for finite N, $\sin(\omega NT/2)/\sin(\omega T/2)$ is a continuous function of frequency, and the convolution of $\sin(\omega NT/2)/\sin(\omega T/2)$ with $O[\underline{k}_0,\omega;t_0 + (N - 1)T/2]$ cannot produce exact replicates of $O[\underline{k}_0,\omega;t_0 + (N - 1)T/2]$.

Given that the conditions of equations (8-118) and (8-119) are satisfied and that N is chosen sufficiently large that the estimate $\tilde{O}[\underline{k}_0,\omega;t_0 + (N - 1)T/2]$ provides a good approximation to the true wavevector-frequency transform, $O[\underline{k}_0,\omega;t_0 + (N - 1)T/2]$, of the time-shifted field $o[\underline{x},t + t_0 + (N - 1)T/2]$, then an estimate of the true wavevector-frequency transform, $O(\underline{k},\omega)$, of the field $o(\underline{x},t)$ can easily be obtained. That is, because

$$\tilde{O}[\underline{k}_0,\omega;t_0 + (N - 1)T/2] = \tilde{O}(\underline{k}_0,\omega)\exp\{i\omega[t_0 + (N - 1)T/2]\} \ . \tag{8-122}$$

it follows from equations (8-111) and (8-121) that

$$\tilde{O}(\underline{k},\omega) = \tilde{O}[\underline{k}_0,\omega;t_0 + (N-1)T/2]\exp\{-i\omega[t_0 + (N-1)T/2]\} \approx O(\underline{k},\omega) ,$$

$$|\omega| \leq \pi/T . \qquad (8\text{-}123)$$

Therefore, given the wavevector-frequency response, $G(\underline{k},\omega)$, of the identical sensors used to measure the pressure field $p(\underline{x},t)$, the wavevector-frequency transform of the pressure field can be estimated by use of equations (8-7) and (8-123). That is,

$$\tilde{P}(\underline{k},\omega) = \begin{Bmatrix} \dfrac{\tilde{O}(\underline{k},\omega)}{G(-\underline{k},\omega)} , & |\omega| \leq \pi/T \\ 0, & \text{otherwise} \end{Bmatrix} \approx \frac{O(\underline{k},\omega)}{G(-\underline{k},\omega)} \approx P(\underline{k},\omega) . \qquad (8\text{-}124)$$

Consider now the estimation of the space-time or wavevector-frequency characteristics of a stationary, random pressure field, $p(\underline{x},t)$, from knowledge of N uniformly spaced temporal samples of the output field, $o(\underline{x},t)$, measured synchronously over all space and over all possible realizations of the experiment. If we assume that, at each spatial location, N temporal samples of the output field are taken at intervals T, starting at time t_0, for each realization of the measurement, the resultant data comprise the ensemble of functions $o(\underline{x},t_0 + nT)$ over all $\underline{x}$ and over the integer values of n between zero and $N - 1$. Therefore, by equation (6-52), our knowledge of the autocorrelation function of the stationary output field is limited to

$$Q_{oo}(\underline{x},\underline{\xi},sT) = E\{o[\underline{x},t_0 + nT]o[\underline{x} + \underline{\xi},t_0 + (n + s)T]\} \qquad (8\text{-}125)$$

over all $\underline{x}$ and $\underline{\xi}$, and over all integer values of s between $-N + 1$ and $N - 1$. If the pressure and output fields are homogeneous as well as stationary, we instead have knowledge of $Q_{oo}(\underline{\xi},sT)$ over all $\underline{\xi}$ and for integer s between $-N + 1$ and $N - 1$.

Owing to our incomplete knowledge of the temporal behavior of the autocorrelation function of the output field, we can only estimate the appropriate wavevector-frequency spectrum of the output field. These estimates are formed by approximating the temporal integrations in the definitions of the wave-

vector-frequency spectrum (equation (6-78)) and two wavevector-frequency spectrum (equation (6-121)) by appropriate summations. Thus, we write the estimate, $\tilde{\Phi}_0(\underline{k},\omega)$, of the wavevector-frequency spectrum, $\Phi_0(\underline{k},\omega)$, of the homogeneous and stationary sensor output field as

$$\tilde{\Phi}_0(\underline{k},\omega) = \int_{-\infty}^{\infty}\int_{-\infty}^{\infty} T \sum_{n=-N+1}^{N-1} Q_{00}(\underline{\xi},nT)\exp\{-i(\underline{k}\cdot\underline{\xi} + \omega nT)\}\, d\underline{\xi} \ , \qquad (8\text{-}126)$$

and the estimate, $\tilde{S}_{00}(\underline{\mu},\underline{k},\omega)$, of the two wavevector-frequency spectrum, $S_{00}(\underline{\mu},\underline{k},\omega)$, of the nonhomogeneous, stationary output field as

$$\tilde{S}_{00}(\underline{\mu},\underline{k},\omega) = \int_{-\infty}^{\infty}\int_{-\infty}^{\infty}\int_{-\infty}^{\infty}\int_{-\infty}^{\infty} T \sum_{n=-N+1}^{N-1} Q_{00}(\underline{x},\underline{\xi},nT)\exp\{-i(\underline{\mu}\cdot\underline{x} + \underline{k}\cdot\underline{\xi} + \omega nT)\}\, d\underline{x}\, d\underline{\xi} \ .$$

(8-127)

By again using the sampling property of the Dirac delta function, we can rewrite equations (8-126) and (8-127) in the forms

$$\tilde{\Phi}_0(\underline{k},\omega) = \int_{-\infty}^{\infty}\int_{-\infty}^{\infty}\int_{-\infty}^{\infty} Q_{00}(\underline{\xi},\tau)\exp\{-i(\underline{k}\cdot\underline{\xi} + \omega\tau)\}\left\{T \sum_{n=-N+1}^{N-1} \delta(\tau - nT)\right\} d\underline{\xi}\, d\tau$$

(8-128)

and

$$\tilde{S}_{00}(\underline{\mu},\underline{k},\omega) = \int_{-\infty}^{\infty}\int_{-\infty}^{\infty}\int_{-\infty}^{\infty}\int_{-\infty}^{\infty}\int_{-\infty}^{\infty} Q_{00}(\underline{x},\underline{\xi},\tau)\exp\{-i(\underline{\mu}\cdot\underline{x} + \underline{k}\cdot\underline{\xi} + \omega\tau)\}$$

$$\left\{T \sum_{n=-N+1}^{N-1} \delta(\tau - nT)\right\} d\underline{x}\, d\underline{\xi}\, d\tau \ . \qquad (8\text{-}129)$$

However, by a change of index, we can write

$$T \sum_{n=-N+1}^{N-1} \delta(\tau - nT) = T \sum_{s=0}^{2(N-1)} \delta[\tau + (N-1)T - sT] = v_f[\tau + (N-1)T;2N-1] \ .$$

(8-130)

Therefore,

$$\tilde{\Phi}_0(\underline{k},\omega) = \int_{-\infty}^{\infty}\int_{-\infty}^{\infty}\int_{-\infty}^{\infty} Q_{00}(\underline{\xi},\tau)v_f[\tau + (N - 1)T;2N - 1]\exp\{-i(\underline{k}\cdot\underline{\xi} + \omega\tau)\}\, d\underline{\xi}\, d\tau \tag{8-131}$$

and

$$\tilde{S}_{00}(\underline{\mu},\underline{k},\omega) = \int_{-\infty}^{\infty}\int_{-\infty}^{\infty}\int_{-\infty}^{\infty}\int_{-\infty}^{\infty}\int_{-\infty}^{\infty} Q_{00}(\underline{x},\underline{\xi},\tau)v_f[\tau + (N - 1)T;2N - 1]$$

$$\exp\{-i(\underline{\mu}\cdot\underline{x} + \underline{k}\cdot\underline{\xi} + \omega\tau)\}\, d\underline{x}\, d\underline{\xi}\, d\tau \;. \tag{8-132}$$

By substituting equation (6-79) into equation (8-131), and equation (6-124) into equation (8-132), we obtain, after performing the integrals over the spatial, wavevector, and temporal variables,

$$\tilde{\Phi}_0(\underline{k},\omega) = (2\pi)^{-1} \int_{-\infty}^{\infty} \Phi_0(\underline{k},\Omega)V_f[\omega - \Omega,2N - 1]\exp\{i(\omega - \Omega)(N - 1)T\}\, d\Omega \tag{8-133}$$

and

$$\tilde{S}_{00}(\underline{\mu},\underline{k},\omega) = (2\pi)^{-1} \int_{-\infty}^{\infty} S_{00}(\underline{\mu},\underline{k},\Omega)V_f[\omega - \Omega;2N - 1]\exp\{i(\omega - \Omega)(N - 1)T\}\, d\Omega \;. \tag{8-134}$$

However, by equation (8-109),

$$V_f[\Omega;2N - 1] = T\exp[-i\Omega(N - 1)T]\, \frac{\sin[\Omega(2N - 1)T/2]}{\sin[\Omega T/2]} \;. \tag{8-135}$$

Thus, by substitution of equation (8-135) into equations (8-133) and (8-134), we find that the estimates of the single and two wavevector-frequency spectra are related to their true values by

$$\tilde{\Phi}_0(\underline{k},\omega) = \frac{T}{2\pi} \int_{-\infty}^{\infty} \Phi_0(\underline{k},\Omega)\, \frac{\sin[(\omega - \Omega)(2N - 1)T/2]}{\sin[(\omega - \Omega)T/2]}\, d\Omega \tag{8-136}$$

and

$$\tilde{S}_{oo}(\underline{\mu},\underline{k},\omega) = \frac{T}{2\pi} \int_{-\infty}^{\infty} S_{oo}(\underline{\mu},\underline{k},\Omega) \frac{\sin[(\omega - \Omega)(2N - 1)T/2]}{\sin[(\omega - \Omega)T/2]} d\Omega \ . \tag{8-137}$$

Equations (8-136) and (8-137) show that, for the finite temporal sampling of the sensor output field, the estimated wavevector-frequency spectra are given by convolutions of the true spectra with the periodic function $\sin[\Omega(2N - 1)T/2]/\sin[\Omega T/2]$. Recall that for an infinite number of temporal samples, the estimated wavevector-frequency spectra were given by convolutions of the true spectra with an infinite, periodic train of Dirac delta functions. The period of the function $\sin[\Omega(2N - 1)T/2]/\sin[\Omega T/2]$ is $2\pi/T$, the same as the period of the train of delta functions associated with the infinite temporal sampling. This mathematical effect of finite temporal sampling on the relation between the estimated and true wavevector-frequency spectra of a random sensor output field is similar to that observed between the estimated and true wavevector-frequency transforms of the deterministic output field. Indeed, the mathematical forms of equations (8-136) and (8-137) are mathematically similar to that of equation (8-112), which relates the estimated and true wavevector-frequency transforms for the finite temporal sampling of a deterministic sensor output field.

As a result of the above cited mathematical similarities, we can apply the analysis and interpretation of equation (8-112) to equations (8-136) and (8-137) to determine the effects of a finite number of temporal samples on the estimate of the wavevector-frequency spectra of the sensor output and surface pressure fields. From these similarity arguments, we can deduce that the true wavevector-frequency spectrum of the sensor output field cannot be recovered exactly from a finite temporal sampling of that field. However, we can also demonstrate that if (1) the true wavevector-frequency spectrum of the output field is band limited in frequency such that either

$$\Phi_o(\underline{k},\omega) = 0, \quad |\omega| > \omega_c \ , \tag{8-138}$$

or

$$S_{oo}(\underline{\mu},\underline{k},\omega) = 0, \quad |\omega| > \omega_c \ , \tag{8-139}$$

(2) N temporal samples of the band-limited output field are taken at uniform temporal increments, T, which are smaller than π/ω_c, and (3) the number of temporal samples, N, is sufficiently large that the bandwidth, $4\pi/[(2N - 1)T]$, of the major acceptance lobe of $\sin[\Omega(2N - 1)T/2]/\sin[\Omega T/2]$ is small in comparison to the bandwidth of any variation, in frequency, of $\Phi_o(\underline{k},\omega)$ or $S_{oo}(\underline{\mu},\underline{k},\omega)$, as appropriate, then

$$\tilde{\Phi}_o(\underline{k},\omega) \approx \sum_{n=-\infty}^{\infty} \Phi_o(\underline{k},\omega - 2n\pi/T) \tag{8-140}$$

or

$$\tilde{S}_{oo}(\underline{\mu},\underline{k},\omega) \approx \sum_{n=-\infty}^{\infty} S_{oo}(\underline{\mu},\underline{k},\omega - 2n\pi/T) \ . \tag{8-141}$$

Under these conditions,

$$\tilde{\Phi}_o(\underline{k},\omega) \approx \Phi_o(\underline{k},\omega), \quad |\omega| \leq 2\pi/T \tag{8-142}$$

or

$$\tilde{S}_{oo}(\underline{\mu},\underline{k},\omega) \approx S_{oo}(\underline{\mu},\underline{k},\omega), \quad |\omega| \leq 2\pi/T \ , \tag{8-143}$$

and, by equations (8-14) and (8-15), the appropriate single or two wavevector-frequency spectrum of the random surface pressure field is estimated by

$$\tilde{\Phi}_p(\underline{k},\omega) = \begin{Bmatrix} \dfrac{\tilde{\Phi}_o(\underline{k},\omega)}{|G(-\underline{k},\omega)|^2} \ , & |\omega| \leq 2\pi/T \\ \\ 0, & \text{otherwise} \end{Bmatrix} \approx \frac{\Phi_o(\underline{k},\omega)}{|G(-\underline{k},\omega)|^2} = \Phi_p(\underline{k},\omega) \tag{8-144}$$

or

$$\tilde{S}_{pp}(\underline{\mu},\underline{k},\omega) = \begin{Bmatrix} \dfrac{\tilde{S}_{oo}(\underline{\mu},\underline{k},\omega)}{G(\underline{k} - \underline{\mu},-\omega)G(-\underline{k},\omega)} \ , & |\omega| \leq 2\pi/T \\ \\ 0, & \text{otherwise} \end{Bmatrix}$$

$$\approx \frac{S_{oo}(\underline{\mu},\underline{k},\omega)}{G(\underline{k} - \underline{\mu},-\omega)G(-\underline{k},\omega)} = S_{oo}(\underline{\mu},\underline{k},\omega) \ , \tag{8-145}$$

respectively. It should be noted that the quality of the estimates given by equations (8-140) through (8-145) improves with increasing numbers of temporal samples.

The analysis presented in this section demonstrates that the finite limits, imposed by practical considerations on the number of temporal samples of the sensor output field, significantly inhibit our ability to estimate the space-time or wavevector-frequency characteristics of the acoustic field of interest. To avoid aliasing errors in the estimate, the acoustic field being measured must be band limited in frequency and the temporal sampling period must be chosen to be less than one-half the period associated with the frequency of the band limit. These constraints are identical to those imposed for an infinite number of temporal samples, and are therefore a consequence of any uniform temporal sampling process. Given that the acoustic field of interest is frequency band limited and that the temporal sampling period is chosen to avoid aliasing, we previously demonstrated that the true space-time or wavevector-frequency characteristics of the acoustic field could be exactly recovered from an infinite number of temporal samples of the sensor output field. However, given any finite subset of those temporal samples of that output field, we can obtain only some approximation to the true space-time or wavevector-frequency characteristics of the acoustic field. The quality of that approximation depends on the bandwidth, $4\pi/(NT)$, of the main response lobe of the Fourier transform of the finite temporal sampling function relative to the bandwidth of any fluctuation, in frequency, of the transform or spectrum (as appropriate) of the sensor output field. Only when N is sufficiently large that the bandwidth of the Fourier transform of the temporal sampling function is small in comparison to the bandwidth of any frequency fluctuation in the transform or spectrum of the output field can a good estimate of the space-time or wavevector-frequency characteristics of the acoustic field of interest be obtained.

8.3.2 Finite Spatial Sampling

Just as finite limits on the number of temporal samples inhibit our ability to estimate the temporal or frequency characteristics of an acoustic field, finite limits on the number of spatial samples inhibit our ability to

estimate the spatial or wavevector characteristics of that acoustic field.

Assume that, for practical reasons, we are constrained to measure the surface pressure field, $p(\underline{x},t)$, with the M by N rectangular array of sensors depicted in figure 8-14. For each realization of the measurement, the outputs of the sensors comprising the array are measured over all time. Thus, our knowledge of the sensor output field is limited to the ensemble of functions $o(x_{01} + md_1, x_{02} + nd_2, t)$ over all time for integer values of m and n between $0 \leq m \leq M - 1$ and $0 \leq n \leq N - 1$.

If the pressure field is deterministic, we can estimate the wavevector-frequency transform of the output field from any member function of the ensemble by approximating the spatial integrals in equation (8-6) by appropriate summations. That is,

$$\tilde{O}(\underline{k},\omega) = d_1 d_2 \sum_{m=0}^{M-1} \sum_{n=0}^{N-1} \int_{-\infty}^{\infty} o(x_{01} + md_1, x_{02} + nd_2, t)$$

$$\exp\{-i[k_1(x_{01} + md_1) + k_2(x_{02} + nd_2) + \omega t]\}\, dt \, . \qquad (8\text{-}146)$$

By defining the finite spatial sampling function, $s_f(\underline{x})$, by

$$s_f(\underline{x};M,N) = d_1 d_2 \sum_{m=0}^{M-1} \sum_{n=0}^{N-1} \delta(x_1 - md_1)\delta(x_2 - nd_2) \, . \qquad (8\text{-}147)$$

we can write equation (8-146) in the form

$$\tilde{O}(\underline{k},\omega) = \int_{-\infty}^{\infty}\int_{-\infty}^{\infty}\int_{-\infty}^{\infty} o(\underline{z},t) s_f(\underline{z} - \underline{x}_0;M,N) \exp\{-i[\underline{k}\cdot\underline{z} + \omega t]\}\, d\underline{z}\, dt \, . \qquad (8\text{-}148)$$

If we write $o(\underline{z},t)$ in the form of its inverse wavevector-frequency transform, it follows that

$$\tilde{O}(\underline{k},\omega) = (2\pi)^{-2} \int_{-\infty}^{\infty}\int_{-\infty}^{\infty} O(\underline{\mu},\omega) S_f(\underline{k} - \underline{\mu};M,N) \exp\{-i(\underline{k} - \underline{\mu})\cdot\underline{x}_0\}\, d\underline{\mu} \, . \qquad (8\text{-}149)$$

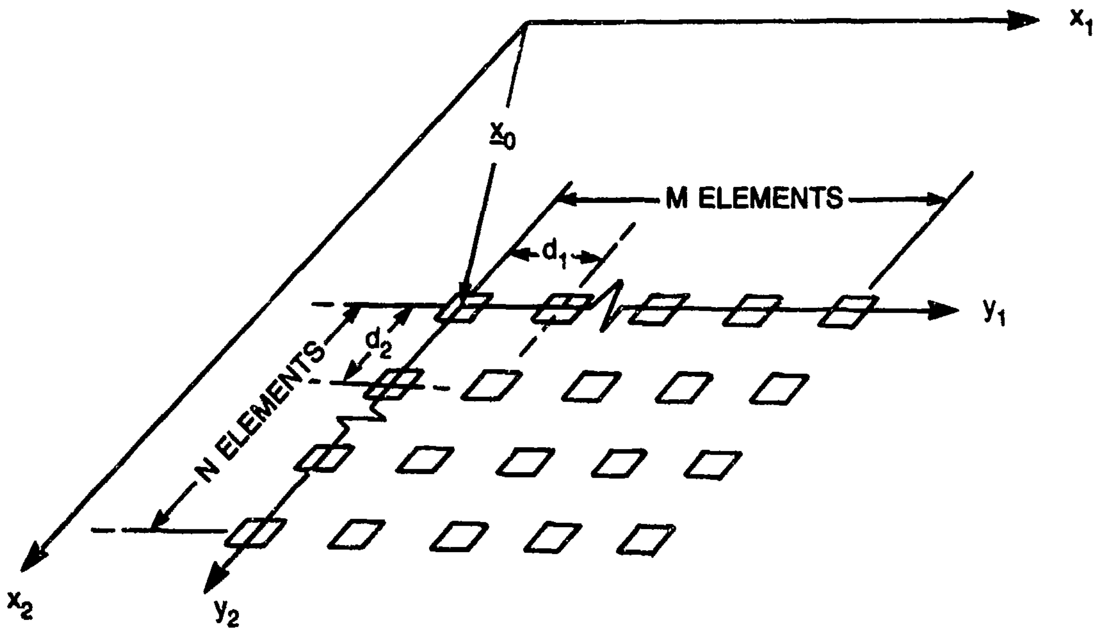

Figure 8-14. M by N Array of Sensors

where $S_f(\underline{k};M,N)$, the wavevector transform of $s_f(\underline{x};M,N)$, is given by

$$S_f(\underline{k};M,N) = d_1 d_2 \exp[-i[k_1(M-1)d_1/2 + k_2(N-1)d_2/2]]$$

$$\frac{\sin(k_1 M d_1/2)}{\sin(k_1 d_1/2)} \frac{\sin(k_2 N d_2/2)}{\sin(k_2 d_2/2)} . \qquad (8\text{-}150)$$

Substitution of equation (8-150) into equation (8-149) yields

$$\tilde{O}(\underline{k},\omega) = \frac{d_1 d_2}{(2\pi)^2} \int_{-\infty}^{\infty} \int_{-\infty}^{\infty} O(\underline{\mu},\omega) \frac{\sin(k_1 M d_1/2)}{\sin(k_1 d_1/2)} \frac{\sin(k_2 N d_2/2)}{\sin(k_2 d_2/2)}$$

$$\exp(-i([k_1 - \mu_1][x_{01} + (M-1)d_1/2]$$

$$+ [k_2 - \mu_2][x_{02} + (N-1)d_2/2])) \, d\underline{\mu} . \qquad (8\text{-}151)$$

From our experience with the analysis of finite temporal sampling, we recognize that

$$O(\underline{k},\omega)\exp(i(\underline{k}\cdot\underline{r})) = O[\underline{k},\omega;\underline{r}] . \qquad (8\text{-}152)$$

where $O[\underline{k},\omega;\underline{r}]$ designates the wavevector-frequency transform of the spatially shifted output field $o(\underline{x} + \underline{r},t)$. By denoting the estimate of $O[\underline{k},\omega;\underline{r}]$ by $\tilde{O}[\underline{k},\omega;\underline{r}]$, it is straightforward to demonstrate that equation (8-151) can be written in the form

$$\tilde{O}\{\underline{k},\omega;[x_{01} + (M - 1)d_1/2, x_{02} + (N - 1)d_2/2]\} =$$

$$\frac{d_1 d_2}{(2\pi)^2} \int_{-\infty}^{\infty} \int_{-\infty}^{\infty} O\{\underline{\mu},\omega;[x_{01} + (M - 1)d_1/2, x_{02} + (N - 1)d_2/2]\}$$

$$\frac{\sin[(k_1 - \mu_1)Md_1/2]}{\sin[(k_1 - \mu_1)d_1/2]} \frac{\sin[(k_2 - \mu_2)Nd_2/2]}{\sin[(k_2 - \mu_2)d_2/2]} \, d\underline{\mu} \, . \qquad (8\text{-}153)$$

From equation (8-153), we can demonstrate that the estimate of the wavevector-frequency transform of the spatially shifted sensor output field, $o[x_1 + x_{01} + (M - 1)d_1/2, x_2 + x_{02} + (N - 1)d_2/2, t]$, is proportional to the convolution of the true transform of that spatially shifted field with the product of the periodic functions $\sin(\mu_1 Md_1/2)/\sin(\mu_1 d_1/2)$ and $\sin(\mu_2 Nd_2/2)/\sin(\mu_2 d_2/2)$. Recall that, for the case of sampling over infinite space, the estimate of the wavevector-frequency transform of the output field was proportional to the convolution of the true transform with a product of infinite, periodic trains of Dirac delta functions in the μ_1 and μ_2 coordinate directions. For given spatial separations, d_1 and d_2, between samples of the output field, the periods of the trains of Dirac delta functions in the μ_1 and μ_2 domains are the same as the respective periods between the major acceptance lobes of $\sin(\mu_1 Md_1/2)/\sin(\mu_1 d_1/2)$ and $\sin(\mu_2 Nd_2/2)/\sin(\mu_2 d_2/2)$.

The differences between the estimates of the wavevector-frequency transform of the space-shifted output field obtained from infinite and finite numbers of spatial samples are mathematically analogous to the differences between the estimates of the transforms of the time-shifted output field obtained from infinite and finite numbers of temporal samples. Indeed, it is easily determined that equations (8-79) and (8-81), which relate the estimated and true wavevector-frequency transforms for an infinite spatial sampling of the output field, are the two-dimensional mathematical analogs of equations (8-48) and (8-51), which relate the estimated and true wavevector-frequency

transforms for an infinite temporal sampling of the output field. Similarly, equation (8-153), which relates the estimated and true wavevector-frequency transforms for a finite spatial sampling of the output field, is the mathematical analog, in the two-dimensional wavevector domain, of equation (8-112), which relates the estimated and true wavevector-frequency transforms for a finite temporal sampling of the output field.

Given that equation (8-153) is the analog, in the wavevector domain, of equation (8-112), we can interpret the effects of finite spatial sampling on the relationship (equation (8-153)) between the wavevector characteristics of the estimated and true transforms as the analog of the effects of finite temporal sampling on the relationship (equation (8-112)) between the frequency characteristics of the estimated and true transforms. By applying such analogical reasoning, we conclude that if (1) the sensor output field is band limited in the wavevector domain such that

$$O(\underline{k},\omega) = 0, \quad |k_1| > k_{1c} \text{ and } |k_2| > k_{2c} \ , \tag{8-154}$$

(2) the spatial sampling intervals are chosen such that

$$d_1 < \pi/k_{1c} \text{ and } d_2 < \pi/k_{2c} \ , \tag{8-155}$$

and (3) the numbers, M and N, of spatial samples in the x_1 and x_2 coordinate directions are chosen sufficiently large that the bandwidths, $4\pi/(Md_1)$ and $4\pi/(Nd_2)$, of the major acceptance lobes of $\sin(k_1Md_1/2)/\sin(k_1d_1/2)$ and $\sin(k_2Md_2/2)/\sin(k_2d_2/2)$ are smaller than the bandwidths of any variations of $O(\underline{k},\omega)$ in k_1 and k_2, respectively, then

$$\begin{aligned}\tilde{O}(\underline{k},\omega;[x_{01} + (M-1)d_1/2, x_{02} + (N-1)d_2/2]) &\approx \\ O(\underline{\mu},\omega;[x_{01} + (M-1)d_1/2, x_{02} + (N-1)d_2/2]) \ , \\ |k_1| \le \pi/d_1 \text{ and } |k_2| \le \pi/d_2 \ . \end{aligned} \tag{8-156}$$

Given that equation (8-153) is true, it then follows (see equation (8-152)) that

$$\tilde{O}(\underline{k},\omega) = \tilde{O}\{\underline{k},\omega;[x_{01} + (M - 1)d_1/2, x_{02} + (N - 1)d_2/2]\}$$

$$\exp(-i\{k_1[x_{01} + (M - 1)d_1/2] + k_2[x_{02} + (N - 1)d_2/2]\}) \approx O(\underline{k},\omega) \ ,$$

$$|k_1| \le \pi/d_1 \text{ and } |k_2| \le \pi/d_2 \ , \qquad (8\text{-}157)$$

and therefore, by equation (8-7),

$$\tilde{P}(\underline{k},\omega) = \begin{Bmatrix} \dfrac{\tilde{O}(\underline{k},\omega)}{G(-\underline{k},\omega)}, & \begin{matrix}|k_1| \le \pi/d_1 \\ |k_2| \le \pi/d_2\end{matrix} \\ & \\ 0, & \text{otherwise} \end{Bmatrix} \approx \frac{O(\underline{k},\omega)}{G(-\underline{k},\omega)} \approx P(\underline{k},\omega) \ . \qquad (8\text{-}158)$$

Thus, we see that when the acoustic field of interest is band limited in the wavevector domain and measured at proper intervals in the spatial domain, an approximation to the wavevector-frequency transform of that field can be obtained from a finite number of spatial samples of the sensor output field. The quality of this approximation depends on both the wavevector character of the acoustic field being measured and the numbers of spatial samples obtained in both the x_1 and x_2 coordinate directions. For any specific acoustic field, the quality of the approximation improves with increasing numbers of spatial samples.

If the pressure field of interest is random, the ensemble of sample functions $o(x_{01} + md_1, x_{02} + nd_2, t)$, measured over all time for integer values of m and n between $0 \le m \le M - 1$ and $0 \le n \le N - 1$, provides knowledge of the (assumed stationary) autocorrelation function

$$Q_{oo}[x_{01} + md_1, x_{02} + nd_2; (q - m)d_1, (s - n)d_2, \tau] =$$

$$E\{o(x_{01} + md_1, x_{02} + nd_2, t)o(x_{01} + qd_1, x_{02} + sd_2, t + \tau)\} \quad (8\text{-}159)$$

over all τ and for integer values of m and q between 0 and $M - 1$ and integer values of n and s between 0 and $N - 1$. If the pressure field is homogeneous as well as stationary, the ensemble of sample functions provides knowledge of the autocorrelation function of the homogeneous sensor output field

$$Q_{oo}(ud_1, vd_2, \tau) =$$

$$E\{o[x_{01} + md_1, x_{02} + nd_2, t]o[x_{01} + (m + u)d_1, x_{02} + (n + v)d_2, t + \tau]\} \tag{8-160}$$

over all τ for integer values of u and v between $1 - M \leq u \leq M - 1$ and $1 - N \leq v \leq N - 1$, respectively.

For the case of the homogeneous, stationary output field, the above stated knowledge of the autocorrelation function supports an estimate, $\tilde{\Phi}_o(\underline{k},\omega)$, of the wavevector-frequency spectrum, $\Phi_o(\underline{k},\omega)$, of the sensor output field in the form

$$\tilde{\Phi}_o(\underline{k},\omega) = d_1 d_2 \sum_{u=-M+1}^{M-1} \sum_{v=-N+1}^{N-1} \int_{-\infty}^{\infty} Q_{oo}(ud_1, vd_2, \tau)$$

$$\exp\{-i(k_1 ud_1 + k_2 vd_2 + \omega\tau)\}\, d\tau \ . \tag{8-161}$$

Alternatively, by making use of the sampling property of the Dirac delta function, we can write

$$\tilde{\Phi}_o(\underline{k},\omega) = \int_{-\infty}^{\infty}\int_{-\infty}^{\infty}\int_{-\infty}^{\infty} Q_{oo}(\underline{\xi},\tau)\exp\{-i(\underline{k}\cdot\underline{\xi} + \omega\tau)\}$$

$$\left\{d_1 \sum_{u=-M+1}^{M-1} \delta(\xi_1 - ud_1)\right\}\left\{d_2 \sum_{v=-N+1}^{N-1} \delta(\xi_2 - vd_2)\right\} d\underline{\xi}\, d\tau \ . \tag{8-162}$$

However, by applying arguments similar to those employed in equation (8-130) to equation (8-147), we can show that

$$\left\{d_1 \sum_{u=-M+1}^{M-1} \delta(\xi_1 - ud_1)\right\}\left\{d_2 \sum_{v=-N+1}^{N-1} \delta(\xi_2 - vd_2)\right\} =$$

$$\left\{d_1 \sum_{m=0}^{2(M-1)} \delta[\xi_1 + (M - 1)d_1 - md_1]\right\}\left\{d_2 \sum_{n=0}^{2(N-1)} \delta[\xi_2 + (N - 1)d_2 - nd_2]\right\} =$$

$$s_f[\xi_1 + (M - 1)d_1, \xi_2 + (N - 1)d_2; 2M - 1, 2N - 1] \ . \tag{8-163}$$

Thus, it follows that

$$\tilde{\Phi}_0(\underline{k},\omega) = \int_{-\infty}^{\infty}\int_{-\infty}^{\infty}\int_{-\infty}^{\infty} Q_{00}(\underline{\xi},\tau) s_f[\xi_1 + (M-1)d_1, \xi_2 + (N-1)d_2; 2M-1, 2N-1]$$

$$\exp\{-i(\underline{k}\cdot\underline{\xi} + \omega\tau)\}\, d\underline{\xi}\, d\tau \ . \qquad (8\text{-}164)$$

By substituting equation (6-79) into equation (8-164) and performing the integrations over the spatial, temporal, and frequency variables, we obtain

$$\tilde{\Phi}_0(\underline{k},\omega) = (2\pi)^{-2} \int_{-\infty}^{\infty}\int_{-\infty}^{\infty} \Phi_0(\underline{\mu},\omega) S_f(\underline{k} - \underline{\mu}; 2M-1, 2N-1)$$

$$\exp\{i[(k_1 - \mu_1)(M-1)d_1 + (k_2 - \mu_2)(N-1)d_2]\}\, d\underline{\mu} \ . \qquad (8\text{-}165)$$

Substitution of equation (8-150) into equation (8-165) then yields the following relationship between the true wavevector-frequency spectrum of the sensor output field and the estimate of that spectrum obtained from a finite number of spatial samples of the output field:

$$\tilde{\Phi}_0(\underline{k},\omega) = \frac{d_1 d_2}{(2\pi)^2} \int_{-\infty}^{\infty}\int_{-\infty}^{\infty} \Phi_0(\underline{\mu},\omega)\, \frac{\sin[(k_1 - \mu_1)(2M-1)d_1/2]}{\sin[(k_1 - \mu_1)d_1/2]}$$

$$\frac{\sin[(k_2 - \mu_2)(2N-1)d_2/2]}{\sin[(k_2 - \mu_2)d_2/2]}\, d\underline{\mu} \ . \qquad (8\text{-}166)$$

Comparison of equation (8-166) with equation (8-136) reveals that the relationship between the wavevector-frequency spectrum estimated from a finite spatial sampling of the output field and the true wavevector-frequency spectrum of that field is the analog, in the wavevector domain, of the relationship between the wavevector-frequency spectrum estimated from a finite temporal sampling of the output field and the true wavevector-frequency spectrum of the output field. Furthermore, it is easily established, by comparison of equations (8-64) and (8-91), that the relationship between the wavevector-frequency spectrum estimated from a uniform sampling of the output

field over all space and the true spectrum of that field is the analog, in the wavevector domain, of the relationship between the wavevector-frequency spectrum estimated from a uniform sampling of the output field over all time and the true wavevector-frequency spectrum. Owing to these mathematical analogies, we can employ arguments, in the wavevector domain, analogous to those presented in section 8.3.1, in the time domain, to interpret the relationship between the estimated and true wavevector-frequency spectrum described by equation (8-166). By such arguments, we conclude that if (1) the true wavevector-frequency spectrum of the sensor output field is band limited in the wavevector domain such that

$$\Phi_0(\underline{k},\omega) = 0, \quad |k_1| > k_{1c} \text{ and } |k_2| > k_{2c} \; . \tag{8-167}$$

(2) the uniform separations, d_1 and d_2, between the spatial samples in the x_1 and x_2 coordinate directions, respectively, are chosen such that

$$d_1 < \pi/k_{1c} \text{ and } d_2 < \pi/k_{2c} \; , \tag{8-168}$$

and (3) the numbers, M and N, of spatial samples obtained in the x_1 and x_2 coordinate directions, respectively, are sufficiently large that the wavevector bandwidths, $4\pi/[(2M - 1)d_1]$ and $4\pi/[(2N - 1)d_2]$, of the major acceptance lobes of the functions $\sin[\mu_1(2M - 1)d_1/2]/\sin[\mu_1 d_1/2]$ and $\sin[\mu_2(2N - 1)d_2/2]/\sin[\mu_2 d_2/2]$ are small in comparison to the bandwidth, in k_1 or k_2, of any variation of $\Phi_0(\underline{k},\omega)$.

then

$$\tilde{\Phi}_0(\underline{k},\omega) \approx \sum_{m=-\infty}^{\infty} \sum_{n=-\infty}^{\infty} \Phi_0(k_1 - 2m\pi/d_1, k_2 - 2n\pi/d_2, \omega) \; . \tag{8-169}$$

so

$$\tilde{\Phi}_0(\underline{k},\omega) \approx \Phi_0(\underline{k},\omega), \quad |k_1| \leq 2\pi/d_1 \text{ and } |k_2| \leq 2\pi/d_2 \; . \tag{8-170}$$

Under these conditions, an approximation to the wavevector-frequency spectrum of the pressure field (see equation (8-15)) can be recovered from the estimate of the spectrum of the sensor output field. That is,

$$\tilde{\Phi}_p(\underline{k},\omega) = \begin{cases} \dfrac{\tilde{\Phi}_o(\underline{k},\omega)}{|G(-\underline{k},\omega)|^2} , & |k_1| \le 2\pi/d_1 \\ & |k_2| \le 2\pi/d_2 \\ 0, & \text{otherwise} \end{cases} \approx \frac{\Phi_o(\underline{k},\omega)}{|G(-\underline{k},\omega)|^2} = \Phi_p(\underline{k},\omega) \ . \quad (8\text{-}171)$$

The quality of the estimates of the wavevector-frequency spectra of the sensor output and surface pressure fields improves with increasing numbers (i.e., M and N) of spatial samples of the output field.

Consider now the estimation of the two wavevector-frequency spectrum of the nonhomogeneous, stationary output field from the limited spatial samples of the autocorrelation function described by equation (8-159). According to equation (6-121), this sampling of the autocorrelation function supports an estimate, $\tilde{S}_{oo}(\underline{\mu},\underline{k},\omega)$, of the two wavevector-frequency spectrum of the sensor output field of the form

$$\tilde{S}_{oo}(\underline{\mu},\underline{k},\omega) = d_1^2 d_2^2$$

$$\sum_{m=0}^{M-1} \sum_{n=0}^{N-1} \sum_{q-m=-m}^{M-m-1} \sum_{s-n=-n}^{N-n-1} \int_{-\infty}^{\infty} Q_{oo}[x_{01} + md_1, x_{02} + nd_2; (q-m)d_1, (s-n)d_2, \tau]$$

$$\exp\{-i[\mu_1(x_{01} + md_1) + \mu_2(x_{02} + nd_2) + k_1(q-m)d_1 + k_2(s-n)d_2 + \omega\tau]\}\, d\tau \ .$$

(8-172)

By defining

$$\underline{x}_{mn} = (x_{01} + md_1, x_{02} + nd_2) \ , \quad (8\text{-}173)$$

we can rewrite equation (8-172) in the form

$$\tilde{S}_{oo}(\underline{\mu},\underline{k},\omega) = d_1^2 d_2^2 \sum_{m=0}^{M-1} \sum_{n=0}^{N-1} \sum_{u=0}^{M-1} \sum_{v=0}^{N-1} \int_{-\infty}^{\infty} Q_{oo}(\underline{x}_{mn}, \underline{x}_{uv} - \underline{x}_{mn}, \tau)$$

$$\exp\{-i[\underline{\mu}\cdot\underline{x}_{mn} + \underline{k}\cdot(\underline{x}_{uv} - \underline{x}_{mn}) + \omega\tau]\}\, d\tau \ . \quad (8\text{-}174)$$

By making use of the sampling property of the Dirac delta function, we can

write equation (8-174) in the form

$$\tilde{S}_{00}(\underline{\mu},\underline{k},\omega) = d_1^2 d_2^2 \int_{-\infty}^{\infty}\int_{-\infty}^{\infty}\int_{-\infty}^{\infty}\int_{-\infty}^{\infty}\int_{-\infty}^{\infty} Q_{00}(\underline{x},\underline{\xi},\tau)\exp\{-i(\underline{\mu}\cdot\underline{x} + \underline{k}\cdot\underline{\xi} + \omega\tau)\}$$

$$\left\{\sum_{m=0}^{M-1}\sum_{n=0}^{N-1}\sum_{u=0}^{M-1}\sum_{v=0}^{N-1} \delta(\underline{x} - \underline{x}_{mn})\delta(\underline{\xi} - \underline{x}_{uv} + \underline{x}_{mn})\right\} d\underline{x}\, d\underline{\xi}\, d\tau \ . \qquad (8\text{-}175)$$

However, it is easily demonstrated that

$$d_1^2 d_2^2 \sum_{m=0}^{M-1}\sum_{n=0}^{N-1}\sum_{u=0}^{M-1}\sum_{v=0}^{N-1} \delta(\underline{x} - \underline{x}_{mn})\delta(\underline{\xi} - \underline{x}_{uv} + \underline{x}_{mn}) =$$

$$d_1^2 d_2^2 \sum_{m=0}^{M-1}\sum_{n=0}^{N-1}\sum_{u=0}^{M-1}\sum_{v=0}^{N-1} \delta(\underline{x} - \underline{x}_{mn})\delta(\underline{x} + \underline{\xi} - \underline{x}_{uv}) =$$

$$\left\{d_1 d_2 \sum_{m=0}^{M-1}\sum_{n=0}^{N-1} \delta(x_1 - x_{01} - md_1)\delta(x_2 - x_{02} - nd_2)\right\}$$

$$\left\{d_1 d_2 \sum_{u=0}^{M-1}\sum_{v=0}^{N-1} \delta(x_1 - x_{01} + \xi_1 - ud_1)\delta(x_2 - x_{02} + \xi_2 - vd_2)\right\} =$$

$$s_f(\underline{x} - \underline{x}_0;M,N)s_f(\underline{x} - \underline{x}_0 + \underline{\xi};M,N) \ . \qquad (8\text{-}176)$$

Thus,

$$\tilde{S}_{00}(\underline{\mu},\underline{k},\omega) = \int_{-\infty}^{\infty}\int_{-\infty}^{\infty}\int_{-\infty}^{\infty}\int_{-\infty}^{\infty}\int_{-\infty}^{\infty} Q_{00}(\underline{x},\underline{\xi},\tau)s_f(\underline{x} - \underline{x}_0;M,N)s_f(\underline{x} - \underline{x}_0 + \underline{\xi};M,N)$$

$$\exp\{-i(\underline{\mu}\cdot\underline{x} + \underline{k}\cdot\underline{\xi} + \omega\tau)\}\, d\underline{x}\, d\underline{\xi}\, d\tau \ . \qquad (8\text{-}177)$$

To obtain a relationship between the estimated and true two wavevector-frequency spectra of the sensor output field, we substitute the inverse

Fourier transformation of equation (6-124) into equation (8-177) and perform the integrals over the temporal and frequency variables to obtain

$$\tilde{S}_{00}(\underline{\mu},\underline{k},\omega) = \frac{1}{(2\pi)^4}\int_{-\infty}^{\infty}\int_{-\infty}^{\infty}\int_{-\infty}^{\infty}\int_{-\infty}^{\infty}\int_{-\infty}^{\infty}\int_{-\infty}^{\infty}\int_{-\infty}^{\infty}\int_{-\infty}^{\infty} S_{00}(\underline{\alpha},\underline{\beta},\omega)s_f(\underline{x} - \underline{x}_0;M,N)$$

$$s_f(\underline{x} - \underline{x}_0 + \underline{\xi};M,N)\exp\{-i[(\underline{\mu} - \underline{\alpha})\cdot\underline{x} + (\underline{k} - \underline{\beta})\cdot\underline{\xi}]\}\, d\underline{x}\, d\underline{\xi}\, d\underline{\alpha}\, d\underline{\beta} \;. \tag{8-178}$$

By performing the integrals over the spatial variables, it follows that

$$\tilde{S}_{00}(\underline{\mu},\underline{k},\omega) = \frac{1}{(2\pi)^4}\int_{-\infty}^{\infty}\int_{-\infty}^{\infty}\int_{-\infty}^{\infty}\int_{-\infty}^{\infty} S_{00}(\underline{\alpha},\underline{\beta},\omega)S_f(\underline{\mu} - \underline{\alpha} + \underline{\beta} - \underline{k};M,N)S_f(\underline{k} - \underline{\beta};M,N)$$

$$\exp\{-i(\underline{\mu} - \underline{\alpha})\cdot\underline{x}_0\}\, d\underline{\alpha}\, d\underline{\beta} \;. \tag{8-179}$$

Substitution of equation (8-150) into equation (8-179) subsequently yields

$$\tilde{S}_{00}(\underline{\mu},\underline{k},\omega) = \frac{d_1^2 d_2^2}{(2\pi)^4}\int_{-\infty}^{\infty}\int_{-\infty}^{\infty}\int_{-\infty}^{\infty}\int_{-\infty}^{\infty} S_{00}(\underline{\alpha},\underline{\beta},\omega)$$

$$\frac{\sin[(k_1 - \beta_1)Md_1/2]}{\sin[(k_1 - \beta_1)d_1/2]}\;\frac{\sin[(k_2 - \beta_2)Nd_2/2]}{\sin[(k_2 - \beta_2)d_2/2]}$$

$$\frac{\sin[(\mu_1 - \alpha_1 + \beta_1 - k_1)Md_1/2]}{\sin[(\mu_1 - \alpha_1 + \beta_1 - k_1)d_1/2]}\;\frac{\sin[(\mu_2 - \alpha_2 + \beta_2 - k_2)Nd_2/2]}{\sin[(\mu_2 - \alpha_2 + \beta_2 - k_2)d_2/2]}$$

$$\exp(-i\{[\mu_1 - \alpha_1][x_{01} + (M - 1)d_1/2] + [\mu_2 - \alpha_2][x_{02} + (N - 1)d_2/2]\})\, d\underline{\alpha}\, d\underline{\beta} \;. \tag{8-180}$$

Note that the two wavevector-frequency spectrum of the space-shifted autocorrelation function $Q_{00}(\underline{x} + \underline{x}_0,\underline{\xi},\tau)$, which we denote by $S_{00}[\underline{\mu},\underline{k},\omega;\underline{x}_0]$, is given by

$$S_{oo}[\underline{\mu},\underline{k},\omega;\underline{x}_0] = \int_{-\infty}^{\infty}\int_{-\infty}^{\infty}\int_{-\infty}^{\infty}\int_{-\infty}^{\infty}\int_{-\infty}^{\infty} Q_{oo}(\underline{x} + \underline{x}_0,\underline{\xi},\tau)$$

$$\exp\{-i(\underline{\mu}\cdot\underline{x} + \underline{k}\cdot\underline{\xi} + \omega\tau)\}\, d\underline{x}\, d\underline{\xi}\, d\tau$$

$$= \int_{-\infty}^{\infty}\int_{-\infty}^{\infty}\int_{-\infty}^{\infty}\int_{-\infty}^{\infty}\int_{-\infty}^{\infty} Q_{oo}(\underline{y},\underline{\xi},\tau)\exp\{-i[\underline{\mu}\cdot(\underline{y} - \underline{x}_0) + \underline{k}\cdot\underline{\xi} + \omega\tau]\}\, d\underline{y}\, d\underline{\xi}\, d\tau$$

$$= S_{oo}(\underline{\mu},\underline{k},\omega)\exp\{i\underline{\mu}\cdot\underline{x}_0\} \; . \tag{8-181}$$

If we denote the product $\tilde{S}_{oo}(\underline{\mu},\underline{k},\omega)\exp\{i\underline{k}\cdot\underline{x}_0\}$ by $\tilde{S}_{oo}[\underline{\mu},\underline{k},\omega;\underline{x}_0]$, it follows from equations (8-180) and (8-181) that

$$\tilde{S}_{oo}[\underline{\mu},\underline{k},\omega;\underline{x}_c] = \frac{d_1^2 d_2^2}{(2\pi)^4}\int_{-\infty}^{\infty}\int_{-\infty}^{\infty}\int_{-\infty}^{\infty}\int_{-\infty}^{\infty} S_{oo}[\underline{\alpha},\underline{\beta},\omega;\underline{x}_c]$$

$$\frac{\sin[(\mu_1 - \alpha_1 + \beta_1 - k_1)Md_1/2]}{\sin[(\mu_1 - \alpha_1 + \beta_1 - k_1)d_1/2]}\,\frac{\sin[(\mu_2 - \alpha_2 + \beta_2 - k_2)Nd_2/2]}{\sin[(\mu_2 - \alpha_2 + \beta_2 - k_2)d_2/2]}$$

$$\frac{\sin[(k_1 - \beta_1)Md_1/2]}{\sin[(k_1 - \beta_1)d_1/2]}\,\frac{\sin[(k_2 - \beta_2)Nd_2/2]}{\sin[(k_2 - \beta_2)d_2/2]}\, d\underline{\alpha}\, d\beta \; , \tag{8-182}$$

where $\underline{x}_c$ denotes the spatial location of the geometric center of the M by N array of sensors. That is,

$$\underline{x}_c = [x_{01} + (M - 1)d_1/2, x_{02} + (N - 1)d_2/2] \; . \tag{8-183}$$

Equation (8-182) shows the estimate, $\tilde{S}_{oo}[\underline{\mu},\underline{k},\omega;\underline{x}_c]$, of the two wavevector-frequency spectrum associated with the space-shifted autocorrelation function $Q_{oo}(\underline{x} + \underline{x}_c,\underline{\xi},\tau)$ to be proportional to a double convolution, in the wavevector variables $\underline{\alpha}$ and $\underline{\beta}$, of the true two wavevector-frequency spectrum, $S_{oo}[\underline{\alpha},\underline{\beta},\omega;\underline{x}_c]$, with functions of the form $\sin[(\alpha_1 - \beta_1)Md_1/2]/\sin[(\alpha_1 - \beta_1)d_1/2]$, $\sin(\beta_1 Md_1/2)/\sin(\beta_1 d_1/2)$, $\sin[(\alpha_2 - \beta_2)Md_2/2]/\sin[(\alpha_2 - \beta_2)d_2/2]$, and $\sin(\beta_2 Md_2/2)/\sin(\beta_2 d_2/2)$. This convolution cannot be illustrated in the

four wavenumber variables α_1, α_2, β_1, and β_2. However, we can gain some insight into the relationship between the estimated and true two wavevector-frequency spectra by examining the behavior of the product of $\sin[(\mu_1 - \alpha_1 + \beta_1 - k_1)Md_1/2]/\sin[(\mu_1 - \alpha_1 + \beta_1 - k_1)d_1/2]$ and $\sin[(k_1 - \beta_1)Md_1/2]/\sin[(k_1 - \beta_1)d_1/2]$, which, in the convolution process, filters the true spectrum, $S_{oo}[\underline{\alpha},\underline{\beta},\omega;\underline{x}_c]$, in the α_1 and β_1 wavenumber variables.

We have previously observed that $\sin(Mk_1d_1)/\sin(k_1d_1)$ is a periodic function of k_1, with major acceptance lobes located at $k_1 = 2n\pi/d_1$ for all positive and negative integer values of n. The amplitudes of these major lobes are proportional to M and the bandwidths are inversely proportional to M. It therefore follows that the product of $\sin[(\beta_1 - \alpha_1)Md_1/2]/\sin[(\beta_1 - \alpha_1)d_1/2]$ and $\sin(\beta_1Md_1/2)/\sin(\beta_1d_1/2)$, which is equal to the product of $\sin[(\mu_1 - \alpha_1 + \beta_1 - k_1)Md_1/2]/\sin[(\mu_1 - \alpha_1 + \beta_1 - k_1)d_1/2]$ and $\sin[(k_1 - \beta_1)Md_1/2]/\sin[(k_1 - \beta_1)d_1/2]$ evaluated at $\mu_1 = k_1 = 0$, is characterized by major acceptance lobes at the intersections of $\beta_1 = 2m\pi/d_1$ and $\alpha_1 - \beta_1 = 2n\pi/d_1$ for all positive and negative integer values of m and n. The amplitudes of these major lobes are proportional to M^2 and the bandwidths, in both the α_1 and β_1 coordinate directions, can be shown to be inversely proportional to M. The locations of these major acceptance lobes in the (α_1,β_1) domain are illustrated in figure 8-15. The shaded region shown in figure 8-15 defines, for future reference, the primary (or unaliased) wavevector range of the M by N array in the (α_1,β_1) domain. This primary acceptance region is bounded by $|\beta_1| \leq \pi/d_1$ and $|\alpha_1 - \beta_1| \leq \pi/d_1$.

If we assume that M is sufficiently large that the bandwidths, in α_1 and β_1, of the major acceptance lobes of the product of $\sin[(\mu_1 - \alpha_1 + \beta_1 - k_1)Md_1/2]/\sin[(\mu_1 - \alpha_1 + \beta_1 - k_1)d_1/2]$ and $\sin[(k_1 - \beta_1)Md_1/2]/\sin[(k_1 - \beta_1)d_1/2]$ are small in comparison to the bandwidth of any variation of $S_{oo}[\underline{\alpha},\underline{\beta},\omega;\underline{x}_c]$ in α_1 and β_1, then we can approximate the convolution of $S_{oo}[\underline{\alpha},\underline{\beta},\omega;\underline{x}_c]$ with the product of $\sin[(\mu_1 - \alpha_1 + \beta_1 - k_1)Md_1/2]/\sin[(\mu_1 - \alpha_1 + \beta_1 - k_1)d_1/2]$ and $\sin[(k_1 - \beta_1)Md_1/2]/\sin[(k_1 - \beta_1)d_1/2]$ as a weighted summation of the sample values of $S_{oo}[\underline{\alpha},\underline{\beta},\omega;\underline{x}_c]$ at the locations of all major acceptance lobes in α_1 and β_1.

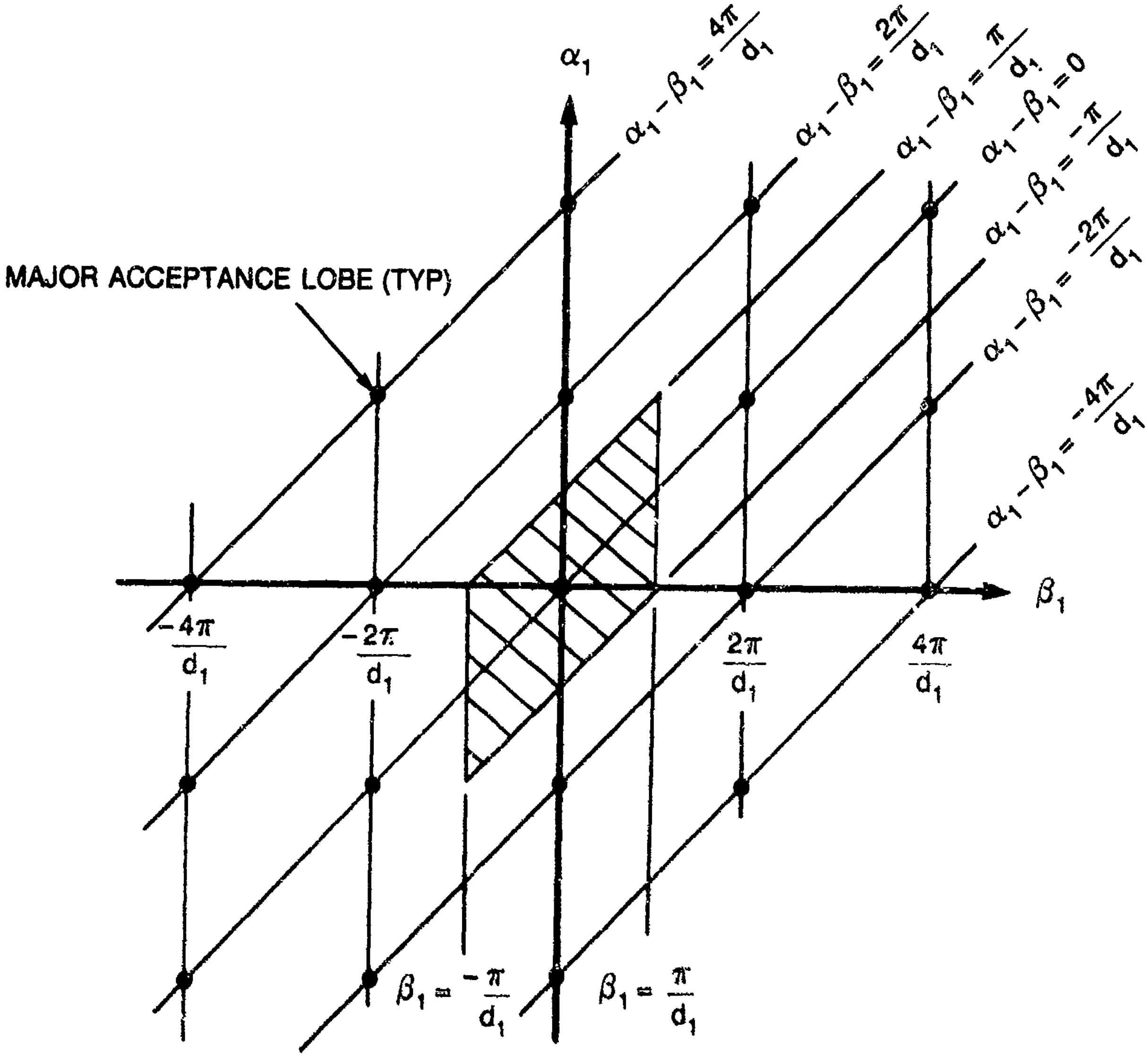

Figure 8-15. Locations of the Major Acceptance Lobes of the Product

$$\frac{\sin[\beta_1 M d_1/2]}{\sin[\beta_1 d_1/2]} \; \frac{\sin[(\beta_1 - \alpha_1) M d_1/2]}{\sin[(\beta_1 - \alpha_1) d_1/2]}$$

The locations of the major acceptance lobes of the product of $\sin[(\mu_1 - \alpha_1 + \beta_1 - k_1)Md_1/2]/\sin[(\mu_1 - \alpha_1 + \beta_1 - k_1)d_1/2]$ and $\sin[(k_1 - \beta_1)Md_1/2]/\sin[(k_1 - \beta_1)d_1/2]$ are illustrated in figure 8-16. Also illustrated, in dashed lines, is the primary wavevector range in the (α_1,β_1) domain. According to figure 8-16 and the above stated approximation, the estimate of $S_{oo}[\underline{\alpha},\underline{\beta},\omega;\underline{x}_c]$ at the wavevector components μ_1 and k_1, for any given values of μ_2 and k_2, will comprise, in general, a weighted summation of the spectral samples $S_{oo}[\mu_1 + 2m\pi/d_1,\alpha_2;k_1 + 2n\pi/d_1,\beta_2;\omega;\underline{x}_c]$ over all positive

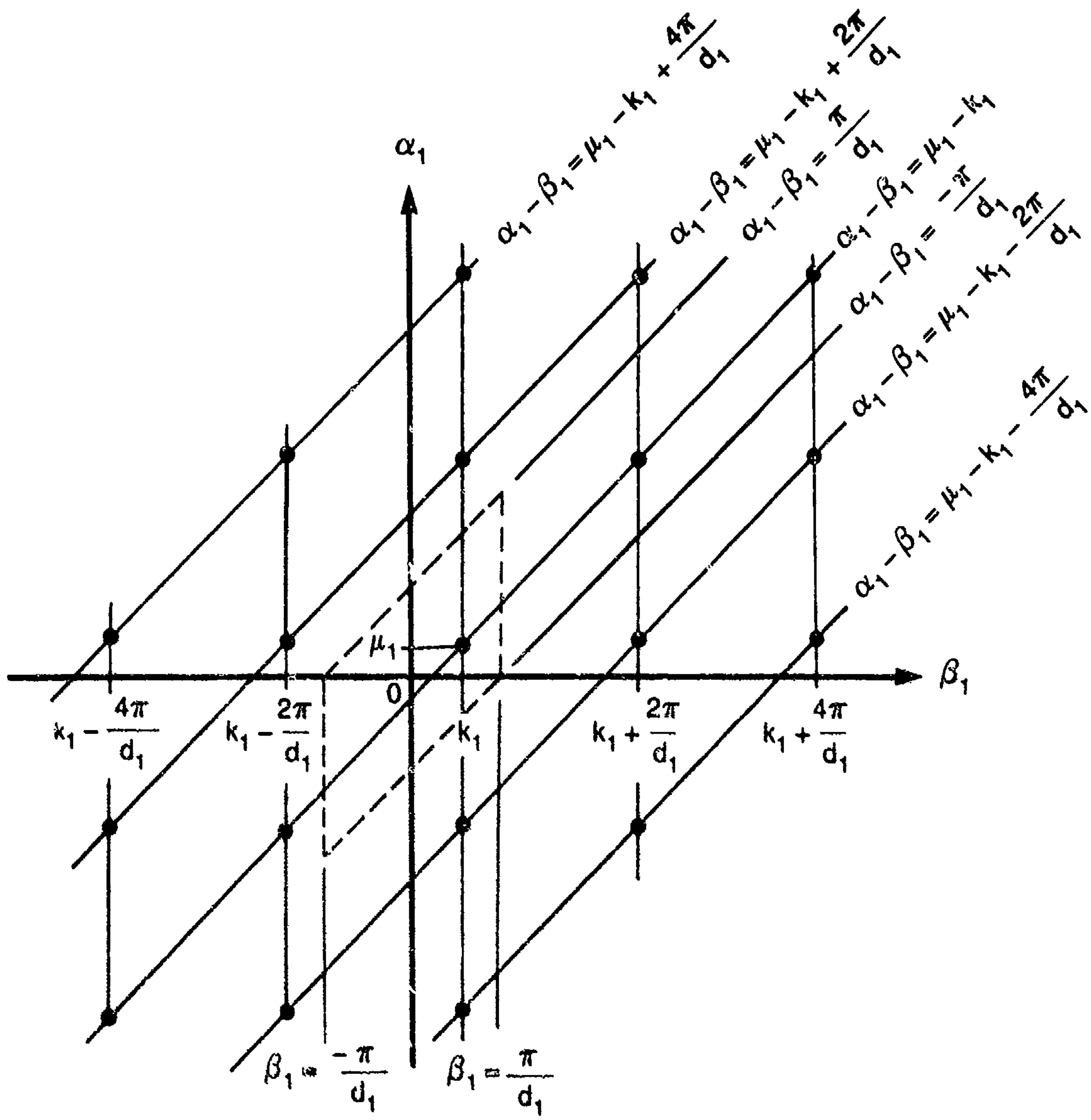

Figure 8-16. Locations of the Major Acceptance Lobes of the Product

$$\frac{\sin[(k_1 - \beta_1)Md_1/2]}{\sin[(k_1 - \beta_1)d_1/2]}\,\frac{\sin[(\mu_1 - \alpha_1 + \beta_1 - k_1)Md_1/2]}{\sin[(\mu_1 - \alpha_1 + \beta_1 - k_1)d_1/2]}$$

and negative integer values of m and n. In this summation, the contributions from the spectral samples associated with nonzero values of m and n are aliased contributions that contaminate the desired value of the estimate: that desired value being $S_{oo}(\mu_1,\alpha_2;k_1,\beta_2;\omega)$. Note, however, that if $S_{oo}(\underline{\mu},\underline{k},\omega)$ is wavenumber band limited in both μ_1 and k_1 such that

$$S_{oo}(\underline{\mu},\underline{k},\omega) = 0, \quad |k_1| > k_{1c} \text{ and } |\mu_1 - k_1| > \epsilon_{1c} \tag{8-184}$$

and d_1 is selected such that

$$d_1 < \mathrm{MIN}\{\pi/k_{1c}, \pi/\epsilon_{1c}\} , \qquad (8\text{-}185)$$

where MIN{} denotes the minimum of the two arguments, then the summation that approximates the estimate of $S_{oo}[\mu_1,\alpha_2;k_1,\beta_2;\omega;\underline{x}_c]$ comprises only a single sample term: that sample term being proportional to $S_{oo}[\alpha_1,\alpha_2;\beta_1,\beta_2;\omega;\underline{z}_c]$ evaluated at $\alpha_1 = \mu_1$ and $\beta_1 = k_1$.

It is evident from figure 8-16 and the above arguments that if the band limits and sampling criteria of equations (8-184) and (8-185) are met, then the estimate of $S_{oo}[\mu_1,\alpha_2;k_1,\beta_2;\omega;\underline{x}_c]$ is a periodic function of the variables $\mu_1 - k_1$ and k_1.

Arguments similar to the above can also be made for the convolution of equation (8-182) in the variables α_2 and β_2.

By the arguments presented above, it is evident that the estimate of the two wavevector-frequency spectrum of the space-shifted output field will be affected by aliasing errors unless (1) the true wavevector-frequency spectrum of the output field is wavevector band limited in both $\underline{\mu}$ and $\underline{k}$ such that

$$S_{oo}(\underline{\mu},\underline{k},\omega) = 0: \quad |k_1| > k_{1c}, |k_2| > k_{2c} \text{ and}$$

$$|\mu_1 - k_1| > \epsilon_{1c}, |\mu_2 - k_2| > \epsilon_{2c} , \qquad (8\text{-}186)$$

and (2) the spacings of the M by N element array are chosen such that

$$d_1 < \mathrm{MIN}\{\pi/k_{1c}, \pi/\epsilon_{1c}\} \text{ and } d_2 < \mathrm{MIN}\{\pi/k_{2c}, \pi/\epsilon_{2c}\} . \qquad (8\text{-}187)$$

Given that these conditions are satisfied, and that M and N are chosen sufficiently large that the bandwidths of the major acceptance lobes of the products $\{\sin(\beta_1 Md_1/2)/\sin(\beta_1 d_1/2)\}\{\sin[(\alpha_1 - \beta_1)Md_1/2]/\sin[(\alpha_1 - \beta_1)d_1/2]\}$ and $\{\sin(\beta_2 Md_2/2)/\sin(\beta_2 d_2/2)\}\{\sin[(\alpha_2 - \beta_2)Md_2/2]/\sin[(\alpha_2 - \beta_2)d_2/2]\}$ are much smaller than the bandwidths of any variation of $S_{oo}[\underline{\alpha},\underline{\beta};\omega;\underline{x}_c]$ in α_1, α_2, β_1, or β_2, then we can approximate equation (8-182) by

$$\tilde{S}_{oo}[\underline{\mu},\underline{k},\omega;\underline{x}_c] = \frac{d_1^2 d_2^2}{(2\pi)^4} S_{oo}[\underline{\mu},\underline{k},\omega;\underline{x}_c]$$

$$\int_{-\pi/d_1}^{\pi/d_1} \int_{\beta_1-\pi/d_1}^{\beta_1+\pi/d_1} \frac{\sin[(\mu_1 - \alpha_1 + \beta_1 - k_1)Md_1/2]}{\sin[(\mu_1 - \alpha_1 + \beta_1 - k_1)d_1/2]} \frac{\sin[(k_1 - \beta_1)Md_1/2]}{\sin[(k_1 - \beta_1)d_1/2]} \, d\alpha_1 \, d\beta_1$$

$$\int_{-\pi/d_2}^{\pi/d_2} \int_{\beta_2-\pi/d_2}^{\beta_2+\pi/d_2} \frac{\sin[(\mu_2 - \alpha_2 + \beta_2 - k_2)Nd_2/2]}{\sin[(\mu_2 - \alpha_2 + \beta_2 - k_2)d_2/2]} \frac{\sin[(k_2 - \beta_2)Nd_2/2]}{\sin[(k_2 - \beta_2)d_2/2]} \, d\alpha_2 \, d\beta_2 \, . \tag{8-188}$$

However, by a change of variable and use of equation (8-116), we can easily show that

$$\int_{-\pi/d_1}^{\pi/d_1} \int_{\beta_1-\pi/d_1}^{\beta_1+\pi/d_1} \frac{\sin[(\mu_1 - \alpha_1 + \beta_1 - k_1)Md_1/2]}{\sin[(\mu_1 - \alpha_1 + \beta_1 - k_1)d_1/2]} \frac{\sin[(k_1 - \beta_1)Md_1/2]}{\sin[(k_1 - \beta_1)d_1/2]} \, d\alpha_1 \, d\beta_1$$

$$= \left\{ \int_{-\pi/d_1}^{\pi/d_1} \frac{\sin[(\mu_1 - k_1 - \theta_1)Md_1/2]}{\sin[(\mu_1 - k_1 - \theta_1)d_1/2]} \, d\theta_1 \right\} \left\{ \int_{-\pi/d_1}^{\pi/2} \frac{\sin[(k_1 - \beta_1)Md_1/2]}{\sin[(k_1 - \beta_1)d_1/2]} \, d\beta_1 \right\}$$

$$= \frac{4\pi^2}{d_1^2} \tag{8-189}$$

for M odd. Equation (8-189) is also approximately true for M even. Consequently, it follows from equations (8-188) and (8-189) that

$$\tilde{S}_{oo}[\underline{\mu},\underline{k},\omega;\underline{x}_c] = S_{oo}[\underline{\mu},\underline{k},\omega;\underline{x}_c]: \quad |k_1| \le \pi/d_1, |k_2| \le \pi/d_2 \text{ and}$$

$$|\mu_1 - k_1| \le \pi/d_1, |\mu_2 - k_2| \le \pi/d_2 \, . \tag{8-190}$$

By the above arguments, it is evident that if (1) $S_{oo}(\underline{\mu},\underline{k},\omega)$ is wavenumber band limited in both μ_1 and k_1 such that

$$S_{oo}(\underline{\mu},\underline{k},\omega) = 0: \quad |k_1| > k_{1c}, |k_2| > k_{2c} \text{ and}$$

$$|\mu_1 - k_1| > \varepsilon_{1c}, |\mu_2 - k_2| > \varepsilon_{2c} , \qquad (8\text{-}191)$$

(2) the spatial sampling periods, d_1 and d_2, are selected such that

$$d_1 < \text{MIN}\{\pi/k_{1c}, \pi/\varepsilon_{1c}\} \text{ and } d_2 < \text{MIN}\{\pi/k_{2c}, \pi/\varepsilon_{2c}\} , \qquad (8\text{-}192)$$

and (3) the numbers of spatial samples, M and N, in the x_1 and x_2 coordinate directions, respectively, are chosen sufficiently large that the bandwidths of the major acceptance lobes of the $\{\sin(\beta_1 Md_1/2)\sin[(\alpha_1 - \beta_1)Md_1/2]\}/\{\sin(\beta_1 d_1/2)\sin[(\alpha_1 - \beta_1)d_1/2]\}$ and $\{\sin(\beta_2 Md_2/2)\sin[(\alpha_2 - \beta_2)Md_2/2]\}/\{\sin(\beta_2 d_2/2)\sin[(\alpha_2 - \beta_2)d_2/2]\}$ are much smaller than the bandwidths of any variation of $S_{oo}[\underline{\alpha},\underline{\beta};\omega;\underline{x}_c]$ in α_1, α_2, β_1, or β_2, then the estimate, $\tilde{S}_{oo}[\underline{\mu},\underline{k},\omega;\underline{x}_c]$, of the two wavevector-frequency spectrum associated with the space-shifted autocorrelation function $Q_{oo}(\underline{x} + \underline{x}_c,\underline{\xi},\tau)$ affords an approximation to the true two wavevector-frequency spectrum, $S_{oo}[\underline{\mu},\underline{k},\omega;\underline{x}_c]$, within the primary (or unaliased) range of the array. The quality of that approximation improves with increasing numbers of spatial samples in the x_1 and x_2 coordinate directions.

Inasmuch as $\tilde{S}_{oo}[\underline{\mu},\underline{k},\omega;\underline{x}_c] = \tilde{S}_{oo}(\underline{\mu},\underline{k},\omega)\exp(i\underline{k}\cdot\underline{x}_c)$, it follows from equation (8-190) that, under the above stated conditions,

$$\tilde{S}_{oo}(\underline{\mu},\underline{k},\omega) = \tilde{S}_{oo}[\underline{\mu},\underline{k},\omega;\underline{x}_c]\exp(-i\underline{k}\cdot\underline{x}_c) \approx$$

$$S_{oo}[\underline{\mu},\underline{k},\omega;\underline{x}_c]\exp(-i\underline{k}\cdot\underline{x}_c) = S_{oo}(\underline{\mu},\underline{k},\omega):$$

$$|k_1| \le \pi/d_1, |k_2| \le \pi/d_2 \text{ and } |\mu_1 - k_1| \le \pi d_1, |\mu_2 - k_2| \le \pi/d_2 .$$

$$(8\text{-}193)$$

In this instance, given the wavevector-frequency response, $G(\underline{k},\omega)$, of the (identical) sensors of the array, we can use equation (8-14) to obtain an approximation, $\tilde{S}_{pp}(\underline{\mu},\underline{k},\omega)$, to the two wavevector-frequency spectrum of the nonhomogeneous pressure field being measured. That is,

$$\tilde{S}_{pp}(\underline{\mu},\underline{k},\omega) = \begin{cases} \dfrac{\tilde{S}_{oo}(\underline{\mu},\underline{k},\omega)}{G(\underline{k}-\underline{\mu},-\omega)G(-\underline{k},\omega)}, & |k_1| \le \pi/d_1, |k_2| \le \pi/d_2 \text{ and } \\ & |\mu_1 - k_1| \le \pi d_1, |\mu_2 - k_2| \le \pi/d_2 \\ 0, & \text{otherwise} \end{cases}$$

$$\approx \frac{S_{oo}(\underline{\mu},\underline{k},\omega)}{G(\underline{k}-\underline{\mu},-\omega)G(-\underline{k},\omega)} \approx S_{pp}(\underline{\mu},\underline{k},\omega) \ . \tag{8-194}$$

Another metric of interest for the nonhomogeneous, stationary field is the space-averaged wavevector-frequency spectrum, $\Phi_o^a(\underline{k},\omega)$, which (from equations (6-142) and (6-149)) is defined by

$$\Phi_o^a(\underline{k},\omega) = \lim_{L\to\infty} \frac{1}{4L^2} \int_{-\infty}^{\infty}\int_{-\infty}^{\infty}\int_{-\infty}^{\infty}\int_{-L}^{L}\int_{-L}^{L} Q_{oo}(\underline{x},\underline{\xi},\tau)\exp[-i(\underline{k}\cdot\underline{\xi} + \omega\tau)]\, d\underline{x}\, d\underline{\xi}\, d\tau \ . \tag{8-195}$$

However, the ensemble of sample functions described by equation (8-159) supports only an estimate of the space-averaged wavevector-frequency spectrum. That estimate, which we denote by $\tilde{\Phi}_o^a(\underline{k},\omega)$, is

$$\tilde{\Phi}_o^a(\underline{k},\omega) = \frac{d_1 d_2}{MN} \sum_{m=0}^{M-1}\sum_{n=0}^{N-1}\sum_{q-m=-m}^{M-m-1}\sum_{s-n=-n}^{N-n-1}\int_{-\infty}^{\infty} Q_{oo}[x_{01} + md_1, x_{02} + nd_2; (q-m)d_1, (s-n)d_2; \tau]$$

$$\exp\{-i[k_1(q-m)d_1 + k_2(s-n)d_2 + \omega\tau]\}\, d\tau \ . \tag{8-196}$$

However, by reasoning similar to that following equation (8-172), we can rewrite equation (8-196) in the form

$$\tilde{\Phi}_o^a(\underline{k},\omega) = \frac{1}{MNd_1 d_2}\int_{-\infty}^{\infty}\int_{-\infty}^{\infty}\int_{-\infty}^{\infty}\int_{-\infty}^{\infty}\int_{-\infty}^{\infty} Q_{oo}(\underline{x},\underline{\xi},\tau)s_f(\underline{x}-\underline{x}_0;M,N)s_f(\underline{x}-\underline{x}_0+\underline{\xi};M,N)$$

$$\exp[-i(\underline{k}\cdot\underline{\xi} + \omega\tau)]\, d\underline{x}\, d\underline{\xi}\, d\tau \ . \tag{8-197}$$

Substitution of the Fourier inverse of $Q_{oo}(\underline{x},\underline{\xi},\tau)$ and performance of the integrations over the temporal and frequency variables then yields

$$\tilde{\Phi}_0^a(\underline{k},\omega) = \frac{1}{(2\pi)^4 MNd_1d_2} \int_{-\infty}^{\infty}\int_{-\infty}^{\infty}\int_{-\infty}^{\infty}\int_{-\infty}^{\infty}\int_{-\infty}^{\infty}\int_{-\infty}^{\infty}\int_{-\infty}^{\infty}\int_{-\infty}^{\infty} S_{00}(\underline{\alpha},\underline{\beta},\tau)$$

$$s_f(\underline{x} - \underline{x}_0;M,N)s_f(\underline{x} - \underline{x}_0 + \underline{\xi};M,N)$$

$$\exp\{i[\underline{\alpha}\cdot\underline{x} - (\underline{k} - \underline{\beta})\cdot\underline{\xi} - \omega\tau]\}\, d\underline{x}\, d\underline{\xi}\, d\underline{\alpha}\, d\underline{\beta} \,. \qquad (8\text{-}198)$$

By integrating over the spatial variables, we obtain

$$\tilde{\Phi}_0^a(\underline{k},\omega) = \frac{1}{(2\pi)^4 MNd_1d_2} \int_{-\infty}^{\infty}\int_{-\infty}^{\infty}\int_{-\infty}^{\infty}\int_{-\infty}^{\infty} S_{00}(\underline{\alpha},\underline{\beta},\tau)S_f(\underline{\beta} - \underline{\alpha} - \underline{k};M,N)$$

$$S_f(\underline{k} - \underline{\beta};M,N)\exp(i\underline{\alpha}\cdot\underline{x}_0)\, d\underline{\alpha}\, d\underline{\beta} \,. \qquad (8\text{-}199)$$

By substituting equation (8-150) for $S_f(\underline{k};MN)$, and utilizing the definitions of equations (8-181) and (8-183), we can show that

$$\tilde{\Phi}_0^a(\underline{k},\omega) = \frac{d_1d_2}{(2\pi)^4 MN} \int_{-\infty}^{\infty}\int_{-\infty}^{\infty}\int_{-\infty}^{\infty}\int_{-\infty}^{\infty} S_{00}[\underline{\alpha},\underline{\beta},\omega;\underline{x}_c]$$

$$\frac{\sin[(\beta_1 - \alpha_1 - k_1)Md_1/2]}{\sin[(\beta_1 - \alpha_1 - k_1)d_1/2]} \frac{\sin[(\beta_2 - \alpha_2 - k_2)Nd_2/2]}{\sin[(\beta_2 - \alpha_2 - k_2)d_2/2]}$$

$$\frac{\sin[(k_1 - \beta_1)Md_1/2]}{\sin[(k_1 - \beta_1)d_1/2]} \frac{\sin[(k_2 - \beta_2)Nd_2/2]}{\sin[(k_2 - \beta_2)d_2/2]}\, d\underline{\alpha}\, d\underline{\beta} \,. \qquad (8\text{-}200)$$

Equation (8-200) establishes a relationship between the estimate of the space-averaged wavevector-frequency spectrum of the sensor output field and the true two wavevector-frequency spectrum of that field. Recall by equation (8-155), that the true space-averaged wavevector-frequency spectrum, $\Phi_0^a(\underline{k},\omega)$, is equal to the integral, over all $\underline{\mu}$, of the product of the two wavevector-frequency spectrum, $S_{00}(\underline{\mu},\underline{k},\omega)$, with $\sin(\mu_1 L)/(\mu_1 L)$ and $\sin(\mu_2 L)/(\mu_2 L)$. Consequently, it is evident from equation (8-200) that we cannot establish an exact relationship between the estimated and true

space-averaged wavevector-frequency spectra. Rather, we can only relate the estimate of the space-averaged spectrum, $\tilde{\Phi}_o^a(\underline{k},\omega)$, to the true two wavevector-frequency spectrum, $S_{oo}(\underline{\mu},\underline{k},\omega)$, as shown in equation (8-200).

If it is known that (1) $S_{oo}(\underline{\mu},\underline{k},\omega)$ is band limited as described in equation (8-186), (2) the interelement spacings of the array are selected in accordance with equation (8-187), and (3) the numbers of sensors, M and N, in the x_1 and x_2 coordinate directions are chosen sufficiently large that the bandwidths of the acceptance lobes of $\sin[(\beta_1 - \alpha_1)Md_1/2]/\sin[(\beta_1 - \alpha_1)d_1/2]$, $\sin[\beta_1 Md_1/2]/\sin[\beta_1 d_1/2]$, $\sin[(\beta_2 - \alpha_2)Nd_2/2]/\sin[(\beta_2 - \alpha_2)d_2/2]$, and $\sin[\beta_2 Nd_2/2]/\sin[\beta_2 d_2/2]$ in α_1, α_2, β_1, and β_2 are small in comparison to the bandwidths of any fluctuations of $S_{oo}(\underline{\mu},\underline{k},\omega)$ in these wavenumber variables, then we can employ previous arguments to show that

$$\tilde{\Phi}_o^a(\underline{k},\omega) \approx \frac{1}{MNd_1d_2} S_{oo}[\underline{0},\underline{\beta},\omega;\underline{x}_c] \; , \quad |k_1| \le \pi/d_1 \text{ and } |k_2| \le \pi/d_2 \; . \tag{8-201}$$

In this case, we can employ equation (8-15) to obtain an estimate of the space-averaged wavevector-frequency spectrum, $\tilde{\Phi}_p^a(\underline{k},\omega)$, of the surface pressure field, $p(\underline{x},t)$. That is,

$$\tilde{\Phi}_p^a(\underline{k},\omega) = \left\{ \begin{array}{ll} \dfrac{\tilde{\Phi}_o^a(\underline{k},\omega)}{|G(-\underline{k},\omega)|^2} \, , & \begin{array}{l} |k_1| \le \pi/d_1 \\ |k_2| \le \pi/d_2 \end{array} \\ & \\ 0, & \text{otherwise} \end{array} \right\}$$

$$= \frac{S_{oo}[\underline{0},\underline{\beta},\omega;\underline{x}_c]}{MNd_1d_2|G(-\underline{k},\omega)|^2} = \frac{S_{pp}[\underline{0},\underline{\beta},\omega;\underline{x}_c]}{MNd_1d_2} \; . \tag{8-202}$$

As a final example, consider the random pressure field characterized by the two wavevector-frequency spectrum

$$S_{pp}(\underline{\mu},\underline{k},\omega) = (2\pi)^2\delta(\underline{\mu})\Phi_p(\underline{k},\omega) + W_{pp}(\underline{\mu},\underline{k},\omega) \; , \tag{8-203}$$

where $\Phi_p(\underline{k},\omega)$ characterizes a homogeneous component of the pressure field

and $W_{pp}(\underline{\mu},\underline{k},\omega)$ characterizes the nonhomogeneous components. By equations (8-14) and (8-15), it follows that the two wavevector-frequency spectrum of the sensor output field has the form

$$S_{oo}(\underline{\mu},\underline{k},\omega) = \frac{(2\pi)^2\delta(\underline{\mu})\Phi_p(\underline{k},\omega)}{|G(-\underline{k},\omega)|^2} + \frac{W_{pp}(\underline{\mu},\underline{k},\omega)}{G(\underline{k}-\underline{\mu},-\omega)G(-\underline{k},\omega)}$$

$$= (2\pi)^2\delta(\underline{\mu})\Phi_o(\underline{k},\omega) + W_{oo}(\underline{\mu},\underline{k},\omega) \ . \qquad (8\text{-}204)$$

We assume that (1) $S_{oo}(\underline{\mu},\underline{k},\omega)$ is band limited in $\underline{\mu}$ and $\underline{k}$ as prescribed by equation (8-186), (2) the spatial sampling intervals are chosen in accordance with equation (8-187), and (3) M and N are chosen such that the bandwidths of the major response lobes of $S(\underline{k};M,N)$ and $S(\underline{\mu}-\underline{k};M,N)$ are much smaller than the bandwidths of any variation of either $\Phi_o(\underline{k},\omega)$ in k_1 or k_2 or $W_{oo}(\underline{\mu},\underline{k},\omega)$ in μ_1, μ_2, k_1, and k_2. Under these restrictions, we can employ the arguments developed previously to show that the estimate of the space-averaged wavevector-frequency spectrum of the sensor output field can be approximated by

$$\tilde{\Phi}_o^a(\underline{k},\omega) \approx \frac{W_{oo}(\underline{0},\underline{k},\omega)}{MNd_1d_2} + \frac{d_1d_2}{(2\pi)^2MN}\Phi_o(\underline{k},\omega)$$

$$\left\{\int_{-\pi/d_1}^{\pi/d_1}\left|\frac{\sin[(k_1-\beta_1)Md_1/2]}{\sin[(k_1-\beta_1)d_1/2]}\right|^2 d\beta_1\right\}\left\{\int_{-\pi/d_2}^{\pi/d_2}\left|\frac{\sin[(k_2-\beta_2)Nd_2/2]}{\sin[(k_2-\beta_2)d_2/2]}\right|^2 d\beta_2\right\} .$$

(8-205)

However, by use of equations (8-147) and (8-150), it is straightforward to show that

$$\left\{\int_{-\pi/d_1}^{\pi/d_1}\left|\frac{\sin[(k_1-\beta_1)Md_1/2]}{\sin[(k_1-\beta_1)d_1/2]}\right|^2 d\beta_1\right\}\left\{\int_{-\pi/d_2}^{\pi/d_2}\left|\frac{\sin[(k_2-\beta_2)Nd_2/2]}{\sin[(k_2-\beta_2)d_2/2]}\right|^2 d\beta_2\right\} =$$

$$\int_{-\pi/d_1}^{\pi/d_1}\int_{-\pi/d_2}^{\pi/d_2}|S_f(\underline{k}-\underline{\beta};M,N)|^2\, d\beta_1\, d\beta_2 = \frac{(2\pi)^2MN}{d_1d_2} \ . \qquad (8\text{-}206)$$

Thus, we see that when the true two wavevector-frequency spectrum of the sensor output field has the form of equation (8-204), and the above listed wavevector band-limit and spatial sampling restrictions are satisfied, then the estimate of the space-averaged wavevector-frequency spectrum is approximated by

$$\tilde{\Phi}_o^a(\underline{k},\omega) \approx \Phi_o(\underline{k},\omega) + \frac{W_{oo}(\underline{0},\underline{k},\omega)}{MNd_1d_2}, \quad |k_1| \le \pi/d_1 \text{ and } |k_2| \le \pi/d_2 . \tag{8-207}$$

It follows that the estimate of the space-averaged wavevector-frequency spectrum of the surface pressure field is approximated by

$$\tilde{\Phi}_p^a(\underline{k},\omega) = \begin{cases} \dfrac{\tilde{\Phi}_o^a(\underline{k},\omega)}{|G(-\underline{k},\omega)|^2}, & \begin{matrix}|k_1| \le \pi/d_1 \\ |k_2| \le \pi/d_2\end{matrix} \\[2ex] 0, & \text{otherwise} \end{cases}$$

$$\approx \frac{1}{|G(-\underline{k},\omega)|^2}\left\{\Phi_o(\underline{k},\omega) + \frac{W_{oo}(\underline{0},\underline{k},\omega)}{MNd_1d_2}\right\} \approx \Phi_p(\underline{k},\omega) + \frac{W_{pp}(\underline{0},\underline{k},\omega)}{MNd_1d_2} . \tag{8-208}$$

Thus, we see that the estimate of the space-averaged wavevector-frequency spectrum of the pressure field approximates the sum of the wavevector-frequency spectrum of the homogeneous component of the field and the average, over the effective area of the array, of the two wavevector-frequency spectrum of the nonhomogeneous component evaluated at $\underline{\mu} = (0,0)$. Recall (see equation (5-158)) that the exact space-averaged wavevector-frequency spectrum of the pressure field characterized by equation (8-203) was equal to the wavevector-frequency spectrum of the homogeneous component of the field: that is, $\Phi_p^a(\underline{k},\omega) = \Phi_p(\underline{k},\omega)$.

Clearly, the finite limits on spatial sampling significantly restrict our ability to estimate the space-time and wavevector-frequency characteristics of any acoustic field of interest. To avoid aliasing errors in such estimates, the output field from the sensors used to measure the acoustic field of interest must be band limited in all wavevector variables of interest, and the spatial intervals between sensors, in each coordinate direction, must be less

than one-half of the wavelengths associated with the largest corresponding wavenumber components c :he band limits. Given that these wavevector band limits and spatial sampling requirements are met, we can obtain only an approximation to the true wavevector-frequency characteristics of the sensor output field, and thereby of the acoustic field of interest, from any finite number of spatial samples of the field. The quality of that approximation depends on the wavenumber bandwidths of the main lobe of the response function of the array relative to the bandwidths, in the corresponding wavenumber directions, of fluctuations in the transform or spectrum of the sensor output field. In general, the quality of the approximation improves with increasing numbers of spatial samples.

8.4 SUMMARY

A complete characterization of any acoustic field requires knowledge of that field over all space and time for all possible realizations of that field. In the measurement of an acoustical field, practical limitations preclude any such complete characterization. Therefore, measurements can provide only some estimate of the space-time or wavevector-frequency character of the field. In this chapter, we have examined the effects of certain measurement limitations and decisions on the quality of such estimates.

In measurements, it is rare that the acoustic parameter of interest can be measured directly. Rather, most measurements utilize transducers or sensors that convert the acoustic parameter of interest to an electrical variable. Transducers are resonant devices and have finite spatial extent. The resonant character of the sensor causes the ratio of the amplitudes of the sensor output and the acoustic variable to vary as a function of frequency at any fixed location within the field. In addition, the phase between the sensor output and the acoustic variable at the sensor location varies as a function of frequency. The finite spatial extent of the sensor results in the various wave components of the acoustic field being spatially "averaged" over the active surface of the sensor. If the acoustic field of interest was measured over all space and time with identical sensors, these resonance and spatial characteristics of the sensor would cause the wavevector-frequency characteristics of the resulting sensor output field to differ from the wavevector-

frequency characteristics of the acoustic field. As shown and discussed in section 8.1, the measured sensor output field is a filtered version, in both the wavevector and frequency domains, of the acoustic field of interest. Given knowledge of the wavevector-frequency response of the sensor, the space-time or wavevector-frequency characteristics of the acoustic field can be recovered from the corresponding characteristics of the sensor output field. Inasmuch as the purpose of the measurement is to characterize the acoustic field in the space-time or wavevector-frequency domains, it is imperative that the sensors selected for any measurement have either (1) known response as a function of wavevector and frequency or (2) resonance frequencies much higher than any acoustic frequency of interest and spatial dimensions much less than the wavelength associated with the highest wavenumber component in the acoustic field.

To take advantage of the computationally efficient fast Fourier transform techniques, it is common practice to sample each sensor output at uniform increments of time. Further, because the finite spatial dimensions of practical sensors preclude temporally synchronous measurements of the acoustic field over all space, the acoustic field is usually measured by arrays of sensors, uniformly separated in each spatial coordinate of interest. If the sensor output field is sampled at uniform intervals T over all time, and at uniform intervals d_1 and d_2 over all space, it is demonstrated in section 8.2 that the exact space-time or wavevector-frequency description of the sensor output field can be recovered from the sampled data if (1) the sensor output field is band limited in frequency and in all wavevector variables such that either

$$O(\underline{k},\omega) = 0: \quad |\omega| > \omega_c,\ |k_1| > k_{1c},\ \text{and } |k_2| > k_{2c}, \tag{8-209}$$

$$\Phi_o(\underline{k},\omega) = 0: \quad |\omega| > \omega_c,\ |k_1| > k_{1c},\ \text{and } |k_2| > k_{2c}, \tag{8-210}$$

or

$$S_{oo}(\underline{\mu},\underline{k},\omega) = 0: \quad |\omega| > \omega_c,\ |k_1| > k_{1c},\ |k_2| > k_{2c},$$

$$|\mu_1 - k_1| > \epsilon_{1c},\ \text{and } |\mu_2 - k_2| > \epsilon_{2c}, \tag{8-211}$$

and (2) the temporal and spatial sampling intervals are selected such that

$$T \leq \pi/\omega_c \tag{8-212}$$

and

$$d_1 \leq \mathrm{MIN}(\pi/\epsilon_{1c}, \pi/k_{1c}) \text{ and } d_2 \leq \mathrm{MIN}(\pi/\epsilon_{2c}, \pi/k_{2c}) \ . \tag{8-213}$$

In equation (8-213), ϵ_{1c} and ϵ_{2c} are taken to be zero for deterministic or homogeneous sensor output fields. Given that equation (8-209), (8-210), or (8-11), as appropriate, and equations (8-12) and (8-13) are satisfied, and given the wavevector-frequency response of the (assumed identical) sensors comprising the measurement array, then the exact space-time or wavevector-frequency description of the acoustic field can be recovered from the sampled output field over all space and time.

Sampling of the sensor output field over infinite limits of space and time is, of course, a physically impossible task. Practically, we can obtain some finite number, Q, of temporal samples of the sensor output field over some finite interval of time. Similarly, we can, at best, utilize some M by N array of sensors to spatially sample the output field within some bounded region of space. Given that the sensor output field is band limited in both the wavevector and frequency domains according to equation (8-209), (8-210), or (8-11), as appropriate, and that the temporal and spatial sampling intervals are chosen in accordance with equations (8-12) and (8-13), we established in section 8.3 that the true space-time or wavevector-frequency description of the sensor output field could not be recovered from the finite numbers of spatial and temporal samples of the output field. Rather, the finite numbers of spatial and temporal samples provide only sufficient information to support an approximation to the true wavevector-frequency descriptor of the sensor output field. As more fully described in section 8.3, the quality of this approximation depends on the bandwidths of the primary response lobes of the wavevector and frequency transforms of the spatial and temporal sampling functions relative to the bandwidths of the fluctuations, in the respective wavevector and frequency domains, of the descriptor of the output field. Inasmuch as the bandwidths of the primary response lobes of the wavevector and frequency transforms of the spatial and

temporal sampling functions decrease with increasing numbers of samples, the quality of the approximation of the desired wavevector-frequency descriptor of the sensor output field generally improves with increasing numbers of spatial and temporal samples. Obviously, given only an approximation to the wavevector-frequency description of the sensor output field, we can, at best, recover only an approximation to the space-time or wavevector-frequency description of the acoustic field of interest.

Given that the purpose of any measurement of an acoustic field is to describe, as accurately as possible, the space-time or wavevector-frequency characteristics of that field, it is evident that careful consideration must be given, during the planning phase of the experiment, to the choice of sensors, the number of sensors and the geometry of their spatial disposition, and the number and period of the temporal samples. Intelligent choices of these experimental variables can be made given reliable estimates of (1) the wavevector and frequency content of the acoustic field to be measured and (2) the material resources available for the measurement.

8.5 REFERENCES

1. M. S. Uberoi and L. S. G. Kovasznay, "On Mapping and Measurement of Random Fields," Quarterly of Applied Mathematics, vol. 10, no. 4, 1953, pp. 375-393.

2. W. A. Strawderman, "Effects of Non-Instantaneous Transducer Response on the Measurement of Turbulent Pressures," Journal of the Acoustical Society of America, vol. 46, no. 5, November 1969, pp. 1289-1293.

3. R. B. Gilchrist and W. A. Strawderman, "Experimental Hydrophone Size Correction for Boundary-Layer Pressure Fluctuations," Journal of the Acoustical Society of America, vol. 38, no. 2, August 1965, pp. 298-302.

4. J. M. Powers, "A Piezoelectric Polymer Evanescent Wave Generator," Journal of the Acoustical Society of America, suppl. 1, vol. 68, 1980, p. S67.

5. R. J. Bobber, Underwater Electroacoustic Measurements, Naval Research Laboratory, Underwater Sound Reference Division, Orlando, Florida, 1970, p. 64.

6. R. V. Churchill, Fourier Series and Boundary Value Problems, McGraw-Hill Book Co., New York, 1941, pp. 62-63.

7. L. R. Rabiner and R. W. Schafer, Digital Processing of Speech Signals, Prentice Hall, Englewood Cliffs, NJ, 1978, pp. 25-26.

8. J. S. Bendat and A. G. Piersol, Measurement and Analysis of Random Data, John Wiley and Sons, Inc., New York, 1966, p. 279.

CHAPTER 9

ESTIMATION OF WAVEVECTOR-FREQUENCY SPECTRA

In chapter 8, we established that measurements of acoustic fields can be obtained only over finite limits in space, time, and possible realizations of the field of interest. We further established that measurements of acoustic fields are normally made with sensors that convert the local acoustic field variable to an electrical variable. Consequently, the data obtained from the measurement of any acoustic field usually consist of some sampling of the sensor output field over limited ranges of space, time, and possible realizations.

By definition, specification of the wavevector-frequency transform of a deterministic field requires knowledge of that field over all space and time; specification of the wavevector-frequency spectrum of a random field requires knowledge of that field over all space and time for all possible realizations of the field. Clearly, data obtained from practicable measurements of any acoustic field of interest are insufficient to determine the true wavevector-frequency transform or spectrum of that field. Therefore, as we argued in chapter 8, any set of measured data can yield only an approximation to the wavevector-frequency descriptor appropriate to the field of interest. The quality of that estimate depends on the specific limitations imposed on the experiment.

The use of sensors and limitations on spatial and temporal sampling are problems common to measurements of deterministic and random fields. The consequences of these common problems on the quality of the estimates of wavevector-frequency descriptors of deterministic and random acoustic fields were treated in the previous chapter.

The limited number of replications of apparatus or trials affordable in any practicable experiment is a problem specific to the measurement of random fields. Recall, from chapter 6, that statistical metrics of random space-time

fields are defined in terms of average values over all possible realizations of that field. Given that we can afford only a limited number of trials or replications of any experiment, it is evident that we cannot observe all possible outcomes of any random space-time field. Therefore, measurements of any random space-time field can produce only an estimate of the desired statistics of that field.

This chapter addresses the estimation of the wavevector-frequency spectra of stationary random space-time fields from measured data, and examines the effects of measurement decisions on the quality of the resulting estimate.

9.1 PERSPECTIVE

Consider an experiment designed to characterize the statistics of the stationary random acoustic field $p(\underline{x},t)$. Owing to practical limitations, the data resulting from even the most carefully designed experiment will comprise some finite number of realizations of sample functions, over finite limits of time and space, of the output field, $o(\underline{x},t)$, of the (identical) sensors used to measure the field. The consequences of the use of sensors, and of finite space and time limitations, on our ability to estimate the wavevector-frequency spectrum of $p(\underline{x},t)$ were examined in the previous chapter. We now wish to examine the consequences of limited trials or replications of the experiment on the quality of our estimate of the statistics of $p(\underline{x},t)$.

To conduct this examination, we must first define

(1) the statistical metric we wish to estimate,

(2) the specific mathematical procedure to be used to produce the desired estimate from the measured data, and

(3) the measure of the quality of the estimate.

In keeping with the focus of this text, we define the desired statistical metric to be the wavevector-frequency spectrum appropriate to the statistical nature of the acoustic field, $p(\underline{x},t)$. However, inasmuch as the experimental

data only provide samples of the output field, $o(\underline{x},t)$, from the sensors employed in the measurement, we can directly estimate only the wavevector-frequency spectrum appropriate to the sensor output field. Given this estimate of the wavevector-frequency spectrum of the sensor output field and knowledge of the wavevector-frequency response of the (presumed identical) sensors employed in the measurement, the desired estimate of the wavevector-frequency spectrum of the acoustic field can then be obtained by use of equation (8-14) or (8-15).

Recall that an estimate of the wavevector-frequency spectrum of a random space-time field is defined as some approximation to the true spectrum of that field. We now define an estimator of the wavevector-frequency spectrum to be a specific mathematical procedure for obtaining such an approximation to the true spectrum from some given set of data. To develop an estimator of the wavevector-frequency spectrum of a stationary random space-time field, we require knowledge of (1) the format of the measured data, (2) the homogeneity of the field of interest, and (3) the specific form of wavevector-frequency spectrum to be estimated.

Several experiments designed to investigate the wavevector-frequency characteristics of pressure fluctuations in a turbulent boundary layer have been conducted since Maidanik and Jorgensen[1] proposed their direct measurement technique in 1967. However, these experiments employed a variety of types and configurations of sensors and produced measured data in a variety of formats. Consequently, these experiments produced a variety of estimators of the wavevector-frequency spectrum of the (presumed) stationary and homogeneous turbulent pressure field. In contrast, only one estimator[2] of the two wavevector-frequency spectrum of a stationary, nonhomogeneous field has been described in the open literature as of this writing.

Clearly, no single estimator of the wavevector-frequency spectrum can accommodate all random fields, experimental designs, and formats of measured data. Therefore, in practice, we are faced with two alternatives; we either develop an estimator to suit each design of experiment and field of interest or we design the experiment to be compatible with an existing estimator appropriate to the field of interest. In the next section, we address the

development of estimators of wavevector-frequency spectra of homogeneous and nonhomogeneous, stationary fields suitable to measured data in the format of limited numbers of realizations of discrete spatial and temporal samples of the sensor output field over limited regions of space and time.

The quality of estimates of statistical descriptors of random temporal fields has been addressed by signal processing specialists. To define metrics of the quality of estimates of wavevector-frequency spectra of stationary random space-time fields, we apply arguments similar to those advanced by Bendat and Piersol[3] for quantifying errors in estimates of statistical descriptors of random temporal fields.

Assume that an experiment designed to measure a stationary random acoustic field $p(\underline{x},t)$ produces N independent realizations of the stationary random sensor output field, $o(\underline{x},t)$, over some finite limits of space and time. Let Γ_0 denote the true value of the wavevector-frequency spectrum appropriate to the sensor output field at some particular wavevector(s) and frequency of interest, and let $\tilde{\Gamma}_0$ denote some estimate of this spectral value formed from the measured data. That is, for a homogeneous field, Γ_0 represents $\Phi_0(\underline{k}_0,\omega_0)$ and $\tilde{\Gamma}_0$ represents $\tilde{\Phi}_0(\underline{k}_0,\omega_0)$. For a nonhomogeneous field, Γ_0 denotes either $S_{00}(\underline{\mu}_0,\underline{k}_0,\omega_0)$ or $\Phi_0^a(\underline{k}_0,\omega_0)$, and $\tilde{\Gamma}_0$ represents their respective estimates: that is, $\tilde{S}_{00}(\underline{\mu},\underline{k},\omega)$ or $\tilde{\Phi}_0^a(\underline{k},\omega)$. Here, $\underline{\mu}_0$, $\underline{k}_0$, and ω_0 represent the (fixed) wavevectors and frequency of interest. Given that the measured data comprise only N sample functions of $o(\underline{x},t)$ over finite limits of space and time, it is evident that these measured data represent some subset of the ensemble of all possible sample functions of $o(\underline{x},t)$ over those limits of space and time. Inasmuch as it is highly improbable that any subsequent repetition of this experiment would produce the identical N sample functions of $o(\underline{x},t)$, the estimate of the wavevector-frequency spectrum of the output field, $\tilde{\Gamma}_0$, will vary randomly from experiment to experiment. Consequently, for any fixed values of $\underline{\mu}_0$, $\underline{k}_0$, and ω_0, the estimate of the value of the wavevector-frequency spectrum, $\tilde{\Gamma}_0$, is a random variable. Therefore, the question of whether $\tilde{\Gamma}_0$ provides a good estimate of Γ_0 can be addressed only from a statistical viewpoint.

Clearly, it is desirable that, if the experiment were repeated many times,

the mean value of the resultant spectral estimates would approach the true value of the wavevector-frequency spectrum at the wavevector(s) and frequency of interest. Thus, if J represents the number of independent estimates of Γ_0, we desire that

$$\lim_{J\to\infty} E\{\tilde{\Gamma}_0\} = \Gamma_0 \ . \tag{9-1}$$

An estimate that satisfies equation (9-1) is said to be unbiased. If $E\{\tilde{\Gamma}_0\}$ does not satisfy equation (9-1), then the estimate is said to be biased. We define the bias error, $B\{\tilde{\Gamma}_0\}$, to be

$$B\{\tilde{\Gamma}_0\} = E\{\tilde{\Gamma}_0\} - \Gamma_0 = E\{\tilde{\Gamma}_0\} - E\{\Gamma_0\} = E\{\tilde{\Gamma}_0 - \Gamma_0\} \ . \tag{9-2}$$

Here we have used the facts that (1) the true wavevector-frequency spectrum at any fixed wavevector(s) and frequency is a constant, (2) the mean value of a constant is equal to that constant, and (3) the sum of the means is equal to the mean of the sum. Note, from equation (9-2), that the bias error is simply the mean value of the difference between the estimated and true values of the wavevector-frequency spectrum. It should be recognized that, when $\tilde{\Gamma}_0$ and Γ_0 represent the estimated and true values of the two wavevector-frequency spectrum, $B\{\tilde{\Gamma}_0\}$ is a complex quantity.

Bendat and Piersol[4] point out that, inasmuch as the bias of an estimate addresses the average properties of all possible realizations of that estimate, the fact that $\tilde{\Gamma}_0$ provides an unbiased estimate of Γ_0 does not imply that the value of $\tilde{\Gamma}_0$ resulting from any particular realization of the experiment will be equal, or even close in value, to the true value, Γ_0. Therefore, it appears desirable, given an ensemble of (possibly complex) values of $\tilde{\Gamma}_0$ from many repetitions of the experiment, that the mean value of the squared magnitude of the difference between the estimated and the true values of the spectrum approach zero as the number of repetitions of the experiment increases. That is, we desire that the mean square error (MSE), defined by

$$MSE = E\{|\tilde{\Gamma}_0 - \Gamma_0|^2\} \ , \tag{9-3}$$

approach zero as the number (say J) of independent estimates of Γ_0 becomes large. An estimate having this property is said to be consistent. Mathematically stated, a spectral estimate is said to be consistent if

$$\lim_{J\to\infty} E\{|\tilde{\Gamma}_0 - \Gamma_0|^2\} = 0 \ . \tag{9-4}$$

Note that, by adding and subtracting the mean of $\tilde{\Gamma}_0$, we can write

$$\tilde{\Gamma}_0 - \Gamma_0 = (\tilde{\Gamma}_0 - E\{\tilde{\Gamma}_0\}) + (E\{\tilde{\Gamma}_0\} - \Gamma_0) \ . \tag{9-5}$$

Thus, the mean square error can be expressed as

$$\begin{aligned} MSE &= E\{|(\tilde{\Gamma}_0 - E\{\tilde{\Gamma}_0\}) + (E\{\tilde{\Gamma}_0\} - \Gamma_0)|^2\} \\ &= E\{|\tilde{\Gamma}_0 - E\{\tilde{\Gamma}_0\}|^2\} + E\{|E\{\tilde{\Gamma}_0\} - \Gamma_0|^2\} \\ &\quad + 2E\{Re(\tilde{\Gamma}_0 - E\{\tilde{\Gamma}_0\})Re(E\{\tilde{\Gamma}_0\} - \Gamma_0)\} + 2E\{Im(\tilde{\Gamma}_0 - E\{\tilde{\Gamma}_0\})Im(E\{\tilde{\Gamma}_0\} - \Gamma_0)\} \ . \end{aligned} \tag{9-6}$$

According to Papoulis,[5] the first term on the right-hand side is the variance of the generally complex random variable $\tilde{\Gamma}_0$. By the recognition that $E\{\tilde{\Gamma}_0\}$ and Γ_0 are constants, the second term on the right-hand side of equation (9-6) can be identified (from equation (9-2)) as the squared magnitude of the bias error, and the last two terms can be shown to be identically zero. Thus, if we denote the variance of $\tilde{\Gamma}_0$ by $Var\{\tilde{\Gamma}_0\}$, it follows that

$$MSE = Var\{\tilde{\Gamma}_0\} + |B\{\tilde{\Gamma}_0\}|^2. \tag{9-7}$$

The bias error and the mean square error provide the desired metrics for assessing the quality of estimates of the wavevector-frequency spectrum at any desired wavevector(s) and frequency. Given several alternative procedures for estimating the wavevector-frequency spectral density, it follows from equations (9-2) and (9-7) that the best estimate will result from the procedure that, for increasing numbers of independent observations, tends toward the smallest bias error and variance. By the definition of equation (9-7), this ideal spectral estimate is one that is consistent.

9.2 ESTIMATORS AND THEIR DEVELOPMENT

Assume that we wish to estimate the wavevector-frequency spectrum of a sensor output field from some given set of measured data. Obviously, we desire to employ the estimator that produces the best possible approximation to the desired true wavevector-frequency spectrum at each wavevector and frequency of interest. By the arguments presented in the previous section, the best estimator is one that accommodates the format of the measured data and produces a consistent estimate of the desired spectrum. Clearly then, a logical first step in our selection of an estimator is to determine whether any estimators of the desired wavevector-frequency spectrum exist that can accommodate the format of the measured data.

If such estimators exist, we must then assess the bias and mean square errors associated with each candidate estimator. If an existing estimator can be shown to produce a consistent estimate of the desired spectrum from the available measured data, that estimator is, by definition, the best choice. Otherwise, the choice is limited to those candidates that exhibit acceptable combinations of bias and mean square errors.

If, on the other hand, no existing estimator can approximate the desired true spectrum from the measured data, or if the bias or mean square errors associated with existing estimators are unacceptably large, we are then faced with the prospect of formulating a suitable estimator for the desired spectrum. This prospect presents two major problems. The first of these is that there is no "best" procedure for formulating an estimator; an estimator founded on a serendipitous guess can be as good or better than one founded on deductive or inductive reasoning. The second problem is that an estimator cannot be formulated to meet prespecified bias and mean square errors. Rather, an estimator of the desired spectrum is first formulated, and the bias and mean square errors associated with that estimator are evaluated subsequently.

As stated previously, a variety of estimators of the wavevector-frequency spectrum of stationary, homogeneous fields were developed for experiments designed to study the wavevector-frequency characteristics of turbulent

pressure fields.[1,6,7,8,9] However, the majority of these estimators were formulated to accommodate a data format specific to a single experiment, and any attention to quality was limited to the bias of the spectral estimates.

In 1977, Dynatron Corporation of Waltham, Massachusetts, developed the first general purpose wavevector-frequency analysis system. This hybrid analog and digital system[10] produced estimates of wavevector-frequency spectra of stationary and homogeneous space-time fields from the continuous time outputs from sensors of a two-dimensional array. The hybrid design was driven by cost considerations; an all digital system required either high computational power or large bulk memory, both of which were expensive in 1977. The estimator of the wavevector-frequency spectrum employed in this system was specific to the hybrid design. If the bias or mean square errors of this estimator were investigated, they were not published.

The Dynatron system demonstrated the feasibility of a general purpose system for wavevector-frequency spectral estimation. However, since 1977, the computational power, data transfer rates, and storage capabilities of digital computers have increased substantially while computer costs (relative to performance) have decreased. These advances make completely digital systems an affordable option for general purpose wavevector-frequency analysis of stationary random space-time fields. In recognition of this option, estimators of the wavevector-frequency spectra of both homogeneous[11] and nonhomogeneous,[12] stationary fields have been developed that accommodate measured data in the format of some finite number of realizations of discrete, uniform spatial and temporal sample functions of the sensor output field. The remainder of this chapter describes the development of these estimators and explores the quality of the resultant approximations to the true spectra.

The motivation for such a detailed examination of these estimators is twofold. The first is to illustrate one deductive process for formulating estimators. The second is to detail the development of estimators of the wavevector-frequency spectra of both homogeneous and nonhomogeneous, stationary fields that are suitable for general purpose implementation on modern computer systems.

9.2.1 Foundation for the Estimator

We know that any practical measurement of a space-time field can produce only a limited number of independent sample functions of the output field of the sensors used for the measurement over some finite limits of space and time. Let us start by considering the extreme case in which the data available from the measurement of a stationary random space-time field consist of a single sample function, say $o_\alpha(\underline{x},t)$, of the sensor output field. Because our primary concern in this chapter is the effect of limited numbers of independent realizations on the quality of the estimate of the wavevector-frequency spectrum, we will assume, initially, that this measured sample function of the output field defines $o_\alpha(\underline{x},t)$ continuously over the space $x_{01} - L_1/2 \le x_1 \le x_{01} + L_1/2$ and $x_{02} - L_2/2 \le x_2 \le x_{02} + L_2/2$, and over the time $t_0 - T_0/2 \le t \le t_0 + T_0/2$. We wish to formulate an estimate of the wavevector-frequency spectrum of the sensor output field from this space- and time-limited portion of a single sample function.

We know from chapter 6 that the wavevector-frequency spectrum of a random space-time field is defined as the multiple Fourier transform of the autocorrelation function of that field on all spatial and temporal variables. We know further that the autocorrelation function of the stationary random sensor output field is the mean of the product $o(\underline{x},t)o(\underline{x} + \underline{\xi},t + \tau)$ over all possible realizations of that field. However, we have knowledge only of a single realization, $o_\alpha(\underline{x},t)$, and that knowledge is restricted in both space and time. Consequently, the product $o_\alpha(\underline{x},t)o_\alpha(\underline{x} + \underline{\xi},t + \tau)$ is undefined over the spatial regions $|x_1 - x_{01}| > L_1/2$ and $|x_2 - x_{02}| > L_2/2$, $|\xi_1| > L_1$ and $|\xi_2| > L_2$, and over the temporal regions $|t - t_0| > T_0/2$ and $|\tau| > T_0$.

If we wish to estimate the wavevector-frequency spectrum by Fourier transformation of an estimate of the autocorrelation function, that estimate of the autocorrelation function must be defined over infinite ranges of all spatial and temporal variables. Let us therefore define a function over all space and time that incorporates our limited knowledge of $o_\alpha(\underline{x},t)$. That is, let

$$\epsilon_\alpha(\underline{x},t) = a(t - t_0)b(\underline{x} - \underline{x}_0)o_\alpha(\underline{x},t) \; , \qquad (9\text{-}8)$$

where

$$a(t) = \begin{cases} 1, & -T_0/2 \le t \le T_0/2 \, , \\ 0, & \text{otherwise}, \end{cases} \tag{9-9}$$

and

$$b(\underline{x}) = \begin{cases} 1, & -L_1/2 \le x_1 \le L_1/2 \text{ and } -L_2/2 \le x_2 \le L_2/2 \, , \\ 0, & \text{otherwise}. \end{cases} \tag{9-10}$$

Note from equations (9-8) through (9-10) that the sample function $\epsilon_\alpha(\underline{x},t)$, defined over all space and time, is equal to the sample function $o_\alpha(\underline{x},t)$ within the spatial and temporal limits of the measurement, and is zero elsewhere. Consequently, the product $\epsilon_\alpha(\underline{x},t)\epsilon_\alpha(\underline{x} + \underline{\xi},t + \tau)$ is defined over all $\underline{x}$, $\underline{\xi}$, t, and τ, and is equal to the function $o_\alpha(\underline{x},t)o_\alpha(\underline{x} + \underline{\xi},t + \tau)$ within the ranges of spatial variables specified by $|x_1 - x_{01}| \le L_1/2$, $|x_2 - x_{02}| \le L_2/2$, $|x_1 + \epsilon_1 - x_{01}| \le L_1/2$, and $|x_2 + \epsilon_2 - x_{02}| \le L_2/2$, and within the temporal ranges $|t - t_0| \le T_0/2$ and $|t + \tau - t_0| \le T_0/2$. However, inasmuch as we are given only the single sample function $o_\alpha(\underline{x},t)$, we have knowledge of only a single sample of the function $\epsilon_\alpha(\underline{x},t)\epsilon_\alpha(\underline{x} + \underline{\xi},t + \tau)$. Given that statistical metrics are defined in terms of averages over the ensemble of all possible outcomes, we are faced with the problem of estimating the autocorrelation function of $o(\underline{x},t)$ from the single member function, $\epsilon_\alpha(\underline{x},t)\epsilon_\alpha(\underline{x} + \underline{\xi},t + \tau)$, of such an ensemble.

Recall, from chapter 6, that the autocorrelation function of a stationary, nonhomogeneous random process is a function of the absolute spatial variable $\underline{x}$, the spatial separation vector $\underline{\xi}$, and the time difference τ, but is independent of the absolute temporal variable, t. The single available sample of the function $\epsilon_\alpha(\underline{x},t)\epsilon_\alpha(\underline{x} + \underline{\xi},t + \tau)$, on the other hand, is an explicit function of t (as well as $\underline{x}$, $\underline{\xi}$, and τ). We exploit this absolute time dependence of $\epsilon_\alpha(\underline{x},t)\epsilon_\alpha(\underline{x} + \underline{\xi},t + \tau)$ to formulate an estimate of the autocorrelation function of the sensor output field. That is, we note that the average of $\epsilon_\alpha(\underline{x},t)\epsilon_\alpha(\underline{x} + \underline{\xi},t + \tau)$ over some appropriate interval of absolute time is a function only of $\underline{x}$, $\underline{\xi}$, and τ, and provides some estimate of the

average properties of the function $\varepsilon(\underline{x},t)\varepsilon(\underline{x} + \underline{\xi},t + \tau)$ over the entire range of these variables. These are precisely the properties we desire for an estimator of the autocorrelation function of the stationary, nonhomogeneous sensor output field. Thus, to approximate the autocorrelation function of a stationary, nonhomogeneous sensor output field, we choose an estimator of the form

$$\tilde{Q}_{00}(\underline{x},\underline{\xi},\tau) = \frac{1}{T_B - T_A} \int_{T_A}^{T_B} \varepsilon_\alpha(\underline{x},t)\varepsilon_\alpha(\underline{x} + \underline{\xi},t + \tau)\, dt \, . \tag{9-11}$$

Here, $\tilde{Q}_{00}(\underline{x},\underline{\xi},\tau)$ denotes the estimator for the autocorrelation function of the sensor output field, and T_A and T_B denote the lower and upper limits, respectively, for the averaging over absolute time. It remains to determine the appropriate values of T_A and T_B.

Note, from equations (9-8) and (9-9), that the function $\varepsilon_\alpha(\underline{x},t)\varepsilon_\alpha(\underline{x} + \underline{\xi},t + \tau)$ is identically zero where either $a(t - t_0)$ or $a(t + \tau - t_0)$ is zero. By equation (9-9), $a(t - t_0)$ is zero for $|t - t_0| > T_0/2$, and $a(t + \tau - t_0)$ is zero for $|t + \tau - t_0| > T_0/2$. One obvious option is to average the function $\varepsilon_\alpha(\underline{x},t)\varepsilon_\alpha(\underline{x} + \underline{\xi},t + \tau)$ over that range of t where that product is nonzero, which is equivalent to the range of t over which the product $a(t - t_0)a(t + \tau - t_0)$ is nonzero. The nonzero range of $a(t - t_0)a(t + \tau - t_0)$ is depicted in figure 9-1. Here we see that the range of t over which the product $a(t - t_0)a(t + \tau - t_0)$ is nonzero varies with the choice of the time delay, τ. Thus, if we choose to average the function $\varepsilon_\alpha(\underline{x},t)\varepsilon_\alpha(\underline{x} + \underline{\xi},t + \tau)$ over its range of nonzero values for each value of τ, the limits T_A and T_B are

$$T_A = \begin{cases} t_0 - T_0/2 \, , & \tau \geq 0 \, , \\ t_0 - \tau - T_0/2 \, , & \tau < 0 \, , \end{cases} \tag{9-12}$$

and

$$T_B = \begin{cases} t_0 - \tau + T_0/2 \, , & \tau \geq 0 \, , \\ t_0 + T_0/2 \, , & \tau < 0 \, . \end{cases} \tag{9-13}$$

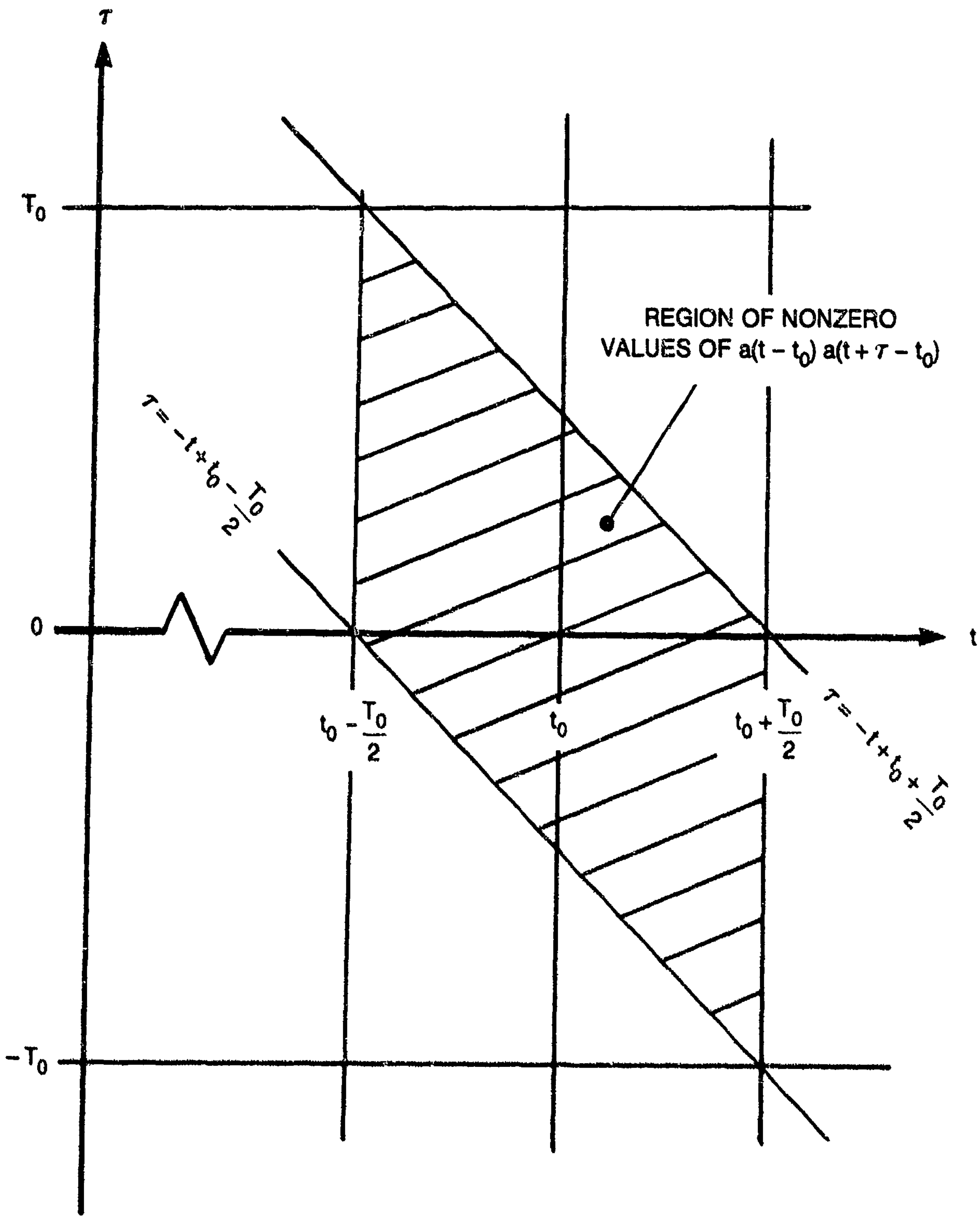

Figure 9-1. Nonzero Region of $a(t - t_0)a(t + \tau - t_0)$

In this case,

$$T_B - T_A = T_0 - |\tau| \ . \tag{9-14}$$

An alternative option is to select

$$T_A = t_0 - T_0/2 \tag{9-15}$$

and

$$T_B = t_0 + T_0/2 \tag{9-16}$$

so that

$$T_B - T_A = T_0 \ . \tag{9-17}$$

Whether the limits are chosen to be those in equations (9-12) and (9-13) or those in (9-15) and (9-16), the only nonzero contributions to the integral of the function $\epsilon_\alpha(\underline{x},t)\epsilon_\alpha(\underline{x} + \underline{\xi},t + \tau)$ over t will be those within the nonzero range of the product $a(t - t_0)a(t + \tau - t_0)$. That nonzero range is specified by the limits in equations (9-12) and (9-13). However, for the choice of limits specified by equations (9-12) and (9-13), the average is formed by dividing the resulting integral by $T_0 - |\tau|$, whereas for the choice specified by equations (9-15) and (9-16), the integral is divided by T_0.

We intend to form an estimator of the two wavevector-frequency spectrum by Fourier transforming the estimate of the autocorrelation function of the stationary, nonhomogeneous sensor output field on the variables $\underline{x}$, $\underline{\xi}$, and τ. The temporal Fourier transform (on τ) is anticipated to be less complicated if we choose $T_B - T_A$ to be T_0 rather than $T_0 - |\tau|$. For that reason, we choose the limits specified by equations (9-15) and (9-16). By this choice, our estimate of the autocorrelation function of the stationary, nonhomogeneous sensor output field can be written in the form

$$\tilde{Q}_{00}(\underline{x},\underline{\xi},\tau) = \frac{1}{T_0} \int_{-\infty}^{\infty} \epsilon_\alpha(\underline{x},t)\epsilon_\alpha(\underline{x} + \underline{\xi},t + \tau)\, dt \ . \tag{9-18}$$

Here, we can use infinite limits on the integral over absolute time because the product $\epsilon_\alpha(\underline{x},t)\epsilon_\alpha(\underline{x} + \underline{\xi},t + \tau)$ is zero outside the temporal limits specified by equations (9-12) and (9-13).

Before proceeding to Fourier transform equation (9-18) in order to obtain an estimate of the two wavevector-frequency spectrum, let us consider how the above described estimation procedure must be modified if the sensor output field is known to be stationary, but homogeneous, rather than nonhomogeneous. Recall from chapter 6 that the average properties of a stationary, homogeneous field, over all possible realizations of that field, are independent of the absolute spatial and temporal variables, $\underline{x}$ and t, and depend only on the spatial and temporal separation variables, $\underline{\xi}$ and τ. However, the value of the function $\epsilon_\alpha(\underline{x},t)\epsilon_\alpha(\underline{x} + \underline{\xi},t + \tau)$ formed from a space- and time-limited portion of a single sample function of the sensor output field, $o(\underline{x},t)$, is likely to vary with both the absolute spatial and temporal variables. We desire that our estimate of the autocorrelation function of the stationary, homogeneous sensor output field be a function of only $\underline{\xi}$ and τ, and reflect some average properties of $\epsilon_\alpha(\underline{x},t)\epsilon_\alpha(\underline{x} + \underline{\xi},t + \tau)$. Both these objectives can be realized if we formulate our estimate of the autocorrelation of the stationary and homogeneous sensor output field as an average of the function $\epsilon_\alpha(\underline{x},t)\epsilon_\alpha(\underline{x} + \underline{\xi},t + \tau)$ over some appropriate ranges of the absolute spatial and temporal variables. Inasmuch as space and time are independent variables, the choice of an appropriate average over absolute time does not affect the selection of an appropriate average over absolute space, and vice-versa. Consequently, the average over absolute time selected for the nonhomogeneous field is also appropriate for the estimate of the autocorrelation function of the homogeneous field. On the basis of these arguments, we formulate the estimate of the autocorrelation function of the stationary, homogeneous sensor output field by

$$\tilde{Q}_{oo}(\underline{\xi},\tau) = \frac{1}{T_0(X_{1B} - X_{1A})(X_{2B} - X_{2A})}$$

$$\int_{-\infty}^{\infty} \int_{X_{1A}}^{X_{1B}} \int_{X_{2A}}^{X_{2B}} \epsilon_\alpha(\underline{x},t)\epsilon_\alpha(\underline{x} + \underline{\xi},t + \tau)\, dx_1\, dx_2\, dt \ . \qquad (9\text{-}19)$$

Here, $\tilde{Q}_{00}(\underline{\xi},\tau)$ denotes the estimate of the autocorrelation function of the stationary and homogeneous sensor output field, X_{1A} and X_{1B} denote the lower and upper limits of the average over x_1, and X_{2A} and X_{2B} denote the lower and upper limits of the average over x_2. It remains to specify appropriate values of X_{1A}, X_{1B}, X_{2A}, and X_{2B}.

From equations (9-8) and (9-10), it is evident that the function $\epsilon_\alpha(\underline{x},t)\epsilon_\alpha(\underline{x} + \underline{\xi},t + \tau)$ is nonzero only over that region of space where the product $b(\underline{x} - \underline{x}_0)b(\underline{x} + \underline{\xi} - \underline{x}_0)$ is nonzero. From equation (9-10), the nonzero range of $b(\underline{x} - \underline{x}_0)b(\underline{x} + \underline{\xi} - \underline{x}_0)$ is defined by $|x_1 - x_{01}| \le L_1/2$, $|x_2 - x_{02}| \le L_2/2$, $|x_1 + \xi_1 - x_{01}| \le L_1/2$, and $|x_2 + \xi_2 - x_{02}| \le L_2/2$. The nonzero range of $b(\underline{x} - \underline{x}_0)b(\underline{x} + \underline{\xi} - \underline{x}_0)$ in the variables x_1 and ξ_1 is illustrated in figure 9-2; the nonzero range in the variables x_2 and ξ_2 is geometrically similar. If we choose to spatially average the function $\epsilon_\alpha(\underline{x},t)\epsilon_\alpha(\underline{x} + \underline{\xi},t + \tau)$ over its range of nonzero values, the spatial limits X_{1A}, X_{1B}, X_{2A}, and X_{2B} are given by

$$X_{1A} = \begin{cases} x_{01} - L_1/2 \,, & \xi_1 \ge 0 \,, \\ x_{01} - \xi_1 - L_1/2 \,, & \xi_1 < 0 \,, \end{cases} \tag{9-20}$$

$$X_{1B} = \begin{cases} x_{01} - \xi_1 + L_1/2 \,, & \xi_1 \ge 0 \,, \\ x_{01} + L_1/2 \,, & \xi_1 < 0 \,, \end{cases} \tag{9-21}$$

$$X_{2A} = \begin{cases} x_{02} - L_2/2 \,, & \xi_2 \ge 0 \,, \\ x_{02} - \xi_2 - L_2/2 \,, & \xi_2 < 0 \,, \end{cases} \tag{9-22}$$

$$X_{2B} = \begin{cases} x_{02} - \xi_2 + L_2/2 \,, & \xi_2 \ge 0 \,, \\ x_{02} + L_2/2 \,, & \xi_2 < 0 \,, \end{cases} \tag{9-23}$$

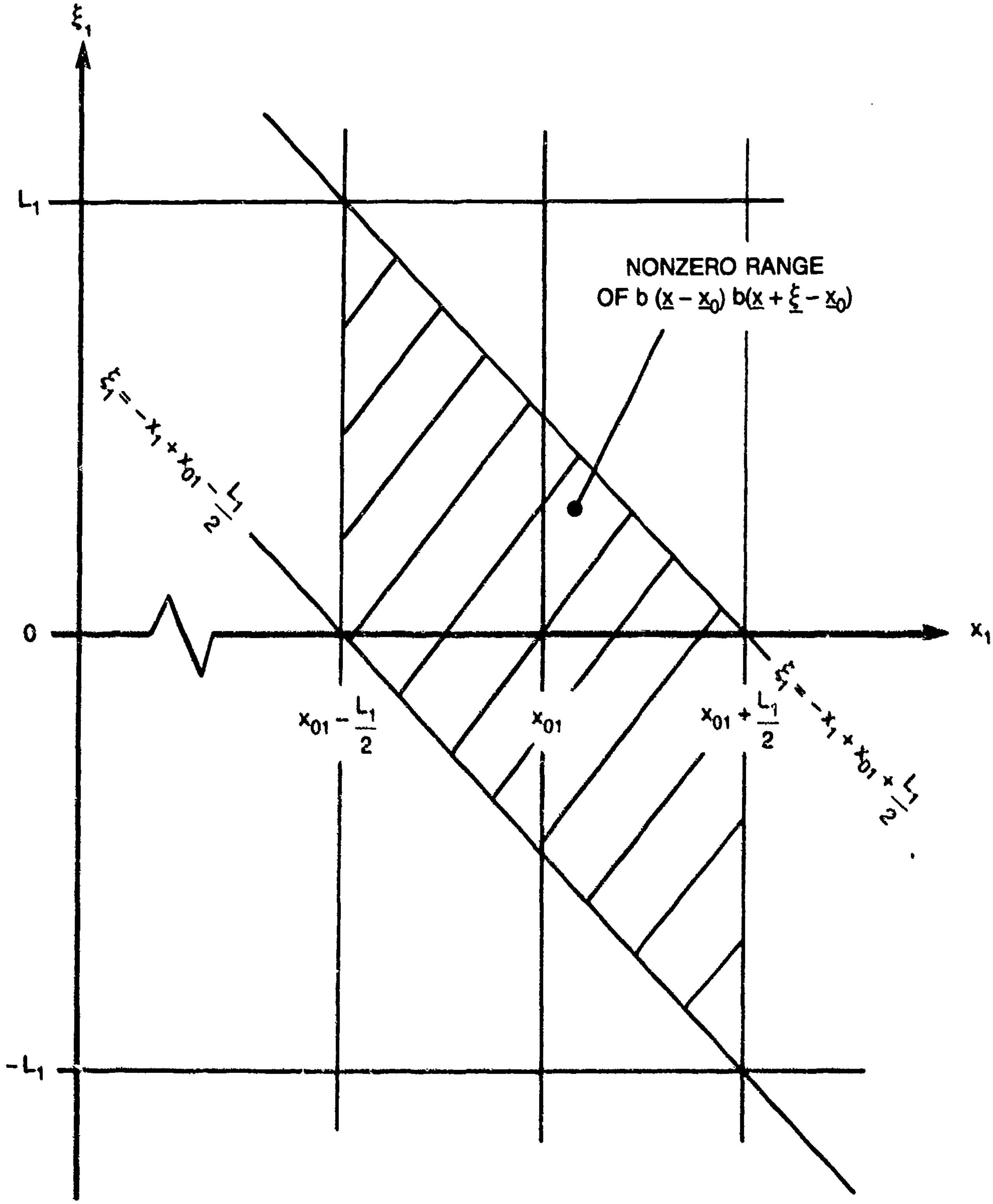

Figure 9-2. Nonzero Range of $b(\underline{x} - \underline{x}_0)b(\underline{x} + \underline{\xi} - \underline{x}_0)$ as a Function of x_1 and ξ_1

so

$$X_{1B} - X_{1A} = L_1 - |\xi_1| \tag{9-24}$$

and

$$X_{2B} - X_{2A} = L_2 - |\xi_2| \; . \tag{9-25}$$

Note here that, because the limits of integration in x_1 and x_2 depend on ξ_1 and ξ_2, the averaging area is also a function of these spatial separations.

An alternative choice of spatial limits is

$$X_{1A} = -L_1/2 \; , \tag{9-26}$$

$$X_{1B} = L_1/2 \; , \tag{9-27}$$

$$X_{2A} = -L_2/2 \; , \tag{9-28}$$

$$X_{2B} = L_2/2 \; , \tag{9-29}$$

so that

$$X_{1B} - X_{1A} = L_1 \tag{9-30}$$

and

$$X_{2B} - X_{2A} = L_2 \; . \tag{9-31}$$

Either choice of limits produces an identical value of the integral in equation (9-19) inasmuch as all nonzero contributions to the integral are confined within the limits specified by equations (9-20) to (9-23). For the limits of equations (9-20) to (9-23), the estimate of the autocorrelation function is obtained by dividing this integral by the product $(L_1 - |\xi_1|)(L_2 - |\xi_2|)$; for the alternative limits of equations (9-26) to (9-29), the estimate is obtained by dividing the integral by L_1L_2. We intend to estimate the wavevector-frequency spectrum of the stationary, homogeneous sensor output field by Fourier transforming the estimate of the autocorrelation function of this field on the variables $\underline{\xi}$ and τ. We

anticipate that this Fourier transformation will be a simpler mathematical exercise if we choose the alternative limits specified by equations (9-26) through (9-29). Consequently, by use of equations (9-26) through (9-31) in equation (9-19), we estimate the autocorrelation function of the stationary, homogeneous sensor output field by

$$\tilde{Q}_{00}(\underline{\xi},\tau) = \frac{1}{T_0 L_1 L_2} \int_{-\infty}^{\infty} \int_{-\infty}^{\infty} \int_{-\infty}^{\infty} \varepsilon_{\alpha}(\underline{x},t)\varepsilon_{\alpha}(\underline{x} + \underline{\xi},t + \tau)\, dx_1\, dx_2\, dt \ . \qquad (9\text{-}32)$$

Here, we can use infinite limits on the integrals over x_1 and x_2 because $\varepsilon_{\alpha}(\underline{x},t)\varepsilon_{\alpha}(\underline{x} + \underline{\xi},t + \tau)$ is identically zero outside the spatial limits specified by equations (9-20) through (9-23).

We should note that the space-averaged autocorrelation function, $Q_{00}^{a}(\underline{\xi},\tau)$, of a stationary, nonhomogeneous sensor output field is defined (see chapter 6) as the average of the stationary, nonhomogeneous autocorrelation function, $Q_{00}(\underline{x},\underline{\xi},\tau)$, over all absolute space, $\underline{x}$. We therefore estimate the space-averaged autocorrelation function of the stationary, nonhomogeneous sensor output field in the form of a spatial average of the estimate of the autocorrelation function of the stationary, nonhomogeneous sensor output field given by equation (9-18). That is,

$$\tilde{Q}_{00}^{a}(\underline{\xi},\tau) = \frac{1}{T_0(X_{1B} - X_{1A})(X_{2B} - X_{2A})}$$

$$\int_{-\infty}^{\infty} \int_{X_{2A}}^{X_{2B}} \int_{X_{1A}}^{X_{1B}} \varepsilon_{\alpha}(\underline{x},t)\varepsilon_{\alpha}(\underline{x} + \underline{\xi},t + \tau)\, dx_1\, dx_2\, dt \ . \qquad (9\text{-}33)$$

Here, X_{1A} and X_{1B} are the (as yet undefined) lower and upper limits of integration for the component x_1 of the absolute spatial vector $\underline{x}$, and X_{2A} and X_{2B} are the lower and upper limits of integration for the component x_2 of that absolute spatial vector, $\underline{x}$.

Comparison of equation (9-33) with equation (9-19) reveals that the

estimate of the space-averaged autocorrelation function has the same mathematical form as the estimate of the autocorrelation function of a stationary, homogeneous field. Recall from chapter 6 that the true space-averaged wavevector-frequency spectrum, defined as the Fourier transform of $Q^a_{00}(\underline{\xi},\tau)$ on the variables $\underline{\xi}$ and τ, represents the wavevector-frequency spectrum of the homogeneous constituents of a generally nonhomogeneous, stationary field. Because we will estimate the space-averaged wavevector-frequency spectrum by Fourier transformation of the estimate of the space-averaged autocorrelation function, it is reasonable to select the spatial limits (and thereby the spatial average) in equation (9-33) to be consistent with the limits chosen for the estimate of the autocorrelation function of the homogeneous, stationary field. Those limits are listed in equations (9-26) to (9-29). By applying these limits to equation (9-33), we obtain the following estimate of the space-averaged autocorrelation function of the nonhomogeneous, stationary sensor output field:

$$\tilde{Q}^a_{00}(\underline{\xi},\tau) = \frac{1}{T_0 L_1 L_2} \int_{-\infty}^{\infty} \int_{-\infty}^{\infty} \int_{-\infty}^{\infty} \varepsilon_\alpha(\underline{x},t)\varepsilon_\alpha(\underline{x} + \underline{\xi}, t + \tau)\, dx_1\, dx_2\, dt \ . \qquad (9\text{-}34)$$

Note that this estimate is identical to the estimate of the autocorrelation function of the stationary, homogeneous sensor output field given by equation (9-32).

We estimate the wavevector-frequency spectra of homogeneous and nonhomogeneous, stationary fields by Fourier transforming the estimates of the autocorrelation functions of these fields according to the spectral definitions presented in chapter 6. Thus, by equations (6-121) and (9-18), we estimate the two wavevector-frequency spectrum of the stationary, nonhomogeneous sensor output field by

$$\tilde{S}_{00}(\underline{\mu},\underline{k},\omega) = \frac{1}{T_0} \int_{-\infty}^{\infty} \int_{-\infty}^{\infty} \int_{-\infty}^{\infty} \int_{-\infty}^{\infty} \int_{-\infty}^{\infty} \int_{-\infty}^{\infty} \varepsilon_\alpha(\underline{x},t)\varepsilon_\alpha(\underline{x} + \underline{\xi}, t + \tau)$$

$$\exp[-i(\underline{\mu}\cdot\underline{x} + \underline{k}\cdot\underline{\xi} + \omega\tau)]\, d\underline{x}\, d\underline{\xi}\, d\tau\, dt \ . \qquad (9\text{-}35)$$

Here, $\tilde{S}_{00}(\underline{\mu},\underline{k},\omega)$ denotes the estimate of the two wavevector-frequency spectrum, and $\underline{\mu}$, $\underline{k}$, and ω are the respective Fourier conjugate variables of the spatial vectors $\underline{x}$ and $\underline{\xi}$ and the time delay τ. A simplification in the form of equation (9-35) can be realized by defining $\mathcal{E}_\alpha(\underline{k},\omega)$ to be the wavevector-frequency transform of $\epsilon_\alpha(\underline{k},\omega)$. That is,

$$\mathcal{E}_\alpha(\underline{k},\omega) = \int_{-\infty}^{\infty}\int_{-\infty}^{\infty}\int_{-\infty}^{\infty} \epsilon_\alpha(\underline{x},t)\exp\{-i(\underline{k}\cdot\underline{x} + \omega t)\}\, d\underline{x}\, dt \tag{9-36}$$

and

$$\epsilon_\alpha(\underline{x},t) = \frac{1}{(2\pi)^3}\int_{-\infty}^{\infty}\int_{-\infty}^{\infty}\int_{-\infty}^{\infty} \mathcal{E}_\alpha(\underline{k},\omega)\exp\{i(\underline{k}\cdot\underline{x} + \omega t)\}\, d\underline{k}\, d\omega\ . \tag{9-37}$$

By use of equation (9-37), we can write equation (9-35) in the form

$$\begin{aligned}\tilde{S}_{00}(\underline{\mu},\underline{k},\omega) = \frac{1}{(2\pi)^3 T_0}&\int_{-\infty}^{\infty}\int_{-\infty}^{\infty}\int_{-\infty}^{\infty}\int_{-\infty}^{\infty}\int_{-\infty}^{\infty}\int_{-\infty}^{\infty}\int_{-\infty}^{\infty}\int_{-\infty}^{\infty}\int_{-\infty}^{\infty} \epsilon_\alpha(\underline{x},t)\mathcal{E}_\alpha(\underline{\beta},\Omega)\\ &\exp\{i[\underline{\beta}\cdot(\underline{x} + \underline{\xi}) + \Omega(t + \tau)]\}\exp\{-i(\underline{\mu}\cdot\underline{x} + \underline{k}\cdot\underline{\xi} + \omega\tau)\}\\ &d\underline{x}\, d\underline{\xi}\, d\tau\, dt\, d\underline{\beta}\, d\Omega\ .\end{aligned} \tag{9-38}$$

By employing equations (2-38) and (9-36), we can easily show that

$$\tilde{S}_{00}(\underline{\mu},\underline{k},\omega) = \frac{1}{T_0}\,\mathcal{E}_\alpha(\underline{\mu} - \underline{k},-\omega)\mathcal{E}_\alpha(\underline{k},\omega)\ . \tag{9-39}$$

By equations (9-36) and (9-39), we see that our estimate of the two wavevector-frequency spectrum of a stationary, nonhomogeneous sensor output field is proportional to a product of Fourier transforms of the single space- and time-continuous sample function $\epsilon_\alpha(\underline{x},t)$ on both the spatial and temporal variables.

By reference to equations (6-78) and (6-149), we estimate the wavevector-frequency spectrum of the stationary, homogeneous sensor output field and of

the space-averaged wavevector-frequency spectrum of the stationary, nonhomogeneous sensor output field by Fourier transforming the mathematically identical estimates of the autocorrelation functions specified by equations (9-32) and (9-34) on the variables $\underline{\xi}$ and τ. That is,

$$\tilde{\Phi}_0(\underline{k},\omega) = \tilde{\Phi}^a_0(\underline{k},\omega) = \frac{1}{T_0 L_1 L_2} \int_{-\infty}^{\infty}\int_{-\infty}^{\infty}\int_{-\infty}^{\infty}\int_{-\infty}^{\infty}\int_{-\infty}^{\infty}\int_{-\infty}^{\infty} \epsilon_\alpha(\underline{x},t)\epsilon_\alpha(\underline{x}+\underline{\xi},t+\tau)$$

$$\exp[-i(\underline{k}\cdot\underline{\xi}+\omega\tau)]\, d\underline{x}\, d\underline{\xi}\, d\tau\, dt \ . \qquad (9\text{-}40)$$

By writing $\epsilon_\alpha(\underline{x}+\underline{\xi},t+\tau)$ in the form of equation (9-37), we can then use equations (2-38) and (9-36) to show that

$$\tilde{\Phi}_0(\underline{k},\omega) = \tilde{\Phi}^a_0(\underline{k},\omega) = \frac{1}{T_0 L_1 L_2} \left|\mathcal{E}_\alpha(\underline{k},\omega)\right|^2 \ . \qquad (9\text{-}41)$$

Thus, the estimate of the wavevector-frequency spectrum of the stationary, homogeneous sensor output field and the estimate of the space-averaged wavevector-frequency spectrum of a stationary, nonhomogeneous sensor output field are mathematically identical, and are proportional to the squared magnitude of the Fourier transform of the single space- and time-continuous sample function $\epsilon_\alpha(\underline{x},t)$ on both the spatial and temporal variables.

The estimators of the wavevector-frequency spectra given by equations (9-39) and (9-41) have a very desirable property; they depend only on the wavevector-frequency transform of the (assumed continuous) measured output field over the spatial and temporal extent of the measurement. That is, by equations (9-8), (9-9), (9-10), and (9-36), it is easily demonstrated that

$$\mathcal{E}_\alpha(\underline{k},\omega) = \int_{t_0-T_0/2}^{t_0+T_0/2}\int_{x_{01}-L_1/2}^{x_{01}+L_1/2}\int_{x_{02}-L_2/2}^{x_{02}+L_2/2} o_\alpha(\underline{x},t)\exp[-i(\underline{k}\cdot\underline{x}+\omega t)]\, d\underline{x}\, dt \ . \qquad (9\text{-}42)$$

Consequently, these estimators of the wavevector-frequency spectra from a single continuous, but spatially and temporally limited, sample function of

the sensor output field are computationally simple. Further, for a single, spatially and temporally discrete, but limited, sample function of the output field, the forms of these estimators appear to be suitable to the application of the computationally efficient fast Fourier transform. However, before we adapt the estimators of equations (9-39) and (9-41) to a discrete, rather than continuous, sample function of the sensor output field, we should first examine the quality of these estimators. Let us start with the estimator having the simplest mathematical form: that is, the estimator, $\tilde{\Phi}_0(\underline{k},\omega)$, of the wavevector-frequency spectrum of the homogeneous, stationary sensor output field.

For any fixed values of $\underline{k}$ and ω, we can show (from equations (9-8), (9-9), (9-10), and (9-41)) that the mean value of the estimate $\tilde{\Phi}_0(\underline{k},\omega)$ is given by

$$E\{\tilde{\Phi}_0(\underline{k},\omega)\} = \frac{1}{T_0L_1L_2}\int_{-\infty}^{\infty}\int_{-\infty}^{\infty}\int_{-\infty}^{\infty}\int_{-\infty}^{\infty}\int_{-\infty}^{\infty}\int_{-\infty}^{\infty} a(t - t_0)a(t + \tau - t_0)b(\underline{x} - \underline{x}_0)b(\underline{x} + \underline{\xi} - \underline{x}_0)$$

$$E\{o_\alpha(\underline{x},t)o_\alpha(\underline{x} + \underline{\xi},t + \tau)\}\exp\{-i(\underline{k}\cdot\underline{\xi} + \omega\tau)\}\, d\underline{x}\, d\underline{\xi}\, d\tau\, dt \;. \tag{9-43}$$

Here, we have used the fact that the expectation operator is commutative with linear operations. However, for the homogeneous and stationary sensor output field, it follows from equations (6-65) and (6-79) that

$$E\{o_\alpha(\underline{x},t)o_\alpha(\underline{x} + \underline{\xi},t + \tau)\} = Q_{00}(\underline{\xi},\tau)$$

$$= (2\pi)^{-3}\int_{-\infty}^{\infty}\int_{-\infty}^{\infty}\int_{-\infty}^{\infty} \Phi_0(\underline{k},\omega)\exp\{i(\underline{k}\cdot\underline{\xi} + \omega\tau)\}\, d\underline{k}\, d\omega \;. \tag{9-44}$$

By substituting equation (9-44) into equation (9-43), we can show that

$$E\{\tilde{\Phi}_0(\underline{k},\omega)\} = \frac{1}{(2\pi)^3T_0L_1L_2}\int_{-\infty}^{\infty}\int_{-\infty}^{\infty}\int_{-\infty}^{\infty} \Phi_0(\underline{\beta},\Omega)|A(\omega - \Omega)|^2|B(\underline{k} - \underline{\beta})|^2\, d\underline{\beta}\, d\Omega \;. \tag{9-45}$$

where

$$A(\omega) = \int_{-\infty}^{\infty} a(t)\exp(-i\omega t)\, dt \tag{9-46}$$

and

$$B(\underline{k}) = \int_{-\infty}^{\infty}\int_{-\infty}^{\infty} b(x)\exp(-i\underline{k}\cdot\underline{x})\, d\underline{x} \ . \tag{9-47}$$

Recall that the spectral estimates of equations (9-39) and (9-41) were obtained by appropriate Fourier transformations of estimates of the auto correlation functions of the respective nonhomogeneous and homogeneous, stationary sensor output fields. The estimate of the autocorrelation function of the nonhomogeneous field was formed by averaging a single sample function of the product $\epsilon_\alpha(\underline{x},t)\epsilon_\alpha(\underline{x} + \underline{\xi},t + \tau)$ over the limited temporal extent, T_0, of the measurement of the sensor output field. The estimate of the autocorrelation function of the homogeneous field was formed by averaging the same single sample function of that product over both the limited temporal extent, T_0, and the limited spatial area, L_1L_2, of the measurement. In formulating the estimates of the autocorrelation function of the nonhomogeneous field by such a temporal average, we are hoping that the function of $\underline{x}$, $\underline{\xi}$, and τ obtained by evaluating $\epsilon_\alpha(\underline{x},t)\epsilon_\alpha(\underline{x} + \underline{\xi},t + \tau)$ at absolute time t_1 will be statistically independent of the function of $\underline{x}$, $\underline{\xi}$, and τ that results from evaluating $\epsilon_\alpha(\underline{x},t)\epsilon_\alpha(\underline{x} + \underline{\xi},t + \tau)$ at absolute time t_2. Similarly, in the estimate of the autocorrelation function of the homogeneous field, we hope that the function of $\underline{\xi}$ and τ that results from evaluating $\epsilon_\alpha(\underline{x},t)\epsilon_\alpha(\underline{x} + \underline{\xi},t + \tau)$ at the absolute time t_1 and absolute spatial location $\underline{x}_1$ will be statistically independent of the function of $\underline{\xi}$ and τ obtained by evaluating the same product at absolute time t_2 and absolute spatial location $\underline{x}_2$. Thus, in the estimation of the autocorrelation function and the two wavevector-frequency spectrum of the nonhomogeneous field, the number of independent observations contributing to the estimate is assumed to be proportional to the absolute time interval, T_0, over which the sample function $\epsilon_\alpha(\underline{x},t)\epsilon_\alpha(\underline{x} + \underline{\xi},t + \tau)$ is averaged. Similarly, in the estimation of the autocorrelation function and wavevector-frequency spectrum of the homogeneous field, the number of independent observations contributing to the estimate is presumed to be proportional to the product of

the absolute time interval (T_0) and the area (L_1L_2) in absolute space over which the sample function $\varepsilon_\alpha(\underline{x},t)\varepsilon_\alpha(\underline{x} + \underline{\xi},t + \tau)$ is averaged.

It should be recognized that, in most experiments, the areal extent of and the intervals between spatial samplings are fixed and limited by the numbers of sensors and attendant amplifiers or line drivers affordable within the budget of the experiment. The temporal extent of an observation is limited by the storage capacity of the data recording system affordable to, and compatible with the requirements of, the experiment. Generally speaking, modern data recording systems have storage capacities in excess of the requirements of most experiments. Conversely, the cost of sensors and their requisite amplifiers and filters is sufficiently high that the intervals between, and the extent of, spatial samplings are usually barely adequate for the objectives of the experiment. In consequence of these arguments, we assert that the only variable that can practicably affect the number of (hopefully) independent samples contributing to the estimate of the auto-correlation function of either a nonhomogeneous or homogeneous field is the absolute time of observation, T_0. Consequently, for the analysis of the bias and mean square error of the spectral estimate, we will assume that the number of independent observations contributing to estimates of the auto-correlation function and wavevector-frequency spectrum is proportional only to T_0.

To investigate the bias of the estimate of $\Phi_0(\underline{k},\omega)$, we wish (according to equation (9-1)) to determine the relationship between $E\{\tilde{\Phi}_0(\underline{k},\omega)\}$ and $\Phi_0(\underline{k},\omega)$ as the number of independent observations (i.e., T_0) approaches infinity. By equation (9-45),

$$\lim_{T_0\to\infty} E\{\tilde{\Phi}_0(\underline{k},\omega)\} = \lim_{T_0\to\infty} \frac{1}{(2\pi)^3 T_0 L_1 L_2} \int_{-\infty}^{\infty}\int_{-\infty}^{\infty}\int_{-\infty}^{\infty} \Phi_0(\underline{\beta},\Omega)$$

$$|A(\omega - \Omega)|^2 |B(\underline{k} - \underline{\beta})|^2 \, d\underline{\beta} \, d\Omega \, . \tag{9-48}$$

Inspection of equations (9-45) to (9-47) and equations (9-9) and (9-10) reveals that the only term in the integrand of equation (9-48) that depends on T_0 is $|A(\omega - \Omega)|^2$. Indeed, by equations (9-9) and (9-46),

$$A(\omega - \Omega) = T_0 \frac{\sin[(\omega - \Omega)T_0/2]}{[(\omega - \Omega)T_0/2]} . \tag{9-49}$$

Therefore, we can write equation (9-48) in the form

$$\lim_{T_0 \to \infty} E\{\tilde{\Phi}_0(\underline{k},\omega)\} = \frac{1}{(2\pi)^3 L_1 L_2} \int_{-\infty}^{\infty} \int_{-\infty}^{\infty} \int_{-\infty}^{\infty} \Phi_0(\underline{\beta},\Omega) |B(\underline{k} - \underline{\beta})|^2$$

$$\left\{ \lim_{T_0 \to \infty} T_0 \frac{\sin^2[(\omega - \Omega)T_0/2]}{[(\omega - \Omega)T_0/2]^2} \right\} d\underline{\beta}\, d\Omega . \tag{9-50}$$

However, by arguments advanced by Papoulis,[12]

$$\lim_{T_0 \to \infty} T_0 \frac{\sin^2[(\omega - \Omega)T_0/2]}{[(\omega - \Omega)T_0/2]^2} = 2\pi\delta(\omega - \Omega) . \tag{9-51}$$

Therefore, it follows that

$$\lim_{T_0 \to \infty} E\{\tilde{\Phi}_0(\underline{k},\omega)\} = \frac{1}{(2\pi)^2 L_1 L_2} \int_{-\infty}^{\infty} \int_{-\infty}^{\infty} \Phi_0(\underline{\alpha},\omega) |B(\underline{k} - \underline{\beta})|^2 \, d\underline{\beta} . \tag{9-52}$$

Clearly, by equation (9-52), the limit of the expected value of $\tilde{\Phi}_c(\underline{k},\omega)$ does not approach $\Phi_0(\underline{k},\omega)$ as the number of (hopefully) independent observations (i.e., T_0) contributing to the estimate approaches infinity. Therefore, according to equation (9-1), the estimate of the wavevector-frequency spectrum of the stationary and homogeneous sensor output field provided by equation (9-41) is a biased one. However, it is easily shown from equations (9-10) and (9-47) that

$$B(\underline{k}) = L_1 L_2 \left\{ \frac{\sin(k_1 L_1/2)}{k_1 L_1/2} \right\} \left\{ \frac{\sin(k_2 L_2/2)}{k_2 L_2/2} \right\} . \tag{9-53}$$

In chapter 8 (see figure 8-3a) we showed that the function $\sin(k_1 L_1/2)/(k_1 L_1/2)$

was characterized by a major response lobe of width $4\pi/L_1$ at $k_1 = 0$ and that, outside this primary lobe, the envelope of the function decreased inversely with the magnitude of k_1. Consequently, we can deduce that $|B(\underline{k} - \underline{\beta})|^2$ has a primary response lobe at $\underline{\beta} = \underline{k}$. The width of this primary lobe in the β_1 and β_2 coordinate directions is $4\pi/L_1$ and $4\pi/L_2$, respectively. Outside this primary lobe, $|B(\underline{k} - \underline{\beta})|^2$ decreases inversely with the square of the product $(k_1 - \beta_1)(k_2 - \beta_2)$. Note that, if L_1 and L_2 are sufficiently large that the bandwidths, in β_1 and β_2, of the major acceptance lobe of $|B(\underline{k} - \underline{\beta})|^2$ are much narrower than any fluctuation of $\Phi_0(\underline{\beta},\omega)$ in β_1 and β_2, then the role of $|B(\underline{k} - \underline{\beta})|^2$ in integral of equation (9-52) is (to first order) to sample $\Phi_0(\underline{\beta},\omega)$ at the wavevector $\underline{k}$. In this case, we can approximate equation (9-52) by

$$\lim_{T_0\to\infty} E\{\tilde{\Phi}_0(\underline{k},\omega)\} \approx \frac{\Phi_0(\underline{k},\omega)}{(2\pi)^2 L_1 L_2} \int_{-\infty}^{\infty}\int_{-\infty}^{\infty} |B(\underline{k} - \underline{\beta})|^2 \, d\underline{\beta} \; . \tag{9-54}$$

However, by use of equations (9-47), (2-38), and (9-10), we can easily show that

$$\int_{-\infty}^{\infty}\int_{-\infty}^{\infty} |B(\underline{k} - \underline{\beta})|^2 \, d\underline{\beta} = \int_{-\infty}^{\infty}\int_{-\infty}^{\infty} B(\underline{\mu})B(-\underline{\mu}) \, d\underline{\mu} = (2\pi)^2 \int_{-\infty}^{\infty}\int_{-\infty}^{\infty} b(\underline{x})b(\underline{x}) \, d\underline{x}$$

$$= (2\pi)^2 \int_{-\infty}^{\infty}\int_{-\infty}^{\infty} b(\underline{x}) \, d\underline{x} = (2\pi)^2 L_1 L_2 \; . \tag{9-55}$$

Consequently, if L_1 and L_2 are sufficiently large that equation (9-54) is a valid approximation, then

$$\lim_{T_0\to\infty} E\{\tilde{\Phi}_0(\underline{k},\omega)\} \approx \Phi_0(\underline{k},\omega) \; , \tag{9-56}$$

and the estimate provided by equation (9-41) is essentially unbiased.

It remains to assess the mean square error as $T_0 \to \infty$. From equation (9-7), the mean square error is the sum of the variance and the squared magnitude of the bias error. We can evaluate the bias error from either equation (9-54) or (9-56). Consequently, to assess the mean square error, we need to evaluate

only the variance of $\tilde{\Phi}_0(\underline{k},\omega)$ as $T_0 \to \infty$. For a homogeneous and stationary sensor output field, the true and estimated wavevector-frequency spectra are real. Therefore, the variance of $\tilde{\Phi}_0(\underline{k},\omega)$ is given by

$$\mathrm{Var}\{\tilde{\Phi}_0(\underline{k},\omega)\} = E\{(\tilde{\Phi}_0(\underline{k},\omega) - E\{\tilde{\Phi}_0(\underline{k},\omega)\})^2\}$$

$$= E\{\tilde{\Phi}_0^2(\underline{k},\omega)\} - (E\{\tilde{\Phi}_0(\underline{k},\omega)\})^2 , \qquad (9\text{-}57)$$

where $E\{\tilde{\Phi}_0(\underline{k},\omega)\}$ is given by equation (9-45). Therefore, it remains to formulate and evaluate $E\{\tilde{\Phi}_0^2(\underline{k},\omega)\}$.

From equation (9-41), and using the definitions of equations (9-36) and (9-8), we can demonstrate that

$$E\{\tilde{\Phi}_0^2(\underline{k},\omega)\} = \frac{1}{(T_0 L_1 L_2)^2} \int_{-\infty}^{\infty}\int_{-\infty}^{\infty}\int_{-\infty}^{\infty}\int_{-\infty}^{\infty}\int_{-\infty}^{\infty}\int_{-\infty}^{\infty}\int_{-\infty}^{\infty}\int_{-\infty}^{\infty}\int_{-\infty}^{\infty}\int_{-\infty}^{\infty}\int_{-\infty}^{\infty}\int_{-\infty}^{\infty} a(t_1 - t_0)a(t_2 - t_0)$$

$$a(t_3 - t_0)a(t_4 - t_0)b(\underline{x}_1 - \underline{x}_0)b(\underline{x}_2 - \underline{x}_0)b(\underline{x}_3 - \underline{x}_0)b(\underline{x}_4 - \underline{x}_0)$$

$$E\{o_\alpha(\underline{x}_1,t_1)o_\alpha(\underline{x}_2,t_2)o_\alpha(\underline{x}_3,t_3)o_\alpha(\underline{x}_4,t_4)\}$$

$$\exp[i(\underline{k}\cdot\underline{x}_1 + \omega t_1)]\exp[-i(\underline{k}\cdot\underline{x}_2 + \omega t_2)]\exp[i(\underline{k}\cdot\underline{x}_3 + \omega t_3)]$$

$$\exp[-i(\underline{k}\cdot\underline{x}_4 + \omega t_4)]\, d\underline{x}_1\, d\underline{x}_2\, d\underline{x}_3\, d\underline{x}_4\, dt_1\, dt_2\, dt_3\, dt_4 . \qquad (9\text{-}58)$$

Here again, we have commuted the expectation and integration operations.

Equation (9-58) presents a problem in that we cannot, for an arbitrary random process, evaluate the fourth-order moment of the form $E\{o_\alpha(\underline{x}_1,t_1)o_\alpha(\underline{x}_2,t_2)o_\alpha(\underline{x}_3,t_3)o_\alpha(\underline{x}_4,t_4)\}$. However, if we make the (not unreasonable) assumption that $o_\alpha(\underline{x},t)$ is a member function of a zero mean Gaussian random process, then we can employ the relationship given by Bendat and Piersol:[13]

$$E\{o_\alpha(\underline{x}_1,t_1)o_\alpha(\underline{x}_2,t_2)o_\alpha(\underline{x}_3,t_3)o_\alpha(\underline{x}_4,t_4)\} =$$

$$E\{o_\alpha(\underline{x}_1,t_1)o_\alpha(\underline{x}_2,t_2)\}E\{o_\alpha(\underline{x}_3,t_3)o_\alpha(\underline{x}_4,t_4)\}$$

$$E\{o_\alpha(\underline{x}_1,t_1)o_\alpha(\underline{x}_3,t_3)\}E\{o_\alpha(\underline{x}_2,t_2)o_\alpha(\underline{x}_4,t_4)\}$$

$$E\{o_\alpha(\underline{x}_1,t_1)o_\alpha(\underline{x}_4,t_4)\}E\{o_\alpha(\underline{x}_2,t_2)o_\alpha(\underline{x}_3,t_3)\} \ . \tag{9-59}$$

For the stationary and homogeneous sensor output field of interest, we can rewrite equation (9-44) in the form

$$E\{o_\alpha(\underline{x}_1,t_1)o_\alpha(\underline{x}_2,t_2)\} = Q_{oo}(\underline{x}_2 - \underline{x}_1,t_2 - t_1)$$

$$= (2\pi)^{-3} \int_{-\infty}^{\infty}\int_{-\infty}^{\infty}\int_{-\infty}^{\infty} \Phi_o(\underline{k},\omega)\exp\{i[\underline{k}\cdot(\underline{x}_2 - \underline{x}_1) + \omega(t_2 - t_1)]\} \, d\underline{k} \, d\omega \ . \tag{9-60}$$

From equations (9-59) and (5-60), it follows that

$$E\{o_\alpha(\underline{x}_1,t_1)o_\alpha(\underline{x}_2,t_2)o_\alpha(\underline{x}_3,t_3)o_\alpha(\underline{x}_4,t_4)\} =$$

$$(2\pi)^{-6} \int_{-\infty}^{\infty}\int_{-\infty}^{\infty}\int_{-\infty}^{\infty}\int_{-\infty}^{\infty}\int_{-\infty}^{\infty}\int_{-\infty}^{\infty} \Phi_o(\underline{\mu},\Omega)\Phi_o(\underline{\beta},\Gamma)$$

$$\{\exp[i\underline{\mu}\cdot(\underline{x}_2 - \underline{x}_1)]\exp[i\Omega(t_2 - t_1)]\exp[i\underline{\beta}\cdot(\underline{x}_4 - \underline{x}_3)]\exp[i\Gamma(t_4 - t_3)]$$

$$+ \exp[i\underline{\mu}\cdot(\underline{x}_3 - \underline{x}_1)]\exp[i\Omega(t_3 - t_1)]\exp[i\underline{\beta}\cdot(\underline{x}_4 - \underline{x}_2)]\exp[i\Gamma(t_4 - t_2)]$$

$$+ \exp[i\underline{\mu}\cdot(\underline{x}_4 - \underline{x}_1)]\exp[i\Omega(t_4 - t_1)]\exp[i\underline{\beta}\cdot(\underline{x}_3 - \underline{x}_2)]\exp[i\Gamma(t_3 - t_2)]\}$$

$$d\underline{\mu} \, d\Omega \, d\underline{\beta} \, d\Gamma \ . \tag{9-61}$$

Substitution of equation (9-61) into equation (9-58) yields, through careful

bookkeeping and use of equations (9-46) and (9-47), the following result:

$$E\{\tilde{\Phi}_0^2(\underline{k},\omega)\} = \frac{1}{(2\pi)^6(T_0L_1L_2)^2} \int_{-\infty}^{\infty}\int_{-\infty}^{\infty}\int_{-\infty}^{\infty}\int_{-\infty}^{\infty}\int_{-\infty}^{\infty}\int_{-\infty}^{\infty} \Phi_0(\underline{\mu},\Omega)\Phi_0(\underline{\beta},\Gamma)$$

$$\{|A(\omega - \Omega)|^2|B(\underline{k} - \underline{\mu})|^2|A(\omega - \Gamma)|^2|B(\underline{k} - \underline{\beta})|^2$$

$$+ A^*(\omega - \Omega)A^*(\omega + \Omega)B^*(\underline{k} - \underline{\mu})B^*(\underline{k} + \underline{\mu})A(\omega - \Gamma)A(\omega + \Gamma)B(\underline{k} - \underline{\beta})B(\underline{k} + \underline{\beta})$$

$$+ |A(\omega - \Omega)|^2|B(\underline{k} - \underline{\mu})|^2|A(\omega + \Gamma)|^2|B(\underline{k} + \underline{\beta})|^2\} \, d\underline{\mu} \, d\Omega \, d\underline{\beta} \, d\Gamma \ . \tag{9-62}$$

By recalling, from equations (6-83) and (6-84), that

$$\Phi_0(\underline{k},\omega) = \Phi_0^*(\underline{k},\omega) = \Phi_0(-\underline{k},-\omega) \ , \tag{9-63}$$

we can show that

$$E\{\tilde{\Phi}_0^2(\underline{k},\omega)\} = \frac{1}{(2\pi)^6(T_0L_1L_2)^2}$$

$$\Bigg\{2 \int_{-\infty}^{\infty}\int_{-\infty}^{\infty}\int_{-\infty}^{\infty} \Phi_0(\underline{\mu},\Omega)|A(\omega - \Omega)|^2|B(\underline{k} - \underline{\mu})|^2 \, d\underline{\mu} \, d\Omega$$

$$\int_{-\infty}^{\infty}\int_{-\infty}^{\infty}\int_{-\infty}^{\infty} \Phi_0(\underline{\beta},\Gamma)|A(\omega - \Gamma)|^2|B(\underline{k} - \underline{\beta})|^2 \, d\underline{\beta} \, d\Gamma$$

$$+\left|\int_{-\infty}^{\infty}\int_{-\infty}^{\infty}\int_{-\infty}^{\infty} \Phi_0(\underline{\beta},\Gamma)A(\omega - \Gamma)A(\omega + \Gamma)B(\underline{k} - \underline{\beta})B(\underline{k} + \underline{\beta}) \, d\underline{\beta} \, d\Gamma\right|^2\Bigg\} \ . \tag{9-64}$$

From equation (9-45), we recognize that the first term on the right-hand side is $2[E\{\tilde{\Phi}_0(\underline{k},\omega)\}]^2$. It then follows, from equations (9-57) and (9-64), that

$$\mathrm{Var}\{\tilde{\Phi}_0(\underline{k},\omega)\} = [E\{\tilde{\Phi}_0(\underline{k},\omega)\}]^2 +$$

$$\left| \frac{1}{(2\pi)^3(T_0L_1L_2)} \int_{-\infty}^{\infty}\int_{-\infty}^{\infty}\int_{-\infty}^{\infty} \Phi_0(\underline{\beta},\Gamma)A(\omega - \Gamma)A(\omega + \Gamma)B(\underline{k} - \underline{\beta})B(\underline{k} + \underline{\beta})\, d\underline{\beta}\, d\Gamma \right|^2 . \tag{9-65}$$

Note from equation (9-65) that, independent of the value of T_0, the variance of our estimate of the wavevector-frequency spectrum of a homogeneous, stationary sensor output field is greater than, or equal to, the square of its expected value. Consequently, even when the areal extent of the (continuous) spatial sampling is sufficiently large (see equation (9-56)) that our estimate is essentially unbiased, the mean square error of our estimate is greater than, or equal to, the square of the mean of the estimate as $T_0 \to \infty$. That is, according to equations (9-7), (9-56), and (9-65),

$$\lim_{T_0 \to \infty} \mathrm{MSE}\{\tilde{\Phi}_0(\underline{k},\omega)\} \geq [E\{\tilde{\Phi}_0(\underline{k},\omega)\}]^2 . \tag{9-66}$$

Clearly, the estimate of the wavevector-frequency spectrum of the stationary and homogeneous sensor output field provided by equation (9-41) is not a consistent one. Therefore, equation (9-41) is not an acceptable estimator of the wavevector-frequency spectrum.

This result is a disappointment, especially in light of the mathematically attractive form of equation (9-41). We are now faced with two options; we can attempt to develop an alternative estimator by utilizing a different approach, or we can attempt to identify and correct the fault in the estimator provided by equation (9-41). We choose the latter option.

9.2.2 Refinement of the Estimators for a Single, Continuous Sample Function

The estimators of the wavevector-frequency spectra of the nonhomogeneous and homogeneous, stationary fields specified by equations (9-39) and (9-41), respectively, are obtained by Fourier transforming estimates of the autocorrelation functions of the corresponding fields, given by equations (9-18)

(or (9-34)) and (9-32), according to the definitions of the various forms of wavevector-frequency spectra specified by equations (6-78), (6-121), and (6-149). Inasmuch as (1) Fourier transforms are linear operations and (2) no approximations were made in the Fourier transformations of equation (9-18), (9-32), or (9-34) that yielded equations (9-39) and (9-41), we are led to suspect that the lack of consistency in our estimate of the wavevector-frequency spectrum of the homogeneous, stationary sensor output field results from some lack of quality in our estimate of the autocorrelation function of that field. Let us therefore examine the bias and mean square errors of this estimate of the autocorrelation function.

The estimate of the autocorrelation function of the stationary, homogeneous sensor output field is given by equation (9-32). By use of equations (9-8), (9-9), and (9-10), it is easily demonstrated that, for any fixed values of $\underline{\xi}$ and τ, the mean value of the estimate $\tilde{Q}_{00}(\underline{\xi},\tau)$ is given by

$$E\{\tilde{Q}_{00}(\underline{\xi},\tau)\} = \frac{1}{T_0 L_1 L_2} \int_{-\infty}^{\infty} \int_{-\infty}^{\infty} \int_{-\infty}^{\infty} a(t - t_0) a(t + \tau - t_0) b(\underline{x} - \underline{x}_0) b(\underline{x} + \underline{\xi} - \underline{x}_0)$$

$$E\{o_\alpha(\underline{x},t) o_\alpha(\underline{x} + \underline{\xi}, t + \tau)\} \, d\underline{x} \, dt \ . \qquad (9\text{-}67)$$

However, we recognize $E\{o_\alpha(\underline{x},t) o_\alpha(\underline{x} + \underline{\xi}, t + \tau)\}$ to be the true autocorrelation function, $Q_{00}(\underline{\xi},\tau)$, of the stationary and homogeneous sensor output field. With this substitution, equation (9-67) can be rewritten in the form

$$E\{\tilde{Q}_{00}(\underline{\xi},\tau)\} = v(\tau) w(\underline{\xi}) Q_{00}(\underline{\xi},\tau) \ , \qquad (9\text{-}68)$$

where

$$v(\tau) = \frac{1}{T_0} \int_{-\infty}^{\infty} a(t - t_0) a(t + \tau - t_0) \, dt \qquad (9\text{-}69)$$

and

$$w(\underline{\xi}) = \frac{1}{L_1 L_2} \int_{-\infty}^{\infty} \int_{-\infty}^{\infty} b(\underline{x} - \underline{x}_0) b(\underline{x} + \underline{\xi} - \underline{x}_0) \, d\underline{x} \ . \tag{9-70}$$

By equations (9-9) and (9-69), it can be demonstrated that

$$v(\tau) = \begin{cases} 1 - |\tau|/T_0 \ , & |\tau| \leq T_0 \ , \\ 0, & \text{otherwise.} \end{cases} \tag{9-71}$$

In a similar fashion, we can demonstrate, from equations (9-10) and (9-70), that

$$w(\underline{\xi}) = \begin{cases} (1 - |\xi_1|/L_1)(1 - |\xi_2|/L_2), & |\xi_1| \leq L_1 \text{ and } |\xi_2| \leq L_2 \ , \\ 0, & \text{otherwise.} \end{cases} \tag{9-72}$$

Consequently, we can write the mean of the estimate as

$$E\{\tilde{Q}_{00}(\underline{\xi},\tau)\} = \begin{cases} (1 - |\tau|/T_0)(1 - |\xi_1|/L_1)(1 - |\xi_2|/L_2) Q_{00}(\underline{\xi},\tau) \ , \\ \qquad \text{for } |\tau| \leq T_0 \text{ and } |\xi_1| \leq L_1 \text{ and } |\xi_2| \leq L_2 \ , \\ 0, \quad \text{otherwise.} \end{cases} \tag{9-73}$$

Recall that, because the areal extent (i.e., $L_1 L_2$) of most experiments is limited, we have assumed that the number of independent observations contributing to the estimate of the autocorrelation function is proportional only to the (presumedly more flexible) time of observation, T_0. Consequently, to assess the bias of the estimate of the autocorrelation function of the stationary, homogeneous sensor output field at any fixed values of $\underline{\xi}$ and τ, we evaluate equation (9-73) in the limit as T_0 approaches infinity. This yields

$$\lim_{T_0 \to \infty} E\{\tilde{Q}_{00}(\underline{\xi},\tau)\} = \begin{cases} Q_{00}(\underline{\xi},\tau)(1 - |\xi_1|/L_1)(1 - |\xi_2|/L_2) \ , \\ \qquad \text{for } |\xi_1| \leq L_1 \text{ and } |\xi_2| \leq L_2 \ , \\ 0, \quad \text{otherwise.} \end{cases} \tag{9-74}$$

Here, we see that this estimate of the autocorrelation function is generally biased. However, it is evident that the bias results only from the limited spatial extent of our observations. That is, if L_1 and L_2 are either (1) much larger than ξ_1 and ξ_2, respectively, or (2) sufficiently large that the true autocorrelation function, $Q_{oo}(\underline{\xi},\tau)$, tends to zero as $\xi_1 \rightarrow L_1$ and $\xi_2 \rightarrow L_2$, then the estimate of the autocorrelation function tends to become unbiased.

It can be shown, under the assumption that $o_\alpha(\underline{x},t)$ is a member function of a zero mean Gaussian random process, that the variance of $\tilde{Q}_{oo}(\underline{\xi},\tau)$, at any fixed values of $\underline{\xi}$ and τ, approaches zero in the limit as $T_0 \rightarrow \infty$. However, the demonstration of this result is a tedious and trying mathematical exercise that will be left to the curious reader.

By the arguments presented above, it is evident that our estimate of the autocorrelation function of the stationary and homogeneous sensor output field tends toward a consistent one as $T_0 \rightarrow \infty$ if L_1 and L_2 are much greater than the largest respective spatial separations, say ξ_{1max} and ξ_{2max}, associated with any significant contribution to the true autocorrelation function of the field. Consequently, we are led to deduce that the quality of our estimate of the autocorrelation function is not the source of the large variance in our estimate of the wavevector-frequency spectrum.

Unfortunately, this deduction is flawed. Jenkins and Watts[14] state the following: "In fact, it is usually not true that, if there is a consistent estimator of a statistical parameter, its Fourier transform is a consistent estimator of the Fourier transform of that parameter." This observation arouses our curiosity regarding the relationship between the bias and variance of the spectral estimate and the bias and variance of the autocorrelation function. The estimate of the wavevector-frequency spectrum of the homogeneous and stationary field was formed from the estimate of the autocorrelation function of that field by

$$\tilde{\Phi}_0(\underline{k},\omega) = \int_{-\infty}^{\infty}\int_{-\infty}^{\infty}\int_{-\infty}^{\infty} \tilde{Q}_{oo}(\underline{\xi},\tau)\exp[-i(\underline{k}\cdot\underline{\xi} + \omega\tau)]\, d\underline{\xi}\, d\tau \ . \tag{9-75}$$

From equations (9-2), (9-75), and the definition of the true wavevector-frequency spectrum, $\Phi_0(\underline{k},\omega)$, of equation (6-78), we can show the following relation between the bias error of the wavevector-frequency spectrum and the bias error of the autocorrelation function:

$$\beta\{\tilde{\Phi}_0(\underline{k},\omega)\} = \int_{-\infty}^{\infty}\int_{-\infty}^{\infty}\int_{-\infty}^{\infty} \beta\{\tilde{Q}_{00}(\underline{\xi},\tau)\}\exp[-i(\underline{k}\cdot\underline{\xi} + \omega\tau)\} \, d\underline{\xi} \, d\tau \; . \qquad (9\text{-}76)$$

Further, by the definition of the variance given by equation (6-9) and the use of equation (9-75), we can show that the variance of the estimate of the wavevector-frequency spectrum is related to the statistics of the estimate of the autocorrelation function by

$$\mathrm{Var}\{\tilde{\Phi}_0(\underline{k},\omega)\} = \int_{-\infty}^{\infty}\int_{-\infty}^{\infty}\int_{-\infty}^{\infty} \mathrm{Cov}\{\tilde{Q}_{00}(\underline{\xi},\tau),\tilde{Q}_{00}(\underline{z},\theta)\}$$

$$\exp[-i[\underline{k}\cdot(\underline{\xi} + \underline{z}) + \omega(\tau + \theta)]] \, d\underline{\xi} \, d\underline{z} \, d\tau \, d\theta \; , \qquad (9\text{-}77)$$

where Cov{A,B} denotes the covariance of A and B, as defined by equation (6-21).

Equation (9-76) states that the bias of the spectral estimate is a multiple Fourier transform of the bias of the estimate of the autocorrelation function. Consequently, a condition sufficient to ensure an unbiased estimate of the wavevector-frequency spectrum at all wavevectors and frequencies is that the bias error of the autocorrelation function be zero for all $\underline{\xi}$ and τ. Note that the variance of the spectral estimate is expressed in terms of a multiple Fourier transform of the covariance, rather than the variance, of the estimate of the autocorrelation function. Clearly then, a requirement that the variance of the estimate of the autocorrelation function be zero for all $\underline{\xi}$ and τ is not sufficient to ensure that the variance of the spectral estimate be zero for all $\underline{k}$ and ω. It therefore follows that the Fourier transform of an estimate of the autocorrelation function that is consistent for all $\underline{\xi}$ and τ will not necessarily produce a consistent estimate of the wavevector-frequency spectrum over all $\underline{k}$ and ω.

Although the above observations demonstrate that a consistent estimate of

the autocorrelation function of a homogeneous, stationary field does not ensure a consistent estimate of the associated wavevector-frequency spectrum, they do not provide useful guidance for reducing the variance of the spectral estimate. Indeed, our efforts toward deducing the specific defect in our estimate of the autocorrelation function responsible for the large variance of our spectral estimate have been singularly unsuccessful. We therefore turn to standard texts on signal processing in the hope of finding a treatment of an analogous problem in the estimation of the frequency spectrum from a sample function of a time series.

This review of standard texts is somewhat more productive than our own deductive efforts. According to Davenport and Root,[15] a common way to estimate the frequency spectral density, $\phi(\omega)$, from a sample function, x(t), known over the interval $0 \leq t \leq T$ is by means of a function called the periodogram. That function is defined by

$$\phi(\omega) = \frac{1}{T} |X(\omega)|^2 , \tag{9-78}$$

where

$$X(\omega) = \int_0^T x(t)\exp(-i\omega t)\, dt . \tag{9-79}$$

If we recall (from equations (9-8) through (9-10)) that $\epsilon(\underline{x},t)$ is zero outside the variable ranges $t_0 - T_0/2 \leq t \leq t_0 + T_0/2$, $x_{01} - L_1/2 \leq x_1 \leq x_{01} + L_1/2$, and $x_{02} - L_2/2 \leq x_2 \leq x_{02} + L_2/2$, it is evident by comparison of equations (9-41) and (9-36) with equations (9-78) and (9-79) that, with the exception of the choice of spatial and temporal origins, our estimate of the wavevector-frequency spectrum of the homogeneous, stationary sensor output field is a three-dimensional analog of the periodogram.

Davenport and Root[16] show that, in the limit as the observation time (T) approaches infinity, the periodogram provides an unbiased estimate of the true frequency spectrum. However, they also show that, when x(t) is a sample function of a real Gaussian random process, the variance of the estimate provided by the periodogram does not approach zero as $T \to \infty$; rather, the

variance of the estimate is equal to or greater than the square of the mean of the estimate. These characteristics of the bias and variance of the periodogram in the limit as $T \to \infty$ are analogous to those observed in the bias and variance of the estimate of the wavevector-frequency spectrum of the stationary, homogeneous field given by equation (9-41) in the limit as $T_0 \to \infty$.

Davenport and Root do not address the cause of the instability (i.e., the large variance) of the estimate provided by the periodogram. Indeed, although most standard texts in signal processing treat the periodogram and note the large variance in the estimate of the frequency spectrum when the periodogram is applied to random fields, they do not provide a cogent explanation of the cause of that instability. However, several texts describe procedures for reducing the variance of the spectral estimate associated with the periodogram. Collectively, these procedures are referred to as "spectral smoothing" or simply "smoothing."

Many procedures have been developed to smooth spectral estimates. However, most of these smoothing procedures are variants of two basic methods. One method, proposed by Blackman and Tukey,[17] convolves the spectral estimate provided by the periodogram with a spectral window. The resulting "smoothed" spectral estimate, at any frequency, is a weighted average of the estimate provided by the periodogram over an effective bandwidth dictated by the spectral window. As a result of this averaging over frequency, the variance of the smoothed spectral estimate is much smaller than that provided by the periodogram. Recall that a convolution in the frequency domain is the result of a product in the time domain. Therefore, it can be demonstrated that the smoothing proposed by Blackman and Tukey can be achieved by multiplying the estimate of the autocorrelation function associated with the periodogram by a "lag window" in the variable τ prior to Fourier transformation on that variable. The purpose of the lag window is to time-limit the estimate of the autocorrelation function in the time delay (or time "lag") variable to $|\tau| \le \tau_{max}$, where τ_{max} is much less than the temporal length of the sample function and is inversely proportional to the desired bandwidth of the spectral window.

The second method of smoothing is that proposed by Bartlett.[18] In this

method, the single sample function of temporal extent T_0 is divided into J segments, thereby creating J sample functions, each of temporal extent T_0/J. A periodogram is computed for each of the J sample functions, and the spectral estimate is formulated by averaging the J periodograms. Oppenheim and Schafer[19] demonstrate that if the J periodograms are statistically independent, then the variance of the spectral estimate obtained from their average is inversely proportional to J, and therefore approaches zero as $J \to \infty$.

Either of the above described smoothing procedures can be applied to reduce the variance of our wavevector-frequency spectral estimates. However, it appears that the smoothing of our spectral estimates by the Bartlett procedure can be implemented by relatively minor modifications of our current estimates. Further, inasmuch as the smoothed spectral estimate resulting from the Bartlett procedure is expressed in the form of an average of periodograms, we anticipate that, for measured data in the form of discrete and uniform spatial and temporal samples of the sensor output field, the smoothed spectral estimate can be efficiently evaluated through the use of fast Fourier transforms. Consequently, we choose to smooth our spectral estimates by employing a variant of the Bartlett procedure. That variant is known as the Welch method.

9.2.3 Smoothing of the Estimators for a Single, Continuous Sample Function by the Welch Method

The Welch method[20] is a modification of the Bartlett procedure in which the smoothing is affected by averaging modified periodograms. In this method, the sample function is first partitioned in time to create J sample functions, each of length T_0/J. Identical temporal weightings are then applied to each of the J sample functions, and modified periodograms are formed by Fourier transforming each of these windowed sample functions. The smoothed spectral estimate is then formed by averaging the J modified periodograms. The use of the temporal weighting affords some degree of control of the shape of the spectral window applied in the frequency domain.

We implement the Welch smoothing method to our estimates of wavevector-frequency spectra as follows. Recall that we are given a single sample

function, $o_\alpha(\underline{x},t)$, of the sensor output field that (for the present) is assumed to have been measured continuously over the space within $x_{01} - L_1/2 \le x_1 \le x_{01} + L_1/2$ and $x_{02} - L_2/2 \le x_2 \le x_{02} + L_2/2$, and over the time $t_0 - T_0/2 \le t \le t_0 + T_0/2$. We first partition the single sample function in time, thereby creating J sample functions of equal temporal length, $T = T_0/J$. The J sample functions, $o_{\alpha j}(\underline{x},t)$, $j = 1,\ldots J$, resulting from this temporal partitioning are defined continuously over the space within $x_{01} - L_1/2 \le x_1 \le x_{01} + L_1/2$ and $x_{02} - L_2/2 \le x_2 \le x_{02} + L_2/2$, and over the temporal intervals $t_0 - T_0/2 + (j - 1)T \le t \le t_0 + T_0/2 + jT$. We next apply identical temporal weightings to each of the J sample functions. The temporal partitioning and weighting is illustrated in figure 9-3. The temporal weighting, which we denote by $a_W(t)$, is a real and even function of time within the temporal range $|t| \le T/2$, and is zero for $|t| > T/2$. A temporal weighting function satisfying these requirements is illustrated in figure 9-4.

We presume that the spatial extent of practical measurements will, owing to fiscal constraints, be barely adequate for the objectives of the experiment. Consequently, we do not propose to partition the data in space. However, it is evident from equations (9-48) and (9-65) that the mean and variance of the spectral estimate depend on $B(\underline{k})$, the wavevector transform of the spatial window, $b(\underline{x})$. Therefore, it appears prudent to provide for spatial weighting of the sample functions so as to offer an additional means of influencing the bias and variance of the spectral estimates. To that end, we apply identical spatial weightings, $b_W(\underline{x} - \underline{x}_0)$, to each of the J sample functions. Here, $b_W(\underline{x})$ is a real and even function of both x_1 and x_2 within $|x_1| \le L_1/2$ and $|x_2| \le L_2/2$, and is zero outside these spatial bounds.

Let us now define, in a fashion similar to equation (9-8), a function over all space and time that incorporates our knowledge of each of the J spatially and temporally weighted sample functions. That is, let

$$\varepsilon_{\alpha j}(\underline{x},t) = a_W[t - t_0 + T_0/2 - (2j - 1)T/2]b_W(\underline{x} - \underline{x}_0)o_\alpha(\underline{x},t),\ j = 1,2,\ldots J\ , \tag{9-80}$$

for all $\underline{x}$ and t. Note by equation (9-80) that $\varepsilon_{\alpha p}(\underline{x},t)$ is equal to the meas-

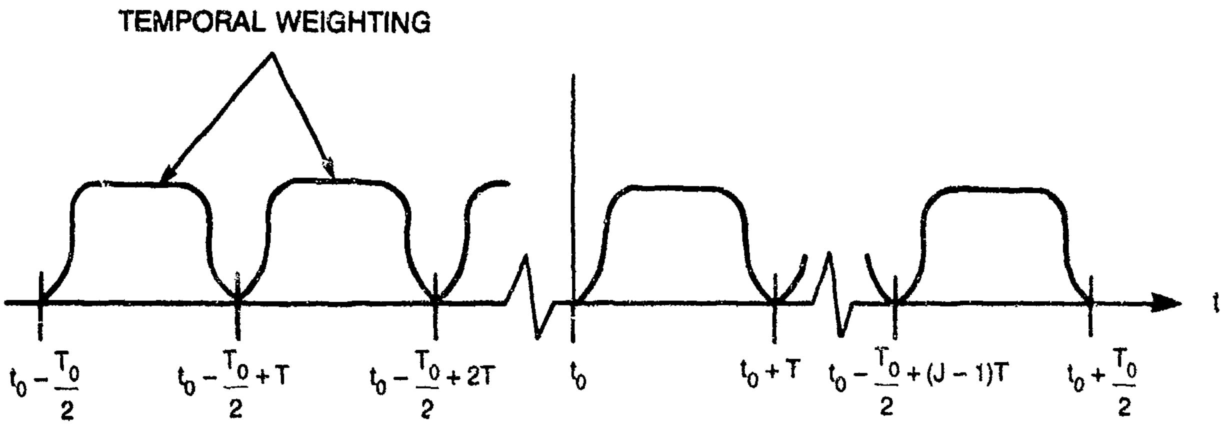

Figure 9-3. Illustration of Temporal Partitioning and Weighting

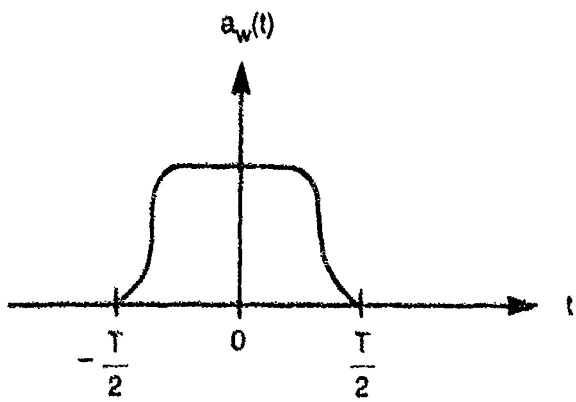

Figure 9-4. Illustration of a Temporal Weighting Function, $a_w(t)$

ured sample function $o_\alpha(\underline{x},t)$, subject to the desired spatial and temporal weightings, within the spatial area defined by $x_{01} - L_1/2 \le x_1 \le x_{01} + L_1/2$ and $x_{02} - L_2/2 \le x_2 \le x_{02} + L_2/2$, and within the temporal interval $t_0 - T_0/2 + (p - 1)T \le t \le t_0 + T_0/2 + pT$. Outside these spatial and temporal regions, $\epsilon_{\alpha p}(\underline{x},t)$ is identically zero.

We now proceed to define estimates of the autocorrelation functions of the sensor output field from each of the J sample functions by applying arguments similar to those advanced in section 9.2.1. If the sensor output field is known to be stationary, but nonhomogeneous, we form an estimate of the autocorrelation function from the j-th sample function by a form similar to that given by equation (9-11). That is,

$$\tilde{Q}_{oo}(\underline{x},\underline{\xi},\tau)_j = \frac{1}{T_{Bj} - T_{Aj}} \int_{T_{Aj}}^{T_{Bj}} \epsilon_{\alpha j}(\underline{x},t)\epsilon_{\alpha j}(\underline{x} + \underline{\xi},t + \tau)\, dt \qquad (9\text{-}81)$$

for all $\underline{x}$, $\underline{\xi}$, and τ. Here, $\tilde{Q}_{oo}(\underline{x},\underline{\xi},\tau)_j$ denotes the estimate of the autocorrelation function of the sensor output field formed from the j-th sample function, and T_{Aj} and T_{Bj} denote the lower and upper limits, in absolute time, over which the product $\epsilon_{\alpha j}(\underline{x},t)\epsilon_{\alpha j}(\underline{x} + \underline{\xi},t + \tau)$ is averaged to form the estimate.

We choose the limits T_{Aj} and T_{Bj} by applying arguments similar to those used in section 9.2.1. As is evident from equation (9-80), the function $\epsilon_{\alpha j}(\underline{x},t)\epsilon_{\alpha j}(\underline{x} + \underline{\xi},t + \tau)$ is identically zero over that range of absolute time where the product $a_w[t - t_0 + T_0/2 - (2j - 1)T/2]a_w[t + \tau - t_0 + T_0/2 - (2j - 1)T/2]$ is zero. The nonzero range of this product is illustrated in figure 9-5 as a function of t and τ. Note that the range in t over which the product $a_w[t - t_0 + T_0/2 - (2j - 1)T/2]a_w[t + \tau - t_0 + T_0/2 - (2j - 1)T/2]$, and thereby the function $\epsilon_{\alpha j}(\underline{x},t)\epsilon_{\alpha j}(\underline{x} + \underline{\xi},t + \tau)$, is nonzero varies with the choice of the time delay, τ. Thus, if we select T_{Aj} and T_{Bj} to correspond to the range of absolute time over which the function $\epsilon_{\alpha j}(\underline{x},t)\epsilon_{\alpha j}(\underline{x} + \underline{\xi},t + \tau)$ is nonzero for each τ, then it is evident from figure 9-5 that $T_{Bj} - T_{Aj}$ will equal $T - |\tau|$ for all j between unity and J. Alternatively, if we select T_{Aj} and T_{Bj} to

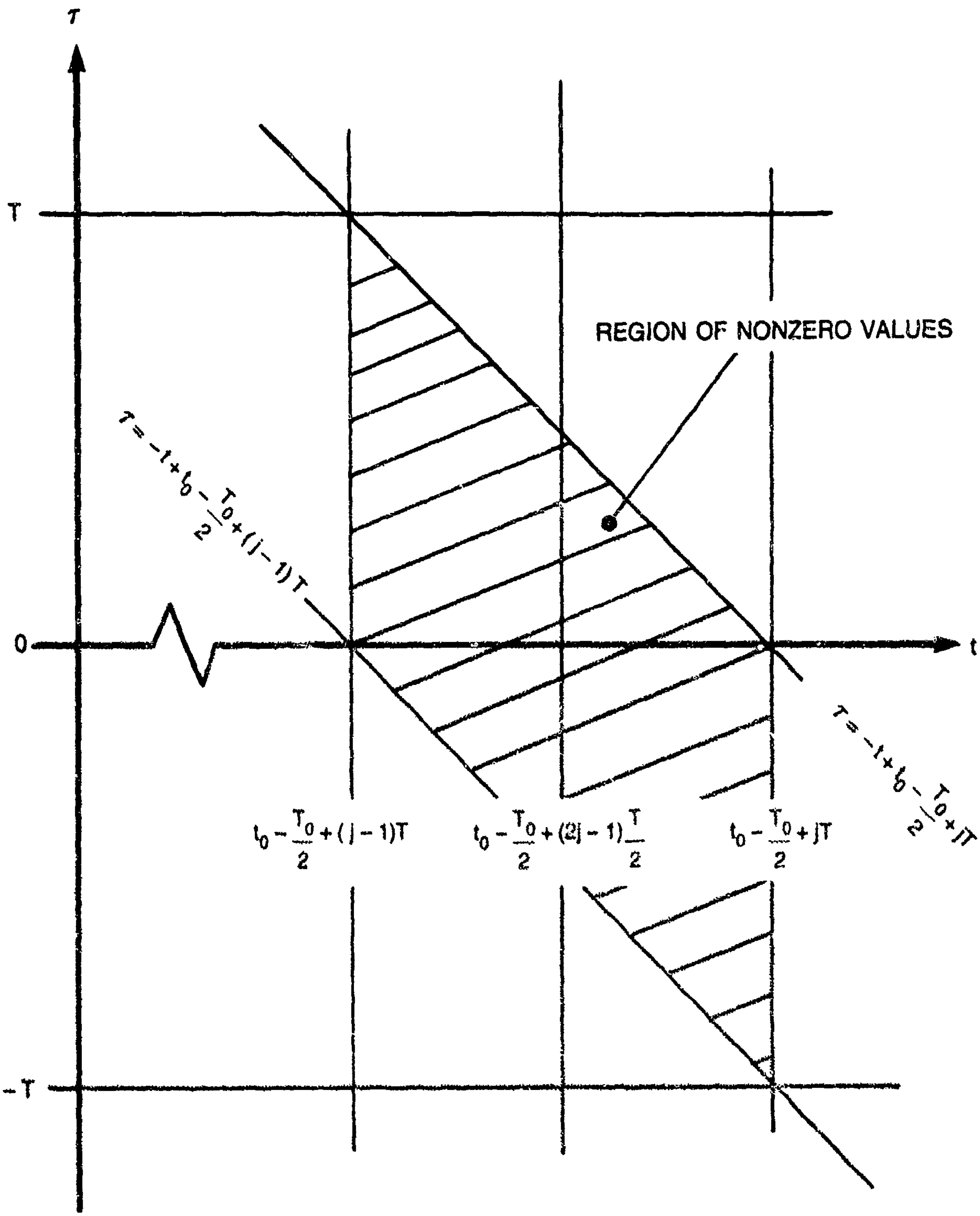

Figure 9-5. Region of Nonzero Values of the Product
$a_w[t - t_0 + T_0/2 - (2j - 1)T/2]a_w[t + \tau + T_0/2 - (2j - 1)T/2]$

be $t_0 - T_0/2 + (j - 1)T$ and $t_0 - T_0/2 + jT$, respectively, the nonzero contributions to the integral of equation (9-81), for any given value of τ, will still be confined to that range of t where the product $a_w[t - t_0 + T_0/2 - (2j - 1)T/2]a_w[t + \tau - t_0 + T_0/2 - (2j - 1)T/2]$ is nonzero, but $T_{Bj} - T_{Aj}$ will be equal to T, regardless of the choice of either j or τ. For reasons consistent with those advanced in section 9.2.1, we select those limits that render $T_{Bj} - T_{Aj}$ independent of τ; that is, we choose T_{Aj} to be $t_0 - T_0/2 + (j - 1)T$ and T_{Bj} to be $t_0 - T_0/2 + jT$. Accordingly, it follows from equation (9-81) that the estimate of the autocorrelation function obtained from the j-th sample function of a stationary, nonhomogeneous sensor output field can be written in the form

$$\tilde{Q}_{oo}(\underline{x},\underline{\xi},\tau)_j = \frac{1}{T}\int_{-\infty}^{\infty} \varepsilon_{\alpha j}(\underline{x},t)\varepsilon_{\alpha j}(\underline{x} + \underline{\xi},t + \tau)\,dt \tag{9-82}$$

for all $\underline{x}$, $\underline{\xi}$, and τ. Here, the infinite limits on the integral over absolute time are permissible because, for any choice of j and τ, the function $\varepsilon_{\alpha j}(\underline{x},t)\varepsilon_{\alpha j}(\underline{x} + \underline{\xi},t + \tau)$ is identically zero outside of the range $t_0 - T_0/2 + (j - 1)T \leq t \leq t_0 - T_0/2 + jT$.

For any given values of $\underline{x}$, $\underline{\xi}$, and τ, we formulate an estimate of the autocorrelation function of the stationary, nonhomogeneous sensor output field by averaging the estimates of the autocorrelation functions obtained from the J sample functions at corresponding values of $\underline{x}$, $\underline{\xi}$, and τ. That is,

$$\begin{aligned}\tilde{Q}_{oo}(\underline{x},\underline{\xi},\tau) &= \frac{1}{J}\sum_{j=1}^{J} \tilde{Q}_{oo}(\underline{x},\underline{\xi},\tau)_j \\ &= \frac{1}{JT}\sum_{j=1}^{J}\int_{-\infty}^{\infty} \varepsilon_{\alpha j}(\underline{x},t)\varepsilon_{\alpha j}(\underline{x} + \underline{\xi},t + \tau)\,dt\ .\end{aligned} \tag{9-83}$$

If the sensor output field is known to be stationary and homogeneous, we argue, as we did in section 9.2.1, that an estimate of the autocorrelation function from the j-th sample function can be obtained by averaging the

function $\varepsilon_{\alpha j}(\underline{x},t)\varepsilon_{\alpha j}(\underline{x} + \underline{\xi},t + \tau)$ over some appropriate ranges of space and time. We assert that the average over absolute time utilized to obtain the autocorrelation function from the j-th sample function of the stationary, nonhomogeneous field is also appropriate for estimating the autocorrelation function from the j-th sample function of the stationary, homogeneous field. Therefore, the estimate of the autocorrelation function from the j-th sample function of a stationary, homogeneous sensor output field can be written in a form similar to that in equation (9-19). That is,

$$\tilde{Q}_{00}(\underline{\xi},\tau)_j = \frac{1}{T(X_{1B} - X_{1A})(X_{2B} - X_{2A})}$$

$$\int_{-\infty}^{\infty} \int_{X_{1A}}^{X_{1B}} \int_{X_{2A}}^{X_{2B}} \varepsilon_{\alpha j}(\underline{x},t)\varepsilon_{\alpha j}(\underline{x} + \underline{\xi},t + \tau)\, dx_1\, dx_2\, dt \ . \qquad (9\text{-}84)$$

Here, $\tilde{Q}_{00}(\underline{\xi},\tau)_j$ denotes the estimate of the autocorrelation function of the stationary and homogeneous sensor output field obtained from the j-th sample function, X_{1A} and X_{1B} denote the lower and upper limits of the average over x_1, and X_{2A} and X_{2B} denote the lower and upper limits of the average over x_2.

By equation (9-80), it is evident that the function $\varepsilon_{\alpha j}(\underline{x},t)\varepsilon_{\alpha j}(\underline{x} + \underline{\xi},t + \tau)$ is nonzero only over that range of $\underline{x}$ where the product $b_w(\underline{x} - \underline{x}_0)b_w(\underline{x} + \underline{\xi} - \underline{x}_0)$ is nonzero. Recall that $b_w(\underline{x})$ is nonzero only within $-L_1/2 \leq x_1 \leq L_1/2$ and $-L_2/2 \leq x_2 \leq L_2/2$. This nonzero range of $b_w(\underline{x})$ is identical (see equation (9-10)) to the nonzero range of $b(\underline{x})$. Thus, the nonzero range of the product $b_w(\underline{x} - \underline{x}_0)b_w(\underline{x} + \underline{\xi} - \underline{x}_0)$ in the variables $\underline{x}$ and $\underline{\xi}$ is identical to the nonzero range of the product $b(\underline{x} - \underline{x}_0)b(\underline{x} + \underline{\xi} - \underline{x}_0)$, which is illustrated in figure 9-2. Inasmuch as (1) equations (9-84) and (9-19) are mathematically similar and (2) the integrands of these equations are nonzero, for any given $\underline{\xi}$, over identical ranges in $\underline{x}$, we can employ arguments identical to those applied to equation (9-19) to define appropriate values of the spatial limits X_{1A}, X_{1B}, X_{2A}, and X_{2B}. These appropriate limits are those specified by equations (9-26) to (9-29). By employing these limits in equation (9-84),

and by noting (see equation (9-80) and figure 9-2) that the function $\epsilon_{\alpha j}(\underline{x},t)\epsilon_{\alpha j}(\underline{x} + \underline{\xi},t + \tau)$ is identically zero for all choices of $\underline{\xi}$ when $|x_1| \geq L_1/2$ and $|x_2| \leq L_2/2$, we obtain the following expression for the estimate of the autocorrelation function of the stationary and homogeneous sensor output field from the j-th sample function:

$$\tilde{Q}_{00}(\underline{\xi},\tau)_j = \frac{1}{TL_1L_2} \int_{-\infty}^{\infty} \int_{-\infty}^{\infty} \int_{-\infty}^{\infty} \epsilon_{\alpha j}(\underline{x},t)\epsilon_{\alpha j}(\underline{x} + \underline{\xi},t + \tau)\, dx_1\, dx_2\, dt . \quad (9\text{-}85)$$

The estimate of the autocorrelation function of the stationary, homogeneous sensor output field, $\tilde{Q}_{00}(\underline{\xi},\tau)$, is formed by averaging the separate estimates formed from each of the J sample functions. That is,

$$\tilde{Q}_{00}(\underline{\xi},\tau) = \sum_{j=1}^{J} \tilde{Q}_{00}(\underline{\xi},\tau)_j$$

$$= \frac{1}{JTL_1L_2} \sum_{j=1}^{J} \int_{-\infty}^{\infty} \int_{-\infty}^{\infty} \int_{-\infty}^{\infty} \epsilon_{\alpha j}(\underline{x},t)\epsilon_{\alpha j}(\underline{x} + \underline{\xi},t + \tau)\, dx_1\, dx_2\, dt . \quad (9\text{-}86)$$

In accordance with the arguments advanced in section 9.2.1, we estimate the space-averaged autocorrelation function of a stationary, nonhomogeneous sensor output field by averaging the estimate of the nonhomogeneous autocorrelation function of that field over some appropriate region of absolute space. By applying this argument to equation (9-83), we obtain

$$\tilde{Q}^{a}_{00}(\underline{\xi},\tau) = \frac{1}{(X_{1B} - X_{1A})(X_{2B} - X_{2A})} \int_{X_{2A}}^{X_{2B}} \int_{X_{1A}}^{X_{1B}} \tilde{Q}_{00}(\underline{x},\underline{\xi},\tau)\, dx_1\, dx_2$$

$$= \frac{1}{(X_{1B} - X_{1A})(X_{2B} - X_{2A})JT} \sum_{j=1}^{J} \int_{-\infty}^{\infty} \int_{X_{2A}}^{X_{2B}} \int_{X_{1A}}^{X_{1B}} \epsilon_{\alpha j}(\underline{x},t)\epsilon_{\alpha j}(\underline{x} + \underline{\xi},t + \tau)\, dt .$$

(9-87)

In section 9.2.1, we argued that it was reasonable to select the limits associated with spatial averaging (i.e., X_{1A}, X_{1B}, X_{2A}, and X_{2B}) to be consistent with those chosen for the estimate of the autocorrelation function of the stationary, homogeneous sensor output field. The spatial limits used to estimate the autocorrelation function of the stationary, homogeneous field are those specified by equations (9-26) through (9-29). By use of these limits in equation (9-87), we obtain the following estimate of the space-averaged autocorrelation function of a stationary, nonhomogeneous sensor output field:

$$\tilde{Q}^{a}_{oo}(\underline{\xi},\tau) = \frac{1}{JTL_1L_2} \sum_{j=1}^{J} \int_{-\infty}^{\infty}\int_{-\infty}^{\infty}\int_{-\infty}^{\infty} \epsilon_{\alpha j}(\underline{x},t)\epsilon_{\alpha j}(\underline{x} + \underline{\xi},t + \tau)\, dx_1\, dx_2\, dt \ . \qquad (9\text{-}88)$$

Note that this estimate is mathematically identical to the estimate of the estimate of the autocorrelation function of the stationary, homogeneous sensor output field given by equation (9-86).

Smoothed estimates of the wavevector-frequency spectra of the sensor output field are obtained by appropriate Fourier transformations of the revised estimates of the autocorrelation functions developed above. From the definition of equation (6-121) and equation (9-83), the two wavevector-frequency spectrum of a stationary, nonhomogeneous sensor output field is estimated by

$$\tilde{S}_{oo}(\underline{\mu},\underline{k},\omega) = \frac{1}{JT} \sum_{j=1}^{J} \int_{-\infty}^{\infty}\int_{-\infty}^{\infty}\int_{-\infty}^{\infty}\int_{-\infty}^{\infty}\int_{-\infty}^{\infty}\int_{-\infty}^{\infty} \epsilon_{\alpha j}(\underline{x},t)\epsilon_{\alpha j}(\underline{x} + \underline{\xi},t + \tau)$$

$$\exp[-i(\underline{\mu}\cdot\underline{x} + \underline{k}\cdot\underline{\xi} + \omega\tau)]\, d\underline{x}\, d\underline{\xi}\, d\tau\, dt \ . \qquad (9\text{-}89)$$

A considerable simplification of the mathematical form of equation (9-89) can be realized by defining the Fourier pair

$$\mathcal{E}_{\alpha j}(\underline{k},\omega) = \int_{-\infty}^{\infty}\int_{-\infty}^{\infty}\int_{-\infty}^{\infty} \epsilon_{\alpha j}(\underline{x},t)\exp[-i(\underline{k}\cdot\underline{x} + \omega t)]\, d\underline{x}\, dt \qquad (9\text{-}90)$$

and

$$\varepsilon_{\alpha j}(\underline{x},t) = \frac{1}{(2\pi)^3}\int_{-\infty}^{\infty}\int_{-\infty}^{\infty}\int_{-\infty}^{\infty}\mathcal{E}_{\alpha j}(\underline{k},\omega)\exp\{i(\underline{k}\cdot\underline{x} + \omega t)\}\, d\underline{k}\, d\omega \; . \quad (9\text{-}91)$$

By writing $\varepsilon_{\alpha j}(\underline{x} + \underline{\xi}, t + \tau)$ in the integrand of equation (9-89) in the form of equation (9-91), we can employ equations (2-38) and (9-90) to show that the smoothed estimate of the two wavevector-frequency spectrum of a stationary, nonhomogeneous sensor output field can be expressed by

$$\tilde{S}_{oo}(\underline{\mu},\underline{k},\omega) = \frac{1}{JT}\sum_{j=1}^{J}\mathcal{E}_{\alpha j}(\underline{\mu} - \underline{k}, -\omega)\mathcal{E}_{\alpha j}(\underline{k},\omega) \; . \quad (9\text{-}92)$$

In a similar fashion, we can demonstrate, from equations (6-78) and (9-85) and from equations (6-149) and (9-88), that smoothed estimates of both the wavevector-frequency spectrum of a stationary, homogeneous sensor output field and the space-averaged wavevector-frequency spectrum of a stationary, nonhomogeneous sensor output field are given by

$$\tilde{\Phi}_o(\underline{k},\omega) = \tilde{\Phi}_o^a(\underline{k},\omega) = \frac{1}{JTL_1L_2}\sum_{j=1}^{J}|\mathcal{E}_{\alpha j}(\underline{k},\omega)|^2 \; . \quad (9\text{-}93)$$

Before we modify the Welch-smoothed estimators of wavevector-frequency spectra developed for a continuous sample function to accommodate measured data in the form of one or more discrete sample functions, it would seem prudent to examine the quality of these estimators in order to determine whether the smoothing process has been effective in reducing the variance of the spectral estimate. In section 9.2.1, we examined the bias and variance of our initial (unsmoothed) estimate of the wavevector-frequency spectrum of a stationary, homogeneous sensor output field. To determine the effects of the Welch smoothing process on the quality of the spectral estimates, we will compare the bias and variance of the smoothed estimate of the wavevector-frequency spectrum of the stationary, homogeneous sensor output field to the bias and variance of the unsmoothed estimate.

By use of equations (9-80), (9-90), and (9-93), we can show that the mean value of the smoothed estimate of the wavevector-frequency spectrum of a stationary, homogeneous sensor output field at any fixed values of $\underline{k}$ and ω can be written in the form

$$E\{\tilde{\Phi}_0(\underline{k},\omega)\} = \frac{1}{JTL_1L_2}\sum_{j=1}^{J}\int_{-\infty}^{\infty}\int_{-\infty}^{\infty}\int_{-\infty}^{\infty}\int_{-\infty}^{\infty}\int_{-\infty}^{\infty}\int_{-\infty}^{\infty} b_W(\underline{x} - \underline{x}_0)b_W(\underline{y} - \underline{x}_0)$$

$$a_W[t - t_0 + T_0/2 - (2j - 1)T/2]a_W[\theta - t_0 + T_0/2 - (2j - 1)T/2]$$

$$E\{o_\alpha(\underline{x},t)o_\alpha(\underline{y},\theta)\}\exp\{i(\underline{k}\cdot\underline{x} + \omega\tau)\}\exp\{-i(\underline{k}\cdot\underline{y} + \omega\theta)\}$$

$$d\underline{x}\ d\underline{y}\ dt\ d\theta\ . \tag{9-94}$$

However, for the stationary, homogeneous sensor output field,

$$E\{o_\alpha(\underline{x},t)o_\alpha(\underline{y},\theta)\} = Q_{00}(\underline{y} - \underline{x},\theta - t)$$

$$= \frac{1}{(2\pi)^3}\int_{-\infty}^{\infty}\int_{-\infty}^{\infty}\int_{-\infty}^{\infty} \Phi_0(\underline{\beta},\Omega)\exp\{i[\underline{\beta}\cdot(\underline{y} - \underline{x}) + \Omega(\theta - t)]\}\ d\underline{\beta}\ d\Omega\ . \tag{9-95}$$

By substituting equation (9-95) into equation (9-94), we can easily demonstrate that the mean of the spectral estimate is given by

$$E\{\tilde{\Phi}_0(\underline{k},\omega)\} = \frac{1}{(2\pi)^3TL_1L_2}\int_{-\infty}^{\infty}\int_{-\infty}^{\infty}\int_{-\infty}^{\infty} \Phi_0(\underline{\beta},\Omega)|A_W(\omega - \Omega)|^2\ |B_W(\underline{k} - \underline{\beta})|^2\ d\underline{\beta}\ d\Omega\ , \tag{9-96}$$

where

$$A_W(\omega) = \int_{-\infty}^{\infty} a_W(t)\exp(-i\omega t)\ dt\ , \tag{9-97}$$

$$B_W(\underline{k}) = \int_{-\infty}^{\infty}\int_{-\infty}^{\infty} b_W(\underline{x})\exp(-i\underline{k}\cdot\underline{x})\ d\underline{x}\ . \tag{9-98}$$

Note, from equation (9-96), that the mean of the spectral estimate is independent of the number, J, of (hopefully, statistically independent) estimates of the spectrum, and is equal to the convolution of the true spectrum with spectral windows, $|A_w(\omega - \Omega)|^2$ and $|B_w(\underline{k} - \underline{\beta})|^2$, in both the frequency and wavevector domains. Thus, according to the definition of equation (9-1), the Welch-smoothed estimate of the wavevector-frequency spectrum of the stationary, homogeneous sensor output field is, in general, a biased one.

Recall that the temporal and spatial weighting functions, $a_w(t)$ and $b_w(\underline{x})$, are real and even functions of time and space, respectively. It therefore follows that the spectral windows $|A_w(\omega)|^2$ and $|B_w(\underline{k})|^2$ are real and even functions of their respective independent variables. The temporal and spatial weighting functions are normally specified such that $|A_w(\omega)|^2$ is characterized by a maximum at $\omega = 0$ and $|B_w(\underline{k})|^2$ is characterized by a maximum at $\underline{k} = (0,0)$. If $a_w(t)$ and $b_w(\underline{x})$ are chosen such that the bandwidths associated with the maxima of $|A_w(\omega)|^2$ and $|B_w(\underline{k})|^2$ are narrower than any fluctuation of the true wavevector-frequency spectrum in ω, k_1, and k_2, then we assert that, in the convolution of equation (9-96), the role of the spectral windows, $|A_w(\omega - \Omega)|^2$ and $|B_w(\underline{k} - \underline{\beta})|^2$, is to "sample" the true wavevector-frequency spectrum, $\Phi_0(\underline{\beta},\Omega)$, at the frequency $\Omega = \omega$ and at the wavevector $\underline{\beta} = \underline{k}$. In this case, equation (9-96) is well approximated by

$$E[\tilde{\Phi}_0(\underline{k},\omega)] \approx \Phi_0(\underline{k},\omega)\left\{\frac{1}{2\pi T}\int_{-\infty}^{\infty} |A_w(\Omega)|^2\, d\Omega\right\}$$

$$\left\{\frac{1}{(2\pi)^2 L_1 L_2}\int_{-\infty}^{\infty}\int_{-\infty}^{\infty} |B_w(\underline{\beta})|^2\, d\underline{\beta}\right\} . \qquad (9\text{-}99)$$

However, by arguments similar to those used in equation (9-55), it is straightforward to show that

$$\frac{1}{2\pi T}\int_{-\infty}^{\infty} |A_w(\Omega)|^2\, d\Omega = \frac{1}{T}\int_{-\infty}^{\infty} a_w^2(t)\, dt \qquad (9\text{-}100)$$

and

$$\frac{1}{(2\pi)^2 L_1 L_2} \int_{-\infty}^{\infty} \int_{-\infty}^{\infty} |B_w(\underline{\beta})|^2 \, d\underline{\beta} = \frac{1}{L_1 L_2} \int_{-\infty}^{\infty} \int_{-\infty}^{\infty} b_w^2(\underline{x}) \, d\underline{x} \ . \qquad (9\text{-}101)$$

Note that, if $a_w(t)$ and $b_w(\underline{x})$ are chosen such that (1) equation (9-99) is a valid approximation and (2) the integrals of equations (9-100) and (9-101) are both equal to one, then

$$E\{\tilde{\Phi}_0(\underline{k},\omega)\} \approx \Phi_0(\underline{k},\omega) \ , \qquad (9\text{-}102)$$

and the smoothed estimate is essentially unbiased.

To evaluate the mean square error of the smoothed estimate, we must (by equation (9-7)) evaluate the variance of the estimate. To evaluate the variance of the wavevector-frequency spectrum of the stationary, homogeneous sensor output field, we must first (see equation (9-57)) formulate an expression for $E\{\tilde{\Phi}_0^2(\underline{k},\omega)\}$.

From equation (9-93), by using the definitions of equations (9-90) and (9-80), we can show that

$$E\{\tilde{\Phi}_0^2(\underline{k},\omega)\} = \frac{1}{(JTL_1L_2)^2} \sum_{j=1}^{J} \sum_{m=1}^{J} \int_{-\infty}^{\infty}\int_{-\infty}^{\infty}\int_{-\infty}^{\infty}\int_{-\infty}^{\infty}\int_{-\infty}^{\infty}\int_{-\infty}^{\infty}\int_{-\infty}^{\infty}\int_{-\infty}^{\infty}\int_{-\infty}^{\infty}\int_{-\infty}^{\infty}\int_{-\infty}^{\infty}\int_{-\infty}^{\infty}$$

$$a_w[t_1 - t_0 + T_0/2 - (2j - 1)T/2]a_w[t_2 - t_0 + T_0/2 - (2j - 1)T/2]$$

$$a_w[t_3 - t_0 + T_0/2 - (2m - 1)T/2]a_w[t_4 - t_0 + T_0/2 - (2m - 1)T/2]$$

$$b_w(\underline{x}_1 - \underline{x}_0)b_w(\underline{x}_2 - \underline{x}_0)b_w(\underline{x}_3 - \underline{x}_0)b_w(\underline{x}_4 - \underline{x}_0)$$

$$E\{o_\alpha(\underline{x}_1,t_1)o_\alpha(\underline{x}_2,t_2)o_\alpha(\underline{x}_3,t_3)o_\alpha(\underline{x}_4,t_4)\}$$

$$\exp[i(\underline{k}\cdot\underline{x}_1 + \omega t_1)]\exp[-i(\underline{k}\cdot\underline{x}_2 + \omega t_2)]\exp[i(\underline{k}\cdot\underline{x}_3 + \omega t_3)]$$

$$\exp[-i(\underline{k}\cdot\underline{x}_4 + \omega t_4)] \, d\underline{x}_1 \, d\underline{x}_2 \, d\underline{x}_3 \, d\underline{x}_4 \, dt_1 \, dt_2 \, dt_3 \, dt_4 \ . \qquad (9\text{-}103)$$

Recall, from section 9.2.1, that in order to evaluate the fourth-order moment $E\{o_\alpha(\underline{x}_1,t_1)o_\alpha(\underline{x}_2,t_2)o_\alpha(\underline{x}_3,t_3)o_\alpha(\underline{x}_4,t_4)\}$, we assumed that $o(\underline{x},t)$ was a Gaussian random process. By again assuming $o(\underline{x},t)$ to be a Gaussian random process, and by employing the consequent relationship given by equation (9-61) in equation (9-103), we obtain

$$E\{\tilde{\Phi}_0^2(\underline{k},\omega)\} = \frac{1}{[(2\pi)^3 JTL_1L_2]^2} \sum_{j=1}^{J} \sum_{m=1}^{J} \int_{-\infty}^{\infty}\int_{-\infty}^{\infty}\int_{-\infty}^{\infty}\int_{-\infty}^{\infty}\int_{-\infty}^{\infty}\int_{-\infty}^{\infty} \Phi_0(\underline{\mu},\Omega)\Phi_0(\underline{\beta},\Gamma)$$

$$\{|A_w(\omega - \Omega)|^2 |B_w(\underline{k} - \underline{\mu})|^2 |A_w(\omega - \Gamma)|^2 |B_w(\underline{k} - \underline{\beta})|^2$$

$$+ A_w^*(\omega - \Omega)A_w^*(\omega + \Omega)B_w^*(\underline{k} - \underline{\mu})B_w^*(\underline{k} + \underline{\mu})$$

$$A_w(\omega - \Gamma)A_w(\omega + \Gamma)B_w(\underline{k} - \underline{\beta})B_w(\underline{k} + \underline{\beta})\exp[-i(\Omega + \Gamma)(j - m)T]$$

$$+ |A_w(\omega - \Omega)|^2 |B_w(\underline{k} - \underline{\mu})|^2 |A_w(\omega + \Gamma)|^2 |B_w(\underline{k} + \underline{\beta})|^2$$

$$\exp[-i(\Omega + \Gamma)(j - m)T]\}\, d\underline{\mu}\, d\Omega\, d\underline{\beta}\, d\Gamma \; . \qquad (9\text{-}104)$$

However, by use of equation (9-63), we can demonstrate that equation (9-104) can be rewritten in the form

$$E\{\tilde{\Phi}_0^2(\underline{k},\omega)\} =$$

$$\frac{1}{[(2\pi)^3 JTL_1L_2]^2} \sum_{j=1}^{J} \sum_{m=1}^{J} \Bigg\{ \int_{-\infty}^{\infty}\int_{-\infty}^{\infty}\int_{-\infty}^{\infty} \Phi_0(\underline{\mu},\Omega)|A_w(\omega - \Omega)|^2 |B_w(\underline{k} - \underline{\mu})|^2\, d\underline{\mu}\, d\Omega$$

$$\int_{-\infty}^{\infty}\int_{-\infty}^{\infty}\int_{-\infty}^{\infty} \Phi_0(\underline{\beta},\Gamma)|A_w(\omega - \Gamma)|^2 |B_w(\underline{k} - \underline{\beta})|^2\, d\underline{\beta}\, d\Gamma$$

$$+ \left| \int_{-\infty}^{\infty}\int_{-\infty}^{\infty}\int_{-\infty}^{\infty} \Phi_0(\underline{\beta},\Gamma)A_w(\omega - \Gamma)A_w(\omega + \Gamma)B_w(\underline{k} - \underline{\beta})B_w(\underline{k} + \underline{\beta})\exp[-i\Gamma(j - m)T]\, d\underline{\beta}\, d\Gamma \right|^2$$

$$+ \left| \int_{-\infty}^{\infty}\int_{-\infty}^{\infty}\int_{-\infty}^{\infty} \Phi_0(\underline{\beta},\Gamma)|A_w(\omega - \Gamma)|^2 |B_w(\underline{k} - \underline{\beta})|^2 \exp[-i\Gamma(j - m)T]\, d\underline{\beta}\, d\Gamma \right|^2 \Bigg\} .$$

$$(9\text{-}105)$$

The first term on the right-hand side of equation (9-105) is independent of j and, by reference to equation (9-96), is equal to $[E\{\tilde{\Phi}_0(\underline{k},\omega)\}]^2$. Thus, it follows from equation (9-57) that

$$\mathrm{Var}\{\tilde{\Phi}_0(\underline{k},\omega)\} = \frac{1}{[(2\pi)^3 JTL_1L_2]^2} \sum_{j=1}^{J} \sum_{m=1}^{J} \left\{ \left| \int_{-\infty}^{\infty}\int_{-\infty}^{\infty}\int_{-\infty}^{\infty} \Phi_0(\underline{\beta},\Gamma) A_W(\omega-\Gamma) A_W(\omega+\Gamma) B_W(\underline{k}-\underline{\beta}) B_W(\underline{k}+\underline{\beta}) \exp[-i\Gamma(j-m)T]\, d\underline{\beta}\, d\Gamma \right|^2 + \left| \int_{-\infty}^{\infty}\int_{-\infty}^{\infty}\int_{-\infty}^{\infty} \Phi_0(\underline{\beta},\Gamma) |A_W(\omega-\Gamma)|^2 |B_W(\underline{k}-\underline{\beta})|^2 \exp[-i\Gamma(j-m)T]\, d\underline{\beta}\, d\Gamma \right|^2 \right\}. \qquad (9\text{-}106)$$

We cannot exactly evaluate the variance as stated in equation (9-106). However, by applying arguments analogous to those presented by Nuttall,[21] we can obtain a good approximation to the variance.

Nuttall first argues that if the frequency of interest, ω, is greater than the bandwidth of the primary response lobe of the spectral window $|A_W(\omega)|^2$, then the primary response lobes of $A_W(\omega - \Gamma)$ and $A_W(\omega + \Gamma)$ do not overlap significantly. In this case (for useful spectral windows), the product $A_W(\omega - \Gamma)A_W(\omega + \Gamma)$ is much less than $|A_W(\omega - \Gamma)|^2$. Analogously, if the components (k_1 and k_2) of the wavevector ($\underline{k}$) of interest are greater than the bandwidths of the primary response lobe of the spectral window $|B_W(\underline{k})|^2$ in their respective coordinate directions, then the primary response lobes of $B_W(\underline{k} - \underline{\beta})$ and $B_W(\underline{k} + \underline{\beta})$ do not overlap significantly. In this case, the product $B_W(\underline{k} - \underline{\beta})B_W(\underline{k} + \underline{\beta})$ is much less than $|B_W(\underline{k} - \underline{\beta})|^2$. Thus, for such wavevectors and frequencies, the contribution to the variance from the first term on the right-hand side of equation (9-106) will be much smaller than the contribution from the second term, so the variance is well approximated by

$$\mathrm{Var}\{\tilde{\Phi}_0(\underline{k},\omega)\} \approx \frac{1}{[(2\pi)^3 JTL_1L_2]^2} \sum_{j=1}^{J} \sum_{m=1}^{J} \left| \int_{-\infty}^{\infty}\int_{-\infty}^{\infty}\int_{-\infty}^{\infty} \Phi_0(\underline{\beta},\Gamma) |A_W(\omega-\Gamma)|^2 |B_W(\underline{k}-\underline{\beta})|^2 \exp[-i\Gamma(j-m)T]\, d\underline{\beta}\, d\Gamma \right|^2 . \qquad (9\text{-}107)$$

For $\omega = 0$ and $\underline{k} = (0,0)$, the first and second terms in equation (9-106) are equal, and the variance is twice the value given by equation (9-107).

Nuttall next shows that, by the change of variable $n = j - m$, equation (9-107) can be rewritten in the form

$$\mathrm{Var}\{\tilde{\Phi}_o(\underline{k},\omega)\} \approx \frac{1}{[(2\pi)^3 T L_1 L_2]^2 J} \sum_{n=-(J-1)}^{J-1} (1 - |n|/J) \left| \int_{-\infty}^{\infty}\int_{-\infty}^{\infty}\int_{-\infty}^{\infty} \Phi_o(\underline{\beta},\Gamma) \right.$$

$$\left. |A_w(\omega - \Gamma)|^2 |B_w(\underline{k} - \underline{\beta})|^2 \exp(-i\Gamma nT)\, d\underline{\beta}\, d\Gamma \right|^2 . \qquad (9\text{-}108)$$

If the bandwidths of the primary response lobes of the spectral windows $|A_w(\Gamma)|^2$ and $|B_w(\underline{\beta})|^2$ are narrower than the widths of any fluctuation of $\Phi_o(\underline{\beta},\Gamma)$ in Γ, β_1, and β_2, then equation (9-108) can be approximated by

$$\mathrm{Var}\{\tilde{\Phi}_o(\underline{k},\omega)\} \approx \frac{\Phi_o^2(\underline{k},\omega)}{(2\pi)^6 (T L_1 L_2)^2 J} \sum_{n=-(J-1)}^{J-1} \left(1 - \frac{|n|}{J}\right)$$

$$\left| \int_{-\infty}^{\infty}\int_{-\infty}^{\infty} |B_w(\underline{k} - \underline{\beta})|^2\, d\underline{\beta} \right|^2 \left| \int_{-\infty}^{\infty} |A_w(\omega - \Gamma)|^2 \exp(-i\Gamma nT)\, d\Gamma \right|^2 . \qquad (9\text{-}109)$$

However, we can easily demonstrate that

$$\frac{1}{(2\pi)} \int_{-\infty}^{\infty} |A_w(\omega - \Gamma)|^2 \exp(-i\Gamma nT)\, d\Gamma = \exp(-i\omega nT) \int_{-\infty}^{\infty} a_w(t) a_w(t + nT)\, dt \qquad (9\text{-}110)$$

and that

$$\frac{1}{(2\pi)^2} \int_{-\infty}^{\infty}\int_{-\infty}^{\infty} |B_w(\underline{k} - \underline{\beta})|^2\, d\underline{\beta} = \int_{-\infty}^{\infty}\int_{-\infty}^{\infty} b_w^2(\underline{x})\, d\underline{x} . \qquad (9\text{-}111)$$

Therefore, it follows that

$$\mathrm{Var}\{\tilde{\Phi}_0(\underline{k},\omega)\} \approx \Phi_0^2(\underline{k},\omega)\left\{\frac{1}{L_1L_2}\int_{-\infty}^{\infty}\int_{-\infty}^{\infty} b_w^2\,(\underline{x})\;d\underline{x}\right\}^2$$

$$\frac{1}{J}\sum_{n=-(J-1)}^{J-1}(1-|n|/J)\left\{\frac{1}{T}\int_{-\infty}^{\infty} a_w(t)a_w(t+nT)\;dt\right\}^2. \qquad (9\text{-}112)$$

Recall that the weighting function $a_w(t)$ is a real and even function of time that is nonzero only within $-T/2 \leq t \leq T/2$. Thus,

$$\int_{-\infty}^{\infty} a_w(t)a_w(t+nT)\;dt = \delta_{n0}\int_{-\infty}^{\infty} a_w^2(t)\;dt \quad , \qquad (9\text{-}113)$$

where δ_{nm} denotes the Kronecker delta function, which equals unity when $n = m$ and is zero otherwise.

By substituting equation (9-113) into equation (9-112) and performing the summation on n, we obtain

$$\mathrm{Var}\{\tilde{\Phi}_0(\underline{k},\omega)\} \approx \frac{1}{J}\,\Phi_0^2(\underline{k},\omega)\left\{\frac{1}{L_1L_2}\int_{-\infty}^{\infty}\int_{-\infty}^{\infty} b_w^2(\underline{x})\;d\underline{x}\right\}^2\left\{\frac{1}{T}\int_{-\infty}^{\infty} a_w^2(t)\;dt\right\}^2 . \qquad (9\text{-}114)$$

The weighting function $b_w(\underline{x})$ is a real and even function of k_1 and k_2 that is nonzero only within $|x_1| \leq L_1/2$ and $|x_2| \leq L_2/2$. Further, inasmuch as all practical weightings are finite, $a_w(t)$ and $b_w(\underline{x})$ are finite for all t and $\underline{x}$, respectively. Because $a_w(t)$ and $b_w(\underline{x})$ are both finite, band-limited functions, the integrals of $a_w^2(t)$ and $b_w^2(\underline{x})$ in equation (9-114) are finite constants. Therefore, it follows that the variance of the Welch-smoothed estimate of the wavevector-frequency spectrum of the stationary, homogeneous sensor output field is inversely proportional to the number (J) of independent estimates averaged to form the final spectral estimate, and approaches zero as J tends to infinity.

Given that the variance of the Welch-smoothed estimate of the wavevector-frequency spectrum of the stationary, homogeneous sensor output field tends to

zero as J approaches infinity, it follows from equation (9-7) that the mean square error of the estimate is equal to the square of the bias error. Recall that the mean value of the Welch-smoothed estimate is independent of J, and approximates the value of the true spectrum only when (1) the bandwidths of the spectral windows $|A_W(\omega)|^2$ and $|B_W(\underline{k})|^2$ are narrower than any fluctuation of the true spectrum in ω, k_1, and k_2 and (2) the mean value of $a_W^2(t)$ over time and of $b_W^2(\underline{x})$ over space (see equations (9-100) and (9-101)) are both equal to unity. Given that both of these conditions are satisfied, the bias error is effectively zero, and equation (9-93) provides an essentially consistent estimate of the wavevector-frequency spectrum of a stationary, homogeneous sensor output field.

It is of interest to note (see equations (9-2) and (9-96)) that the bias error depends on the bandwidths of the spectral windows, $|A_W(\omega)|^2$ and $|B_W(\underline{k})|^2$, relative to the bandwidths of the fluctuations of the true wavevector-frequency spectrum, $\Phi_0(\underline{k},\omega)$, in ω, k_1, and k_2, whereas the variance of the spectral estimate (see equation (9-114)) depends on the number, J, of independent estimates of the spectrum that are averaged to form the final spectral estimate. To illustrate the practical implications of this observation, consider the problem of estimating the wavevector-frequency spectrum of a stationary, homogeneous sensor output field from a sample function, $o_\alpha(\underline{x},t)$, observed continuously over the space within $|x_1| \le L_1/2$ and $|x_2| \le L_2/2$, and over the time $|t| \le T_0/2$. We desire to estimate the wavevector-frequency spectrum by utilizing the Welch-smoothed method, and therefore we wish to partition the sample function in time to create J sample functions, each of length $T = T_0/J$. How do we choose J in order to obtain the best estimate of the wavevector-frequency spectrum?

For simplicity, let us assume that the temporal and spatial weighting functions are uniform, and are given by

$$a_W(t) = \begin{cases} 1/T, & |t| \le T/2 , \\ 0, & \text{otherwise}, \end{cases} \qquad (9\text{-}115)$$

and

$$b_w(\underline{x}) = \begin{cases} 1/(L_1L_2), & |x_1| \le L_1/2 \text{ and } |x_2| \le L_2/2 \ , \\ 0, & \text{otherwise.} \end{cases} \tag{9-116}$$

The consequent spectral windows, $|A_w(\omega)|^2$ and $|B_w(\underline{k})|^2$, are

$$|A_w(\omega)|^2 = \frac{\sin^2(\omega T/2)}{(\omega T/2)^2} \tag{9-117}$$

and

$$|B_w(\underline{k})|^2 = \frac{\sin^2(k_1L_1/2)\sin^2(k_2L_2/2)}{(k_1L_1/2)^2(k_2L_2/2)^2} \ . \tag{9-118}$$

The bandwidth of the primary acceptance lobe of $|A_w(\omega)|^2$ can be shown to be $4\pi/T$, and the bandwidths of the primary acceptance lobe of $|B_w(\underline{k})|^2$ in the k_1 and k_2 coordinate directions are $4\pi/L_1$ and $4\pi/L_2$, respectively.

By equation (9-96) and successive arguments, we desire that the primary acceptance lobes of $|A_w(\omega)|^2$ and $|B_w(\underline{k})|^2$ be as narrow as possible in order to minimize the bias error. Inasmuch as the bandwidths of these acceptance lobes are inversely proportional to T and to L_1 and L_2, we clearly wish to select these parameters to be as large as possible in order to minimize the bias of the estimate. However, the mean square error of the estimate is equal to the sum of the variance of the estimate and the square of the bias error, and the variance of the estimate is inversely proportional to J, the number of time partitions of the original sample function. To minimize the bias, we should select the largest possible value of T; that is, $T = T_0$. However, for that choice of T, J would be unity, and the variance of the estimate would be relatively large. Conversely, to minimize the variance of the estimate, we should select J to be large. However, given that T_0 is fixed, a large value of J results in a small value of T, a consequent wide bandwidth of the primary acceptance lobe of $|A_w(\omega)|^2$, and thereby a (potentially) large bias error.

Clearly, in choosing a temporal partitioning of a sample function, one

must make some tradeoff between the bias error and variance of the estimate. Given some preknowledge of the wavevector-frequency characteristics of the true spectrum and some control of the temporal extent of the measurement, one can often partition the measured data in such a fashion that the bias error and variance of the spectral estimate are kept within acceptable limits.

By applying arguments similar to those used above, one can evaluate the bias and variance of Welch-smoothed estimates of the two wavevector-frequency spectrum and the space-averaged wavevector-frequency spectrum. These estimates, like that of the wavevector-frequency spectrum of the stationary, homogeneous field, are generally biased and have variances that decrease with increasing J. Detailed analyses of the bias and variance of these spectral forms are left as an exercise for the interested reader.

Let us now adapt the smoothed estimators developed for a single, continuous, space-time sample function to the more realistic data format of one or more, spatially and temporally discrete, sample functions of the sensor output field.

9.3 ESTIMATORS OF WAVEVECTOR-FREQUENCY SPECTRA FROM DISCRETE SPACE-TIME SAMPLE FUNCTIONS

As we explained in chapter 8, practical considerations prohibit us from observing the sensor output field over any continuous portion of time and space. Rather, practical measurements of acoustic fields are made by using arrays of sensors. From such arrays, we are provided with continuous knowledge, over some finite interval of time, of the sensor output field at discrete locations in space. To accommodate modern digital signal processing techniques, the continuous outputs from all sensors of the array are synchronously sampled at discrete intervals in time.

We assume that the acoustic field of interest is spatially sampled by the M x N array of sensors illustrated in figure 9-6. Here, the sensors are uniformly separated by d_1 in the x_1 coordinate direction and by d_2 in the x_2 coordinate direction. The choice of the spatial origin is an

arbitrary one and, for mathematical convenience, we choose it coincident with the geometric center of the array. The vector location, $\underline{x}_{mn}$, of the center of the mn-th sensor is therefore given by

$$\underline{x}_{mn} = \left\{ \left[m - \left(\frac{M+1}{2} \right) \right] d_1 ,\ \left[n - \left(\frac{N+1}{2} \right) \right] d_2 \right\} . \qquad (9\text{-}119)$$

For nonhomogeneous fields, the estimate of the two wavevector-frequency spectrum referred to the spatial origin at the array center can be transformed to an estimate referred to any other spatial origin by use of equation (8-181).

Because we intend to estimate the wavevector-frequency spectrum by means of a digital computer, the outputs of all sensors are assumed to be sampled synchronously at uniform increments in time. Figure 9-7 illustrates the temporal sampling of the output, $o(\underline{x}_{mn},t)$, of the mn-th sensor of the array. As indicated in this figure, the output of each sensor is sampled at uniform increments of T_s seconds. We assume that a single discrete sample function of the sensor output field comprises P temporal samples from all MN sensors in the array. We further assume that the temporal extent of the measurement is sufficient to yield J discrete sample functions.

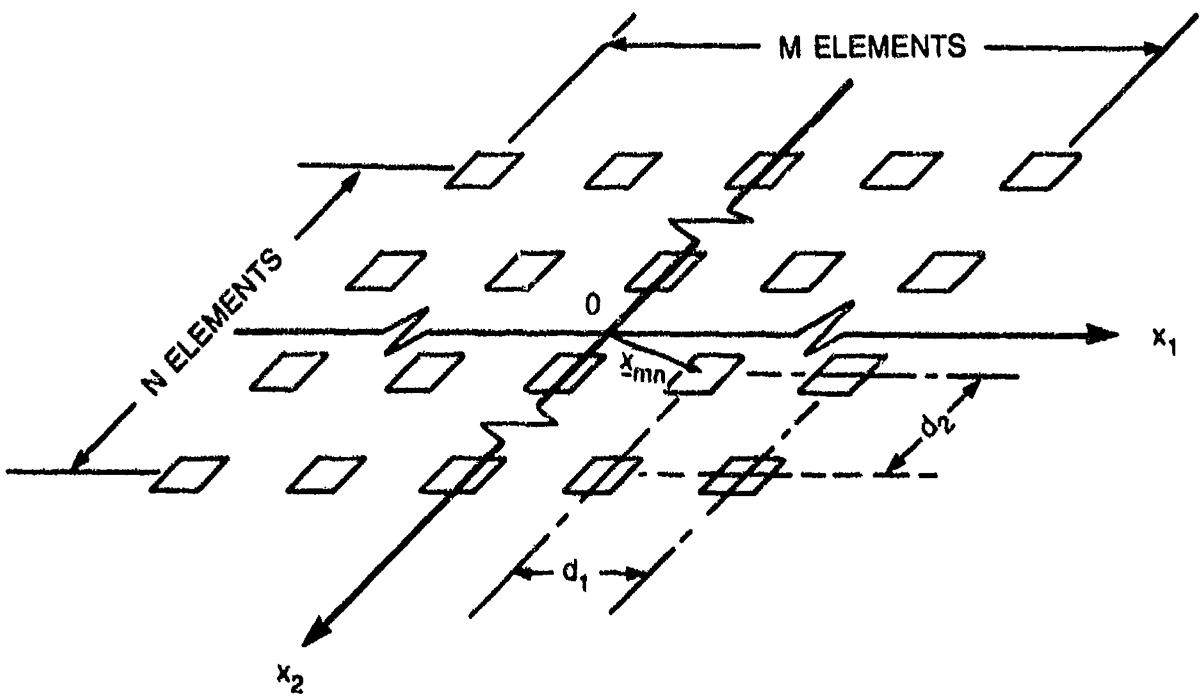

Figure 9-6. The Array Geometry

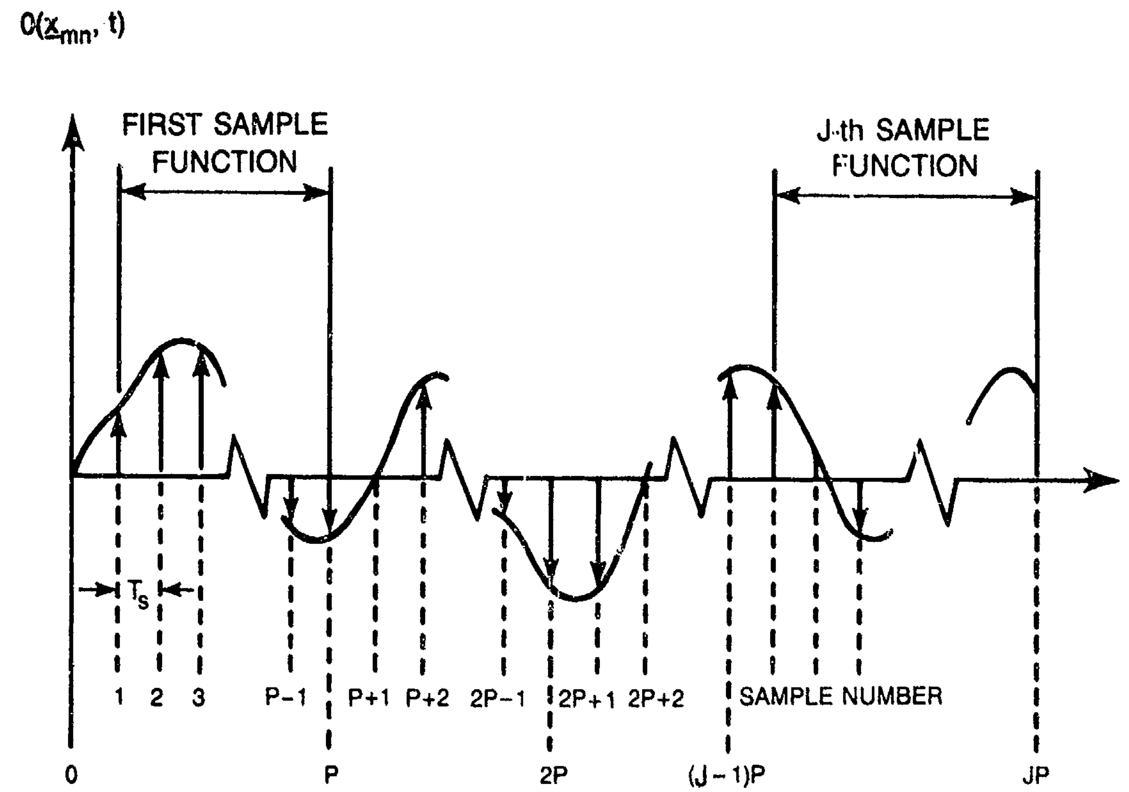

Figure 9-7. Temporal Sampling of the mn-th Sensor

We will assume that the true wavevector-frequency spectrum of the sensor output field is, or has been rendered (by appropriate lowpass filtering), band limited in both the wavevector and frequency domains. We will further assume that the spatial and temporal sampling increments have been selected to preclude aliasing errors in the spectral estimate. There remains one other sampling issue that should be addressed.

Recall that the Welch-smoothed estimate of the wavevector-frequency spectrum is formed by averaging the ensemble of wavevector-frequency spectra estimated from each of the J sample functions of the sensor output field. Ideally, we desire that the spectral estimates formed from each of the J individual sample functions be statistically independent of each other inasmuch as the bias and consistency of the estimate (see equations (9-1) and (9-4)) are defined on the basis of the behavior of the mean and mean square errors with increasing numbers of statistically independent estimates. We note from equations (9-80), (9-90), (9-92), and (9-93) that spectral estimates formed from the j-th sample function are functions of $o_{\alpha j}(\underline{x},t)$, the j-th sample function of the random process $o_{\alpha}(\underline{x},t)$. It can therefore be

demonstrated, from arguments presented in chapter 6 (see section 6.1.2), that spectral estimates formed from the j-th and k-th sample functions will be statistically independent if the sample functions $o_{\alpha j}(\underline{x},t)$ and $o_{\alpha k}(\underline{x},t)$ are independent random processes.

If we assume that $o(\underline{x},t)$ is a Gaussian random process, then it follows[22] that the j-th and k-th sample functions, $o_j(\underline{x},t)$ and $o_k(\underline{x},t)$, are jointly Gaussian random processes. Papoulis[23] shows that two jointly random variables are statistically independent if the random variables are uncorrelated. Therefore, if we make the (not unreasonable) assumption that $o(\underline{x},t)$ is a zero mean Gaussian random process, a sufficient condition for the statistical independence of the spectral estimates formed from the j-th and k-th sample functions is that the j-th and k-th sample functions, $o_j(\underline{x},t)$ and $o_k(\underline{x},t)$, be uncorrelated for all $\underline{x}$ and t.

Let us define τ_{max} to be the largest time delay required for the true autocorrelation function, $Q_{oo}(\underline{x},\underline{\xi},\tau)$ or $Q_{oo}(\underline{\xi},\tau)$, of the sensor output field to become effectively zero over the range of $\underline{x}$ and $\underline{\xi}$ afforded by the array. To ensure statistical independence of adjacent (and thereby all) sample functions, we require a temporal interval equal to or greater than τ_{max} between the last temporal sample of one sample function and the first temporal sample of the succeeding sample function. Clearly, such a temporal interval between sample functions reduces the total number (J) of sample functions attainable from any measurement of a fixed time duration.

In practice, one can effectively eliminate the requirement for such intervals between sample functions by choosing the temporal length (PT_s) of each of the J sample functions to be much greater than the maximum correlation time (τ_{max}) of the sensor output field. By this choice (1) only adjacent sample functions are substantially correlated, (2) the temporal extent over which a given sample function is correlated with its adjacent sample functions is small compared to the temporal length of the sample function, and (3) such correlation occurs only at the beginning and end of the sample function. Inasmuch as each of the J sample functions is uncorrelated with most other sample functions, and inasmuch as the correlation that exists between adjacent sample functions occurs only in regions at the ends of each sample function

that are small in comparison to the total length of the sample function, we assert that this choice for the length of the sample functions renders them, for practical purposes, essentially statistically independent.

We therefore assume that the temporal lengths, PT_s, of the sample functions are chosen to be much greater than τ_{max} so that all sample functions are, for practical purposes, statistically independent of each other.

Note that if the sample functions obtained by temporally partitioning each realization of an experiment are statistically independent, then additional realizations or repetitions of the experiment simply increase the number of sample functions and, thereby, the number of sample spectral estimates to be averaged.

For the spatial and temporal samplings described above, our knowledge of the sensor output field from any single realization of the measurement is limited to the J discrete sample functions $o_{\alpha j}\{\underline{x}_{mn},[p + (j - 1)P]T_s\}$, specified over the integer values $1 \leq m \leq M$, $1 \leq n \leq N$, $1 \leq p \leq P$, $1 \leq j \leq J$. However, given that the J sample functions are statistically independent of each other, we can interpret each sample function as an independent realization of the measurement. With this interpretation, we do not require knowledge of the temporal behavior of each discrete sample function relative to the absolute temporal origin of the sampling process. Rather, for each independent realization, we require only temporal knowledge of the associated sample function relative to a temporal origin defined for that realization. If we choose the temporal origin of each statistically independent sample function to be the center of the P samples and define

$$t_p = [p - (P + 1)2]T_s \ , \qquad (9\text{-}120)$$

we can interpret our knowledge of the sensor output field to be the J statistically independent sample functions $o_j(\underline{x}_{mn},t_p)$ specified over the integer values $1 \leq m \leq M$, $1 \leq n \leq N$, $1 \leq p \leq P$, $1 \leq j \leq J$.

Recall that in the Welch-smoothing process, temporal and spatial weightings $a_w(t)$ and $b_w(\underline{x})$, respectively, are applied to each sample

function. We require $a_w(t)$ to be an even function of t and $b_w(\underline{x})$ to be an even function of both x_1 and x_2. By applying these weightings to each of the discrete sample functions of the sensor output field, we form the discrete analog, $\epsilon_j(\underline{x}_{mn},t_p)$, of $\epsilon_{\alpha j}(x,t)$ defined by equation (9-80). That is,

$$\epsilon_j(\underline{x}_{mn},t_p) = \begin{cases} a_w(t_p)b_w(\underline{x}_{mn})o_{\alpha j}(\underline{x}_{mn},t_p) \ , & \text{for } 1 \le m \le M \ , \ 1 \le n \le N \ , \\ & 1 \le p \le P \ , \ 1 \le j \le J \ , \\ 0, & \text{otherwise.} \end{cases} \tag{9-121}$$

The Welch-smoothed estimates of wavevector-frequency spectra given by equations (9-92) and (9-93) are expressed in terms of products of the wavevector-frequency transform of $\epsilon_{\alpha j}(\underline{x},t)$. However, our knowledge of $\epsilon_{\alpha j}(\underline{x},t)$ is limited to the set of discrete sample functions defined by equation (9-121). Therefore, we cannot obtain the exact wavevector-frequency transform of $\epsilon_{\alpha j}(\underline{x},t)$. Rather, at best, we can approximate the wavevector-frequency transform of $\epsilon_{\alpha j}(\underline{x},t)$ by the discrete wavevector-frequency transform of $\epsilon_j(\underline{x}_{mn},t_p)$. That discrete wavevector-frequency transform, which we denote by $\mathcal{E}_{jd}(\underline{k},\omega)$, is obtained by replacing the integrals in equation (9-90) by appropriate summations, and is given by

$$\mathcal{E}_{jd}(\underline{k},\omega) = d_1 d_2 T_s \sum_{m=1}^{M} \sum_{n=1}^{N} \sum_{p=1}^{P} \epsilon_j(\underline{x}_{mn},t_p)\exp[-i(k\cdot\underline{x}_{mn} + \omega t_p)] \ . \tag{9-122}$$

Welch-smoothed estimates of wavevector-frequency spectra from measured data in the format of discrete spatial and temporal samples of the sensor output field are formulated by substituting appropriate forms of $\mathcal{E}_{jd}(\underline{k},\omega)$ in place of $\mathcal{E}_{\alpha j}(\underline{k},\omega)$ in equations (9-92) and (9-93). By applying this substitution to equation (9-92), and by recognizing that the temporal length (T) of each continuous sample function in equation (9-92) must be replaced by the effective temporal length (PT_s) of each discrete sample function, we obtain the following smoothed estimate for the two wavevector-frequency spectrum of a stationary, nonhomogeneous sensor output field:

$$\tilde{S}_{oo}(\underline{\mu},\underline{k},\omega) = \frac{1}{JPT_s} \sum_{j=1}^{J} \mathcal{E}_{jd}(\underline{\mu} - \underline{k},-\omega)\mathcal{E}_{jd}(\underline{k},\omega) \ . \tag{9-123}$$

By applying similar arguments to equation (9-93), and by recognizing that the area of continuous observation (L_1L_2) must be replaced by the effective area of discrete observations (Md_1Nd_2), we obtain Welch-smoothed estimates for both the wavevector-frequency spectrum of a homogeneous, stationary sensor output field and the space-averaged wavevector-frequency spectrum of a nonhomogeneous, stationary sensor output field. These estimators are mathematically identical, and are given by

$$\tilde{\Phi}_o(\underline{k},\omega) = \tilde{\Phi}_o^a(\underline{k},\omega) = \frac{1}{JMd_1Nd_2PT_s} \sum_{j=1}^{J} |\mathcal{E}_{jd}(\underline{k},\omega)|^2 \ . \qquad (9\text{-}124)$$

It remains to determine the quality of these estimators of wavevector-frequency spectra that have been formulated to accommodate measured data in the format of discrete spatial and temporal samples of the sensor output field.

9.3.1 Bias of the Estimators Formulated to Accommodate Discrete Space-Time Sample Functions

To assess the bias of the estimators of wavevector-frequency spectra specified by equations (9-123) and (9-124), we must first (see equation (9-2)) determine the mean values of these estimates.

By substituting appropriate forms of equations (9-121) and (9-122) in equation (9-123), it is straightforward to show that the mean of the estimate of the two wavevector-frequency spectrum can be written in the form

$$E\{\tilde{S}_{oo}(\underline{\mu},\underline{k},\omega)\} = \frac{d_1^2d_2^2T_s}{JP} \sum_{j=1}^{J} \sum_{m=1}^{M} \sum_{n=1}^{N} \sum_{p=1}^{P} \sum_{q=1}^{M} \sum_{r=1}^{N} \sum_{s=1}^{P} a_w(t_p)a_w(t_s)$$

$$b_w(\underline{x}_{mn})b_w(\underline{x}_{qr})E\{o_j(\underline{x}_{mn},t_p)o_j(\underline{x}_{qr},t_s)\}$$

$$\exp\{-i[(\underline{\mu} - \underline{k})\cdot\underline{x}_{mn} - \omega t_p]\}\exp\{-i(\underline{k}\cdot\underline{x}_{qr} + \omega t_s)\} \ . \qquad (9\text{-}125)$$

Here, we have commuted the summation and expectation operations. However, for

a stationary, nonhomogeneous sensor output field, it follows from equations (6-52) and (6-124) that

$$E\{o_j(\underline{x}_{mn},t_p)o_j(\underline{x}_{qr},t_s)\} = Q_{oo}(\underline{x}_{mn},\underline{x}_{qr} - \underline{x}_{mn},t_s - t_p)$$

$$= (2\pi)^{-5} \int_{-\infty}^{\infty}\int_{-\infty}^{\infty}\int_{-\infty}^{\infty}\int_{-\infty}^{\infty}\int_{-\infty}^{\infty} S_{oo}(\underline{\beta},\underline{\sigma},\Omega)$$

$$\exp\{i[\underline{\beta}\cdot\underline{x}_{mn} + \underline{\sigma}\cdot(\underline{x}_{qr} - \underline{x}_{mn}) + \Omega(t_s - t_p)]\}\, d\underline{\beta}\, d\underline{\sigma}\, d\Omega \;, \tag{9-126}$$

independent of the value of j. By substituting equation (9-126) into equation (9-125), we can show that

$$E\{\tilde{S}_{oc}(\underline{\mu},\underline{k},\omega)\} = \frac{1}{(2\pi)^5 PT_s} \int_{-\infty}^{\infty}\int_{-\infty}^{\infty}\int_{-\infty}^{\infty}\int_{-\infty}^{\infty}\int_{-\infty}^{\infty} S_{oo}(\underline{\beta},\underline{\sigma},\Omega)\,|A_{wd}(\omega - \Omega)|^2$$

$$B_{wd}(\underline{\mu} - \underline{k} + \underline{\sigma} - \underline{\beta})B_{wd}(\underline{k} - \underline{\sigma})\, d\underline{\beta}\, d\underline{\sigma}\, d\Omega \;, \tag{9-127}$$

where

$$A_{wd}(\omega) = T_s \sum_{p=1}^{P} a_w(t_p)\exp(-i\omega t_p) \tag{9-126}$$

and

$$B_{wd}(\underline{k}) = d_1 d_2 \sum_{m=1}^{M}\sum_{n=1}^{N} b_w(\underline{x}_{mn})\exp(-i\underline{k}\cdot\underline{x}_{mn}) \;. \tag{9-129}$$

The mean values of the estimates of the wavevector-frequency spectrum of a stationary, homogeneous field and the space-averaged wavevector-frequency spectrum of a stationary, nonhomogeneous field are obtained by similar arguments. That is, by substituting appropriate forms of equations (9-121) and (9-122) in equation (9-124), we can show that

$$E\{\tilde{\Phi}_o(\underline{k},\omega)\} = E\{\tilde{\Phi}_o^a(\underline{k},\omega)\} =$$

$$\frac{d_1 d_2 T_s}{JMNP} \sum_{j=1}^{J} \sum_{m=1}^{M} \sum_{n=1}^{N} \sum_{p=1}^{P} \sum_{q=1}^{M} \sum_{r=1}^{N} \sum_{s=1}^{P} a_w(t_p) a_w(t_s)$$

$$b_w(\underline{x}_{mn}) b_w(\underline{x}_{qr}) E\{o_j(\underline{x}_{mn},t_p) o_j(\underline{x}_{qr},t_s)\}$$

$$\exp\{i(\underline{k}\cdot\underline{x}_{mn} + \omega t_p)\}\exp\{-i(\underline{k}\cdot\underline{x}_{qr} + \omega t_s)\} \ . \qquad (9\text{-}130)$$

Here, it must be recognized that the equal sign between $E\{\tilde{\Phi}_o(\underline{k},\omega)\}$ and $E\{\tilde{\Phi}_o^a(\underline{k},\omega)\}$ denotes only equality between the mathematical forms of these means and not equality of the means. That is, for a nonhomogeneous field, $E\{o_j(\underline{x}_{mn},t_p)o_j(\underline{x}_{qr},t_s)\}$ is related (see equation (9-126)) to the two wavevector-frequency spectrum of the sensor output field, whereas, for a homogeneous field,

$$E\{o_j(\underline{x}_{mn},t_p)o_j(\underline{x}_{qr},t_s)\} = Q_{oo}(\underline{x}_{qr} - \underline{x}_{mn}, t_s - t_p)$$

$$= (2\pi)^{-3} \int_{-\infty}^{\infty}\int_{-\infty}^{\infty}\int_{-\infty}^{\infty} \Phi_o(\underline{\sigma},\Omega)\exp\{i[\underline{\sigma}\cdot(\underline{x}_{qr} - \underline{x}_{mn}) + \Omega(t_s - t_p)]\} \, d\underline{\sigma} \, d\Omega \ . \qquad (9\text{-}131)$$

By substituting equation (9-126) into equation (9-130), we obtain the following expression for the mean value of the estimate of the space-averaged wavevector-frequency spectrum of a stationary, nonhomogeneous field:

$$E\{\tilde{\Phi}_o^a(\underline{k},\omega)\} = \frac{1}{(2\pi)^5 N d_1 N d_2 P T_s} \int_{-\infty}^{\infty}\int_{-\infty}^{\infty}\int_{-\infty}^{\infty}\int_{-\infty}^{\infty}\int_{-\infty}^{\infty} S_{oo}(\underline{\beta},\underline{\sigma},\Omega)\,|A_{wd}(\omega - \Omega)|^2$$

$$B_{wd}(\underline{\sigma} - \underline{k} - \underline{\beta}) B_{wd}(\underline{k} - \underline{\sigma}) \, d\underline{\beta} \, d\underline{\sigma} \, d\Omega \ , \qquad (9\text{-}132)$$

where $A_{wd}(\omega)$ and $B_{wd}(\underline{k})$ are given by equations (9-128) and (9-129), respectively.

Substitution of equation (9-131) into equation (9-130) produces a

relationship between the mean value of the estimated wavevector-frequency spectrum of a stationary, homogeneous field and the true wavevector-frequency spectrum of that field. That relationship is given by

$$E[\tilde{\Phi}_0(\underline{k},\omega)] = \frac{1}{(2\pi)^3 Md_1 Nd_2 PT_s} \int_{-\infty}^{\infty}\int_{-\infty}^{\infty}\int_{-\infty}^{\infty} \Phi_0(\underline{\sigma},\Omega)\,|A_{wd}(\omega - \Omega)|^2$$

$$|B_{wd}(\underline{k} - \underline{\sigma})|^2 \, d\underline{\sigma} \, d\Omega \, . \tag{9-133}$$

Note, by inspection of equations (9-127), (9-132), and (9-133), that the mean values of the estimates of all forms of the wavevector-frequency spectra are independent of the number, J, of spectral estimates, formed from statistically independent sample functions, that were averaged to obtain the final estimates of these wavevector-frequency spectra. Further inspection of these equations reveals that the mean values of the estimates of all forms of wavevector-frequency spectra differ from the true values of the respective spectra. Therefore, we must conclude that the estimates provided by equations (9-123) and (9-124) for the two wavevector-frequency spectrum and the space-averaged wavevector-frequency spectrum, respectively, of the stationary, nonhomogeneous sensor output field are biased. The estimate of the wavevector-frequency spectrum of the stationary, homogeneous sensor output field provided by equation (9-124) is also biased. To determine the degree of bias of these estimates, it is necessary to examine the characteristics of $A_{wd}(\omega)$ and $B_{wd}(\underline{k})$.

By the definition of $A_{wd}(\omega)$ in equation (9-128) and the definition of t_p in equation (9-120), one can easily confirm that

$$A_{wd}(\omega + 2u\pi/T_s) = (-1)^{u(P+1)} A_{wd}(\omega) \tag{9-134}$$

for all positive and negative integer values of u. Thus, it follows that the frequency window $|A_{wd}(\omega)|^2$ is an even, positive periodic function of ω, with period $2\pi/T_s$. To illustrate the characteristics of $|A_{wd}(\omega)|^2$, consider the example of uniform temporal weighting: that is, $a_w(t)$ equal to unity. For this temporal weighting, it is easily shown that the frequency window $|A_{wd}(\omega)|^2$ is given by

$$|A_{wd}(\omega)|^2 = (PT_s)^2 \left\{ \frac{\sin(\omega PT_s/2)}{P\sin(\omega T_s/2)} \right\}^2 . \tag{9-135}$$

As illustrated in figure 9-8, this frequency window is characterized by periodic major acceptance lobes centered at the frequencies $2u\pi/T_s$, for all positive and negative integer values of u. The bandwidths of these major acceptance lobes are seen to be inversely proportional to the temporal length, PT_s, of the sample function. Weightings other than uniform can produce different widths of the major acceptance lobes and higher ratios of amplitudes of major to minor acceptance lobes. However, for uniform intervals (T_s) between temporal samples, the locations of the major acceptance lobes are independent of the specific form of the temporal weighting, $a_w(t)$.

With regard to the wavevector window $B_{wd}(\underline{k})$, it is easily demonstrated from equations (9-119) and (9-129) that

$$B_{wd}(k_1 + 2\pi v/d_1, k_2 + 2\pi w/d_2) = (-1)^{[v(M+1)+w(N+1)]} B_{wd}(k_1, k_2) \tag{9-136}$$

for all positive and negative integer values of v and w. Clearly, $|B_{wd}(\underline{k})|^2$ is a real, even periodic function of both k_1 and k_2, with periods of $2\pi/d_1$ in the k_1 coordinate direction and $2\pi/d_2$ in the k_2 coordinate direction. To further illustrate the wavevector characteristics of $B_{wd}(\underline{k})$, consider the case of uniform spatial weighting where $b_w(\underline{x}) = 1$. For this weighting, the wavevector window $B_{wd}(\underline{k})$ is given by

$$B_{wd}(k_1, k_2) = Md_1Nd_2 \left\{ \frac{\sin(Mk_1d_1/2)}{M\sin(k_1d_1/2)} \right\} \left\{ \frac{\sin(Nk_2d_2/2)}{N\sin(k_2d_2/2)} \right\} . \tag{9-137}$$

Figure 9-9 illustrates the k_1 dependence of this wavevector window at $k_2 = 0$ for an odd number (M) of sensors in the x_1 coordinate direction of the array. Here it is evident that $B_{wd}(k_1, 0)$ is characterized by periodic major acceptance lobes centered at the wavenumbers $2v\pi/d_1$, for all positive and negative integer values of v. The bandwidths of these major acceptance lobes are inversely proportional to the spatial aperture, Md_1, of the array in the x_1 coordinate direction. When the array comprises an odd number (M) of

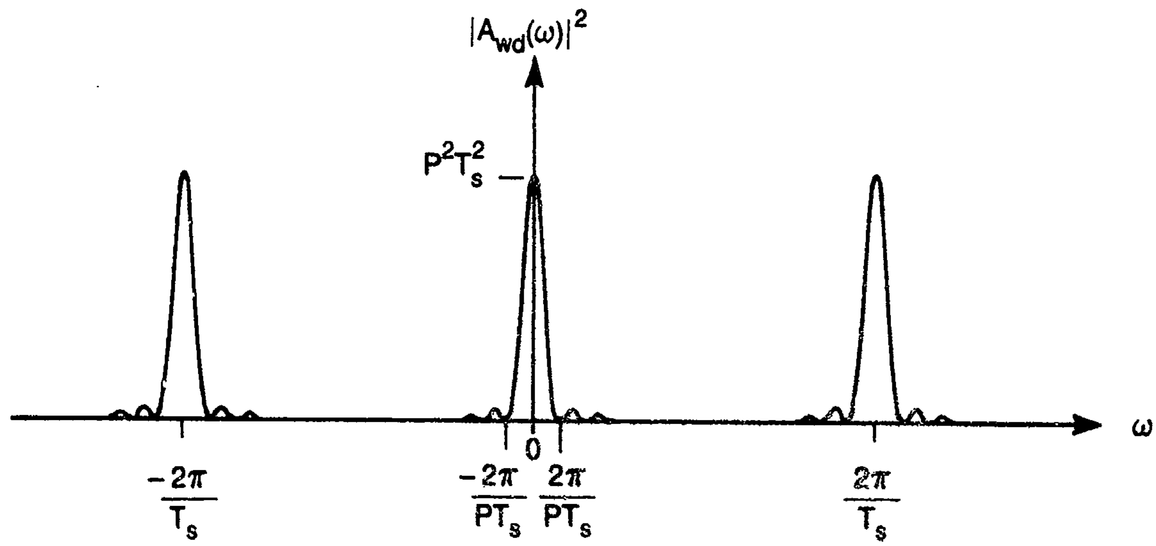

Figure 9-8. The Frequency Window $|A_{wd}(\omega)|^2$ Associated With Uniform Temporal Weighting

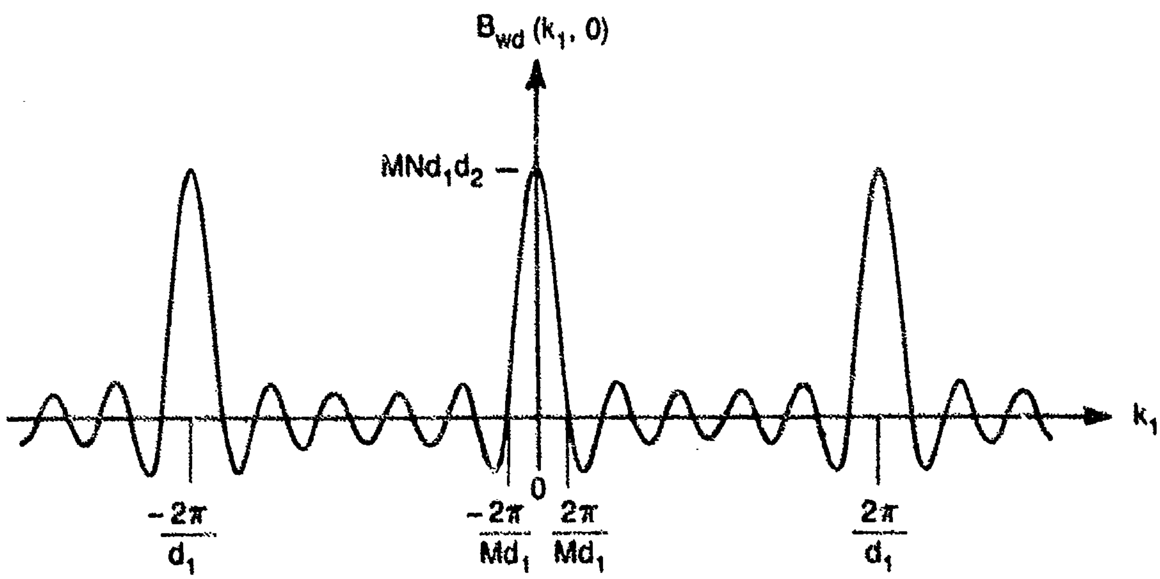

Figure 9-9. The k_1 Dependence of the Wavevector Window $B(\underline{k})$ at $k_2 = 0$ for M Odd

sensors in the x_1 coordinate direction, all major acceptance lobes (at $k_2 = 0$) are positive. On the other hand, if the array comprises an even number (M) of sensors in the x_1 coordinate direction, the major acceptance lobe at the origin is positive, and successive major lobes alternate in sign. Spatial weightings other than uniform can be used to alter the bandwidth of the major acceptance lobes and the ratio of the amplitudes of major to minor acceptance lobes. However, the locations of the major acceptance lobes are independent of the specific form of the spatial weighting, $b_w(\underline{x})$, and depend only on the spatial interval (d_1) between sensors. By similar arguments, it can be shown that $B_{wd}(2\pi v/d_1, k_2)$ is characterized by major acceptance lobes centered at the wavenumbers $2w\pi/d_2$, for all positive and negative integer values of w. The bandwidths of these major acceptance lobes are inversely proportional to the spatial aperture, Nd_2, of the array in the x_2 coordinate direction. By equation (9-136), it is evident that the sign of the vw-th major acceptance lobe will be positive when $[v(M + 1) + w(N + 1)]$ is even and will be negative when $[v(M + 1) + w(N + 1)]$ is odd.

Let us now apply our knowledge of the characteristics of these spectral windows in the frequency and wavevector domains to the evaluation of the bias of our estimates of the various forms of wavevector-frequency spectra. We recognize from the previous chapter that the periods between the major acceptance lobes of the spectral windows $A_{wd}(\omega)$ and $B_{wd}(\underline{k})$ are dictated solely by the intervals between the discrete temporal and spatial samplings of the sensor output field. The shapes and bandwidths of the major acceptance lobes and the ratios of the amplitudes of major to minor lobes of these spectral windows are dictated by the temporal and spatial extent (i.e., PT_s, Md_1, and Nd_2) of the discrete sample functions and temporal and spatial weightings, $a_w(t)$ and $b_w(\underline{x})$, applied to the sample functions. The effects of such finite temporal and spatial samplings on spectral estimates were treated in the previous chapter, and we will draw on those treatments to assess the extent of the bias of our spectral estimates.

By equation (9-127), we note that the mean value of our estimate of the two wavevector-frequency spectrum of the stationary, nonhomogeneous sensor output field is given by the integral, over all $\underline{\beta}$, $\underline{\sigma}$, and Ω, of the true two wavevector-frequency spectrum of that field, $S_{oo}(\underline{\beta},\underline{\sigma},\Omega)$, with the

spectral windows $|A_{wd}(\omega - \Omega)|^2$ and $B_{wd}(\underline{\mu} - \underline{k} + \underline{\sigma} - \underline{\beta})B_{wd}(\underline{k} - \underline{\sigma})$. The locations of the major acceptance lobes of $|A_{wd}(\Omega)|^2$ are illustrated in figure 9-8, and the pattern of the major acceptance lobes of the spectral window $B_{wd}(\underline{\mu} - \underline{k} + \underline{\sigma} - \underline{\beta})B_{wd}(\underline{k} - \underline{\sigma})$ is illustrated in figure 8-16 (if α_1 represents β_1 and $\underline{\beta}_1$ represents σ_1). We assumed at the outset that the true wavevector-frequency spectrum $S_{oo}(\underline{\beta},\underline{\sigma},\Omega)$ was, or was rendered, band limited in both the wavevector and frequency domains and that temporal and spatial sampling intervals were chosen to avoid aliasing errors in the spectral estimate. By the arguments presented in sections 8.3.1 and 8.3.2 of chapter 8, this implies, at the least, that

$$S_{oo}(\underline{\beta},\underline{\sigma},\Omega) = 0\ , \quad |\Omega| \geq \pi/T_s, \quad |\sigma_1| \geq \pi/d_1, \quad |\sigma_2| \geq \pi/d_2,$$

$$|\beta_1 - \sigma_1| \geq \pi/d_1, \quad |\beta_2 - \sigma_2| \geq \pi/d_2\ . \tag{9-138}$$

If (1) the temporal length (PT_s) and weighting $a_w(t)$ of the discrete sample function are selected such that the bandwidths of the major acceptance lobes of $A_{wd}(\Omega)$ are narrower than the bandwidth of any fluctuation of $S_{oo}(\underline{\beta},\underline{\sigma},\Omega)$ in Ω and (2) the spatial extent (Md_1Nd_2) and weighting $b_w(\underline{x})$ of the discrete sample function are selected such that the bandwidths of the major acceptance lobes of $B_{wd}(\underline{\sigma} - \underline{\beta})B_{wd}(\underline{\sigma})$ in β_1, σ_1, β_2, and σ_2 are much narrower than any fluctuation of $S_{oo}(\underline{\beta},\underline{\sigma},\Omega)$ in these wavevector variables, then it follows from equations (9-127) and (9-138) that, within the frequency range $|\omega| \leq \pi/T_s$ and within the wavenumber ranges $|k_1| \leq \pi/d_1$, $|k_2| \leq \pi/d_2$, $|\mu_1 - k_1| \leq \pi/d_1$, and $|\mu_2 - k_2| \leq \pi/d_2$, the mean value of $\tilde{S}_{oo}(\underline{\mu},\underline{k},\omega)$ is well approximated by

$$E[\tilde{S}_{oo}(\underline{\mu},\underline{k},\omega)] \approx \frac{S_{oo}(\underline{\mu},\underline{k},\omega)}{(2\pi)^5 PT_s} \int_{-\pi/T_s}^{\pi/T_s} |A_{wd}(\omega - \Omega)|^2\, d\Omega$$

$$\int_{-\pi/d_1}^{\pi/d_1}\int_{-\pi/d_2}^{\pi/d_2}\int_{-\pi/d_1}^{\pi/d_1}\int_{-\pi/d_2}^{\pi/d_2} B_{wd}(\underline{\mu} - \underline{k} + \underline{\sigma} - \underline{\beta})B_{wd}(\underline{k} - \underline{\sigma})\, d\underline{\beta}\, d\underline{\sigma}\ . \tag{9-139}$$

However, from equations (9-120) and (9-128), it can be demonstrated that

$$\int_{-\pi/T_s}^{\pi/T_s} |A_{wd}(\omega - \Omega)|^2 \, d\Omega = 2\pi T_s \sum_{p=1}^{P} a_w^2(t_p) \ . \qquad (9\text{-}140)$$

Further, by use of equations (9-119) and (9-129), we can write

$$\int_{-\pi/d_1}^{\pi/d_1} \int_{-\pi/d_2}^{\pi/d_2} \int_{-\pi/d_1}^{\pi/d_1} \int_{-\pi/d_2}^{\pi/d_2} B_{wd}(\underline{\sigma} - \underline{\beta}) B_{wd}(\underline{\sigma}) \, d\underline{\beta} \, d\underline{\sigma} = (2\pi)^4 \Gamma(\underline{\mu};M,N)$$

$$= (2\pi)^4 \sum_{m=1}^{M} \sum_{n=1}^{N} b_w^2(\underline{x}_{mn}) \exp[-i\underline{\mu}\cdot\underline{x}_{mn}] \theta(m,M)\theta(n,N) \ , \qquad (9\text{-}141)$$

where

$$\theta(j,J) = \begin{cases} \delta_{j,(J+1)/2} \ , & \text{for } J \text{ odd,} \\[2ex] \dfrac{\sin\{[j - (J+1)/2]\pi\}}{[j - (J+1)/2]\pi} \ , & \text{for } J \text{ even.} \end{cases} \qquad (9\text{-}142)$$

By equations (9-139), (9-140), and (9-141), it follows that

$$E\{\tilde{S}_{oo}(\underline{\mu},\underline{k},\omega)\} \approx S_{oo}(\underline{\mu},\underline{k},\omega)\Gamma(\underline{\mu};M,N)\left\{\frac{1}{P}\sum_{p=1}^{P} a_w^2(t_p)\right\} \ ,$$

$$\text{for } |\omega| \le \pi/T_s, \quad |k_1| \le \pi/d_1, \quad |k_2| \le \pi/d_2 \ ,$$

$$|\mu_1 - k_1| \le \pi/d_1, \quad |\mu_2 - k_2| \le \pi/d_2 \ . \qquad (9\text{-}143)$$

Clearly, if

$$\frac{1}{P}\sum_{p=1}^{P} a_w^2(t_p) = 1 \qquad (9\text{-}144)$$

and

$$\Gamma(\underline{\mu};M,N) = 1 \ , \qquad (9\text{-}145)$$

then the mean value of the estimate of the two wavevector-frequency spectrum

provides a good approximation to the true two wavevector-frequency spectrum within the ranges of frequency and wavevectors specified by equation (9-143).

We should note, from equations (9-141) and (9-142), that if M and N are both odd,

$$\Gamma(\underline{\mu};M,N) = b_w^2(0,0) \quad . \tag{9-146}$$

However, if either M or N is even, $\Gamma(\underline{\mu};M,N)$ is a function of $\underline{\mu}$. For purposes of illustration, figure 9-10 depicts the μ_1 dependence, at $\mu_2 = 0$, of $\Gamma(\underline{\mu};M,N)$ for an array in which $b_w(\underline{x}) = 1$, $M = 10$, and $N = 9$. Note that, except near the limits of the fundamental range (i.e., near $\mu_1 = -\pi/d_1$ and $\mu_1 = \pi/d_1$), $\Gamma(\mu_1,0;10,9)$ is approximately equal to $b_w^2(0,0)$, which equals unity. Note, in this example, that the mathematical expression for $\Gamma(\mu_1,0;10,9)$ obtained from equations (9-141) and (9-142) resembles a 10-term Fourier series approximation to a unit amplitude square wave of period $4\pi/d_1$.

Thus, given that (1) the true two wavevector-frequency spectrum of the sensor output field is band limited in both the wavevector and frequency domains, (2) the temporal and spatial sampling intervals (T_s, d_1, and d_2) are chosen such that equation (9-138) is satisfied, (3) the temporal length (PT_s) and weighting $a_w(t)$ of the discrete sample function are selected such that the bandwidth of the major acceptance lobes of $A_{wd}(\Omega)$ are narrower than the bandwidth of any fluctuation of $S_{oo}(\underline{\beta},\underline{\sigma},\Omega)$ in Ω, (4) the spatial extent (Md_1Nd_2) and weighting $b_w(\underline{x})$ of the discrete sample function are selected such that the bandwidths of the major acceptance lobes of $B_{wd}(\underline{\sigma} - \underline{\beta})B_{wd}(\underline{\sigma})$ in β_1, σ_1, β_2, and σ_2 are much narrower than any fluctuation of $S_{oo}(\underline{\beta},\underline{\sigma},\Omega)$ in the respective wavevector variables, (5) the temporal weights are chosen to satisfy the restriction of equation (9-144), and (6) the spatial weights are chosen to satisfy equation (9-145), then the estimate of the two wavevector-frequency spectrum provided by equation (9-123) will be, for practical purposes, an unbiased one.

Recall, from the arguments presented in section 6.5.2.3 of chapter 6, that the true space-averaged wavevector-frequency spectrum represents the homogeneous constituents of a generally nonhomogeneous field. Therefore, to evaluate the bias of our estimate of the space-averaged wavevector-frequency

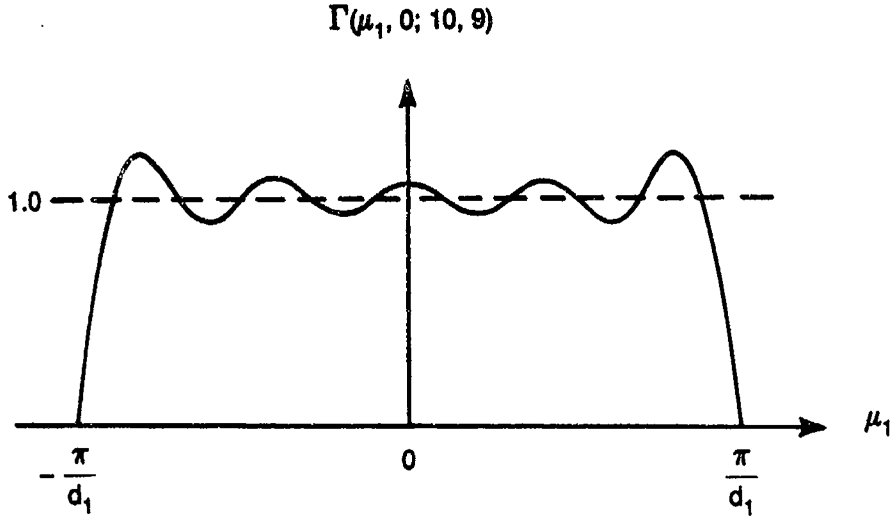

Figure 9-10. The μ_1 Dependence of $\Gamma(\underline{\mu};MN)$ for a 10-by-9 Element Unweighted Array

spectrum, we assume the true two wavevector-frequency spectrum, $S_{00}(\underline{\beta},\underline{\sigma},\Omega)$, of the sensor output field is of the form

$$S_{00}(\underline{\beta},\underline{\sigma},\Omega) = (2\pi)^2\delta(\underline{\beta})\Phi_0(\underline{\sigma},\Omega) + N_{00}(\underline{\beta},\underline{\sigma},\Omega) \ , \tag{9-147}$$

where $\Phi_0(\underline{\sigma},\Omega)$ represents the stationary and homogeneous contributions to the field and $N_{00}(\underline{\beta},\underline{\sigma},\Omega)$ characterizes the stationary, but nonhomogeneous, contributions to the field. By substituting equation (9-147) into equation (9-132), we obtain the following expression for the mean value of the estimate of the space-averaged wavevector-frequency spectrum:

$$E(\tilde{\Phi}_0^a(\underline{k},\omega)) = \frac{1}{(2\pi)^3 Md_1Nd_2PT_s} \int_{-\infty}^{\infty}\int_{-\infty}^{\infty}\int_{-\infty}^{\infty} \Phi_0(\underline{\sigma},\Omega)|A_{wd}(\omega - \Omega)|^2$$

$$|B_{wd}(\underline{k} - \underline{\sigma})|^2 \, d\underline{\sigma} \, d\Omega$$

$$+ \frac{1}{(2\pi)^5 Md_1Nd_2PT_s} \int_{-\infty}^{\infty}\int_{-\infty}^{\infty}\int_{-\infty}^{\infty}\int_{-\infty}^{\infty}\int_{-\infty}^{\infty} N_{00}(\underline{\beta},\underline{\sigma},\Omega)|A_{wd}(\omega - \Omega)|^2$$

$$B_{wd}(\underline{\sigma} - \underline{k} - \underline{\beta})B_{wd}(\underline{k} - \underline{\sigma}) \, d\underline{\beta} \, d\underline{\sigma} \, d\Omega \ . \tag{9-148}$$

We have assumed all true wavevector-frequency spectra to be band limited

in both the wavevector and frequency domains. Further, we have assumed that the spatial and temporal samplings were selected to avoid aliasing errors in the spectral estimates. Therefore, it follows (see sections 8.3.1 and 8.3.2 of chapter 8) that

$$\Phi_o(\underline{\sigma},\Omega) = 0, \quad |\Omega| \geq \pi/T_s, \quad |\sigma_1| \geq \pi/d_1, \quad |\sigma_2| \geq \pi/d_2 \ , \tag{9-149}$$

and that the two wavevector-frequency spectrum, $N_{oo}(\underline{\beta},\underline{\sigma},\Omega)$, satisfies the constraints of equation (9-138).

If (1) the temporal length and weighting of the discrete sample function are selected such that the bandwidth of the major acceptance lobes of $|A_{wd}(\Omega)|^2$ are much narrower than the bandwidth of any fluctuation of $\Phi_o(\underline{\sigma},\Omega)$ or $N_{oo}(\underline{\beta},\underline{\sigma},\Omega)$ in Ω and (2) the spatial extent $(Md_1 Nd_2)$ and weighting $b_w(\underline{x})$ of the discrete sample function are selected such that the bandwidths of the major acceptance lobes of $|B_{wd}(\underline{\sigma})|^2$ are much narrower than those of any fluctuation of $\Phi_o(\underline{\sigma},\Omega)$ in σ_1 and σ_2, and the bandwidths of the major acceptance lobes of $B_{wd}(\underline{\sigma} - \underline{\beta})B_{wd}(\underline{\sigma})$ in the variables β_1, σ_1, β_2, and σ_2 are much narrower than the bandwidths of any fluctuation of $N_{oo}(\underline{\beta},\underline{\sigma},\Omega)$ in the corresponding variables, then it follows from equations (9-138), (9-148), and (9-149) that, within $|\omega| \leq \pi/T_s$, $|k_1| \leq \pi/d_1$, $|k_2| \leq \pi/d_2$, $|\mu_1 - k_1| \leq \pi/d_1$, and $|\mu_2 - k_2| \leq \pi/d_2$, the mean value of the estimate of the space-averaged wavevector-frequency spectrum is well approximated by

$$E[\tilde{\Phi}_o^a(\underline{k},\omega)] \approx \frac{\Phi_o(\underline{k},\omega)}{(2\pi)^3 Md_1 Nd_2 PT_s} \int_{-\pi/T_s}^{\pi/T_s} |A_{wd}(\omega - \Omega)|^2 \, d\Omega$$

$$\int_{-\pi/d_1}^{\pi/d_1} \int_{-\pi/d_2}^{\pi/d_2} |B_{wd}(\underline{k} - \underline{\sigma})|^2 \, d\underline{\sigma}$$

$$+ \frac{N_{oo}(\underline{0},\underline{k},\omega)}{(2\pi)^5 Md_1 Nd_2 PT_s} \int_{-\pi/T_s}^{\pi/T_s} |A_{wd}(\omega - \Omega)|^2 \, d\Omega$$

$$\int_{-\pi/d_1}^{\pi/d_1} \int_{-\pi/d_2}^{\pi/d_2} \int_{-\pi/d_1}^{\pi/d_1} \int_{-\pi/d_2}^{\pi/d_2} B_{wd}(\underline{\sigma} - \underline{k} - \underline{\beta}) B_{wd}(\underline{k} - \underline{\sigma}) \, d\underline{\beta} \, d\underline{\sigma} \ , \tag{9-150}$$

where $\underline{0}$ denotes the vector (0,0).

By use of equations (9-119) and (9-129), we can demonstrate that

$$\int_{-\pi/d_1}^{\pi/d_1} \int_{-\pi/d_2}^{\pi/d_2} |B_{wd}(\underline{k} - \underline{\sigma})|^2 \, d\underline{\sigma} = (2\pi)^2 \, d_1 d_2 \sum_{m=1}^{M} \sum_{n=1}^{N} b_w^2(\underline{x}_{mn}) \; . \tag{9-151}$$

This result, in combination with equations (9-140) and (9-141), allows us to rewrite equation (9-150) in the form

$$E\{\tilde{\Phi}_o^a(\underline{k},\omega)\} \approx \Phi_o(\underline{k},\omega)\left\{\frac{1}{P}\sum_{p=1}^{P} a_w^2(t_p)\right\}\left\{\frac{1}{MN}\sum_{m=1}^{M}\sum_{n=1}^{N} b_w^2(\underline{x}_{mn})\right\}$$

$$+ \frac{N_{oo}(\underline{\mu},\underline{k},\omega)}{Md_1 Nd_2} \, \Gamma(\underline{0};M,N)\left\{\frac{1}{P}\sum_{p=1}^{P} a_w^2(t_p)\right\} ,$$

$$\text{for } |\omega| \le \pi/T_s, \quad |k_1| \le \pi/d_1, \quad |k_2| \le \pi/d_2 \; . \tag{9-152}$$

Inasmuch as the true space-averaged wavevector-frequency spectrum represents the homogeneous constituents of a generally nonhomogeneous field, the estimate of the space-averaged wavevector-frequency spectrum provided by equation (9-124) will be unbiased only if

$$\frac{1}{P}\sum_{p=1}^{P} a_w^2(t_p) = 1 \; , \tag{9-153}$$

$$\frac{1}{MN}\sum_{m=1}^{M}\sum_{n=1}^{P} b_w^2(\underline{x}_{mn}) = 1 \; , \tag{9-154}$$

and

$$\frac{\Gamma(\underline{0};M,N)}{Md_1 Nd_2} = 0 \; . \tag{9-155}$$

However, by reference to equations (9-141) and (9-142), it is evident that the

conditions of equations (9-154) and (9-155) are mutually incompatible. If we enforce the conditions of equations (9-153) and (9-154), and if we denote the function $\Gamma(\underline{0};M,N)$ that results from the enforcement of equation (9-154) by $\Gamma_r(\underline{0};M,N)$, we can write equation (9-152) in the form

$$E\{\tilde{\Phi}_0^a(\underline{k},\omega)\} \approx \Phi_0(\underline{k},\omega) + N_{oo}(\underline{\mu},\underline{k},\omega)\,\frac{\Gamma_r(\underline{0};M,N)}{Md_1Nd_2}\ ,$$

$$|\omega| \le \pi/T_s,\quad |k_1| \le \pi/d_1,\quad |k_2| \le \pi/d_2\ . \tag{9-156}$$

Clearly, the mean value of the estimate of the space-averaged wavevector-frequency spectrum differs from the true wavevector-frequency spectrum, $\Phi_0(\underline{k},\omega)$, of the homogeneous contribution to the generally nonhomogeneous field. Therefore, the estimate of the space-averaged wavevector-frequency spectrum provided by equation (9-124) is a biased one. By equations (9-2) and (9-156), the bias error is well approximated by

$$B\{\tilde{\Phi}_0^a(\underline{k},\omega)\} \approx N_{oo}(\underline{\mu},\underline{k},\omega)\,\frac{\Gamma_r(\underline{0};M,N)}{Md_1Nd_2} \tag{9-157}$$

and decreases with increasing aperture (Md_1Nd_2) of the array.

Given that all wavevector-frequency spectra are band limited in both the frequency and wavevector domains, and given that the temporal and spatial sampling intervals have been selected to avoid aliasing errors, then it follows that the true wavevector-frequency spectrum, $\Phi_0(\underline{k},\omega)$, of the stationary, homogeneous field satisfies the condition of equation (9-149). If the temporal length and weighting of the discrete sample function are selected such that the bandwidths of the major acceptance lobes of $|A_{wd}(\Omega)|^2$ are much narrower than the bandwidth of any fluctuation of $\Phi_0(\underline{\sigma},\Omega)$ in Ω, and the spatial extent (Md_1Nd_2) and weighting $b_w(\underline{x})$ of the discrete sample function are selected such that the bandwidths of the major acceptance lobes of $|B_{wd}(\underline{\sigma})|^2$ are much narrower than those of any fluctuation of $\Phi_0(\underline{\sigma},\Omega)$ in σ_1 and σ_2, then it follows from equation (9-133) that, within the variable ranges $|\omega| \le \pi/T_s$, $|k_1| \le \pi/d_1$, and $|k_2| \le \pi/d_2$, the mean value of the estimate of the wavevector-frequency spectrum of a stationary, homogeneous field is well approximated by

$$E\{\tilde{\Phi}_0(\underline{k},\omega)\} = \frac{\Phi_0(\underline{k},\omega)}{(2\pi)^3 Md_1 Nd_2 PT_s} \int_{-\pi/T_s}^{\pi/T_s} |A_{wd}(\omega - \Omega)|^2$$

$$\int_{-\pi/d_1}^{\pi/d_1} \int_{-\pi/d_2}^{\pi/d_2} |B_{wd}(\underline{k} - \underline{\sigma})|^2 \, d\underline{\sigma} \, d\Omega \ . \qquad (9\text{-}158)$$

By employing equations (9-140) and (9-151), it follows that

$$E\{\tilde{\Phi}_0(\underline{k},\omega)\} = \Phi_0(\underline{k},\omega)\left\{\frac{1}{P}\sum_{p=1}^{P} a_w^2(t_p)\right\}\left\{\frac{1}{MN}\sum_{m=1}^{M}\sum_{n=1}^{N} b_w^2(\underline{x}_{mn})\right\} ,$$

$$|\omega| \le \pi/T_s, \quad |k_1| \le \pi/d_1, \quad |k_2| \le \pi/d_2 \ . \qquad (9\text{-}159)$$

If $a_w(t_p)$ and $b_w(\underline{x}_{mn})$ are selected to satisfy the conditions of equations (9-153) and (9-154), respectively, then

$$E\{\tilde{\Phi}_0(\underline{k},\omega)\} = \Phi_0(\underline{k},\omega) \qquad (9\text{-}160)$$

within $|\omega| \le \pi/T_s$, $|k_1| \le \pi/d_1$, $|k_2| \le \pi/d_2$. Thus, within this variable range, equation (9-124), with suitable restrictions, provides an unbiased estimate of the wavevector-frequency spectrum of a stationary, homogeneous sensor output field.

By the arguments presented in this section, we have shown that if

(1) the true wavevector-frequency spectrum is band limited in both the wavevector and frequency domains,

(2) the spatial and temporal sampling intervals are selected to avoid aliasing errors,

(3) the temporal length and weighting of each discrete sample function is selected such that the bandwidths of the major acceptance lobes of

$|A_{wd}(\omega)|^2$ are narrower than the bandwidth of any fluctuation of the true wavevector-frequency spectrum in the frequency domain,

(4) the spatial extent and weighting of the discrete sample function are selected such that the bandwidths of the major acceptance lobes of $B_{wd}(\underline{\sigma} - \underline{\beta})B_{wd}(\underline{\sigma})$ are much narrower than any fluctuation of the true wavevector-frequency spectrum in any wavevector variable,

(5) the temporal weights satisfy the restriction of equation (9-144), and

(6) the spatial weights satisfy, as appropriate, the restriction of either equation (9-145) or (9-154),

then equation (9-123) provides an unbiased estimate of the two wavevector-frequency spectrum of a stationary, nonhomogeneous sensor output field, and equation (9-124) provides an unbiased estimate of the wavevector-frequency spectrum of a stationary, homogeneous sensor output field. However, under these same conditions, the estimate of the space-averaged wavevector-frequency spectrum provided by equation (9-124) is biased by nonhomogeneous contributions existing at $\underline{\mu} = (0,0)$. By reference to section 6.5.2.3 of chapter 6, it can be shown that this bias is a consequence of the finite aperture of the measurement array, and is therefore unavoidable in practical measurements. However, as is evident from equation (9-157), this bias error decreases with increasing aperture of the measurement array.

9.3.2 Variance of the Estimators Formulated to Accommodate Discrete Space-Time Sample Functions

According to Papoulis,[15] the variance of a complex random variable, say Γ, is given by

$$\mathrm{Var}\{\Gamma\} = E\{|\Gamma - E\{\Gamma\}|^2\} \ . \tag{9-161}$$

However, inasmuch as $E\{\Gamma\}^* = E\{\Gamma^*\}$, it can easily be shown that

$$\mathrm{Var}\{\Gamma\} = E\{|\Gamma|^2\} - |E\{\Gamma\}|^2 \ . \tag{9-162}$$

Clearly, therefore, to evaluate the variance of our wavevector-frequency

spectral estimates, we must first evaluate the mean values of the squared magnitudes of these estimates.

According to equation (9-123), the squared magnitude of the estimate of the two wavevector-frequency spectrum of the stationary, nonhomogeneous sensor output field is given by

$$|\tilde{S}_{oo}(\underline{\mu},\underline{k},\omega)|^2 = \frac{1}{(JPT_s)^2}\sum_{g=1}^{J}\sum_{j=1}^{J} \mathcal{E}_{gd}(\underline{\mu} - \underline{k},-\omega)\mathcal{E}_{gd}(\underline{k},\omega)$$

$$\mathcal{E}^*_{jd}(\underline{\mu} - \underline{k},-\omega)\mathcal{E}^*_{jd}(\underline{k},\omega) \ . \qquad (9\text{-}163)$$

From equation (9-124), it is evident that the estimates of the wavevector-frequency spectrum of the stationary, homogeneous sensor output field and the space-averaged wavevector-frequency spectrum of the stationary, nonhomogeneous sensor output field are real and positive. Thus, it follows that

$$|\tilde{\Phi}_o(\underline{k},\omega)|^2 = |\tilde{\Phi}^a_o(\underline{k},\omega)|^2 = \tilde{\Phi}^2_o(\underline{k},\omega) = \tilde{\Phi}^{a2}_o(\underline{k},\omega)$$

$$= \frac{1}{(JMd_1Nd_2PT_s)^2}\sum_{g=1}^{J}\sum_{j=1}^{J} |\mathcal{E}_{gd}(\underline{k},\omega)|^2|\mathcal{E}_{jd}(\underline{k},\omega)|^2 \ . \qquad (9\text{-}164)$$

By use of equations (9-121) and (9-122), we can demonstrate that $E\{|\tilde{S}_{oo}(\underline{\mu},\underline{k},\omega)|^2\}$ can be written in the form

$$E\{|\tilde{S}_{oo}(\underline{\mu},\underline{k},\omega)|^2\} = \frac{(d_1d_2)^4T_s^2}{(JP)^2}\sum_{g=1}^{J}\sum_{j=1}^{J}\sum_{m=1}^{M}\sum_{n=1}^{N}\sum_{p=1}^{P}\sum_{q=1}^{M}\sum_{r=1}^{N}\sum_{s=1}^{P}$$

$$\sum_{u=1}^{M}\sum_{v=1}^{N}\sum_{w=1}^{P}\sum_{y=1}^{M}\sum_{z=1}^{N}\sum_{\theta=1}^{P} a_w(t_p)a_w(t_s)a_w(t_w)a_w(t_\theta)$$

$$b_w(\underline{x}_{mn})b_w(\underline{x}_{qr})b_w(\underline{x}_{uv})b_w(\underline{x}_{yz})$$

$$E\{o_{\alpha g}(\underline{x}_{mn},t_p)o_{\alpha g}(\underline{x}_{qr},t_s)o_{\alpha j}(\underline{x}_{uv},t_w)o_{\alpha j}(\underline{x}_{yz},t_\theta)\}$$

$$\exp\{-i[(\underline{\mu} - \underline{k})\cdot\underline{x}_{mn} + \underline{k}\cdot\underline{x}_{qr} + \omega(t_s - t_p)]\}$$

$$\exp\{i[(\underline{\mu} - \underline{k})\cdot\underline{x}_{uv} + \underline{k}\cdot\underline{x}_{yz} + \omega(t_\theta - t_w)]\} \ . \qquad (9\text{-}165)$$

Similarly, by using equations (9-121) and (9-122) in equation (9-164), we can show that $E\{\tilde{\Phi}_0^2(\underline{k},\omega)\}$ and $E\{\tilde{\Phi}_0^{a2}(\underline{k},\omega)\}$ can be written in the identical mathematical forms

$$E\{\tilde{\Phi}_0^2(\underline{k},\omega)\} = E\{\tilde{\Phi}_0^{a2}(\underline{k},\omega)\}$$

$$= \frac{(d_1 d_2 T_s)^2}{(JMNP)^2} \sum_{g=1}^{J} \sum_{j=1}^{J} \sum_{m=1}^{M} \sum_{n=1}^{N} \sum_{p=1}^{P} \sum_{q=1}^{M} \sum_{r=1}^{N} \sum_{s=1}^{P}$$

$$\sum_{u=1}^{M} \sum_{v=1}^{N} \sum_{w=1}^{P} \sum_{y=1}^{M} \sum_{z=1}^{N} \sum_{\theta=1}^{P} a_w(t_p) a_w(t_s) a_w(t_w) a_w(t_\theta)$$

$$b_w(\underline{x}_{mn}) b_w(\underline{x}_{qr}) b_w(\underline{x}_{uv}) b_w(\underline{x}_{yz})$$

$$E\{o_{\alpha g}(\underline{x}_{mn}, t_p) o_{\alpha g}(\underline{x}_{qr}, t_s) o_{\alpha j}(\underline{x}_{uv}, t_w) o_{\alpha j}(\underline{x}_{yz}, t_\theta)\}$$

$$\exp\{-i[\underline{k}\cdot(\underline{x}_{qr} - \underline{x}_{mn}) + \omega(t_s - t_p)]\}$$

$$\exp\{-i[\underline{k}\cdot(\underline{x}_{yz} - \underline{x}_{uv}) + \omega(t_\theta - t_w)]\} . \qquad (9\text{-}166)$$

Recall that we have assumed that the temporal length of each sample function is much greater than the largest time delay required for the true autocorrelation function to become zero over the range of $\underline{x}$ and $\underline{\xi}$ afforded by the spatial sampling of the sensor output field. By this assumption, each sample function of the sensor output field is rendered, for practical purposes, statistically independent of all other sample functions. Given this statistical independence of the sample functions, it follows that

$$E\{o_{\alpha g}(\underline{x}_{mn}, t_p) o_{\alpha g}(\underline{x}_{qr}, t_s) o_{\alpha j}(\underline{x}_{uv}, t_w) o_{\alpha j}(\underline{x}_{yz}, t_\theta)\}$$

$$= \delta_{gj} E\{o_{\alpha j}(\underline{x}_{mn}, t_p) o_{\alpha j}(\underline{x}_{qr}, t_s) o_{\alpha j}(\underline{x}_{uv}, t_w) o_{\alpha j}(\underline{x}_{yz}, t_\theta)\}$$

$$+ (1 - \delta_{gj}) E\{o_{\alpha g}(\underline{x}_{mn}, t_p) o_{\alpha g}(\underline{x}_{qr}, t_s)\}$$

$$E\{o_{\alpha j}(\underline{x}_{uv}, t_w) o_{\alpha j}(\underline{x}_{yz}, t_\theta)\} . \qquad (9\text{-}167)$$

If we further assume that each statistically independent sample function, $o_{\alpha j}(\underline{x},\theta)$, is a member function of a zero mean Gaussian random process, then it follows from equations (9-59) and (9-167) that

$$E\{o_{\alpha g}(\underline{x}_{mn},t_p)o_{\alpha g}(\underline{x}_{qr},t_s)o_{\alpha j}(\underline{x}_{uv},t_w)o_{\alpha j}(\underline{x}_{yz},t_\theta)\}$$

$$= \delta_{gj}[E\{o_{\alpha j}(\underline{x}_{mn},t_p)o_{\alpha j}(\underline{x}_{qr},t_s)\}E\{o_{\alpha j}(\underline{x}_{uv},t_w)o_{\alpha j}(\underline{x}_{yz},t_\theta)\}$$

$$+ E\{o_{\alpha j}(\underline{x}_{mn},t_p)o_{\alpha j}(\underline{x}_{uv},t_w)\}E\{o_{\alpha j}(\underline{x}_{qr},t_s)o_{\alpha j}(\underline{x}_{yz},t_\theta)\}$$

$$+ E\{o_{\alpha j}(\underline{x}_{mn},t_p)o_{\alpha j}(\underline{x}_{yz},t_\theta)\}E\{o_{\alpha j}(\underline{x}_{qr},t_s)o_{\alpha j}(\underline{x}_{uv},t_w)\}]$$

$$+ (1 - \delta_{gj})E\{o_{\alpha g}(\underline{x}_{mn},t_p)o_{\alpha g}(\underline{x}_{qr},t_s)\}E\{o_{\alpha j}(\underline{x}_{uv},t_w)o_{\alpha j}(\underline{x}_{yz},t_\theta)\} \ . \tag{9-168}$$

For a stationary, nonhomogeneous field, we know from equation (6-69) that

$$E\{o_{\alpha j}(\underline{x}_{mn},t_p)o_{\alpha j}(\underline{x}_{qr},t_s)\} = Q_{oo}(\underline{x}_{mn},\underline{x}_{qr} - \underline{x}_{mn},t_s - t_p) \ , \tag{9-169}$$

independent of the index j. Thus, for a stationary, nonhomogeneous field, we can write equation (9-168) in the form

$$E\{o_{\alpha g}(\underline{x}_{mn},t_p)o_{\alpha g}(\underline{x}_{qr},t_s)o_{\alpha j}(\underline{x}_{uv},t_w)o_{\alpha j}(\underline{x}_{yz},t_\theta)\}$$

$$= Q_{oo}(\underline{x}_{mn},\underline{x}_{qr} - \underline{x}_{mn},t_s - t_p)Q_{oo}(\underline{x}_{uv},\underline{x}_{yz} - \underline{x}_{uv},t_\theta - t_w)$$

$$+ \delta_{gj}[Q_{oo}(\underline{x}_{mn},\underline{x}_{uv} - \underline{x}_{mn},t_w - t_p)Q_{oo}(\underline{x}_{qr},\underline{x}_{yz} - \underline{x}_{qr},t_\theta - t_s)$$

$$+ Q_{oo}(\underline{x}_{mn},\underline{x}_{yz} - \underline{x}_{mn},t_\theta - t_p)Q_{oo}(\underline{x}_{qr},\underline{x}_{uv} - \underline{x}_{qr},t_w - t_s)] \ . \tag{9-170}$$

However, according to equation (6-124),

$$Q_{oo}(\underline{x}_{mn},\underline{x}_{qr} - \underline{x}_{mn},t_s - t_p) = (2\pi)^{-5} \int_{-\infty}^{\infty}\int_{-\infty}^{\infty}\int_{-\infty}^{\infty}\int_{-\infty}^{\infty}\int_{-\infty}^{\infty} S_{oo}(\underline{\beta},\underline{\sigma},\Omega)$$

$$\exp\{i[\underline{\beta}\cdot\underline{x}_{mn} + \underline{\sigma}\cdot(\underline{x}_{qr} - \underline{x}_{mn}) + \Omega(t_s - t_p)]\}\ d\underline{\beta}\ d\underline{\sigma}\ d\Omega \ . \qquad (9\text{-}171)$$

Therefore, for a stationary, nonhomogeneous field,

$$E\{o_{\alpha g}(\underline{x}_{mn},t_p)o_{\alpha g}(\underline{x}_{qr},t_s)o_{\alpha j}(\underline{x}_{uv},t_w)o_{\alpha j}(\underline{x}_{yz},t_\theta)\}$$

$$= \frac{1}{(2\pi)^{10}} \int_{-\infty}^{\infty}\int_{-\infty}^{\infty}\int_{-\infty}^{\infty}\int_{-\infty}^{\infty}\int_{-\infty}^{\infty}\int_{-\infty}^{\infty}\int_{-\infty}^{\infty}\int_{-\infty}^{\infty}\int_{-\infty}^{\infty}\int_{-\infty}^{\infty} S_{oo}(\underline{\beta}_1,\underline{\sigma}_1,\Omega_1)S_{oo}(\underline{\beta}_2,\underline{\sigma}_2,\Omega_2)$$

$$[\exp\{i[\underline{\beta}_1\cdot\underline{x}_{mn} + \underline{\sigma}_1\cdot(\underline{x}_{qr} - \underline{x}_{mn}) + \Omega_1(t_s - t_p)]\}$$

$$\exp\{i[\underline{\beta}_2\cdot\underline{x}_{uv} + \underline{\sigma}_2\cdot(\underline{x}_{yz} - \underline{x}_{uv}) + \Omega_2(t_\theta - t_w)]\}$$

$$+ \delta_{gj}(\exp\{i[\underline{\beta}_1\cdot\underline{x}_{mn} + \underline{\sigma}_1\cdot(\underline{x}_{uv} - \underline{x}_{mn}) + \Omega_1(t_w - t_p)]\}$$

$$\exp\{i[\underline{\beta}_2\cdot\underline{x}_{qr} + \underline{\sigma}_2\cdot(\underline{x}_{yz} - \underline{x}_{qr}) + \Omega_2(t_\theta - t_s)]\}$$

$$+ \exp\{i[\underline{\beta}_1\cdot\underline{x}_{mn} + \underline{\sigma}_1\cdot(\underline{x}_{yz} - \underline{x}_{mn}) + \Omega_1(t_\theta - t_p)]\}$$

$$\exp\{i[\underline{\beta}_2\cdot\underline{x}_{qr} + \underline{\sigma}_2\cdot(\underline{x}_{uv} - \underline{x}_{qr}) + \Omega_2(t_w - t_s)]\})]$$

$$d\underline{\beta}_1\ d\underline{\sigma}_1\ d\Omega_1\ d\underline{\beta}_2\ d\underline{\sigma}_2\ d\Omega_2 \ . \qquad (9\text{-}172)$$

If the sensor output field is stationary, but homogeneous rather than nonhomogeneous, we know (see equation (6-73)) that

$$E\{o_{\alpha j}(\underline{x}_{mn},t_p)o_{\alpha j}(\underline{x}_{qr},t_s)\} = Q_{oo}(\underline{x}_{qr} - \underline{x}_{mn},t_s - t_p) \ , \qquad (9\text{-}173)$$

independent of the index j. Therefore, for a stationary, homogeneous field, equation (6-168) can be rewritten in the form

$$E\{o_{\alpha g}(\underline{x}_{mn},t_p)o_{\alpha g}(\underline{x}_{qr},t_s)o_{\alpha j}(\underline{x}_{uv},t_w)o_{\alpha j}(\underline{x}_{yz},t_\theta)\}$$

$$= Q_{oo}(\underline{x}_{qr} - \underline{x}_{mn},t_s - t_p)Q_{oo}(\underline{x}_{yz} - \underline{x}_{uv},t_\theta - t_w)$$

$$+ \delta_{gj}[Q_{oo}(\underline{x}_{uv} - \underline{x}_{mn},t_w - t_p)Q_{oo}(\underline{x}_{yz} - \underline{x}_{qr},t_\theta - t_s)$$

$$+ Q_{oo}(\underline{x}_{yz} - \underline{x}_{mn},t_\theta - t_p)Q_{oo}(\underline{x}_{uv} - \underline{x}_{qr},t_w - t_s)] \ . \quad (6\text{-}174)$$

However, according to equation (6-88),

$$Q_{oo}(\underline{x}_{qr} - \underline{x}_{mn},t_s - t_p) = \frac{1}{(2\pi)^3} \int_{-\infty}^{\infty}\int_{-\infty}^{\infty}\int_{-\infty}^{\infty} \Phi_o(\underline{\sigma},\Omega)$$

$$\exp\{i[\underline{\sigma}\cdot(\underline{x}_{qr}- \underline{x}_{mn}) + \Omega(t_s - t_p)]\}\ d\underline{\sigma}\ d\Omega \ . \quad (9\text{-}175)$$

Consequently, for a stationary, homogeneous sensor output field,

$$E\{o_{\alpha g}(\underline{x}_{mn},t_p)o_{\alpha g}(\underline{x}_{qr},t_s)o_{\alpha j}(\underline{x}_{uv},t_w)o_{\alpha j}(\underline{x}_{yz},t_\theta)\}$$

$$= \frac{1}{(2\pi)^6} \int_{-\infty}^{\infty}\int_{-\infty}^{\infty}\int_{-\infty}^{\infty}\int_{-\infty}^{\infty}\int_{-\infty}^{\infty}\int_{-\infty}^{\infty}\int_{-\infty}^{\infty}\int_{-\infty}^{\infty}\int_{-\infty}^{\infty}\int_{-\infty}^{\infty} \Phi_o(\underline{\sigma}_1,\Omega_1)\Phi_o(\underline{\sigma}_2,\Omega_2)$$

$$[\exp\{i[\underline{\sigma}_1\cdot(\underline{x}_{qr} - \underline{x}_{mn}) + \Omega_1(t_s - t_p)]\}$$

$$\exp\{i[\underline{\sigma}_2\cdot(\underline{x}_{yz} - \underline{x}_{uv}) + \Omega_2(t_\theta - t_w)]\}$$

$$+ \delta_{gj}\exp\{i[\underline{\sigma}_1\cdot(\underline{x}_{uv} - \underline{x}_{mn}) + \Omega_1(t_w - t_p)]\}$$

$$\exp\{i[\underline{\sigma}_2\cdot(\underline{x}_{yz} - \underline{x}_{qr}) + \Omega_2(t_\theta - t_s)]\}$$

$$+ \delta_{gj}\exp\{i[\underline{\sigma}_1\cdot(\underline{x}_{yz} - \underline{x}_{mn}) + \Omega_1(t_\theta - t_p)]\}$$

$$\exp\{i[\underline{\sigma}_2\cdot(\underline{x}_{uv} - \underline{x}_{qr}) + \Omega_2(t_w - t_s)]\}]\ d\underline{\sigma}_1\ d\Omega_1\ d\underline{\sigma}_2\ d\Omega_2 \quad (9\text{-}176)$$

Both the two wavevector-frequency spectrum and the space-averaged wavevector-frequency spectrum are descriptors of nonhomogeneous fields. By

substituting equation (9-172) into equation (9-165) and performing the summations on g and j, we can demonstrate, through careful bookkeeping, that

$$E\{|\tilde{S}_{oo}(\underline{\mu},\underline{k},\omega)|^2\} = \frac{1}{(2\pi)^{10}P^2T_s^2}$$

$$\Bigg\{\int_{-\infty}^{\infty}\int_{-\infty}^{\infty}\int_{-\infty}^{\infty}\int_{-\infty}^{\infty}\int_{-\infty}^{\infty} S_{oo}(\underline{\beta}_1,\underline{\sigma}_1,\Omega_1)|A_{wd}(\omega-\Omega_1)|^2$$

$$B_{wd}(\underline{\mu}-\underline{k}+\underline{\sigma}_1-\underline{\beta}_1)B_{wd}(\underline{k}-\underline{\sigma}_1)\ d\underline{\beta}_1\ d\underline{\sigma}_1\ d\Omega_1$$

$$\int_{-\infty}^{\infty}\int_{-\infty}^{\infty}\int_{-\infty}^{\infty}\int_{-\infty}^{\infty}\int_{-\infty}^{\infty} S_{oo}(\underline{\beta}_2,\underline{\sigma}_2,\Omega_2)|A_{wd}(\omega+\Omega_2)|^2$$

$$B^*_{wd}(\underline{\mu}-\underline{k}-\underline{\sigma}_2+\underline{\beta}_2)B^*_{wd}(\underline{k}+\underline{\sigma}_2)\ d\underline{\beta}_2\ d\underline{\sigma}_2\ d\Omega_2$$

$$+\frac{1}{J}\int_{-\infty}^{\infty}\int_{-\infty}^{\infty}\int_{-\infty}^{\infty}\int_{-\infty}^{\infty}\int_{-\infty}^{\infty} S_{oo}(\underline{\beta}_1,\underline{\sigma}_1,\Omega_1)|A_{wd}(\omega-\Omega_1)|^2$$

$$B_{wd}(\underline{\mu}-\underline{k}+\underline{\sigma}_1-\underline{\beta}_1)B^*_{wd}(\underline{\mu}-\underline{k}+\underline{\sigma}_1)\ d\underline{\beta}_1\ d\underline{\sigma}_1\ d\Omega_1$$

$$\int_{-\infty}^{\infty}\int_{-\infty}^{\infty}\int_{-\infty}^{\infty}\int_{-\infty}^{\infty}\int_{-\infty}^{\infty} S_{oo}(\underline{\beta}_2,\underline{\sigma}_2,\Omega_2)|A_{wd}(\omega+\Omega_2)|^2$$

$$B_{wd}(\underline{k}+\underline{\sigma}_2-\underline{\beta}_2)B^*_{wd}(\underline{k}+\underline{\sigma}_2)\ d\underline{\beta}_2\ d\underline{\sigma}_2\ d\Omega_2$$

$$+\frac{1}{J}\int_{-\infty}^{\infty}\int_{-\infty}^{\infty}\int_{-\infty}^{\infty}\int_{-\infty}^{\infty}\int_{-\infty}^{\infty} S_{oo}(\underline{\beta}_1,\underline{\sigma}_1,\Omega_1)A^*_{wd}(\omega+\Omega_1)A^*_{wd}(\omega-\Omega_1)$$

$$B^*_{wd}(\underline{k}+\underline{\sigma}_1)B_{wd}(\underline{\mu}-\underline{k}+\underline{\sigma}_1-\underline{\beta}_1)\ d\underline{\beta}_1\ d\underline{\sigma}_1\ d\Omega_1$$

$$\int_{-\infty}^{\infty}\int_{-\infty}^{\infty}\int_{-\infty}^{\infty}\int_{-\infty}^{\infty}\int_{-\infty}^{\infty} S_{oo}(\underline{\beta}_2,\underline{\sigma}_2,\Omega_2)A_{wd}(\omega-\Omega_2)A_{wd}(\omega+\Omega_2)$$

$$B_{wd}(\underline{k}+\underline{\sigma}_2-\underline{\beta}_2)B^*_{wd}(\underline{\mu}-\underline{k}+\underline{\sigma}_2)\ d\underline{\beta}_2\ d\underline{\sigma}_2\ d\Omega_2\Bigg\}\ . \qquad (9\text{-}177)$$

where $A_{wd}(\omega)$ and $B_{wd}(\underline{k})$ are given by equations (9-128) and (9-129), respectively.

By substituting equation (9-172) into equation (9-166) and performing the summations on g and j, we can similarly show that the mean value of the square of the estimate of the space-averaged wavevector-frequency spectrum can be written in the form

$$E\{\tilde{\Phi}_0^{a2}(\underline{k},\omega)\} = \frac{1}{(2\pi)^{10}(Md_1Nd_2PT_s)^2}$$

$$\left\{\int_{-\infty}^{\infty}\int_{-\infty}^{\infty}\int_{-\infty}^{\infty}\int_{-\infty}^{\infty}\int_{-\infty}^{\infty} S_{oo}(\underline{\beta}_1,\underline{\sigma}_1,\Omega_1)|A_{wd}(\omega-\Omega_1)|^2\right.$$

$$B_{wd}(-\underline{k}+\underline{\sigma}_1-\underline{\beta}_1)B_{wd}(\underline{k}-\underline{\sigma}_1)\,d\underline{\beta}_1\,d\underline{\sigma}_1\,d\Omega_1$$

$$\int_{-\infty}^{\infty}\int_{-\infty}^{\infty}\int_{-\infty}^{\infty}\int_{-\infty}^{\infty}\int_{-\infty}^{\infty} S_{oo}(\underline{\beta}_2,\underline{\sigma}_2,\Omega_2)|A_{wd}(\omega-\Omega_2)|^2$$

$$B_{wd}(-\underline{k}+\underline{\sigma}_2-\underline{\beta}_2)B_{wd}(\underline{k}-\underline{\sigma}_2)\,d\underline{\beta}_2\,d\underline{\sigma}_2\,d\Omega_2$$

$$+\frac{1}{J}\int_{-\infty}^{\infty}\int_{-\infty}^{\infty}\int_{-\infty}^{\infty}\int_{-\infty}^{\infty}\int_{-\infty}^{\infty} S_{oo}(\underline{\beta}_1,\underline{\sigma}_1,\Omega_1)A_{wd}^*(\omega+\Omega_1)A_{wd}^*(\omega-\Omega_1)$$

$$B_{wd}(-\underline{k}+\underline{\sigma}_1-\underline{\beta}_1)B_{wd}(-\underline{k}-\underline{\sigma}_1)\,d\underline{\beta}_1\,d\underline{\sigma}_1\,d\Omega_1$$

$$\int_{-\infty}^{\infty}\int_{-\infty}^{\infty}\int_{-\infty}^{\infty}\int_{-\infty}^{\infty}\int_{-\infty}^{\infty} S_{oo}(\underline{\beta}_2,\underline{\sigma}_2,\Omega_2)A_{wd}(\omega-\Omega_2)A_{wd}(\omega+\Omega_2)$$

$$B_{wd}(\underline{k}+\underline{\sigma}_2-\underline{\beta}_2)B_{wd}(\underline{k}-\underline{\sigma}_2)\,d\underline{\beta}_2\,d\underline{\sigma}_2\,d\Omega_2$$

$$+\frac{1}{J}\int_{-\infty}^{\infty}\int_{-\infty}^{\infty}\int_{-\infty}^{\infty}\int_{-\infty}^{\infty}\int_{-\infty}^{\infty} S_{oo}(\underline{\beta}_1,\underline{\sigma}_1,\Omega_1)|A_{wd}(\omega-\Omega_1)|^2$$

$$B_{wd}(\underline{k}-\underline{\sigma}_1)B_{wd}(-\underline{k}+\underline{\sigma}_1-\underline{\beta}_1)\,d\underline{\beta}_1\,d\underline{\sigma}_1\,d\Omega_1$$

$$\int_{-\infty}^{\infty}\int_{-\infty}^{\infty}\int_{-\infty}^{\infty}\int_{-\infty}^{\infty}\int_{-\infty}^{\infty} S_{oo}(\underline{\beta}_2,\underline{\sigma}_2,\Omega_2)|A_{wd}(\omega+\Omega_2)|^2$$

$$\left.B_{wd}(\underline{k}+\underline{\sigma}_2-\underline{\beta}_2)B_{wd}(-\underline{k}-\underline{\sigma}_2)\,d\underline{\beta}_2\,d\underline{\sigma}_2\,d\Omega_2\right\}. \qquad (9\text{-}178)$$

The mean value of the square of the estimate of the wavevector-frequency spectrum of a stationary, homogeneous sensor output field can be expressed in terms of the true wavevector-frequency spectrum of that field by substituting equation (9-176) into equation (9-166). By making this substitution and performing the summations over g and j, we can show that

$$E\{\tilde{\Phi}_o^2(\underline{k},\omega)\} = \frac{1}{(2\pi)^6(Md_1Nd_2PT_s)^2}$$

$$\Bigg\{\int_{-\infty}^{\infty}\int_{-\infty}^{\infty}\int_{-\infty}^{\infty} \Phi_o(\underline{\sigma}_1,\Omega_1)|A_{wd}(\omega - \Omega_1)|^2|B_{wd}(\underline{k} - \underline{\sigma}_1)|^2\, d\underline{\sigma}_1\, d\Omega_1$$

$$\int_{-\infty}^{\infty}\int_{-\infty}^{\infty}\int_{-\infty}^{\infty} \Phi_o(\underline{\sigma}_2,\Omega_2)|A_{wd}(\omega - \Omega_2)|^2|B_{wd}(\underline{k} - \underline{\sigma}_2)|^2\, d\underline{\sigma}_2\, d\Omega_2$$

$$+ \frac{1}{J}\int_{-\infty}^{\infty}\int_{-\infty}^{\infty}\int_{-\infty}^{\infty} \Phi_o(\underline{\sigma}_1,\Omega_1)A_{wd}^*(\omega + \Omega_1)A_{wd}^*(\omega - \Omega_1)$$

$$B_{wd}^*(\underline{k} - \underline{\sigma}_1)B_{wd}^*(\underline{k} + \underline{\sigma}_1)\, d\underline{\sigma}_1\, d\Omega_1$$

$$\int_{-\infty}^{\infty}\int_{-\infty}^{\infty}\int_{-\infty}^{\infty} \Phi_o(\underline{\sigma}_2,\Omega_2)A_{wd}(\omega - \Omega_2)A_{wd}(\omega + \Omega_2)$$

$$B_{wd}(\underline{k} + \underline{\sigma}_2)B_{wd}(\underline{k} - \underline{\sigma}_2)\, d\underline{\sigma}_2\, d\Omega_2$$

$$+ \frac{1}{J}\int_{-\infty}^{\infty}\int_{-\infty}^{\infty}\int_{-\infty}^{\infty} \Phi_o(\underline{\sigma}_1,\Omega_1)|A_{wd}(\omega - \Omega_1)|^2|B_{wd}(\underline{k} - \underline{\sigma}_1)|^2\, d\underline{\sigma}_1\, d\Omega_1$$

$$\int_{-\infty}^{\infty}\int_{-\infty}^{\infty}\int_{-\infty}^{\infty} \Phi_o(\underline{\sigma}_2,\Omega_2)|A_{wd}(\omega + \Omega_2)|^2|B_{wd}(\underline{k} + \underline{\sigma}_2)|^2\, d\underline{\sigma}_2\, d\Omega_2\Bigg\}. \quad (9\text{-}179)$$

We can achieve considerable simplification of equations (9-177), (9-178), and (9-179) by making use of certain properties of the true wavevector-frequency spectra and of the spectral windows $A_{wd}(\omega)$ and $B_{wd}(\underline{k})$. That is, by equations (6-224) and (6-227), we know that

$$S_{oo}(\underline{\mu},\underline{k},\omega) = S^*_{oo}(-\underline{\mu},-\underline{k},-\omega) = S_{oo}(\underline{\mu},\underline{\mu} - \underline{k},-\omega) \ . \tag{9-180}$$

Further, as demonstrated in equations (6-82) and (6-83),

$$\Phi_o(\underline{k},\omega) = \Phi_o(-\underline{k},-\omega) = \Phi^*_o(\underline{k},\omega) \ . \tag{9-181}$$

Finally, inasmuch as $a_w(t_p)$ and $b_w(\underline{x}_{mn})$ are real, it follows from equations (9-128) and (9-129) that

$$A_{wd}(-\omega) = A^*_{wd}(\omega) \tag{9-182}$$

and

$$B_{wd}(-\underline{k}) = B^*_{wd}(\underline{k}) \ . \tag{9-183}$$

By employing equations (9-180), (9-182), and (9-183) in equation (9-177), we can demonstrate, with suitable changes of variables, that

$$E\{|\tilde{S}_{oo}(\underline{\mu},\underline{k},\omega)|^2\} = \frac{1}{(2\pi)^{10}P^2T_s^2}$$

$$\Bigg\{\Bigg|\int_{-\infty}^{\infty}\int_{-\infty}^{\infty}\int_{-\infty}^{\infty}\int_{-\infty}^{\infty}\int_{-\infty}^{\infty} S_{oo}(\underline{\beta}_1,\underline{\sigma}_1,\Omega_1)|A_{wd}(\omega - \Omega_1)|^2$$

$$B_{wd}(\underline{\mu} - \underline{k} + \underline{\sigma}_1 - \underline{\beta}_1)B_{wd}(\underline{k} - \underline{\sigma}_1) \ d\underline{\beta}_1 \ d\underline{\sigma}_1 \ d\Omega_1\Bigg|^2$$

$$+ \frac{1}{J}\int_{-\infty}^{\infty}\int_{-\infty}^{\infty}\int_{-\infty}^{\infty}\int_{-\infty}^{\infty}\int_{-\infty}^{\infty} S_{oo}(\underline{\beta}_1,\underline{\sigma}_1,\Omega_1)|A_{wd}(\omega - \Omega_1)|^2$$

$$B_{wd}(\underline{\mu} - \underline{k} + \underline{\sigma}_1 - \underline{\beta}_1)B_{wd}(\underline{k} - \underline{\mu} - \underline{\sigma}_1) \ d\underline{\beta}_1 \ d\underline{\sigma}_1 \ d\Omega_1$$

$$\int_{-\infty}^{\infty}\int_{-\infty}^{\infty}\int_{-\infty}^{\infty}\int_{-\infty}^{\infty}\int_{-\infty}^{\infty} S_{oo}(\underline{\beta}_2,\underline{\sigma}_3,\Omega_3)|A_{wd}(\omega - \Omega_3)|^2$$

$$B_{wd}(\underline{k} - \underline{\sigma}_3)B_{wd}(-\underline{k} + \underline{\sigma}_3 - \underline{\beta}_2) \ d\underline{\beta}_2 \ d\underline{\sigma}_3 \ d\Omega_3$$

$$+ \frac{1}{J}\Bigg|\int_{-\infty}^{\infty}\int_{-\infty}^{\infty}\int_{-\infty}^{\infty}\int_{-\infty}^{\infty}\int_{-\infty}^{\infty} S_{oo}(\underline{\beta}_2,\underline{\sigma}_2,\Omega_2)A_{wd}(\omega - \Omega_2)A_{wd}(\omega + \Omega_2)$$

$$B_{wd}(\underline{k} + \underline{\sigma}_2 - \underline{\beta}_2)B^*_{wd}(\underline{\mu} - \underline{k} + \underline{\sigma}_2) \ d\underline{\beta}_2 \ d\underline{\sigma}_2 \ d\Omega_2\Bigg|^2\Bigg\} . \tag{9-184}$$

From equation (9-127), we recognize the first term on the right-hand side of equation (9-184) to be $|E\{\tilde{S}_{00}(\underline{\mu},\underline{k},\omega)\}|^2$, and the second term to be the product $E\{\tilde{S}_{00}(\underline{0},\underline{k} - \underline{\mu},\omega)\}E\{\tilde{S}_{00}(\underline{0},\underline{k},\omega)\}$. However, from equations (9-123) and (9-124),

$$\tilde{S}_{00}(\underline{0},\underline{\alpha},\omega) = Md_1Nd_2\tilde{\Phi}_0^a(\underline{\alpha},\omega) \ . \tag{9-185}$$

Therefore, by reference to equation (9-162), it follows that

$$\begin{aligned}\mathrm{Var}\{\tilde{S}_{00}(\underline{\mu},\underline{k},\omega)\} &= \frac{1}{J}(Md_1Nd_2)^2E\{\tilde{\Phi}_0^a(\underline{k} - \underline{\mu},\omega)\}E\{\tilde{\Phi}_0^a(\underline{k},\omega)\} \\ &+ \frac{1}{(2\pi)^{10}P^2T_s^2J}\left|\int_{-\infty}^{\infty}\int_{-\infty}^{\infty}\int_{-\infty}^{\infty}\int_{-\infty}^{\infty}\int_{-\infty}^{\infty} S_{00}(\underline{\beta}_2,\underline{\sigma}_2,\Omega_2)A_{wd}(\omega - \Omega_2)A_{wd}(\omega + \Omega_2)\right. \\ &\left. B_{wd}(\underline{k} + \underline{\sigma}_2 - \underline{\beta}_2)B_{wd}^*(\underline{\mu} - \underline{k} + \underline{\sigma}_2)\, d\underline{\beta}_2\, d\underline{\sigma}_2\, d\Omega_2\right|^2 \ .\end{aligned} \tag{9-186}$$

Note that if $E\{\tilde{\Phi}_0^a(\underline{k} - \underline{\mu},\omega)\}$, $E\{\tilde{\Phi}_0^a(\underline{0},\underline{k},\omega)\}$, and the multiple integrals on the right-hand side of equation (9-186) are finite, then

$$\lim_{J\to\infty} \mathrm{Var}\{\tilde{S}_{00}(\underline{\mu},\underline{k},\omega)\} = 0 \ . \tag{9-187}$$

The multiple integral of equation (9-186) has the general form

$$I(\underline{\mu},\underline{k},\omega) = \int_{-\infty}^{\infty}\int_{-\infty}^{\infty}\int_{-\infty}^{\infty}\int_{-\infty}^{\infty}\int_{-\infty}^{\infty} S_{00}(\underline{\beta}_2,\underline{\sigma}_2,\Omega_2)G(\underline{\beta}_2,\underline{\sigma}_2,\Omega;\underline{\mu},\underline{k},\omega)\, d\underline{\beta}_2\, d\underline{\sigma}_2\, d\Omega_2 \ , \tag{9-188}$$

where

$$G(\underline{\beta}_2,\underline{\sigma}_2,\Omega;\underline{\mu},\underline{k},\omega) = A_{wd}(\omega - \Omega_2)A_{wd}(\omega + \Omega_2)B_{wd}(\underline{k} + \underline{\sigma}_2 - \underline{\beta}_2)B_{wd}^*(\underline{\mu} - \underline{k} + \underline{\sigma}_2) \ . \tag{9-189}$$

If the integral $I(\underline{\mu},\underline{k},\omega)$ is to be finite, we require that $|I(\underline{\mu},\underline{k},\omega)| < \infty$.

It is well known that

$$\left| \int_{-\infty}^{\infty}\int_{-\infty}^{\infty}\int_{-\infty}^{\infty}\int_{-\infty}^{\infty}\int_{-\infty}^{\infty} S_{oo}(\underline{\beta}_2,\underline{\sigma}_2,\Omega_2)G(\underline{\beta}_2,\underline{\sigma}_2,\Omega;\underline{\mu},\underline{k},\omega)\ d\underline{\beta}_2\ d\underline{\sigma}_2\ d\Omega_2 \right|$$

$$\leq \int_{-\infty}^{\infty}\int_{-\infty}^{\infty}\int_{-\infty}^{\infty}\int_{-\infty}^{\infty}\int_{-\infty}^{\infty} |S_{oo}(\underline{\beta}_2,\underline{\sigma}_2,\Omega_2)||G(\underline{\beta}_2,\underline{\sigma}_2,\Omega;\underline{\mu},\underline{k},\omega)|\ d\underline{\beta}_2\ d\underline{\sigma}_2\ d\Omega_2\ . \quad (9\text{-}190)$$

Moreover, it is easily established from equations (9-128) and (9-129) that

$$|A_{wd}(\omega)| \leq T_s \sum_{p=1}^{P} |a_w(t_p)| \quad (9\text{-}191)$$

and

$$|B_{wd}(\underline{k})| \leq d_1 d_2 \sum_{m=1}^{M}\sum_{n=1}^{N} |b_w(\underline{x}_{mn})|\ . \quad (9\text{-}192)$$

Therefore, it follows from equations (9-189), (9-191), and (9-192) that

$$|G(\underline{\beta}_2,\underline{\sigma}_2,\Omega;\underline{\mu},\underline{k},\omega)| \leq G_{max} = \text{constant}\ , \quad (9\text{-}193)$$

where

$$G_{max} = \left\{T_s \sum_{p=1}^{P} |a_w(t_p)|\right\}^2 \left\{d_1 d_2 \sum_{m=1}^{M}\sum_{n=1}^{N} |b_w(\underline{x}_{mn})|\right\}^2 . \quad (9\text{-}194)$$

From equations (9-190) and (9-193), it is evident that

$$|I(\underline{\mu},\underline{k},\omega)| \leq G_{max} \int_{-\infty}^{\infty}\int_{-\infty}^{\infty}\int_{-\infty}^{\infty}\int_{-\infty}^{\infty}\int_{-\infty}^{\infty} |S_{oo}(\underline{\beta}_2,\underline{\sigma}_2,\Omega_2)|\ d\underline{\beta}_2\ d\underline{\sigma}_2\ d\Omega_2\ . \quad (9\text{-}195)$$

For realistic weightings, G_{max} is finite. Therefore, if $|I(\underline{\mu},\underline{k},\omega)|$ is to be finite, we require

$$\int_{-\infty}^{\infty}\int_{-\infty}^{\infty}\int_{-\infty}^{\infty}\int_{-\infty}^{\infty}\int_{-\infty}^{\infty} |S_{oo}(\underline{\beta}_2,\underline{\sigma}_2,\Omega_2)|\ d\underline{\beta}_2\ d\underline{\sigma}_2\ d\Omega_2 \leq \infty\ . \quad (9\text{-}196)$$

By applying arguments similar to those employed above to equation (9-132), we can demonstrate that equation (9-196) is also the requisite condition for $E\{\tilde{\Phi}_o^a(\underline{k} - \underline{\mu},\omega)\}$ and $E\{\tilde{\Phi}_o^a(\underline{0},\underline{k},\omega)\}$ to be finite. According to Sneddon,[24] equation (9-196) is a sufficient condition for the existence of the Fourier transform of $S_{oo}(\underline{\beta}_2,\underline{\sigma}_2,\Omega)$ on the variables $\underline{\beta}_2$, $\underline{\sigma}_2$, and Ω. Thus, we conclude that if the multiple Fourier transform of $S_{oo}(\underline{\mu},\underline{k},\omega)$ exists, then the variance of the estimate of $\tilde{S}_{oo}(\underline{\mu},\underline{k},\omega)$ tends to zero as the number (J) of independent observations approaches infinity.

By appropriate use of equations (9-180), (9-182), and (9-183) in equation (9-178), we can show that

$$E\{\tilde{\Phi}_o^{a2}(\underline{k},\omega)\} = \frac{1}{(2\pi)^{10}(Md_1Nd_2PT_s)^2}$$

$$\Bigg\{\Bigg[\int_{-\infty}^{\infty}\int_{-\infty}^{\infty}\int_{-\infty}^{\infty}\int_{-\infty}^{\infty}\int_{-\infty}^{\infty} S_{oo}(\underline{\beta}_1,\underline{\sigma}_1,\Omega_1)|A_{wd}(\omega - \Omega_1)|^2$$

$$B_{wd}(-\underline{k} + \underline{\sigma}_1 - \underline{\beta}_1)B_{wd}(\underline{k} - \underline{\sigma}_1)\, d\underline{\beta}_1\, d\underline{\sigma}_1\, d\Omega_1\Bigg]^2$$

$$+ \frac{1}{J}\Bigg|\int_{-\infty}^{\infty}\int_{-\infty}^{\infty}\int_{-\infty}^{\infty}\int_{-\infty}^{\infty}\int_{-\infty}^{\infty} S_{oo}(\underline{\beta}_2,\underline{\sigma}_2,\Omega_2)A_{wd}(\omega - \Omega_2)A_{wd}(\omega + \Omega_2)$$

$$B_{wd}(\underline{k} + \underline{\sigma}_2 - \underline{\beta}_2)B_{wd}(\underline{k} - \underline{\sigma}_2)\, d\underline{\beta}_2\, d\underline{\sigma}_2\, d\Omega_2\Bigg|^2$$

$$+ \frac{1}{J}\Bigg|\int_{-\infty}^{\infty}\int_{-\infty}^{\infty}\int_{-\infty}^{\infty}\int_{-\infty}^{\infty}\int_{-\infty}^{\infty} S_{oo}(\underline{\beta}_1,\underline{\sigma}_1,\Omega_1)|A_{wd}(\omega - \Omega_1)|^2$$

$$B_{wd}(\underline{k} - \underline{\sigma}_1)B_{wd}(-\underline{k} + \underline{\sigma}_1 - \underline{\beta}_1)\, d\underline{\beta}_1\, d\underline{\sigma}_1\, d\Omega_1\Bigg|^2\Bigg\} . \qquad (9\text{-}197)$$

However, from equation (9-132), we recognize the first term on the right to be $E\{\tilde{\Phi}_o^a(\underline{k},\omega)\}^2$, and the last term on the right to be $|E\{\tilde{\Phi}_o^a(\underline{k},\omega)\}|^2$. Therefore, according to equation (9-162), it follows that

$$\mathrm{Var}\{\tilde{\Phi}_o^a(\underline{k},\omega)\} = \frac{1}{J}\, |E\{\tilde{\Phi}_o^a(\underline{k},\omega)\}|^2$$

$$+ \frac{1}{(2\pi)^{10}(Md_1 Nd_2 PT_s)^2 J} \left| \int_{-\infty}^{\infty}\int_{-\infty}^{\infty}\int_{-\infty}^{\infty}\int_{-\infty}^{\infty}\int_{-\infty}^{\infty} S_{oo}(\underline{\beta}_2,\underline{\sigma}_2,\Omega_2) \right.$$

$$\left. A_{wd}(\omega - \Omega_2)A_{wd}(\omega + \Omega_2)B_{wd}(\underline{k} + \underline{\sigma}_2 - \underline{\beta}_2)B_{wd}(\underline{k} - \underline{\sigma}_2)\; d\underline{\beta}_2\, d\underline{\sigma}_2\, d\Omega_2 \right|^2 . \tag{9-198}$$

By arguments similar to those employed in assessing the variance of the estimate of the two wavevector-frequency spectrum, we can show that if the multiple Fourier transform of $S_{oo}(\underline{\mu},\underline{k},\omega)$ on the variables $\underline{\mu}$, $\underline{k}$, and ω exists, then it follows from equation (9-198) that the variance of the estimate of the space-averaged wavevector-frequency spectrum tends to zero as the number (J) of independent estimates approaches infinity.

By appropriate use of equations (9-181), (9-182), and (9-183) in equation (9-179), and by employing equations (9-133) and (9-162), we can use arguments similar to those used to assess the variances of the estimates of the two wavevector-frequency spectrum and the space-averaged wavevector-frequency spectrum to demonstrate that the variance of the estimate of the wavevector-frequency spectrum of the stationary, homogeneous sensor output field is given by

$$\mathrm{Var}\{\tilde{\Phi}_o(\underline{k},\omega)\} = \frac{1}{J}\, |E\{\tilde{\Phi}_o(\underline{k},\omega)\}|^2$$

$$+ \frac{1}{(2\pi)^{6}(Md_1 Nd_2 PT_s)^2 J} \left| \int_{-\infty}^{\infty}\int_{-\infty}^{\infty}\int_{-\infty}^{\infty} \Phi_o(\underline{\sigma}_2,\Omega_2)A_{wd}(\omega + \Omega_2)A_{wd}(\omega - \Omega_2) \right.$$

$$\left. B_{wd}(\underline{k} - \underline{\sigma}_2)B_{wd}(\underline{k} + \underline{\sigma}_2)\; d\underline{\sigma}_2\, d\Omega_2 \right|^2 . \tag{9-199}$$

It can be demonstrated, by arguments similar to those employed previously, that if the multiple Fourier transform of $\Phi_o(\underline{k},\omega)$ exists, then

$$\lim_{J\to\infty} \mathrm{Var}\{\tilde{\Phi}_o(\underline{k},\omega)\} = 0 . \tag{9-200}$$

9.3.3 Some Practical Observations Regarding the Quality of the Estimators

Recall (see section 9.1) that our metrics of the quality of an estimate are the bias and mean square error. Recall further (see equation (9-7)) that the mean square error of an estimate is the sum of the variance and the squared magnitude of the bias error of that estimate. Clearly, the ideal estimator is one that is unbiased and has zero variance.

In section 9.3.1, we showed that the estimates of the two wavevector-frequency spectrum and the space-averaged wavevector-frequency spectrum of a stationary, nonhomogeneous field given by equations (9-123) and (9-124) and the estimate of the wavevector-frequency spectrum of the homogeneous field given by equation (9-124) were generally biased, and that the bias errors were independent of the number (J) of statistically independent sample functions used in the estimates. However, given that all true wavevector-frequency spectra were band limited in the wavevector and frequency domains, we also showed that the bias error of any estimator was significantly reduced when the bandwidths of the primary acceptance lobes of the spectral filters $A(\omega)$ and $B(\underline{k})$ were substantially narrower than the bandwidths of any fluctuation of the associated true wavevector-frequency spectrum in the respective frequency and wavevector domains.

For uniform temporal weighting of the discrete space-time sample function, we showed that the bandwidth of the primary acceptance lobes of $A(\omega)$ were inversely proportional to the temporal length (PT_s) of the sample function. Similarly, for uniform spatial weighting of the discrete sample function, we showed that the bandwidths of the primary acceptance lobes of $B(\underline{k})$ in the k_1 and k_2 coordinate directions were inversely proportional to the spatial lengths (Md_1 and Nd_2) of the sample function in the respective x_1 and x_2 coordinate directions. It can be demonstrated (although we will not do so here) that these inverse relationships between bandwidths of the primary acceptance lobes of $A(\omega)$ and $B(\underline{k})$ and the temporal and spatial dimensions of the discrete space-time sample function also hold for practical weighting functions, $a_w(t_p)$ and $b_w(\underline{x}_{mn})$, other than uniform.

Clearly, given some preliminary knowledge of the wavevector and frequency

characteristics of the true wavevector-frequency spectrum of the sensor output field of interest, the bias error of the estimate of that wavevector-frequency spectrum can, within pra cal constraints, be controlled by judicious design of the experiment.

In the previous section, we demonstrated that the variance of the estimates of all forms of wavevector-frequency spectra decreased as the number (J) of statistically independent space-time sample functions comprising that estimate increased. It should be recalled that, given the discrete space-time sample function resulting from any single realization of an experiment of time duration T_0, some finite number (J) of (essentially) statistically independent, discrete sample functions can be realized by appropriately partitioning the measured sample function in the time domain. To ensure the practical statistical independence of the sample functions resulting from this partitioning, the temporal length (PT_s) of each sample function must be much greater than the maximum time delay (τ_{max}) required f the autocorrelation function to become effectively zero within the ranges of the spatial variables $\underline{x}$ and $\underline{\xi}$ afforded by the array of sensors utilized for the measurement.

Clearly, to reduce the bias of our spectral estimate and to ensure statistical independence of the space-time sample functions used in that estimate, we desire the temporal length (PT_s) of these discrete sample functions to be large. However, given that the temporal duration of any realization of the experiment is limited to T_0, it is evident that the number (J) of statistically independent sample functions available from that realization is an integer less than or equal to $T_0/(PT_s)$. Consequently, as the temporal length (PT_s) of the sample function increases, the number (J) of statistically independent sample functions decreases, and the variance of the estimate increases. Thus, given a discrete space-time field resulting from a single realization of an experiment, it is evident that a decrease in the bias of an estimate can usually be achieved only at the expense of an increase in the variance of the estimate.

Inasmuch as the mean square error of an estimate is the sum of the variance and the squared magnitude of the bias error, it is desirable to

select the number and the temporal lengths of the statistically independent sample functions to achieve that mix of variance and bias error that results in the minimum mean square error. However, because the bias error and the variance are both functions of the (unknown) true wavevector-frequency spectrum of interest, this optimization can only be addressed by a process of trial and error.

9.3.4 Computational Forms of the Spectral Estimates

Numerical evaluation of the wavevector-frequency spectral estimates given by equations (9-123) and (9-124) is facilitated by shifting the origins of the spatial and temporal coordinates. To this end, we choose the new spatial origin to be at the location of the (1,1)-th sensor of the array and the new temporal origin to be coincident with the first time sample. The spatial vector from the (1,1) sensor to the geometric center of the array, which we denote by $\underset{\sim}{x}_c$, is

$$\underset{\sim}{x}_c = \left[\frac{(M-1)d_1}{2}, \frac{(N-1)d_2}{2}\right], \tag{9-201}$$

and the time between the first temporal sample and the center of the P samples, which we denote by t_c, is

$$t_c = \frac{(P-1)T_s}{2} . \tag{9-202}$$

If we denote the spatial vector relative to the (1,1) sensor by $\tilde{\underset{\sim}{x}}$ and the time relative to the first temporal sensor by $\tilde{t}$, we can establish the following relationships:

$$\tilde{\underset{\sim}{x}}_{mn} = \underset{\sim}{x}_{mn} + \underset{\sim}{x}_c = [(m-1)d_1, \ (n-1)d_2], \quad 1 \le m \le M, \quad 1 \le n \le N , \tag{9-203}$$

and

$$\tilde{t}_p = t_p + t_c = (p-1)T_s, \quad 1 \le p \le P . \tag{9-204}$$

Let us now define

$$\tilde{o}_{j\alpha}(\tilde{\underline{x}}_{mn},\tilde{t}_p) = o_{j\alpha}(\underline{x}_{mn},t_p) \ , \tag{9-205}$$

$$\tilde{a}_w(\tilde{t}_p) = a_w(t_p) \ , \tag{9-206}$$

and

$$\tilde{b}_w(\tilde{\underline{x}}_{mn}) = b_w(\underline{x}_{mn}) \ , \tag{9-207}$$

for $1 \leq m \leq M$, $1 \leq n \leq N$, and $1 \leq p \leq P$. If we then define

$$\tilde{\varepsilon}_j(\tilde{\underline{x}}_{mn},\tilde{t}_p) = \tilde{a}_w(\tilde{t}_p)\tilde{b}_w(\tilde{\underline{x}}_{mn})\tilde{o}_{j\alpha}(\tilde{\underline{x}}_{mn},\tilde{t}_p) \ , \tag{9-208}$$

it is evident that

$$\tilde{\varepsilon}_j(\tilde{\underline{x}}_{mn},\tilde{t}_p) = \varepsilon_j(\underline{x}_{mn},t_p), \quad 1 \leq m \leq M, \quad 1 \leq n \leq N, \quad 1 \leq p \leq P \ . \tag{9-209}$$

By substitution of equation (9-209) into equation (9-122), we can easily show that

$$\mathcal{E}_{jd}(\underline{k},\omega) = \tilde{\mathcal{E}}_{jd}(\underline{k},\omega)\exp\{i(\underline{k}\cdot\underline{x}_c + \omega t_c)\} \ , \tag{9-210}$$

where

$$\tilde{\mathcal{E}}_{jd}(\underline{k},\omega) = d_1 d_2 T_s \sum_{m=1}^{M}\sum_{n=1}^{N}\sum_{p=1}^{P} \tilde{\varepsilon}_j(\tilde{\underline{x}}_{mn},\tilde{t}_p)\exp\{-i(\underline{k}\cdot\tilde{\underline{x}}_{mn} + \omega\tilde{t}_p)\} \ . \tag{9-211}$$

However, by use of equation (9-208) and a change of the indices of summation, we can rewrite equation (9-211) in the computationally convenient form

$$\tilde{\mathcal{E}}_{jd}(\underline{k},\omega) = d_1 d_2 T_s \sum_{q=0}^{M-1}\sum_{r=0}^{N-1}\sum_{u=0}^{P-1} \tilde{a}_w(uT_s)\tilde{b}_w(qd_1,rd_2)\tilde{o}_{j\alpha}(qd_1,rd_2,uT_s)$$

$$\exp\{-i(k_1 qd_1 + k_2 rd_2 + \omega uT_s)\} \ . \tag{9-212}$$

To avail ourselves of this computationally efficient form for $\tilde{\mathcal{E}}_{jd}(\underline{k},\omega)$, we make use of equation (9-210) to write the estimate of the two wavevector-

frequency spectrum of the stationary, nonhomogeneous sensor output field, given by equation (9-213), in the form

$$\tilde{S}_{oo}(\underline{\mu},\underline{k},\omega) = \frac{\exp(i\underline{\mu}\cdot\underline{x}_c)}{JPT_s} \sum_{j=1}^{J} \tilde{\mathcal{E}}_{jd}(\underline{\mu} - \underline{k},-\omega)\tilde{\mathcal{E}}_{jd}(\underline{k},\omega) \ ,$$

$$|\omega| \le \pi/T_s, \quad |k_1| \le \pi/d_1, \quad |k_2| \le \pi/d_2, \quad |\mu_1 - k_1| \le \pi/d_1, \quad |\mu_2 - k_2| \le \pi/d_2 \ . \tag{9-213}$$

Similarly, by substituting equation (9-210) into equation (9-124), the mathematically identical estimates of the space-averaged wavevector-frequency spectrum of the stationary, nonhomogeneous sensor output field and the wavevector-frequency spectrum of the stationary, homogeneous sensor output field can be expressed in the form

$$\tilde{\Phi}_o(\underline{k},\omega) = \tilde{\Phi}_o^a(\underline{k},\omega) = \frac{1}{JMd_1Nd_2PT_s} \sum_{j=1}^{J} |\tilde{\mathcal{E}}_{jd}(\underline{k},\omega)|^2 \ ,$$

$$|\omega| \le \pi/T_s, \ |k_1| \le \pi/d_1, \ |k_2| \le \pi/d_2 \ . \tag{9-214}$$

Equations (9-213) and (9-214), in conjunction with equation (9-212), are relatively efficient computational forms for estimating wavevector-frequency spectra from discrete space-time sample functions of the sensor output field.

9.4 REFERENCES

1. G. Maidanik and D. W. Jorgensen, "Boundary Wave-Vector Filters for the Study of the Pressure Field in a Turbulent Boundary Layer," Journal of the Acoustical Society of America, vol. 42, no. 2, August 1967, pp. 494-501.

2. R. M. Kennedy and W. A. Strawderman, "Examples of Two Wavenumber Spectra in Nonhomogeneous One-Dimensional Structures," NUSC Technical Document 8429, Naval Underwater Systems Center, New London, CT, 16 November 1988.

3. J. S. Bendat and A. G. Piersol, The Measurement and Analysis of Random Data, John Wiley and Sons, Inc., New York, 1966, pp. 182-183.

4. Ibid., p. 183.

5. A. Papoulis, Probability, Random Variables, and Stochastic Processes, McGraw-Hill Book Co., New York, 1965, p. 241.

6. W. K. Blake and D. M. Chase, "Wavenumber-Frequency Spectra of Turbulent-Boundary-Layer Pressure Measured by Microphone Arrays," Journal of the Acoustical Society of America, vol. 49, no. 3, March 1971, pp. 862-877.

7. P. W. Jameson, "Measurement of Low-Wavenumber Component of Turbulent Boundary Layer Wall Pressure Spectrum," BBN Report No. 1937, Bolt Beranek and Newman, Cambridge, MA, 1970.

8. T. M. Farabee and F. E. Geib, "Measurement of Boundary Layer Pressure Fields With an Array of Transducers in a Subsonic Flow," DTRDC Report 76-0031, David Taylor Research and Development Center, Bethesda, MD, 1976.

9. N. C. Martin and P. Leehey, "Low Wavenumber Wall Pressure Measurements Using a Rectangular Membrane as a Spatial Filter," Journal of Sound and Vibration, vol. 52, no. 1, 1977, pp. 95-120.

10. W. A. Strawderman, "Development of a Prototype Wavevector-Frequency Spectral Analysis System," NUSC Technical Document 7295, Naval Underwater Systems Center, New London, CT, 12 December 1984.

11. W. A. Strawderman, "Wavevector-Frequency Spectral Estimation: A Review of Conventional Signal Processing Techniques," NUSC Technical Document 8469, Naval Underwater Systems Center, New London, CT, 14 February 1989.

12. A. Papoulis, The Fourier Integral and Its Applications, McGraw-Hill Book Co., New York, 1962, p. 32.

13. J. S. Bendat and A. G. Piersol, op. cit., p. 94.

14. G. M. Jenkins and D. G. Watts, Spectral Analysis and Its Applications, Holden-Day, Inc., San Francisco, 1968, pp. 222-223.

15. W. B. Davenport and W. L. Root, An Introduction to the Theory of Random Signals and Noise, McGraw-Hill Book Co., New York, 1958, p. 107.

16. Ibid., pp. 107-108.

17. R. B. Blackman and J. W. Tukey, The Measurement of Power Spectra, Dover Publications, Inc., New York, 1959, p. 11.

18. M. S. Bartlett, An Introduction to Stochastic Processes With Special Reference to Methods and Applications, Cambridge University Press, Cambridge, UK, 1955, pp. 280-281.

19. A. V. Oppenheim and R. W. Schafer, Digital Signal Processing, Prentice Hall, Inc., Englewood Cliffs, NJ, 1975, pp. 548-549.

20. P. D. Welch, "The Use of Fast Fourier Transforms for the Estimation of Power Spectra: A Method Based on Time Averaging Over Short, Modified Periodograms," IEEE Transactions on Audio and Electroacoustics, vol. AU15, no. 2, June 1967, pp. 70-73.

21. A. H. Nuttall, "Spectral Estimation By Means of Overlapped Fast Fourier Transform Processing of Windowed Data," NUSC Technical Report 4169, Naval Underwater Systems Center, New London, CT, 13 October 1971.

22. A. Papoulis, Probability, Random Variables, and Stochastic Processes, McGraw-Hill Book Co., New York, 1965, pp. 474-475.

23. Ibid., p. 221.

24. I. N. Sneddon, Fourier Transforms, McGraw-Hill Book Co., New York, 1951, pp. 15-19.